Light Scattering, Size Exclusion Chromatography and Asymmetric Flow Field Flow Fractionation

Powerful Tools for the Characterization of Polymers, Proteins, and Nanoparticles

Stepan Podzimek

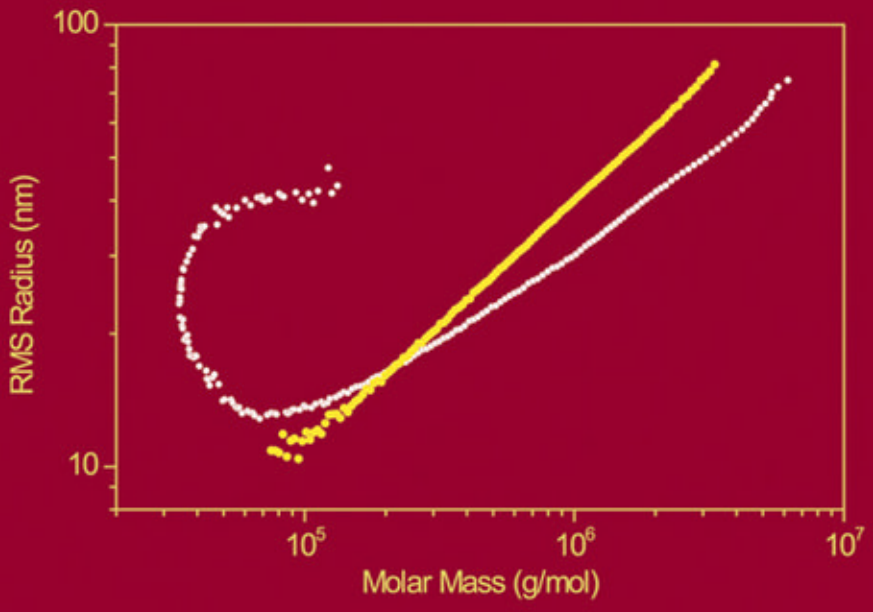

WILEY

Light Scattering, Size Exclusion Chromatography and Asymmetric Flow Field Flow Fractionation

Light Scattering, Size Exclusion Chromatography and Asymmetric Flow Field Flow Fractionation

Powerful Tools for the Characterization of Polymers, Proteins and Nanoparticles

Stepan Podzimek

A John Wiley & Sons, Inc., Publication

Published by John Wiley & Sons, Inc., Hoboken, New Jersey.
Published simultaneously in Canada.

Library of Congress Cataloging-in-Publication Data:

Podzimek, Stepan, 1955–
Light scattering, size exclusion chromatography and asymmetric flow field flow fractionation : powerful tools for the characterization of polymers, proteins and nanoparticles / Stepan Podzimek.
p. cm.
Includes bibliographical references and index.
ISBN 978-0-470-38617-0 (cloth)
1. Polymers–Analysis. 2. Polymers–Separation. 3. Light–Scattering. 4. Chromatographic analysis. I. Title.
QD139.P6P625 2010
543′.8–dc22
2010010798

Printed in Singapore.

10 9 8 7 6 5 4 3 2 1

Contents

Preface

This book brings together three powerful methods of polymer analysis and characterization, namely light scattering and two analytical separation techniques, size exclusion chromatography and asymmetric flow field flow fractionation. Each of these methods has been known and used in polymer research for several decades, and each of them has its specific advantages and limitations. Many of the limitations can be overcome by combination of light scattering with one of the separation methods. Bringing together three different techniques into a single book, showing their advantages and limitations and explaining how they complement each other and how their combinations overcome the limitations, should be the main benefit for readers, who might include university students, analysts in manufacturing quality control, and scientists in academic and industrial research laboratories. The application area of the methods that are presented includes various synthetic and natural polymers, proteins, and nanoparticles. The ability of these methods to characterize and study biomacromolecules makes them particularly attractive, because detailed knowledge of structure and structure–properties relationships is a pathway to new materials capable of replacing traditional crude-oil-based raw materials. The importance of these methods is evident in their numerous applications in medical and pharmaceutical research, including drugs, drug delivery systems, and materials for medical devices.

Molar mass is a characteristic that distinguishes polymers from low-molar-mass organic compounds. Unlike organic compounds, which have a single molar mass corresponding to their chemical formula, polymers typically consist of molecules covering a specific molar mass range. The molar mass distribution of a given polymer sample is related to many important properties and also yields information about the production process or the changes brought about during polymer application or degradation. In protein chemistry, the ability of proteins to form various oligomers affects their capability to crystallize and their possible therapeutic applications, and such demonstration of the absence of oligomers is of vital importance. The size distribution of nanoparticles, which have a wide variety of potential applications in material and biomedical fields, is crucial for their applicability and properties of final products.

Light scattering is one of the few physical techniques that provide absolute molar mass. The term *absolute* means that the molar mass is determined on the basis of fundamental physical principles using an exactly derived relationship

between the intensity of light scattered by a dilute polymer solution and the molar mass of scattering molecules. In addition to molar mass, the light scattering measurements yield valuable information about the molecular size and intensity of interactions of polymer molecules with solvent. Light scattering technique is also able to provide information about branching of polymer molecules, which is another important type of nonuniformity of synthetic and natural polymers having significant impact on their various properties. The most serious limitation of the classical light scattering of nonfractionated polydisperse polymers is that it yields average quantities that are often unable to distinguish among different polymer samples or describe structure–properties relationships.

Size exclusion chromatography (SEC) has been used in polymer research since the mid-sixties and since that time has found great popularity among polymer chemists. The instrumental development of the method has been driven by the development of other types of liquid chromatography. Today's SEC instruments are highly reliable and relatively easy to use. However, it may be just the relative simplicity that often results in poor reproducibility of the method, especially in the sense of long-term reproducibility within a laboratory or reproducibility among various laboratories. The poor reproducibility is a consequence of high sensitivity of the results to numerous operational parameters, which is often overlooked by inexperienced users. In addition, the SEC results are often misinterpreted in the sense of the absolute correctness of the obtained molar masses. The most serious limitation of SEC is that the method does not measure any physical quantity directly related to molar mass. The method solely separates polymer molecules according to their hydrodynamic volume; to transfer the obtained chromatograms to molar mass information the SEC columns must be calibrated, that is, one has to establish the relation between the elution volume and molar mass. This procedure, called *calibration*, has several pitfalls, and finding true calibration for many synthetic and natural polymers is uncertain or even impossible. It has become common practice that a calibration curve established with polymer standards of a given chemical composition is used for processing the data of other polymers of significantly different chemical composition or molecular architecture. As a consequence of that, the resulting molar masses may differ from the true ones quite significantly. This fact is often not understood by SEC users. Although the apparent values obtained by incorrect calibration may be useful for a simple comparison of polymer samples and finding the effect of polymerization conditions on molar mass distribution, the molar masses obtained by this approach cannot be used for detailed polymer characterization. Thus the calibration of SEC columns remains the most serious limitation of the SEC method.

The most effective solution of the calibration issue is the combination of SEC with a method capable of direct measurement of molar mass. Light scattering, especially in the form of multi-angle light scattering (MALS), has been proved to be the most suitable method for this purpose. The MALS detector not

only effectively solves the calibration problem, but also significantly improves the reproducibility and repeatability of the measurements. In addition, the combination of SEC and MALS allows very detailed characterization of branching and detection of even minute amounts of aggregates. The latter ability makes SEC-MALS highly attractive for protein characterization. However, even in the case of SEC-MALS there are still several potential limitations resulting from the nature of SEC separation that is achieved in columns packed by porous materials. The passage of polymer molecules through the porous column bed is a possible source of several problems, namely degradation of polymer molecules by shearing forces, interaction of polymer molecules with column packing, and anchoring of branched molecules in pores of column packing.

Asymmetric flow field flow fractionation (A4F) is one of the field flow fractionation techniques. The method has coexisted with SEC for several decades. However, until now it has not achieved the popularity or as wide an application range as SEC. The reason for that has been mainly more complicated instrumentation and even more uncertain determination of molar mass calibration. Recent developments in A4F instrumentation have brought a new generation of commercially available instruments that are as easy to use as SEC. The modern A4F instruments even allow easy switching from A4F to SEC mode and vice versa. The combination of A4F with a MALS detector allows efficient determination of molar mass and size distribution, identification of aggregates, and characterization of branching. The separation in A4F is achieved by a flow of polymer molecules or particles in an empty channel, which strongly reduces or even completely eliminates SEC limitations such as shearing degradation, interactions with column packing, or anchoring in pores. The A4F-MALS hyphenated method has been recently finding its way into many pharmaceutical, polymer, and nano-related research and quality control laboratories.

This book minimizes theory to the explanation of basic principles and emphasizes the practical approach of achieving reproducible and correct results. The focus is on giving guidelines for using the instruments properly, planning the experiments, acquiring reliable data, data processing, and the proper interpretation of the obtained results. The book draws from my long experience based on my own work in the laboratories of industrial research, academia, and an instrument manufacturer, as well as experience gained by my visits to many laboratories and interactions with users of light scattering, SEC, and A4F. This book presents a selection of interesting and informative examples from thousands of experimental data files collected during my experimental work. The book targets novices who are about to perform their first experiments and need to learn basic principles and methodology, as well as experienced users who may need to confirm their own understanding or help in interpreting their results.

This book would have been impossible without my 20-months' stay with Wyatt Technology Corporation in Santa Barbara and without long cooperation and support from this company. All MALS and A4F results presented in the

book were acquired using instruments from Wyatt Technology Corporation. My special thanks go to Dr. Philip Wyatt, CEO and founder of Wyatt Technology Corporation, his sons, Geofrey and Clifford, president and vice president of the company, and Dr. Christoph Johann, director of Wyatt Technology Europe.

STEPAN PODZIMEK
November 2010, Pardubice, Czech Republic

Chapter 1

Polymers

1.1 INTRODUCTION

Polymers can be characterized by many methods that find applications in organic chemistry, such as, for example, nuclear magnetic resonance, infrared spectroscopy, or liquid chromatography. On the other hand, there are several methods that find utilization almost exclusively in the field of polymer chemistry. Examples include light scattering, dilute solution viscometry, size exclusion chromatography, and flow field flow fractionation.

Polymer is a substance composed of macromolecules, that is, molecules built of a big number of small molecules linked together by covalent bonds. The entirely manmade polymers (synthetic polymers) are relatively new materials that did not exist a hundred years ago. The first synthetic polymer, phenol-formaldehyde resin, Bakelite, appeared shortly before World War I. Further synthetic polymers, developed before World War II, were neoprene, nylon, poly(vinyl chloride), polystyrene, polyacrylonitrile, and poly(vinyl butyral); poly(vinyl butyral) was first used in automotive safety glass to prevent flying glass during car accidents and continues to be used for this important application. World War II encouraged further development of polymers as a result of war shortages and demands for new materials with enhanced properties. Other important polymers included polytetrafluoroethylene (Teflon), polysiloxanes (silicones), polyester fibers and plastics such as poly(ethylene terephthalate) (PET), aromatic polyamides (Kevlar), and polyetheretherketone (PEEK). Nowadays, the synthetic polymers are used in a variety of applications covering, for example, electronics, medical uses, communications, food, printing inks, aerospace, packaging, and automobiles.

Synthetic polymers can be classified as *thermoplasts*, which soften under heat and can be reversibly melted and dissolved, and *thermosets*, which, by the action of heat or chemical substances, undergo chemical reaction and form insoluble materials that cannot be melted or dissolved. Mixtures of molecules of

Light Scattering, Size Exclusion Chromatography and Asymmetric Flow Field Flow Fractionation: Powerful Tools for the Characterization of Polymers, Proteins and Nanoparticles, by Stepan Podzimek

relatively low molar mass (hundreds to thousands g/mol) that are able to react mutually or with other compounds and form cross-linked materials are often called *synthetic resins*. The term *oligomer* refers to a polymer molecule with relatively low molar mass (roughly below 10,000 g/mol) whose properties vary significantly with the removal of one or a few of the units. Besides synthetic polymers, many polymers can be found in the nature. Various polysaccharides (e.g., cellulose, starch, dextran, hyaluronic acid) represent an important group of biopolymers (natural polymers); some of them are an essential part of food or have other important applications. Proteins are other examples of biopolymers, which represent a specific and tremendously rising field of research, where the use of efficient analytical tools is necessary for the characterization and process development of protein therapeutics.

1.2 MOLECULAR STRUCTURE OF POLYMERS

The terms configuration and conformation are used to describe the geometric structure of a polymer and are often confused. *Configuration* refers to the molecular structure that is determined by chemical bonds. The configuration of a polymer cannot be altered unless chemical bonds are broken and reformed. *Conformation* refers to the order that arises from the rotation of molecules about the single bonds. If two atoms are joined by a single bond, then rotation about that bond is possible since it does not require breaking the bond. However, a rotation about a double bond is impossible. The term conformation refers to spatial structure of a macromolecule in dilute solution. Depending on the thermodynamic quality of solvent and properties of a polymer chain, the polymer may adopt a random coil, compact sphere-like shape or highly extended rod-like conformation. The terms *topology* or *architecture* often refer to the polymer chain arrangement with respect to branching.

The part of a macromolecule from which the macromolecule is built is called a *monomer unit* while the smallest part of a macromolecule that repeats periodically is called a *structural repeating unit*. Polymers can consist of one or more kinds of monomer unit. The former are called *homopolymers*, the latter *copolymers*. Synthetic polymers are usually varied mixtures of molecules of different molar mass (M) and often also of different chemical composition and/or molecular architecture. That is, they are nonuniform (polydisperse) materials. *Polydispersity* means that a given property, such as molar mass, spans a continuous range. Various possible nonuniformities are outlined in the following:

- Molar mass.
- Chemical composition: A *random copolymer* contains a random arrangement of the monomers and can be denoted schematically as -A-B-A-B-A-A-B-B-B-B-A-B-B-A-B-. The particular macromolecules can differ in their overall chemical composition as well as in the sequential arrangement of monomers in the polymer chain. A *block copolymer* contains

linear blocks of monomers of the same type -A-A-A-A-A-A-A-A-A-B-B-B-B-B-B- and the possible heterogeneity includes various block length or existence of homopolymer fractions. A *graft copolymer* contains a linear main chain consisting of one type of monomer with branches made up of other monomers, when the molecules may differ in the number, position, and length of the branches. An *alternating copolymer* consists of regularly alternating units -A-B-A-B-A-B-A-B-A-B- such as, for example, in the well-known Nylon 66 $(-CO-(CH_2)_4-CO-NH-(CH_2)_6-NH-)_n$ and the heterogeneity is limited to the molar mass and end groups. The characterization of a copolymer is always much more complex than that of a homopolymer.

- End groups: X-A-A-A-A-A-A-A-X, Y-A-A-A-A-A-A-A-Y, X-A-A-A-A-A-A-A-Y.
- *Cis* and *trans* isomerization: The *cis* configuration arises when substituent groups are on the same side of a carbon–carbon double bond. *Trans* refers to the substituents on opposite sides of the double bond. These structures cannot be changed by rotation. Technically important examples include polybutadiene or unsaturated polyesters based on maleic acid.
- Branching: A branched polymer is formed when there are side chains attached to a main polymer chain. There are many ways in which a branched polymer can be arranged. Possible branching topology includes randomly branched polymers, stars, combs, hyperbranched polymers, and dendrimers.
- Tacticity: spatial arrangement on chiral centers within a macromolecule (atactic, isotactic, syndiotactic polymers, such as polypropylene).
- Head-to-tail or head-to-head (tail-to-tail) configuration of vinyl polymers: $-CH_2-CHR-CH_2-CHR-$, $-CH_2-CHR-CHR-CH_2-$.

Polymers can be nonuniform in one or more properties. It is worth mentioning that monodisperse polymers (i.e., uniform with respect to all properties) are exceptional for synthetic polymers and most of the natural polymers. A polystyrene sample prepared by anionic polymerization that has a very narrow molar mass distribution is the most common example of an almost monodisperse polymer in the field of synthetic polymers. Examples of polymers that are heterogeneous in more than one distributed property are copolymers and branched polymers. Although the term *polydisperse* can apply to various heterogeneities, it is often understood only with respect to polydispersity of molar mass. The importance of a given heterogeneity may depend on molar mass and application. For example, the end groups are of primary importance for synthetic resins, like, for example, epoxies, where the end epoxy groups are essential for curing process. However, the influence of end groups diminishes with increasing molar mass and for most of the polymers the effect of end groups on their properties is negligible. Besides molar mass, chemical composition is another important characteristic governing polymer properties and applications.

The two most important sources of chemical heterogeneity are: (1) *statistical heterogeneity*, when compositional variation arises from random combinations of comonomers in polymer chains, and (2) *conversion heterogeneity*, when differences in the reactivity of the comonomers cause the change of monomer mixture composition with conversion and such molecules with different composition are formed at different conversion. While the former type of heterogeneity is almost negligible, the latter is usually the main source of the compositional heterogeneity in polymers.

It is of utmost importance for polymer chemists and analysts to be aware of all possible nonuniformities of polymers in order to choose a suitable experimental method for the characterization, interpret the experimental data, and understand the polymer properties and behavior. Two polymer samples may be identical in one or more properties but differ in others. Although the polymer properties are generally distributed, solely average values can be often obtained by the analysis. Two polymer samples can be identical in an average property but the property distributions can be different. However, average properties are often used instead of distributions in order to simplify the description of a polymer sample or because the distribution cannot be determined due to time or instrumental limitations. In addition to nonuniformity resulting from the randomness of the polymerization process, many commercially important polymer-based materials are polymer blends, that is, mixtures of two or more polymeric components; also various low-molar-mass compounds are added to polymers to modify their properties and protect them against degradation.

1.2.1 Macromolecules in Dilute Solution

Understanding the shape, size, and hydrodynamic behavior of polymer molecules in dilute solutions is essential not only for understanding the property–structure relationships, but also for understanding the principles of polymer characterization, such as column calibration in size exclusion chromatography or the characterization of branching. In a dilute solution the polymer molecules are isolated from each other so that the interactions of polymer–solvent prevail over the intermolecular interactions of polymer–polymer. The macromolecules take the most statistically probable conformations and usually form so-called *random coils* (coiled polymeric domains swollen with the solvent). The polymer coil must not be assumed to be a rigid, motionless object, but due to rotation about single bonds the coil can create a large number of various conformations. That means a polymer chain shows a dynamic behavior with fast and randomly changing conformations. It is impossible to study the number of various conformers and their corresponding conformations, but the experimental measurements always provide statistical averages of macromolecular dimensions. The polymers that can easily transform from one conformation to another and that can form a large number of various conformations are flexible, while those polymers for which the transition from one conformation to another is restricted by high potential

barrier and the number of possible conformations is limited are rigid. The flexible polymers typically consist of only single C-C bonds in the main chain and no or small chain substituents, while double bonds or cyclic structures in the main chain as well as large chain substituents increase chain rigidity.

The conformation of a real chain is defined by valence angles and restricted torsion due to different potential energy associated with different torsion angles (*trans* position being at minimum potential energy). In addition, two segments cannot occupy the same space element at the same time, and the chain expands due to the *excluded volume* effect. The excluded volume is a result of materiality of the polymer chain. It refers to the fact that one part of a long-chain molecule cannot occupy space that is already occupied by another part of the same molecule. Excluded volume causes the ends of a polymer chain in a solution to be further apart than they would be were there no excluded volume. The effect of excluded volume decreases with increasing chain rigidity and decreasing chain length, because the bonds in a polymer chain are to a certain extent stiff and such a collision of two segments of the same chain can only occur when the chain between the two segments can create a sufficiently large loop. In thermodynamically good solvents, the interactions between polymer segments and solvent molecules are energetically favorable and the solvent creates a solvating envelope around the polymer chain, which results in further expansion of the polymer coil. In a thermodynamically poor solvent, the intramolecular interactions between polymer segments are intensive and under specific conditions can precisely compensate the effect of excluded volume. Such conditions (solvent and temperature) are called *theta conditions* and polymer coil dimensions under these conditions *unperturbed dimensions* (zero subscript is used to indicate unperturbed dimensions). In theta conditions, the long-range interactions arising from excluded volume are eliminated and the chain conformation is defined solely by bond angles and short-range interactions given by the hindrances to rotation about bonds (i.e., steric or other interactions involving neighboring groups). A characteristic feature of theta conditions is that the second virial coefficient is zero. Commonly all theoretical calculations are done under the assumption of unperturbed chain dimensions, while the real experiments are mostly carried out far from theta point. This fact must be considered when the experimental results are being compared with the theoretical predictions.

The dimensions of a linear chain can be described by the *mean square end-to-end distance* $\langle r^2 \rangle$ or the square root of this quantity $\langle r^2 \rangle^{\frac{1}{2}}$. The angle brackets denote the average over all conformations. In a three-dimensional space, the distance between the two ends is a vector, which fluctuates with regard to the dimension and direction. The scalar product of the vector with itself is a quantity fluctuating only with respect to the dimension. Note that squares of vector quantities are usually used in theoretical calculations to eliminate the directional part of the vectors. However, the end-to-end distance becomes completely meaningless in the case of branched polymers that have more than two ends. Another parameter describing the size of the polymer chain, which can be effectively used for the characterization of branched molecules, is the *mean square* (MS)

radius $\langle R^2 \rangle$ and the *root mean square* (RMS) *radius* $\langle R^2 \rangle^{\frac{1}{2}}$. The RMS radius can be used generally for the size description of a particle of any shape. The RMS radius is frequently called *radius of gyration* and symbols $\langle r_g^2 \rangle^{\frac{1}{2}}$ or $\langle s^2 \rangle^{\frac{1}{2}}$ are also used in scientific literature. For the sake of simplicity, the symbol R is mostly used for the RMS radius in this book. The RMS radius is often mistakenly associated with the term *gyration*, although there is no gyration involved in the RMS radius definition. The integration is over the mass elements of the molecule with respect to the center of gravity of the molecule (i.e., the subscript g refers to the center of gravity and not to gyration). For the RMS radius definition and the determination, see Chapter 2.

The mean square end-to-end distance of a real chain in solution is expressed as:

$$\langle r^2 \rangle = \alpha^2 \langle r^2 \rangle_0 \tag{1.1}$$

where α is the *expansion factor*, which represents the effect of long-range interactions, that is, the effect of excluded volume, and swelling of the chain by the polymer–solvent interactions. The effect of bond angle restriction and steric hindrances to rotation about single bonds is represented by unperturbed dimension $\langle r^2 \rangle_0$. The expansion factor expresses the deviation of a polymer chain from theta state. Besides the expansion factor based on the end-to-end distance there are other expansion factors defined by other dimensional characteristics, namely by the RMS radius and intrinsic viscosity:

$$\alpha_R = \sqrt{\frac{\langle R^2 \rangle}{\langle R^2 \rangle_0}} \tag{1.2}$$

$$\alpha_\eta = \left(\frac{[\eta]}{[\eta]_0} \right)^{\frac{1}{3}} \tag{1.3}$$

It is worth noting that expansion factors defined by Equations 1.1–1.3 are not expected to be exactly equal.

The simplest model of a polymer in solution is a *freely jointed*, or *random flight*, chain[1] (Figure 1.1). It is a hypothetical model based on the assumptions that (1) chain consists of n immaterial segments of identical length l; and (2) $(i + 1)$th segment freely moves around its joint with the ith segment. The angles at the segment junctions are all of equal probability and the rotations about segments are free. That means a polymer molecule is formed by a random walk of fixed-length, linearly connected segments that occupy zero volume and have all bond and torsion angles equiprobable. Since the segments are assumed to be of zero volume, two or more segments can occupy the same volume element in the space.

For a sufficiently long chain, the value of $\langle r^2 \rangle_0$ for a freely jointed chain is directly proportional to the number of segments:

$$\langle r^2 \rangle_{0,j} = nl^2 \tag{1.4}$$

$$\langle r^2 \rangle_{0,j}^{1/2} = \sqrt{n} \times l \tag{1.5}$$

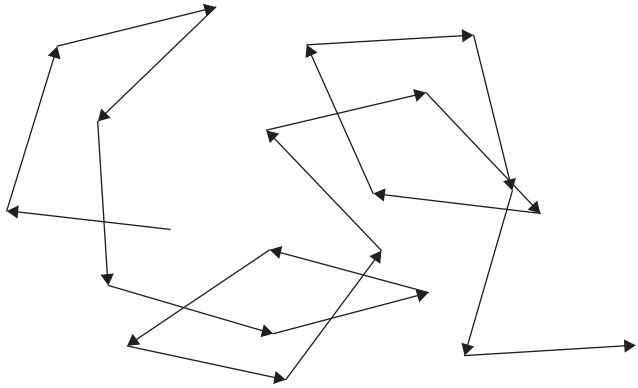

Figure 1.1 Schematic representation of freely jointed model of polymer chain formed by a random walk of 20 segments in two-dimensional space.

Here n is the number of segments (rigid sections) of the length l, and the subscripts zero and j are used to indicate unperturbed dimensions and freely jointed model, respectively. In simple single-strand chains, bonds are taken as the rigid sections. The MS radius is in a simple relation to the mean square end-to-end distance:

$$\langle R^2 \rangle_0 = \frac{\langle r^2 \rangle_0}{6} \tag{1.6}$$

A *freely rotating* chain is a hypothetical model consisting of n segments of fixed length l jointed at fixed angles. It assumes free internal rotation under fixed bond angles (i.e., all torsion angles are equally likely). For a chain consisting of only one kind of bond of length l and for $n \to \infty$, the mean square end-to-end distance is:

$$\langle r^2 \rangle_{0,r} = nl^2 \times \frac{(1 + \cos\theta)}{(1 - \cos\theta)} \tag{1.7}$$

where θ is the supplement of the valence bond angle and subscript r indicates a freely rotating chain. For carbon polymer chains the valence angle is 109.5° (i.e., $\cos\theta = 1/3$) and thus the mean square end-to-end distance is a double that of the freely jointed chain. Although the freely rotating chain represents a more realistic model of polymer chains, the state of entirely free rotation is rare. The freely rotating behavior diminishes with increasing size of the main chain substituents. The ratio of the root mean square end-to-end distance of a real polymer chain with unperturbed dimensions to that of a freely rotating chain with the same structure:

$$\sigma = \left(\frac{\langle r^2 \rangle_0}{\langle r^2 \rangle_{0,r}} \right)^{\frac{1}{2}} \tag{1.8}$$

is called the *steric factor*, which reflects the effect of hindrance to free rotation.

The unperturbed dimensions of a flexible polymer chain can be characterized by the so-called *characteristic ratio*:

$$C_n = \frac{\langle r^2 \rangle_0}{nl^2} \tag{1.9}$$

where n is the number of rigid sections in the chain, each of length l. The characteristic ratio is the ratio of the mean square end-to-end distance in the theta state divided by the value expected from the freely jointed chain. C_n approaches an asymptotic value as n increases (i.e., $C_n = C_\infty$ for $n \to \infty$). In simple chains, the bonds can be taken as the segments and the number of segments can be calculated from the degree of polymerization P or the molar mass M and the molar mass of the monomer unit M_0. For vinyl polymers, $n = 2P$ or $2M/M_0$ and $l = 0.154$ nm. If all of the segments are not of equal length, the mean square value of l is used:

$$l^2 = \frac{1}{n} \sum_i l_i^2 \tag{1.10}$$

For the freely jointed chain, $C_\infty = 1$, and for real polymer chains, $C_\infty > 1$. The increasing value of C_∞ indicates greater deviation from freely jointed behavior. For a polymer with N' chain bonds per monomer unit, Equation 1.9 can be rearranged as:

$$C_\infty = \frac{\langle r^2 \rangle_0}{M} \frac{M_0}{N' l^2} \tag{1.11}$$

Unperturbed chain dimensions of polystyrene can be used as concrete examples of the previous characteristics: $K_0 = (82 \pm 5) \times 10^{-3}$ mL/g, $\langle r^2 \rangle_0^{\frac{1}{2}} / M^{\frac{1}{2}} = (670 \pm 15) \times 10^{-4}$ nm, $\sigma = 2.22 \pm 0.05$, $C_\infty = 9.85$. The data were determined in various solvents at a temperature around 30°C.

The determination of unperturbed dimensions of polymer chains can be achieved by means of the Flory-Fox equation:[3]

$$[\eta] = K_0 M^{0.5} \alpha_\eta^3 \tag{1.12}$$

where

$$K_0 = \Phi_0 \left(\frac{\langle r^2 \rangle_0}{M} \right)^{1.5} \tag{1.13}$$

and $[\eta]$ is the intrinsic viscosity.

Under theta conditions, there is no excluded volume effect, $\alpha_\eta = 1$, and Equation 1.12 can be written as:

$$[\eta]_0 = K_0 M^{0.5} \tag{1.14}$$

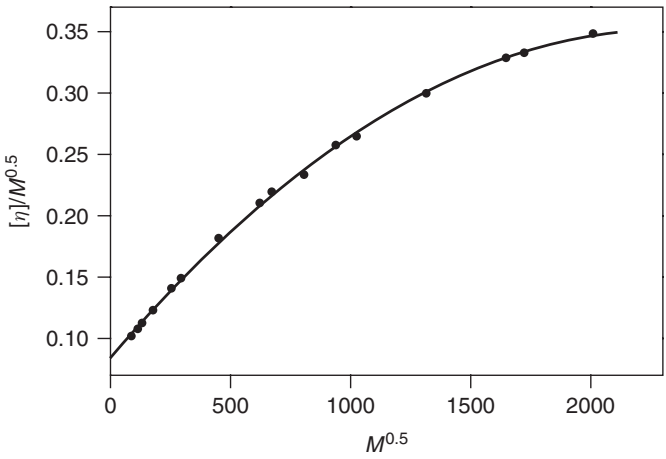

Figure 1.2 Plot of $[\eta]/M^{0.5}$ versus $M^{0.5}$ for polystyrene in THF (intrinsic viscosity expressed in mL/g). The intercept $(K_0) = 84.3 \times 10^{-3}$ mL/g.

Equations 1.12 and 1.14 correspond to the Mark-Houwink equation, but the exponent a has a constant value of 0.5. Flory constant Φ_0 is a universal constant for linear flexible chain molecules under theta conditions. In fact, Φ_0 is not a real constant, because different values were reported in the literature, the range being somewhere in the limits of 2.1×10^{21} to 2.87×10^{21} (for end-to-end distance expressed in centimeters and intrinsic viscosity in deciliters per gram). The Flory-Fox equation can be used outside θ conditions (see Section 1.4.3.2). The measurement of intrinsic viscosity under θ conditions yields K_0. The ratio $\langle r^2 \rangle_0 / M$ is obtained from Equation 1.13, which then yields C_∞ from Equation 1.11. Measurements of intrinsic viscosity at theta conditions can encounter experimental difficulties and various procedures that allow determination of K_0 from the intrinsic viscosities determined in thermodynamically good solvents (i.e., $T \neq \theta$) were proposed. The estimation of K_0 can be obtained by measurements in thermodynamically good solvents using, for example, the Burchard-Stockmayer-Fixman method:[4,5]

$$[\eta] = K_0 M^{0.5} + 0.51 \Phi_0 B M \tag{1.15}$$

where B is a constant. Linear extrapolation of the relation $[\eta]/M^{0.5}$ versus $M^{0.5}$ yields K_0 as the intercept. However, in very good solvents, especially if the molar mass range is broad, the $[\eta]/M^{0.5}$ versus $M^{0.5}$ plot is markedly curved, which makes extrapolation rather uncertain. An example of a Burchard-Stockmayer-Fixman plot for a polymer in thermodynamically good solvent is shown in Figure 1.2. The obtained constant K_0 of 84.3×10^{-3} mL/g yields ratios $\langle r^2 \rangle_0^{1/2} / M^{\frac{1}{2}} = 696 \times 10^{-4}$ nm and $C_\infty = 10.6$, which are in good agreement with literature values.[2]

It must be emphasized that the extrapolation procedures for the estimation of K_0 are valid for flexible chains and should not be applied to polymers with semiflexible chains (Mark-Houwink exponent $a > 0.85$). A wormlike chain model[6] is used to describe the behavior of semiflexible polymers such as some types of polysaccharides, aromatic polyesters, aromatic polyamides, and polypeptides in helical conformation. The value of $\langle r^2 \rangle_0 / M$ and other characteristics of the semiflexible polymers can be obtained, for example, by a procedure developed by Bohdanecky.[7]

Contour length is another term that can be used to describe chain molecules. It is the maximum end-to-end distance of a linear polymer chain, which for a single-strand polymer molecule usually means the end-to-end distance of the chain extended to the all-*trans* conformation.

A real polymer chain consisting of n segments of the length l can be approximated by a freely jointed chain consisting of n' segments of the length l' under the condition that the values of $\langle r^2 \rangle_0$ and the totally expanded chain lengths for the freely jointed chain and the real chain are identical:

$$\langle r^2 \rangle_0 = n' l'^2 \tag{1.16}$$

$$nl = n' l' \tag{1.17}$$

Such a model chain is called an *equivalent chain* and its segment a *statistical segment* (Kuhn segment). The number of segments (bonds) in a statistical segment is proportional to chain rigidity.

1.3 MOLAR MASS DISTRIBUTION

It is the high molar mass that distinguishes polymers from organic low-molar-mass compounds. The molar mass and molar mass distribution of synthetic and natural polymers are their most important characteristics with a strong relation to various properties and industrial applications. The polymer properties influenced by molar mass include melt and solution viscosity, tensile strength, toughness, impact strength, adhesive strength, elasticity, brittleness, abrasion resistance, flex life, softening temperature, solubility, chemical resistance, cure time, diffusion coefficient, film and fiber forming ability, ability to be fabricated, and processing temperature. The ability of a polymer to form fibers and films is possible from a certain molar mass and the film and fiber properties are related to molar mass.

A polymer containing high-molar-mass fractions shows greater elastic effect. However, the relation of some properties to molar mass may not be straightforward. A certain property may be related more to a certain molar mass average, and polydispersity usually plays an important role. Different molar mass averages can be related to different polymer properties since either high-molar-mass or low-molar-mass fractions can primarily influence specific properties. For example, the tensile strength is particularly related to the weight-average molar mass (M_w) since it is most influenced by the large molecules in the material. The flex life (ability of a polymer material to bend many times before breaking) is

more related to z-average molar mass (M_z), because extremely large molecules are most important for this property. The number-average molar mass (M_n) is needed for kinetics studies and stoichiometric calculations. Relatively narrow molar mass distribution and high molar mass are beneficial for fiber-forming polymers, where molecules with high molar mass increase the tensile strength, while polymers for pressure-sensitive adhesives benefit from broad polydispersity since the high-molar-mass fractions enhance the material strength and the lower-molar-mass fractions have a desirable plasticizing effect. Resistance of plastics to the surface-initiated failure of stressed polymers in the presence of surface active substances such as alcohols or soaps (environmental stress cracking) increases with increasing molar mass, and is considerably decreased by the presence of low-molar-mass chains. The molar mass distribution is also important for polymers used as plasma expanders (e.g., hydroxyethyl starch, dextran), because the circulation time in blood depends on it, and the adverse effects are caused by too high levels of the low-molar-mass fractions. Many times the positive influence of increasing molar mass must be balanced with the ability of a polymer to be processed (e.g., tensile strength versus melt or solution viscosity). Solubility of polymers decreases with increasing molar mass because of the decrease of the second virial coefficient (see Equation 2.4). It is important to note that there are no commonly good molar mass averages or molar mass distributions for a polymer sample. The optimum values depend on the nature of the polymer, the way of processing, and especially on the required end-use properties. A molar mass distribution of a polymer sample that is known as a good one for a given application can serve as a reference to which other samples are compared.

The viscosity of polymer melts is proportional to the 3.4-power of M_w:

$$\eta = k \times M_w^{3.4} \tag{1.18}$$

where k is a proportionality constant. For some polymers, the melt viscosity may become related to an average somewhere between the M_w and M_z. Polymer melts typically show non-Newtonian behavior (i.e., their viscosity decreases with increasing shear stress). The rate of viscosity reduction with shear is related to molar mass and polydispersity; generally it is enhanced by the presence of high-molar-mass components. The glass transition temperature (T_g) is related to the M_n according to the relation:

$$T_g = T_g(\infty) - \frac{K}{M_n} \tag{1.19}$$

where $T_g(\infty)$ is a glass transition temperature of a polymer with indefinite molar mass and K is a constant. In a solution of macromolecules, the diffusion rate decreases with increasing molar mass according to relation:

$$D = K_D M^{-\beta} \tag{1.20}$$

where D is the translational diffusion coefficient characterizing the ability of molecules to move in solution and K_D and β are constants for a given polymer, solvent, and temperature.

The exponent β generally lies in the range of $0.33 < \beta < 1.0$, the value depending on the molecular conformation and thermodynamic quality of solvent. Example of molar mass dependence of diffusion coefficient is shown in Figure 1.3.

Although the molar mass and molar mass distribution affect many polymer properties in bulk, the determination of molar mass is possible only in the form of dilute polymer solution. That means the solubility of a polymer is a necessary condition for the determination of its molar mass. The requirement of solubility may not be fulfilled for some important technical polymers such as Teflon or PEEK. In addition, a polymer in a certain solvent may not form a true solution where all molecules are dispersed in the form of individual molecules, but the solution may also contain supermolecular structures that have a significant effect on the average value of molar mass. Obviously, in the case of thermosets, the characterization of molar mass is possible only before their crosslinking.

Several notations are used in polymer science to express molar mass, namely *molar mass* or *molecular mass* (mass of polymer divided by the amount of polymer expressed in moles, dimension g/mol), and *relative molecular mass* or *molecular weight* (mass of the polymer related to 1/12 of the mass of the ^{12}C atom, dimensionless). A relative unit, *Dalton* (Da), is also sometimes used. The molar mass expressed in different units is numerically identical, which means a polymer having molar mass 10^5g/mol has relative molecular mass 10^5 or 10^5 Da. The number of monomeric units in a macromolecule or oligomer molecule is called *polymerization degree* (P). The relation between the molar mass and polymerization degree is:

$$M = P \times M_0 \tag{1.21}$$

where M_0 is the molar mass of a monomeric unit.

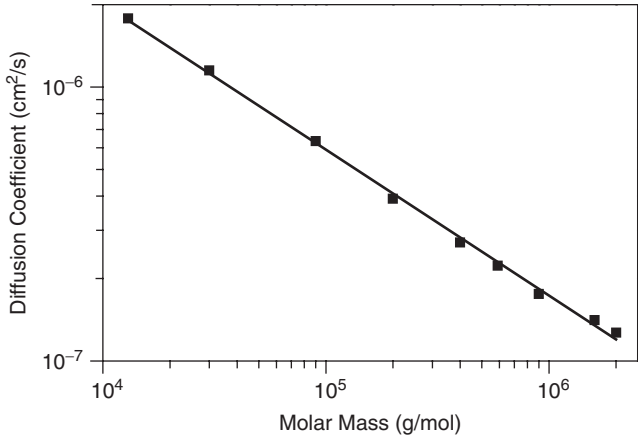

Figure 1.3 Molar mass dependence of diffusion coefficient of polystyrene in THF at room temperature. Data obtained by DLS of narrow polystyrene standards.
$D = 0.00027 \times M^{-0.533}$ (cm^2/s).

1.3.1 Description of Molar Mass Distribution

In contrast to low-molar-mass compounds a polymer does not have a single molar mass and almost all synthetic and natural polymers are *polydisperse* in molar mass. Frequencies of particular molar masses in a given polymer sample are described by the *molar mass distribution*. The *differential*, $f(M)$, and *cumulative* (*integral*), $I(M)$, molar mass distribution functions are used for the description of molar mass distribution. The differential distribution is often preferred in the polymer community over the cumulative molar mass distribution. However, the cumulative molar mass distribution allows easy determination of the weight fraction of polymer below or above a certain molar mass limit or the weight fraction of polymer in a specific molar mass range. Such information cannot be readily deducted from the differential distribution, which is more convenient for the assessment of the molar mass distribution symmetry, revealing multimodal distribution or the determination of the molar mass minimum and maximum and the molar mass of the most abundant fractions.

The molar mass distribution can be described graphically by a distribution curve or mathematically by a distribution function. Although the molar mass is a discrete quantity, the discreteness of molar mass is usually ignored[i] and the distribution is treated as a continuous one. The distribution function expressing the amount of material as weight fraction is called the *weight molar mass distribution*. It is also possible to use mole fraction (number fraction) and the distribution is called the *number molar mass distribution*. The subscripts w and n are used to differentiate between the weight and number distributions, respectively. The weight distributions are mostly used in routine practice. It is usual practice to express the molar mass axis in logarithmic scale or as a logarithm of M. The notations $f_w(M)$ and $F_w(\log M)$ can be used in order to distinguish the distributions based on normal and logarithmic scale, respectively. The function $F_w(\log M)$ is typically more symmetrical and better descriptive than $f_w(M)$. *Note:* Expression of the axis in $\log M$ is significantly less convenient for reading than using the molar mass axis in logarithmic scale (compare, for example, Figures 1.4 and 3.20).

The following equations describe various distribution functions and relations between them:

$$f_w(M)dM = F_w(\log M)d\ \log M \tag{1.22}$$

$$f_w(M) = \frac{F_w(\log M)}{2.303 \times M} \tag{1.23}$$

$$\int_0^\infty f_w(M)dM = 1 \tag{1.24}$$

[i]Oligomers that can be at least partly separated by a chromatographic technique or mass spectroscopy may be exceptions from the continuous expression of molar mass distribution.

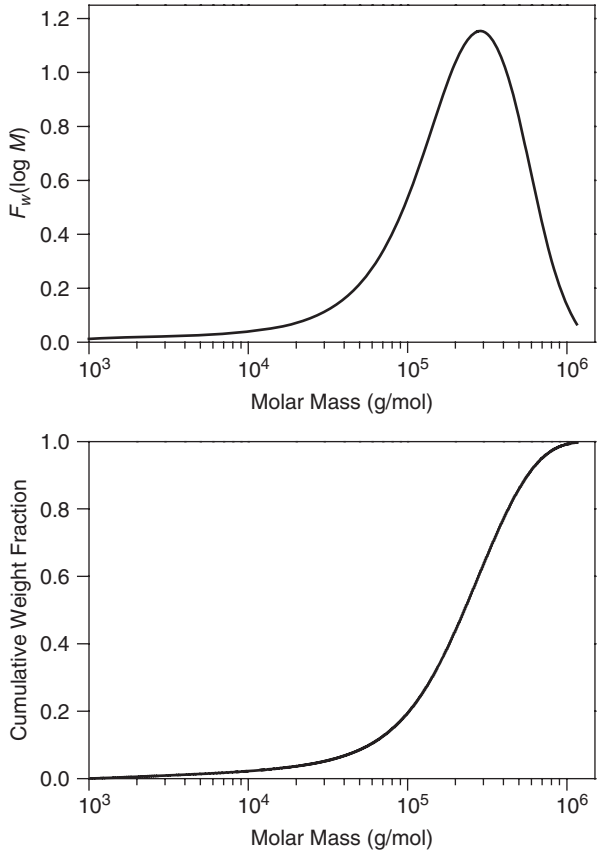

Figure 1.4 Differential weight distribution (top) and cumulative weight distribution (bottom) of NIST SRM 706 polystyrene. $M_n = 66{,}000$ g/mol, $M_w = 279{,}000$ g/mol, $M_z = 442{,}000$ g/mol, $M_{z+1} = 588{,}000$ g/mol.

$$\int_0^\infty f_n(M)dM = 1 \tag{1.25}$$

$$f(M) = \frac{dI(M)}{dM} \tag{1.26}$$

$$I_w(M) = \int_0^M f_w(M)\,dM \tag{1.27}$$

$$I_n(M) = \int_0^M f_n(M)\,dM \tag{1.28}$$

The weight fraction w of polymer material having molar mass between M and $M + dM$ is $f_w(M)\,dM$, and alternatively for the distribution expressed in

the logarithmic scale $F_w(\log M)\, d(\log M)$. The weight fraction of molecules with molar mass smaller than or equal to M_1 is given by $\int_0^{M_1} f_w(M)\, dM$ or $I_w(M_1)$. The weight fraction of molecules with molar mass between M_1 and M_2 is given by: $\int_{M_1}^{M_2} f_w(M)\, dM$ or $I_w(M_2) - I_w(M_1)$. In the graphical representation by differential distribution curve, this fraction equals the area bounded by the curve, abscissa, and two vertical lines at the position of M_1 and M_2. Similarly, using the number distributions yields the same information expressed in the number fractions: for example, the number (mole) fraction of molecules with molar mass $\leq M_1$ is $\int_0^{M_1} f_n(M)\, dM$ or $I_n(M_1)$.

The relation between the weight and number distribution can be derived using the definition of the weight fraction:

$$w_i = \frac{m_i}{\sum\limits_i m_i} = \frac{n_i M_i}{\sum\limits_i n_i M_i} \tag{1.29}$$

After extension of the above expression by $1/\sum\limits_i n_i$ we get:

$$w_i = \frac{M_i}{M_n} x_i \tag{1.30}$$

which allows transformation of the weight fraction w to the number fraction x and vice versa. In the above equations, m_i, n_i, w_i, and x_i are the weight (mass), number of moles, weight fraction, and number (mole) fraction of molecules having molar mass M_i, respectively. The number fraction is defined as:

$$x_i = \frac{n_i}{\sum n_i} \tag{1.31}$$

Alternatively to Equation 1.30, the relation between the weight and number distribution can be expressed as:

$$f_w(M) = \frac{M}{M_n} f_n(M) \tag{1.32}$$

An example of the cumulative and differential distribution curves is shown in Figure 1.4 and Table 1.1. Using the data in Figure 1.4 and Table 1.1, one can easily read the following information: (1) The sample contains about 1.6% wt molecules with molar mass below 10,000 g/mol; (2) the most abundant fractions around the apex of the distribution have molar mass around 287,000 g/mol; for example, the weight fraction of the molecules having the molar mass in the range of about $285{,}200 - 287{,}500$ g/mol is $1.1609 \times (\log 287454 - \log 285154) = 0.0041$, that is, about 0.41% wt.; (3) the minimum molar mass is about 2,000, the maximum is about 1.3×10^6 g/mol; and (4) the weight fraction of molecules with molar mass in the range of 10,000 g/mol to 100,000 g/mol is about $0.1888 - 0.0156 = 0.173$, i.e., 17.3% wt.

Graphical overlay of distribution curves can serve for comparison of a series of samples and finding even subtle differences among them. The distribution

Table 1.1 Tabular Data for Differential and Cumulative Distribution Curves Shown in Figure 1.4

Molar Mass (g/mol)	Differential Weight Distribution	Cumulative Weight Distribution
9688	0.0382	0.0152
9766	0.0384	0.0153
9845	0.0387	0.0150
9924	0.0389	0.0155
10005	0.0391	0.0156
10085	0.0393	0.0158
10167	0.0396	0.0159
~	~	~
97961	0.5231	0.1830
98751	0.5283	0.1849
99547	0.5335	0.1868
100350	0.5387	0.1888
101160	0.5440	0.1907
101976	0.5494	0.1927
102798	0.5547	0.1947
~	~	~
278364	1.1598	0.5943
280609	1.1603	0.5983
282872	1.1606	0.6022
285154	1.1608	0.6062
287454	1.1609	0.6102
289773	1.1608	0.6142
292110	1.1606	0.6181
294466	1.1603	0.6221
296841	1.1598	0.6261
299235	1.1592	0.6301
301649	1.1585	0.6340
304082	1.1576	0.6380
306535	1.1566	0.6419
309007	1.1554	0.6459
~	~	~

functions can also provide information about the polymer composition or polymerization process. Two or more peaks on the differential distribution indicate a blend of two or more polymers with different molar mass distributions. Multimodal distribution may also indicate the presence of a single polymer prepared under polymerization conditions (temperature, concentration of monomers, or initiator) that were changed in the course of polymerization. Tails or shoulders at

the high-molar-mass regions of molar mass distribution are signs of appreciable amounts of species with very high molar masses. It is important to note that these species can significantly affect the polymer properties. A high-molar-mass tail on the distribution curve often indicates the presence of branched molecules. A substantial level of oligomers in a polymer sample is indicated by a tail running to low molar masses (see, for example, Figure 1.4).

1.3.1.1 Distribution Functions

The molar mass distribution of polymers can be described by an analytical function of two or more parameters. Several molar mass distribution functions were derived from the kinetics of polymerization or estimated empirically to fit the experimentally determined distribution curves. At the beginning of polymer science, the empirical distribution functions were often used to estimate the entire distribution from the knowledge of two molar mass averages. With the development of size exclusion chromatography, the importance of the distribution functions as the means of the estimation of molar mass distribution dropped significantly, but they still can find utilization in theoretical modeling and calculations. In addition, the discrepancy between the experimental and theoretical distribution functions can indicate side reactions. Several examples of various distribution functions are given here:

Schulz-Zimm distribution:

$$f_w(M) = \frac{a^{b+1}}{\Gamma(b+1)} M^b e^{-aM} \tag{1.33}$$

where a and b are two positive parameters, and $\Gamma(b+1)$ is the gamma function of $(b+1)$. The parameters a and b can be adjusted to fit the real distribution of a polymer sample. The average molar masses of the Schulz-Zimm distribution can be expressed in terms of the two parameters:

$$M_n = \frac{b}{a} \tag{1.34}$$

$$M_w = \frac{b+1}{a} \tag{1.35}$$

The distribution function proposed by *Tung* is expressed as:

$$f_w(M) = npM^{n-1} e^{-pM^n} \tag{1.36}$$

The main advantage of the distribution function expressed by Equation 1.36 is that it can be integrated analytically to the cumulative distribution form:

$$I_w(M) = 1 - e^{-pM^n} \tag{1.37}$$

The average molar masses for those polymers that follow Equation 1.36 are:

$$M_n = \frac{p^{-1/n}}{\Gamma(1-1/n)} \tag{1.38}$$

$$M_w = \Gamma(1+1/n)p^{-1/n} \tag{1.39}$$

Another distribution function of interest is the *log-normal distribution* with two parameters M_0 and β:

$$f_w(M) = \frac{1}{\sqrt[\beta]{\pi}} \frac{1}{M} \exp\left(-\frac{1}{\beta^2} \ln^2 \frac{M}{M_0}\right) \tag{1.40}$$

The average molar masses expressed in terms of M_0 and β are:

$$M_n = M_0 e^{\frac{-\beta^2}{4}} \tag{1.41}$$

$$M_w = M_0 e^{\frac{\beta^2}{4}} \tag{1.42}$$

It is obvious that in the above equations the molar mass can be replaced by the polymerization degree.

Molar mass distribution can be calculated theoretically for various polymerization reactions. The distribution of molar mass in polymers prepared by polycondensation has been derived by Flory, assuming that the functional group reactivities are independent of the chain length. For the polycondensation of monomer type A-B (e.g., hydroxy acid) or the equimolar mixture of monomers A-A and B-B (e.g., dicarboxylic acid with glycol), the probability that a randomly selected functional group has reacted is equal to the reaction conversion q:

$$q = \frac{n_o - n}{n_o} \tag{1.43}$$

where n and n_0 are the number of moles of functional groups at the reaction time t and at the beginning of reaction, respectively. The conversion q ranges within 0 and 1 and can be equaled with the probability that a randomly selected functional group has reacted (i.e., it is incorporated in the polymer chain). Similarly, the probability that a randomly selected functional group has not reacted is $(1 - q)$. The fraction of molecules having the polymerization degree P equals the probability that a randomly selected molecule has the polymerization degree P, that is, contains $(P - 1)$ reacted functional groups and one unreacted functional group at the end of polymer chain. The total probability is given as the product of partial probabilities, and for the mole fraction of molecules having the polymerization degree P one gets:

$$x_P = q^{P-1}(1-q) \tag{1.44}$$

Expression 1.44 fulfils the condition $\sum_{P=1}^{\infty} x_P = 1$ (sum of infinite series). The number average polymerization degree is obtained as:

$$P_n = \sum_{P=1}^{\infty} x_P P = \sum_{P=1}^{\infty} (1-q) P q^{P-1} = \frac{1}{1-q} \tag{1.45}$$

The weight fraction of molecules having the polymerization degree P is obtained using Equation 1.30 as:

$$w_P = \frac{P}{P_n} x_P = (1-q)^2 P q^{P-1} \tag{1.46}$$

Equation 1.46 leads to the expression for the weight-average polymerization degree:

$$P_w = (1-q)^2 \sum_{P=1}^{\infty} P^2 q^{P-1} = \frac{1+q}{1-q} \tag{1.47}$$

and polydispersity:

$$\frac{P_w}{P_n} = 1 + q \tag{1.48}$$

The obtained distribution is usually called the *Flory distribution* or *most probable distribution*. The following arrangement of the above relations can be beneficial for practical applications: For large P it is true that $P = (P-1)$, $(1-q)^2 = \frac{1}{P_n^2}$, $\ln q = q - 1 = -\frac{1}{P_n}$, and $q = e^{\ln q}$, which leads to:

$$f_w(P) = \frac{P}{P_n^2} e^{-\frac{P}{P_n}} \tag{1.49}$$

$$f_w(M) = \frac{M}{M_n^2} e^{-\frac{M}{M_n}} \tag{1.50}$$

Using the definition of the cumulative distribution and Equations 1.49 and 1.50, and integration by parts, one gets:

$$I_w(P) = 1 - e^{-\frac{P}{P_n}} \left(1 + \frac{P}{P_n}\right) \tag{1.51}$$

$$I_w(M) = 1 - e^{-\frac{M}{M_n}} \left(1 + \frac{M}{M_n}\right) \tag{1.52}$$

Once the value of M_n is determined experimentally, it can be used for the calculation of the theoretical distribution function of a polymer prepared by polycondensation. In the case of polycondensation of monomers with average functionality larger than 2, the average polymerization degrees are:

$$P_n = \frac{1}{1 - \frac{qf}{2}} \tag{1.53}$$

$$P_w = \frac{1+q}{1-q(f-1)} \tag{1.54}$$

where f is an average monomer functionality

$$f = \frac{\sum n_i f_i}{\sum n_i} = \sum_i x_i f_i \tag{1.55}$$

where n_i and x_i are the number of moles and number fraction of f functional monomer, respectively.

An addition of a small amount of monomer B+B[i] to monomer A-B or equimolar mixture of monomers A-A and B-B results in the decrease of the polymerization degree:

$$P_n = \frac{1+r}{r-2qr+1} \tag{1.56}$$

where $r = n_A/n_B$ is the ratio of the number of moles of functional groups A and B and q is the conversion of functional group A. For example, 1% excess of monomer B-B (i.e., $r = 0.99$) decreases the maximum polymerization degree at 100% conversion to $P = 199$.

The above equations lead to following conclusions concerning the molar mass of polymers prepared by polycondensation:[ii]

- One of the most critical factors to achieve a high degree of polymerization is a strict stoichiometric balance of the two functional groups. An imbalanced ratio of the two functional groups leads to a lower degree of polymerization.
- The maximum polydispersity M_w/M_n of the polymers prepared by polycondensation of monomer A-B or an equimolar mixture of monomers A-A and B-B is two. This polydispersity is achieved at 100% conversion.
- In the case of functionality larger than 2.0, the polycondensation can reach the gel point (i.e., the conversion when P_w achieves indefinite value).

The molar mass distribution of polymers prepared by free radical polymerization is governed by the termination process. Polymers formed by free radical polymerization with termination by disproportionation have the molar mass distribution expressed as:

$$f_w(P) = \frac{P}{P_n^2} e^{-\frac{P}{P_n}} \tag{1.57}$$

And for products with termination by combination (coupling):

$$f_w(P) = \frac{4P^2}{P_n^3} e^{-\frac{2P}{P_n}} \tag{1.58}$$

[i]It can be identical with monomer B-B, but not necessarily.

[ii]The same conclusions can be applied to the polymers prepared by polyaddition.

The polydispersities of polymers prepared by free radical polymerization are either 2.0 or 1.5 for the termination by disproportionation or combination, respectively. Termination by combination results in narrower polydispersity, because radicals of various lengths (i.e., also short and long) are combined. The values of polydispersity and distributions according to Equations 1.57 and 1.58 apply to products formed during a short time period when the concentrations of monomer and initiator are constant. Commercial polymers, which are always polymerized to high conversions, have distributions different from those described by Equations 1.57 and 1.58, because in the course of free radical polymerization the monomer and initiator concentrations usually vary with conversion and consequently the polydispersity of final product is broader. The final distribution function is superposition of partial distribution functions having arisen at various conversions. Indication of whether termination occurs by combination or disproportionation can be obtained from the measurements of polydispersity of polymers prepared during a short time period for which the monomer-to-initiator ratio remains constant (in practice, this requirement is achieved by measurement at low conversion when the polymerization goes to only 5 or 10% conversion). However, both termination reactions usually occur concurrently.

Molar mass distribution of polymers prepared by free radical polymerization can be influenced by chain transfer to polymer, which results in branching of polymer chains and markedly increased polydispersity. Also the change of reaction conditions (temperature, concentration of monomer, initiator or chain transfer agent) increases the broadness of the molar mass distribution. Let us also remember that the molar mass of polymers made by free radical polymerization decreases with increasing temperature and increasing initiator concentration.

1.3.1.2 Molar Mass Averages

Several average molar masses are used in polymer science. Different instrumental techniques provide different kinds of molar mass averages. They are defined as follows:

Number-average:

$$M_n = \int_0^\infty M f_n(M)\, dM = \sum_i x_i M_i = \frac{\sum_i n_i M_i}{\sum_i n_i} = \frac{\sum_i m_i}{\sum_i m_i / M_i} = \frac{1}{\sum_i w_i / M_i} \quad (1.59)$$

Weight-average:

$$M_w = \int_0^\infty M f_w(M)\, dM = \sum_i w_i M_i = \frac{\sum_i m_i M_i}{\sum_i m_i} = \frac{\sum_i n_i M_i^2}{\sum_i n_i M_i} \quad (1.60)$$

Z-average:

$$M_z = \frac{\int_0^\infty M^2 f_w(M)\, dM}{\int_0^\infty M f_w(M)\, dM} = \frac{\sum_i m_i M_i^2}{\sum_i m_i M_i} = \frac{\sum_i n_i M_i^3}{\sum_i n_i M_i^2} \tag{1.61}$$

$Z+1$-average:

$$M_{z+1} = \frac{\int_0^\infty M^3 f_w(M)\, dM}{\int_0^\infty M^2 f_w(M)\, dM} = \frac{\sum_i m_i M_i^3}{\sum_i m_i M_i^2} = \frac{\sum_i n_i M_i^4}{\sum_i n_i M_i^3} \tag{1.62}$$

Viscosity-average:

$$M_v = \left[\int_0^\infty M^a f_w(M)\, dM\right]^{\frac{1}{a}} = \left[\sum_i w_i M_i^a\right]^{\frac{1}{a}} \tag{1.63}$$

In the above equations, n_i is the number of moles (or the number of molecules N_i), m_i is the mass, x_i is the mole fraction, and w_i is the weight fraction of molecules with molar mass M_i. The exponent a is the exponent of the Mark-Houwink equation. If the exponent a becomes unity, the viscosity-average becomes identical to the weight-average. Commonly the M_v value lies between M_n and M_w (closer to M_w). The different averages are differently sensitive to different molar masses. Namely, M_n is sensitive mainly to the fractions with low molar masses while M_w and particularly M_z and even more M_{z+1} are sensitive to high-molar-mass fractions. For monodisperse polymers all molar averages are identical. The mutual relation of molar mass averages for polydisperse polymers is $M_n < M_v < M_w < M_z < M_{z+1}$. To illustrate the sensitivity of particular averages to low and high molar masses, let us consider a hypothetical sample consisting of 1% by weight of molecules with molar mass $M = 10^7$ g/mol, 98% wt molecules with $M = 10^5$ g/mol, and 1% molecules with $M = 10^3$ g/mol. The molar mass averages for this sample are: $M_n = 50{,}500$ g/mol, $M_w = 198{,}000$ g/mol, $M_z = 5{,}100{,}000$ g/mol, and $M_{z+1} = 9{,}904{,}000$ g/mol. Note that from the viewpoint of number of molecules the most abundant fraction is that with $M = 10^3$ g/mol (50.5 molar %).

The ratio of M_w/M_n is a measure of the broadness of the molar mass distribution and is often called *polydispersity* or *polydispersity index*. If a polymer is truly monodisperse, the ratio M_w/M_n is unity because all molar mass averages are identical. The ratio M_w/M_n increases as the polymer polydispersity increases. The ratio M_z/M_w can be used as an additional parameter or can be alternatively applied instead of M_w/M_n if the M_n value cannot be reliably determined. Other indices of polydispersity are the ratio M_z/M_n and index $U = M_w/M_n - 1$.

1.4 METHODS FOR THE DETERMINATION OF MOLAR MASS

Molar mass of polymers can be determined by various methods that differ in the type of molar mass average and applicable molar mass range. With the development of size exclusion chromatography, the importance of some traditional techniques, such as, for example, osmometry or analytical ultracentrifugation, decreased markedly. SEC gives not only molar mass averages, but also a complete description of molar mass distribution. The disadvantage of SEC in its conventional form is that it is a relative technique that requires a careful calibration; that is, SEC is not an absolute technique for measuring polymer molar mass. The term *absolute* means that molar mass is related to an exactly determinable physical quantity such as vapor pressure lowering, osmotic pressure, or intensity of scattered light. Ebullioscopy (measuring the boiling point elevation of a solution) and cryoscopy (measuring the freezing point depression of a solution), once widely used and still listed in some polymer textbooks, nowadays have no real applicability and their meaning is solely in the sense of understanding basic physical principles and historical perspectives.

1.4.1 Method of End Groups

The end-group method, which provides M_n, is applicable solely to linear polymers with easily determinable end groups such as epoxy resins, polyesters, or polyamides. The end groups are determined by titration or using UV, IR, or NMR spectroscopy. The concentration of end groups in a polymer sample decreases with increasing molar mass, which limits the applicability of the method to polymers with M_n below about 10,000 g/mol. The obtained results may be influenced by the presence of chain defects or cyclization (overestimation of M_n) and by the branching (underestimation of M_n). On the other hand, the discrepancies of M_n obtained by the method of end groups and by another suitable method may identify branching or chain end defects. In the case of linear polyesters prepared by the polycondensation of hydroxy carboxylic acids, that is, polyesters with the equal number of hydroxyl and carboxyl ends, the determination of M_n is according to the equation:

$$M_n = \frac{56 \times 1000}{AN} \tag{1.64}$$

For polyesters prepared by polycondensation of dicarboxylic acids and diols, the relation is:

$$M_n = \frac{2 \times 56 \times 1000}{AN + HN} \tag{1.65}$$

where AN and HN are acid number and hydroxyl number, respectively. They are determined by titration and expressed in mg KOH per gram of sample. Factor 56 is the molar mass of potassium hydroxide that is used for titration. Despite

several limitations, the method of end groups is still relatively frequently used for the characterization of various oligomeric materials. The main advantage is given by simplicity and low demand for instrumental equipment.

1.4.2 Osmometry

Osmometry yields values of M_n. There are two types of osmometry applicable to polymers of different molar mass range. They are *vapor pressure osmometry* (vapor phase osmometry) (VPO) and *membrane osmometry* (MO). Vapor pressure and osmotic pressure are colligative properties, that is, properties that depend on the number of molecules in a given volume of solvent and not on the properties (e.g., size or mass) of the molecules. Unlike MO, VPO requires calibration with a standard of known molar mass, and it may not be considered an absolute method of molar mass determination in a precise sense of the term. However, in contrast to SEC, a low-molar-mass compound of accurately known molar mass is used for the calibration of VPO apparatus. A general advantage of osmometry is independency of the chemical nonuniformity; VPO and MO are very suitable for the characterization of heterogeneous copolymers. However, the practical meaning of both methods has declined tremendously with the development of SEC and nowadays they find only limited applications.

1.4.2.1 Vapor Pressure Osmometry

The principle of VPO is based on the fact that the vapor pressure of a solution is lower than that of the pure solvent at the same temperature and pressure. At sufficiently low concentrations, the magnitude of the vapor pressure decrease is directly proportional to the molar concentration of dissolved compound. Vapor pressure is not measured directly, but is measured indirectly by using thermistors (resistors whose resistance varies with temperature) that are connected in a Wheatstone bridge. The thermistors are placed in a measuring chamber that contains a reservoir of solvent and porous paper wicks to provide a saturated solvent atmosphere around the thermistors. If drops of solvent are placed on both thermistors, the thermistors will be at the same temperature. When a drop of solution is placed on one thermistor and solvent is placed on the other, the temperature difference is created. Due to lower solvent pressure above the solution, condensation of solvent into the solution from the saturated solvent atmosphere occurs. Solvent condensation releases heat that increases the solution temperature. Condensation continues until the solution temperature rises enough to compensate the decrease of solvent pressure. In the system equilibrium, the decrease of solvent pressure by the presence of dissolved compound is compensated by the increase of pressure due to increased temperature. The measurements are made at multiple concentrations and M_n is obtained by the extrapolation of the relation $\Delta R/c$ versus c to zero concentration:

$$M_n = \frac{K}{\left(\frac{\Delta R}{c}\right)_{c\to 0}} \tag{1.66}$$

where c is the concentration, ΔR is the difference in resistance of the thermistors that is measured instead of temperature difference, and K is a calibration constant of the instrument obtained by measuring a compound of known molar mass (e.g., sucrose octaacetate for organic solutions or sucrose for aqueous solutions).

A serious disadvantage of VPO is excessive sensitivity to the presence of low-molar-mass compounds, such as residual monomers, solvents, or moisture, which can result in serious underestimation of M_n. For example, presence of solely 0.1% wt of water in a polymer with $M_n = 2,000$ g/mol decreases the experimental value of M_n to about 1,800 g/mol. VPO is applicable to M_n of about 20,000 g/mol (some instruments claim applicability up to 10^5 g/mol). In the past, VPO replaced ebullioscopy and cryoscopy and enjoyed widespread use, but nowadays the VPO method is relatively rarely used and it has been replaced by SEC. Besides polymer chemistry, osmometers are used for determining the concentration of dissolved salts or sugar in blood or urine samples.

1.4.2.2 Membrane Osmometry

Membrane osmometry is an absolute method for the determination of M_n. In an MO instrument, a solution of a polymer is separated from pure solvent by a semipermeable membrane, which allows the solvent to pass through while being impermeable for the polymer. Due to the difference of chemical potential of pure solvent and solvent in solution, there is a solvent flow from the pure solvent side to the solution side. This solvent flow can be eliminated by applying pressure to the solution side. The applied pressure equals the osmotic pressure of the solution. A schematic illustration of the osmometer is shown in Figure 1.5. Solvent diffuses to the solution until the osmotic pressure is balanced by the hydrostatic pressure:

$$p = \Delta h d g \tag{1.67}$$

where Δh is the difference in the heights of the columns of solvent and solution, d is the density, and g is the gravitational acceleration.

The osmotic pressure π is related to the molar mass by the equation:

$$\frac{\pi}{c} = RT\left(\frac{1}{M_n} + A_2 c + A_3 c^2 + \cdots\right) \tag{1.68}$$

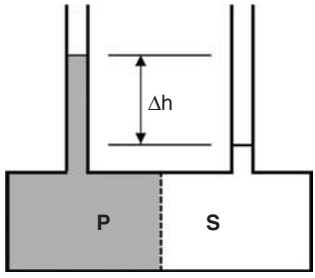

Figure 1.5 Schematic representation of membrane osmometer. P = polymer solution, S = pure solvent, Δh = height difference. Dashed line represents semipermeable membrane.

where A_2 and A_3 are the second and third virial coefficients, c is the concentration of polymer (g/mL), R is the gas constant, and T is the absolute temperature. At low concentrations the higher terms in Equation 1.68 are negligible and a plot of π/c versus c is linear with the intercept yielding M_n. The ratio of π/c is called the *reduced osmotic pressure*. The second virial coefficient is an additional result from the measurement of osmotic pressure that provides information about the polymer–solvent interactions and thus about the thermodynamic quality of solvent. Upward curvature on the π/c versus c plot indicates contributions from the third and higher virial coefficients. Membrane osmometry has a potential of the determination of theta conditions for a given solvent–polymer pair, but this potential is limited by solubility problems.

The apparatus outlined in Figure 1.5 may require several hours or even days to achieve equilibrium. The automated osmometers introduced in the early 1960s allowed measurements of osmotic pressure in only a few minutes.

The low-molar-mass limit of MO is given by membrane permeability, which is around 5,000 g/mol. Consequently, if a sample contains oligomeric species that can permeate through the membrane, the osmotic pressure is too low and the obtained M_n is overestimated. Generally, polydisperse polymers with pronounced oligomeric tail are not suitable for the MO method. The upper limit is about 5×10^5 g/mol.

1.4.3 Dilute Solution Viscometry

The dimensions of the polymer coils in a dilute solution affect the viscous properties of the solution. As a matter of fact, viscometry is not a method of the determination of molar mass, because the molar mass is not measured directly. Using the viscometric data, the molar mass can be obtained indirectly using the previously established Mark-Houwink relation. Viscometry of dilute solutions is an important method of the characterization of polymers with significant advantage given by simple and cheap instrumentation. In addition to the determination of molar mass, measurements of dilute solution viscosities can provide information about polymer branching, polymer size and its temperature dependence, and chain flexibility. Besides classical measurements of polymer solutions by a capillary viscometer, viscometry has become an important type of detection for SEC. Therefore, the viscometric characterization of dilute polymer solutions requires special attention. In order to characterize polymer molecules, the increase of viscosity brought about by the polymer molecules is measured instead of the absolute viscosity of the polymer solution. Classical viscometric measurements are performed using a capillary viscometer (Ubbelohde, Ostwald). The measured quantity is the *specific viscosity* (η_{sp}) or *relative viscosity* (η_{rel}):

$$\eta_{sp} = \frac{\eta - \eta_0}{\eta_0} = \frac{t - t_0}{t_0} = \eta_{rel} - 1 \tag{1.69}$$

where η and η_0 are the viscosities of dilute polymer solution and pure solvent, respectively. In practice, the measurement of viscosity is replaced with the

measurement of time (t) needed for a certain volume of the solvent or solution to flow from one mark to the other. The specific viscosity is a measure of the increase of viscosity due to the addition of polymer, and according to Einstein it is proportional to the volume fraction (φ) of a polymer in solution:

$$\eta_{sp} = 2.5 \times \varphi \tag{1.70}$$

where $\varphi = \frac{V_{polymer}}{V_{solution}}$ (i.e., fraction of volume occupied by polymer molecules to the entire solution volume). The factor 2.5 assumes that polymer molecules behave like hard spheres.

Another quantity of interest is the *reduced viscosity* (*viscosity number*):

$$\eta_{red} = \frac{\eta_{sp}}{c} \tag{1.71}$$

or the *inherent viscosity* (*logarithmic viscosity number*):

$$\eta_{inh} = \frac{\ln \eta_{rel}}{c} \tag{1.72}$$

In the limit of infinite dilution, the reduced viscosity is known as the *intrinsic viscosity* (*limiting viscosity number*):

$$[\eta] = \lim_{c \to 0} \frac{\eta_{sp}}{c} \tag{1.73}$$

or alternatively

$$[\eta] = \lim_{c \to 0} \frac{\ln \eta_{rel}}{c} \tag{1.74}$$

The intrinsic viscosity reflects the ability of a polymer molecule to enhance the viscosity and depends on the size and shape of the polymer molecule. It is an important quantity describing the behavior of a polymer in solution and the polymer molecular structure. The concentration dependence of the specific viscosity can be described by the Huggins equation:

$$\frac{\eta_{sp}}{c} = [\eta] + k_H [\eta]^2 c + \cdots \tag{1.75}$$

where c is the concentration (g/mL or g/dL), k_H is the Huggins constant for a given polymer, solvent, and temperature, and $[\eta]$ is the intrinsic viscosity. For a sufficiently low concentration, the plot of η_{sp}/c versus c is linear with intercept equal to the intrinsic viscosity. The term k_H is obtained from the slope of the plot. For polymers in thermodynamically good solvents, k_H usually has a value around 1/3, while larger values of 0.5−1 are typical of poor solvents. Thus the Huggins constant can be used as a measure of solvent quality for a given polymer. An alternative expression was proposed by Kraemer:

$$\frac{\ln \eta_{\mathrm{rel}}}{c} = [\eta] + k_K [\eta]^2 \, \mathrm{c} + \cdots \tag{1.76}$$

where k_K is the Kraemer constant. For polymers in good solvents, k_K is negative and the mutual relation of the two constants is $k_H - k_K = 0.5$. The most accurate procedure of the determination of the intrinsic viscosity is to plot according to both Equations 1.75 and 1.76 and to take the mutual intercept as $[\eta]$. A small discrepancy of the intercept can be eliminated by taking an average value. An example of the determination of the intrinsic viscosity according to the Huggins and Kraemer procedures is depicted in Figure 1.6. Although various other extrapolation procedures were proposed, those according to Huggins and Kraemer represent the most often used and most reliable ones. When constant k_H or k_K is known, Equations 1.75 and 1.76 allow the calculation of intrinsic viscosity from a single point measurement. However, the measurements at multiple concentrations and extrapolation procedures should be preferred for precise determination of intrinsic viscosity. For the measurement the sample is typically prepared as a stock solution that is diluted by addition of solvent to prepare low concentrations. A more accurate procedure, which eliminates random errors during the preparation of stock solution, involves separate preparation of each solution. The initial concentration should provide $\eta_{sp} \approx 0.8$ and the specific viscosity for the most dilute solution should be about 0.1. However, the most important parameter is the linearity of the dependence of η_{sp}/c versus c or ln η_{rel}/c versus c with no indication of curvature at higher concentrations. It can be seen from Figure 1.6 that even the points that do not fulfill the requirement of $\eta_{sp} < 0.8$ show no deviation from the linearity. Another important requirement is that the solution can be considered dilute (i.e., consisting of mutually isolated polymeric coils

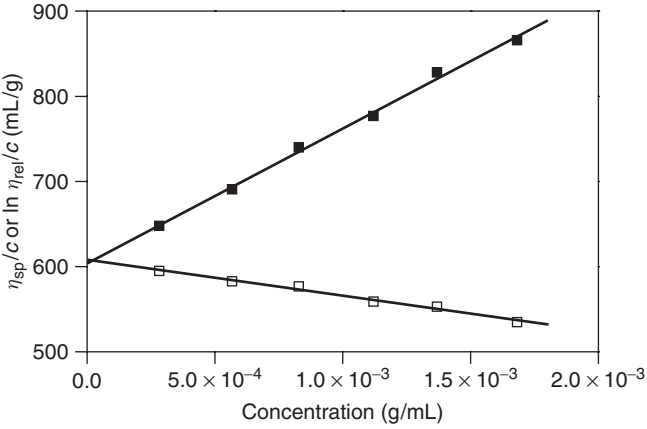

Figure 1.6 Plots of η_{sp}/c (■) and ln η_{rel}/c (□) versus c for a sample of hyaluronic acid sodium salt of $M_w = 335{,}000$ g/mol in aqueous 0.1 M sodium phosphate buffer pH 7 at 25°C. The mutual intercept is $[\eta]$. The intercepts are 604 mL/g and 608 mL/g for Huggins and Kraemer plots, respectively. The slopes allow calculation of Huggins and Kraemer constants: $k_H = 0.43$, $k_K = -0.11$.

Source: Courtesy Martina Hermannova, Contipro C, Czech Republic.

without significant polymer–polymer intermolecular interactions). The concentration when the solution is completely filled with the polymer coils and the coils start to penetrate each other is called *critical concentration* (c^*). Critical concentration is reached when the volume fraction of polymer $\varphi = 1$. Then, using Equation 1.70, the critical concentration can be estimated as:

$$c^* \approx \frac{2.5}{[\eta]} \tag{1.77}$$

The critical concentration is indirectly proportional to the intrinsic viscosity, and the determination of the intrinsic viscosity should be performed below c^* to assure exact linear extrapolation. The two highest concentrations in Figure 1.6 do not fulfill the requirement of $\eta_{sp} < 0.8$, but they are still well below the critical concentrations, which appears a more relevant requirement since the two points do not show any deviation from linear fit.

The viscometer should be selected so that $t_0 \approx 100$ sec. The solutions must be filtered to remove dust and other insoluble matters. Precise temperature control is very important for the determination of intrinsic viscosity. However, maintaining the constant temperature is of greater importance than absolute temperature itself.

The relation between the intrinsic viscosity and molar mass[i] is given by the Mark-Houwink equation (also called Mark-Houwink-Kuhn or Mark-Houwink-Kuhn-Sakurada):

$$[\eta] = KM^a \tag{1.78}$$

where K and a are the constants for a given polymer, solvent, and temperature. The intrinsic viscosity of a polydisperse polymer is related to the molar mass distribution and the obtained intrinsic viscosity is the weight-average:

$$[\eta] = \sum_i w_i [\eta]_i \tag{1.79}$$

where w_i is the weight fraction of polymer with the intrinsic viscosity $[\eta]_i$. Replacing the intrinsic viscosity in Equation 1.79 with Equation 1.78 and calculating M from Equation 1.78 shows that the molar mass obtained from the intrinsic viscosity is the viscosity average:

$$M = \left(\sum_i w_i M_i^a \right)^{\frac{1}{a}} = M_v \tag{1.80}$$

Once K and a values are reliably established, the molar mass can be determined from the value of $[\eta]$ for a polymer under investigation. For many polymers, the

[i]The use of this equation with the relative molecular weight is recommended by IUPAC Compendium of Chemical Terminology to avoid awkward and variable dimensions of constant K in the case that molar mass in g/mol is used.

parameters K and a can be found in the literature.[2] The experimental determination of K and a requires a series of samples with narrow molar mass distribution and known values of the intrinsic viscosity and molar mass. The intrinsic viscosity is plotted in a double logarithmic scale against molar mass, and the Mark-Houwink constant K and exponent a are obtained from the intercept and slope, respectively. The traditional method of determination of the parameters of the Mark-Houwink equation included fractionation of a polydisperse sample into a series of narrow fractions and the characterization of the obtained fractions by viscometry and light scattering and/or membrane osmometry. The requirement of narrow polydispersity was often not fulfilled. Equation 1.78 yields the viscosity average molar mass only if the constants K and a were determined by the measurements of monodisperse fractions. For all other cases, when the Mark-Houwink relationship was determined using polymer samples of polydispersity $M_w/M_n > 1$ and the average molar mass M_n or M_w was used, the Mark-Houwink equation should be corrected with a correction factor (correction factors are listed, for example, in *Polymer Handbook*[2]). However, the influence of polydispersity is relatively small when $[\eta]$ is correlated with M_w and $M_w/M_n < 1.5$. Although the Mark-Houwink relation of linear polymers is linear over a broad range of molar masses, one should be cautious when the parameters K and a are used beyond the molar mass range over which they were determined. The molar mass range of polymer samples used for the determination of the $[\eta]-M$ relationship should cover at least one order of magnitude. The parameters K and a should always be quoted not only with the solvent and temperature, but also with the number of samples and their molar mass range and polydispersity, and the method of the molar mass determination. As a rule of thumb, the values obtained with narrow polymers using light scattering should be preferred.

1.4.3.1 Properties of Mark-Houwink Exponent

The literature shows relatively significant differences of the values K and a even for polymers measured under identical conditions. The low K values are associated with the high a values and vice versa, which means the differences are to a certain level mutually compensated when the constants are used to calculate the molar mass averages.

An important property of the exponent a is that it bears information about the polymer conformation. Generally, for flexible polymer molecules in thermodynamically good solvents the exponent a ranges from about 0.65 to about 0.75. In theta solvent, $a = 0.5$, while higher values of a, equaling or even exceeding unity, can be found for less flexible rodlike macromolecules, such as some polysaccharides or polyelectrolytes. Especially polyelectrolytes are able to create expanded rodlike macromolecules due to the repulsive electrostatic forces of charges within the polymer chain. The maximum value of a is two, which corresponds to rigid rods. On the other hand, the increasing compactness of the macromolecules results in decreasing a, which in the ultimate case of compact spheres equals zero and so the intrinsic viscosity becomes independent of the

molar mass. Although compact sphere-like macromolecules are rare, the decrease of the exponent a is observed for branched polymers that often show an evenly decreasing slope of the Mark-Houwink plot with increasing molar mass (see examples and further discussion in Chapter 6).

The Mark-Houwink relations established for high-molar-mass polymers are not valid for oligomers. In the region of low molar masses, the Mark-Houwink relations show a break where the slope drops to about 0.5, no matter the polymer composition and thermodynamic quality of the solvent. This is a consequence of short polymer chains that have no excluded volume effect, because the situation where a polymer chain segment cannot take the exact place of another segment cannot happen for too-short chains. Different Mark-Houwink exponents of oligomers and polymers are illustrated in Figure 1.7, which shows log – log plot of $[\eta]$ against M for polystyrene in THF. The exponent a obtained for lower-molar-mass polystyrene is markedly lower than that for polystyrene of high molar mass, yet it is a larger-than-expected value of 0.5, which may reflect the fact that the chains consisting of 13–125 monomeric units are not short enough to completely eliminate the effect of excluded volume.

1.4.3.2 Molecular Size from Intrinsic Viscosity

The dimension of intrinsic viscosity, mL/g, suggests this quantity to be related to the volume occupied by the polymer molecules in solution. The hydrodynamic volume of a polymer coil is expressed as:

$$V_h = \frac{[\eta]M}{\gamma N_A} \tag{1.81}$$

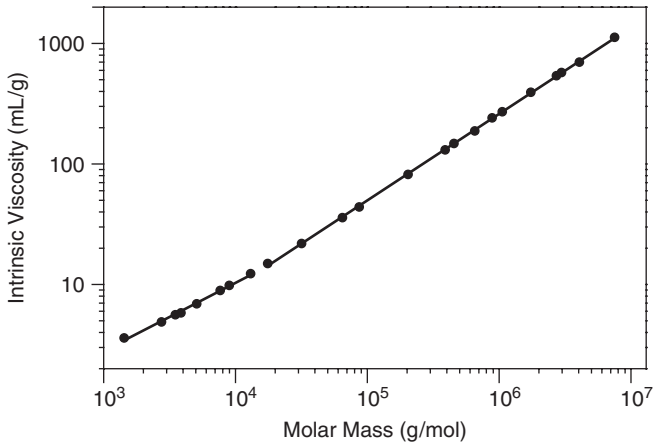

Figure 1.7 Mark-Houwink plot for polystyrene in THF at 35°C. Mark-Houwink parameters $a = 0.565$, $K = 5.66 \times 10^{-2}$ mL/g (M from 1400 to 13,000 g/mol); $a = 0.719, K = 1.27 \times 10^{-2}$ mL/g (M from 17,500 to 7.5×10^6 g/mol). The data were obtained by SEC-MALS-VIS analysis of narrow polystyrene standards.

where M is the molar mass, N_A is Avogadro's number, and γ is Simha's parameter related to the shape of a particle, which equals 2.5 for a hard sphere. Using $\gamma = 2.5$, the hydrodynamic volume is the volume of a hydrodynamically equivalent sphere (i.e., a hypothetical sphere that would have the same intrinsic viscosity as the actual polymer molecule). The hydrodynamically equivalent sphere can be similarly defined on the basis of diffusion coefficient. The size of a hydrodynamically equivalent sphere may be different for different types of motion of the macromolecules (i.e., viscous flow or diffusion), and thus the hydrodynamic radii calculated on the basis of intrinsic viscosity and diffusion coefficient need not be absolutely identical. The hydrodynamic radius (radius of hydrodynamically equivalent sphere) is then calculated as:

$$R_h = \left(\frac{3[\eta]M}{10\pi N_A}\right)^{\frac{1}{3}} \tag{1.82}$$

The hydrodynamic radius calculated from the intrinsic viscosity is often called the *viscometric radius* (R_η) and the term *hydrodynamic radius* is reserved for the radius based on the diffusion coefficient. However, the difference between the two radii is usually negligible. The intrinsic viscosity also can yield the RMS radius using the Flory-Fox and Ptitsyn-Eizner equations:[3,8]

$$R = \frac{1}{\sqrt{6}}\left(\frac{[\eta]M}{\Phi}\right)^{\frac{1}{3}} \tag{1.83}$$

$$\Phi = 2.86 \times 10^{21}(1 - 2.63\varepsilon + 2.86\varepsilon^2) \tag{1.84}$$

$$\varepsilon = \frac{2a - 1}{3} \tag{1.85}$$

where a is the exponent of Mark-Houwink equation. Equation 1.84 expresses Flory's universal constant Φ_0 after correction for non-theta conditions. The correction parameter $\varepsilon = 0$ at theta conditions, whereas at thermodynamically good solvents it is related to the exponent of the Mark-Houwink equation. Equation 1.83 yields the RMS radius in cm using the intrinsic viscosity expressed in dL/g. For example, for polystyrene molecules of molar mass 10^6 g/mol, using the parameters of the Mark-Houwink equation $a = 0.717$ and $K = 1.17 \times 10^{-4}$ dL/g, one gets $\varepsilon = 0.145$, $\Phi = 1.94 \times 10^{21}$, and $R = 4.4 \times 10^{-6}$ cm (i.e., 44 nm). The practical meaning of Equation 1.83 is that it can provide RMS radii for smaller polymers that are not accessible directly by the light scattering measurements. Equation 1.83 also can be used in reversed direction for the calculation of intrinsic viscosity from the RMS radius and molar mass. Since both RMS radius and molar mass are obtained by light scattering, a light scattering photometer can yield the intrinsic viscosity without a viscometer. Equation 1.83 also shows the relation between the exponents of the Mark-Houwink equation and the

relationship RMS radius versus molar mass:

$$R = k \times M^{b} \tag{1.86}$$

$$b = \frac{1 + a}{3} \tag{1.87}$$

The exponent a can range from zero for compact spheres to two for rigid rods and thus the values of exponent b are in a narrower interval of 0.33−1.0. This fact explains why the conformation plots of branched polymers are usually significantly less curved than the corresponding Mark-Houwink plots. A typical value for the exponent $a \approx 0.7$ corresponds to $b \approx 0.57$. In contrast to the Mark-Houwink parameters K and a, which were published for many polymers in various solvents, the literature values of k and b are significantly less frequent. Since these parameters are needed for the characterization of branching, the possibility of calculating them on the basis of the Mark-Houwink parameters using Equation 1.83 is of practical importance.

Using Equation 1.82 and the Stokes-Einstein equation, one can get the relation for the exponent of the molar mass dependence of the diffusion coefficient (Equation 1.20):

$$\beta = \frac{1 + a}{3} \tag{1.88}$$

1.4.3.3 Dependence of Intrinsic Viscosity on Polymer Structure, Temperature, and Solvent

The influence of the chemical composition of a polymer on the intrinsic viscosity is not straightforward. Double bonds and cycles in the main chain and large side groups decrease the chain flexibility and affect the ability of the chain to form a random coil and so result in increased intrinsic viscosity. However, the chemical structure of the polymer also affects the interactions of the polymer with the solvent, and it may not be easy to distinguish between the influence of solvation and the steric hindrance of different chain structures. The solvation of a polymer chain has a significant impact on the expansion of the polymer coil. The solvent interacting with a polymer chain creates a solvating envelope that increases with increasing thermodynamic quality of the solvent and thus the intrinsic viscosity increases with increasing thermodynamic quality of the solvent.

Ionic groups along the polymer chain have a strong effect on the intrinsic viscosity. A polymer coil of polyelectrolyte can expand due to the electrostatic repulsive forces between the ionic groups compared to a neutral polymer of a similar chemical structure (e.g., polyacrylic acid sodium salt versus polyacrylamide, hyaluronic acid sodium salt versus pullulan). The coil expansion of the polyelectrolyte is determined by the degree of dissociation of the ionic groups, which depends on pH. The expansion of the polyelectrolyte chain is strongly affected by addition of salt, which shields charged groups. The coil expansion and thus the intrinsic viscosity decreases with an increasing salt concentration.

The viscosity of a polymer solution decreases exponentially with temperature according to the equation:

$$\eta = A \times e^{\frac{E}{RT}} \tag{1.89}$$

where E is the flow activation energy, T is the absolute temperature, R is the gas universal constant, and A is a constant. The behavior of the intrinsic viscosity is different, and the temperature coefficient $\mathrm{d}[\eta]/\mathrm{d}T$ can be positive, negative, or zero. Increased temperature can increase chain flexibility due to the lower potential barrier of the transition from one conformation to another, which decreases the intrinsic viscosity due to a more coiled macromolecular structure. On the other hand, the rising temperature increases the thermodynamic quality of the solvent. The intrinsic viscosity is more sensitive to temperature in the vicinity of theta temperature. The increase of the intrinsic viscosity with temperature is used for an interesting and important application of some copolymers as additives for motor oils. These polymers dissolved in the oil at room temperature are closed to theta conditions and their molecules are highly coiled. Due to the relatively low hydrodynamic volume of the macromolecules, their contribution to solution viscosity is low. During the oil application at high temperatures, the thermodynamic quality of the oil increases, leading to high solvation of the macromolecules, their strong expansion, and thus a partial compensation for the overall decrease of the oil viscosity and thus the lubrication efficiency.

1.4.4 Matrix-Assisted Laser Desorption Ionization Time-of-Flight Mass Spectrometry

Matrix-assisted laser desorption ionization time-of-flight mass spectrometry (MALDI-TOF MS) is a relatively new technique of the determination of molar mass with accuracy and resolution unachievable with other methods. A mixture of a UV-light-absorbing matrix and a polymer sample is irradiated by a nanosecond laser pulse. Most of the laser energy is absorbed by the matrix, which prevents unwanted fragmentation of the polymer. Another purpose of the matrix is to isolate the analyte molecules from each other and thus to prevent clustering of the analyte into high-mass complexes that would be too large for desorption and analysis. The ionized macromolecules are accelerated in an electric field and enter the TOF tube. During the flight in the tube, the molecules are separated according to their mass-to-charge ratio and reach the detector at different times. In this way, each molar mass gives a distinct signal in the mass spectrum. In addition to the molar mass distribution MALDI-TOF MS can also provide compositional information concerning end groups and chemical composition. However, in the case of polydisperse polymers the method commonly fails due to the mass-dependent desorption ionization process and/or mass-dependent detection efficiency due to the signal intensity discrimination against higher-molar-mass components. As a consequence of that, the most abundant ions in the obtained spectrum may not coincide with the apex of

the molar mass distribution and the fractions with the highest molar mass can be completely missing. The inability of MALDI to provide reliable molar mass distribution for polydisperse polymers can be overcome by combination with SEC by collecting fractions and performing MALDI-TOF MS analysis offline. In a SEC-MALDI-TOF MS combination, the refractive index detector of the SEC instrument determines the polymer concentration in each fraction and the corresponding molar masses are measured by MALDI-TOF MS. The determination of the average molar mass of each fraction allows establishing the SEC calibration, which can then be used to compute molar mass distribution by conventional SEC. However, the speed of the analysis and the expensive instrumentation are the limitations of the SEC-MALDI methodology. For more information about the MALDI-TOF technique, refer to reference 9.

1.4.5 Analytical Ultracentrifugation

Analytical ultracentrifugation (UC) represents a traditional technique of polymer characterization that played an important role at the beginning of polymer science in the 1920s. The method was invented by Theodor Svedberg, who introduced both the *sedimentation velocity method* and the *sedimentation equilibrium method*. The method of sedimentation velocity is used to measure the sedimentation coefficient that can be used for the calculation of molar mass. The method is based on monitoring the movement of concentration boundary in dilute polymer solution placed in the ultracentrifuge cell under high centrifugal field (e.g., 70,000 rotations per minute). The determination of sedimentation coefficient is performed at multiple concentrations to allow the extrapolation of sedimentation coefficient to zero concentration. The molar mass can be calculated from the Svedberg equation:

$$M = \frac{RTs}{D(1 - \bar{v}d)} \tag{1.90}$$

where R is the gas constant, T is the temperature (K), s is the sedimentation coefficient (second), D is the diffusion coefficient, $\bar{v}$ is the partial specific volume (mL/g), and d is the density.

The sedimentation equilibrium experiment yields both weight-average M_w and the centrifuge-average M_z. The centrifugal field is significantly lower compared to the former method (e.g., 15,000 rpm). When the sedimentation equilibrium is reached, the molecules are distributed in the centrifuge cell according to their molar mass. Although the method can provide valuable information about sample purity, characterize assembly and disassembly mechanisms of biomacromolecular complexes, characterize macromolecular conformational changes, or measure equilibrium constants for self- and hetero-associating systems, in the area of synthetic polymers it has been completely replaced with size exclusion chromatography. Major limitations for routine applications are analysis time needed for the experiments (time needed to reach equilibrium can be up to several days) and expensive instrumentation.

1.5 KEYNOTES

- There are several types of nonuniformities that can occur in most synthetic and natural polymers. The most frequently studied nonunifiormity is that of molar mass, but the others should be kept in mind when polymers are being characterized.
- Freely jointed chain represents the basic model of polymer chain in dilute solution.
- Excluded volume refers to the fact that one part of a long chain molecule cannot occupy space that is already occupied by another part of the same molecule. Excluded volume causes the polymer chain to expand to a larger size compared to what it would be were there no excluded volume effect.
- The effect of excluded volume can be neutralized by specific conditions (solvent and temperature) that are called theta conditions.
- Besides excluded volume, the size and shape of a polymer chain is affected by chain structure (i.e., bond angles, bond length, ability to rotate about the single bonds, and presence of double bonds or cycles in the main chain).
- The size and properties of polymer chains must be evaluated by averaging over all possible conformations given by all angles of rotation about the bonds.
- Molar mass distribution can be described by cumulative and differential distribution functions. Both distributions can be expressed in term of number fraction and weight fraction.
- The molar mass moments used in polymer science are the number-average, weight-average, z-average, $(z+1)$-average, and viscosity average. The type of average should be stated whenever talking about the polymer molar mass.

1.6 REFERENCES

1. Flory, P. J., *Statistical Mechanics of Chain Molecules*, John Wiley & Sons, New York (1969).
2. Brandrup, J., Immergut, E. H., Grulke, E. A. (editors), *Polymer Handbook*, 4th Edition, John Wiley & Sons, New York (1999).
3. Flory, P. J. and Fox, T. G., *J. Am. Chem. Soc*., **73**, 1904 (1951).
4. Burchard, W., *Makromol. Chem*., **50**, 20 (1960).
5. Stockmayer, W. H. and Fixman, M., *J. Polym. Sci., Part C*, **1**, 137 (1963).
6. Kratky, O. and Porod, G., *Rec. Trav. Chim*., **68**, 1106 (1949).
7. Bohdanecky, M., *Macromolecules*, **16**, 1483 (1983).
8. Ptitsyn, O. B. and Eizner, Yu. E., *Sov. Phys. Tech. Phys*., **4**, 1020 (1960).
9. Pasch, H. and Schrepp, W., *MALDI-TOF Mass Spectrometry of Synthetic Polymers*, Springer, Berlin (2003).

Chapter 2

Light Scattering

2.1 THEORY AND BASIC PRINCIPLES

This chapter describes basic principles of scattering of light by dilute solutions of macromolecules or dispersions of colloidal particles and presents various examples of the application of light scattering for the characterization of unfractionated polymer solutions. Principles and applications of the light scattering hyphenated with a separation technique are presented in Chapters 4 and 5. Generally, it is not necessary to distinguish between the solutions of macromolecules or dispersions of particles. In fact, many real systems may contain dissolved macromolecules along with highly compact branched macromolecules or supermolecular structures and the borderline between *dissolved* and *dispersed* may not always be clear. The importance of light scattering is obvious because it is one of the few absolute methods available for the determination of molar mass of polymers. In addition, light scattering can provide information about the macromolecular size and structure and interactions of macromolecules with solvent and with each other.

An important advantage of light scattering is its applicability over an extremely broad range of molar masses. The first experiments focused on the application of light scattering for polymer characterization were carried out in the 1940s and 1950s, that is, before availability of personal computers, lasers, membrane filters, and size exclusion chromatography. Several important technological developments, including lasers and advances in personal computers and software, converted light scattering from an originally tedious and uncertain method of limited applicability to a routine and easy-to-use modern analytical technique. The advent of size exclusion chromatography and other separation techniques and development of light scattering instruments capable of working as chromatography detectors tremendously extended obtainable information as well as application areas.

Light Scattering, Size Exclusion Chromatography and Asymmetric Flow Field Flow Fractionation: Powerful Tools for the Characterization of Polymers, Proteins and Nanoparticles, by Stepan Podzimek

Light scattering can be simply defined as a natural phenomenon, namely a result of the interaction of light with matter. The light is the oscillating field consisting of electric and magnetic parts. The oscillating electric field interacting with a neutral molecule creates a dipole, which, due to the oscillation of the incident radiation, oscillates as well. The oscillating dipole becomes a source of new radiation. The schematic illustration is shown in Figure 2.1. It is obvious that the ability of a molecule to scatter light is in relation to the tendency of the electron cloud of the molecule to be displaced from its normal shape by an external electric field. This tendency is called *polarizability*, which is directly proportional to the specific refractive index increment (dn/dc).

A perfect crystal that is much larger than the wavelength of the incident light can be considered as composed of identical small elements that are much smaller compared to the wavelength. Every small element can be considered to be a point source of scattered light. In any direction of observation it is possible to find two identical volume elements distant from each other such that the light beams scattered by these two elements reach the detector phase shifted by exactly $\lambda/2$. In a perfect crystal, identical volume elements contain an identical number of molecules and therefore the intensities of light scattered by the two volume elements are identical. Two light beams of identical intensity, shifted by $\lambda/2$, cancel each other completely due to interference. Consequently, large perfect crystals do not scatter light. Real crystals scatter light due to local inhomogeneities and surface layers. Pure liquids scatter light much more intensively than the same number of molecules in the form of crystal. The explanation for this fact is that the number of molecules in a volume element of a liquid fluctuates with time. Consequently, the intensities scattered by the same volume elements are not identical and are not completely canceled by interference. Although the macroscopic density of a liquid is constant with time, the microscopic density fluctuations explain the non-zero intensity of light scattered by pure liquids.

The intensity of light scattered by a dilute polymer solution consists of two contributions: (1) intensity scattered by a solvent itself, and (2) intensity scattered by macromolecules. The difference between the two scattered intensities is called *excess scattering*, which bears information about the dissolved macromolecules. Similarly to the case of pure liquids, small volume elements of solution contain different numbers of macromolecules and thus the fluctuation of solute concentration accounts for the excess scattering.

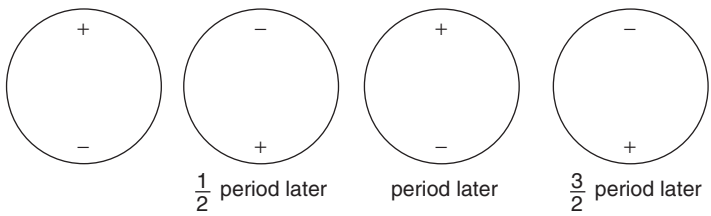

Figure 2.1 Oscillation of induced dipole due to the oscillation of incident light.

2.2 TYPES OF LIGHT SCATTERING

There are three different types of light scattering:

1. *Static light scattering* (also called *elastic*, *Rayleigh*, or *classical* light scattering) occurs at the same wavelength as the incident light. Static light scattering refers to an experiment in which the scattered light intensity is determined at a given scattering angle by averaging the fluctuating intensity over a long time scale compared with the time scale of the intensity fluctuation. The information about the scattering macromolecules is obtained from the measurement of angular and concentration dependence of the intensity of scattered light. This type of experiment yields the molar mass, molecular size expressed as the root mean square (RMS) radius, and the second virial coefficient. This book deals mostly with the static type of light scattering.
2. *Dynamic light scattering* (*quasielastic* light scattering) also occurs at the same wavelength as that of the incident light, but the fluctuations of the scattered light intensity are studied instead of the average intensity. Due to the Brownian motion of the scattering particles, the intensity of scattered light fluctuates. The fluctuation is over extremely short time intervals. In fact, static and dynamic light scattering apply to the same phenomena and the only difference is in the way of collecting and processing the experimental data. In static light scattering we measure the time-averaged intensity of scattered light while in dynamic light scattering we analyze how the scattered light intensity fluctuates with time. Today's light scattering instruments allow performing both types of light scattering experiments simultaneously. *Note:* The photodiodes used to detect the scattering light intensity at the static experiments are not able to follow extremely rapid changes of the intensity and thus monitor an average intensity of the scattered light. The difference between the static and dynamic light scattering measurements is illustrated in Figure 2.2. The dynamic light scattering experiment yields information about the diffusion coefficient of scattering particles and consequently about the hydrodynamic radius.
3. *Raman scattering* occurs at a wavelength different from that of incident light. Raman spectroscopy can provide structural information and is not a topic of this book.

Several examples of light scattering can be found in nature. The most visible example of light scattering is the blue color of sky. As will be shown later, the intensity of scattered light strongly depends on the light wavelength. The blue color is the most intensively scattered light from the incident sunlight, which is scattered by dust and ice particles and molecules at the upper layers of atmosphere. Since the blue part of sunlight is scattered with the highest intensity, the sky ultimately appears as blue. Similar effects are responsible for red sunset or

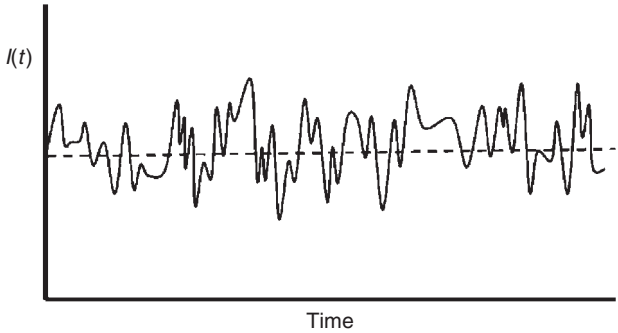

Figure 2.2 Sketch of fluctuation of scattered light intensity with time. For a static light scattering experiment the average scattered intensity (indicated by the dotted line) is measured, while for dynamic light scattering the intensity fluctuations are analyzed.

sunrise. The only difference is that the incident light comes to the atmosphere from a different angle and travels a longer path in the atmosphere compared to the sunlight that one can see during the day. In the longer path, the scattering actually has a filtering effect and one can see the least scattered light as red.

2.2.1 Static Light Scattering

The fundamental description of the theory, instrumentation including assembly of a flow cell in multi-angle light scattering (MALS) photometers, and applications of light scattering were reviewed in an extensive article by Wyatt.[1] A book by Pavel Kratochvil can become a source of valuable information about light scattering from polymer solutions.[2]

The basic equation that relates the intensity of scattered light with the properties of the macromolecules in solution is:[3]

$$\frac{R_\theta}{K^* c} = MP(\theta) - 2A_2 cM^2 P^2(\theta) + \cdots \tag{2.1}$$

where R_θ is the excess Rayleigh ratio, c is the concentration of polymer in solution (g/mL), M is the molar mass, A_2 is the second virial coefficient, K^* is the optical constant, and $P(\theta)$ is the *particle scattering function* (also called *particle scattering factor*). The properties of some of the quantities are discussed in the following text.

The excess Rayleigh ratio describes the angle-dependent intensity of light scattered by a sample. As a matter of fact, the light scattering intensity is measured as voltage yielded by photodiodes:

$$R_\theta = \frac{(I_\theta - I_{\theta,solvent})r^2}{I_0 V} = f\frac{V_\theta - V_{\theta,solvent}}{V_{laser}} \tag{2.2}$$

where I_θ is the scattered light intensity of the solution; $I_{\theta,solvent}$ is the scattered light intensity of the solvent; I_0 is the intensity of the incident radiation; V is the volume of the scattering solution; r is the distance between the scattering volume and detector; $V_\theta, V_{\theta,solvent}$, and V_{laser} are detector signal voltages of the solution, solvent, and laser, respectively; and f is an instrumental constant related to the geometry of the apparatus, structure of the scattering cell, and the refractive indices of the solvent and scattering cell. The constant f is usually determined by a solvent of the well-known Rayleigh ratio. Note that dividing by the laser signal compensates for any change of laser intensity due to power supply instability and temperature fluctuations or laser aging. The subscript θ implies the angle between the scattering direction and the incident light beam ($\theta = 0^\circ$ being straightforward from the perspective of the incident light). The word *excess* means that one measures the contribution of dissolved molecules to the Rayleigh ratio of the entire solution, that is, the difference between the Rayleigh ratios of solution and pure solvent. The dimension of R_θ is length^{-1}, mostly cm^{-1}. The advantage of the Rayleigh ratio is that it is independent of the incident light intensity and the geometrical arrangement of the apparatus. *Note:* Equation 2.2 assumes a vertically polarized light source. The constant K^* is an optical constant that is defined for the vertically polarized incident light as:

$$K^* = \frac{4\pi^2 n_0^2}{\lambda_0^4 N_A}(dn/dc)^2 \tag{2.3}$$

where n_0 is the refractive index of the solvent at the incident wavelength, λ_0 is the incident radiation wavelength at vacuum, N_A is Avogadro's number, and dn/dc is the specific refractive index increment of scattering macromolecules. The second virial coefficient A_2 is related to the thermodynamic quality of solvent. Note that Equation 2.1 has further terms with the third and higher virial coefficients that can be neglected at very low concentrations. Generally, the R_θ/K^*c versus c plot is linear at the region of low concentrations with the slope directly proportional to the second virial coefficient and deviating from linearity at higher concentrations. Modern light scattering photometers are sufficiently sensitive to allow working at low concentrations where the effect of the term with the third virial coefficient is negligible.

The A_2 is a quantity that is sometimes overlooked as a result of polymer characterization by light scattering. It characterizes the intensity of interactions between the solvent and dissolved polymer. The positive values of the order of magnitude of $\geq 10^{-4}$ mol mL/g^2 are typical for so-called thermodynamically good solvents, where the polymer–solvent interactions are stronger than mutual interactions among individual polymer molecules or intramolecular interactions among different segments of a macromolecule. In other words, in thermodynamically good solvents the dissolved macromolecules prefer to interact with the solvent over interacting with themselves. In so-called *theta* solvents, the A_2 equals zero and the strength of polymer–solvent interactions is identical with that of polymer–polymer interactions.

Slightly negative values indicate the tendency of polymer to precipitate from solution, because the interactions of polymer–polymer are stronger than those of polymer–solvent, or we can say that the molecules prefer themselves to the solvent. Solutions with larger negative A_2 do not exist, because such thermodynamically poor solvents do not dissolve polymers at all. The value of A_2 depends on temperature and polymer molar mass. With the increasing temperature the A_2 increases, which explains the well-known fact that polymers dissolve more rapidly at elevated temperatures. The increasing temperature, as a matter of fact, increases the thermodynamic quality of the solvent. The molar mass dependence of A_2 is given by a simple expression:

$$A_2 = kM^{-\vartheta} \tag{2.4}$$

where k is a constant and exponent ϑ is mostly in the range of 0.15 to 0.35. For instance, using the data from reference 4 for polystyrene in THF at room temperature, the following relationship is obtained:

$$A_2 = 0.01 \times M^{-0.25}(\text{mol mL/g}^2) \tag{2.5}$$

Decreasing value of A_2 with increasing molar mass explains why polymer solubility decreases as molar mass increases. In contrast to solutions of monodisperse polymers, where only identical macromolecules interact with each other, in solutions of polydisperse polymers all different macromolecules interact with each other with the frequencies given by the molar mass distribution of a given polymer. Therefore, in the case of polydisperse samples the A_2 obtained by a light scattering experiment is an average that is not as clearly defined as the averages of molar mass and RMS radius.

For a polydisperse polymer, the total Raileigh ratio can be expressed as a sum of the particular Rayleigh ratios corresponding to scattering by each molar mass:

$$R_\theta = K^* \sum_i c_i M_i \tag{2.6}$$

which can be rearranged as

$$\frac{R_\theta}{K^* c} = \frac{\sum c_i M_i}{c} = \sum_i w_i M_i = M_w \tag{2.7}$$

where c_i and w_i are the concentration and the weight fraction of molecules with molar mass M_i, respectively. That means the Rayleight ratio of a dilute solution of a polydisperse polymer is directly proportional to the weight-average molar mass (M_w), and thus the batch light scattering measurements of polydisperse polymers yield the values of M_w.

The particle scattering function $P(\theta)$ describes the decrease of the scattered light intensity with increasing angle of observation. It is defined as the ratio of

the intensity of radiation scattered at an angle of observation θ to the intensity of radiation scattered at zero angle:

$$P(\theta) = \left(\frac{R_\theta}{R_0}\right)_{c=0} \tag{2.8}$$

The decline of light scattering intensity with increasing angle is due to intramolecular interference of light beams scattered by different points of the same particle. A small scattering particle with the maximum distance of two points of the particle below about $\lambda/20$ behaves as a point source of scattered light for which all scattered beams are in phase. In contrast, the light beams scattered by different parts of a large particle reach the photodetector phase shifted. Phase-shifted light beams interfere destructively and thus the intensity is lower than would correspond to the intensities of individual light beams. The destructive interference depends on the scattering angle, as demonstrated in Figure 2.3. At zero scattering angle, the path lengths of the scattered beams are identical and there is no destructive interference, while due to the interference of the two phase-shifted beams the intensity of the resulting radiation at an angle θ is smaller than at zero angle with decreasing trend toward higher angles. For very large colloidal particles, the particle scattering function can even show maxima and minima.

For small angles, the particle scattering function can be approximated as:

$$\lim_{\theta \to 0} P(\theta) = 1 - \frac{16\pi^2}{3\lambda^2} R^2 \sin^2(\theta/2) = 1 - \frac{\mu^2}{3} R^2 \tag{2.9}$$

where $\lambda = \lambda_o / n_o$ is the wavelength of the incident light in a given solvent, R^2 is the mean square radius, and μ is the scattering vector:

$$\mu = \frac{4\pi}{\lambda} sin(\theta/2) \tag{2.10}$$

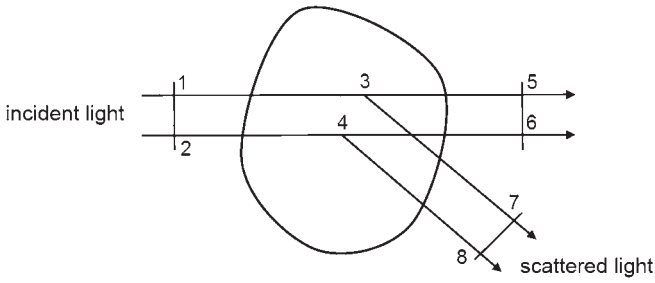

Figure 2.3 Scattering of light by a large particle. The path length 1–3–5 equals the path 2–4–6, but path 1–3–7 is longer than 2–4–8. The different path lengths of light scattered by different parts of a large particle cause reduction of scattering intensity due to intramolecular interference.

As for $x \to 0 \lim[1/(1-x)] = 1 + x$, Equation 2.9 can be for $\theta \to 0$ written as

$$\lim_{\theta \to 0} \frac{1}{P(\theta)} = 1 + \frac{16\pi^2}{3\lambda^2} R^2 \sin^2(\theta/2) = 1 + \frac{\mu^2}{3} R^2 \tag{2.11}$$

According to Equations 2.9 and 2.11, the plots of $P(\theta)$ or $P^{-1}(\theta)$ against $\sin^2(\theta/2)$ are straight lines with the slopes proportional to the R^2. This very important fact tells us that the slope of the angular variation of the scattered light intensity at angle zero yields the root mean square (RMS) radius (R). It is also worth noting that the information about the size of scattering particles can be revealed solely from the measurement of the angular variation of scattered light intensity. The RMS radius describes the distribution of mass around the center of gravity. A particle can be assumed to consist of mass elements of mass m_i and the RMS radius is defined as the square root of the weight-average of r_i^2 for all the mass elements:

$$R = \left(\frac{\sum m_i r_i^2}{\sum m_i} \right)^{1/2} \tag{2.12}$$

where r_i is the distance of the ith mass element of mass m_i from the center of gravity. In contrast to other size parameters, the RMS radius makes no assumption of particle shape. As already mentioned, the RMS radius is a quantity purely derived from the light scattering data, which can be determined even if the concentration and dn/dc of the scattering particles are unknown. Equation 2.12 is valid for a rigid particle. A random coil, which is by far the most frequent shape for synthetic and natural polymers, is a flexible structure that can create a large number of various conformations, each of them having its particular RMS radius. The quantity measurable experimentally is an average value—that is, for a non-rigid macromolecule the distance r_i is an average over all possible conformations.

The RMS radius is in simple relationships with other size parameters characteristic for various particle shapes:

For a random coil:

$$R^2 = \frac{\langle r^2 \rangle}{6} \tag{2.13}$$

For a rod:

$$R^2 = \frac{L^2}{12} \tag{2.14}$$

For a compact sphere:

$$R^2 = \frac{3D^2}{20} = \frac{3}{5} a^2 \tag{2.15}$$

For a hollow sphere (spherical shell):

$$R^2 = a^2 \tag{2.16}$$

where $\langle r^2 \rangle$, L, D, and a are the mean square end-to-end distance of random coil, rod length, sphere diameter, and sphere radius, respectively.

Equations 2.9 and 2.11 describe how the intensity of scattered light decreases with the increasing angle of observation at the region of very low angles. This angular dependence becomes more pronounced with increasing size of scattering molecules. On the other hand, small molecules with the RMS radius roughly below 10 nm scatter light with the same intensity in all scattering angles. That means no size information can be obtained from elastic light scattering measurement for small molecules. It must be emphasized at this point that the 10 nm RMS radius is not a magical borderline below which the molecules scatter with equal intensity in all directions and above which the measurement of RMS radius is feasible. The diminution of the angular dependence is gradual and the limit for which the RMS radius can be or cannot be measured depends also on the signal-to-noise ratio of the light scattering signal. Scattering intensities for small molecules that scatter evenly in all angles and for larger molecules that scatter with declining intensity are compared in Figure 2.4. Note that although the scattering intensity of larger molecules decreases with increasing angle, its absolute value is markedly larger than that of small molecules.

An important property of the RMS radius is that for polydisperse polymers the experimental value is the z-average as shown in the following: For an infinitely dilute solution of a polydisperse polymer, the intensity of scattered light is given as the sum of the contributions of particular polymer molecules:

$$R_\theta = \sum_i R_{\theta,i} = K^* \sum_i c_i M_i P_i(\theta) = K^* c M_w P(\theta)_{average} \tag{2.17}$$

where $P(\theta)_{average}$ is an average particle scattering function. The comparison of the last two terms of Equation 2.17 defines the average particle scattering function of polydisperse polymer to be the z-average:

$$\begin{aligned} P(\theta)_{average} &= \frac{\sum c_i M_i P_i(\theta)}{c M_w} = \frac{1}{M_w} \sum_i w_i M_i P_i(\theta) \\ &= \frac{1}{M_w} \int_0^\infty f_w(M) M P_M(\theta)\, dM = P_z(\theta) \end{aligned} \tag{2.18}$$

The average particle scattering function for a polydisperse polymer of known distribution function $f_w(M)$ can be derived using the particle scattering function for a given particle shape on condition that the integral in Equation 2.18 can be solved analytically.

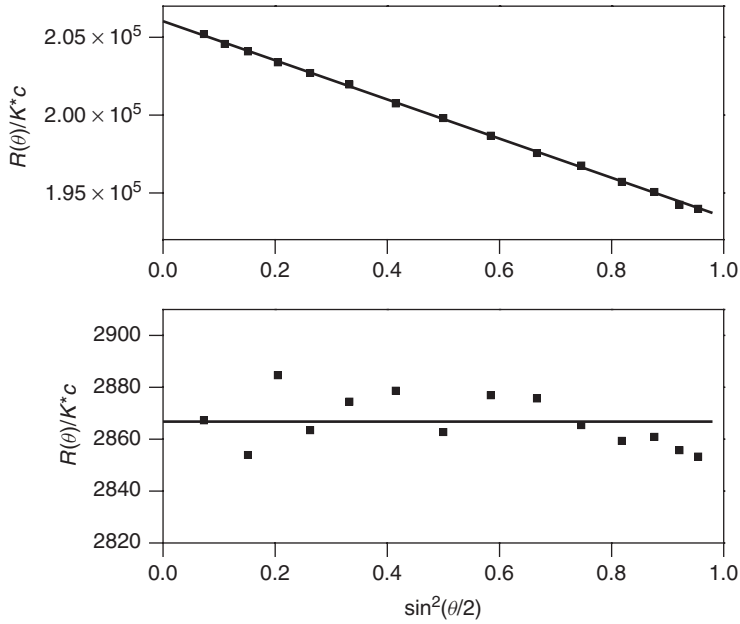

Figure 2.4 Angular variation of intensity of scattered light for polystyrene with nominal molar mass of 200,000 g/mol (top) and 2500 g/mol (bottom). Note the scattering of experimental data points for the bottom plot corresponds to the molar mass of less than 50 g/mol.

For small angles, the particle scattering function can be expressed using Equation 2.9:

$$P_z(\theta) = \frac{1}{M_w}\sum_i w_i M_i \left(1 - \frac{\mu^2}{3}R_i^2\right) = 1 - \frac{\mu^2}{3}\frac{1}{M_w}\sum_i w_i M_i R_i^2 \tag{2.19}$$

$$\frac{1}{M_w}\sum_i w_i M_i R_i^2 = R_z^2 \tag{2.20}$$

That means the initial slope of the scattered light intensity on $\sin^2(\theta/2)$ is proportional to the z-average RMS radius. The fact that light scattering yields the molar mass and the RMS radius of different moments, that is, the weight-average molar mass against the z-average RMS radius, is very important for the interpretation of the light scattering results. It was shown in Section 1.3.1.2 that the two averages are sensitive to the presence of small amounts of fractions with very high molar mass, and that this effect is more pronounced for the z-average.

The particle scattering function describes the decrease of light scattering intensity with the observation angle for large particles due to destructive interference of phase-shifted light beams and must not be confused with the angular dependence due to the use of unpolarized light. The scattering of unpolarized light can be considered as scattering of light polarized in two perpendicular directions:

vertically polarized light for which the scattering intensity is independent of angle, and horizontally polarized light for which the scattering intensity depends on scattering angle. The intensity of a wave is proportional to the square of its amplitude, but in the case of light polarized in a horizontal plane the intensity is not given by the whole amplitude, but solely by its projection to the direction of observation as illustrated in Figure 2.5. In the case of unpolarized light, the scattering intensity depends on scattering angle by the term $(1 + \cos^2\theta)$, where unity corresponds to the vertical component, which is angularly independent, and $\cos^2\theta$ reflects the angular dependence of the horizontal component. The maximum scattering intensity is at $\theta = 0^\circ$, while the minimum scattering intensity is at $\theta = 90^\circ$. The optical constant as described by Equation 2.3 is valid for vertically polarized incident light for which the angular dependence is solely due to the intramolecular interference. The measurements are typically carried out using a vertically polarized light source.

2.2.1.1 Particle Scattering Functions

The particle scattering functions were calculated for various particle shapes, such as random coils, rods, and spheres. A general form of the particle scattering function for a particle consisting of N identical scattering elements can be expressed as:[5]

$$P(\theta) = \frac{1}{N^2} \sum_i \sum_j \frac{\sin(\mu r_{ij})}{\mu r_{ij}} \tag{2.21}$$

where μ is the scattering vector expressed by Equation 2.10, and r_{ij} is the distance between the ith and jth scattering element. For small products of $\mu r_{i,j}$ (i.e., when the scattering molecule is small or the angle is low), Equation 2.21 can be approximated by Equation 2.9. From Equation 2.21 the particle scattering functions can be calculated for a specific particle shape. For linear random coils, the particle scattering function is:[6]

$$P(\theta) = \frac{2}{x^2}(e^{-x} - 1 + x) \tag{2.22}$$

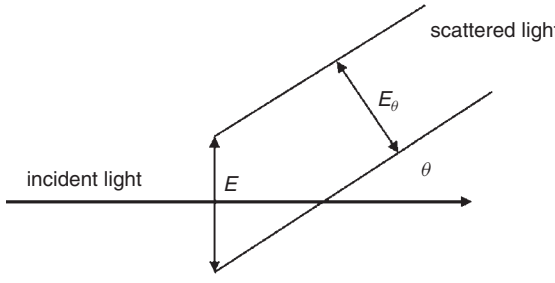

Figure 2.5 Schematic depiction of scattering of light polarized in horizontal plane (top view). E is the amplitude of scattered light, E_θ is the projection of E to the direction of observation θ : $E_\theta = E \sin\left(\frac{\pi}{2} - \theta\right) = E\cos\theta$.

where

$$x = \frac{8\pi^2}{3\lambda^2}\langle r^2\rangle \sin^2(\theta/2) \tag{2.23}$$

where λ is the wavelength of the light in a given solvent and $\langle r^2\rangle$ is the mean square end-to-end distance of the chain related to the RMS radius according to the Equation 2.13. Figure 2.6 compares particle scattering functions for linear random coils of various size calculated by means of Equations 2.22 and 2.9. It is obvious that the difference of the two particle scattering functions for relatively small molecules is negligible even for scattering angles far from zero. For large molecules, the two scattering functions overlap as the angle approaches zero. It should be noted that Equation 2.22 is valid for polymers dissolved in a theta solvent, in which the second and higher virial coefficients are zero. In thermodynamically good solvents ($A_2 > 0$), the expansion of the polymer coils affects the particle scattering function.

For homogeneous spheres, the particle scattering function is:

$$P(\theta) = \left[\frac{3}{x^3}(\sin x - x\cos x)\right]^2 \tag{2.24}$$

where

$$x = a\mu = \frac{2\pi D}{\lambda}\sin(\theta/2) \tag{2.25}$$

where μ is the scattering vector, D is the diameter, and a is the radius of the sphere. In the case of real samples, spheres can be represented by solid polymer particles prepared by emulsion polymerization, various kinds of organic and

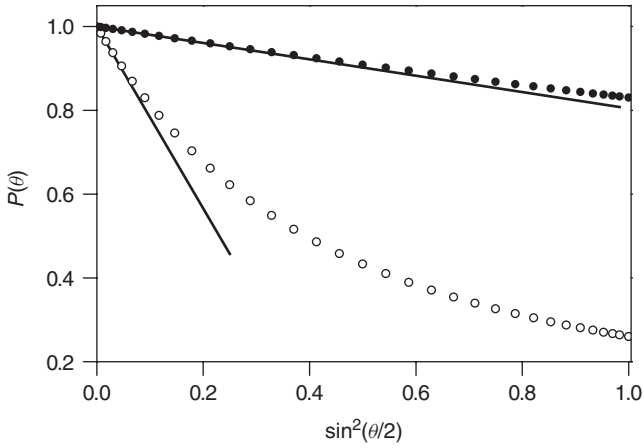

Figure 2.6 Particle scattering functions for monodisperse linear random coils of RMS radius 30 nm (•) and 100 nm (○) calculated by means of Equation 2.22. Solid lines represent approximate function represented by Equation 2.9.

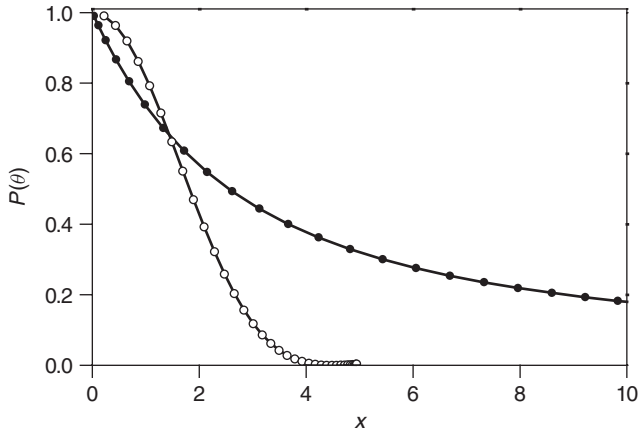

Figure 2.7 Particle scattering functions for monodisperse linear random coils (•) and homogeneous spheres (○) according to Equations 2.22 and 2.24.

inorganic nanoparticles, incompletely soluble polymer fractions (usually called *microgels*), or highly branched molecules such as stars with a high number of arms or dendritic and hyperbranched polymers. *Note:* Equations 2.22 and 2.24 are valid for monodisperse systems of given R or a.

The particle scattering functions according to Equations 2.22 and 2.24 are functions of only one variable x, which includes a dimensional parameter characteristic for a given particle shape and angle of observation. The dimension of a particle is related to the wavelength of light in a given solvent and the angular parameter is expressed as $sin(\theta/2)$. Note that the same value of x, and thus also of $P(\theta)$, can be obtained by an infinite number of combinations of dimensional and angular factors. Graphical representations of particle scattering functions for the two most common particle shapes (random coils and solid spheres) are given in Figure 2.7. Plots of $P^{-1}(\theta)$ versus $\sin^2(\theta/2)$ for random coils and solid spheres of different size are contrasted in Figure 2.8. A significant difference between the particle scattering functions of the two most common shapes can be found for large particles while for smaller particles the plots almost overlap. The RMS radius of 30 nm for linear random coils corresponds to molar mass of roughly 500,000 g/mol. Note the strong curvature of the particle scattering function for large solid spheres, which in some special cases may provide further information about the sample under analysis.

Various coordinates can be used to describe the angular variation of the scattered light intensity, for instance, $P^{-1}(\theta)$ versus μ^2R^2, $P^{-1}(\theta)$ versus $\sin^2(\theta/2)$, or $P(\theta)$ versus x. Alternatively, instead of $P^{-1}(\theta)$, the ratio K^*c/R_θ is plotted against $\sin^2(\theta/2)$. Both dependences are completely equivalent, because K^*c/R_θ is directly proportional to $P^{-1}(\theta)$ with the proportionality constant $1/M$ or $1/M_w$. The plot K^*c/R_θ or R_θ/K^*c versus $\sin^2(\theta/2)$ is usually used for simultaneous determination of molar mass from the intercept and R from the slope, while

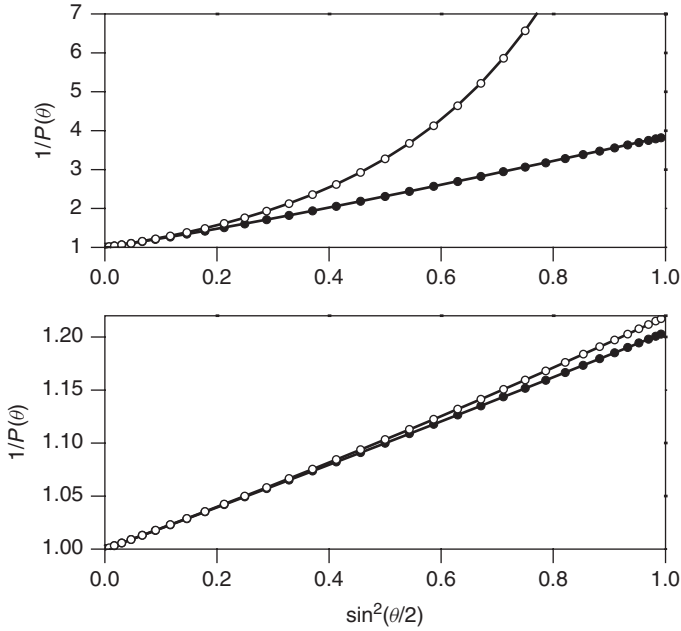

Figure 2.8 Reciprocal particle scattering function $P^{-1}(\theta)$ for monodisperse linear random coils (•) and homogeneous spheres (○) of RMS radius 100 nm (top) and 30 nm (bottom).

$P^{-1}(\theta)$ or $P(\theta)$ versus $\sin^2(\theta/2)$ can be beneficial for the comparison of angular dependences of samples of different molar mass.

Besides random coils and solid spheres, the particle scattering functions were derived for other particle shapes, such as infinitely thin rods, hollow spheres, infinitely thin discs, ellipsoids, cylinders, polydisperse coils, coils outside theta temperature, regular stars, polydisperse stars, monodisperse regular combs, and so on. A review of particle scattering functions for different particle models can be found, for example, in references 7 and 8. In principle, the comparison of an experimentally determined particle scattering function with $P(\theta)$ calculated theoretically allows the determination of particle shape. However, the practical meaning of such determination is limited due to the following reasons: The great majority of natural and synthetic polymers form random coils, and other shapes, such as rods or ellipsoids, are rare. In other words, polymer chemists mostly characterize random coils, whose diversity is given by their contraction or expansion due to polymer–solvent interactions or size reduction due to the presence of branches. However, these parameters cannot be simply inferred from the shape of particle scattering function. Another limitation of the estimation of the particle shape from the $P(\theta)$ function is given by the fact that the comparison of experimental and theoretical particle scattering functions requires a wide range of $P(\theta)$ values, which are accessible solely for very large particles. Let us consider the wavelength of 690 nm, tetrahydrofuran of $n = 1.401$, maximum angle of

observation of about 155°, and a polymer molecule of molar mass of 10^6 g/mol, which corresponds to the RMS radius of about 45 nm.

The maximum value of $x \approx 1.3$ can be calculated for this molecule. That means the experimentally accessible x values for small and mid-sized molecules are too small to get into the range where different particle shapes can be reliably distinguished from each other (see Figure 2.7). It can be concluded that information about the particle shape can be obtained only for polymers of very large molar mass (order of magnitude several millions g/mol). Moreover, the investigated polymer must be monodisperse in order to eliminate the influence of polydispersity on $P(\theta)$, because the effect of polydispersity may overwhelm the effect of particle shape. It can be concluded that the ability of classical light scattering to characterize polymer shape and conformation is limited and can be enhanced only by combination with a separation technique that reduces the effect of polydispersity and provides a relation between the RMS radius and molar mass.

The most typical shapes of the particle scattering function are as follows: (1) For small particles, with the RMS radius <10 nm, the Rayleigh ratio does not depend on the angle of observation; (2) linear or slightly curved particle scattering functions are typical for molecules with the RMS radii of several tens of nm; and (3) strongly curved particle scattering functions are characteristic of very large polymers (RMS radius >100 nm), very broad polymers, or systems containing macromolecules of a common molar mass of the order of 10^5 g/mol plus small amounts of very large particles. These large particles can be macromolecules of ultra-high molar mass, supermolecular aggregates consisting of a large number of individual macromolecules, or crosslinked swollen particles (microgels). Even a trace weight fraction of species with molar mass and molecular dimensions much larger than the rest of the molecules strongly affects the intensity and angular variation of the scattered light. This phenomenon occurs because the large macromolecules scatter light very intensely mainly at low scattering angles, due to very high molar mass, but the scattering intensity diminishes quickly with increasing angle of observation due to the very large size (i.e., intensive intramolecular interference).

On the other hand, smaller macromolecules with lower molar mass scatter light less intensely than the large molecules at low angles, but the decrease of the scattering intensity toward high angles is not that steep. That means in the case of a mixture of smaller and large macromolecules, the light scattering intensities at low angles are governed mainly by large particles, while the contribution of smaller molecules becomes more important at high angles. The superposition of angular dependencies of smaller and very large particles yields a strongly curved angular dependence as shown in Figure 2.9. As seen in this figure, the presence of solely 0.02% wt of a component with very high molar mass results in strongly curved plots regardless of the light scattering formalism used for data processing. The slopes at low angles are significantly higher than those at high angles. This is because very large macromolecules (10^7 g/mol in this particular example) contribute to scattering intensity relatively more at low angles, while

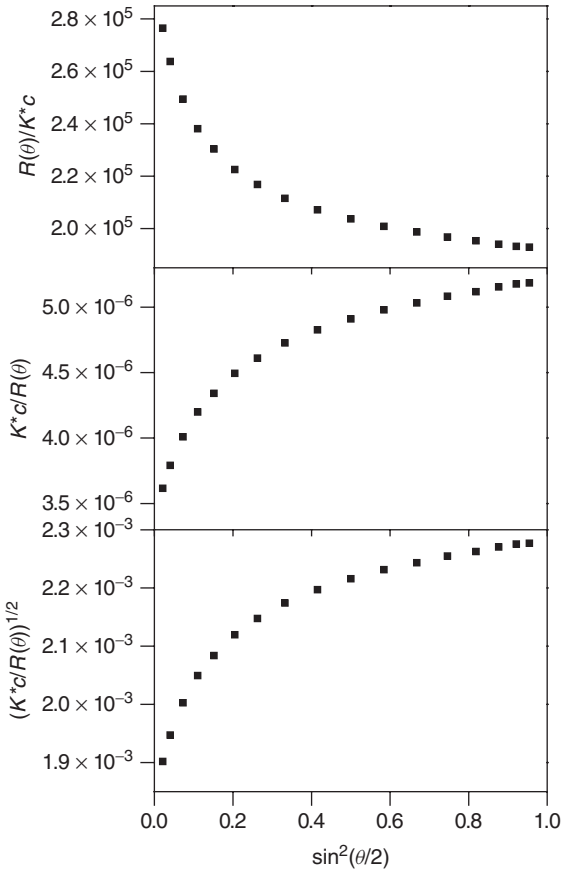

Figure 2.9 Debye plots (from top to bottom: Debye, Zimm, and Berry formalism) for a mixture of PS standards of nominal molar mass 2×10^5 and 10×10^6 g/mol prepared at concentrations of approximately 500 μg/mL and 0.1 μg/mL, respectively.

the smaller molecules (200,000 g/mol in this example) contribute more at higher angles. The data in Figure 2.9 were obtained by a model mixture, but a similar situation occurs in the case of very broad continuous distribution and the angular dependences of extremely polydisperse polymers are strongly curved. In batch measurements it may be difficult to remove the large fractions from solutions, and in fact it is often not obvious what exactly should be removed, since it may be difficult to distinguish what is still an integral part of the sample and what is dust and other impurities.

The large structures may have a strong effect on the sample properties and their identification and characterization may bring important information about the polymerization process. On the other hand, they have strong effect on the molar mass and especially on the RMS radius and their presence in solution can completely disturb the information inferred about the major polymeric part of the sample. It must be emphasized that supermolecular aggregates are often found in polymers of very high molar mass (10^6 g/mol and more), in highly

branched polymers, crystalline polymers, or stereolegular polymers capable of crystallization. The aggregates often can be destroyed by a long period of dissolution (several days, a week, or even longer) or at elevated temperatures. However, intensive mechanical agitation should be avoided because of possible shearing degradation.

The light scattering theory outlined in the preceding text is based on the Rayleigh-Gans-Debye (RGD) approximation:

$$|m - 1| \ll 1 \text{ and } 2ka|m - 1| \ll 1 \tag{2.26}$$

where a is a characteristic radius of the molecules, m is the relative refractive index of scattering molecules n/n_0, n is the refractive index of the solvated molecules, n_0 is the refractive index of the solvent, λ_0 is the vacuum wavelength of the light, $k = 2\pi n_0/\lambda_0$. Inequalities 2.26 mean that the relative refractive index of scattering particles is close to unity, that is, the particle refractive index is almost indistinguishable from that of solvent, and the total phase shift of the incident light wave is negligible.

These conditions are fulfilled for many common samples, but they will not be true for some very large, dense molecules and particles. As a matter of fact, the RGD theory is often applied to large particles where its validity is uncertain. For instance, the aqueous polymer latex (refractive index $\approx 1.6, a \approx 100$ nm), $m = 1.6/1.33 \approx 1.2$ does not exactly satisfy the RGD conditions. However, the comparison of results obtained by MALS with those determined by dynamic light scattering or electron microscopy suggests that the theory works even when RGD requirements are not strictly satisfied. It was also shown that RGD approximation becomes more valid in the limit of $\theta \to 0$.[9] Finally, the more general and more complex Mie theory, valid for spheres of any size and refractive index, can be applied to the particles that do not comply with RGD approximation.

The basic light scattering Equation 2.1 can be summarized into two fundamental light scattering principles:

1. The intensity of light scattered by a dilute polymer solution is directly proportional to the concentration and molar mass of polymer molecules.
2. The angular variation of the scattered light intensity is related to the size of scattering molecules.

These principles are important not only for proper understanding and interpretation of the experimental data, but also for planning and performing the measurements. Even trace amounts of particles with enormously high molar mass (aggregates, highly compact particles, or dust) generate very intensive light scattering signals. On the other hand, investigation of oligomers requires preparation of solutions with sufficiently high concentrations. It is sometimes not well understood that appropriate concentrations for batch light scattering measurement of dissolved polymers can vary over a very broad concentration range, such as 10^{-5} to 10^{-2} g/mL, depending only on the molar mass of the polymer under investigation. The concentration needed for the characterization of dispersed particles

can be several orders of magnitude lower compared to that needed for the measurement of macromolecular solutions.

Incipient users of light scattering sometimes ask about the detection limit of a MALS detector. The first light scattering principle explains that a MALS detector has no detection limit in the sense of minimum detectable concentration, because the response of a light scattering photometer is proportional not only to the concentration, but also to the molar mass. Each molar mass has its own detection limit and the detection limits can differ by many orders of magnitude. As a matter of fact, a MALS detector is rather used to characterize than to detect. That means the concentration of analyzed sample should be appropriate in order to get an intensive signal-to-noise ratio and thus proper characterization.

2.2.1.2 Light Scattering Formalisms

Equation 2.1 can be rearranged into the following alternative forms:[3,10]

$$\frac{K^*c}{R_\theta} = \frac{1}{MP(\theta)} + 2A_2c + \cdots \tag{2.27}$$

$$\sqrt{\frac{K^*c}{R_\theta}} = \frac{1}{\sqrt{MP(\theta)}} + A_2c\sqrt{MP(\theta)} + \cdots \tag{2.28}$$

Similarly to the case of Equation 2.1, the above equations have higher concentration terms. The particular formalisms describe the same phenomenon (i.e., the concentration and angular variation of light scattered by a polymer solution or a colloidal dispersion). Equations 2.1, 2.27, and 2.28 represent different ways of the processing of the experimental data and are usually called *Debye, Zimm*, and *Berry formalisms*, respectively.

Frequently used light scattering terminology can be sort of confusing since the term *Debye* is used for the plot of the light scattering intensity versus angle of observation at a given concentration and also for one of the possible light scattering formalisms. The light scattering intensities acquired at a single concentration can be extrapolated to zero angle, neglecting the concentration dependence. This procedure, called a *Debye plot*, can be done using Zimm, Debye, or Berry formalism. The Debye plot is always used for processing the data acquired in an online mode, but can be also applied for a batch measurement. A *Zimm plot* means processing the light scattering data that were collected at multiple angles and multiple concentrations. In contrast to the Debye plot, the concentration dependence is taken into account and the obtained data are extrapolated not only to zero angle, but also to zero concentration. This processing can be performed using Zimm, Debye, or Berry formalisms. For discussion of the influence of the light scattering formalism on the molar mass and RMS radius, see also Section 4.2.1.5.

2.2.1.3 Processing the Experimental Data

Raw data generated by a light scattering photometer are voltages yielded by photodiodes at various angles. However, the requested physical quantity is the

intensity of scattered light, which is expressed as the *Rayleigh ratio*. The conversion of voltages into Rayleigh ratios is done by means of the instrumental constant f, which in addition takes account of the scattering volume and the distance of the scattering volume from the detector. In routine practice, the constant f is determined by a standard liquid, a solution of standard polymer of known molar mass, or a dispersion of standard colloids. To convert voltage recorded by a light scattering photometer to the Rayleigh ratio, the instrument must by calibrated by a standard under identical conditions (wavelength, temperature, and geometrical arrangement of the cell).

Calibration of the light scattering photometer involves the measurement of the voltage of the standard of known Rayleigh ratio and the determination of the constant f from the measured voltage and the Rayleigh ratio. The voltages generated by a sample are then converted to the Rayleigh ratios using the constant f. It is worth mentioning that the instrumental constant f is independent of solvent that is used for the measurements of real samples, but it slightly depends on temperature. The absolute scattering power of the standard must be determined by an absolute method. The calibration by pure liquids has the advantage that the scattering power depends only on the temperature and wavelength of the incident light and there is no other compound involved. Toluene is an example of a liquid that was carefully characterized with respect to its absolute scattering power and that is easy to purify and stable at room temperature. The formerly often-used benzene cannot be recommended, due to high toxicity. 1,2,4-Trichlorobenzene, a frequently used solvent for high-temperature SEC, can be used as a standard for calibration of high-temperature MALS photometers. Calibration using solution of a polymer standard may be uncertain in the sense of absolute correctness of the molar mass of standard and the method of its determination. The M_w of standard used for the calibration of a light scattering photometer is often measured by another light scattering photometer. An even worse situation might be the case where the standard would be characterized by conventional SEC with column calibration. The calibration constant of a light scattering photometer, once properly determined, usually remains constant for several months or even years and there is no need for frequent recalibration. That is one of the advantages of light scattering. However, the calibration constant may be affected by a stray light scattered by dirt in the flow cell or caused by a misaligned laser beam. The stray light causes the calibration constant to be too small, resulting in calculated molar masses that are also too small (the percentage errors in the calibration constant and molar mass are identical).

Note that the molar masses are affected only through the calibration constant, because the stray light added to the sample measurement is included also in the baselines and thus it is eliminated during data processing. Using solvent with a high Rayleigh ratio, the possible effect of stray light is minimized and thus low-Rayleigh-ratio solvents, such as water, methanol, or THF, cannot be recommended for the calibration of MALS photometers.

Normalization is another procedure that is needed in the case of a MALS photometer. The normalization provides a set of coefficients, one for each of the

detectors placed at various angles around the cell of a MALS detector. Unlike calibration constant f, the normalization coefficients are valid for a given solvent and a change to a solvent of different refractive index requires determination of another set of normalization coefficients. The principle of normalization is explained in the following.

Assuming vertical polarization of incident light, small particles scatter with the same intensity at all angles. That means the particular photodiodes placed at various angles around the cell of a MALS photometer should yield identical voltages when the flow cell is filled with a dilute solution of a small polymer. However, in reality, the voltages are not identical for the following reasons: (1) The photodiodes are not identical and they can produce slightly different voltages for identical light intensity, and (2) the photodiodes monitor different scattering volumes. This effect is sketched in Figure 2.10, which shows that each photodiode views a different illuminated volume. The photodiodes at low and high angles look along the beam and see a larger illuminated volume, while the intermediate photodiodes look across the beam and see a smaller illuminated volume (the smallest observed volume is at 90°). Therefore, a set of normalization coefficients relating each detector to the 90° detector must be determined.

The normalization coefficient for a given angle (N_θ) becomes a part of Equation 2.2, where the right side becomes equal to $N_\theta f(V_\theta - V_{\theta,solvent})/V_{laser}$. The normalization coefficient of the 90°degree detector is always unity and only this detector is calibrated. The normalization involves measurement of a solution of a small polymer that scatters equally in all angles. The light scattering software records voltages corresponding to particular photodetectors and calculates a series of normalization coefficients. The voltages yielded by particular photodiodes become identical and equal to 90° voltage after multiplication with corresponding normalization coefficients. The obtained normalization coefficients are solvent related, because the scattered light beam is refracted when passing from solvent into the flow cell glass. Due to the refraction of scattered light passing from the solvent into the glass, the photodiode monitors light scattered at a different angle than the fixed angle at which the photodiode is placed (Figure 2.11). As a matter of fact, the refraction explains why the MALS photometers can measure at relatively small scattering angles with minimized effect of transmitted light. Polymers suitable for normalization are those with molar

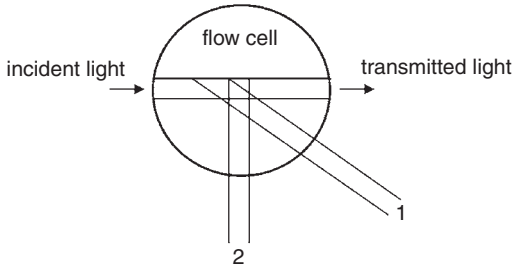

Figure 2.10 Schematic illustration of different scattering volumes monitored by two photodetectors (1, 2) placed at different positions around the flow cell (top view). The arrows indicate inlet and outlet from the flow cell. Larger scattering volume is viewed by detector 1.

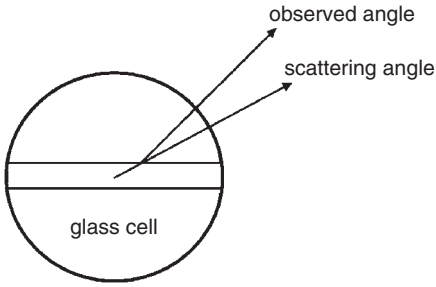

Figure 2.11 Sketch of flow cell refraction (top view).

mass high enough to scatter intensively, but small enough to scatter equally in all directions. To make the normalization more accurate the light scattering software can correct for a non–infinitely small molecular size of the polymer used for normalization using a theoretical particle scattering function and known RMS radius of the polymer. Polystyrene of molar mass 20,000–30,000 g/mol is a good example of sufficiently small polymer for organic solvents. Bovine serum albumin (BSA) or about 30,000 g/mol pullulan, dextran, or poly(ethylene glycol) can be used in aqueous solvents. The polymer used for normalization should be preferentially of narrow molar mass distribution, because fractions with very low molar mass undesirably decrease the light scattering intensity while fractions with very high molar mass do not fulfill the requirement for small, evenly scattering molecules. The requirement of narrow molar mass distribution is of primary importance in the case of batch measurements, while in the case of combination of a MALS detector with a separation technique a part of a chromatogram corresponding to small molecules can be selected for the normalization. An example of using a proper part of a chromatogram for normalization is shown in Figure 2.12 for BSA that fulfills the requirement of small molecules, but typically contains a certain amount of larger aggregates. The peaks of dimer and trimer as well as lower-intensity data points at the descending part of the peak are not used for the normalization as indicated by the two vertical lines.

Processing the light scattering data requires correction for two effects: (1) Due to the interference of light beams scattered by different mass points of a large particle, the intensity of the resulting radiation is smaller than the sum of particular intensities of light scattered by all the individual mass points of that particle. This phenomenon is called *intramolecular (intraparticle) interference of scattered light*. The decrease of the scattered light intensity due to the intramolecular interference is described by the particle scattering function. (2) In a polymer solution of a finite concentration, the light scattered by different macromolecules also interferes. This effect, which is called *intermolecular interference*, causes the intensity of light scattered by a solution to be smaller than the sum of scattered intensities by the individual macromolecules. The extent of the intermolecular interference is related to thermodynamic properties of the polymer–solvent system and is characterized by the second and higher

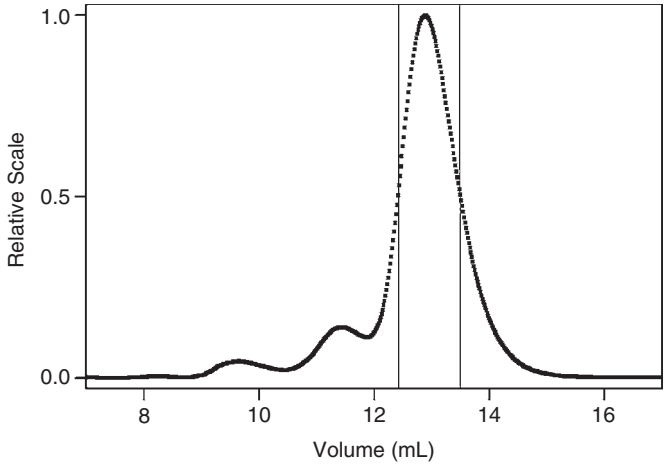

Figure 2.12 Normalization of a MALS photometer in an SEC mode using BSA. Only the data points between the vertical lines are used for normalization to avoid influence of aggregates and data points with low intensities.

virial coefficients. To process the data acquired by a light scattering experiment and to determine true characteristics of the dissolved polymer, the two non-ideality effects (the effect of terms with A_2 and higher virial coefficients and the effect of intramolecular interference) have to be eliminated.

To correct for the non-ideal solution behavior, we can neglect terms beyond the A_2 and plot K^*c/R_θ as a function of c. For low concentrations the relation is linear, giving the second virial coefficient from the slope (slope $= 2A_2$) and the weight-average molar mass from the intercept (intercept $= 1/M_w$). However, the obtained results are valid solely for small polymer molecules since the concentration extrapolation ignores the effect of intramolecular interference. To eliminate the scattered light intensity reduction due to the intramolecular interference, the light scattering experiment would have to be carried out at zero angle. However, it is impossible to measure the intensity of scattered light at zero angle, because the intensity of transmitted light is several orders of magnitude higher than that of scattered light. Instead, the light scattering intensity is measured at multiple angles and then extrapolated to zero angle, for which the particle scattering function equals unity.

The concentration and angular variation of the intensity of scattered light can be simultaneously processed using the so-called Zimm plot, which is a relation between K^*c/R_θ and $\sin^2(\theta/2) + kc$. The constant k is chosen to spread out the experimental data points and affects solely the visual appearance of the plot, but has no influence on the obtained results. Details of the processing and examples of a Zimm plot for various polymers are presented further in Section 2.7.

2.2.2 Dynamic Light Scattering

Macromolecules or colloidal particles dissolved or dispersed in solvent undergo Brownian motion. The light beams scattered at a given time by different particles are to a certain extent phase shifted and mutually interfere. The interference can be either positive or negative depending on the mutual position of the scattering particles. After a time delay the scattering particles move to another position and the intensity of light receipted by the detector is different, because the mutual position of the particles is different and the phase shift of scattered beams is different as well (see Figure 2.13). The distance among the scattering particles in solution is therefore constantly changing with time, which results in the fluctuation of the intensity of scattered light. The fluctuation of intensity reflects the motion of the scattering particles. In the case of large particles, which move slowly, the intensity fluctuates slowly too, while for small particles moving rapidly the intensity fluctuation is rapid too. That means the fluctuation of the intensity bears information about the moving particles.

The information about the moving particles is obtained by the analysis of the intensity fluctuation, which is done by transformation into the intensity autocorrelation function using a piece of hardware called a *correlator*. The time scale of the scattered light intensity fluctuations is analyzed by a mathematical process called *autocorrelation*. The autocorrelation function expresses the mutual relationship of the signal with itself (i.e., it reports how quickly on average the light intensity changes with time). The autocorrelation function expresses the probability that after time delay τ the intensity of the scattered light will be identical

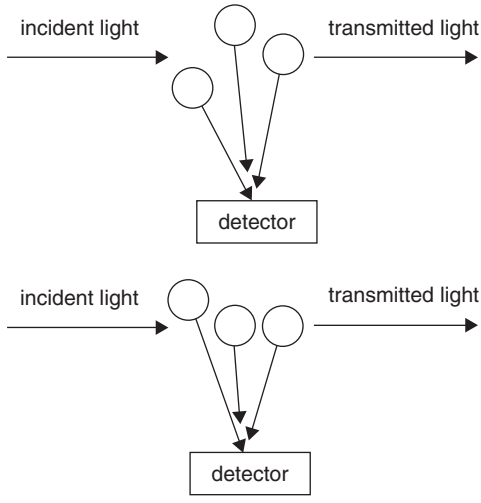

Figure 2.13 Illustration of scattering of light by particles undergoing Brownian motion. Position of particles at time t (top) and $t + \tau$ (bottom). Light beams scattered by particles at two different times travel different distances to the detector and thus their mutual phase shift is different.

to that in the initial time. At short time delays, the correlation is high because the scattering particles do not have enough time to change their mutual position to a great extent compared to the original state. The two signals are almost identical when compared after a very short time interval. With the increasing time delay, the correlation starts to exponentially decrease. After a certain time delay, there is no correlation between the scattering intensity at the initial time t and the final time $t + \tau$. Figure 2.14 shows an example of different profiles of autocorrelation functions for particles of different hydrodynamic radius. A faster decay corresponds to smaller molecules, while a slower decay indicates larger molecules. The normalized intensity autocorrelation function is defined as:

$$g(\tau) = \frac{\langle I(t)I(t+\tau)\rangle}{\langle I(t)\rangle^2} \tag{2.29}$$

where $I(t)$ is the detected intensity as a function of time t, $\langle I(t)\rangle^2$ is the average scattered intensity squared, τ is a delay time, and the brackets indicate averaging over all t. The autocorrelation function is established by multiplying the scattered intensity as a function of time with itself after shifting by a delay time τ, and the obtained products are averaged over a sufficiently long time period. The autocorrelation function is calculated for various values of τ, ranging typically from about 1 μs to several seconds, and plotted against τ (usually on a log-scale time axis).

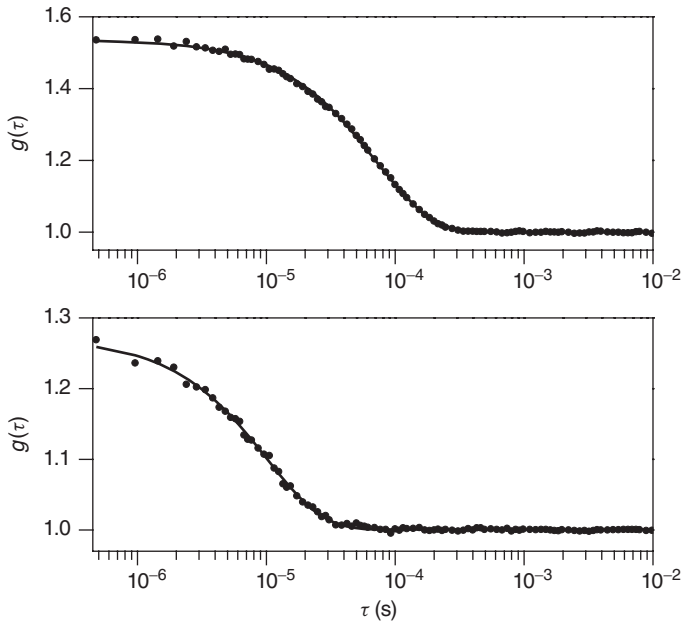

Figure 2.14 Autocorrelation function for polystyrene of $R_h = 30$ nm (top) and 4 nm (bottom). Tetrahydrofuran at ambient temperature.

For a monodisperse sample, the normalized autocorrelation function is described by an exponential function:

$$g(\tau) = 1 + \beta e^{-2D\mu^2\tau} \tag{2.30}$$

where $\mu = \frac{4\pi}{\lambda} \sin(\theta/2)$, D is the translational diffusion coefficient, β is the signal amplitude of the autocorrelation function, λ is the wavelength of light in a given solvent, and θ is the detection angle with respect to the direction of the incident beam. The analysis of the autocorrelation function allows determination of the translation diffusion coefficient of the macromolecules or particles. Using the diffusion coefficient and assuming the spherical shape of the molecules, one can calculate the hydrodynamic radius using the Stokes-Einstein relation:

$$R_h = \frac{kT}{6\pi\eta D} \tag{2.31}$$

where k is Boltzman's constant, T is the absolute temperature, and η is the solvent viscosity.

The hydrodynamic radius R_h is the radius of the so-called hydrodynamically equivalent sphere that would have the same diffusion coefficient as the molecules or particles under investigation. It must be stressed that the hydrodynamic radius is by definition a different size parameter from the RMS radius. The mutual relation of the two radii depends on the particle shape and thus the comparison of R_h and R allows, at least in principle, the estimation of particle shape. For a compact sphere, the hydrodynamic radius equals the geometric radius and can be related to the RMS radius using the following equation (compare Equation 2.15):

$$R^2 = \frac{3}{5}R_h^2 \tag{2.32}$$

It can be mentioned that there is another method for the determination of hydrodynamic radius based on the intrinsic viscosity as shown in Section 1.4.3.2. A significant advantage of R_h compared to R is that it can be measured also for small particles down to about 1 nm. On the other hand, the characterization of larger particles requires longer acquisition time, which limits the applicability of the method in the online mode, because in SEC or A4F of polydisperse samples the size of particles flowing through the flow cell changes with time. That means the autocorrelation function is not acquired for a rigorously monodisperse fraction and this effect becomes more pronounced with increasing acquisition time. If the relation between the diffusion coefficient and molar mass is known, the diffusion coefficient can be used for the estimation of molar mass. However, such calculation is meaningful only for polymers of given chemical composition under given experimental conditions (solvent, temperature) and dynamic light scattering cannot be considered to be the absolute method of molar mass determination.

The diffusion coefficient and the hydrodynamic radius can be accurately determined only for dilute solutions or dispersions, because in the case of more concentrated samples the particle mobility is influenced by interactions with

neighboring particles. However, in the case of concentrated dispersions such as those prepared by emulsion polymerization the necessity to dilute the sample may question the obtained results, because both aggregation and disaggregation can accompany the dilution.

Although dynamic light scattering represents an absolute method for the determination of hydrodynamic radius, the measurement of polydisperse systems in batch mode offers only limited possibility to characterize the size distribution. For a mixture of small and large particles, the autocorrelation function may show two decays—a faster one representing smaller particles and a slower one representing larger particles. The autocorrelation function of light scattered from a polydisperse population of particles is described by the sum of the autocorrelation functions of all particles, weighed by their normalized intensities. Information about the size distribution is obtained by the analysis of the autocorrelation function under a few assumptions.

Generally two methods are used to extract the size distribution data from the batch DLS measurement: The method of *cumulants* assumes a Gaussian distribution of diffusion rates and uses the first and second cumulant only to calculate a mean and Gaussian width of the diffusion rates. The cumulants of a distribution are closely related to distribution's moments and they are used to calculate the corresponding values of hydrodynamic radius. The *regularization* method assumes a smooth distribution of hydrodynamic radius. The software determines a number of R_h distributions that all fit the experimental data equally well, and chooses between them based on the smoothness of the distribution, favoring smooth distributions over spiked distributions. The obtained size distribution is weighted by scattered light intensity and can be converted to mass or number distribution as follows:

According to the basic light scattering equation, the scattering intensity of the ith particle (I_i) can be written in a simplified form as:

$$I_i = KM_i c_i = KM_i^2 N_i \tag{2.33}$$

where K is the proportionality constant, and M_i, c_i, and N_i are the molar mass, the concentration (g/mL), and the number concentration (particle number/mL) of scattering particles, respectively. The relation between the molar mass M and the radius a for a spherical particle is:

$$M_i = a_i^3 N_A \frac{4\pi}{3\overline{v}} \tag{2.34}$$

where N_A is Avogadro's number, $\overline{v}$ the partial specific volume (mL/g). After substitution of M_i Equation 2.33 can be rearranged into the following form:

$$I_i = K' a_i^3 c_i = K'' a_i^6 N_i \tag{2.35}$$

which relates the scattering intensity to the mass concentration or the number concentration of the ith particle. To determine the mass fraction, the intensity fraction $I_i / \sum I_i$ is divided by $R_{h,i}^3$, and to determine the number fraction, by

$R_{h,i}^6$. It is worth mentioning that different types of distribution are measured by different analytical methods and thus the type of distribution (intensity %, mass % or number %) must be taken into account when the results from different analytical techniques are compared. The mass % and number % distributions are shifted toward lower hydrodynamic radii compared to the intensity distributions. The results from the batch DLS are often expressed using a bar diagram. The number of bars and their heights can serve as an estimation of the size distribution, but they are not the true distribution—for instance, three bars do not mean a mixture of three species of distinct size.

2.3 LIGHT SCATTERING INSTRUMENTATION

A classical light scattering instrument is called *goniometer*. In the goniometer the sample is placed in a glass or quartz cell and the detector photodiode is mounted on a bearing allowing measurements of light scattering intensity at various angles. That means each scattering angle is measured separately in a sequence. Modern instruments mostly allow performing both static and dynamic light scattering experiments. The most serious disadvantage of the goniometer is the relatively long time required for a single measurement of angular intensity dependence. For this reason, goniometers cannot be used for online measurements in combination with analytical separation techniques.

Another approach offers instruments that allow simultaneous measurements of the scattered light intensity at multiple angles. Simultaneous measurement can cover the whole range of angles at once, which is a principal difference from the goniometer-based technique. Such instruments are usually called *multi-angle light scattering (MALS) detectors* or *photometers* (see scheme in Figure 2.15) and they have achieved great popularity due to their ability to perform rapid batch measurements of unfractionated samples, but more frequently they are used as online detectors for size exclusion chromatography or other separation techniques. Unlike the goniometer, where a single photodetector moves around the cell, the cell of a MALS photometer is surrounded by an array of photodiodes. Each photodiode is placed at a fixed angle, but depending on the solvent refractive index the observed angles change as shown in Figure 2.11. Alternatively, a set of optical fibers can be used to collect the scattered light and transfer it for the detection and processing. MALS photometers can measure static and dynamic light scattering simultaneously. To perform the dynamic light scattering experiment the light scattered in the flow cell is collected by an optical fiber, detected by an avalanche photodiode and analyzed by a digital correlator that measures the autocorrelation function of the intensity signal carried by the optical fiber.

A Brookhaven Instruments BI-200SM system allowing studies of both static and dynamic light scattering is an example of goniometer. A Wyatt Technology Corporation DAWN® HELEOS™ is an example of a MALS photometer with currently the highest available number (18) of photodetectors. Wyatt Technology Corporation is also the manufacturer of MALS photometers operating at eight or

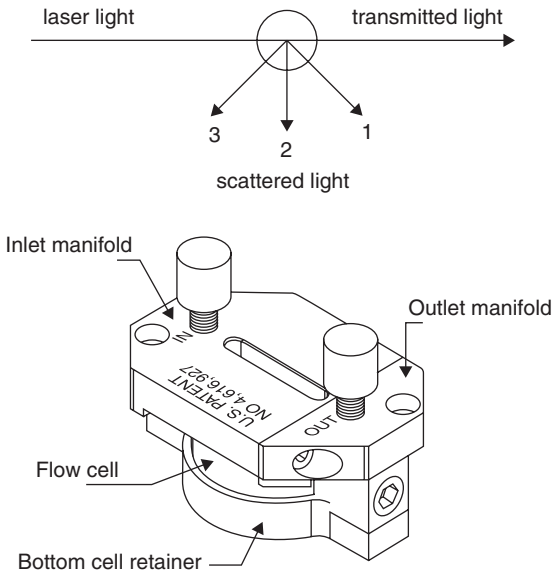

Figure 2.15 Top: Scheme of a MALS photometer. Flow cell is surrounded by photodetectors (1, 2, 3) placed at various angles. Bottom: The flow cell assembly consists of a glass cylinder with a bored channel assembled in a channel holder allowing continuous inlet and outlet flow. *Source:* Courtesy of Wyatt Technology Corporation.

three angles, namely HELEOS™ 8 and miniDAWN™ TREOS. The light scattering instrumental portfolio of this company is completed by various dynamic light scattering instruments capable of measurement in chromatography or batch mode. Brookhaven Instruments manufactures a fiber-optic seven-angle MALS photometer, BI-MwA. A two-angle light scattering photometer PD2020 with scattering angles of 15° and 90° is available from Precision Detectors (acquired by Varian). A serious disadvantage of the two-angle system is that the extrapolation using solely two angles is highly uncertain.

Single-angle photometers operating at 90° or a very low angle close to zero (e.g., 7°) are other types of light scattering instruments. The former instruments are limited to the characterization of small polymers such as proteins with negligible angular variation of the scattered light intensity. The latter instruments, often called *low-angle laser light scattering (LALLS)*, do not require extrapolation of scattered light intensity to zero angle, because the particle scattering function at a very low angle approaches unity. The LALLS approach completely ignores the particle scattering function, which can be seen as an advantage since the reduction of measurement to a single angle simplifies the processing of data compared to multi-angle detectors. However, very high sensitivity to dust particles present in solvent or shedding from SEC columns is a serious limitation of these instruments, which typically suffer from a significantly lower signal-to-noise ratio compared to the MALS photometers. In addition, the size information is completely missing, because of ignoring the angular variation of scattered light intensity, which represents a serious obstacle in branching studies.

2.4 SPECIFIC REFRACTIVE INDEX INCREMENT

The specific refractive index increment is an important parameter necessary for processing the light scattering data. The dn/dc appears in the optical constant K^*, and it is also needed to calculate the absolute concentration of polymer molecules in online experiments using MALS or viscometric detectors. The specific refractive index increment is also associated with the sensitivity of the light scattering measurement, because at a given molar mass and concentration the intensity of scattered light increases with dn/dc squared. That means the same polymer will scatter light with different intensities at different solvents. In some cases it may be necessary to change solvent to get dn/dc high enough to be able to perform light scattering measurements. According to my experience, dn/dc as low as 0.05 mL/g allows reliable measurement of polymers with molar masses down to about 1,000 g/mol. However, measurements at very low molar masses and low dn/dc require solutions of sufficiently high concentration. The optical constant K^* is proportional to the square of dn/dc and thus the error of $N\%$ in the dn/dc results in about $2N\%$ error of molar mass. Consequently, accurate dn/dc is essential for accurate determination of molar mass. This is especially valid in the case of batch measurements. In online experiments, where the dn/dc is used also for the determination of concentration, the $N\%$ error in dn/dc results in the same percentage error in molar mass, because of partial compensation (see Equations 2.1 and 2.37).

The dn/dc is a constant for a given polymer in a given solvent and depends on the wavelength and temperature. It decreases with increasing wavelength and this dependence becomes less pronounced toward higher wavelengths. The differences of dn/dc between most recently employed wavelengths of 633 nm, 658 nm, and 690 nm are negligible. The dn/dc can be defined as the slope of the dependence of refractive index of polymer solution on its concentration. The determination of dn/dc is accurate to about ± 0.001 mL/g when properly performed. Experimentally it can be measured with a differential refractometer. The measurement is relatively easy; nevertheless, several requirements must be fulfilled in order to obtain correct results. The most important requirement is purity of the polymer sample that is used for the measurement. The sample must be free of solvents, residual monomers, moisture, or other impurities. The percentage of impurities results in the same percentage error in dn/dc, and consequently the same error in molar mass from online experiment, and in double error in molar mass determined using the batch technique. If the purity of the sample is questionable, the sample should be purified by a suitable purification process such as drying or precipitation. Another requirement is that the solvent used for the preparation of polymer solutions must be identical with the solvent that is injected into the reference cell of the differential refractometer. That means the content of the impurities must be the same in the polymer solutions and the solvent used for their preparation.

Note: Absolute purity of the solvents used for the *dn/dc* determination is not an imperative and regularly a purity >99% is sufficient. The really crucial requirement is solvent identity and thus the solvent used for the preparation of polymer solutions should be from the same bottle as the solvent in the reference cell.

Great caution must be taken in the case of solvents that are chemically unstable and/or highly hygroscopic. Tetrahydrofuran (THF), which is widely used in organic SEC due to its relatively low toxicity, low viscosity, and ability to dissolve many synthetic polymers, is also a typical example of solvent vulnerable to chemical changes due to exposure to light even if it is stabilized. In addition, it is highly hygroscopic. However, the determination of *dn/dc* in THF is quite feasible using the following procedure:

1. Use volumetric flasks of the same type. However, there is no need for colored glass (i.e., regular clear laboratory glass is sufficient).
2. Take the needed volume of THF into a large flask (e.g., 250 mL). Do not degas the solvent.
3. Prepare stock solution in a 50- or 100-mL flask; use analytical balance with the precision of 0.1 mg. Fill the flask carefully to the mark. *Note:* The error in concentration of the stock solution will result in the same error of *dn/dc*, so pay close attention to this step.
4. Immediately after sample dissolution use serial dilution to prepare at least four more samples with concentration covering about one order of magnitude. Weigh the stock solution and THF rather than using the volumetric method. However, it is possible to use, for example, a 10-mL syringe to facilitate dosing the stock. The example procedure is as follows: add 1 mL of stock into a 10-mL volumetric flask, take a weight using analytical balance, fill the flask to the mark with THF, and take the total weight. The diluted concentration equals the concentration of stock solution times the weight of stock solution divided by the total weight. *Note:* Although the time between the sample preparation and the measurement should be as short as possible, some polymer samples may need several hours or even days to dissolve properly. If the solution contains insoluble impurities, filter it with about 1 μm filter (filtration can be easily done with a 10-mL syringe and a syringe filter). Be aware that a significant amount of insolubles affects the accuracy of the measurement.
5. Keep all solutions and THF in the same place with the same light conditions. Seal all the flasks properly.
6. Inject the solutions into the cell of RI detector starting and ending with pure THF. The injection can be made with a syringe pump (e.g., from Razel Scientific, the same arrangement as that used for the microbatch MALS measurements). Use different syringes for different solutions. It is possible to use disposable plastic syringes, but without a rubber tip. Since injections with the syringe pump require 5 to 10 min for each solution, it

is possible to make injections and dilutions simultaneously. Alternatively, THF and particular solutions can be injected using an HPLC pump and injector with a sample loop large enough (≈1 mL) to create flat plateaus for each concentration.

The determination should be repeated at least twice to assure accuracy of the result. It is important to emphasize that once the reliable *dn*/*dc* is obtained, its measurement need not be repeated. An example of the measurement in THF is depicted in Figure 2.16. The decent appearance of the plot proves the feasibility of the measurement in THF. *Note:* The determination of *dn*/*dc* in water and aqueous salt solutions is typically easier than measurements in THF.

An alternative determination of *dn*/*dc* can be performed in an online mode when the sample is injected into the SEC columns and the *dn*/*dc* is calculated

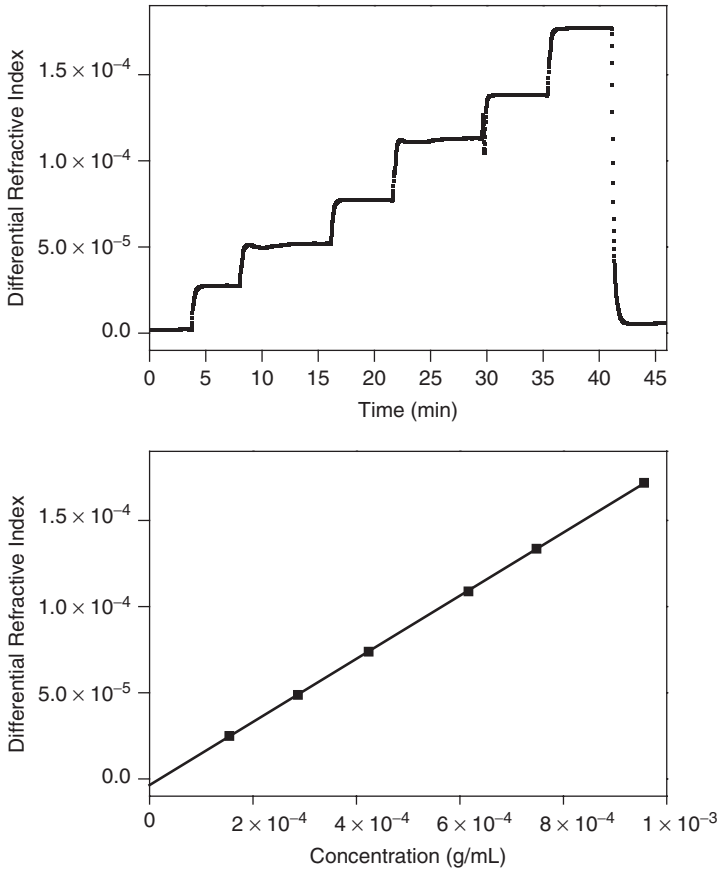

Figure 2.16 Determination of *dn*/*dc* of polystyrene in THF at 633 nm and 25°C. Plots of differential refractive index versus time (top) and differential refractive index versus concentration (bottom): $dn/dc = 0.183 \pm 0.001$ mL/g; RI detector calibrated by means of NaCl aqueous solutions using $dn/dc = 0.174$ mL/g.

from the injected mass and the response of an RI detector. In this case, the determination of *dn*/*dc* and sample characterization with respect to the molar mass and size distribution can be done simultaneously within one analysis. However, it can be recommended to focus first on the determination of *dn*/*dc*. Besides the requirement of sample purity the sample must elute from SEC columns with 100% mass recovery. Although this requirement is fulfilled for many polymers, adsorption of a part of sample in the columns may be a source of significant error. Therefore, multiple injections shall provide identical results and deviations larger than ±0.002 mL/g may indicate adsorption issue. In the online mode, the accuracy of the *dn*/*dc* measurement is also affected by the accuracy of the injection device, because the injected mass is calculated from the sample concentration and the injected volume. It can be noted that some manual injectors add about 10 μL volume to the sample loop volume. Since typical injection volume in SEC is 100 μL, 10% erroneous *dn*/*dc* are determined using such injectors. Therefore, the injection of samples with an autosampler should be preferred. The accuracy of the injected volume by an autosampler can be easily checked by mass difference after multiple injections of a specified volume (e.g., 5 × 100 μL injection of pure water in several-minute time intervals). The *dn*/*dc* from SEC data can be calculated using an appropriate template of light scattering software (e.g., Wyatt Technology Corporation ASTRA® V offers such calculation), and it can be also rapidly determined by the following procedure:

1. Inject known volume of exactly known concentration into SEC columns (e.g., 100 μL of 0.2% w/v solution, which yields 0.2 mg total injected mass). Enter apparent *dn*/*dc* of 0.1 mL/g into the light scattering software.
2. Compare injected mass (calculated from the sample concentration and injected volume, i.e., 0.2 mg in our example) with the mass calculated using the apparent *dn*/*dc* of 0.1 mL/g.
3. Calculate sample $dn/dc = 0.1 \times$ (calculated mass)/(injected mass).

Although the offline method of injecting solutions directly into the cell of an RI detector may be considered more accurate, it must be stressed that both procedures yield identical results. This fact is illustrated in Table 2.1, which lists *dn*/*dc* of three polysiloxanes of different composition determined by online and offline methods.

The determination of *dn*/*dc* in multicomponent solvents (solvent blends or salt solutions) requires dialysis of solution against the solvent. The dialysis results in the osmotic equilibrium and thus even distribution of low-molar-mass components between the solution and solvent. The dialysis may be of particular importance in the case of polyelectrolytes that are mostly measured in aqueous salt solutions to suppress the electrostatic repulsive forces. The aqueous salt solutions are mixed solvents and thus the dialysis becomes a necessary step in the accurate determination of *dn*/*dc*. The need for dialysis is given by the selective sorption of one of the components of a multicomponent solvent. A dilute polymer solution is in fact a two-phase system, one phase being the polymer

Table 2.1 Comparison of *dn*/*dc* of Polysiloxanes in THF Determined in SEC Mode Assuming 100% Mass Recovery and Using Optilab® RI Detector in Offline Mode

	dn/*dc* (mL/g)	
Sample	100% Mass Recovery	Offline Mode
1	0.050 0.049	0.0495 ± 0.0006
2	0.153 0.154	0.1533 ± 0.0004
3	0.061 0.062	0.0616 ± 0.0005

coils (i.e., the polymer domains highly swollen with the solvent), and the second phase being the bulk solvent occupying the space among polymer coils. In the case of two-component (multicomponent) solvents, the ratio of the two solvents is generally different in each phase, because of different thermodynamic quality of the particular components with regard to a polymer. The solvent that is thermodynamically better for a given polymer is preferentially solvated in the polymer domains and thus the solvent phase becomes enriched with the thermodynamically poorer solvent, which means the polymer is in fact dissolved in a different solvent than that used for sample preparation. Consequently, the differential refractive index measurement of the solution against the mixed solvent of the original composition yields incorrect *dn*/*dc*.

The compositional difference between the solvent in the polymer domains and the solvent in the surrounding space increases as the polymer concentration increases, because more thermodynamically better solvent is sorbed by polymer coils. To reestablish the original composition of the solvent outside the polymer domains, the polymer solution and the mixed solvent must be brought into contact through a semipermeable membrane. The necessary condition is that the volume of solution is finite while the volume of solvent is infinite. The driving force of the solvent transport is the concentration gradient. When the equilibrium is reached, the solvent in the polymer coils is still enriched with the thermodynamically better component, but the composition of the bulk solvent among the polymer molecules is identical with that used for sample preparation. Since the volume of pure solvent used for the dialysis is infinite, or in practice significantly larger than the volume of solution, the redistribution of molecules does not affect the solvent composition.

Dialysis can be performed using a dialysis cassette (e.g., Pierce) or seamless dialysis tubing (e.g., Sigma), which allow dialysis of polymer solution in mixed solvent against significantly larger volume of pure mixed solvent in a suitable vessel. Dialysis eliminates the change of the bulk solvent composition caused by the preferential sorption. In the absence of selective sorption, the dialysis is not necessary because the overall composition of the solvent in solution is

not changed. Dialysis is also not needed in SEC, because the equilibrium is achieved during the elution of sample through SEC columns. That means the *dn*/*dc* determined in the online mode is equivalent to the *dn*/*dc* value measured in the offline mode with the dialysis step.

Note that the preferential sorption affects also the light scattering intensity, because the polymer–solvent complex with selectively sorbed solvent molecules has different *dn*/*dc* than the polymer itself. In mixed solvents, the intensity of scattered light is given by the *dn*/*dc* of the complex polymer–solvent, whereas the intensity corresponding to the *dn*/*dc* of the polymer alone is needed in order to get true molar mass. That means the light scattering measurement of a polymer in a multicomponent solvent yields an apparent molar mass instead of the true molar mass. The ratio of the correct molar mass (determined by the measurement in a single component solvent) to the apparent molar mass (determined in the mixed solvent) can provide a certain measure of the preferential sorption.

For polymer blends and copolymers, the average *dn*/*dc* can be calculated from the *dn*/*dc* values of particular homopolymers and the composition:

$$dn/dc = (dn/dc)_A w_A + (dn/dc)_B w_B \tag{2.36}$$

where w is the weight fraction of homopolymers in the blend or monomers in the copolymer.

In the case of heterogeneous copolymers, the *dn*/*dc* according to Equation 2.36 is correct only for polymer molecules having the average chemical composition. Other molecules of the chemical composition different from the bulk composition have *dn*/*dc* corresponding to their actual chemical composition. Note that the solution of a chemically heterogeneous copolymer scatters light even if the average *dn*/*dc* is zero, because due to the polydispersity of chemical composition most of the molecules have non-zero *dn*/*dc*. In contrast to homopolymers, the intensity of light scattered by the solution of a chemically heterogeneous copolymer depends not only on the molar mass, but also on the distribution of chemical composition. That means the molar mass of heterogeneous copolymer determined by the light scattering measurement is generally incorrect, and only an apparent value is obtained. On the other hand, the measurements of molar mass in several solvents of different refractive index can provide correct molar mass and two parameters characteristic of the chemical heterogeneity.[11]

Selected *dn*/*dc* values for various polymers are listed in Table 2.2. In general, the *dn*/*dc* depends on both the polymer composition and solvent. It increases with decreasing refractive index of solvent. If reliable *dn*/*dc* cannot be found in the literature or determined experimentally, it can be estimated from the value in one solvent and difference of the refractive indices of given solvent and the solvent for which the *dn*/*dc* is to be estimated. Let us illustrate the procedure for polystyrene and tetrahydrofuran and toluene: *dn*/*dc* of polystyrene in THF at 633 nm is 0.185 mL/g, $n_{\text{THF}} = 1.401$, $n_{\text{toluene}} = 1.488$, and estimated *dn*/*dc* of polystyrene in toluene $= 0.185 - (1.488 - 1.401) = 0.098$ mL/g is close to the real value of 0.105 mL/g. A review of *dn*/*dc* for different polymers and solvents can be found in references 12 and 13.

Table 2.2 Selected *dn*/*dc* Values (Room Temperature, 633–690 nm)

Polymer	Solvent	*dn*/*dc* (mL/g)
Polystyrene	THF	0.185
Polystyrene	Toluene	0.105
Polystyrene	$TCB^{135^\circ C}$	0.047
Poly(methyl acrylate)	THF	0.068
Poly(methyl methacrylate)	THF	0.084
Poly(butyl acrylate)	THF	0.064
Poly(butyl methacrylate)	THF	0.076
Poly(isobutyl methacrylate)	THF	0.075
Poly(cyclohexyl acrylate)	THF	0.095
Poly(benzyl acrylate)	THF	0.138
Poly(benzyl methacrylate)	THF	0.144
Poly(lauryl methacrylate)	THF	0.079
Poly(methoxyethyl methacrylate)	THF	0.077
Polyisoprene	THF	0.127
Polybutadiene	THF	0.130
Polyisobutylene	THF	0.112
Polyvinylacetate	THF	0.059
Polyethylene	$TCB^{135^\circ C}$	−0.104
Poly(*1*-hexene)	THF	0.076
Polycarbonate	THF	0.186
Bisphenol A epoxy resin	THF	0.183 ($M_w > 9000$ g/mol)
		0.178 ($M_w \approx 3000$ g/mol)
Phenol-formaldehyde novolac	THF	0.220
Poly(phenyl acetylene)	THF	0.286
Poly(DL-lactic acid)	THF	0.049
Polybutandiol	THF	0.069
Poly(ethylene glycol)	Water	0.135
Bovine serum albumin (BSA)	Water, aqueous buffers	0.185
Dextran	Water, aqueous buffers	0.145
Pullulan	Water, aqueous buffers	0.145
Hyaluronic acid sodium salt	Water, aqueous buffers	0.155

In the case of lack of literature and experimental data, the *dn*/*dc* can be estimated from the value for a polymer of similar chemical composition and the difference in chemical composition between the reference and polymer under investigation. General rules are as follows: The aromatic segments in the polymer chain increase *dn*/*dc* while long aliphatic chains have the opposite effect, double bonds slightly increase the *dn*/*dc*, but the effect is moderate compared to aromatic rings. Probably the maximum value of *dn*/*dc* in THF of 0.286 mL/g was reported for poly(phenyl acetylene),[14] which is due to the highly aromatic structure and

double bonds in the polymer chain. On the other hand, aliphatic polymers with no double bonds and no aromatic rings have *dn*/*dc* several times lower. The *dn*/*dc* depends on the polymer chemical composition, but slight changes of chemical composition typically have minor effects on *dn*/*dc*. In the range of low molar masses, the *dn*/*dc* increases with increasing molar mass. However, from molar masses of several thousands the *dn*/*dc* becomes constant and the molar mass dependence of *dn*/*dc* can be safely neglected. The *dn*/*dc* of a polymer in certain solvents can be close to zero (e.g., polydimethyl siloxane in THF). Also negative values of *dn*/*dc* are possible (e.g., polyethylene in TCB). The negative *dn*/*dc* has no impact on the light scattering signal, but the RI peak appears negative and requires changing the RI detector polarity.

2.5 LIGHT SCATTERING IN BATCH AND CHROMATOGRAPHY MODE

There are two types of light scattering experiments: *batch* measurement and *chromatography* (online) measurement. In the batch mode, the MALS detector is used as a standalone instrument to characterize an unfractionated polymer sample. The advantage of the batch mode is that it can eliminate possible problems arising from chromatographic separations (e.g., interactions of sample with column packing or shearing degradation of large molecules in SEC columns). It is also possible to work in solvents that may be difficult for chromatography, such as dimethylsulfoxide or concentrated acids. Batch mode is also suitable for solvent studies, because in the SEC mode it takes a relatively long time to switch from one solvent to another. However, substantially more information is typically obtained when the MALS detector is connected to a separation system (mostly SEC, but other types of chromatography or field flow fractionation are applicable as well) and used as an online detector having the capability of determining the molar mass and RMS radius distributions. A significant advantage of the MALS detectors over goniometers is that they allow easy switching from batch to chromatography mode and vice versa, while goniometers can be used for batch measurements only.

A typical example of the batch measurement is shown in Figure 2.17. For the sake of simplicity, Figure 2.17 shows only the signal recorded by a photodiode at position 90°, but signals of light scattered at other angles were recorded simultaneously as well. The sample was prepared at multiple concentrations covering about one order of magnitude. The sample preparation can be done by the serial dilutions of a stock solution or by the separate preparations of each concentration. The procedure is similar to that used for the determination of *dn*/*dc*, but the small difference of composition of solvent used for sample preparation and solvent injected for the determination of solvent offset does not affect the obtained results.

The sample solutions can be injected directly into the flow cell of the MALS detector or they can be measured in scintillation vials. To distinguish

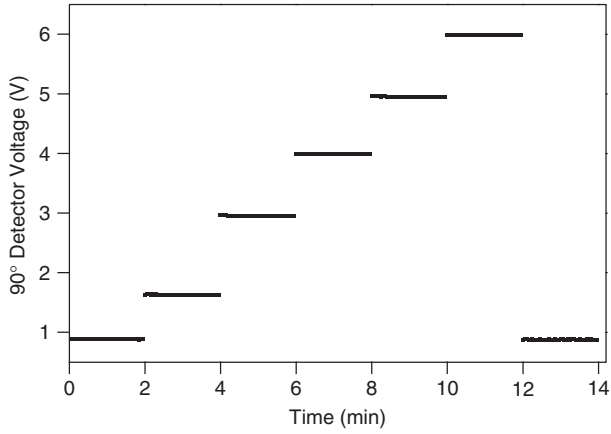

Figure 2.17 Detector voltages for 90° photodiode obtained by microbatch measurement of polystyrene NIST SRM 706. For corresponding Zimm plot, see Figure 2.21. Sample concentrations: 5.152e-5, 1.450e-4, 2.207e-4, 2.938e-4, 3.760e-4 g/mL.

the two types of measurements, the former is usually called a microbatch, the latter a batch. Both experiments have specific advantages and disadvantages. The scintillation vials are easy to use and they are well suitable for long-term time-dependent experiments. In the period between the two measurements the sample can be stored directly in the scintillation vials under requested conditions and re-measured.

Another advantage of the scintillation vials is that they are cheap and disposable and therefore especially suitable for samples that have a tendency to deposit in the flow cell (e.g., some proteins or nanoparticles). A microcuvette may become an option for samples available only in small quantities. The microbatch experiment takes full advantage of the perfect optical quality of the flow cell and thus more consistent Zimm plots are usually obtained. A syringe pump and single-use syringes with attached filters represents the most efficient way of sample injection in the microbatch mode. A typical example of a syringe pump setup is shown in Figure 2.18. An alternative method of measurement of a Zimm plot in the microbatch mode uses an HPLC pump and sample injections with a large sample loop.

Another rarely used method employs a binary HPLC pump connected to two solvent reservoirs. One reservoir is filled with a sample solution of exactly known concentration and the second reservoir is filled with a solvent. The pump gradient is programmed stepwise to generate different sample concentrations by mixing solvent and sample solution in different ratios, typically from 100% solvent to 100% sample solution. A sample and solvent filtration must be performed by an inline filter connected before the MALS detector inlet.

The batch or microbatch experiment provides three important quantities: M_w, R_z, and A_2. The molar masses and RMS radii measured in chromatography

Figure 2.18 Photograph of a syringe pump with a syringe attached to a membrane filter and a luer adaptor. Connection to a detector inlet is with finger-tight PEEK fittings and PEEK tubing.

and batch mode are typically well comparable. In principle, it is also possible to measure the A_2 in chromatography mode, but the upper concentration range in the SEC-MALS experiment is limited regarding the possible overloading effect of columns, whereas at very low concentrations the effect of A_2 is negligible. Thus significantly more reliable values of A_2 are determined using a traditional batch arrangement.

It is of ultimate importance to realize that any light scattering experiment can be completely discarded by submicrometer dust particles scattering more intensely than the polymer molecules themselves. The clarification of polymer solutions is therefore of primary importance for successful batch/microbatch measurements. The clarification includes either centrifugation or filtration. Filtration using a disposable syringe filter unit is an easy and fast way of clarification with mostly satisfactory results. Several companies manufacture membrane filters (e.g., Millipore, Whatman) that are available in various membrane materials and pore sizes. The available pore sizes include 0.02 μm, 0.1 μm, 0.2 μm, 0.45 μm, 1 μm, and 5 μm.

The signal noise decreases with decreasing pore size of the filter used for sample clarification and thus the pore size of the filter should be as low as possible for a given sample. However, a polymer sample can contain a fraction of molecules or supermolecular structures that can be removed by filtration when a too-small filter size is used.

Special attention must be paid to the filtration of highly polydisperse polymers containing molar masses spanning several orders of magnitude. The fractions of very high molar mass can be completely removed from solution by filtration, which has significant effect on the obtained molar mass and especially

on the RMS radius. Filters of 0.45 μm pore size usually work well for samples containing molecules up to molar mass of order of magnitude 10^7 g/mol. *Note:* For typical random coils in thermodynamically good solvents, the RMS radius of the molar mass of 10^7 g/mol is about 170 nm. Filters of pore size 1 μm or even 5 μm should be used for polymers that are expected to contain fractions with molar masses up to order of magnitude several tens or even hundreds of millions g/mol. The previous numbers represent only rough guidelines and for unknown samples that are suspected to contain ultra-high-molar-mass fractions test measurements using filters of various pore size should be performed.

The upper limit of molar mass for which a given filter pore size can be safely used for sample clarification depends also on the thermodynamic quality of solvent, because polymer molecules are more expanded and thus larger in thermodynamically good solvents. That means the same macromolecules can be removed when filtered in a thermodynamically good solvent and may pass using the same filter in a thermodynamically poor solvent. Sample filtration is usually performed using a disposable syringe attached to a disposable filter unit.

Clogging of the filter and increased syringe backpressure are obvious evidence of removing a part of sample. Besides removing a part of sample due to the presence of particles larger than filter size, sample adsorption to a filter membrane can occur. The change of concentration due to the adsorption on filter membrane has a strongly negative effect in the case of batch experiments, while in the online experiments the actual concentration of eluting molecules is measured with a concentration-sensitive detector. In the case of adsorption, using different filter material or conditioning the filter with several mL of sample solution before collecting the sample solution for measurement can eliminate this effect. An important recommendation for batch experiments is discarding the first few drops of the sample solution because of possible elution of dust particles from the filter itself during the early stage of filtration. Another aspect to consider is that during hand filtration with a syringe a relatively high pressure may occur, which can result in shearing degradation of large molecules during their passage through the filter membrane.

The sample clarification procedure is quite different in the case of online SEC experiments. As a matter of fact, the filtration of polymer solutions is carried out only to protect the columns from mechanical impurities that may be present in samples. The columns themselves function as very efficient filters that clarify the injected sample before it reaches the cell of the light scattering detector. However, the SEC columns are not only filters, but a potential source of dust particles as well. The dust particles eluting from SEC columns have two sources. They are residues from the manufacturing process or particles that were filtered out from the mobile phase during the previous measurements.

Especially new columns bleed submicrometer particles. The bleeding effect can diminish almost completely after several days of continuous flushing, but it usually appears again when the columns are exposed to a flow rate change. The source of particles from the column structure can be eliminated by innovative techniques yielding packing materials that exhibit very low particle shedding.

SEC columns specifically designed for use with light scattering detectors are available, for example, from Polymer Laboratories, part of Varian (PLgel LS), or Wyatt Technology Corporation (Wyatt MALS columns).

Since excessive baseline noise arising from small particles in the eluent can significantly deteriorate the quality of the light scattering data it is imperative to flush the columns properly before measurements. Usually the SEC columns must be flushed for several hours or even several days before the measurement can be performed in order to completely minimize the noise generated by particles. An important requirement is flushing the columns at a constant flow rate that is used for real measurements. Some experimentalists have a tendency to reduce the flow rate or even completely stop the pump when the SEC-MALS setup is not in use. However, it must be stressed that any change of the flow rate creates a pressure pulse that may release particles from columns and it may take again several hours to achieve a stable MALS signal. It is not widely known that when the pump is stopped the created pressure drop releases particles from the column that reach the MALS detector. If left for a long period of time the particles may adhere to the flow cell walls and may not be flushed out when the flow is switched on again. Therefore, for the sake of keeping the flow cell clean, it is highly recommended to disconnect the MALS photometer before switching off the pump, and when the pump is started again to bypass the MALS for at least several hours to flush the columns first. After several hours of flushing, the column outlet should be connected to the MALS detector inlet without stopping the pump. The use of PEEK finger-tight fittings can facilitate the connections of a column outlet and a MALS detector inlet. It may be noted that finger-tight PEEK fittings work well also with stainless-steel tubings.

In connection with the spurious effect of dust particles in chromatography eluent it is necessary to emphasize the importance of perfect cleanliness of the flow cell of a MALS detector. Bright red light spots visible in the flow cell are a clear indication of the particles trapped in the flow cell. Also increase of the solvent background voltage indicates that there is an additional source of scattered light in the flow cell. However, a slight increase of the light scattering intensity during the day can be due to the warmup of the light scattering instrument or due to the change of laboratory temperature. A rigorous test of the flow cell can be easily performed in the chromatography mode by measurement of a small polymer. It can be the same polymer as used for the normalization and both normalization and test of the flow cell cleanliness can be performed from one data file. The principle of the test is that a small polymer scatters light with equal intensities in all directions and thus, assuming proper normalization, all chromatograms recorded by particular photodetectors are identical. That means, viewing the chromatograms in a three-dimensional plot with rotation and elevation angles set to 0°, all signals from particular photodetectors should superimpose on each other and appear as a single chromatogram. Any stray light in the flow cell causes the signals at different angles to not perfectly overlay on either the leading or trailing edge of a peak. The procedure is illustrated in Figure 2.19,

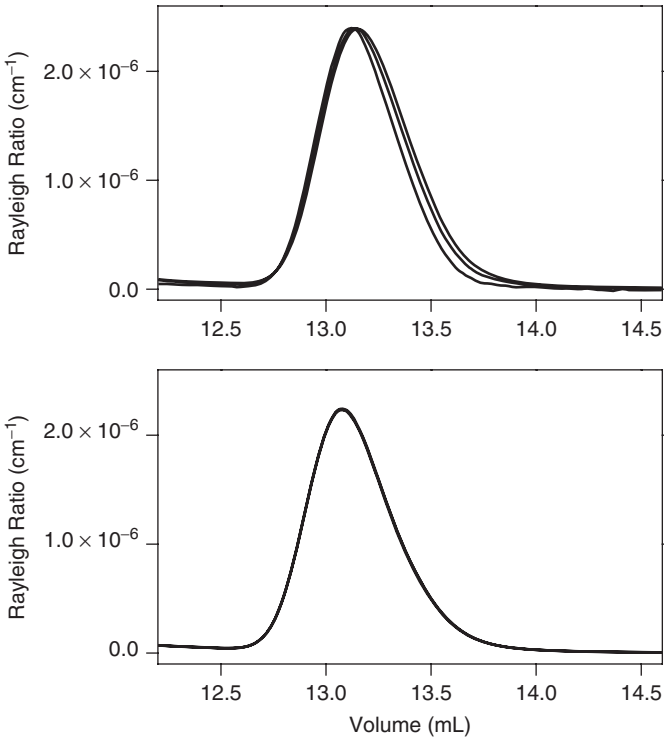

Figure 2.19 Detecting stray light in the flow cell of a MALS detector: three-dimensional plot of MALS chromatograms recorded at 45°, 90°, and 135° viewed with rotation and elevation angles set to 0°. Top: Symptoms of stray light in the flow cell. Bottom: Perfect overlay of all three signals proves clean flow cell. Sample: narrow polystyrene standard of $M = 30{,}000$ g/mol.

and since it is very beneficial, every light scattering software should offer this kind of test (available in ASTRA® software of Wyatt Technology Corporation).

The negative effect of particles shedding from the SEC columns is illustrated in Figure 2.20, which compares signals corresponding to a clean filtered aqueous buffer injected into the flow cell with a syringe filter and the same buffer eluting from an SEC column. The buffer was pre-filtered with a 0.2-μm filter and online filtered using a 0.1-μm filter, which means the noise can be attributed mostly to the particles generated from the columns. Note that the particles eluting from the SEC column not only increase the signal noise but also markedly increase the absolute signal offset.

Pre-filtration of SEC solvents and connection of an inline filter between the HPLC pump and injector may significantly reduce the level of particles in the mobile phase. Pre-filtration is especially important in the case of aqueous solvents containing inorganic salts, because the salts are typically a significant source of dust particles. In addition, highly polar water is a great absorber of dust. On the other hand, the pre-filtration of organic solvents such as THF or

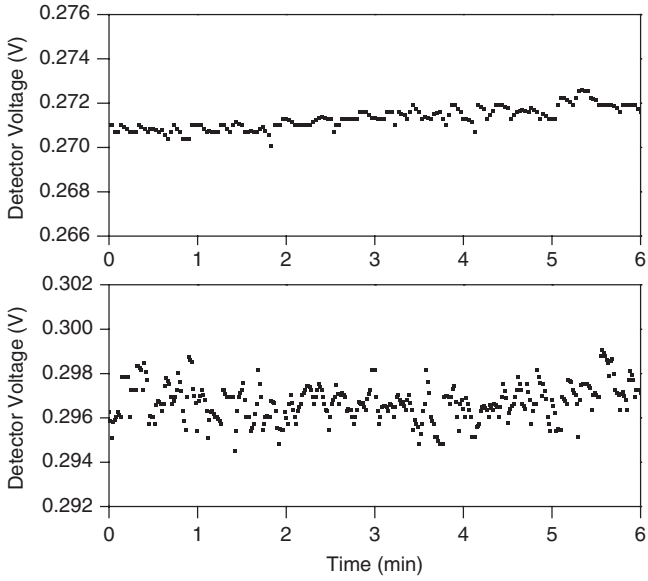

Figure 2.20 Effect of particles bleeding from SEC column on the MALS detector signal. MALS 90° signal corresponding to solvent filtered with 0.02 μm filter (top) and to solvent eluting from SEC column (bottom). The continuous bleeding of particles from column increases not only the noise level, but also the baseline voltage.

toluene is not necessary with the exception of organic solvents containing salts (e.g., dimethylformamide with LiBr). Generally, from the viewpoint of dust it is easier to work with organic solvents than with water and aqueous salt solutions. It is also necessary to stress that the electronic noise generated by a modern light scattering detector itself is significantly below the noise level generated by the chromatography system.

It must be pointed out that the filtering effect of columns can also remove a part of ultra-high-molar-mass fractions from the analyzed sample and thus significantly affect the obtained results. Crosschecks with batch measurement or the use of field flow fractionation can reveal a column filtration effect and/or shearing degradation. Another recommendation is that samples that may contain fractions with very high molar mass should be characterized with SEC columns packed with larger particles (10 μm or 20 μm instead of 5 μm) in order to minimize shearing degradation.

2.6 PARAMETERS AFFECTING ACCURACY OF MOLAR MASS DETERMINED BY LIGHT SCATTERING

Equations 2.1, 2.27, and 2.28 relate the molar mass and the intensity of light scattered by a polymer solution. They were rigorously derived and from this viewpoint the light scattering is undoubtedly an absolute method of molar mass

determination, absolute in the sense that the molar mass is directly related to a measurable physical quantity. However, the method is as absolute as absolute constants and other parameters are used for the calculation. The following three quantities influence the absolute accuracy of the light scattering experiment: (1) the instrumental constant f, (2) the specific refractive index increment dn/dc, and (3) the concentration of polymer molecules in solution.

The instrumental constant f is related to the method employed for the calibration of a light scattering instrument. As already mentioned, light scattering instruments are often calibrated with toluene and thus the accuracy of the Rayleigh ratio of toluene is in direct relation to the accuracy of the molar mass. The Rayleigh ratio of 1.404×10^{-5} cm^{-1} at wavelength 633 nm and 25°C is used by Wyatt Technology Corporation software ASTRA. The origin of this number is reference 15. According my experience, this value provides reliable molar masses well comparable with other methods of molar mass determination. A very similar value of toluene Rayleigh ratio of 1.39×10^{-5} cm^{-1} (633 nm, 20°C) is given in Huglin's monograph.[11] The Rayleigh ratios of toluene for other recently used wavelengths 690 nm and 658 nm are 9.780×10^{-6} cm^{-1} and 1.193×10^{-5} cm^{-1}, respectively.

For batch experiments, polymer solutions can be prepared at highly accurate concentrations using analytical balance. However, the impurities present in polymer such as residual monomers, solvents, or moisture result in incorrect concentrations. Another crucial requirement for the preparation of sample solutions is 100% solubility of a polymer sample. It must be stressed that polymers generally dissolve slowly and it usually takes several hours for polymer to dissolve completely. Fractions with very high molar mass may require even several days. Solutions containing a measurable level of incompletely dissolved supermolecular structures even after a week in solution are not exceptional. The dissolution can be promoted by elevated temperature, but intensive shaking or sonication cannot be recommended due to possible degradation of large polymer chains by shearing forces. Even in the case of thermodynamically good solvents industrial polymers can contain insoluble fractions created by various side reactions.

In the case of online experiments the situation is quite different. The exact concentration of injected polymer need not be known, because it is calculated from the response of a concentration-sensitive detector. However, in contrast to the conventional SEC, where only relative slice areas are needed, the absolute concentrations of polymer molecules eluting at particular elution volume slices must be determined by a concentration-sensitive detector. An RI detector is the most widely used concentration detector for the SEC-MALS experiments. The signal of the RI detector in volts is converted to refractive index units by means of the RI detector calibration constant and the obtained refractive index difference is further used with dn/dc to calculate the concentration according to the following equation:

$$c_i = \frac{\alpha(V_i - V_{i,baseline})}{dn/dc} \tag{2.37}$$

where α is the RI detector calibration constant (in RI units per volt), and V_i and $V_{i,baseline}$ are the RI detector sample and baseline voltages, respectively. The calibration constant α is determined by injections of solutions of exactly known concentration of a compound of accurately known dn/dc. Aqueous sodium chloride can be recommended for the RI detector calibration using the procedure exactly equivalent to that used for the determination of dn/dc. The online RI detector calibration is carried out by injection of an exactly known mass of a polymer of known dn/dc into SEC columns. The RI detector calibration constant is calculated from the RI peak area, injected mass, and polymer dn/dc. This procedure is equivalent to the online determination of dn/dc. Polystyrene is the most suitable polymer for THF due to its perfect solubility and no tendency to interactions with styrene-divinylbenzene column packing. In addition, it is available in the form of narrow standards that elute as sharp peaks that are easy to integrate. Pullulan or dextran can be used for online RI detector calibration in aqueous solvents. The accuracy of the obtained RI calibration constant is directly related to the accuracy of dn/dc of the compound used for the calibration.

Most of the RI detectors operate at a wavelength different from that of MALS photometer. Widely used Waters RI detectors 2414 operating at a wavelength of 880 nm or the previous model 410 operating at 930 nm can be given as examples. However, most of the literature dn/dc values are listed for wavelength 633 nm or lower. The following equation shows the wavelength dependence of aqueous sodium chloride solution calculated using the data from reference 16:

$$dn/dc = 1.673 \times 10^{-7}\lambda_0^2 - 2.237 \times 10^{-4}\lambda_0 + 0.2487 \qquad (2.38)$$

The above equation yields dn/dc of aqueous sodium chloride of 0.174 mL/g for the two commonly used wavelengths of 633 nm and 690 nm. An important fact is that the difference between the two wavelengths is negligible. A slightly different dn/dc of aqueous sodium chloride of 0.179 mL/g can be found in reference 13. A difference less than 3% between the dn/dc values of 0.174 and 0.179 mL/g indicates possible uncertainty associated with the calibration of an RI detector. Since the wavelength dependence of dn/dc diminishes with the increasing wavelength, the RI detectors working at high wavelengths should be preferred over those operating with polychromatic light. Unfortunately, there is a lack of extensive study of the effect of the difference between the wavelength of the RI detector and the wavelength at which the dn/dc of the compound used for the RI detector calibration is valid. It can be hypothesized that the error of RI detector calibration constant α caused by the erroneous dn/dc of the compound used for the detector calibration is compensated by the same error of dn/dc of polymer under investigation.

To give a concrete example for the previous sentence: an RI detector operating at 930 nm is calibrated by polystyrene in THF using dn/dc of 0.185 mL/g valid at 633 nm; the RI detector is then used for the analysis of poly(methyl methacrylate) with dn/dc of 0.084 mL/g that is valid at 633 nm as well. The idea is that the dn/dc difference due to the wavelength difference is identical

for both polymers and thus the effect on concentration is mutually canceled. Although this concept sounds speculative, results of a short study published in reference 17 did not indicate significant error when a Waters 410 RI detector operating at a wavelength of 930 nm was calibrated using polystyrene *dn*/*dc* valid for 633 nm, and then used for SEC-MALS characterization of various polymers. Anyway, the use of an RI detector with a wavelength identical with that of a MALS detector yields more trustworthy results. A Wyatt Technology Corporation Optilab® rEX is an example of an RI detector whose operating wavelength matches the wavelength of the MALS detectors manufactured by the company.

Another possible source of inaccuracy is the difference between the RI detector temperature and the reference temperature at which the *dn*/*dc* of a polymer under investigation or a compound used for the RI detector calibration was determined. Many RI detectors have heating, but no cooling ability. In order to stabilize the detector flow cell temperature it is necessary to set the operating temperature of the RI detector 5–10°C above the room temperature. That means the RI detector is typically working at 35°C, while the literature *dn*/*dc* was determined at 25°C. The temperature coefficient of the specific refractive index increment, $d(dn/dc)/dt$ is 1×10^{-4} to 5×10^{-4} mL/g°C. That means that a change of temperature by 1°C results in *dn*/*dc* change of 0.0001–0.0005 mL/g. Results published in reference 17 did not indicate significant errors due to the temperature of RI detector. The temperature dependence of *dn*/*dc* affects not only the concentration determined by the RI detector, but also the molar mass calculated from the intensity of scattered light, because the *dn*/*dc* is in the optical constant K^*. In a less-favorable case of the temperature coefficient the change of *dn*/*dc* due to a temperature difference of 10°C may be around 0.005 mL/g. For *dn*/*dc* of 0.185 mL/g (e.g., polystyrene in THF or BSA in aqueous salt solution), the error of *dn*/*dc* due to a 10° temperature difference is likely less than 3%.

A UV detector is another concentration detector that can be used in combination with the MALS detector in the online mode. To determine the concentration by the UV detector the following parameters must be known: (1) the UV response factor in absorbance units per volt (typically 1 AU/volt), (2) the cell length (typically 1 cm), and (3) the extinction coefficient in $\text{mLg}^{-1}\ \text{cm}^{-1}$. In the ideal case, the concentrations determined by RI and UV detectors can be crosschecked. If the extinction coefficient of the analyzed polymer is known, it is possible to calculate the mass from the UV peak area and then to use this mass to calculate the unknown *dn*/*dc* of the polymer from the RI peak area (the reverse procedure, when the *dn*/*dc* is known and the extinction coefficient unknown, is the same). The obtained *dn*/*dc* can be then used for the determination of molar mass from the light scattering intensity. The advantage of this procedure is that it does not require 100% sample purity or 100% mass recovery from the SEC columns. However, most of the synthetic and natural polymers have no UV response, styrene-containing polymers and proteins being important exceptions.

Possible uncertainty of results associated with the *dn*/*dc* and RI detector calibration constant is depicted in Table 2.3. In this experiment, a Waters 2414

Table 2.3 M_w of Polystyrene NIST SRM 706 Measured by SEC-MALS with UV and RI Detection and by Batch Measurement

	Determination of polystyrene UV extinction coefficient @ 254 nm and determination of RI calibration constant using 90,000 and 170,000 polystyrene narrow standards			
1	No. of injections	Extinction coefficient (mLg^{-1} cm^{-1})		RI calibration constant relative uncertainty(%)
	8	1595 ± 14		0.7
	Analysis of broad polystyrene NIST 706 by SEC-MALS (10 injections)			
	M_w (10^3 g/mol)		Mass recovery (%)	
2	RI detection 283.4 ± 0.2 $(287.5 \pm 0.1)^*$	UV detection 276.0 ± 0.3	RI detection 100	UV detection 102.6 ± 0.1
3	Batch mode (average from three measurements) $M_w = (288.1 \pm 2.2) \times 10^3$ g/mol			
4	Nominal $M_w = (285 \pm 23) \times 10^3$ g/mol			

Notes:

Row 1: Waters 2414 RI detector working at 880 nm was calibrated online by PS standards using *dn*/*dc* of 0.185 mL/g; Waters 2487 UV detector was used online to determine extinction coefficient of polystyrene.

Row 2: The obtained extinction coefficient and RI calibration constant were used to determine M_w by SEC-MALS using a three-angle miniDAWN™ photometer. *The result obtained by triplicate measurements using an SEC-MALS-RI setup consisting of an 18-angle DAWN® EOS photometer and Optilab® DSP RI detector with wavelength matching that of MALS; RI calibration offline by means of NaCl.

Row 3: Batch mode using an 18-angle DAWN® EOS photometer; measurements using serial dilutions of stock solution; each stock solution was made up independently.

Row 4: According to NIST certificate.

RI detector with operating wavelength of 880 nm was carefully calibrated in SEC mode using eight injections of narrow polystyrene standards and *dn*/*dc* of 0.185 mL/g valid for 633 nm and THF. The instrumental setup also included a Waters 2487 UV detector operating at 254 nm, which was used to determine the extinction coefficient of polystyrene simultaneously with the calibration of the RI detector. The same UV-MALS-RI setup was then used for the characterization of broad polystyrene NIST SRM 706 that was processed using both UV and RI detector signals. The results show about 2.6% difference between the M_w and the calculated mass determined from the signals of UV and RI detectors. The difference may reflect possible errors given by the use of an RI detector of different wavelength than that for which the *dn*/*dc* is valid. However, the

difference may be also due to accuracy of volume delay between the UV and MALS and MALS and RI detectors, and interdetector peak broadening.

An important finding is that the M_w obtained by the online experiment agrees with that determined in the batch mode. This fact verifies both the calibration constant of the RI detector and the UV extinction coefficient.

Another important finding is that the obtained M_w agrees with that determined with another SEC-MALS setup consisting of different MALS and RI detectors. All the obtained M_w values agree well with the reference value no matter whether in batch or chromatography mode or what concentration detector is used. National Institute of Standards and Technology (NIST) Standard Reference Material (SRM) 706a polystyrene is still available and thus a few notes concerning its characterization may be worthwhile. The polystyrene sample (originally labeled as SRM 706) was prepared by thermal polymerization of styrene at 140°C to 37% conversion. The originally reported values (in 1967) were as follows:

Measured by light scattering		$M_w = 257{,}800 \pm 930$ g/mol
Measured by sedimentation equilibrium		$M_w = 288{,}100 \pm 9600$ g/mol
Osmotic pressure measurements		$M_n = 136{,}500$ g/mol
Intrinsic viscosity[i]	(benzene at 25°C)	$[\eta] = 93.7 \pm 0.19$ mL/g
	(cyclohexane at 35°C)	$[\eta] = 39.5 \pm 0.10$ mL/g

The light scattering and sedimentation measurements were carried out in cyclohexane at 35°C and the data were processed using 0.1705 mL/g for the refractive index increment and 0.930 mL/g for the partial specific volume. Ratios of molar masses $M_z : M_w : M_n = 2.9 : 2.1 : 1$ were reported based on a viscometric analysis of 41 fractions. The recertification was carried out by light scattering in 1998 and yielded the following results:

$$M_w = 285{,}000 \pm 23{,}000 \text{ g/mol}$$

The recertification measurement was carried out in toluene at 25°C. The specific refractive index was determined as 0.1089 ± 0.0009 mL/g. The dn/dc was determined using a Chromatix KMX-16 differential refractometer calibrated with sodium chloride solutions. The light scattering measurements of the solutions were made on a Brookhaven Instrument Model BI-200 goniometer, which was calibrated by benzene. The recertification report also provides $A_2 = 0.000411 \pm 0.00003$ mol mL/g^2 and $R_z = 27.8 \pm 1.0$ nm. Another important finding of the NIST SRM 706 recertification is that the SEC study did not indicate any difference between SRM 706 and SRM 706a.

Light absorption and fluorescence represent other potential sources of errors in light scattering measurements. Fortunately, most of the synthetic and natural polymers do not absorb visible light or show fluorescence. However, for some specific polymers both effects must be considered. If polymer yields colored solutions, they must be checked by a spectrometer for absorption at the wavelength

[i]Note the significant influence of the thermodynamic quality of solvent on the intrinsic viscosity.

of the light scattering photometer. Light scattering photometers that monitor the intensity of transmitted light allow easy detection of absorption, and also the light transmitted through the flow cell can be used by the light scattering software to compensate for the absorption. To eliminate the effect of absorption the intensity of scattered light is related to the intensity of transmitted light monitored by the forward photodetector. ASTRA® V (Wyatt Technology Corporation) is an example of the light scattering software that can eliminate the effect of absorption. Fluorescence (i.e., the emission of light after irradiation by visible light) is another source of errors. If it is caused by impurities, the problem can be solved by sample purification or measurement in the online mode when the polymer under investigation is separated from the fluorescing impurities. If the fluorescence is caused by the polymer itself, the emitted light superimposes with the scattered light, which leads to the overestimation of molar mass. The intensity of the fluorescent light may be significantly higher than that of the scattered light and thus the obtained molar masses may be enormously high.

Less intense fluorescence can be eliminated by fluorescence filters, that is, monochromatic filters that are placed between the scattering solution and photodetectors. These filters transmit only the true scattered light that has the wavelength of the incident light. Concerning the absolute accuracy of light scattering, it is necessary to realize that small errors in particular parameters—concentration, calibration constant of light scattering instrument, dn/dc of the polymer under investigation or the compound used for the RI detector calibration, and RI detector calibration constant—can mutually partly or even completely compensate. On the other hand, they can work synergistically.

2.7 EXAMPLES OF LIGHT SCATTERING MEASUREMENT IN BATCH MODE

Processing the light scattering data obtained by the batch experiment is demonstrated on well-known polystyrene NIST SRM 706. Figure 2.21 shows a Zimm plot of NIST 706 polystyrene (the corresponding raw data are depicted in Figure 2.17). The data were obtained by preparation of sample in THF at five different concentrations. The solutions were prepared by dilution of the stock solution. The dilution was done on the basis of weight. The solutions were injected directly into the flow cell of a MALS photometer by means of a syringe pump using disposable syringes attached to 0.45 μm filter units. The Zimm plot allows simultaneous extrapolation of the concentration and angular dependence of the light scattering intensities to zero angle and zero concentration.

It is worth mentioning that the Zimm plot processes the three-dimensional function R_θ versus c and θ using a two-dimensional plot. The first-order polynomials fit both angular and concentration dependencies for the data in Figure 2.21, but higher-order fits may be necessary, especially for angular dependence. As for the concentration dependence, the experiments should be carried out at concentrations low enough that the first-order polynomial is sufficient to fit the data.

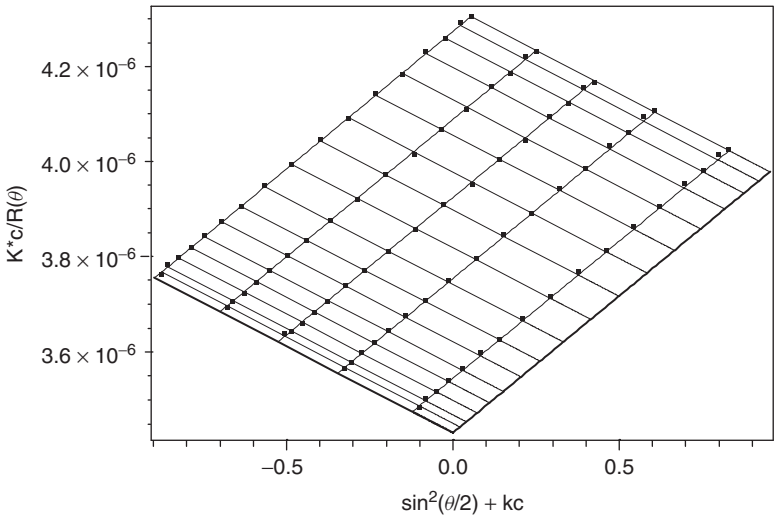

Figure 2.21 Zimm plot for NIST SRM 706 polystyrene. Each of five lines consisting of 17 data points represents angular variation acquired for a particular concentration; thick lines are concentration dependence at zero angle and angular dependence at zero concentration. Formalisms according to Zimm, THF as solvent, room temperature, vertically polarized light 690 nm, negative scale factor k, concentration: 1st-order fit, angle: 1st-order fit. $M_w = 291{,}600 \pm 200$ g/mol; $R_z = 27.8 \pm 0.1$ nm; $A_2 = (4.33 \pm 0.04) \times 10^{-4}$ mol mL/g^2.

The resulting extrapolated lines are the angular dependence of the scattered light intensity at zero concentration and the concentration dependence of scattered light intensity at zero angle. Both lines cross with the K^*c/R_θ axis at the intercept equal to the reciprocal weight-average molar mass $1/M_w$. The slope of the concentration dependence at zero angle yields the second virial coefficient: slope $= 2A_2$.

The angular dependence of scattered light intensity at zero concentration can be expressed using Equations 2.27 and 2.11 as:

$$\left(\frac{K^*c}{R_\theta}\right)_{c=0} = \frac{1}{M_w} + \frac{16\pi^2}{3\lambda^2}\frac{1}{M_w}R_z^2 \sin^2\left(\frac{\theta}{2}\right) \tag{2.39}$$

The slope of this relation at zero angle (m_0) equals:

$$m_0 = \frac{16\pi^2}{3\lambda^2}\frac{1}{M_w}R_z^2 \tag{2.40}$$

and the intercept of this line is equal to $1/M_w$. The z-average RMS radius is calculated from the slope of the angular variation at zero concentration:

$$R_z = \sqrt{\frac{3m_0\lambda^2 M_w}{16\pi^2}} \tag{2.41}$$

Although according to Equation 2.41 the calculation of R_z involves M_w, incorrect M_w due to incorrect dn/dc does not affect the obtained R_z, because the error in M_w generated by the error in dn/dc generates proportional error in the slope m_0 (see Figure 2.22). Using the relation between R and M for linear polystyrene ($R = 0.014 \times M^{0.585}$), the RMS radius of 22 nm corresponds to the M_w obtained by the Zimm plot, which is markedly lower than the value determined experimentally from the angular variation. This fact illustrates that for polydisperse polymers the molar mass and RMS radius cannot be directly compared, because they are of different type and different sensitivity to the polydispersity. Assuming linear topology, the value of M_z of 434,000 g/mol can be estimated from R_z and the R–M relationship. This value is quite comparable to that determined by SEC-MALS or A4F-MALS measurements (see Figure 5.25). The second virial coefficient of order of magnitude 10^{-4} mol.mL/g^2 confirms THF as a thermodynamically good solvent for polystyrene. Note that the R_z determined for NIST 706 in THF equals the reference value obtained in toluene, which indicates similar thermodynamical quality of the two solvents and consequently similar expansion of the polymer chain.

Figure 2.23 depicts corresponding Debye plots for the lowest and highest concentrations. In this case the information about the second virial coefficient is missing and the M_w and R_z are calculated from the intercept and slope of the angular dependence, respectively. The M_w determined at the lowest and highest concentrations are 98.7% and 91.4% of the value obtained by means of the

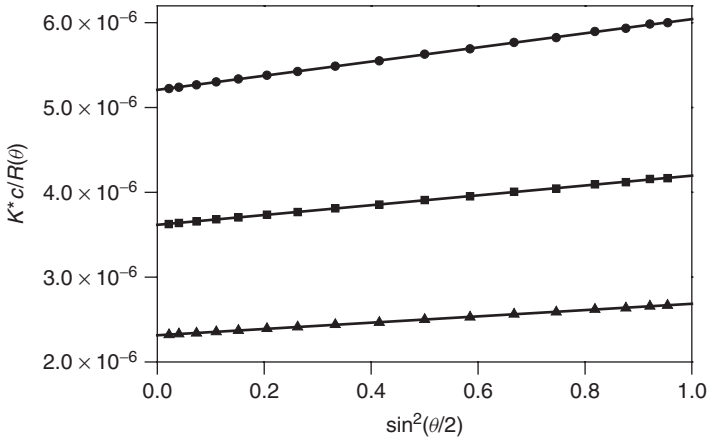

Figure 2.22 Influence of the accuracy of dn/dc on the Debye plot (Zimm formalism) of polystyrene: (■) correct $dn/dc = 0.185$ mL/g, intercept = 3.616E-6, slope = 5.795E-7, (▲) incorrect $dn/dc = 0.148$ mL/g, intercept = 2.314E-6, slope = 3.709E-7, (●) incorrect $dn/dc = 0.222$ mL/g, intercept = 5.207E-6, slope = 8.345E-7. The molar mass (reciprocal intercept) calculated by erroneous dn/dc is incorrect, while the RMS radius calculated from the slope according to Equation 2.41 is independent of dn/dc, because the ratio slope/intercept remains constant.

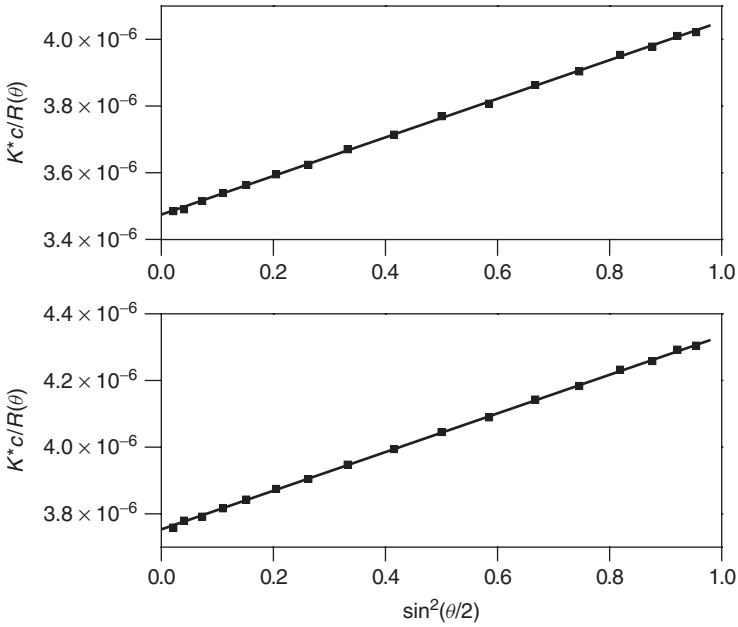

Figure 2.23 Deby plots obtained from data presented in Figure 2.21 for the lowest (top) and the highest (bottom) concentration: $c = 5.152$e-5 g/mL: $M_w = 287,900 \pm 100$ g/mol, $R_z = 27.7 \pm 0.1$ nm; $c = 3.760$e-4 g/mL: $M_w = 266{,}400 \pm 100$ g/mol, $R_z = 26.7 \pm 0.1$ nm.

Zimm plot. In the case of the Debye plot, the R_z is slightly concentration dependent due to the concentration dependence of M_w. The Debye plot at a single concentration has practical meaning in the case of a limited sample amount or when the sample throughput is to be increased. The error due to neglecting the concentration dependence increases with increasing concentration and thus the Debye experiments should be performed at the lowest possible concentrations.

Figure 2.24 shows the same data for NIST SRM 706 polystyrene processed using the so-called Debye and Berry formalisms (i.e., Equations 2.1 and 2.28, respectively). It can be concluded that for this polymer various formalisms yield almost identical results. However, this is not a generally valid conclusion as shown further.

The effect of processing the data with various formalisms is further demonstrated in Table 2.4, which compares results determined by particular mechanisms for several polymers of different molar mass and size. In conclusion, one can say that the results for small polymers with no or moderate angular dependency of scattered light intensity are independent of the formalism.

For larger polymers, the differences of molar masses and RMS radii determined by particular mechanisms are quite significant and can reach several tens of percent. The quantity that matters is the size and not the molar mass as evident from the results obtained for poly(methyl methacrylate) with significantly larger M_w but smaller R_z compared to hyaluronic acid.

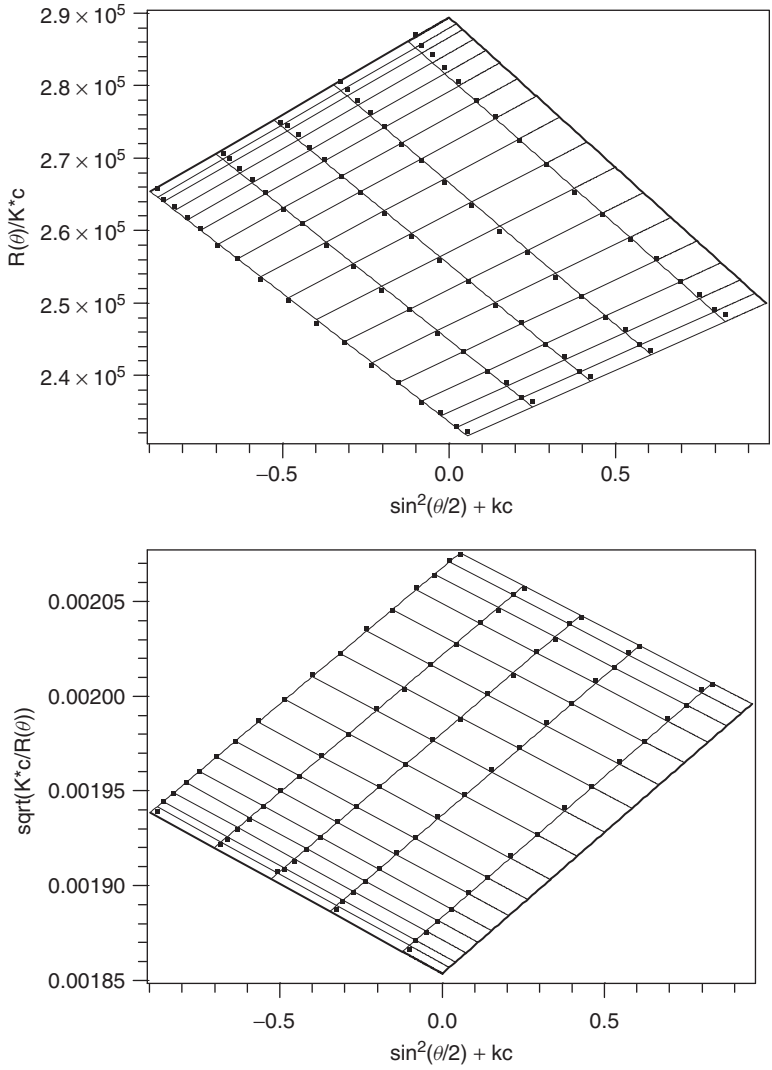

Figure 2.24 Zimm plot for NIST SRM 706 polystyrene obtained using Debye formalism (top) and Berry formalism (bottom). THF, room temperature, vertically polarized light 690 nm; negative scale factor, concentration: 1st-order fit, angle: 1st-order fit. Debye: $M_w = 289{,}400 \pm 400$ g/mol; $R_z = 25.6 \pm 0.2$ nm; $A_2 = (3.82 \pm 0.07) \times 10^{-4}$ mol mL/g^2. Berry: $M_w = 291{,}000 \pm 200$ g/mol; $R_z = 27.2 \pm 0.1$ nm; $A_2 = (4.19 \pm 0.04) \times 10^{-4}$ mol mL/g^2. (Zimm formalism, see Figure 2.21.)

Table 2.4 Characteristics of Polymers Determined in Batch Mode Using Various Light Scattering Formalisms

	M_w (10^3 g/mol)			R_z (nm)			A_2 (10^{-4} mol mL/g^2)		
Sample	Z	B	D	Z	B	D	Z	B	D
PS	2.9	2.9	2.8	—	—	—	17.8	16.0	12.3
EP (2)	8.4	8.3	8.1	—	—	—	14.5	13.2	10.4
PS (A)	337	336	336$^{(2)}$	33.8	32.9	34.4$^{(2)}$	4.1	3.9	3.6
HA	437	382	315$^{(3)}$	72.0	61	58$^{(3)}$	27.4	19.8	10.6
PMMA (Y)	612	609	609$^{(2)}$	41.6	39.9	41.4$^{(2)}$	2.6	2.5	2.2
PS	4340	3953$^{(2)}$	3237$^{(3)}$	133	122$^{(2)}$	101$^{(3)}$	2.8	2.1	1.1

PS = linear polystyrene, EP = epoxy resin based on bisphenol A, HA = hyaluronic acid sodium salt, PMMA = poly(methyl methacrylate), Z = Zimm, B = Berry, D = Debye, $^{(2),(3)}$2nd respective 3rd-order polynomial used to fit angular data; otherwise linear fit.

Choosing the proper formalisms may not be always obvious. A fitness of the formalism to the experimental data points and uncertainty calculated by the software can be used as guidance. Generally, the Zimm formalism is linear even for large molecules, but compared to other formalisms it yields larger M_w and R_z. The effect of the light scattering formalism is presented in more detail in Section 4.2.1.

A Zimm plot for sodium salt of hyaluronic acid is depicted in Figure 2.25. Compared to M_w the sample has high R_z, which in this particular case indicates extended chain conformation. However, high R_z can be also due to very high polydispersity and presence of fractions with very high molar mass. The A_2 of order of magnitude 10^{-3} mol mL/g^2 suggests intensive polymer–solvent interactions. The high A_2 accounts for significant inaccuracy of the molar mass determined by means of the Debye plot method, which gives errors in M_w of about 10% and 62% for the lowest and highest concentration, respectively.

Figure 2.26 shows an example of a Zimm plot for highly branched polystyrene with M_w substantially higher compared to NIST polystyrene. The second-order polynomial is necessary to fit the angular data points. The slope of the concentration dependence is close to zero although the A_2 of 2.7×10^{-4} mol.mL/g^2 corresponds to the M_w according to Equation 2.5, which can be attributed to the presence of highly branched molecules and the fact that A_2 decreases with increasing degree of branching. The decrease of A_2 due to branching is given by a more compact structure of branched macromolecules where polymer segments are forced to intramolecular interactions. The A_2 equal to zero allows accurate determination of molar mass using the Debye plot technique at a single concentration. In this case, even the Debye plot at the highest concentration yields M_w virtually identical with that determined by means of the Zimm plot. The experimental R_z is larger than the value of

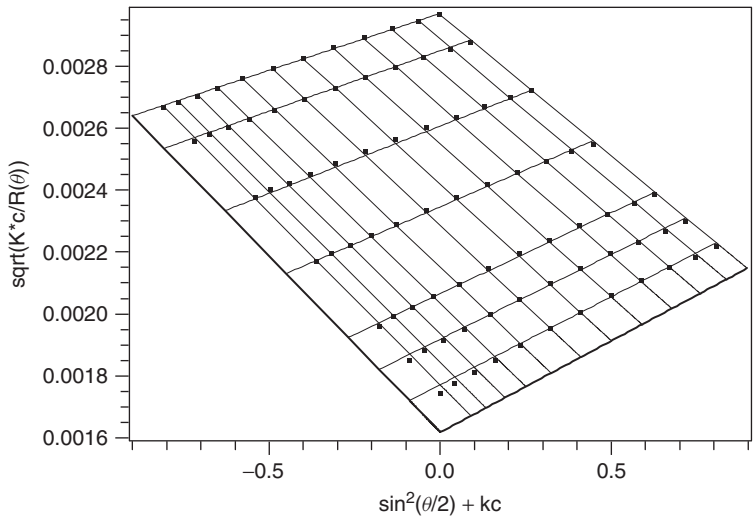

Figure 2.25 Zimm plot for hyaluronic acid sodium salt. Berry formalism, phosphate buffer, room temperature, vertically polarized light 690 nm; negative scale factor k, concentration: 1st-order fit, angle: 1st-order fit. Concentrations: 8.345e-5, 1.656e-4, 2.497e-4, 4.176e-4, 5.833e-4, 7.478e-4, 8.334e-4 g/mL. $M_w = 382,000 \pm 2000$ g/mol; $R_z = 61.1 \pm 0.4$ nm; $A_2 = (1.98 \pm 0.01) \times 10^{-3}$ mol mL/g^2.
Source: Courtesy Martina Hermannova, Contipro C, Czech Republic.

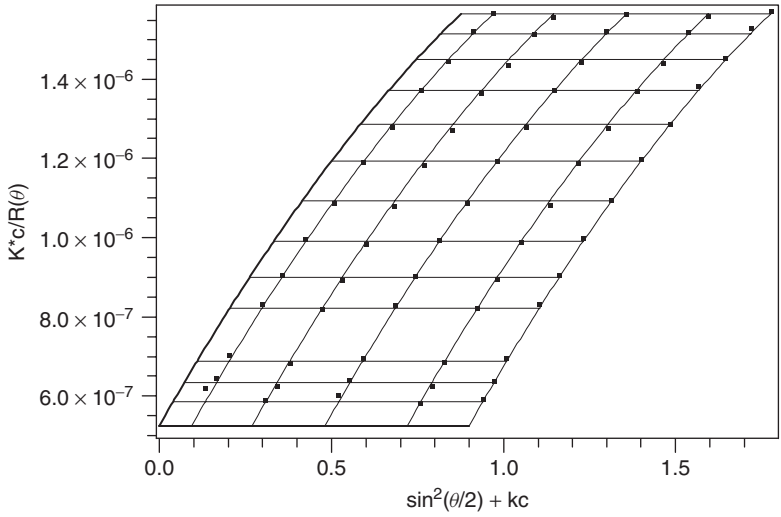

Figure 2.26 Zimm plot for randomly branched polystyrene. Zimm formalism, THF, room temperature, vertically polarized light 690 nm, positive scale factor k, concentration: zero-order fit, angle: 2nd-order fit. Concentrations: 9.866e-6, 2.830e-5, 5.054e-5, 7.555e-5, 9.448e-5 g/mL. $M_w = 1,908,000 \pm 7000$ g/mol; $R_z = 116.2 \pm 0.6$ nm; $A_2 \to 0$ mol mL/g^2.

66 nm calculated for the given M_w from the R-versus-M relationship for linear polystyrene.

Branching reduces the molecular size and the information about branching can be generally revealed from the comparison of RMS radii of linear and branched polymers of the same molar mass. However, randomly branched polymers with a high degree of branching are characterized by very broad molar mass distribution with a high-molar-mass tail. Since the high-molar-mass fractions affect the z-average more than the weight-average, the reducing effect of branching on R_z is overcompensated by the presence of fractions with very high molar mass, which accounts for the R_z larger than would correspond to the linear polymer of the same M_w.

Figure 2.27 shows another example of a Zimm plot for branched polymer. In this case the branched polymer was prepared by GTP and has a starlike topology with numerous arms. Highly compact structure corresponds to the high molar mass and relatively small size. The RMS radius of corresponding linear polymer of the same M_w is 63 nm (i.e., markedly larger that the experimental value). In this particular case of highly compact structure and absence of a high-molar-mass tail (confirmed by A4F-MALS), the value of R_z is lower than that of corresponding linear polymer of the same M_w. The data in Figures 2.26 and 2.27 show that the comparison of experimental value of R_z with the theoretical R calculated for linear polymer of the same M_w yields very uncertain and limited information

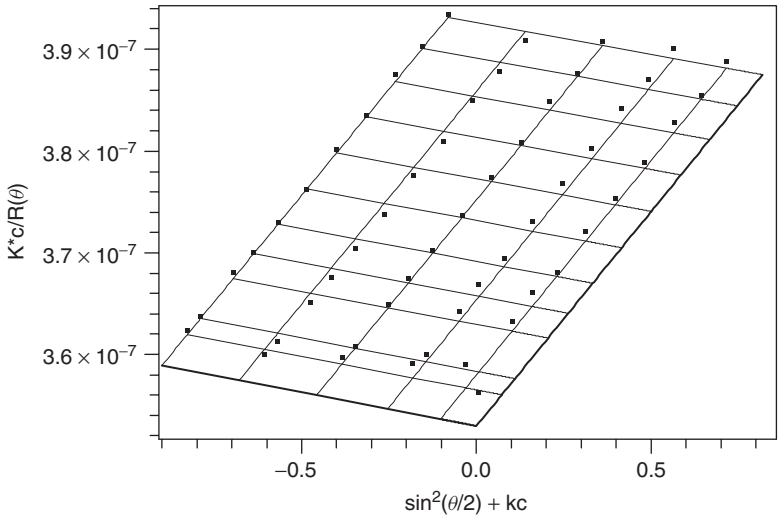

Figure 2.27 Zimm plot for star-branched poly(benzyl methacrylate) with high number of arms. Zimm formalism, THF, room temperature, vertically polarized light 690 nm, negative scale factor k, concentration: 1st-order fit, angle: 1st-order fit. Concentrations: 8.939e-6, 2.213e-5, 3.983e-5, 5.915e-5, 7.843e-5 g/mL. $M_w = 2{,}833{,}000 \pm 6000$ g/mol; $R_z = 23.5 \pm 0.4$ nm; $A_2 = (3.8 \pm 0.6) \times 10^{-5}$ mol mL/g^2.

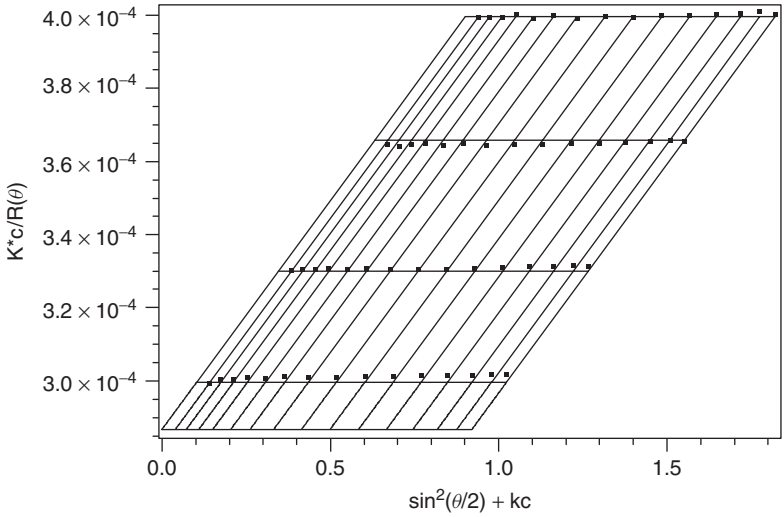

Figure 2.28 Zimm plot for bisphenol A–based epoxy resin. Zimm formalism, THF, room temperature, vertically polarized light 690 nm, positive scale factor k, concentration: 1st-order fit, angle: zero-order fit. Concentrations: 3.678e-3, 1.238e-2, 2.263e-2, 3.226e-2 g/mL. $M_w = 3,490 \pm 10$ g/mol; R_z N/A; $A_2 = (1.75 \pm 0.01) \times 10^{-3}$ mol mL/g^2.

about branching. Only if the experimental R_z is smaller than the R calculated from the relation between the RMS radius and molar mass for a linear polymer can one safely conclude that the polymer is branched. However, even in this case there is no possibility of getting information about the degree of branching unless the polymer is monodisperse. For most of the randomly branched polymers the reduction of RMS radius is partly or completely compensated by the presence of fractions with very high molar mass.

An example of a Zimm plot for an oligomer is shown in Figure 2.28. The sample shows no angular variation of the scattered light intensity due to very small molecules. High A_2 of order of magnitude of 10^{-3} corresponds to relatively low molar mass. The excellent shape of the Zimm plot presented in Figure 2.28 also disproves the sometimes-still-believed perception that light scattering is suitable only for polymers with molar mass above 10,000 g/mol.

An example of a Zimm plot for an ultra-high-molar-mass polymer is shown in Figure 2.29. Despite very high molar mass, the A_2 is at the 10^{-4} mol.mL/g^2 level, roughly corresponding to Equation 2.5. The data show high uncertainty and also significant difference between the results obtained by Zimm and Berry formalisms. The Debye formalism, which is not shown in Figure 2.29, was completely unable to fit the experimental data points. It is worth mentioning that the Zimm formalism yields markedly larger values of M_w and R_z than the Berry formalism. In the case of polymers with very high molar mass, the difference between the highest and lowest value of K^*c/R_θ is large and thus a small inaccuracy of extrapolation to zero angle significantly affects the value of M_w, which

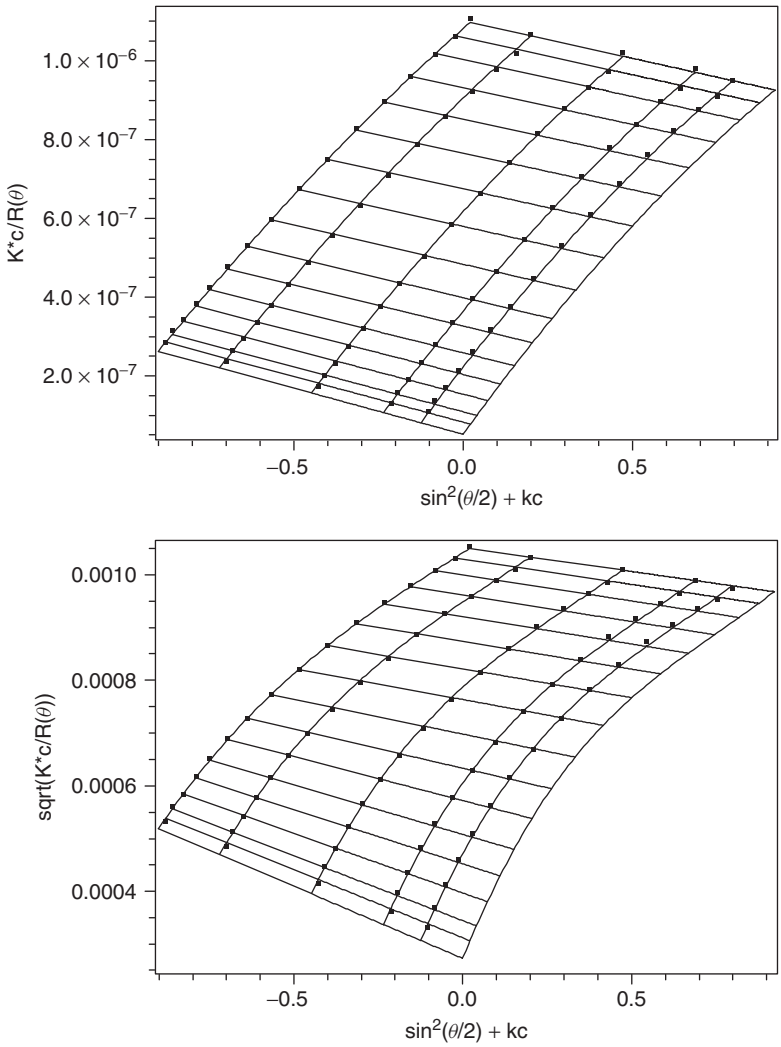

Figure 2.29 Zimm plot for ultra-high-molar-mass polystyrene standard. THF, room temperature, vertically polarized light 690 nm, negative scale factor k. Concentrations: 6.614e-5, 1.250e-4, 2.388e-4, 3.835e-4, 4.795e-4 g/mL. Zimm formalism (top): concentration: 1st-order fit, angle: 2nd-order fit, $M_w = (19.3 \pm 3.6) \times 10^6$ g/mol; $R_z = 325 \pm 33$; $A_2 = (2.20 \pm 0.15) \times 10^{-4}$ mol mL/g^2. Berry formalism (bottom): concentration: 1st-order fit, angle: 3rd-order fit. $M_w = (13.4 \pm 1.4) \times 10^6$ g/mol; $R_z = 230 \pm 14$; $A_2 = (1.40 \pm 0.13) \times 10^{-4}$ mol mL/g^2.

accounts for high M_w uncertainty. The uncertainty of R_z is also much higher compared to smaller polymers. Although very large polymer molecules have steep initial slope of angular dependence that can be measured precisely, the uncertainty and accuracy of R_z are influenced by the value of M_w, as seen from Equation 2.41.

Another application of the batch light scattering method is shown in Figure 2.30. The measurement was carried out using a heated/cooled MALS photometer allowing measurements below room temperature. The sample was a polymer creating supermolecular structures at temperatures close to 0°C. The measurement was carried out in a scintillation vial. The aggregation of individual molecules is indicated by significant increase of scattered light intensity. The data also allow the determination of the size of arisen aggregates. Very high RMS radius of the aggregates yields highly curved angular dependency, and thus only the lower angles are used for data processing.

Light scattering can be used as a fast method of studying protein temperature induced aggregation, as demonstrated in Figure 2.31. In this example,

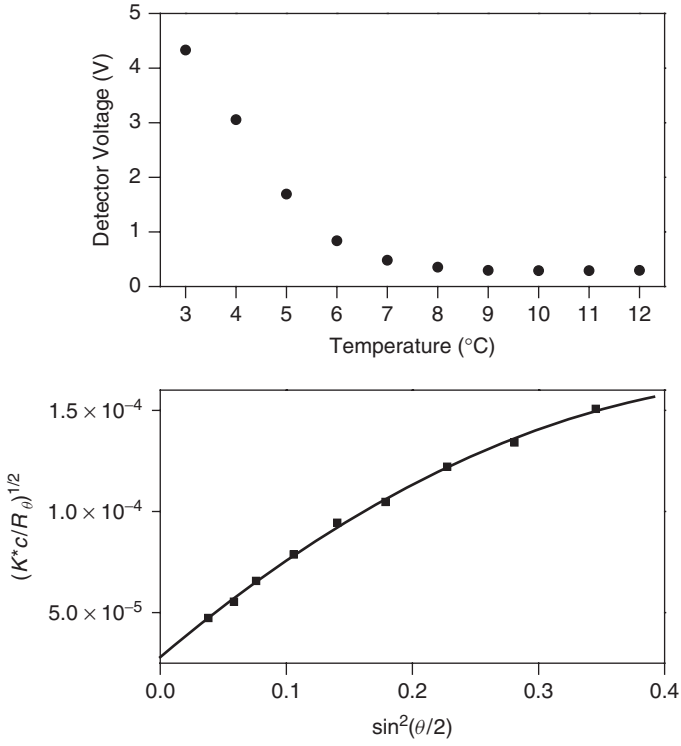

Figure 2.30 Temperature dependence of light scattering intensity of a polymer creating aggregates (top) and Debye plot at 3°C (bottom). Second-order fit using Berry formalism: $R_z = 385 \pm 4$ nm.

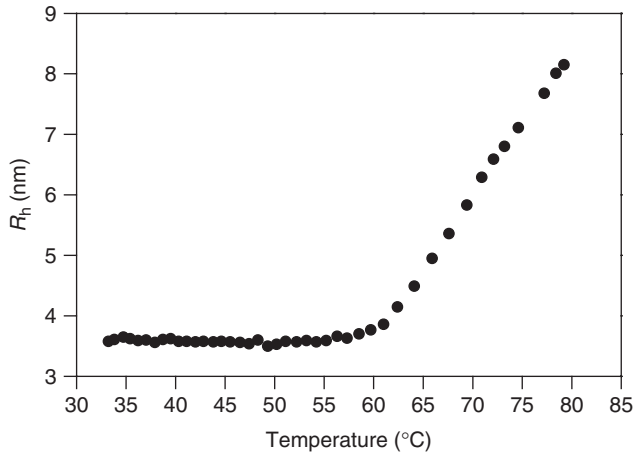

Figure 2.31 Melting study for BSA: hydrodynamic radius of BSA measured as a function of temperature. Onset temperature $= 59.0 \pm 0.1^{\circ}$C.
Source: Courtesy of Roger Scherrers, Wyatt Technology Europe. Measured using photometer Dynapro™ NanoStar.

DLS employing thermal ramping was used to measure changes of hydrodynamic radius. A folded protein can exhibit unfolding with increase in temperature, resulting in the exposure of hydrophobic regions and eventual protein aggregation.

Generally, the light scattering technique can be used for sensitive detection of processes that are associated with the change of molar mass or molecular size. An interesting application is the quantitative characterization of reversible protein–protein association. The method employs static light scattering under different compositions and concentrations of protein and buffer. As protein complexes are formed, scattered light intensity and M_w increase. The method was reported as composition gradient multi-angle light scattering (CG-MALS).[18,19] The procedure of preparing solutions of different compositions and delivering them into a MALS photometer and a concentration detector can be fully automatized by a commercially available instrument called Calypso (Wyatt Technology Corporation). The instrument is based on three computer-controlled syringe pumps that yield different compositions by varying the relative flow rates of the pumps connected to the two sample vials and a buffer reservoir. The specified compositions are delivered via a static mixer into the flow cells of MALS and concentration (UV, RI) detectors.

The previous examples of light scattering measurements in batch/microbatch mode showed several Zimm plots of neat appearance, and demonstrated that the technique is quite applicable over a broad range of molar masses and polymer structure. The batch measurement is relatively fast and does not require more than two hours for one sample, including sample preparation. The particular solutions

can be prepared individually or by dilution of a stock solution. Since the appearance of the Zimm plot strongly depends on the accuracy of the concentrations, usually better-looking Zimm plots are obtained using serial dilutions of a stock solution. The particular dilutions must be made with great care, keeping four significant figures of accuracy. Dilutions on the basis of weight should be used instead of dilutions on the basis of volume.

2.8 KEYNOTES

- Light scattering is the result of interaction of light with matter.
- In static (elastic, Rayleigh) light scattering the time-averaged intensity of the scattered light is measured, whereas in dynamic (quasielastic) light scattering the time-dependent fluctuations are of interest.
- The intensity of scattered light is expressed by the quantity called Rayleigh ratio, which is independent of the intensity of incident light and light scattering apparatus.
- The absolute intensity of scattered light is directly proportional to the molar mass and concentration of scattering molecules. The size of scattering molecules is reflected in the decrease of the scattered light intensity with the angle of detection.
- The angular variation of the scattered light intensity is described by the particle scattering function. The particle scattering function reflects the intramolecular interference, which is eliminated by extrapolation to zero angle.
- In solutions of finite concentration, the light scattered from different molecules interferes. This intermolecular interference is eliminated by extrapolation to zero concentration or by measurement at very low concentrations.
- A light scattering experiment yields three pieces of information: (1) the weight-average molar mass, (2) the z-average RMS radius, and (3) the second virial coefficient. The RMS radius can be determined without knowledge of concentration and/or dn/dc solely from the angular variation of scattered light intensity.
- A light scattering experiment can be performed in batch mode on an unfractionated sample or in chromatography mode when a light scattering detector is placed online after a separation analytical instrument.
- The traditional batch light scattering experiment involves the measurement of a series of solutions of various concentrations at different angles. The obtained angular and concentration dependence of the intensity of scattered light is simultaneously extrapolated to zero angle and zero concentration by means of a Zimm plot. The concentration range should cover about one order of magnitude. Samples with different molar mass require different

concentrations of measured solutions: Figures 2.21–2.29 show appropriate concentrations for various molar masses.

- A simpler way of processing the light scattering data is extrapolation of solely angular intensity at a single concentration. The method is called a Debye plot and usually yields underestimated M_w with error proportional to the concentration.
- The experimental data can be processed using various light scattering formalisms. They are: Debye, Zimm and Berry, which plot $R_\theta/K^*c, K^*c/R_\theta$, and $(K^*c/R_\theta)^{1/2}$ versus $\sin^2(\theta/2)$, respectively.
- Light scattering is an absolute method for determination of molar mass whose absolute accuracy is given by the accuracy of Rayleigh ratio of standard used for the calibration of a light scattering instrument, accuracy of the dn/dc, and accuracy of concentration. In the case of SEC-MALS experiments, the calibration constant of the RI detector is another important parameter affecting the accuracy of the molar mass. Concerning the determination of molar mass, the RI detector plays as important a role as the MALS detector.
- Light scattering experiments are very sensitive to submicrometer particles in solutions measured in batch mode or mobile phase eluting from a separation device. The optical clarification of the sample is of crucial importance for the batch experiments. The clarification should remove dust and other scattering matters not belonging to the polymer under analysis. On the other hand, the clarification should not remove a relevant part of the sample. Clarification of the sample itself is not crucial in the case of online experiment, but possible particle shedding from SEC columns is another source of unwanted signal noise.
- A perfectly clean flow cell of the MALS photometer is crucial for accurate measurements. Bright spots visible in the low cell and increase of the baseline signal are indications of impurities in the cell.
- Although light scattering yields both molar mass and molecular size, the ability to characterize branching of polydisperse polymers by measurements of unfractionated samples is highly limited due to different sensitivity of M_w and R_z to the high-molar-mass fractions. For polydisperse polymers, the reduction of RMS radius due to the branching is compensated by the increase of R_z due to the presence of high-molar-mass fractions.

2.9 REFERENCES

1. Wyatt, P. J., *Analytica Chimica Acta*, **272**, 1 (1993).
2. Kratochvil, P., *Classical Light Scattering from Polymer Solutions, Polymer Science Library*, Jenkins, A. D. (editor), Elsevier, Amsterdam (1987).
3. Zimm, B. H., *J. Chem. Phys*., **16**, 1093 (1948).

4. Schulz, G. V. and Baumann, H., *Makromol. Chem*., **114**, 122 (1968).
5. Debye, P., *Ann. Phys*., **46**, 809 (1915).
6. Debye, P., *J. Phys. Coll. Chem*., **51**, 18 (1947).
7. Burchard, W., *Advances in Polymer Science*, **48**, Springer-Verlag, Berlin Heidelberg (1983), p. 58.
8. Burchard, W., *Macromolecules*, **10**, 919 (1977).
9. Kerker, M., Farone, W. A., and Matijevic, E., *J. Opt. Soc. Am*., **53**, 758 (1963).
10. Berry, G. C., *J. Chem. Phys*., **44**, 4550 (1966).
11. Huglin, M. B. (editor), *Light Scattering from Polymer Solutions*, Academic Press, London (1972).
12. Mori, S. and Barth, H. G., *Size Exclusion Chromatography*, Springer, Berlin (1999).
13. Brandrup, J., Immergut, E. H., Grulke, E. A. (editors), *Polymer Handbook*, 4th Edition, John Wiley & Sons New York (1999).
14. Sedlacek, J., Vohlidal, J., and Grubisic-Gallot, Z., *Makromol. Chem. Rapid Commun*., **14**, 51 (1993).
15. Kaye, W. and McDaniel, J. B., *Applied Optics*, **13**, 1934 (1974).
16. Becker, A., Kohler, W., and Muller, B., *Berichte der Bunsengesellschaft fur Physikalische Chemie*, **99**, 600 (1995).
17. Podzimek, S., in *Multiple Detection in Size-Exclusion Chromatography*, Striegel, A. M. (ed.), ACS Symposium Series **893**, Washington, D.C. (2004), p. 109.
18. Some, D., Hanlon, A., and Kamron, S., *American Biotechnology Laboratory*, **26**, March, 18 (2008).
19. Some, D., Hitchner, E., and Ferullo, J., *American Biotechnology Laboratory*, **27**, February, 16 (2009).

Chapter 3

Size Exclusion Chromatography

3.1 INTRODUCTION

Polymer analysis can be performed in three different modes of column liquid chromatography: (1) size exclusion chromatography (SEC), (2) liquid chromatography (LC)[i] at critical conditions, and (3) various kinds of LC based on enthalpic interactions. Enthalpic interactions represent attractive and repulsive forces between solute, solvent, and stationary phase and include adsorption, partition, ion interactions, and specific biochemical interactions (bioaffinity). The dissolution–precipitation process is another mechanism playing an important role in the separation of polymers and oligomers. The term *adsorption* LC applies to the distribution of solute between the solution and a solid surface; that is, the sample components are separated due to their varying degree of adsorption onto the solid surfaces. The stationary phase in adsorption chromatography is usually silica gel.[ii] The term *partition* (*liquid–liquid*) chromatography describes the distribution of solute between two chemically different liquid phases. In partition chromatography, the stationary phase is usually a liquid, which is mechanically coated or chemically bonded on an inert solid support. The term *normal-phase* HPLC is used for nonpolar solvent and polar column (silica gel), while the term *reversed-phase* HPLC is used for polar solvent/nonpolar column (e.g., silica gel modified with C_{18} or C_8 hydrocarbon).

Besides SEC, reversed-phase HPLC, typically performed in gradient elution mode, is often used in polymer and especially oligomer analysis. SEC is, at

[i]With the development of high-performance columns and advanced instrumentation, the term *high-performance liquid chromatography (HPLC)* has been frequently used.

[ii]The properties and polarity of silica gel can be further modified with polar functional groups such as cyano—C_2H_4CN, diol—$C_3H_6OCH_2CHOHCH_2OH$, or amino—C_3H_6 NH_2.

Light Scattering, Size Exclusion Chromatography and Asymmetric Flow Field Flow Fractionation: Powerful Tools for the Characterization of Polymers, Proteins and Nanoparticles, by Stepan Podzimek

least in its ideal state, governed purely by entropy, whereas the interaction LC is controlled by enthalpic effects, and the balance between enthalpic and entropic effects controls the separation by LC at critical conditions. Interaction LC separates according to both molar mass and chemical composition; the increase in molar mass results in the increase of retention time, while the presence of polar functional groups retention time decreases (reversed-phase LC) or increases (normal-phase LC). LC at critical conditions separates molecules independently of their molar mass according to their chemical composition and the type of end groups. Although this type of separation is attractive for many samples, its wide application is limited by the high sensitivity to experimental conditions.

In contrast to interaction LC and especially LC at critical conditions, where each polymer under analysis requires very specific separation conditions (column, mobile phase, temperature), SEC analysis can be performed using generic conditions for various polymers with the only requirements those of solubility of a polymer in an SEC solvent and an appropriate separation range of the SEC columns. The terms *LC* and *HPLC* include all chromatographic techniques in which the mobile phase is a liquid. Strictly speaking, SEC is one type of liquid chromatography and it is not appropriate to speak of SEC and HPLC as if they were two different methods. However, in common practice the two terms are used in order to distinguish an HPLC method based on interactions and typically applied to oligomeric and low-molar-mass compounds from the SEC method based on entropic separation and typically used for the analysis of polymers.

SEC, which is also well known under the name *gel permeation chromatography* (GPC) or *gel filtration*, represents one of the most important methods of polymer analysis that is widely used for polymer characterization and understanding and predicting polymer performance. SEC has almost completely replaced traditional methods of molar mass determination such as osmometry or ultracentrifugation, and nowadays even light scattering and viscometry are mostly carried out in combination with SEC. The advantages of SEC include relative simplicity, versatility, and ability to determine the complete distribution of molar masses as opposed to other methods providing solely an average molar mass, speed of measurement, and low sample demand. In addition, SEC benefits from intensive development of instrumentation driven by other types of liquid chromatography and from the fact that the instrumentation is available from many manufacturers.

SEC with solely a concentration detector and the calculation of molar mass distribution based on the column calibration can be called *conventional* SEC if there is a need of distinguishing from SEC combined with a light scattering or a viscometric detector. SEC can be defined as one method of molar mass determination even though the molar mass is not measured directly. SEC can be also defined as a special type of column chromatography—special in the sense of the nonexistence of interactions between the analyte and stationary phase. It must be emphasized that the absence of enthalpic interactions makes SEC unique among other types of liquid chromatography. As a consequence of the absence of interactions the method separates compounds purely according to their size in solution. However, the interactions are completely absent under

ideal SEC conditions, and in real SEC, various types of interactions often appear as undesirable side phenomena.

SEC has become the most popular method for determination of molar mass distribution and molar mass moments, and, in combination with light scattering and viscometric detectors, for determination of the distribution of root mean square (RMS) radius and intrinsic viscosity, detections of aggregation, and characterization of the molecular conformation and branching. The requested information is typically obtained in a timeframe of about 30 min. Just for curiosity, obtaining such information by traditional fractionation methods and characterization of the obtained fractions with batch light scattering and viscometry required several weeks of intensive work. SEC is often used to study polymerization kinetics, and for investigation of polymer degradation and ageing, determination of low-molar-mass additives in polymers, and characterization of oligomers. One of the advantages of the method is that it is suitable for use in research laboratories as well as for industrial plant applications.

The method dates back to the 1950s, when Porath and Flodin successfully separated water-soluble compounds using crosslinked dextrane gels.[1] They called the method *gel filtration* and proposed the idea of tailoring preparation of gels for different molecular size ranges. The milestone in the separation of synthetic polymers in nonaqueous solvent was the work by Moore,[2] who prepared a series of gels of different pore sizes based on crosslinked styrene-divinyl benzene copolymers and described efficient separation of polystyrene in the molar mass range of $700–10^6$ g/mol. He suggested the name *gel permeation chromatography*.

The first experiments were carried out using simple devices where the eluent flowed through the gel bed solely by gravitation forces and the fractions were collected for further characterization. The second generation of GPC instruments appeared in the 1960s (Waters GPC 100 and Waters GPC 200). These utilized low-pressure pumps operating at pressure below 10 bars. The 4-ft (120-cm) × 7.8-mm stainless-steel columns were packed with relatively soft gel packing of particle size of several tens of μm. The columns were assembled into sets consisting of three to six columns packed with gel of different pore sizes to cover sufficient molar mass range. The elution volume was determined by a siphon where each pour-out was registered by a count on a chromatogram. A significant improvement of the method was the development of online refractive index (RI) and UV detectors. A chart recorder recorded the detector signals and the obtained chromatograms were manually processed using a pencil and a ruler by drawing several tens of equidistant vertical lines from the baseline to a point on the chromatogram. The calculation of the calibration curves, the molar mass averages, and distribution plots was performed using large computers. The overlay of several chromatograms was typically done manually, using a pen and a sheet of transparent paper. The instruments also offered fraction collectors and simple autoinjectors. The third generation of instruments utilized high-pressure pumps, significantly shorter columns (typically 1 ft (30 cm) × 7.8 mm), smaller column packing of about 10 μm of mostly spherical shape, electronic integrators, and later the first personal computers. Current development is mostly aimed at

new columns with increased separation efficiency and reduced secondary separation mechanisms, advanced detection systems capable of direct measurements of molar mass and other molecular characteristics, increased sample throughput and methodology of processing, and interpretation of the experimental data.

3.2 SEPARATION MECHANISMS

The basic principle of separation by SEC can be described as follows. The chromatographic columns are packed with small particles of porous material. The space among the particles and pores are filled with a mobile phase. The sample is injected in the form of a dilute solution in the same solvent as used in the mobile phase into a series of columns that are continuously flowed with the mobile phase. The concentration of molecules eluting from the column outlet is monitored online by a concentration detector, usually an RI detector. The molecules permeate into the pores; the smaller molecules can permeate deeper into pores and they can permeate into smaller pores while large molecules are excluded from the pores with effective size smaller than the size of the molecules. Consequently, the large molecules elute from the columns first, followed by molecules with decreasing molecular size. This principle is generally known and accepted as the major separation mechanism called *steric exclusion*. However, there are other separation mechanisms that may play a role under specific conditions. The main SEC separation mechanisms are (1) steric exclusion, (2) restricted diffusion, and (3) separation by flow.

3.2.1 Steric Exclusion

The concept of steric exclusion is based on the idea that different a volume of pores in the SEC column is available for polymer molecules of different size. The basic idea is that the molecules have enough time to diffuse into the pores and back. In other words, the diffusion coefficients are large enough that the time necessary for polymer molecules to diffuse in and out of pores is significantly shorter than the residence time in which molecules stay in a given section of the column. Typically, the experimental conditions allow the establishment of the diffusion equilibrium and thus the steric exclusion is the primary separation mechanism in SEC.

The elution volume V_e can be expressed as

$$V_e = V_0 + K_d V_i \tag{3.1}$$

where K_d is the distribution coefficient, V_0 is the total volume of the solvent outside the pores, and V_i is the total volume of the solvent inside the pores. Molecules that are larger than the largest pores elute at elution volume V_0 (*limit of total exclusion*) and small molecules that can permeate into all pores elute at volume $(V_0 + V_i)$ at the *limit of total permeation*. Under ideal conditions

without interactions the distribution coefficient lies in the interval $0 \leq K_d \leq 1$. The distribution coefficient represents a volume fraction of pores that are available for molecules of a given molecular size. In contrast to other types of liquid chromatography, where the retention volumes can achieve very high values, the elution volume in SEC is limited by the interval $V_0 - V_t$, where $V_t = V_0 + V_i$ is the total volume of the mobile phase in the column. The effective volume of an SEC column in which the molecules can elute is approximately in the range of $0.4V_c - 0.8V_c$, where V_c is the volume of the column:

$$V_c = V_0 + V_i + V_g \tag{3.2}$$

where V_g is the volume occupied by the solid matrix (gel). For instance, for a 300 × 8-mm SEC column, the effective volume is within the range of about 6–12 mL. As a consequence of the limited range of the elution volume, the selectivity of SEC is lower than that of other types of liquid chromatography.

The distribution coefficient is independent of the length and inner diameter of the SEC column, but depends on the pore size distribution of the material used as the column packing. Although this property of the distribution coefficient allows good comparison of the results obtained using different packings under different experimental conditions, the distribution coefficient is rarely used and the elution volume itself is mostly used to plot SEC chromatograms.

Much attention was paid to finding a direct relation between the distribution coefficient and the size or even molar mass of eluting macromolecules. This is a very attractive idea, because it would make SEC an absolute method of molar mass determination. However, the obtained theoretical results never found real applications.

3.2.2 Restricted Diffusion

The restricted diffusion separation mechanism is based on the idea that the time needed for macromolecules to diffuse in and out of the pores is comparable with the time that they stay in a given column zone. In such a case, the permeation depth is governed by the diffusion coefficient, which is indirectly related to molecular size. The large molecules penetrate slowly and thus do not stay in a given chromatographic zone long enough to penetrate into the entire available volume. The idea of restricted diffusion implies that the elution volume should depend on the flow rate, which is typically not true. However, separation by restricted diffusion may partially take place at the separation of high-molar-mass polymers or at high flow rates.

3.2.3 Separation by Flow

Separation by flow (hydrodynamic chromatography) is based on the idea of flow through a narrow capillary in which there is a parabolic velocity profile of the

liquid flow. A column packed with small, solid nonporous particles creates a system of narrow capillaries. For each molecule there is an excluded volume in the proximity of the channel walls given by its geometrical dimensions. The large molecules statistically more frequently occur closer to the capillary center and therefore flow faster than the smaller molecules, which can be situated close to the wall where the flow is slow. Although hydrodynamic separation is in principle different from size exclusion, it separates according to the particles' size in the same order as SEC and thus does not destroy steric separation. Separation by flow may take place at the region of very high molar masses. This is probably one of the reasons why the experimental determination of the limit of the total exclusion is not as straightforward as one might expect, because separation by flow can occur beyond the molar mass corresponding to the total exclusion limit.

Although over a certain molar mass all molecules should elute together at elution volume V_0, molecules larger than the column exclusion limit are separated by flow and elute at elution volumes smaller than V_0. An example of concurrent SEC and hydrodynamic separation of polystyrene standards is shown in Figure 3.1. The nominal exclusion limit of the applied column set is about 30,000 g/mol. That means the standards with molar mass 34,500 g/mol and less are separated by SEC, whereas the standards over this limit are separated by flow. The most significant parameters affecting the separation by flow are the ratio of the polymer hydrodynamic diameter to the diameter of the packing particles and the pore diameter related to the diameter of the packing particles.

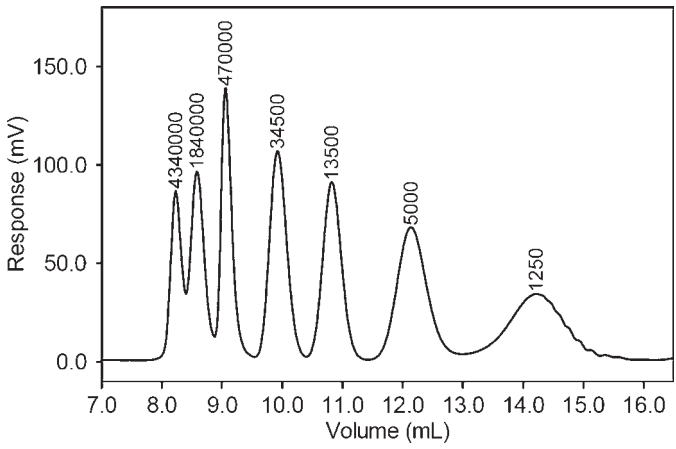

Figure 3.1 Separation of polystyrene standards using 2 × PLgel Mixed-E 300 × 7.5-mm 3-μm columns. THF, 1 mL/min, 40°C. Standards 1250 g/mol, 5000 g/mol, 13,500 g/mol, and 34,500 g/mol are separated by SEC separation, whereas standards 470×10^3 g/mol, 1.84×10^6 g/mol, and 4.34×10^6 g/mol are separated by hydrodynamic chromatography.

3.2.4 Peak Broadening and Separation Efficiency

A monodisperse compound injected into an SEC column should theoretically elute as a narrow rectangular peak of width equal to the injected volume and the area proportional to the detector sensitivity and injected mass. However, in real chromatography the span between the elution volume of the first eluting molecules and the elution volume of the last eluting molecules is much greater than the volume of injected sample and the real peak is of different shape and height compared to the ideal rectangular peak. The explanation is that the peak of the monodisperse solute is spread during the flow through the column. The major sources of peak broadening are diffusion along the column axis, eddy diffusion, limited velocity of the mass transfer between the stationary phase and the mobile phase, and the void volume of the chromatographic system.

A peak of a monodisperse compound can be approximated by a Gaussian function:

$$G(V) = \frac{A}{\sigma\sqrt{2\pi}} e^{-\frac{(V-V_e)^2}{2\sigma^2}} \tag{3.3}$$

where $G(V)$ is the detector response as a function of elution volume, σ is the standard deviation of the Gaussian function, V is the elution volume, V_e is the elution volume of the apex of the chromatographic peak, and A is a parameter related to the sensitivity of the detection system and directly proportional to the injected mass (i.e., it can be understood as the area of the peak). The standard deviation describes the broadness of the peak. Besides σ the broadness of the peak can be characterized by a width at the baseline W or at half height $W_{1/2}$ related to the standard deviation as $W = 4\,\sigma$ and $W_{1/2} = 2.355\sigma$.

A chromatogram of a polydisperse polymer can be assumed to be a superposition of chromatograms of individual macromolecules with different molar masses, each of them being approximated by a Gaussian function. A real chromatogram of a polydisperse polymer is broadened due to the real broadness of the molar mass distribution and due to the peak broadening effects. Because of peak broadening, the real peak width is broader than would correspond to the molar mass distribution and thus processing an SEC chromatogram without peak broadening correction yields broader molar mass distribution. A general relation between the experimental chromatogram $G(V)$ and the true chromatogram $W(y)$ is expressed by Tung's equation:[3]

$$G(V) = \int_0^\infty W(y)G(V,y)\,dy \tag{3.4}$$

where V and y are elution volumes and $G(V,y)$ is the instrumental spreading function. The spreading function can be understood as a response of a given chromatographic column to the infinitesimally short injection of a perfectly monodisperse polymer with molar mass corresponding to the elution volume y.

The chromatogram $W(y)$ would be recorded by means of a hypothetical column with unlimited resolution power.

Peak broadening (band broadening; zone spreading; axial, longitudinal, column, or instrumental dispersion) is an unwanted effect that decreases separation efficiency. In SEC the available elution volumes are limited by the exclusion limit and limit of total permeation and thus the minimization of the sources of peak broadening is of primary importance. Knowledge and understanding of the factors leading to peak broadening are important for the optimization of separation conditions. The most frequent peak broadening is the symmetrical or Gaussian type that broadens the molar mass distribution, decreases M_n, and increases M_w and M_z. In a rigorous manner, the compensation of the peak broadening is necessary for the calculation of the true molar mass distribution and true molar mass averages from the chromatogram obtained by SEC experiment.

To compensate for peak broadening it is necessary to transfer the experimental chromatogram into an ideal chromatogram that would be recorded without peak broadening. The peak width and shape of the corrected chromatogram reflect only the width and shape of the molar mass distribution. Numerous methods were proposed to correct for the effect of peak broadening. Peak broadening correction used to be a very popular subject of scientific papers dedicated to SEC theory. A comprehensive and critical overview of the different methods used to correct band broadening can be found in reference 4. However, none of the published methods is readily adaptable for routine measurements. With the development of high-performance columns, correction for peak broadening became less important and usually is not applied. The effect of peak broadening can be significant in the case of SEC analysis of very narrow polymers where determination of the true polydispersity may be of interest. An interesting question related to the correction for peak broadening may be, "How narrow are narrow polymer standards?" In the case of broad polymer samples, the effect of peak broadening usually can be ignored without significant impact on the accuracy of results.

A simple method of peak broadening correction assumes Gaussian SEC chromatograms and nominal polydispersity of polystyrene standards to be correct. Several standards are measured and a correction factor

$$R = \left[\frac{(M_w/M_n)_{\text{nom}}}{(M_w/M_n)_{\text{exp}}} \right]^{\frac{1}{2}} \tag{3.5}$$

is calculated by simply comparing the nominal (nom) and experimental (exp) polydispersity. The true molar mass averages of samples under analysis are then calculated from the experimental results and R:

$$M_{n,\text{true}} = \frac{M_{n,\text{exp}}}{R} \quad \text{and} \quad M_{w,\text{true}} = RM_{w,\text{exp}} \tag{3.6}$$

Although this procedure is rather simplified, and the correctness of polydispersity of the calibration standards may be questionable, one can see that even in the case of a relatively large difference between nominal and experimental

polydispersities the correction of molar mass averages lies in the range of only a few percent.

The extent of peak broadening and the separation efficiency of the chromatographic column can be characterized by the *number of theoretical plates* and the *height equivalent to a theoretical plate* (*H, plate height*). The plate height is defined as the variance (σ^2) of the eluting peak divided by the length of the column (L):

$$H = \frac{\sigma^2}{L} \tag{3.7}$$

The relation between the separation efficiency and the parameters characterizing the chromatographic separation process was derived by van Deemter et al.[5] and expressed as:

$$H = A + \frac{B}{u} + Cu \tag{3.8}$$

where u is the linear velocity of the mobile phase (cm/s), A is the contribution of eddy diffusion, B is the contribution of axial diffusion and C is related to the mass transfer between the stationary and mobile phases. Equation 3.8 describes three basic processes that contribute to plate height: (1) eddy diffusion, caused by the flow of solute at unequal rates through the tortuous pathways of the bed of the packing particles (which means the packed column functions as some kind of a static mixer); (2) axial diffusion, in which solute molecules diffuse axially from the center of the zone; and (3) nonequilibrium or mass transfer, in which the limited speed of diffusion in and out of the stationary phase causes broadening of the solute zone, because the molecules being at a given time inside the pores are delayed behind those that are already carried by the flow stream.

Linear velocity is easily calculated from the volume flow rate in mL/min dividing by πr^2, where r is the inner radius of the column. Equation 3.8 shows that the axial diffusion becomes less pronounced with increasing flow rate while the effect of the mass transfer between the phases increases. In contrast to low-molar-mass compounds, the polymers have generally low diffusion coefficient and thus the effect of axial diffusion is negligible as shown by the interrupted flow experiment when the polymer was kept in the columns for many hours before the elution continued.[6] The relation H versus u touches minimum at a certain u that represents the most optimum flow rate for a given column. In routine practice the maximum pressure limit for the columns and the analysis time must be considered and a flow rate in the range of 0.5 to 1 mL/min is mostly used with standard 300 × 8-mm SEC columns.

The number of theoretical plates (N) can be calculated from the chromatogram of a monodisperse low-molar-mass compound:

$$N = 16\left(\frac{V_e}{W}\right)^2 = 5.54\left(\frac{V_e}{W_{1/2}}\right)^2 \tag{3.9}$$

where W and $W_{1/2}$ are the peak width in the baseline and in half height, respectively. The peak width W is measured between two crosspoints of the baseline and two tangents drawn from the inflection points of the ascending and descending sides of the peak. The height equivalent to a theoretical plate is calculated as L/N. The peak width is indirectly proportional to the square root of the plate number (Equation 3.9), that is, smaller plate numbers mean broader peaks and less resolution. It may be important to note that the plates do not really exist; they are created by the imagination, which helps to understand the separation process and serves as a way of measuring the column efficiency. The plate height decreases with decreasing particle size and thus columns packed with smaller particles are more efficient, but they are also less suitable for the analysis of polymers with high molar mass owing to high backpressure and possibility of shearing degradation. As shown by semiempirical prediction[7] and confirmed by experimental data,[8] the plate height increases with decreasing distribution coefficient K_d. For example, the H-versus-K_d plot published in reference 7 shows about a triplicate increase of H with the decrease of K_d from 0.4 to 0.2. At very low K_d close to the total exclusion limit the trend is reversed and H starts to decrease. That means the H-versus-K_d plot shows a maximum at low K_d, but the plate height values at low K_d are still significantly higher compared to the region of larger K_d.

Peak symmetry is another parameter that characterizes the quality of column:

$$s = \frac{a}{b} \tag{3.10}$$

where a and b are the peak widths measured at 10% of peak height on either side of the perpendicular from the baseline to the peak apex (a is the distance from the center line to the descending part of peak).

Peak symmetry is a measure of peak tailing that has negative effect on the resolution. A little tailing (roughly $s < 1.2$) is normal, but excessive tailing indicates a damaged column bed, enthalpic interactions of the analyzed molecules with column packing, or other non-SEC effects. Various compounds can be used to measure the number of theoretical plates and symmetry, for example, propyl benzene, acetone, toluene, dicyclohexyl phthalate, ethyleneglycol, glucose, and orthodichlorobenzene. Modern 300 × 7.5-mm SEC columns provide per column more than 24,000 plates, 15,000 plates, 10,000 plates, and 5,000 plates for 3, 5, 10, and 20 μm packing size, respectively. However, the plate number usually decreases with column use.

The separation of two components can be characterized by *resolution*:

$$R_S = \frac{2(V_2 - V_1)}{W_1 + W_2} \tag{3.11}$$

where V and W are elution volume and baseline width of the two components. Resolution is the difference in elution volumes divided by the average peak width. The difference of elution volumes of the two components ($V_2 - V_1$) is a reflection of the selectivity of the separation process, whereas W represents the

zone spreading that is related to the efficiency of the process. At a resolution of 1 the two peaks are not completely separated, but the peak area overlap is only 2%. The complete separation is achieved at a resolution of 1.25.

Equation 3.11 tells us that the resolution is controlled by both selectivity and efficiency, and that with columns of low efficiency (e.g., worn out by excessive or improper use), which provide very broad peaks, one can barely achieve satisfactory resolution; on the other hand, even highly efficient columns cannot provide satisfactory resolution if the separation process is not sufficiently selective. Resolution increases with the square root of column length or number of theoretical plates. If the column length (number of theoretical plates) is doubled, the resolution increases by a factor of $\sqrt{2}$. In SEC the quantity called *specific resolution* (R_{SP}), which takes molar mass of the two compounds into account, provides better characterization of the separation efficiency of SEC columns:

$$R_{SP} = \frac{2(V_2 - V_1)}{(W_1 + W_2)(\log M_1 - \log M_2)} \tag{3.12}$$

The specific resolution can be determined by two monodisperse polymer standards. If the polymer standards are not monodisperse, the widths W_1 and W_2 in the above equation are divided by the polydispersity M_w/M_n.

The resolution of two compounds in the interaction types of liquid chromatography is defined by the equation:

$$R_S = \frac{2(V'_{R2} - V'_{R1})}{W_1 + W_2} = \frac{1}{4}\frac{r_{1,2} - 1}{r_{1,2}}\frac{k_2}{1 + k_2}\sqrt{N} \tag{3.13}$$

where $V'_R = V_R - V_t$ is the net retention volume (the term *retention volume* is used as the equivalent to *elution volume* to differentiate between the interaction and non-interaction separation),

$$r_{1,2} = \frac{V'_{R2}}{V'_{R1}} \tag{3.14}$$

is the relative retention (selectivity), and

$$k = \frac{V_R - V_t}{V_t} \tag{3.15}$$

is the capacity factor.

Equation 3.13 shows that the resolution in interaction liquid chromatography is controlled by selectivity ($r_{1,2}$), capacity (k), and column efficiency (N). In SEC, contrary to other types of liquid chromatography, capacity does not play a role and resolution can be controlled solely by selectivity and column efficiency. The number of theoretical plates is related to the quality of column packing and column length. The usual way of increasing the number of theoretical plates in SEC is connection of two or more columns in series. However, it is necessary to stress that the resolution is proportional only to the square root of the number

of theoretical plates and doubling the number of theoretical plates by using, for example, four columns instead of two improves resolution by a factor of 1.4, but the analysis time increases by a factor of 2. Selectivity in SEC is related to the slope of the calibration curve. That means SEC columns of high plate numbers do not necessarily provide good resolution unless the slope of the calibration curve is sufficiently low. Although the calibration curves are usually slightly curved, they can be approximated by a linear fit at least for a certain range of the elution volume:

$$\log M = a + bV \tag{3.16}$$

Then the slope equals:

$$b = \frac{\log M_1 - \log M_2}{V_2 - V_1} \tag{3.17}$$

where M_1 and M_2 are molar masses eluting in the elution volumes V_1 and V_2. The slope of the linear fit shows how well a column can separate peak apexes of polymers of different molar mass, while the peak widths of monodisperse polymers are related to the number of theoretical plates. The separation increases with decreasing slope, and to achieve good separation the slope should be of minimum value. The slope of the calibration curve is related to the pore volume, which should be as large as possible. Selectivity further depends on the pore size of the column packing material and the selection of SEC columns with separation range appropriate for a given polymer sample is of primary importance. For example, if the pore sizes are too small for the macromolecules to be separated, all molecules elute at the limit of total exclusion. On the other hand, packing material with large pore sizes cannot separate oligomeric mixtures. For a given column set, the slope of the calibration curve and consequently the selectivity can be different for different molar mass regions.

Figure 3.2 compares three column sets of different separation range and selectivity. Note that the column sets (□) and (■) have similar separation range, but their slopes in the region of lower and higher molar masses are different. Figure 3.3 compares the calibration curves established by the same type but a different number of SEC columns. In this case the use of more columns not only improves the selectivity due to lower slope, but also increases the number of theoretical plates. If the columns are properly calibrated and of appropriate separation range, the molar mass results should not depend on the columns employed for the measurements. However, in reality one can often find differences between the distribution curves determined using different column sets even though other separation conditions are identical (e.g., see Figure 3.4).

The reciprocal of the slope of the calibration curve over one molar mass decade (i.e., logarithm of molar mass interval of one) related to the column cross-sectional area is another parameter that can be used to characterize the

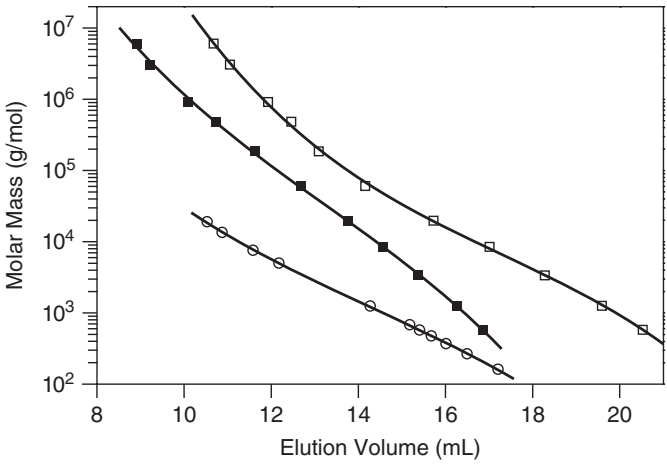

Figure 3.2 Calibration curves of three column sets 2 × 300 × 7.5 mm with different selectivity in the region of high and low molar masses. Set (□) compared to set (■) shows lower selectivity in the region of high molar masses and higher selectivity in the lower-molar-mass region. Set (□): $R_{SP} = 2.86$ and 3.83 for pairs of standards 915,000/60,450 and 60,450/3370, respectively. Set (■) : $R_{SP} = 4.22$ and 3.37 for pairs of standards 915,000/60,450 and 60,450/3370, respectively. Set (◯) has the highest selectivity in the lower-molar-mass region, but the separation range is limited.

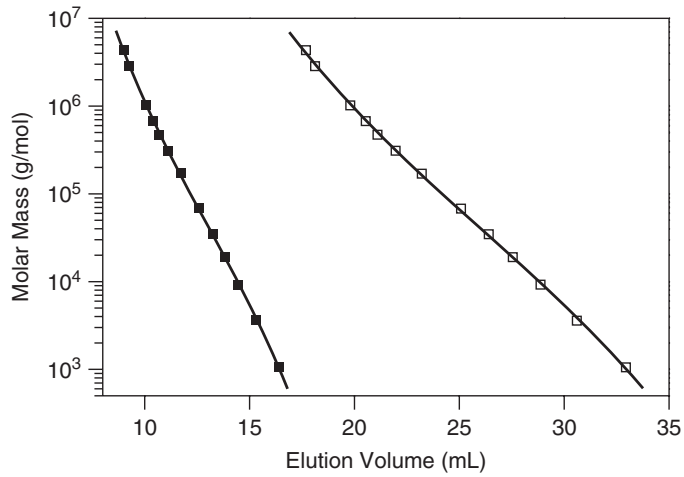

Figure 3.3 Calibration curves obtained by sets of two and four PLgel Mixed-C 300 × 7.5 columns. Two columns (■) : $R_{SP} = 3.88$, $SP = 4.94$; four columns (□): $R_{SP} = 4.39$, $SP = 10.30$. R_{SP} calculated for standards 675,000 and 68,000 g/mol.

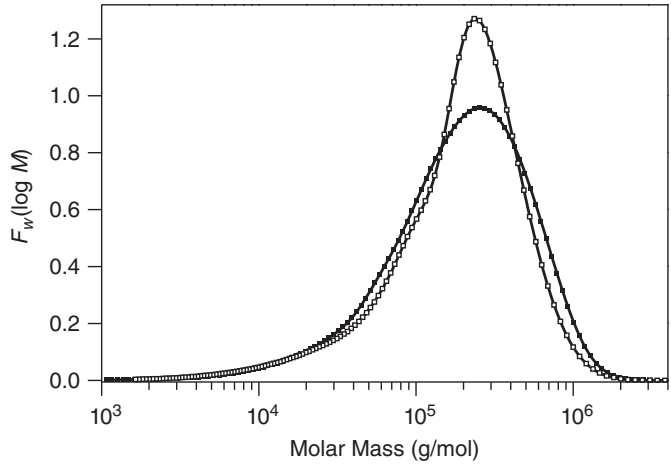

Figure 3.4 Differential distribution plots determined using column sets (■) and (□) from Figure 3.2. Molar mass averages: M_n (g/mol) = 89,900 ± 1200 (Set □), 79,900 ± 900 (Set ■), M_w (g/mol) = 262,800 ± 1000 (Set □), 277,600 ± 500 (Set ■), M_z (g/mol) = 444,000 ± 2000 (Set □), 526,900 ± 2600 (Set ■).

separation performance (*SP*) of SEC columns:[9]

$$SP = \frac{V_M - V_{10M}}{\pi r^2} \tag{3.18}$$

where r is the inner radius of the column (in cm), and V_M and V_{10M} are the elution volumes (in mL) of calibration standards with molar mass M and ten times the value of M, respectively. According to reference 9, the minimum *SP* is six, while the value of R_{SP} should be greater than 2.5.[10] The two parameters defined by Equations 3.12 and 3.18 are not entirely equivalent: R_{SP} reflects both selectivity in the sense of difference of elution volumes and efficiency in the sense of the peak width; *SP* reflects only the column selectivity in terms of the slope of the calibration curve. The limit of separation performance of six was suggested by experience and may not be fulfilled by two mixed columns. For example, separation of two polystyrene standards of molar masses of 675,000 g/mol and 68,000 g/mol using two PLgel Mixed-C 300 × 7.5 columns results in *SP* of about 4.9 and R_{SP} of about 3.9 (i.e., *SP* is below and R_{SP} well above the recommended values). As shown in Section 3.5.6, the increased number of columns need not necessarily have significant effect on the molar mass averages.

SEC resolution decreases with increasing molar mass, as is clearly illustrated by the separation of oligomers, where the resolution of neighboring members of the oligomeric series rapidly diminishes with the increasing polymerization degree (see chromatograms in Section 3.5.5). In the high-molar-mass region large differences in molar mass are reflected in small changes in elution volume.

3.2.5 Secondary Separation Mechanisms

All mechanisms describing the principle of SEC separation assume that the stationary phase acts only as an inert matrix that does not interact with the solute. In real SEC highly skewed chromatograms and even polymer molecules eluting behind the limit of total permeation can occur. However, severe tailing can also result from a possible void at the column inlet, which can be created during long-term usage of the column. Tailing from poor column packing can be easily distinguished from tailing due to column interactions by measuring a few narrow calibration standards. If the peaks of standards are symmetrical, the peak tailing can be explained by interactions. The characteristic feature of the tailing due to damaged column packing is that all peaks in a chromatogram show similar shape. The measurement of molar mass or RMS radius across the peak by a MALS detector often reveals that molar mass and RMS radius decrease only over a part of the peak and then reach a plateau parallel with the volume axis or even show the increase from certain elution volume. Such behavior indicates enthalpic interactions of solute with stationary phase, or a specific anchoring behavior of branched polymers (described in Section 6.2.1).

The term *adsorption* is generally used to describe SEC separation in which enthalpic interactions play a role. The enthalpic interactions can affect the SEC separation to different extents depending on particular properties of SEC column packing, sample, and solvent. In the ultimate case the sample can be irreversibly retained in the SEC columns. The type of interactions may not be always known. They can be dipole–dipole interactions, dispersion forces, $\pi-\pi$ interactions (noncovalent interactions between organic compounds containing aromatic rings), hydrogen bonding, ionic exclusion and inclusion, hydrophobic interactions, or interactions of polar groups with the polar groups of the column packing. Ionic interactions are common in separation of various water-soluble polymers in aqueous solvents. Ion exclusion is a consequence of the presence of anionic groups in the SEC packing, when negatively charged polymers are exluded from the pores due to electrostatic repulsive forces. This effect results in earlier elution than would correspond to hydrodynamic volume and thus in the overestimation of the molar mass calculated on the basis of column calibration. Ion inclusion is interaction of anionic and cationic functionalities, resulting in delayed elution and thus underestimation of molar mass. Reduction of mobile phase pH to prevent dissociation of carboxyl groups and increase of the ionic strength of the mobile phase in order to shield electrostatic interactions are possible ways to eliminate ionic interactions.

Besides solute–column packing interactions the elution volume in SEC can be influenced by incompatibility between solute and packing, which results in early elution. Strong interactions are very common in the case of polymers bearing amino groups analyzed in tertahydrofuran using columns packed with styrene-divinylbenzene gels. Amine-containing polymers have been recently applied for the production of environmentally friendly waterborne paints and thus problems with their SEC characterization may be frequent. The interaction

of amine-containing polymers with styrene-divinylbenzene gels is sort of surprising, because the gels are hydrophobic and they are not supposed to contain polar functional groups capable of interacting with polymer. It appears that the styrene-divinylbenzene gels may contain polar groups from irreversibly adsorbed or chemically bonded auxiliary compounds of the manufacturing process or polar groups that are created during column usage and aging. THF has a tendency to form peroxides and contains a certain level of oxygen even if degassed. Both oxygen and peroxides can contribute to the oxidative formation of carbonyl, carboxyl, or peroxy functional groups. The functional groups in SEC stationary phase can also occur due to irreversibly retained previously analyzed materials. My experience shows that column properties depend on its history and previous applications (i.e., columns have some type of memory effect). Deterioration of separation efficiency is usually faster if the columns are applied to the analysis of polar polymers as compared to when they are used for the characterization of well-soluble neutral polymers. Besides amino groups, carboxyl groups represent another type of group increasing probability of interactions.

Hydrophobic interactions are frequent in the case of water-soluble polymers analyzed on hydrophylic gel packing based on poly(hydroxyethyl methacrylate) (HEMA) crosslinked with ethylenglycol dimethacrylate. The polymer molecules of water-soluble polymers typically consist of hydrophylic polar groups giving water solubility and hydrophobic chains. The HEMA packing shows similar composition and such hydrophobic chains of polymer interact with the hydrophobic backbone of HEMA. The analysis of sulphonated polystyrene is a typical example.

Enthalpic interactions can result in the adsorption of a part of the injected samples on the surface and in the pores of column packing. This effect is often indicated by poor repeatability and by different peak areas obtained by repeated injections. Sometimes the columns can show some kind of saturation effect; that is, after column saturation by several consecutive injections the peak areas become constant and the repeatability of molar mass averages improves.

Various mobile-phase additives can be used to suppress the interactions. Diethanol amine in the amount of 0.1% can be used for the analysis of amine-containing polymers in THF to prevent adsorption. An example is presented in Figure 3.5. Another way of suppressing the interactions is saturation of the column by multiple injections of the problematic polymer or more effectively by the addition of the polymer directly into the mobile phase. Adsorption also can be suppressed by sample derivatization (see Section 3.5.1.1).

3.3 INSTRUMENTATION

There is no principal difference between the instrumental setup used for SEC measurements and other types of liquid chromatography, and a “liquid chromatograph” can be easily converted to an “SEC chromatograph” by a simple

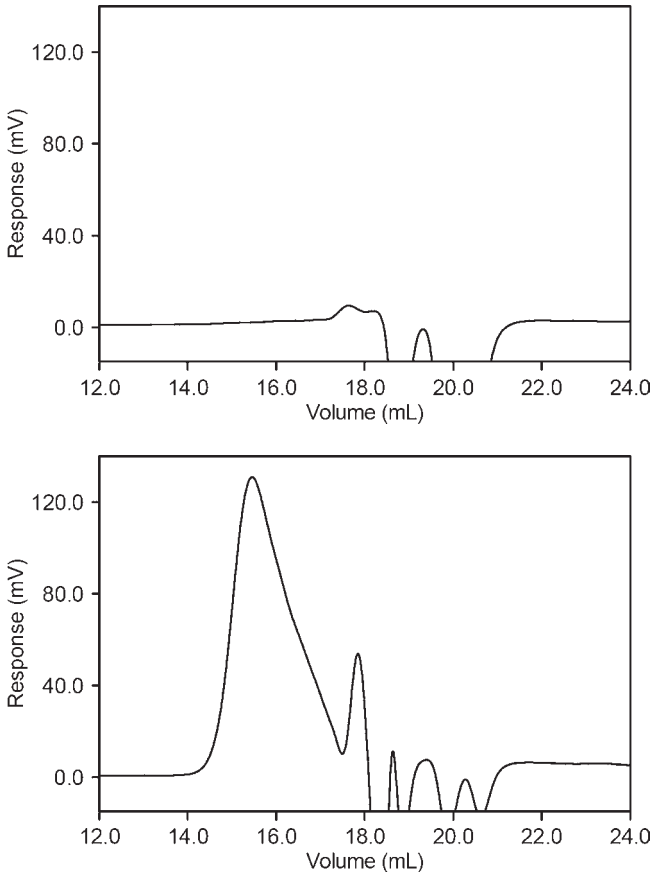

Figure 3.5 RI chromatograms of copolymer 2-ethylhexyl methacrylate (25%) and dimethylaminopropyl methacrylamide (75%) measured in THF (top) and THF containing 0.1% diethanol amine (bottom). In pure THF, the sample was completely retained in the columns due to enthalpic interactions that were suppressed by the addition of diethanol amine.

swapover of columns. In contrast to other types of liquid chromatography, SEC does not use gradient elution. Also some types of detectors are rarely used while other detectors, such as light scattering or viscometry, are almost exclusively used in SEC.

A chromatographic setup for SEC consists of a solvent reservoir, a degassing device, a solvent delivery pump, an injector, columns, a detector system, a waste reservoir, and a PC with SEC software allowing data acquisition and processing. A pulse dampener is another possible part of the solvent delivery system, which may be needed in some applications. The pulse dampener, which is placed between the pump and injector, is usually not needed for RI detectors in the case of a modern HPLC pump, but it may improve the signal of an online viscometer that is extremely sensitive to flow pulsation.

Mobile-phase degassing is necessary to avoid malfunction of the solvent delivery pump. An air bubble in the HPLC pump causes a momentary drop in the backpressure and decrease of the flow rate. The air bubbles that get into the column system stay in solution because of the system pressure, but when they arrive in a detector cell, where the system pressure is low, the bubbles can be released and cause spikes on the chromatogram. The elimination of spikes by a pressure restrictor after the detection system is not the best solution, especially in the case of RI detectors, which are generally not designed to withstand high pressures. Helium sparging, a traditional and effective way of degassing, has been widely replaced with inline vacuum degassers, which have become a part of most of today's solvent delivery systems. In contrast to inline degassing, helium sparging removes the air already in the solvent reservoir, which may be advantageous in the case of oxygen-sensitive solvents such as THF.

The solvent reservoir is typically a glass bottle of 1–2-L volume. Glass solvent containers are usually delivered with the HPLC pump. They are equipped with plastic caps containing several holes for polytetrafluorethylene (PTFE) tubing that delivers solvent to the pump. The end of the PTEF tubing is connected to a glass or stainless-steel frit that protects the pump from mechanical impurities. An original bottle, in which the solvent is supplied, can be used as a solvent container. The holes for the PTFE tubings can be directly drilled into the caps. A brown bottle should be used for THF to prevent degradation caused by light. The solvent reservoir must hold a sufficient amount of solvent to allow measurements of number of runs without the need for solvent refill. This is especially important in the case of an RI detector when the refill of solvent typically results in a significant change of baseline signal. The reservoir should isolate the solvent from contact with the laboratory environment in order to prevent solvent evaporation, reaction with oxygen, light-induced degradation, and absorption of moisture.

These requirements obviously do not apply to all solvents; for example, toluene has almost no tendency to degradation or moisture absorption, whereas THF is a typical example of solvent that requires special attention. Some experimenters recommend some means of agitation (e.g., magnetic stirring) to assure solvent homogeneity. Nevertheless, agitation is usually not needed for most solvents, including aqueous buffers.

A high-quality pump that is able to deliver solvent at a constant, pulse-free and reproducible flow rate is a crucial part of an SEC instrumental setup. Today's HPLC pumps are typically dual-head, having two independently driven pistons for optimal flow control. The pulse-free flow is achieved by a synchronized action of two pistons, where one piston fills the solvent into the chamber while the other provides flow to the columns. Inlet and outlet check valves are an important part of the HPLC pump. The most common check valve is the ball-type check valve, usually consisting of a ruby ball and a saphire seat. The check valve operates in a way such that when the pressure below the ball is higher than above the ball, the ball is lifted off the seat and liquid can flow through the valve. When the pressure above the ball is higher, it closes the valve by pushing the ball back to the seat,

preventing reverse liquid flow. It is worth mentioning that many pump-related problems are caused by improperly working check valves.

The sample solution can be injected by a manual six-port sample injection valve, or by means of an autoinjector (autosampler). The loop of the manual valve is filled with sample solution in the sample load position, and then the valve rotor is manually turned into the injection position to flush the loop into the eluent stream. The volume of the loop is usually 20–200 μL, but smaller or large volumes are also available. An excess volume of sample solution is used to flush the solvent completely out and to fill the loop properly. A typical feature of the manual injection valves is that they typically add about 10 μL of an extra volume corresponding to the inside channels. This fact is not important for conventional SEC or HPLC, but it should be taken into account for the online calibration of RI detectors or the determination of a specific refractive index increment in the case of a light scattering detection.

Automatic injectors called *autosamplers* or *autoinjectors* allow automatic analysis of large sample series and overnight operation. The samples are placed into 1–4 mL vials sealed with septa to avoid solvent evaporation. A significant advantage of most autosamplers over manual injectors is the possibility of changing the injection volume without changing the sample loop. The required volume of sample solution is withdrawn from a vial by a stepper motor–controlled syringe into a sample loop and injected into the eluent flow similarly as in the case of manual injectors. In the case of high-temperature SEC instruments, the autosampler compartment must be kept at high temperature and the sample dissolution is usually performed directly in the autosampler compartment. The autosampler can be programmed to agitate the sample periodically by rotation of a sample tray to promote dissolution, and the sample is then automatically filtered prior to injection.

A temperature-controlled column oven is another optional part of the SEC instrumental setup, which can contribute to results accuracy and repeatability because it maintains the column temperature constant. The column oven may not be necessary in the case of constant room temperature and especially when the molar mass is determined by a light scattering detector instead of column calibration.

An SEC setup can be purchased separately as a modular system or as an integrated apparatus incorporating a pump, an injector, a column oven, and detectors into one system. The integrated form is necessary in the case of high-temperature systems that are used for polymers that are not soluble in any solvent at room temperature. Polyolefins, such as polyethylene and polypropylene, are typical examples of polymers of great industrial importance, which require analysis at high temperatures. High-temperature SEC typically means that the columns are kept at a temperature over 100°C, mostly around 150°C. The temperature in the high-temperature SEC system must be maintained from the injector over columns to the detection system in order to prevent sample precipitation. The detectors are typically placed in the column oven. Should the sample leave the oven to reach

another detector, such as a high-temperature light scattering photometer, the connecting lines must be heated as well. In high-temperature SEC the actual flow rate is higher than the nominal flow rate of the chromatographic pump because of thermal expansion of the mobile phase. In trichlorobenzene at 150°C the flow rate increase is about 10%.

Some solvents may require temperatures of 60–80°C in order to decrease their viscosity. If the sample dissolves at room temperature, or remains in solution after dissolving at elevated temperature, then an ambient SEC system can be used for the measurements with column oven maintaining the requested temperature.

3.3.1 Solvents

A solvent is an important part of the SEC analysis. The solvent for SEC must be compatible with the column packing material and must dissolve the polymer requiring analysis. The solvent must form stable solutions to prevent precipitation of polymer from solution prior to or during analysis. From this viewpoint, thermodynamically good solvents should be preferred. The thermodynamic quality of the solvent increases with increasing temperature and thus analysis above room temperature is necessary for some polymers. The solvent viscosity preferably should be low, because with increasing viscosity the separation efficiency decreases and the backpressure increases. However, some polymers are difficult to dissolve and the only choice may be highly viscous solvent such as dimethyl sulfoxide. Additionally, the solvents for SEC should be of low toxicity, nonflammable, stable, noncorrosive with respect to the chromatography system and columns, cheap, and easily purifyable. An important parameter is the specific refractive index increment of a polymer requiring analysis that is directly proportional to the RI detector response. For UV detection the solvents must have almost no absorption at the wavelength that is to be used. Typically, it is impossible to meet all the previous requirements and mostly the requirement of good solubility prevails over others. Unlike gradient liquid chromatography, solvents of HPLC purity are not necessary and purity over 99% is mostly appropriate for SEC measurements.

Tetrahydrofuran (THF) represents the most common solvent for organic SEC, because it dissolves a wide range of synthetic polymers. THF does not dissolve biopolymers such as proteins or polysaccharides, and some important synthetic polymers such as polyamides, polyolefins, poly(ethylen terephthalate), and poly(vinyl alcohol). Since THF is highly hygroscopic it should be kept in closed bottles to prevent absorption of moisture from the environment. Besides ability to dissolve many polymers, other advantages of THF include low UV cutoff, low viscosity, and acceptable price. Disadvantages include relatively high toxicity, high volatility, high tendency to absorb moisture and air, formation of explosive mixtures with air, and formation of explosive peroxides and other compounds with oxygen. The reactivity of THF with oxygen is potentially dangerous, because the peroxides can concentrate by THF evaporation and they can explode

at temperatures around 120°C. Despite potential danger THF can be safely utilized with no special laboratory precautions. Oxidation is efficiently prevented by stabilization with 0.025% 2,6-ditert-butyl-4-hydroxy toluene (BHT).

Eluent from SEC columns containing small amounts of polymer can be easily distilled and reused in order to reduce analysis costs and environmental burden. The distillation is performed with the addition of copper oxide (about 1 g/L) to remove possibly present peroxides. Water can be removed by molecular sieves 3 Å or by potassium hydroxide prior to distillation, but the distillation itself is mostly sufficient for the purification of waste THF. The distillation is performed using a filled glass distillation column of about 1 m in length placed in a fume hood covered for safety reasons with fencing. Freshly distilled THF can be used for SEC measurements with UV detection or stabilized with BHT. THF forms strong hydrogen bonds with hydroxyl groups and thus creates associates containing one THF molecule per hydroxyl group. The associates have larger dimensions compared to the original compounds and elute at lower elution volumes than would correspond to the dimensions of molecules without association with THF.

Association between sample molecules and THF must be taken into account for the interpretation of chromatograms of some oligomers. A typical feature of RI chromatograms recorded from the analysis in THF is the existence of three solvent peaks. These peaks (Figure 3.6) belong to water, nitrogen, and oxygen. A good resolution of the three peaks is an indication of good separation efficiency of the columns and thus the peaks can be used as a quick check of column separation performance (Figure 3.7). One of the three peaks can be utilized as a flow marker.

Toluene is a traditional SEC solvent that dissolves nonpolar and medium-polar polymers such as polystyrene, polybutadiene, and polyisoprene. It is used

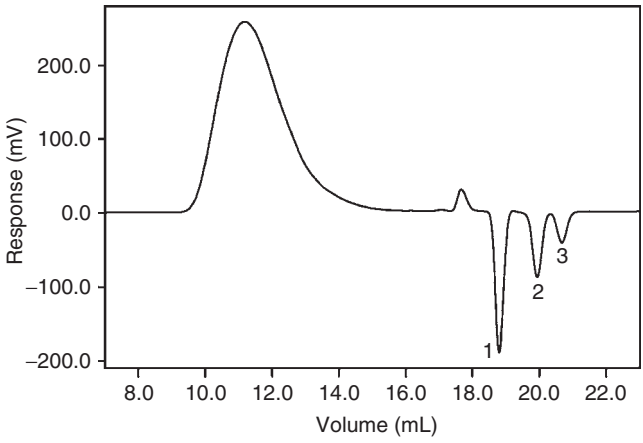

Figure 3.6 RI chromatogram of a polydisperse polymer in THF showing three typical negative peaks: 1 = water, 2 = nitrogen, 3 = oxygen.

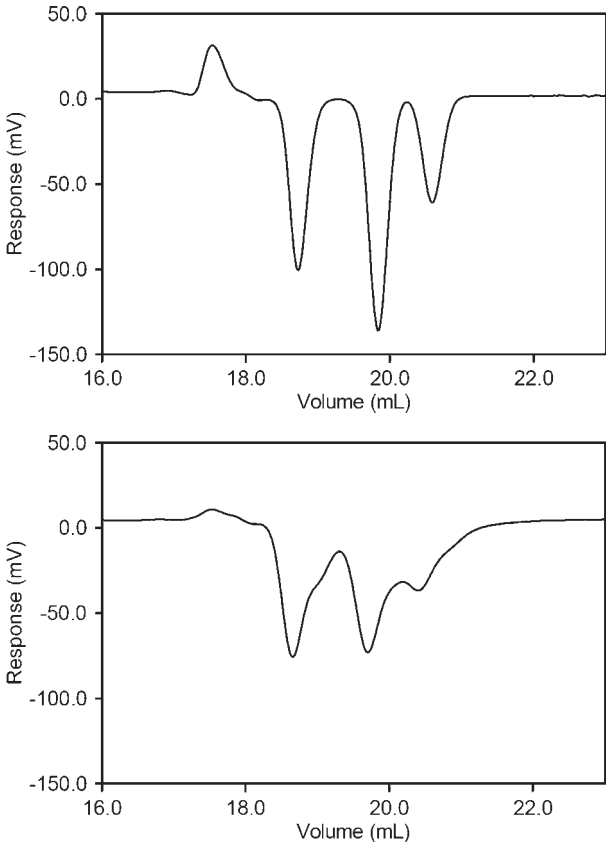

Figure 3.7 Solvent peaks in THF recorded with good columns (top) and the same columns after long-term use (bottom).

instead of THF for the analysis of poly(dimethyl siloxane), which has very low RI response in THF. Advantages include relatively low toxicity and excellent stability, but it cannot be used with UV detection.

Chloroform is another traditionally used SEC solvent. Despite some advantages such as very good ability to dissolve various polymers, UV transparency, and nonflammability, $CHCl_3$ has several serious disadvantages. It is very toxic, which is especially serious due to high volatility. The oxidation leads to extremely dangerous phosgene. The waste disposal cost is high and in addition chloroform is highly corrosive and thus its application is justified only if there is no other appropriate alternative.

THF, toluene, and chloroform represent good solvents for crosslinked polystyrene gels.

1,2,4-Trichlorobenzene (TCB) represents a typical solvent for SEC of polyolefins at temperatures above 135°C. It dissolves polystyrene and thus polystyrene standards can be employed for column calibration.

1,1,1,3,3,3-Hexafluoro-2-propanol (hexafluoroisopropanol, HFIP) is an interesting solvent due to its properties. It exhibits strong hydrogen-bonding properties

and ability to dissolve many polymers, including those insoluble in other organic solvents such as polyamides (e.g., nylon 6), polyacrylonitrile, and poly(ethylene terephthalate). HFIP is corrosive, and UV transparent up to about 190 nm with low refractive index ($n_D = 1.276$), which results in significantly higher polymer dn/dc compared to other solvents. The applicability of HFIP is limited by high price, which can be reduced by redistillation and/or using narrow-bore SEC columns. Addition of about 0.1% sodium trifluoroacetate is used to suppress polyelectrolyte effects of the analyzed polymers. Poly(methyl methacrylate) narrow standards must be used for column calibration instead of the typically used polystyrene, which is insoluble in HFIP. Very low refractive index and consequently dn/dc significantly higher than in other solvents make HFIP an ideal solvent for SEC measurements with a light scattering detector.

Dimethylformamide (DMF) is typically used with the addition of about 0.1% lithium bromide. It is a good solvent for polyacrylonitrile or poly(vinyl alcohol). Polystyrene standards are soluble in DMF, but interaction with polystyrene-based packing can influence the elution and thus poly(ethylene glycol) and poly(ethyle oxide) standards can be used instead.

N-methylpyrrolidone (NMP) has desirable properties such as low volatility, low flammability, relatively low toxicity, and ability to dissolve many polymers. It may represent a good alternative for polymers that are not soluble in THF.

Dimethylsulfoxide (DMSO) is another organic solvent that can be used for polymers that are insoluble in THF or other organic solvents. DMSO represents the best choice for urea formaldehyde resins that are insoluble in most other solvents. It can be also used for the analysis of starch.

o-Chloronaphthalene is an infrequently used solvent that can be used at very high temperatures of about 220°C for the characterization of polyphenylene sulfide and possibly other polymers with limited solubility.

Water, usually with the addition of various salts, is used for the analysis of proteins and other water-soluble polymers such as dextran, pullulan, hyaluronic acid, or poly(acrylic acid). Typical salts are $NaNO_3$ or Na_2SO_4 in concentration of about 0.1 M or phosphate buffer. Other possible additives include surfactants such as sodium dodecyl sulphate (SDS) or urea. The salt concentration and pH of aqueous solvents may alter solubility of biopolymers. The ionic strength affects the conformation and size of polyeclectrolytes that expand at low salt concentrations and create random coil conformation when repulsive electrostatic forces are sufficiently shielded by salt ions.

Mixed eluents can be used in some special cases in order to achieve solubility, and suppress aggregation or interactions of solute with column packing. For example, addition of 10–20% organic solvent (methanol, acetonitrile, THF) to water can suppress hydrophobic interactions of water-soluble polymers with column material. Addition of a small level of methanol to THF can promote solubility of polar compounds. However, the separation process and obtained results can be affected by preferential solvation of the analyzed polymer with one component of the mobile phase. Other possible issues are higher tendency of RI signal to drift due to preferential evaporation of one of the components

and extremely intensive solvent peaks at the end of the chromatogram that can affect the determination of peak limits in the case of imperfect separation from the main polymer peak.

All solvents should be of purity above 99% and free of mechanical impurities. Pre-filtration of solvents such as toluene or THF is not necessary, but it should be always performed in the case of solvents containing salts, because the salts, even if of high chemical purity, often contain a substantial level of particulate matter, such as mechanical impurities from the manufacturing process or bits of plastic generated by rubbing the plastic container during transport and handling.

3.3.2 Columns and Column Packing

SEC columns are the most important part of an SEC instrumental setup that is critical for efficient separation. Today's columns are typically 300 mm in length and 7.5, 7.8, or 8 mm in inner diameter. Stainless steel is the most frequent material for SEC columns. Biocompatible glass columns are used for the separation of biomaterials that can degrade in contact with metals. Narrow-bore columns of 4.6-mm inner diameter allow significant reduction of solvent usage and thus solvent purchasing and disposal costs. To maintain the same linear velocity through the columns, the volume flow rate must be reduced by a factor of about three, which results in significantly lower solvent consumption. A disadvantage of narrow-bore columns is that the band-broadening effects are more severe because the contribution of the outside column volume in connecting tubings and detectors is related to smaller column volume and thus it is relatively more significant. To use the potential of narrow-bore columns it is necessary to minimize the system dispersion and therefore the columns are not well suitable for multiple detection systems. Preparative columns of dimension, for example, 250×25 mm, are generally packed with the same packing materials as those used for the analytical columns. The columns allow fractionation of the sample into several fractions by collecting the eluent and subsequent solvent evaporation. Compared to regular 300×7.5-mm analytical columns, the 250×25-mm columns offer more than 10 times scaleup. The applicability of semipreparative SEC is limited by high column price and significantly smaller load and resolution compared to interaction types of liquid chromatography.

Rapid columns of dimensions 150×7.5 mm or 100×10 mm can be used when significantly reduced run time is requested. They can find utilization in direct manufacturing control when the results are needed in a very short time or for the high-throughput screening measurements of large sample series. The fast SEC columns bring several benefits, such as analysis time less than 7 minutes, increased sample throughput, reduced solvent consumption and consequently reduction of purchase and waste disposal costs, and lower column pressure and consequently reduced possibility of shearing degradation. In addition, the purchase price of a single fast column is markedly below that of several conventional columns, and low solvent consumption allows use of expensive solvents such as

HFIP. However, the selectivity and efficiency of a fast column are significantly lower compared to a system of two or three regular columns and thus their applications are limited.

Guard columns are used to protect the main analytical columns from materials that can irreversibly adhere to column packing. They are generally 50 mm in length of inner diameter as the analytical columns, packed with the same packing material as the main analytical columns. The packing material in the guard column should trap materials that otherwise would bind irreversibly to the top of the analytical column, thus prolonging the analytical column lifetime. Although a guard column can in some cases protect and extend the lifetime of the analytical columns, not all contaminants are commonly trapped by flow through a 50-mm-long guard column. Although one might think that the extra column length added by the guard column should improve the separation, in fact the guard columns do not contribute to or even slightly reduce efficiency and separation. The reason for that may be extra volume added by the additional fittings and tubing. It may also not be unambiguous to decide when the guard column needs to be replaced. Since the guard columns are relatively expensive, it may not be acceptable to change them on regular basis. A substantially cheaper online filter with replaceable stainless-steel frit can be alternatively used to protect the analytical columns from blockage with insoluble impurities. It must be emphasized that blocked frit of the inline filter can significantly increase the shearing degradation of the high-molar-mass polymers, as demonstrated in Figure 3.8. An inline filter can be installed after the injector even if the guard column is used.

Styrene-divinylbenzene gels are the most widely used packing materials for organic applications. HEMA-based gels are frequent materials for aqueous applications. Other packing materials include, for example, polyacrylamide gels, sulfonated polystyrene, poly(vinyl alcohol) gels, and gels based on dextran crosslinked with epichlorohydrin. Silica-based packing materials are highly rigid and allow application in a wide range of solvents including water and organic solvents. The silanol groups on the surface of silica gel can be deactivated by chemical modification using, for example, glycidoxypropyltrimethoxysilane, which is bonded to silanol groups, and consequently the epoxy ring is opened to form a hydrophilic surface covered with dihydroxy groups. The silica-based columns with organic hydroxyl modification are often used for the characterization of proteins. Modification with alkyl chlorosilane can create a hydrophobic surface usable for applications in organic solvents.

In order to analyze polydisperse polymers it is necessary to cover sufficiently broad molar mass range. The traditional approach is to combine several individual pore size columns in series. Individual pore size columns are available in several grades with different separation range. Traditionally, the packing materials are designated as 100, 500, 1000, 10^4, 10^5, and 10^6 Å with corresponding separation limits up to 4×10^3, $500 - 3 \times 10^4$, $500 - 6 \times 10^4$, $10^4 - 6 \times 10^5$, $6 \times 10^4 - 2 \times 10^6$, and $6 \times 10^5 - 10^7$ g/mol. The exclusion limits are approximately valid for polystyrene in THF and can vary depending on polymer chemical and molecular structure, temperature, and solvent. The symbol Å

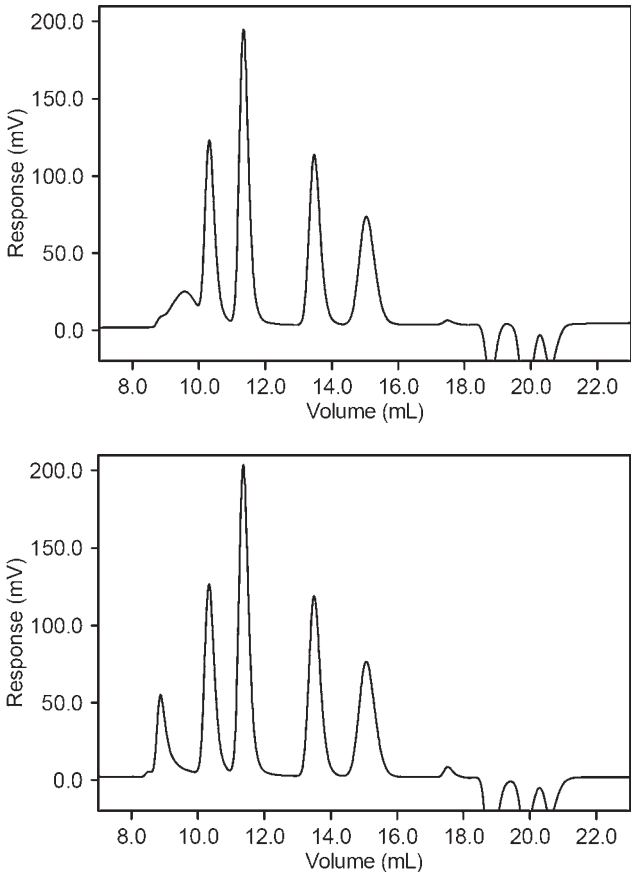

Figure 3.8 Chromatograms of PS standards ($2.85 \times 10^6, 4.7 \times 10^5, 1.7 \times 10^5, 1.9 \times 10^4$, and 3600 g/mol) with blocked (top) and clean (bottom) frit of inline filter.

does not apply to the real pore diameter, but it was historically introduced as the exclusion limit expressed by fully extended polystyrene chain.

The individual pore size columns must be combined so that the separation ranges of the columns overlay, which means there are no gaps in the pore volume distribution. An improper combination of the individual pore size columns may result in false peak shoulders that are due to the mismatch of the pore size and volume. That means the unusual peak shapes are artifacts and not reflections of the true pattern of molar mass distribution. A more recent approach for covering a broad separation range is using mixed columns packed with a mixture of individual pore size materials that are blended to cover a specific molar mass range.

Although the columns are often blended in order to get linear calibration curves, the real calibration curves are slightly curved as in the case of individual

pore size columns. The mixed bed columns are typically available in several types covering different molar mass range. For example, PLgel mixed columns are labeled as E, D, C, B, A and cover the molar mass range up to 3×10^4, $200 - 4 \times 10^5$, $200 - 2 \times 10^6$, $500 - 10^7$, $2000 - 4 \times 10^7$ g/mol, respectively. Packing materials with multipore structure instead of the combination of individual pore size materials is the most recent development in column technology.

Generally, mixed and multipore columns simplify the column selection and reduce the possibility of artifacts in the peak shape. A significant advantage is that very different molar masses and polydispersity can be analyzed on the same column set. To increase the number of theoretical plates the mixed and multipore columns are usually connected in series. For most practical cases the combination of two 5- or 10-μm columns is adequate and using three or four columns usually does not bring more information about the analyzed polymers. Three to four columns should be used in the case of 20-μm packing designed for the analysis of polymers containing fractions with molar mass up to several tens of millions g/mol. The calibration curves for individual and mixed columns are usually available in the manufacturers' brochures and they can be used to choose an appropriate type of columns. The manufacturers of SEC columns include Waters (Ultrastyragel, Ultrahydrogel columns), Polymer Laboratories—a part of Varian (PLgel, PL aquagel-OH), Shodex (KF-800, K-800 series), Tosoh (TSK-GEL), Phenomenex (Phenogel), Jordi, Polymer Standards Service, and MZ Analysentechnik.

Besides pore volume and pore size, the particle size of column packing is another important parameter related to both the number of theoretical plates and backpressure. The two quantities increase with decreasing particle size. Available particle sizes are 3, 5, 10, and 20 μm. The higher the column backpressure the higher the possibility of degradation of high-molar-mass fractions of the sample by shearing forces. Small particle size is used for the analysis of oligomers and lower-molar-mass polymers, whereas 20-μm packing is used for the characterization of high-molar-mass polymers to reduce shearing degradation, which can happen for molar masses in the range of several millions and more.

SEC columns are not only important, but also a relatively expensive part of an SEC setup and proper care and handling is necessary to prolong their lifetime. Columns that are frequently used will not last forever. Experience shows that columns that are in everyday service can show appropriate separation efficiency even after several years although the same type of columns may deteriorate within a few months or even faster. Besides the column handling, the chemical nature of the samples that are analyzed is the most important for column duration. Samples containing microgels and other insoluble fractions and highly polar functional groups are more likely to reduce column lifetime compared to well-soluble neutral polymers.

Excessive peak broadening and tailing due to the use of columns that have already lost efficiency result in erroneous results, usually underestimated M_n and overestimated M_w and polydispersity. SEC column cleaning or regeneration is mostly impossible and columns that have lost resolution should be replaced.

Columns do not lose separation efficiency even when stored for several years assuming they are stored at room temperature with both ends tightly plugged to prevent solvent evaporation. In the case of aqueous columns, the solvent in the columns should be replaced with about 0.02% sodium azide or alternatively with 5% aqueous methanol to prevent growth of microorganisms. Unlike many HPLC columns, SEC columns packed with swollen organic gels must be prevented from drying since deterioration of column performance as a result of drying is irreversible. Maximum flow rate and column pressure are specified by the column manufacturers.

To avoid column damage the maximum operating pressure recommended by a manufacturer should not be exceeded even for a short period of time. The flow direction is labeled directly on the columns. A typical flow rate for regular 7.5-mm inner diameter columns in THF is 1 mL/min. Lower flow rates of 0.5 or 0.8 mL/min are mostly used in aqueous solvents. When using columns with increased or decreased inner diameter, the volumetric flow rate should be adjusted accordingly to maintain an equivalent linear velocity through the column. Higher viscosity eluents such as DMSO should be used at reduced flow rates or elevated temperatures. Columns packed with styrene-divinylbenzene–based gels must not be used in non-solvents for polystyrene such as water, alcohols, or hydrocarbons. Although modern styrene-divinylbenzene packing materials are highly rigid and my own experience indicates that the columns can survive even a short accidental flushing with methanol, the use of the previously stated solvents should be avoided.

Using a stepwise change of the flow rate in several increments or continuous flow rate gradient over several minutes to reach a full flow rate or to stop it was traditionally recommended to protect the columns from mechanical damage. This practice can be still obeyed even though it may not be absolutely necessary with today's rigid packing materials. It must be stressed that even microscopic shrinkage of the gel bed due to the shrinkage by chemical or mechanical exposure or solvent evaporation results in voids that cause severe peak tailing and reduction of plate numbers. One defective column typically causes peak spreading that cannot be overcome by any number of good columns and thus one defective column in a series causes poor separation efficiency of the entire column set.

The columns can be transferred from one solvent to another assuming the solvents are miscible. The transfer should be performed at a low flow rate of about 0.2 mL/min. However, to maintain high column efficiency the solvent replacement should not be done too often. Instead, it is preferable to have several column sets in different solvents. Some manufacturers offer columns directly packed in special solvents such as DMF or HFIP. Styrene-divinylbenzene–packed columns allow working at elevated temperatures around 150°C. The high temperature is necessary for the analysis of polyolefins and other polymers of limited solubility. To avoid an excessive temperature shock the column temperature should be raised or lowered at a reduced rate, such as 1°C per minute, and if the pump is intended to stop it should be stopped after room temperature is achieved. The pH of the mobile phase is important in aqueous silica–based columns, which

should be usually in the pH range of 3–7.5. The pH range of aqueous columns is a part of the manufacturer's recommendations. Although UV detection may demand working in nonstabilized THF, it should be replaced with stabilized THF before storage or when only RI detection is needed.

To eliminate the effect of possible partial solvent evaporation at the column inlet and outlet during long storage, the column can be connected in a reversed direction; that is, the outlet of the column is connected to the solvent delivery system and the pump is activated at a low flow rate of about 0.2 mL/min until a few drops appear at the column inlet. Then the column is connected in a normal direction and the flow rate is increased.

Caution should be taken when connecting columns into series and to an injector and a detector. Leaks in the connections can result in detector noise, drifting baseline, and elution volume irregularities, and leakage inside detectors can even result in their complete damage. It is necessary to keep in mind that improperly tightened fittings may cause leaks, but overtightening should be avoided as well, especially when the fitting is reused. Testing the connections for leaks can be most effectively performed by dabbing with a piece of folded filter paper and identifying the leak as either a dark spot or smell of organic solvent on the paper. A new fitting should be used rather than overtightening when slightly tightening the fitting does not solve the leakage problem.

3.3.3 Detectors

Detectors are used to monitor the molecules of solute eluting from the separation system. The refractive index (RI) detector, the ultraviolet (UV) detector, the light scattering photometer, the viscometer, the infrared (IR) photometer, and the evaporative light scattering detector (ELSD) represent the most important detectors in SEC. The detector monitors the change of the mobile-phase composition and converts it into an electrical signal, which is further acquired and processed by computer and SEC software.

The RI and UV detectors represent concentration-sensitive detectors with the signal proportional solely to the concentration of sample in the eluate. The signal of a light scattering detector is proportional to the product of molar mass and concentration, while the viscometer signal is proportional to the product of concentration and molar mass to the power of the Mark-Houwink exponent. That means that for most polydisperse polymers the peak of the viscometer is after the peak of the light scattering detector, with the exception of polymers with the Mark-Houwink exponent ≥ 1, where the peaks overlay or the viscometer peak can even forego the light scattering one.

The most important parameter for the concentration detectors is the *detection limit*, which represents the minimum injected amount detectable under given chromatographic conditions. The smallest detectable signal is usually considered to be double the height of the largest noise spike. When the baseline signal is zoomed enough, one can see that the baseline is irregular even if no peak elutes

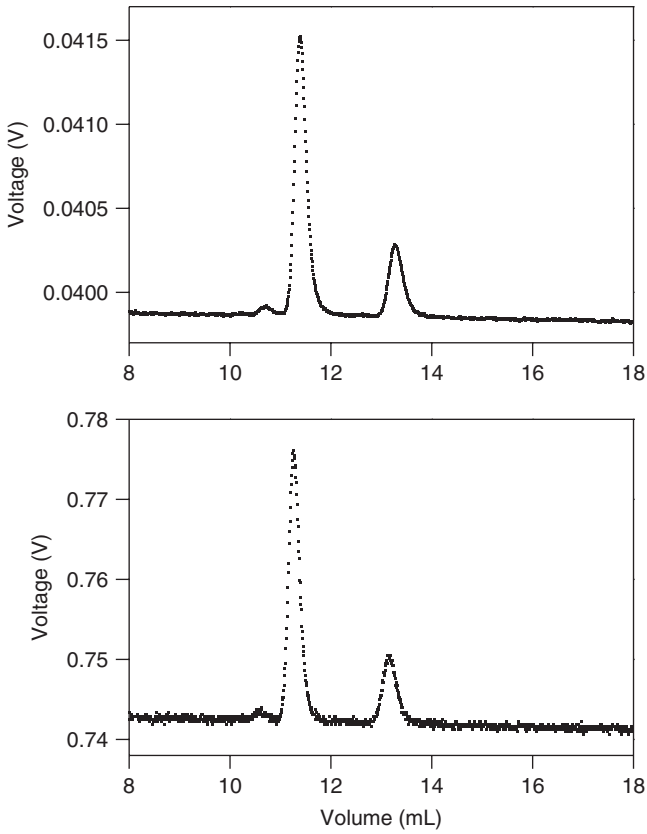

Figure 3.9 Comparison of signal-to-noise ratio for two generations of light scattering detectors. Data measured under identical conditions with the two detectors connected in series.

from the columns. Although the noise should be minimized, its absolute level is not as important as the ratio of the signal compared to the baseline noise (i.e., the *signal-to-noise ratio*). For quantitative analysis the signal-to-noise ratio should be at least ten. If the signal-to-noise ratios of different detectors are to be compared, they should be determined under identical experimental conditions; preferably the two detectors should be connected in series. An example of such a comparison is shown in Figure 3.9 for two generations of light scattering detectors.

Drift is an even increase or decrease of the baseline signal that appears as the slope. It can be normal for a certain period of time due to warming up of the lamps and electronics and column flushing and stabilization. After warmup, the baseline signal should show negligible change with time. The most important sources of drift are elution of the old mobile phase after the refill or change of the eluent, change of the mobile-phase composition due to evaporation of one component in the case of mixed solvents or buffers or chemical instability such as in the case of THF, change of temperature, and elution of compounds adsorbed

in columns from previous injections. The signal noise and drift specified by the detector manufacturers are usually far below the noise and drift that originate from the instability of the chromatographic system.

The *linearity* of detector response means that a detector yields signal with a peak area directly proportional to the injected amount. The plot of peak area versus injected mass should be linear in a wide range with the slope giving the detector *response*. The detector response is different for different compounds depending on the detector type and properties of a specific compound. The extinction coefficient, the specific refractive index increment dn/dc, and the product of $(dn/dc)^2$ and molar mass are the relevant properties for UV, RI, and light scattering detectors, respectively. That means different compounds can show significantly different detector responses when injected in the same amounts.

The *time constant* characterizes how quickly a detector can record a peak. It can be defined as the time needed to reach a certain percentage of full scale (e.g., 98%). It is expressed in seconds and generally the detector noise decreases with increasing time constant, but it should not be too high for detecting very narrow peaks. Most detectors offer a choice of the time constant. In SEC, the polymer peaks are usually broad and there is no need to use small time constants.

Volume of the flow cell and cell path length are other important detector characteristics. The volume of the detector cell contributes to the peak broadening. On the other hand, too short pass length has a negative impact on the sensitivity, whereas detectors with short path lengths can be used for semi-preparative analyses. A standard cell volume of RI or UV detector is 8–10 μL. Regarding peak broadening, the cell volume must be related to peak width of the narrowest peak in the chromatogram. Since SEC chromatograms are usually broad, covering elution volume of several milliliters, detector cell volume is not a serious issue.

Different types of detectors can show significantly different sensitivity to the baseline noise and drift. An RI detector is more sensitive to mobile-phase composition and temperature changes compared to a UV detector. A light scattering detector is very sensitive to bleeding of particles from the column packing, which are completely unseen by RI and UV detectors, whereas its sensitivity to temperature or flow rate fluctuations is negligible. A randomly noisy detector baseline can arise from several sources. These include bubbles caused by improper solvent degassing, pump malfunction, faulty detector lamp, electric power fluctuation, temperature instability, disturbance from the environment (e.g., nearby improperly shielded electrical appliances or air conditioning), or sometimes even slight pulses from a dripping waste tube.

Noise originating in the pump is usually indicated by pressure pulsation and it can be demonstrated by turning off the pump and obtaining a noise-free (yet usually drifting) baseline. The correction of the pump problem usually requires changing the pump seals, check valves, and pistons. If the noise persists when the pump is off, the detector lamp and other possibilities should be checked.

3.3.3.1 UV Detector

A *UV detector* is the most common type of detector used in liquid chromatography and can be used for compounds containing a double bond, conjugated double bonds, an aromatic ring, a carbonyl group C═O, or a nitro group NO_2. Its applicability in SEC is limited by the fact that many important polymers have weak or no absorption of UV light. The applicability of the UV detector is also limited by the fact that THF has a higher UV cutoff of about 230 nm compared to other common HPLC solvents such as methanol or acetonitrile. The applicability of a UV detector includes polystyrene and styrene-containing copolymers, nitrocellulose, bisphenol A–based epoxy resins, phenol-formaldehyde resins, unsaturated polyesters, alkyds, poly(ethylene terephthalate), and proteins. The UV detector measures the absorbance (A) of the eluate, which is defined as the logarithm of the ratio of the intensities of the incident light (I_0) and the transmitted light (I). According to the Lambert-Beer law the absorbance is related to the absorption (extinction) coefficient a ($mLg^{-1}\ cm^{-1}$), the concentration c (g/mL), and the cell length L (cm):

$$A = \log\left(\frac{I_0}{I}\right) = acL \tag{3.19}$$

For most samples, namely those with UV absorbance given by the monomer unit, the response of the UV detector is proportional to the injected mass of the analyzed sample. However, in the case of polymer molecules bearing a single absorbing unit, the UV response is proportional to the number of eluting molecules. In such a specific case the molar mass of molecules at a given elution volume can be determined from the ratio of the signal of a mass-sensitive detector (usually a refractometer) to that of a number-sensitive detector.

The sensitivity of a UV detector is expressed as the response factor in absorbance units (AU) per volt. For example, the response factor one AU per volt means that the absorbance one AU causes the signal output one volt. The path length of a typical UV detector is 10 mm, but the thickness is small in order to keep the total cell volume small. The family of UV detectors includes a fixed-wavelength detector, a variable-wavelength detector, and a photodiode array (PDA) detector. Technical details can differ for the particular models of different manufacturers. Modern UV detectors do not use a reference cell and zero baseline is adjusted electronically using the signal from a reference photodiode.

Some detectors allow simultaneous data acquisition at dual wavelength. A programmable-wavelength UV detector consists of a deuterium lamp, an optical system of mirrors that collects light from the lamp and directs it toward the grating. The operation wavelength is determined by the position of grating. The light of a particular wavelength is focused onto the entrance of the flow cell and the transmitted light is detected by a photodiode. A beamsplitter located in front of the flow cell diverts a portion of the light to a reference photodiode. In the case of a PDA detector the light from the deuterium lamp passes directly through the flow cell. The sample in the flow cell absorbs at specific wavelengths and the

light exiting the flow cell is directed onto the grating. The light from the grating is dispersed into 1.2-nm wavelength beams that are recorded by the array of 512 photodiodes.

Usually, the response from several photodiodes is cumulated, so that the spectral band is larger than 1.2 nm (e.g., 2.4 nm, 4.8 nm). The reference diode receives the light through the beamsplitter assembly. The PDA detector acquires all data in a specified wavelength range and thus UV spectra of compounds eluting at particular elution volumes can be obtained and the chromatograms can be extracted from the collected data at any suitable wavelength.

The UV detectors offer a highly sensitive detection of UV-absorbing compounds, but they cannot be applied for the detection of a wide range of nonabsorbing compounds. For interpretation of the experimental results it is necessary to keep in mind that two peaks of about the same area can correspond to compounds that are present in concentrations different by several orders of magnitude. Similarly, a minor peak in a chromatogram can correspond to a weakly absorbing compound that may represent a substantial part of the analyzed sample.

If the UV detector is used in combination with a light scattering detector or an online viscometer, the absolute concentration c_i of the molecules eluting at the ith elution volume increment i can be determined according to Equation 3.20:

$$c_i = \frac{RF_{UV}\,(V_i - V_{i,baseline})}{aL} = \frac{\alpha_{UV}\,(V_i - V_{i,baseline})}{a} \tag{3.20}$$

where RF_{UV} is the UV detector response factor in absorbance units per volt, L is the flow cell length, a is the extinction coefficient ($\mathrm{mLg^{-1}\ cm^{-1}}$), and V_i and $V_{i,baseline}$ are the detector signals in volts for sample and baseline, respectively. The ratio of RF_{UV}/L represents the calibration constant of the UV detector (α_{UV}). The UV response factor supplied by the manufacturer is generally accurate and can be easily verified. The procedure for determining the UV detector calibration constant is similar to that for determining the RI calibration constant. The only difference is that the extinction coefficient is used instead of the *dn/dc*. *Note:* SEC-MALS analysis with a UV detector requires not only *dn/dc*, but the extinction coefficient as well.

3.3.3.2 Refractive Index Detector

Refractive index (RI) (differential refractive index, DRI) detectors are the most common detectors in SEC. They can be used universally for all compounds with a non-zero specific refractive index increment. Although *dn*/*dc* of different polymers can differ substantially and also negative values are possible, *dn*/*dc* values close to zero are rare. In the case of zero *dn*/*dc* the detector response must be improved by the choice of a different solvent of different refractive index. For compounds with high absorption of UV light, such as those containing aromatic rings, the sensitivity of an RI detector may be significantly lower compared to a UV detector. On the other hand, for many nonabsorbing compounds the RI detector is the only choice.

Compared to UV detectors the RI detectors are highly sensitive to temperature and flow rate fluctuation. To eliminate the influence of the temperature, the cell is incorporated in a massive metal thermostated block. Most RI detectors have no cooling capability and thus the operating temperature must be set about 10°C above room temperature. The eluent passes through relatively long stainless-steel tubing before it reaches the flow cell to equilibrate the temperature with that of the cell. This fact typically results in significantly larger interdetector volume compared to UV detectors. Instability of the flow rate causes a significant increase of noise level. A malfunction of pump seals or check valves results in a regular short-term pulsation of a baseline. Therefore, a properly working pump is essential for keeping the noise level low. The RI detectors are highly sensitive to any changes of the composition of eluate and it typically takes several hours to flush the SEC columns and stabilize the signal. A solvent refill during the pump operation usually results in a significant change of the baseline signal especially in the case of THF. Regular fluctuation with a several-minute period may be due to an online vacuum degasser, which keeps the vacuum level within certain limits. In the case where pressure gets over a maximum limit the pump of the degasser starts working until the pressure drops to the desired limit. Due to the vacuum fluctuation the level of degassing fluctuates as well and the RI detector signal regularly fluctuates because of different levels of solvent degassing. This problem does not appear with degassers working in continuous mode, that is, keeping the chamber pressure at a constant value, or when degassing is achieved with helium sparging.

A typical feature of RI detectors is a low-pressure resistance of the flow cell, which usually does not allow connection of other detectors after the RI detector.

The principle of an RI detector is based on the refraction (bending) of a light beam when passing from one medium into another at an angle that is not perpendicular to the interface surface. The extent of the light refraction is related to the difference of the refractive indices of the two media.

A *deflection*-type RI detector has a flow cell separated into two parts. During the purge period both parts of the flow cell, that is, the reference cell and the measuring cell, are filled with a solvent eluting from the columns. When both parts of the cell are properly flushed the reference part is closed and the eluent passes only through the measuring cell. Shortly after the purge the refractive indices of solvent in the reference cell and measuring cell are identical. The light from the lamp is focused and passes both parts of the flow cell and the deflection of the light beam, which is proportional to the difference of the refractive indices in both cells, is monitored by a photodiode. The zero detector output can be adjusted optically or electronically. As the sample components eluting from the column pass through the measuring cell, the refractive index of solution changes and the light beam passing though the cell is refracted.

Conventionally, a dual-element photodiode is used to measure the light beam angular deflection. The dual-element photodiode contains two photodiode light detectors placed side by side. As the light beam bends, it moves away from one photodetector onto the other. The actual light beam position is characterized

by the voltage difference between the two elements of the photodiode, which is proportional to the refractive index difference between the measuring cell and the reference cell, which is proportional to the concentration of the component in the measuring cell. Once the light beam moves entirely off of one photodetector and onto the other, there is no way to determine the beam position and the detector signal saturates. An innovative way to measure light beam deflection is based on an array of 512 light-measuring elements instead of using two elements (Optilab® rEX of Wyatt Technology Corporation). Each element of the photodiode array, called a pixel, precisely measures the intensity of light impacting it. The data from the 512 pixels are analyzed using mathematical algorithms to determine the position of the light beam on the array. Using a photodiode array and advanced mathematical analysis techniques, the light beam position is measured with very high accuracy. The photodiode array is 1.3 cm long, and so the beam may move more than a centimeter before it slides off the end of the photodiode array.

A significant advantage of this type of RI detector is that it does not require any change of sensitivity setting. In contrast to conventional RI detectors, for which high sensitivity is associated with a limited dynamic range or a great dynamic range is associated with reduced sensitivity, full sensitivity is achieved over the entire range and thus small peaks can be detected alongside huge peaks within a single run with no signal saturation.

Another type of RI detector is an *interferometer*, where the light beam is split into two beams of equal intensity by a beam splitter. One beam passes through a reference cell, the other through a measuring cell. As the beams enter the cells they are in phase with one another. After passage through both cells the two beams are recombined by a second beam splitter. If the refractive indices of the liquids in the reference and measuring cell are different, the two light beams are phase shifted, which results in an attenuation of the light intensity due to interference.

In contrast to conventional SEC, the use of an RI detector with a light scattering photometer or a viscometer requires determination of concentration in absolute units (g/mL). To determine the absolute concentration one must know the RI detector calibration constant (in refractive units per volt). Unlike the response factor of UV detectors, the calibration constant provided by an RI detector manufacturer (with the exception of Optilab® rEX) is not accurate and must be determined (see Section 2.6).

3.3.3.3 Infrared Detector

Infrared (IR) detectors work on a principle similar to UV detectors. The major limitation of the IR detector in SEC is the fact that the solvents used as the mobile phase also have a strong absorption at wavelengths that could be potentially used to monitor eluting polymers. The IR detector currently finds application mainly in the case of SEC of polyolefins in trichlorobenzene, where it can be used not only for monitoring the concentration but also for the determination of chemical heterogeneity of polyethylene copolymers and branching in polyethylene. The

determination of short-chain and long-chain branching distribution across the elution volume axis is based on the simultaneous measurements of a selective absorbance in the CH_3 region and a broad-band absorbance of CH_2 and CH_3. The ratio of these two signals is directly proportional to the number of branches. In the high-temperature SEC of polyolefins, the IR detector can be used as an alternative to an RI detector with the advantage given by high sensitivity and signal stability. An IR detector suitable for a high-temperature SEC analysis of polyolefins is available, for example, from the Spanish company PolymerChar.

In the case of combination with a light scattering detector, the IR detector must be calibrated in order to provide absolute concentration. The calibration is equivalent to the determination of the extinction coefficient by the UV detector in online mode. A significant advantage of the IR detector over the differential refractometer in the combination of SEC with light scattering and viscosity detectors is that the IR detector can be connected as the first detector in the series and thus the measurement of concentration is not affected by the dilution effect of the viscometer.

A possible solution of the limitation caused by solvent absorption is using an interface that permits removing the solvent from the eluent. In such an application the IR detector is not used as the concentration-sensitive detector, but provides information about chemical composition of sample eluting from the SEC columns. The sample can be deposited continuously onto a rotating germanium disk that can be subsequently scanned to provide the polymer composition as a function of molar mass, or strictly speaking, as a function of elution volume. The eluent from the column is sprayed with a nitrogen stream through a nozzle to the disc. The nonvolatile solute from the eluent is deposited on the disc, from which the IR spectra are measured. Alternatively, the sample can be deposited as a series of spots on the surface of a moving stainless-steel belt. The belt continuously transfers the spots into the diffuse reflectance accessory of the FTIR spectrometer, enabling identification of the deposited solutes by measurement of the diffuse reflectance IR spectra.[11] Although the principle appears promising for the characterization of chemically heterogeneous samples, it has not found a wide application.

3.3.3.4 Evaporative Light Scattering Detector

The *evaporative light scattering detector* (ELSD) is another type of universal detector representing a possible alternative to the RI detector. In contrast to the RI detector, the ELSD allows the use of mobile-phase gradient, which may be of interest for other types of liquid chromatography. The ELSD offers some potential advantages, such as no requirement for the sample to have a strong absorbing chromophore, universal response with no effect of absorption coefficient or dn/dc, and high sensitivity. The eluent is sprayed into a stream of gas, the solvent is vaporized, and the solute that is less volatile than the solvent creates an aerosol of small particles. The particles scatter the light from the light source. The scattered light intensity is proportional to the concentration of the eluting polymer. The

response of the detector can be optimized by the temperature of the evaporator and the flow rate of the nebulizing gas (typically nitrogen). The temperature of the evaporator is selected according to the type of sample and mobile phase. Low-molar-mass compounds and lower oligomers can be lost with the nebulizing gas. Compared to UV and RI detectors, the ELSD is destructive and cannot be used for preparative applications. The ELSD is sometimes confused with light scattering detectors.

3.3.3.5 Viscosity Detector

A *viscosity detector* (*online viscometer*, *viscometric detector*) is exclusively used in combination with SEC. It is often considered to be a molar mass–sensitive detector, even though the primary quantity measured by a viscometer is not molar mass, but the specific viscosity, which is, using the concentration from a concentration-sensitive detector, converted into the intrinsic viscosity. Having the intrinsic viscosity, one can read the molar mass from the universal calibration dependence. However, the method suffers from drawbacks similar to conventional SEC, namely sensitivity to the flow rate variations, temperature fluctuations, non-size-exclusion separation mechanisms, and efficiency of the columns. The failure of the universal calibration for polyelectrolytes in aqueous solvents was reported.[12]

An online viscometer measures a pressure drop between a line containing the polymer solution and one containing pure eluent. According to Poiseuille's law for laminar flow, the measurement of viscosity can be replaced by the measurement of pressure difference:

$$\dot{V} = \frac{\Delta P \pi R^4}{8\eta L} \tag{3.21}$$

where $\dot{V}$ is the volumetric flow rate through the tube (mL/min), ΔP is the pressure difference across the tube (i.e., the inlet pressure minus the outlet pressure), R is the radius of the tube, η is the viscosity, and L is the length of the tube.

Online viscometers are available in several different designs. The simplest type, measuring the pressure drop across a capillary, is highly sensitive to flow rate and temperature fluctuations. A significant reduction of signal noise is obtained with the bridge type of viscometer, outlined in Figure 3.10. The fluid stream splits at the top of the bridge, and half of the solvent flows through each arm. Since the bridge is symmetric, the differential pressure transducer in the center of the bridge measures zero. When a sample elutes, it is also split evenly. In the left arm of the bridge is a delay volume, where the eluting sample is retained. At the time of sample elution the sample enters the delay volume, but solvent still exits, causing a pressure imbalance in the bridge. This imbalance pressure, combined with the inlet pressure, gives the specific viscosity (η_{sp}) according to the equation:

$$\eta_{sp} = \frac{\eta}{\eta_0} - 1 = \frac{4\Delta P}{IP - 2\Delta P} \tag{3.22}$$

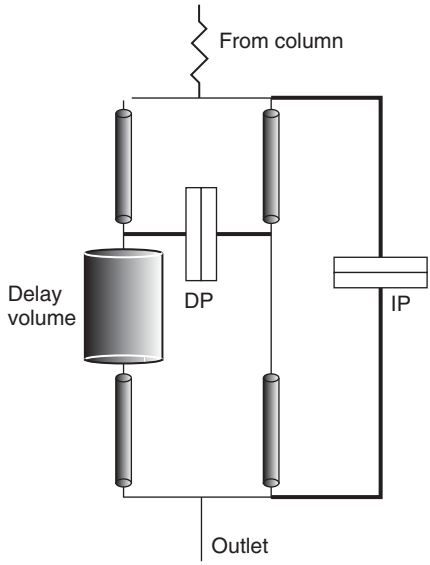

Figure 3.10 Scheme of four-capillary bridge viscometer ViscoStar™. DP = differential pressure transducer, IP = inlet pressure transducer. *Source:* Courtesy of Wyatt Technology Corporation.

where η is the viscosity of the sample solution, η_0 is the viscosity of the solvent, ΔP is the imbalance pressure across the bridge, and IP is the inlet pressure (i.e., pressure difference between the top and the bottom of the bridge).

According to Equation 3.22, the specific viscosity measurement is performed by the two pressure measurements ΔP and IP. That means the accuracy of the specific viscosity is based only on the calibrated transducers. The measurement is independent of the flow rate, but both ΔP and IP are directly proportional to the applied flow rate, which can be in some cases used to improve the signal-to-noise ratio, because most of the HPLC pumps operate better at higher flow rates. However, typical flow rates used for the measurements with an online viscometer do not differ from those used for other types of SEC measurements.

At the end of the run, the delay volume is flushed with new solvent, which causes a negative signal of the viscometer and a positive signal of the RI detector (see Figure 3.11). The volume delay (a set of three empty columns) can be changed by a disconnection of one or two delay columns to match the configuration of the viscometer with the number of SEC columns and type of analyzed samples. The need to flush the delay volume reservoir prolongs the run time and thus the use of narrow-bore 4.6-mm columns requiring lower flow rates is not advisable.

When combined with a concentration detector, the online viscometer can be used to determine the intrinsic viscosity using the well-known relation:

$$[\eta] = \lim_{c \to 0} \frac{\eta_{sp}}{c} \tag{3.23}$$

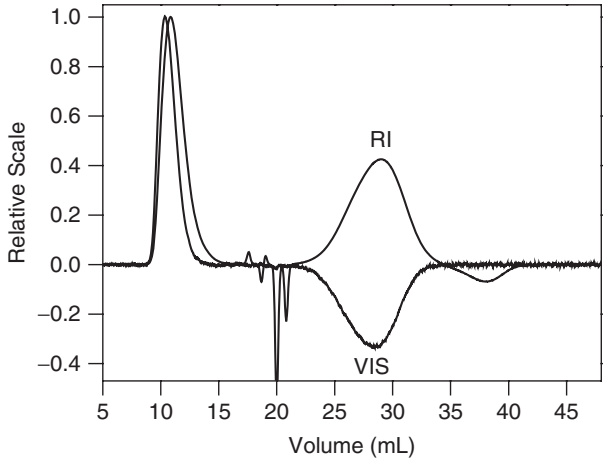

Figure 3.11 Positive and negative signals of RI detector and viscometer caused by flushing the delay volume of the viscometer.

where c is the concentration of polymer molecules eluting from the columns. As in the case of light scattering detectors, the concentration measured by a concentration detector must be expressed in g/mL, which requires the absolute calibration constant of an applied detector to be known. In fact, without correcting for band broadening, the intrinsic viscosity is the weight-average of the molecules eluting at a given elution volume. However, band broadening is mostly neglected and the values of intrinsic viscosity are assumed to be measured for monodisperse elution volume slices.

Since the RI detector is usually connected as the last detector in the series, the concentration of the eluting molecules is decreased by the split ratio between the two sides of the viscometer bridge. That means the sample that exits the viscometer is diluted by a factor of about two. Therefore the RI detector does not measure the same concentrations that flow through the detectors connected before the viscometer. If the two arms were absolutely identical, the dilution factor would be exactly 50%. In practice, the two arms are never exactly identical.

To correct for the change in concentration, it is necessary to determine the exact dilution ratio. The determination of the dilution factor is simple and involves injection of a sample giving an easily processable chromatogram (e.g., narrow standard well separated from the solvent peaks). The exact sample concentration need not be known. The sample is injected with and without the viscometer and the dilution factor is simply computed as the ratio of the two peak areas.

The data from the viscometer and concentration detector allow not only the determination of the molar mass using the universal calibration, but also the computation of the distribution of intrinsic viscosity and intrinsic viscosity averages. Some scientists have suggested using the particular averages of intrinsic viscosity instead of molar mass averages for polymer characterization and relation of the molecular structure with application properties.

Intrinsic viscosity is one of the fundamental characteristics of polymer materials. Its practical application is mainly in combination with molar mass, especially for the characterization of macromolecular size and polymer branching. That means the most efficient application of the viscometric detector is in combination with a light scattering detector that measures molar mass directly without need for universal calibration. The data can be used to generate a Mark-Houwink plot, that is, log–log relation between the intrinsic viscosity and molar mass, and to calculate the hydrodynamic radius through the Einstein-Simha relation (see Equation 1.82).

An interesting application of the viscosity detector is an alternative calculation of the number-average molar mass without a concentration detector. Using the definition of hydrodynamic volume (Equation 1.81):

$$V_h \approx [\eta]M \tag{3.24}$$

the number-average molar mass is calculated as

$$M_n = \frac{\sum\limits_i c_i}{\sum\limits_i \frac{c_i}{M_i}} = \frac{\sum\limits_i c_i}{\sum\limits_i \frac{c_i}{V_{h,i}/[\eta]_i}} \tag{3.25}$$

At low concentrations the intrinsic viscosity at the ith elution volume increment can be replaced by $\eta_{sp,i}/c_i$ and Equation 3.25 can be rearranged as

$$M_n = \frac{\sum\limits_i c_i}{\sum\limits_i \frac{\eta_{sp,i}}{V_{h,i}}} \tag{3.26}$$

The concentration (in g/mL) of molecules eluting at the ith elution volume slice is

$$c_i = \frac{mH_i}{\Delta V \sum\limits_i H_i} \tag{3.27}$$

where m is the injected mass, H_i is the height of the RI chromatogram at volume slice i, and ΔV is the elution volume between two data points. Then

$$\sum_i c_i = m/\Delta V \tag{3.28}$$

and Equation 3.26 can be expressed as

$$M_n = \frac{m}{\Delta V \sum\limits_i \frac{\eta_{sp,i}}{V_{h,i}}} \tag{3.29}$$

The hydrodynamic volumes at particular elution volume slices $V_{h,i}$ are directly determined from the universal calibration curve and the values $\eta_{sp,i}$ are

measured by the viscometer. A significant advantage of Equation 3.29 is that the value of M_n is not influenced by the calibration constant of the RI detector or by the specific refractive index increment and thus the method represents an interesting way of determining M_n or verifying results obtained by other methods. Of course, one has to assume 100% mass recovery of the injected polymer from the columns. According to Equation 3.26, in the case of imperfect SEC separation, that is, when band broadening is not negligible or in the case of complex polymers, the molar mass determined at a given elution volume is the number-average.

For shear-sensitive polymers (i.e., those showing decrease of solution viscosity with increasing shear rate), the results can be affected by the *shear-thinning* effect. For a radial velocity profile $v(r)$ the shear rate $\gamma = dv(r)/dr$. The shear rate in a capillary in the distance r from the center of the capillary is:

$$\gamma = \frac{-4\dot{V}r}{\pi R^4} \tag{3.30}$$

where $\dot{V}$ is the volumetric flow rate and R is the radius of capillary. The negative sign is because the fluid velocity $v(r)$ is at maximum at the capillary center $v(0)$, and zero at the capillary wall $v(R)$. The maximum shear rate at the capillary wall is:

$$\gamma_{max} = \frac{4\dot{V}}{\pi R^3} \tag{3.31}$$

and the average value is:

$$\gamma_{average} = \frac{8\dot{V}}{3\pi R^3} \tag{3.32}$$

For a typical flow rate of 1 mL/min (i.e., 0.0167 mL/s) and a capillary of 0.025 cm, the average shear rate is about 900 cm^{-1}, which can be for very large molecules over the limit of Newtonian flow behavior. The limit of Newtonian behavior increases as concentration and molar mass decrease, and as ionic strength increases for the case of polyelectrolytes. At concentrations typically used in SEC experiments even shear-thinning polymers can be still on their Newtonian plateau. Behind the limit of Newtonian behavior the specific viscosity becomes underestimated. Note that the shear rate effect on the shear-sensitive polymers is the opposite in the case of an online viscometer compared to a capillary viscometer. In the case of the online viscometer, the concentration dependence of the specific viscosity is neglected, and the intrinsic viscosity is equaled with the reduced viscosity ($\frac{\eta sp}{c}$). On the other hand, when the measurement is performed by a capillary viscometer, the intrinsic viscosity is determined from the y-axis intercept of the concentration dependence of reduced viscosity, and the non-Newtonian behavior, being more prominent at higher concentrations, in fact results in the decrease of the slope of the concentration dependence of the reduced viscosity and thus overestimation of the intrinsic viscosity.

3.3.3.6 Light Scattering Detector

Light scattering detectors are almost exclusively used in SEC and also in FFF measurements. In principle, it is possible to use a light scattering detector in combination with other types of liquid chromatography, but the majority of applications lie in the area of SEC. Light scattering detectors represent the most powerful detection in SEC since they eliminate the necessity of column calibration and provide information unavailable by conventional SEC. Three different types of light scattering detectors are used that differ in the method of the determination of molar mass. *Multi-angle* light scattering (MALS) detectors permit extrapolating the light scattering intensities measured at various angles to zero angle where the particle scattering function is unity. *Low-angle* light scattering detectors use an angle low enough to assume that the particle scattering function is equal to one. However, for very large molecules $P(\theta)$ can decrease considerably below one even at low angles. *Right-angle* light scattering (RALS) can be used either for small polymers assuming particle scattering function $P(\theta) = 1$, or as part of a so-called *triple detection* system (sometimes termed *SEC*^{3}) consisting of a RALS detector, a viscometer, and an RI detector. The 90° light intensity is used to estimate the molar mass considering the particle scattering function is unity. The approximate molar mass is used together with the intrinsic viscosity obtained from the online viscometer to estimate the RMS radius from Equations 1.83–1.85. Then the particle scattering function is calculated using the estimated R and the equation for a given particle shape. Increasingly accurate approximations of the particle scattering function and the molar mass can be calculated by iterations until the values obtained can be considered constant. The limitation of this procedure is that it requires using the particle scattering function appropriate to the analyzed molecules. Probably the most serious limitation of the triple detection approach is caused by the generally unknown Flory's constant Φ for a given polymer under given experimental conditions. For example, in the case of branched polymers Φ will vary with the degree of branching.

The theory of light scattering is explained in Chapter 2. The principles and methodology of the combination of SEC with multi-angle light scattering detectors are described in Chapter 4. An interesting application of a light scattering detector was described in reference 13, which suggests improved methodology of the determination of the link between SEC results and polymer rheological properties. The method may be useful for samples with a molar mass distribution skewed toward high molar masses, which show at low elution volumes an intensive signal of a light scattering detector, but a weak RI signal due to very low concentration of the molecules eluting at the beginning of the chromatogram (see Figure 3.12 for a sample of polyethylene). For such samples conventional SEC and SEC combined with light scattering and RI detectors may suffer from weak RI signal at the region of low elution volumes, which can result in poor precision of the higher-order molar mass averages (M_z, M_{z+1}).

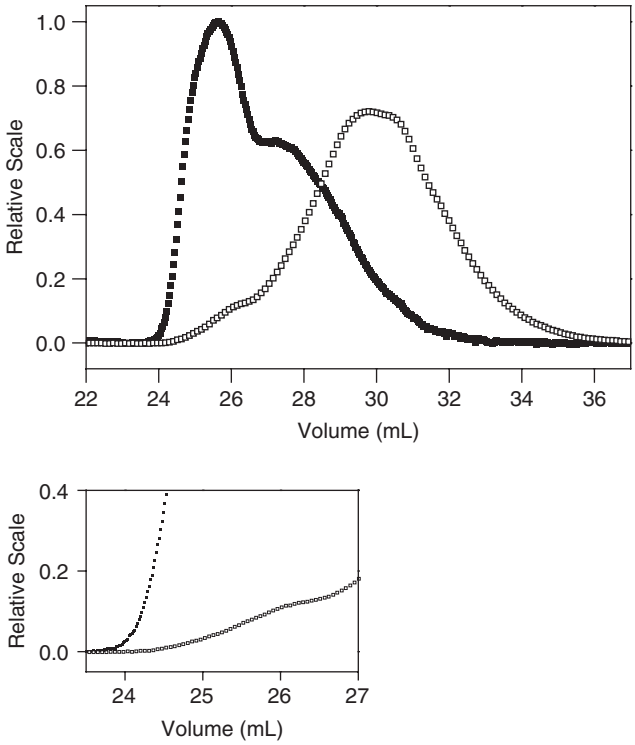

Figure 3.12 RI (□) and 90° MALS (■) signals for a sample of polyethylene illustrating the advantage of the calculation of M_z using solely light scattering signal (Equation 3.36).

The alternative calculation of higher-order molar mass averages requires a simple change of a computational algorithm. The light scattering signal is used instead of the RI signal to calculate the molar mass averages from the conventional SEC calibration curve determined by means of any of the available procedures. The advantage of the method is that it uses the high sensitivity of a light scattering detector to high-molar-mass fractions, but avoids the problem of diminishing RI signal at the region of low elution volumes. The calculation is explained in the following: Using the conventional calibration and RI detection approach, M_z is calculated as:

$$M_z = \frac{\sum c_i M_i^2}{\sum c_i M_i} = \frac{\sum RI_i M_i^2}{\sum RI_i M_i} \tag{3.33}$$

where M_i its the molar mass from the calibration curve at the ith elution volume slice, and c_i is the concentration of the molecules at the ith slice that can be replaced by the RI detector response RI_i. The light scattering signal LS_i is proportional to the concentration and molar mass of molecules eluting at the

SEC slice i:

$$LS_i \approx c_i M_i \approx RI_i M_i \tag{3.34}$$

and thus

$$RI_i \approx \frac{LS_i}{M_i} \tag{3.35}$$

Using Equation 3.35, Equation 3.33 can be written as:

$$M_z = \frac{\sum LS_i M_i}{\sum LS_i} \tag{3.36}$$

The above equation allows the calculation of M_z using only the signal of a light scattering detector. A similar procedure can be used for the calculation of M_{z+1}:

$$M_{z+1} = \frac{\sum LS_i M_i^2}{\sum LS_i M_i} \tag{3.37}$$

Equations 3.36 and 3.37 permit the calculation of higher-order molar mass averages from only the light scattering signal and the SEC calibration curve with no need for an RI detector. A potential advantage of this approach is the fact that the molar mass averages sensitive to the high-molar-mass fractions are calculated solely from the light scattering signal, which is also sensitive to the high-molar-mass fractions. The disadvantage is the necessity of column calibration. Since the method focuses on high-molar-mass fractions that are often branched, the molar masses according to the SEC calibration curve can be significantly erroneous. For many samples the errors given by the incorrect calibration can be larger than those given by a low RI signal when the light scattering detector is used together with an RI detector to calculate the molar mass directly without a calibration curve. A possible solution to this dilemma can be self-calibration, that is, using the data points across the chromatogram where both light scattering and RI signals are sufficiently intensive to establish the calibration curve that is extrapolated toward low elution volumes and used with the light scattering signal for the determination of higher-order molar mass averages.

3.3.3.7 Other Types of Detectors

Online mass spectrometers (MS) are widely used in other types of LC because of high sensitivity and ability to provide qualitative information. Of the many different mass spectrometric methods, matrix-assisted laser desorption ionization time-of-flight (MALDI-TOF) and electrospray ionization (ESI) are the most promising as SEC detectors. Both MALDI and ESI represent soft ionization methods that do not generally lead to fragmentation. Although application of an MS detector in SEC is possible and has been reported in the literature, real applications, especially in the area of synthetic organic soluble polymers, are

rare. *Inductively coupled plasma mass spectrometry* (ICP-MS) has been reported for the detection of various metals along the elution volume profile of biological and environmental samples.[14,15]

Detectors based on *nuclear magnetic resonance* using flowthrough microprobes can provide structural information or the determination of molar mass in the oligomeric region based on the determination of end groups. Besides the substantially high price of such instruments the disadvantages include generally low sensitivity of the online NMR spectrometer, which can be partly solved by using a stop-and-go technique. Note that due to generally low diffusion coefficients of polymers the spreading of the elution zone during the stop period is negligible, and thus the stop-and-go technique is very applicable in SEC.

Various kinds of detectors, specifically designed for combination with SEC, have been reported in the literature, but none of them has found regular applications. A density detector and an osmometric detector have been used in combination with SEC. The density detector, which may be an alternative to an RI detector, is based on the increase of density due to polymer elution. The measurement is based on the change of the period of oscillation of a measuring cell in the form of a U-shaped oscillating tube. Lehmann and Kohler[16] reported the use of membrane osmometry as an online detector in combination with SEC. They designed an osmometer containing cylindrical semipermeable membrane and an outer glass tube. The polymer solution flows through the bore of the membrane capillary. The reference cell filled with solvent is the volume between the membrane and the outer glass tube. The osmometric detector has several limitations such as relatively long response time, impossibility of detecting lower molar mass due to permeation of oligomers through the semipermeable membrane, and decreasing sensitivity toward high molar masses. These limitations are missing in the case of light scattering detectors and thus routine use of online osmometers is unlikely.

3.4 COLUMN CALIBRATION

SEC has become the most intensively used method for the determination of molar mass of synthetic and natural polymers. However, in the conventional form with a concentration-sensitive detector only, SEC is not an absolute method of molar mass determination since there is no direct relation between the measured quantities (i.e., elution volume and detector response, and molar mass). SEC is a method that can easily provide numbers, but the numbers may not always be meaningful. An appropriate column calibration must be established in order to get true information about the molar mass distribution of the analyzed polymers. Since there is no exact theoretical relation between the elution volume and molar mass or size of the eluting molecules, the SEC columns used for the analysis must be calibrated. The calibration relation is then used for the samples requiring characterization to convert the elution volume into the molar mass. The calibration of SEC columns means establishing the relation between the logarithm of

molar mass and elution volume V. The calibration curve can be mostly described by the polynomial:

$$\log M = a + bV + cV^2 + dV^3 \tag{3.38}$$

In the simplest case, the log M is related linearly with the elution volume (i.e., $c = d = 0$), but for most of the available SEC columns the third-order polynomial represents the most appropriate fit. Some SEC softwares offer higher-order polynomials or other types of fits (e.g., point-to-point). However, higher-order polynomials may produce unrealistic maxima or minima on the calibration curve. The applied SEC software should permit the evaluation of the fit in the sense of correlation coefficient and differences between the nominal molar masses of calibration standards and molar masses calculated from the calibration curve.

A straightforward method of calibration of SEC columns is the analysis of a series of standards of accurately known molar mass and very narrow polydispersity under the same experimental conditions as those used for the analysis of real polymer samples. The identical conditions involve mainly the solvent, the flow rate, and the temperature. The obtained calibration curve is valid for a given SEC column set and cannot be used for other columns even in the case of identical column type and manufacturer. Small temperature deviations in the range of about 1°C have no significant impact on the accuracy of the measurement, while the flow rate is the absolutely key parameter, for which even minor fluctuations result in serious errors in molar mass.

The molar mass of the standards used for the column calibration should be determined by a suitable absolute method. The primary methods are light scattering, membrane osmometry, and vapor-phase osmometry. However, it seems that only SEC is used to characterize some of the commercially available standards. The polydispersity of standards should be characterized by SEC, because for narrow standards the values obtained by the combination of light scattering and osmometry are not reliable because of the small differences between M_w and M_n. The requirement of narrow polydispersity is important, because only if this requirement is fulfilled one can assume the validity of the equation $M_n = M_w = M_{PEAK}$. The quantity M_{PEAK} is the molar mass corresponding exactly to the maximum of the chromatogram.

The procedure of the establishment of the calibration curve using narrow standards is illustrated in Figure 3.13. The standards can be analyzed as mixtures of 3–5 standards of molar mass different enough to obtain almost baseline separation. The chromatograms are obtained for each standard mixture, the elution volumes are calculated from the time of injection to the maximum of each peak, and the calibration is established as a plot of log M_{PEAK} versus peak elution volumes.

Establishing a good calibration curve requires standards covering the entire molar mass range of the polymer samples to be analyzed; the analyzed polymers should elute only within the range of the calibration data. Although this requirement may not be always fulfilled, caution should be taken when the polynomial

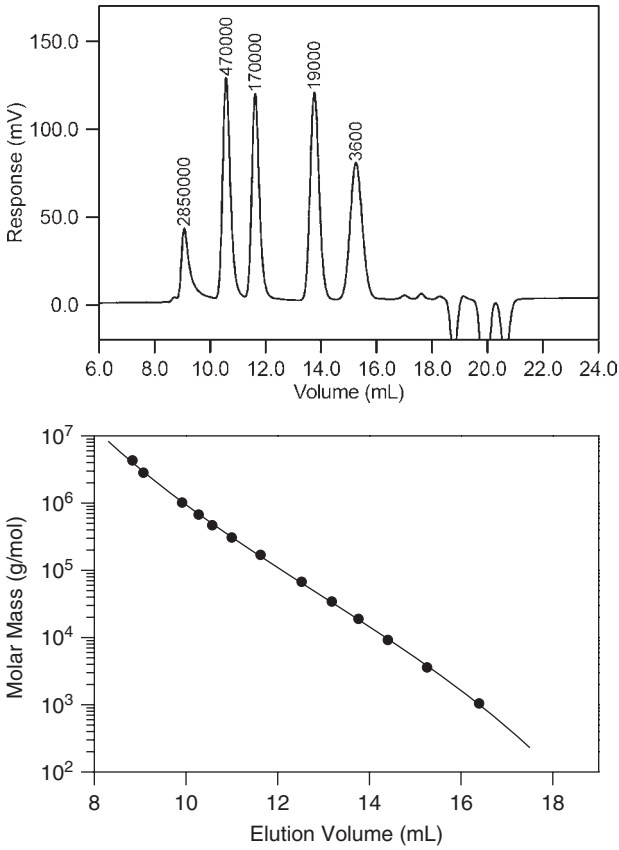

Figure 3.13 Chromatogram of a mixture of polystyrene standards (top) and corresponding calibration curve obtained by the analysis of three standard mixtures (bottom). Molar masses of standards are labeled at the peaks. Calibration curve: $\log M = 16.38664 - 1.86284 \times V + 0.11088 \times \mathrm{V}^2 - 0.00287 \times \mathrm{V}^3$.

is extrapolated outside the first and last data point of the calibration curve. This is especially true in the proximity of the exclusion limit and limit of total permeation. In addition, the standards should be approximately equidistant on the elution volume axis. Typically 10–15 standards are sufficient to establish the calibration curve; using more standards does not increase accuracy.

Calibration standards for polystyrene covering molar mass range of about $600–10^7$ g/mol are available from several suppliers (e.g., Waters, Polymer Laboratories, Pressure Chemical Company, PSS Polymer Standards Service). The polystyrene standards are prepared by anionic polymerization using stringently purified reagents and synthesis conditions. Some standards prepared by anionic polymerization can contain a small amount of polymer with double molar mass, which appears on a chromatogram as a small satellite peak with lower elution

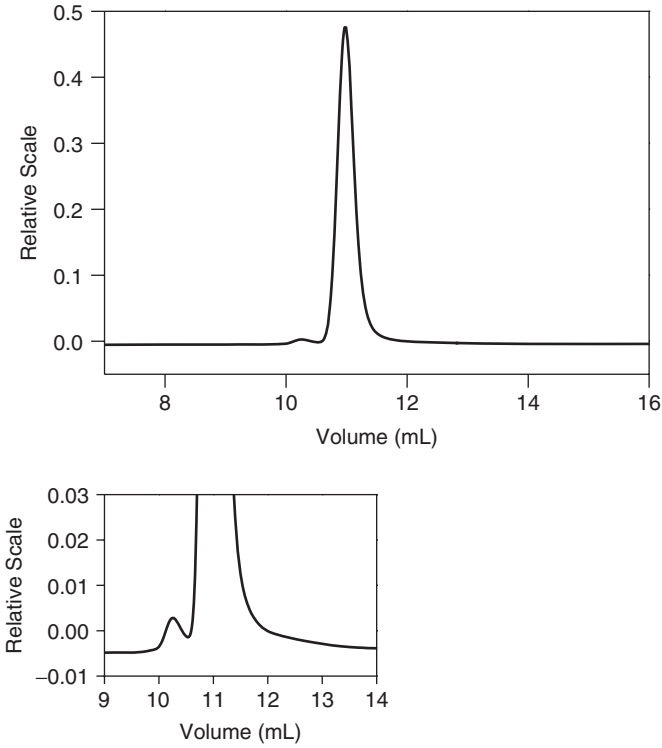

Figure 3.14 RI chromatogram of polystyrene standard of M_{PEAK} 200,000 g/mol showing a small peak of an impurity with about double molar mass.

volume (Figure 3.14). This polymer impurity does not necessarily disturb the determination of a calibration data point, especially when it is well resolved from the main peak, but it influences M_w measured by batch light scattering. The standards are typically characterized with M_{PEAK} and polydispersity M_w/M_n. The nominal polydispersity is mostly less than 1.1. In order to properly characterize the standards, at least one molar mass average should be determined by an absolute method. Unfortunately, this requirement is not always fulfilled. The standards are available as kits or individual molar masses or in the form of mixtures in vials or deposited on small spatulas. With the pre-prepared vial or spatula the calibration solution is easily prepared by addition of an appropriate volume of eluent into a vial or placing a spatula into a vial upon addition of solvent. The pre-prepared kits are available, for example, from Polymer Laboratories (part of Varian), under the trade names EasiVial™ and EasiCal™.

The narrow standards are also available for other homopolymers, for example, poly(methyl methacrylate), poly(ethylene glycol), poly(ethylene oxide), polytetrahydrofuran, dextran, pullulan, sulfonated polystyrene, and poly(acrylic acid). Some standards may not cover a wide molar mass range,

and for many homopolymers and especially copolymers the narrow standards are unavailable. Preparation of standards by precipitation fractionation of a polydisperse polymer and subsequent characterization of the obtained fractions by absolute methods is a very laborious and time-consuming process, which typically yields fractions with polydispersity >1.2.

Polydisperse standards for column calibration can be obtained either by preparation of broad polymer samples covering a broad molar mass range (using, for example, free radical polymerization with different initiator concentration), or by fractionation of a broad polymer. In the latter case the polydispersity of the fractions is lower than that of broad polymers. In either way, at least two molar mass averages must be determined by absolute methods for each polydisperse standard. Alternatively, one molar mass average and the polydispersity estimated by SEC using column calibration established for another polymer can be used. For polydisperse standards, taking M_n, M_v or M_w as M_{PEAK} leads to errors that increase with increasing polydispersity. The correct M_{PEAK} lies somewhere between M_n and M_w and usually the viscosity average M_v is the closest average to M_{PEAK}, but not identical. The relation between the M_{PEAK} and other molar mass averages depends on the type of molar mass distribution. For the Schulz-Zimm type of distribution M_{PEAK} is approximately equal to M_w.

For the logarithmic normal distribution M_{PEAK} is approximately equal to $(M_n \times M_w)^{1/2}$ and there are the following relations between M_n, M_v or M_w and M_{PEAK}:

$$M_n = M_{PEAK}\ e^{-\frac{\beta^2}{4}} \tag{3.39}$$

$$M_v = M_{PEAK}\ e^{\frac{a\beta^2}{4}} \tag{3.40}$$

$$M_w = M_{PEAK}\ e^{\frac{\beta^2}{4}} \tag{3.41}$$

where a is the exponent of the Mark-Houwink equation and β is a parameter related to the polydispersity. The determination of M_{PEAK} of broad standards requires knowledge of not only an average molar mass for each standard, but of distribution type and polydispersity as well.

A single polydisperse polymer with at least two known molar mass averages can be used for the determination of the calibration curve using a trial-and-error search method consisting of comparison of the experimental molar mass averages with those calculated from the SEC chromatogram. A linear calibration curve can be established if only M_n and M_w are known. The procedure may be a part of commercially available SEC software (e.g., Waters Empower™). The broad standards of known molar mass averages can be obtained by SEC-MALS measurements.

Another calibration procedure based on a broad standard uses a polymer sample with a known molar mass distribution curve. The procedure involves comparison of the normalized peak area with the cumulative fraction taken from the distribution curve. The procedure is outlined in Figure 3.15. The particular

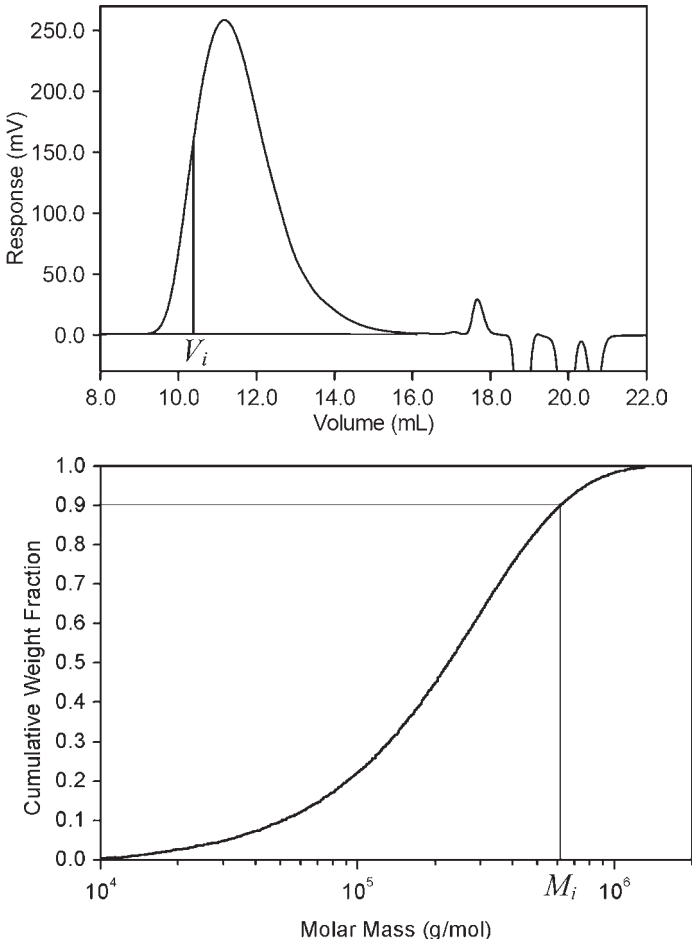

Figure 3.15 Procedure for the determination of calibration curve using a broad polymer standard with known molar mass distribution. RI chromatogram with baseline and a cut at the elution volume corresponding to 10% of total peak area (top) and cumulative distribution curve obtained by SEC-MALS analysis (bottom). The molar mass M_i corresponds to the elution volume V_i, that is, the coordinates of the calibration data point are M_i, V_i. Further data points are obtained by equivalent procedures.

elution volumes V_i are matched with the molar masses M_i taken from the molar mass distribution curve so that the peak area fraction and the weight fraction are identical. The molar mass distribution curve of polydisperse standard is determined experimentally, preferably by means of SEC-MALS, or using two molar mass averages and assuming validity of a theoretical distribution function.

Unlike calibration based on the narrow standards, the calibration curves obtained by broad standards are affected by instrumental peak broadening and thus are more prone to errors when applied to the molar mass characterization of

polymer samples. Nevertheless, although calibration by means of a broad standard is less accurate than that established by a series of narrow standards, it may yield more reliable results than those based on the calibration established by narrow standards of different chemical composition than that of polymer under investigation.

3.4.1 Universal Calibration

In view of the fact that SEC separation is governed by the size of polymer molecules in dilute solution, it can be assumed that the hydrodynamic volumes (Equation 1.81) of all species eluting at the same elution volume are identical and that the product $[\eta]M$ represents a universal calibration parameter. The *universal calibration* is a function of $\log([\eta]M) = f(V)$ that can be, as in the case of conventional calibration, described by the first- to third-order polynomial. The intrinsic viscosity of narrow standards can be determined experimentally or calculated from the Mark-Houwink equation. The idea of universal calibration was proved for the first time by Benoit and co-workers,[17] who plotted $\log([\eta]M)$ versus elution volume and obtained a common plot for polymers of various chemical composition and architecture, namely linear polystyrene, star polystyrene, comb polystyrene, poly(methyl methacrylate), poly(vinyl chloride), copolymer styrene–methyl methacrylate, poly(phenyl siloxane), and polybutadiene. The concept of universal calibration appears to be widely valid with the exception of polymers encountering secondary separation mechanisms that are common in aqueous solvents for ionic polymers, highly polar polymers, or polymers measured in theta solvents. Universal calibration was also shown to fail in the case of low-molar-mass polymers.[18]

The concept of universal calibration allows the transformation of the calibration based on well-defined narrow standards (usually polystyrene in organic solvents or pullulan in aqueous solvents) into a calibration valid for a polymer requiring analysis. The hydrodynamic volumes of the standard and polymer under investigation are identical at each elution volume, which, using the definition of the hydrodynamic volume, gives:

$$\log([\eta]_P M_P) = \log([\eta]_S M_S) \tag{3.42}$$

where S and P refer to standard polymer and polymer under analysis, respectively. Entering the Mark-Houwink equation into Equation 3.42 leads to:

$$\log M_P = \frac{1}{1+a_P} \log \frac{K_S}{K_P} + \frac{1+a_S}{1+a_P} \log M_S \tag{3.43}$$

where K and a are the constants of the Mark-Houwink equation for the standard and the polymer requiring analysis. The molar mass of each standard can be recalculated to the molar mass of the polymer requiring analysis using Equation 3.43 and the constants of the Mark-Houwink equation for the standard and the polymer. The literature often shows several combinations of Mark-Houwink

parameters for a polymer in the same solvent at the same temperature. Even for such common polymers as polystyrene or poly(methyl methacrylate) the literature values may differ noticeably, and the situation is typically worse for other polymers. Generally, small K is related to large a, and vice versa. Any combination of K and a usually can be used to calculate the viscosity-average molar mass from the intrinsic viscosity and the obtained results are similar. However, when the Mark-Houwink constants are to be used for universal calibration, their careful selection for the calibration standard and the polymer under investigation is very important. The parameters to consider are: number of samples used to get the Mark-Houwink plot, molar mass range (at least one order of magnitude), polydispersity of samples ($M_w/M_n < 1.5$), type of molar mass average (M_w preferred), and linearity of the obtained plot.

An alternative universal calibration procedure assumes good thermodynamic quality of the SEC solvent for the standard and polymer under analysis, that is, the state when the two polymers will have similar polymer–solvent interactions. Then the unperturbed root mean square end-to-end distance $\langle r \rangle_0^{1/2}$ can be used as an alternative universal calibration parameter.

The relation between $\langle r \rangle_0^{1/2}$ and $[\eta]$ describes the equation derived by Flory and Fox (Equations 1.12 and 1.13). In thermodynamically good solvents the two polymers have similar polymer–solvent interactions and their expansion factors are almost identical. The calibration curves of a standard and a polymer are then related by:

$$\log M_P = \log M_S + \log \frac{(\langle r^2 \rangle_0 / M)_S}{(\langle r^2 \rangle_0 / M)_P} \tag{3.44}$$

where $(\langle r^2 \rangle_0 / M)^{1/2}$ is a constant for a polymer independent of molar mass, which can be found in the literature.[19] Note that according to Equation 3.44 the calibration curves of the standard and polymer under analysis are assumed to be parallel, which is often not fulfilled.

Besides the transformation of the calibration curve of a standard to the calibration curve of a polymer, the concept of universal calibration can be also used for the determination of the constants of the Mark-Houwink equation using the chromatogram of a broad polymer sample for which at least two molar mass averages or one molar mass average and the intrinsic viscosity are known. The procedure uses two of the following equations:

$$[\eta] = \sum_i w_i [\eta]_i \tag{3.45}$$

$$M_n = \left[\sum_i (w_i / M_i) \right]^{-1} \tag{3.46}$$

$$M_w = \sum_i w_i M_i \tag{3.47}$$

where w_i is the weight fraction of polymer eluting at the elution volume V_i and $[\eta]_i$ and M_i are the corresponding intrinsic viscosity and molar mass. Identifying $J_i = [\eta]_i M_i$, the above equations can be rearranged as:

$$[\eta] = K^{\frac{1}{1+a}} \sum_i w_i J_i^{a/(1+a)} \tag{3.48}$$

$$M_n = \left[K^{\frac{1}{1+a}} \sum_i \frac{w_i}{J_i^{1/(1+a)}} \right]^{-1} \tag{3.49}$$

$$M_w = \left(\frac{1}{K} \right)^{\frac{1}{1+a}} \sum_i w_i J_i^{1/(1+a)} \tag{3.50}$$

The values of w_i can be determined from the experimental chromatogram and J_i from the universal calibration curve. The procedure is theoretically capable of yielding the Mark-Houwink constants, but the obtained values may differ for different samples of the same polymer and the method represents a generally less reliable way of determining the constants K and a.

The most effective application of universal calibration is the use of $\log([\eta]M)$-versus-V dependence with an online viscometer, which continuously measures the intrinsic viscosity as a function of elution volume. Using the intrinsic viscosities determined at particular elution volumes one can calculate the corresponding molar masses from the universal calibration curve. This application of universal calibration generally provides more reliable results than calculation based on Equations 3.43 or 3.44, because it is independent of the accuracy of the universal calibration parameters.

For many real polymer samples reliable universal calibration parameters or well-defined standards are unavailable. The application of a calibration determined by available standards, mostly polystyrene in the case of organic soluble polymers, for processing the chromatograms of other polymers became a routine practice in many laboratories of polymer research and quality control. This practice can be called a bad SEC habit. It must be stressed that the molar masses obtained by the use of calibration prepared with narrow standards of one polymer to polymers of other types are often in error by a factor of several tens percent, and by as much as an order of magnitude in the case of branched polymers (for example, see Figure 3.16).

Although the application of polystyrene calibration to other polymers can be acceptable for a rough estimation of the molar masses and especially for the mutual comparison of samples of identical chemical composition, it should not be used for a fundamental description of polymer samples, stoichiometric calculations, or kinetic studies. The procedure is especially erroneous and even misleading in the case of branched polymers and polymers interacting with column packing. If the polystyrene calibration is applied, this fact should be reported together with the obtained results and they should not be treated as the absolute values. The molar mass averages and the molar mass distribution obtained by

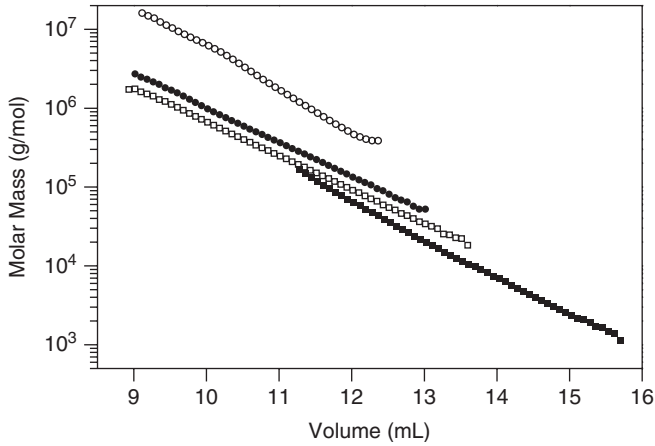

Figure 3.16 Calibration curves of polystyrene (□), epoxy resin based on bisphenol A (■), linear (•) and star-branched (◯) poly(benzyl methacrylate) determined by SEC-MALS. Conditions: 2 × PLgel Mixed-C 300 × 7.5 mm, THF, 30°C.

means of polystyrene calibration represent the values for a hypothetical sample of polystyrene that would have the same distribution of hydrodynamic volume as the polymer under analysis.

3.4.2 Flow Marker

The calibration curve is valid for a given column set and separation conditions used for the chromatography runs. These conditions include solvent, temperature, flow rate, and also current status of the columns, because the separation efficiency of the columns can change with time. An absolutely constant flow rate is essential for further use of calibration curve. Since the calibration curve is a log-M-versus-V relation, small deviations of the elution volume have significant influence on the molar mass calculated from the calibration equation. Even modern HPLC pumps may show slight flow rate fluctuations that are typically insignificant for other types of liquid chromatography but may be significant from the viewpoint of the molar mass determination by SEC.

Flow marker (internal standard) is a low-molar-mass compound that is added to the solutions of standards used to establish the calibration relation and to a solution of a polymer requiring analysis. A reference elution volume and a tolerance window (in %) is entered into the SEC software used to acquire and process the data. The calibration relation is valid for a certain elution volume of the flow marker measured at the time when the calibration was established. If the elution volume of the flow marker varies between the runs, the elution volumes of particular volume slices are shifted by the ratio of $\frac{V_{FM,ref}}{V_{FM}}$, where V_{FM} and $V_{FM,ref}$ are the elution volume of the flow marker and the reference

flow marker position, respectively. Then the molar masses M_i are calculated for elution volumes $V_i \times \frac{V_{FM,ref}}{V_{FM}}$. That means that if the flow marker appears, for example, at lower elution volume compared to the reference value, the entire polymer peak is shifted slice by slice along the elution volume axis toward higher elution volumes to compensate for the faster pump rate. Toluene, benzene, and sulphur have been used as a flow marker in the case of THF, glucose can be an option in aqueous solvents, and many other compounds can be employed as well.

A good flow marker should be readily soluble in SEC solvent, nonreactive with the solvent and polymer sample, low-toxic, stable, and easily available, and it should elute after the polymer peak at elution volume different from those of impurity peaks. The application of flow marker can undoubtedly improve the accuracy and repeatability of the SEC measurements, but it has several potential drawbacks. First, the flow marker can compensate for a deviation of the flow rate from nominal value that is constant during the entire SEC run, but cannot eliminate the influence of short-term flow rate fluctuations. For many polymer samples the flow marker can overlay with the oligomers, residual solvents, and monomers or additives present in the sample. In addition, the flow markers may co-elute with the solvent peaks from the SEC eluent itself. That is especially the case with THF, which usually shows three negative peaks at the end of chromatogram, or aqueous buffer solutions where an intensive salt peak usually appears at the end of chromatogram.

The mutual interference of positive and negative peaks can change the position of the flow marker and thus its application can be counterproductive. In THF, one of the three negative peaks can be used as the flow marker, assuming the sample does not contain a significant amount of impurities co-eluting with the solvent peaks. The effect of the flow marker on the elimination of flow rate deviations is demonstrated in Table 3.1. The data show that a flow rate deviation as low as 0.2% results in a reckonable deviation of molar mass, and 1% deviation causes significant difference of about 10%. Besides flow rate variations the flow marker can partly compensate for the change of SEC column properties. However, the use of flow marker is not always straightforward and alternatively daily establishment of the calibration can be used. Laboratories equipped with an autosampler can implement this approach, because assuming a typical sample run time of 30–45 min and injection of three standard mixtures there is still sufficient instrumental time for numerous analyses. Polystyrene standards in THF are stable for several months with no sign of degradation. The only requirement is to keep the solutions sealed properly to avoid THF evaporation. The samples can be stored directly in the autosampler vials using new nonpunctured seals. Storage in a refrigerator can reduce THF evaporation. Also solutions of water-soluble standards can be kept for several months in a refrigerator especially when microbiological degradation is minimized by addition of 0.02% sodium azide.

Measurement of flow rate can be performed to identify possible sources of errors due to flow rate deviations. The procedure is simple and requires collection of the effluent from the detector outlet into a 5- or 10-mL volumetric flask and

Table 3.1 Influence of Flow Rate on M_w of Polydisperse Polystyrene and Correction of Flow Rate Deviations with Flow Marker

Flow (mL/min)	M_w (g/mol)		Flow Marker Elution Volume (mL)
	No Flow Marker	Flow Marker	
1	273,200 ± 1,000	277,500 ± 500	19.93–19.94
0.998	268,300 ± 300	277,500 ± 300	19.97
0.995	262,800 ± 100	279,800 ± 300	20.02
0.99	249,800 ± 500	279,600 ± 400	20.10
0.98	226,200 ± 1300	279,800 ± 900	20.25–20.28
0.97	199,500 ± 2700	280,800 ± 400	20.46–20.52
0.95	153,900 ± 300	281,300 ± 300	20.95

Conditions: THF at 1 mL/min, column temperature 40°C, 2 × PLgel Mixed-C 300 × 7.5 mm columns, flow marker elution volume for calibration standards = 19.91 mL.

the measurement of time by a stopwatch. The flow rate is then calculated with a precision of ±0.01 mL/min.

Regular analysis of a reference polymer should be included in the analysis of each sample series irrespective of the use of flow marker. The reference polymer should be stable in the SEC solvent and show no interactions with column packing. It need not be necessarily of well-known molar mass averages, because its primary application is to check repeatability of the measurements. The reference sample preferably should have molar mass range similar to typical samples that are to be analyzed, but the chemical composition can be different. A broad polystyrene in THF and dextran in aqueous solvents can be recommended as good reference polymers, but other types according to particular columns, solvent, and application area can be used as well. The reference sample should be available in sufficient amounts so that it can be used over many years and possibly shared with other laboratories when interlaboratory comparability of the results becomes of interest. The reference polymer can be measured repeatedly during long sample series. A deviation of the molar mass averages over an acceptable limit results in the reestablishment of the calibration curve and check of the pump flow rate, temperature stability, and column performance.

3.5 SEC MEASUREMENTS AND DATA PROCESSING

3.5.1 Sample Preparation

Appropriate preparation of sample is an important part of successful SEC measurement. It is not always recognized that an inappropriate sample preparation may result in significant errors in molar masses or in poor repeatability. The ultimate condition for the analysis of a polymer by SEC is its solubility in a suitable solvent. The solubility of a polymer sample in a given solvent can be

predicted according to the solubility parameter δ that is defined as:

$$\delta = \left(\frac{\Delta E}{V} \right)^{\frac{1}{2}} \tag{3.51}$$

where $\Delta E/V$ is the energy of vaporization per unit volume. A polymer dissolves in a solvent if the solubility parameters of the solvent and polymer are identical, whereas the probability of dissolution decreases with increasing difference of solubility parameters. In contrast to solvents, the solubility parameters of polymers cannot be measured directly, because polymers do not vaporize, but they must be measured indirectly from swelling experiments with solvents of known δ. Solubility parameters are available for various polymers and solvents in the literature, but the prediction of solubility on the basis of solubility parameters is limited and a typical approach is empirical testing of a polymer requesting analysis in the solvents that are usually used in a given laboratory.

Commonly, the sample requiring analysis is prepared in the mobile phase and only exceptionally it is dissolved in a different solvent than that used as the mobile phase. Such a procedure can be used if the sample solubility is significantly better in a different solvent than in the mobile phase. To protect SEC columns it is necessary to verify that the sample remains in solution after injection into the SEC columns. Tests can be performed by dilution of a sample solution by SEC solvent. A sample solution at higher concentration than that used for SEC analysis must remain clear with no precipitation after significant dilution with SEC solvent. However, the injection of a sample in a solvent different from the mobile phase should be used only in justified cases. This procedure also results in a very intensive solvent peak at the end of the chromatogram.

It must be stressed that dissolving a polymer often requires several hours or even several days and exceptionally a full dissolution may take even longer. The obtained polymer solution may contain insoluble parts if the dissolution time is not sufficient. The insolubles consist of the high-molar-mass part of the sample and improper sample preparation may result in a loss of part of a sample and consequently an incorrect picture of the molar mass distribution. Generally, the time needed to dissolve a polymer sample completely depends on the thermodynamic quality of the solvent, molar mass of the polymers, polymer branching, and polymer crystallinity. The dissolution rate increases with decreasing molar mass and increasing thermodynamic quality of the solvent, and decreases with increasing branching and crystallinity.

A thermodynamically good solvent can dissolve a polymer up to high concentrations in a wide temperature range, while polymer solubility is limited in thermodynamically poor solvents. The sample solubility increases with dissolution temperature and some polymers are soluble only at elevated temperatures. The samples soluble only at elevated temperatures may either remain in solution even after cooling down to the room temperature and so can be analyzed using ambient SEC, or remain in solution only at high temperature and so must be analyzed at that temperature by means of a high-temperature SEC system.

Although gentle shaking and warming at about 60°C can decrease the dissolution time and help dissolve polymers with limited solubility, intensive manual shaking, high-speed agitation, or dissolution in an ultrasonic bath should be avoided, because polymers can contain fractions with high molar mass that may undergo shearing degradation when exposed to intensive shaking or agitation. The probability of shearing degradation increases with increasing molar mass. The shearing degradation is also more probable in thermodynamically good solvents and at elevated temperatures, because of the expansion of polymer chains.

To prepare a sample for SEC analysis a known amount of polymer is placed in a volumetric flask or other suitable container and filled with the solvent. Although knowledge of the exact sample concentration is not needed for data processing, the sample concentration should be appropriate. The appropriate concentration is a result of counteracting requirements such as detector response, loading capacity of the columns, solution viscosity of the sample, and concentration dependence of the elution volume. The sample should be injected at a concentration and volume that results in sufficiently intensive detector response while column overloading and viscosity effects are minimal. Typical sample concentrations range from 0.1 to 1% w/v. Sample concentrations recommended by column manufacturers are listed in Table 3.2. As a rule of thumb, the optimum sample concentration decreases with increasing molar mass and samples containing fractions with molar mass of several millions g/mol should be injected at the lowest possible concentration. Broad polymers usually can be injected at higher concentrations than narrow polymers, because the sample zone in SEC columns is spread over larger elution volume. The sample concentration of oligomers is typically not a serious issue.

Injected volume is another important operating parameter influencing the accuracy of the obtained results. Polymers creating highly viscous solutions may require injection of larger, more dilute solutions, but the injection of too-large

Table 3.2 Sample Concentration Recommended by Column Manufacturers

Manufacturer	Molar Mass (g/mol)	Sample Concentration (% w/v)
1	Up to 25,000	<0.25
	25,000–200,000	<0.1
	200,000–2,000,000	<0.05
	>2,000,000	<0.02
2	Up to 5,000	<1.0
	5,000–25,000	<0.5
	25,000–200,000	<0.25
	200,000–2,000,000	<0.1
	>2,000,000	<0.05
3	Not specified	0.05–0.5

volumes contributes to peak broadening and reduces separation performance, which is especially true in the case of 4.6-mm narrow-bore columns.

The injection volume in SEC is usually several times larger than in other types of liquid chromatography. A typical injection volume per regular 300 × 8-mm column is 50 to 100 μL, and should be decreased accordingly for narrow-bore 4.6-mm columns. The injection volume for narrow standards can be about half of that used for polydisperse polymers to improve peak shape and resolution. For example, using two 300 × 7.5-mm columns, 50 μL can be used for the injection of standards and 100 μL for the injection of broad polymer samples.

The optimum concentration for narrow polystyrene standards is approximately 0.03% w/v for molar masses up to about 1 million g/mol, 0.015% w/v for standards with molar mass of 1–5 million g/mol, and 0.01% w/v for standards with molar mass around 10^7 g/mol. A polydisperse polymer can be analyzed using a concentration of about 0.2–0.3% w/v and the concentration can be adjusted according to the detector response, peak shape, average molar mass, and sample polydispersity.

Excessive injected mass can result in column overloading, which does not damage the columns, but affects the peak shape and position and thus the molar mass distribution. As shown further in Section 3.5.6, the molar mass averages decrease with the increasing injected mass. Consequently, random changes of injected mass due to improper sample preparations can negatively influence the accuracy and repeatability of the measurements. This can happen when a small piece of sample is dissolved without a proper weighing or if samples containing different amounts of solvents or fillers are prepared at the same amount without taking into account the real concentration of polymer in the sample. Paints, which besides polymer binder contain solvents, fillers, and other additives, are typical materials for which the polymer content should be determined before the sample is prepared for SEC analysis.

Filtration is an important step in sample preparation for SEC measurement. Many industrial polymers contain insoluble materials such as fillers or species created during polymerization such as highly crosslinked microgels. Filtration protects column frits from blockage. The blockage increases the system back pressure and can even distort the chromatographic peaks. In addition, the blockage of column frits increases the probability of shearing degradation. Filtration of the sample through a 0.45-μm disposable filter is an efficient way of removing insoluble species. To reduce the possibility of removing part of a sample by filter membrane, the filter should be flushed with a small amount of sample solution before transferring into the injection device. Although sample filtration protects SEC columns, it should be always performed with caution, because it may remove or degrade high-molar-mass fractions in the sample. Samples containing ultra-high-molar-mass fractions may require filters with larger porosity (e.g., 1 μm). Samples such as calibration standards or pure polymers that show complete dissolution with no indication of particulate matter do not need to be filtered. An alternative procedure of sample clarification is to centrifuge the sample with a benchtop centrifuge for a few minutes and then inject the supernatant.

Most synthetic and also natural polymers show good stability in solutions. Keeping the solutions well sealed at room temperature or in a refrigerator can enhance their stability. Nevertheless, sample stability after dissolution is a potential issue that may have a negative impact on the accuracy of the experimental results. If a polymer sample is suspected of degradation in solution, the measurements should be repeated in suitable time intervals to see whether the molar mass is constant or decreases with time. If the degradation is eminent, then the sample should be prepared in another solvent where the degradation does not occur, or at least measured immediately after dissolution. Water, which is typically present in THF, can promote hydrolysis of polyesters as demonstrated in Figure 3.17. If needed, THF can be effectively dried with molecular sieves. Poly(phenyl acetylene) is a typical polymer that undergoes fast degradation in THF.

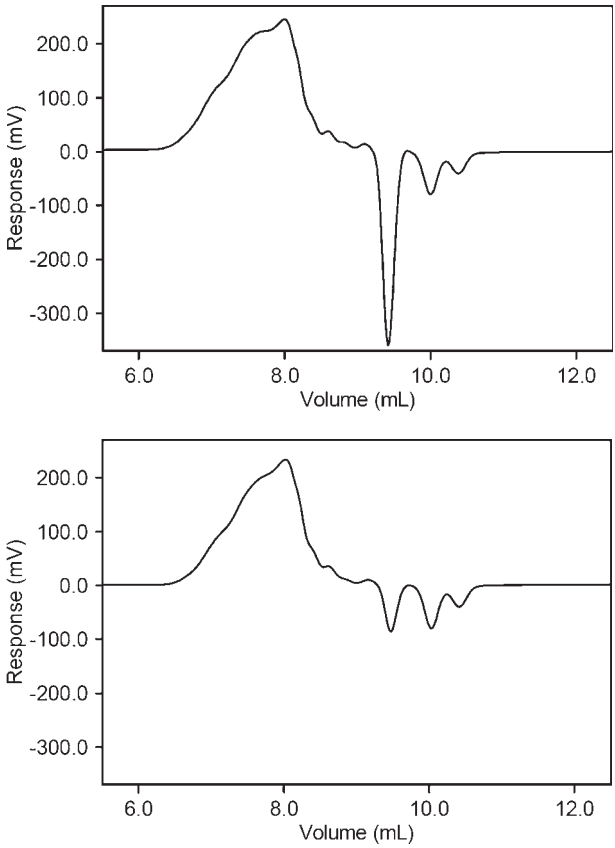

Figure 3.17 RI chromatograms of polyester resin: fresh solution (top) and the same solution after three days (bottom). Note the significant decrease of negative water peak as a result of hydrolysis of the polyester chain. M_n (g/mol) = 2020 (fresh solution), 1900 (after 3 days); M_w (g/mol) = 6480 (fresh solution), 5520 (after 3 days); M_z (g/mol) = 16,100 (fresh solution), 12,700 (after 3 days).

3.5.1.1 Sample Derivatization

Derivatization represents a possible part of sample preparation. In other types of liquid chromatography, derivatization is often used to increase the detection limit, and in gas chromatography the purpose of derivatization is to increase volatility and improve thermal stability. In SEC, derivatization is used significantly less frequently and may improve sample solubility or suppress enthalpic interactions of polymer with the column packing. In principle, the derivatization reaction can be carried out before the analysis or between the column and detector, the former being the most applicable in SEC. The derivatization reactions must not be associated with degradation of the polymer chain. The derivatization changes the molar mass, and the number and mass of bonded molecules should be taken into account at the interpretation of the obtained results. The derivatization involves the reaction of a specific functional group of a polymer with a suitable chemical agent. The chemical composition of a polymer to be analyzed and its solubility govern the choice of the derivatization procedure. Most of the polymers are by their nature not capable of easy derivatization. Fortunately, there is also no need of derivatization of such polymers, because they can be easily analyzed in their net form. Various derivatization reactions and derivatives can be found in an excellent book by Blau and Halket.[20] The following reactions can serve as examples of suitable derivatizations:

- *Silylation* with N,O-Bis(trimethylsilyl)trifluoroacetamide of polymers containing a high level of carboxyl groups can significantly improve the peak shape for analysis in THF on styrene-divinylbenzene gels as demonstrated in Figure 3.18. The silylation can be easily done by addition of 0.3 mL of silylation agent to 3 mL of about 0.3% w/v solution of polymer in THF. The solution is heated up to about 60°C for three hours, filtered, and injected into SEC columns.
- *Acetylation* with acetic anhydride under catalysis with N-methylimidazole can improve THF solubility of polymers containing hydroxyl groups or amine groups. The reaction results in the formation of esters or amides of acetic acid. Acetic anhydride and N-methylimidazole are added in the amount of 20 μL per 1 mL of about 0.3% w/v THF solution, and after one hour at room temperature the solution can be analyzed. The reaction has been successfully applied to the analysis of hyperbranched polyesters based on dimethylol propionic acid, which showed limited solubility in THF with tendency to aggregation.

3.5.2 Determination of Molar Mass and Molar Mass Distribution

A primary result of an SEC experiment is a *chromatogram*, which is a record of a detector signal against elution volume. The chromatogram bears information about the concentration of molecules eluting at various elution volumes, which

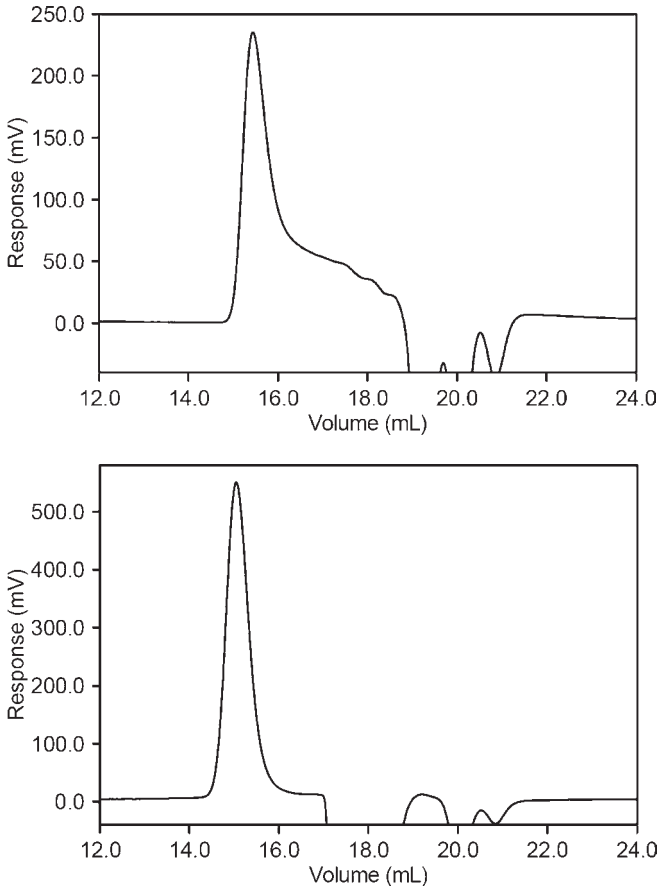

Figure 3.18 Chromatograms of acrylic copolymer containing a high level of carboxyl groups before (top) and after (bottom) silylation with N,O-Bis(trimethylsilyl)trifluoroacetamide. The silylation of the carboxyl groups eliminates the interactions with column packing. Conditions: 2 × PLgel Mixed-C 300 × 7.5 columns, THF, 40°C, 1 mL/min.

is related to the intensity of detector signal, and the molar mass, which is related to the elution volume. Although the chromatogram reflects the molar mass distribution of the sample under analysis, chromatograms of the same sample measured using different columns, and possibly other parameters such as temperature or flow rate, are different. Assuming proper calibration and data processing, the molar mass distributions obtained by processing chromatograms acquired under different chromatographic conditions should be identical within the experimental uncertainties. That means the transformation of the chromatograms into molar mass distribution curves eliminates the differences given by different instrumentation.

The simplest way to determine molar mass from the SEC chromatogram is the determination of M_{PEAK}, which is the molar mass corresponding to the

maximum of the peak. This method is applicable only for monodisperse or very narrow polymers; for polydisperse samples it cannot be recommended. Not only is the method applicable solely to unimodal chromatograms, but it results in the determination of a molar mass average of unknown type for which the relation $M_n < M_{PEAK} < M_w$ is valid. In addition, a single value of M_{PEAK} does not provide any information about sample polydispersity. Consequently, calculation of the entire molar mass distribution and all molar mass averages should be performed for proper description of a polymer under analysis.

A fundamentally correct procedure of the calculation of molar mass distribution from an SEC chromatogram involves correction for peak broadening. Correction for peak broadening is the most complicated and uncertain step in processing SEC data and there are no simple and completely adequate methods. With the development of modern high-performance columns, the need for peak broadening correction has faded for most practical cases. The necessity of peak broadening correction also decreases with the increasing sample polydispersity. In the case of narrow polymers, a possible error is not in the sense of molar mass, but mainly in the sense of sample polydispersity, which is undoubtedly overestimated due to peak broadening. The need for peak broadening correction is also further eliminated in the case of light scattering detection when molar mass is directly determined after the sample elutes from the SEC columns.

The following procedure for processing chromatograms assumes that band broadening can be neglected. The procedure consists of determination of baseline and peak integration interval (i.e., beginning and end of the peak). The chromatogram is separated into regular intervals by vertical lines that are sufficiently close to each other. The relative height of each slice represents the weight fraction of molecules eluting at a given elution volume (the slice area can be used instead of the slice height):

$$w_i = \frac{H_i}{\sum\limits_i H_i} = \frac{A_i}{\sum\limits_i A_i} = \frac{A_i}{A} \tag{3.52}$$

where w_i is the weight fraction of molecules eluting at elution volume V_i, H_i and A_i are the height and the area of the ith slice, respectively, and A is the total peak area. The sampling frequency is typically 0.5–2 seconds and further decrease of the slice width does not benefit the obtained results. The molar mass corresponding to each elution volume slice is calculated from the calibration curve expressed by Equation 3.38. The obtained values of H_i or A_i and M_i are used to calculate the molar mass averages:

$$M_n = \frac{\sum H_i}{\sum \frac{H_i}{M_i}} = \frac{\sum A_i}{\sum \frac{A_i}{M_i}} \tag{3.53}$$

$$M_w = \frac{\sum H_i M_i}{\sum H_i} = \frac{\sum A_i M_i}{\sum A_i} \tag{3.54}$$

$$M_z = \frac{\sum H_i M_i^2}{\sum H_i M_i} = \frac{\sum A_i M_i^2}{\sum A_i M_i} \tag{3.55}$$

$$M_{z+1} = \frac{\sum H_i M_i^3}{\sum H_i M_i^2} = \frac{\sum A_i M_i^3}{\sum A_i M_i^2} \tag{3.56}$$

$$M_v = \left(\frac{\sum H_i M_i^a}{\sum H_i}\right)^{\frac{1}{a}} = \left(\frac{\sum A_i M_i^a}{\sum A_i}\right)^{\frac{1}{a}} \tag{3.57}$$

where a is the exponent of the Mark-Houwink equation. If the number of slices is sufficiently large, the use of area slices or slice heights provides equivalent results. Besides the values of molar mass averages, most of the commercially available SEC softwares report also the value of M_{PEAK}. Although M_{PEAK} does not have an exact definition as do other molar mass averages, it can be understood as the molar mass of the most abundant fractions in a given polymer sample and thus it can provide certain information about the analyzed sample. However, caution should be taken in the case of bimodal samples, where using M_{PEAK} can lead to false conclusions.

The SEC analysis yields not only all molar mass averages, but also the differential and cumulative distribution curves. The normalized chromatogram $g(V)$ is obtained according to the equation:

$$g(V) = \frac{G(V)}{\int_0^\infty G(V)dV} \tag{3.58}$$

where $G(V)$ is the unnormalized detector signal. The relation between the normalized chromatogram and the differential distribution curve is:

$$g(V)\,dV = -f_w(M)\,dM \tag{3.59}$$

where $f_w(M)$ is the weight differential distribution function. The negative sign is because the molar mass decreases with increasing elution volume. In a rigorous manner, Equation 3.59 should use a normalized chromatogram corrected for band broadening $w(y)$ instead of $g(V)$.

Using Equation 3.59, the differential distribution function equals:

$$f_w(M) = \frac{-g(V)}{\frac{dM}{dV}} = \frac{-g(V)}{\frac{d(\log M)}{dV}}\frac{\log e}{M} = \frac{-g(V)}{2.303M\frac{d(\log M)}{dV}} \tag{3.60}$$

The weight fraction of polymer in the molar mass interval M to $(M + dM)$ is $f_w(M)dM$ or in the molar mass interval $\log M$ to $(\log M + d\log M)$ is $F_w(\log M)d\log M$. The differential function $F_w(\log M)$ is calculated according to the equation:

$$F_w(\log M) = \frac{-g(V)}{\frac{d(\log M)}{dV}} \tag{3.61}$$

The differential distribution curve expressed in log M is sometimes labeled as $dw/d(\log M)$ or $dwt/d(\log M)$, where w or wt indicates the weight fraction. The derivatives in Equations 3.60 and 3.61 are obtained analytically by differentiating the calibration curve. If the calibration curve is fitted by the third order polynomial (Equation 3.38), the derivative to be used in Equations 3.60 and 3.61 is:

$$\frac{d(\log M)}{dV} = b + 2cV + 3dV^2 \tag{3.62}$$

In the case where the calibration curve is linear, the derivative is constant over all elution volumes and equals the slope of the calibration curve.

The cumulative distribution expressing the weight fraction less than or equal to M_i is given by the equation:

$$I_w(M_i) = \int_{V_b}^{V_i} g(V)\,dV = \frac{\sum_{1}^{i} A_i}{A} \tag{3.63}$$

where M_i is the molar mass of molecules eluting from the columns at elution volume V_i, V_b is the beginning elution volume of the peak processing, A_i is the slice area, and A is the total peak area. The procedure for processing the chromatogram and calculating the molar mass distribution and molar mass averages is illustrated in Figure 3.19. The corresponding distribution curves calculated by Waters Empower™ software are depicted in Figure 3.20 and the numerical data are listed in Table 3.3. Note that in this particular example the two distribution curves are drawn from high to low molar masses in accordance with the SEC elution order, and the molar mass axis is expressed in log M. Taking, for example, the data at slice number 130, one can read that about 41.1% of molecules have molar mass larger than 251,000 g/mol or alternatively that 58.9% molecules in the analyzed sample have molar mass below this value. The slice fraction $A_{130} = 2.58 \times 10^5/3.56 \times 10^7 = 0.00725$, that is, 0.725% molecules have molar mass corresponding to this slice. The same value is obtained from the differential distribution function: $F_w(\log M) = 0.94632, d(\log M) = (\log 251{,}300 - \log 246,900) = 0.00767$, weight fraction of molecules with molar mass in the range of 246,900 g/mol $-251,300$g/mol $= 0.94632 \times 0.00767 = 0.00726$, that is, 0.726%.

The most important steps in processing the experimental data are the construction of the baseline and the selection of the peak limits. The baseline construction is the easiest part of chromatogram processing, assuming a stable detector signal. The procedure for constructing the baseline is to draw a linear line from a point before the beginning of the polymer peak to the point after the solvent and impurity peaks. If the baseline is stable and properly established, moving the baseline beginning and end points along the elution volume axis should not markedly change the results, as demonstrated in Figure 3.21. Especially in the case of samples containing oligomeric tail, positioning the baseline

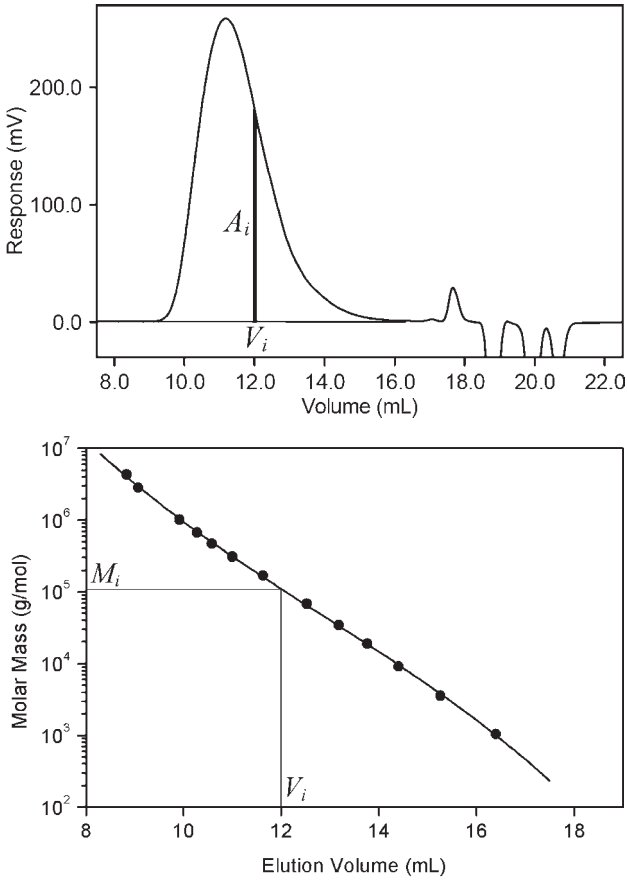

Figure 3.19 Procedure for the calculation of molar mass averages and molar mass distribution curves from an SEC chromatogram and a calibration curve.

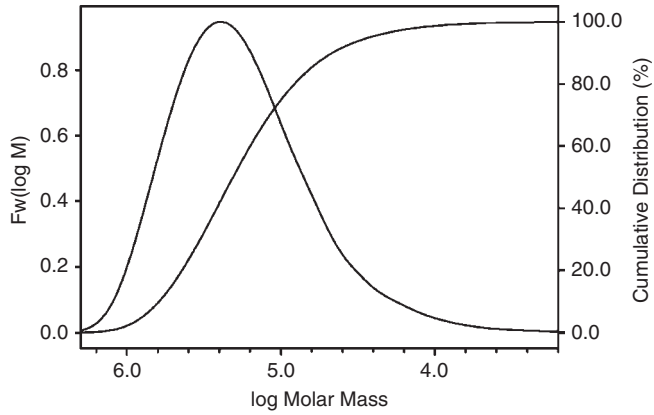

Figure 3.20 Differential and cumulative molar mass distribution plots corresponding to Figure 3.19. Waters Empower™ style.

Table 3.3 Example of Slice Data Corresponding to Figure 3.19

Slice #	V (mL)	M (g/mol)	Area (μVs)	$I_w(M)(\%)$	$F_w(\log M)$
5	9.117	2.787E+06	2.19E+02	0.002	0.00066
6	9.133	2.728E+06	2.48E+02	0.003	0.00075
7	9.150	2.670E+06	2.76E+02	0.004	0.00084
8	9.167	2.614E+06	3.19E+02	0.005	0.00097
9	9.183	2.559E+06	3.62E+02	0.006	0.00110
10	9.200	2.506E+06	4.09E+02	0.007	0.00125
11	9.217	2.453E+06	4.80E+02	0.008	0.00147
12	9.233	2.402E+06	5.51E+02	0.010	0.00169
13	9.250	2.352E+06	6.41E+02	0.012	0.00197
14	9.267	2.303E+06	7.40E+02	0.014	0.00228
15	9.283	2.255E+06	8.62E+02	0.016	0.00266
16	9.300	2.209E+06	9.98E+02	0.019	0.00308
17	9.317	2.163E+06	1.15E+03	0.022	0.00356
18	9.333	2.118E+06	1.33E+03	0.026	0.00413
19	9.350	2.075E+06	1.54E+03	0.030	0.00479
20	9.367	2.032E+06	1.78E+03	0.035	0.00553
21	9.383	1.990E+06	2.04E+03	0.041	0.00636
22	9.400	1.950E+06	2.34E+03	0.048	0.00731
23	9.417	1.910E+06	2.68E+03	0.055	0.00840
24	9.433	1.871E+06	3.05E+03	0.064	0.00957
...	...	...	...	...	...
120	11.033	3.000E+05	2.55E+05	33.849	0.92419
121	11.050	2.947E+05	2.56E+05	34.565	0.92788
122	11.067	2.895E+05	2.56E+05	35.284	0.93129
123	11.083	2.844E+05	2.57E+05	36.004	0.93433
124	11.100	2.794E+05	2.57E+05	36.726	0.93704
125	11.117	2.745E+05	2.58E+05	37.448	0.93937
126	11.133	2.697E+05	2.58E+05	38.172	0.94140
127	11.150	2.649E+05	2.58E+05	38.895	0.94313
128	11.167	2.603E+05	2.58E+05	39.620	0.94447
129	11.183	2.557E+05	2.58E+05	40.344	0.94554
130	11.200	2.513E+05	2.58E+05	41.068	0.94632
131	11.217	2.469E+05	2.58E+05	41.791	0.94667
132	11.233	2.426E+05	2.58E+05	42.514	0.94680
133	11.250	2.384E+05	2.57E+05	43.236	0.94658
134	11.267	2.342E+05	2.57E+05	43.957	0.94606
135	11.283	2.301E+05	2.56E+05	44.676	0.94526
136	11.300	2.261E+05	2.56E+05	45.394	0.94413
137	11.317	2.222E+05	2.55E+05	46.110	0.94268
138	11.333	2.184E+05	2.55E+05	46.824	0.94093
139	11.350	2.146E+05	2.54E+05	47.536	0.93891
...	...	...	...	...	...

Total area= 3.56E+07.

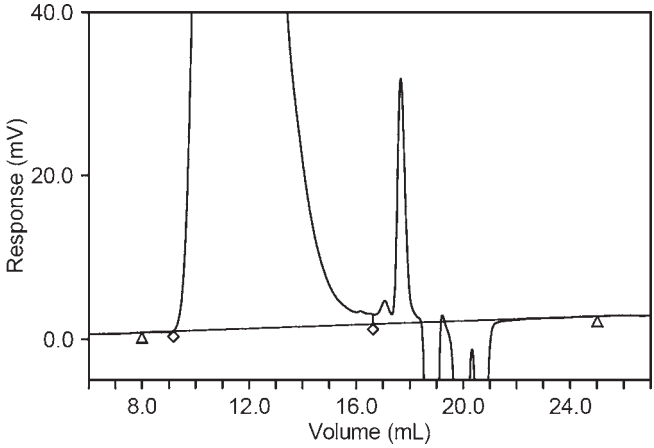

Figure 3.21 Example of stable baseline. Baseline position is marked with triangles; diamonds show integration limits. Baseline is drawn from 8 to 25 mL; moving the baseline 1 mL backward or forward has no impact on the molar mass averages: M_n (g/mol) = 75,600; 76,000; 75,200; M_w (g/mol) = 272,500; 272,500; 272,600; M_z (g/mol) = 499,100; 498,400; 499,800 for the baseline start/end points at 7/26 mL, 8/25 mL, and 9/24 mL, respectively.

end after the solvent peaks should be preferred over drawing the baseline from the peak beginning to the peak end (see Figure 3.22). It is worth mentioning that the automatic data processing algorithms have a strong tendency to position the baseline end point on the oligomeric tail of the chromatogram. Positioning the baseline end on the oligomeric tail has a significant influence on the M_n while the influence on the higher-order molar mass averages is negligible.

To obtain a stable detector signal, the columns must be flushed for several hours before the first injection can be performed. Other necessary conditions for a stable baseline are sufficient warming-up and stabilization of RI detector and constant temperature of RI detector and SEC columns. Most RI detectors are temperature controlled in the sense of heating and stable column temperature can be easily achieved with a column oven, which, however, is not a necessary part of an SEC experimental setup because a stable room environment is mostly sufficient. Keeping the RI detector on continuously even if it is not used for a couple of days improves the signal stability and shortens the time needed to get the SEC setup ready for the measurements. In fact, the entire SEC setup can be kept running even if not used overnight or over the weekend. HPLC pumps are designed to work and they work best when kept running. If an SEC instrument is not to be used for a period of time, the pump can be set to a lower flow rate. To prevent excessive solvent consumption, the column outlet can be recycled back to the solvent reservoir. Some RI detectors enable easy switching between the waste and recycle outlets. The time-life limited components such as the laser of a light scattering detector or the lamp of an UV detector can be switched off since their warmup time is relatively short (sufficient time is usually about 30

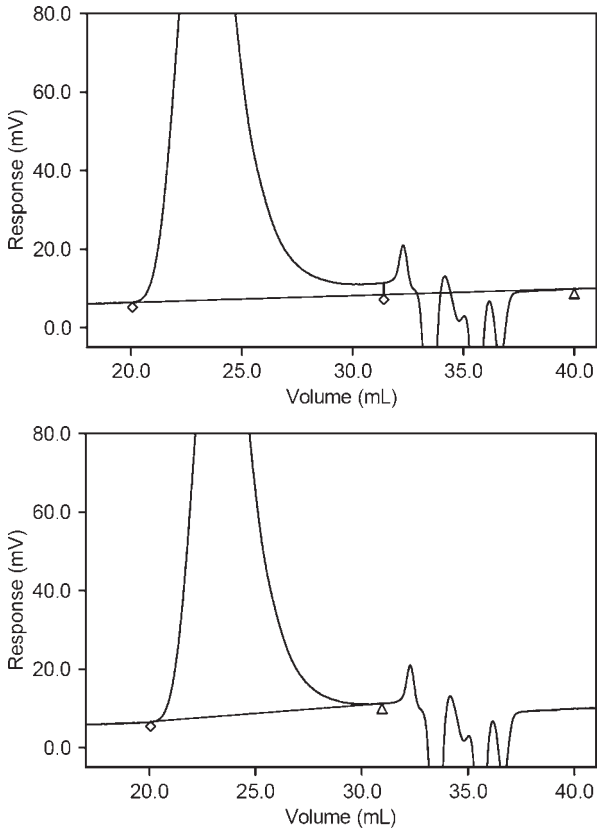

Figure 3.22 Correct (top) and incorrect (bottom) position of the baseline end point for a polymer sample containing oligomeric fractions. Baseline end at 40.0 mL: $M_n = 60{,}000$ g/mol, $M_w = 290{,}000$ g/mol, $M_z = 469{,}000$ g/mol; baseline end at 31.4 mL: $M_n = 134{,}000$ g/mol, $M_w = 298{,}000$ g/mol, $M_z = 463,000$ g/mol. Conditions: 3 × Styragel HR5E 300 × 7.8 mm, THF, 25°C, 1 mL/min, 75 μL 0.25% w/v. Baseline end is marked with a triangle.

minutes). Evenly drifting baseline usually does not represent a serious obstacle in data processing, but the baseline fluctuation makes the baseline construction uncertain and it should be eliminated.

Selection of the peak interval, although it appears to be a simple procedure, is not always straightforward. As mentioned, many synthetic and natural polymers contain fractions with molar masses down to several hundreds g/mol. In such a case the end of the polymer peak is flat and parallel to the baseline. Chromatograms of polymer with and without oligomeric tail are shown in Figures 3.22 and 3.23. For many samples the detector response from oligomeric fractions overlays with the onset of the response from the impurities. The position of the integration end has significant impact on M_n and the inclusion of the oligomeric part of the peak results in significantly lower values.

The issue of baseline construction and selection of the integration end was investigated by Mori et al.,[21] who studied NIST SRM 706 polystyrene and verified that the flat parallel baseline after the polymer peak is really caused by oligomers and that it is not an artifact. They also suggested the use of a special Solvent-Peak Separation column (available from Shodex) that is connected before

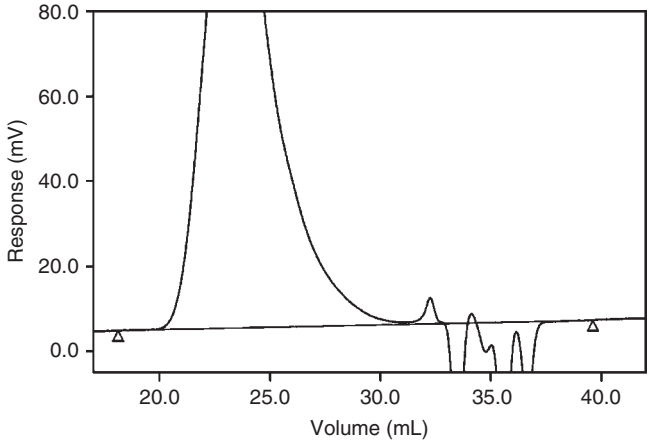

Figure 3.23 RI chromatogram of a polymer sample without oligomeric tail (compare with Figure 3.22).

the regular columns. Such a column can improve separation in the low-molar-mass range without affecting separation in the high-molar-mass range, but it does not solve the problem of the flat parallel signal at the end of the polymer peak. Determination of the peak end is also of particular importance in processing the data of oligomers. Chromatograms of oligomers usually show several peaks at their ends. The insertion or elimination of the last peak usually has a significant impact on the obtained M_n, as demonstrated in Figure 3.24. Making the decision whether to include the last peak in the data processing may not be always

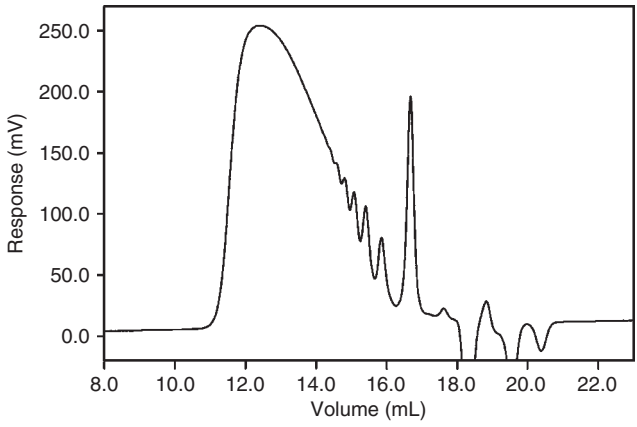

Figure 3.24 RI chromatogram of polyester based on dimethylol propionic acid (DMP) and p-hydroxy benzoic acid (HB). The peak at 16.7 mL has relative area of 6.3% and probably belongs to DMP-HB ester. The molar mass averages with this peak (1) excluded from integration: $M_n = 1960$ g/mol, $M_w = 3490$ g/mol, $M_z = 5170$ g/mol; (2) included in integration: $M_n = 1430$ g/mol, $M_w = 3290$ g/mol, $M_z = 5140$ g/mol.

easy especially when the identity of the peak is unknown, because it can be a member of an oligomeric series, but it can also belong to additives, monomers, or impurities.

There is no magic rule for solving the problem of determination of the peak end. The following recommendations should help get reliable M_n and improve reproducibility of the measurements: (1) The peak end set by a skilled operator is usually more reliable than using automatic peak processing by SEC software. However, intuitive assignment of the peak end by different individuals may result in noticeably different values of M_n. (2) Oligomers, if present, are an integral part of the sample with possibly significant impact on the application properties and shall be included in the determination of molar mass. On the other hand, residual monomers, solvents, and additives are not a part of polymer itself and should be excluded from the calculation of polymer molar mass distribution. However, their presence can be mentioned as a part of the SEC results and illustrated by a chromatogram. They can be characterized and quantified by other more appropriate techniques such as other types of liquid chromatography or by gas chromatography, or simply by the determination of solids. (3) Peak end should be assigned consistently for a series of similar samples to facilitate their mutual comparison. For many polymers the oligomeric tail overlays with the solvent and impurity peaks and the peak end can be positioned at the valley, as shown in Figure 3.25. (4) Zooming the area around the peak baseline is important for proper peak selection. (5) Preparation of sample in the solvent taken from the pump solvent reservoir can minimize the solvent peak on an RI chromatogram. Especially in the case of THF, the use of solvent from different bottles can result in an intensive peak of stabilizer that can overlay with the lowest oligomers and result in significantly lower M_n when included in chromatogram processing.

The influence of the peak end (cutoff elution volume) on the molar mass averages is demonstrated on NIST SRM 706 polystyrene in Figure 3.26 and Table 3.4 In contrast to the determination of the polymer peak end, the determination of the peak beginning is usually straightforward. However, some samples may contain low amounts of high-molar-mass fractions, which cause very low increase of the ascending part of the polymer peak. For such samples it may not be easy to distinguish between the drifting baseline and the rise of the peak due to the elution of small amounts of higher-molar-mass fractions. These fractions can be easily detected by means of SEC columns of lower exclusion limit, as shown in Figure 3.27. Although the columns with low exclusion limit do not provide true molar mass distribution, they can be used for sensitive detection and quantification of higher-molar-mass impurities in oligomers.

An important assumption for the calculation of the true molar mass distribution from SEC data is that the detector response is proportional only to the concentration and that it is independent of elution volume. Only if this assumption is fulfilled the ratio $A_i / \sum A_i$ equals the weight fraction w_i of molecules eluting at the elution volume V_i. This requirement is typically well fulfilled in the case of homopolymers, but it may not be fulfilled in the case of copolymers or polymer blends when the chemical composition may change along the elution volume axis.

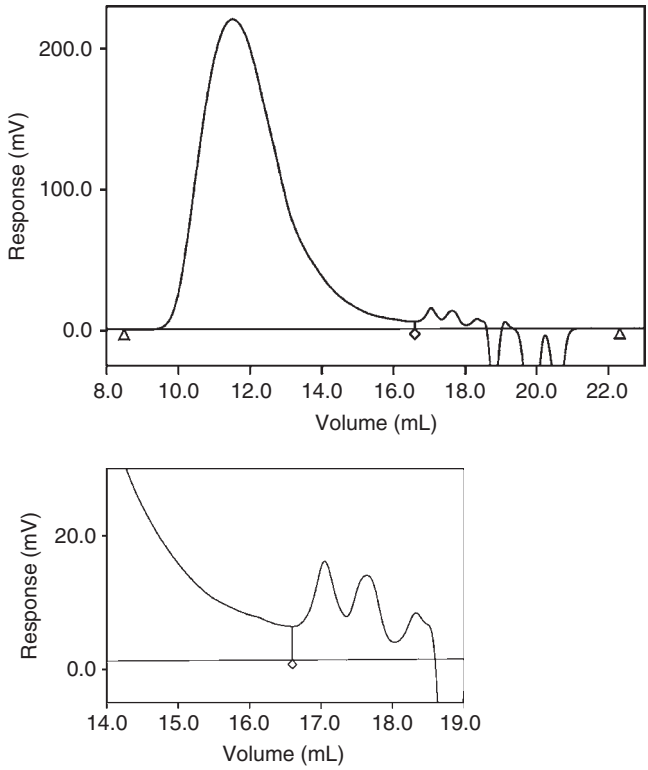

Figure 3.25 Example of positioning the peak end (indicated by diamond) at the valley between the oligomeric tail and solvent and impurity peaks.

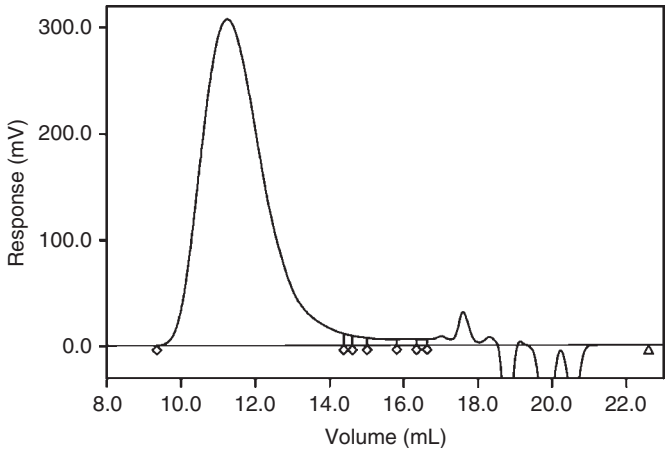

Figure 3.26 RI chromatogram of NIST SRM 706 polystyrene with different peak ends. Molar mass averages corresponding to various peak end positions are listed in Table 3.4. Conditions: columns 2 × PLgel Mixed-C 300 × 7.5 mm, THF at 1 mL/min.

Table 3.4 Effect of Peak End on Molar Mass Averages of Polystyrene NIST SRM 706 See chromatogram in Figure 3.26

Peak End (mL)	M at Peak End (g/mol)	M_n (10^3 g/mol)	M_w (10^3 g/mol)	M_z (10^3 g/mol)
16.64	700	55.3	270.3	464.5
16.35	1000	66.1	271.0	464.5
15.81	2000	85.8	272.4	464.5
15.0	5000	108.5	274.6	464.6
14.62	8000	118.0	275.9	464.6
14.38	10,000	123.9	276.9	464.7

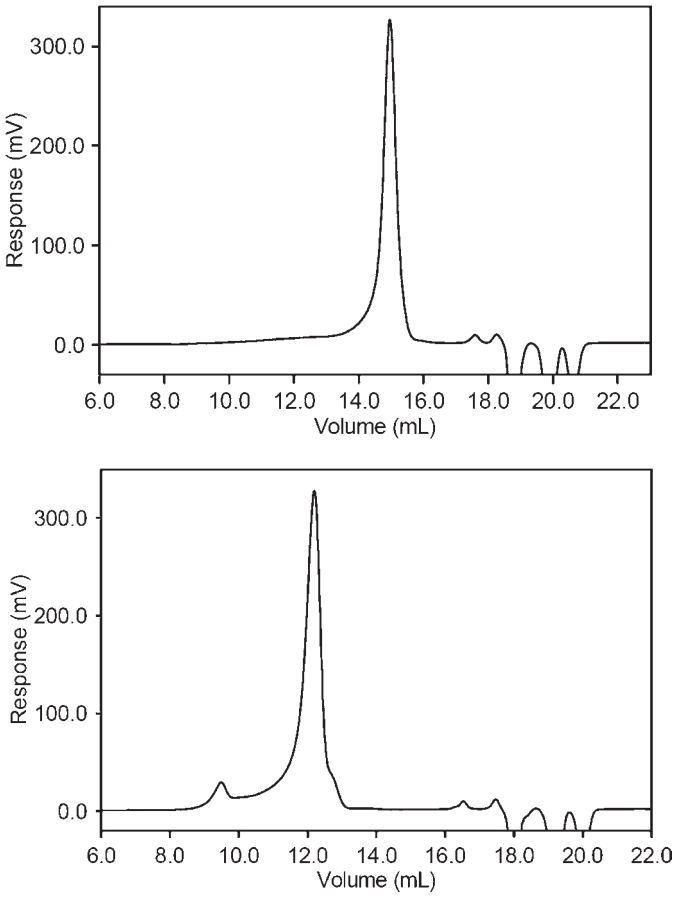

Figure 3.27 Chromatograms of oligomeric sample containing a small amount of higher-molar-mass fractions analyzed on columns with exclusion limit of 2×10^6 g/mol (top) and 30,000 g/mol (bottom). The columns with low exclusion limit visualize fractions with higher molar mass. Columns: 2 × PLgel Mixed-C (top) and 2 × PLgel Mixed-E (bottom), THF at 1 mL/min.

In the case of similar specific refractive index increments of particular homopolymers, neglecting the chemical heterogeneity does not result in significant errors in w_i. However, similar refractive index increments of homopolymers are not always the case: For instance, polystyrene in THF has dn/dc of 0.185 mL/g while most acrylates and methacrylates that are often used for copolymerization with styrene have dn/dc in the range of 0.6–0.84 mL/g. Another possible error in the determination of molar mass of copolymers arises from the column calibration. If the parent homopolymers have significantly different calibration curves, then each elution volume requires different calibration appropriate to the given chemical composition. The rigorous calibration would be the logarithm of molar mass as a function of not only elution volume, but chemical composition as well:

$$\log M = f(V, w_A) \tag{3.64}$$

where w_A is the weight fraction of co-monomer A in the analyzed copolymer. The determination of such a calibration relation is typically impossible. The concept of the universal calibration is theoretically reliable, because the copolymer molecules separate on the basis of hydrodynamic volume as do homopolymers. The limitation is caused by the fact that the hydrodynamic volume of copolymer is generally a function of molar mass and chemical composition and thus the molecules of varied molar mass and chemical composition co-elute at a given elution volume. That means chemical heterogeneity increases polydispersity within the elution volume slice beyond that resulting from peak broadening.

Although the Mark-Houwink parameters have been determined for several copolymers, they are unavailable for most real samples, and even if available, their applicability is limited by the dependence on the chemical composition. Universal calibration with a viscometer eliminates the need for the Mark-Houwink constants and the only remaining sources of errors are compositional dependence of the detector response and increased polydispersity of the particular elution volume slices.

In conventional SEC the chromatograms of copolymers or polymer blends are mostly processed using the same procedure as that for homopolymers with the calibration that appears the most appropriate for the analyzed samples, typically the calibration that is valid for the most abundant homopolymer. If the composition along the elution volume axis is known from the dual detection, the calibration curve can be estimated using the equation:

$$\log M_c = w_B \log M_B + (1 - w_B) \log M_A \tag{3.65}$$

where M_c is the molar mass of copolymer of the composition w_B and M_A and M_B are the molar masses of the corresponding homopolymers at the same elution volume. It has been shown that Equation 3.65 provides suitable results for block copolymers, but does not apply for statistical and alternating copolymers. Nevertheless, chemical composition as a function of elution volume is often unknown and thus the application of Equation 3.65 is rare. Due to the complexity of most

copolymers, the obtained results should be expected to be less correct compared to the characterization of corresponding homopolymers.

Conventional calibration also provides incorrect results for branched polymers, because branched molecules are generally more compact compared to corresponding linear molecules of the same molar mass. Consequently, branched molecules elute later than their linear counterparts and the molar mass determined from column calibration is underestimated.

3.5.3 Reporting Results

Proper reporting of results is an important part of data processing. The primary goal of the SEC experiment is usually the characterization of molar mass distribution. The report should contain not only the characteristics of the sample, but also information that would permit the data to be easily found and, if needed, further reprocessing. The information in the report should include (1) sample information such as sample unanimous name, information about research project and customer, date of data acquisition and processing, and injection volume; (2) RI and/or UV chromatogram showing the baseline and peak limits; (3) table with molar mass averages and possibly other characteristics of the chromatogram useful for the interpretation of results and comparison with other data; and (4) cumulative and differential distribution curves, either in separate plots or overlaid in a single plot.

The raw chromatogram is useful to illustrate the stability of the baseline, to show integration limits, and eventually to indicate presence of other compounds, such as residual monomers, solvents, or oligomers. Molar mass averages are reported by software with accuracy to the last unit. With respect to the repeatability of the measurement, the molar mass averages should be rounded off to hundreds or thousands or even tens of thousands at the molar mass order of 10^6 g/mol. Similarly, the polydispersity M_w/M_n should be rounded off to one or two decimal figures.

The report should also state the total peak area that can reveal concentration inconsistency resulting from improper sample preparation or from different levels of polymer in sample due to solvents, fillers, or other nonpolymeric compounds. The peak area can also indicate adsorption of part of the sample in column packing. For samples of identical chemical composition prepared at the same concentration the peak area must be identical.

End time of peak processing may be important for samples showing oligomeric tail where the determination of peak end is uncertain. This information may improve consistency of results when similar samples are analyzed after some time. Besides molar mass averages and distribution curves it is possible to report other characteristics that may be helpful for the characterization of samples. These may be percentage of fractions below a certain molar mass limit (e.g., fractions below 1,000 g/mol), molar masses at 10 and 90% of the cumulative distribution, or M_w of the lowest 10% fractions and

M_w of the highest 10% fractions. For example, the M_w of the 10% lowest and highest fractions are required for the characterization of dextran samples by the *Pharmacopoeia*.

3.5.4 Characterization of Chemical Composition of Copolymers and Polymer Blends

A complete description of a broad chemically heterogeneous binary copolymer requires two-dimensional function $f_w(M, w_A)$, which provides the weight fraction of molecules with molar mass M and chemical composition w_A. The situation is much more complicated in the case of ternary or even more complex copolymers. Using SEC the only obtainable information about the chemical composition of copolymers and polymer blends is chemical composition as a function of molar mass. The determination of the distribution of chemical composition, that is, function $f_w(w_A)$, requires separation according to the chemical composition by means of other types of liquid chromatography, critical mode of liquid chromatography or combination of various chromatographic modes in two-dimensional chromatography. Details and other literature references can be found, for instance, in a book by Pasch and Trathnigg.[22]

Chemical composition as a function of molar mass can be determined either (1) by fraction collection, using semipreparative/preparative SEC columns and subsequent analysis of the obtained fractions by analytical SEC to determine the molar mass distribution, and spectral or chemical methods to characterize chemical composition, or (2) online, using multiple detection. The former approach is laborious, but generally applicable; the latter is mostly limited to copolymers and polymer blends where one component is UV active while the other is not or where the two components have significantly different UV response at two different wavelengths.

Unsaturated polyesters composed of maleic (fumaric) unsaturated units along with units of aromatic saturated acid are an example of copolymers with different UV response at different wavelengths. The chemical composition at particular elution volumes can be determined from the relation between the absorbance ratio at two wavelengths and the weight fraction of one of the absorbing components:[23]

$$\frac{A_{\lambda_1}}{A_{\lambda_2}} = f(x_A) \tag{3.66}$$

where A_λ is the absorbance at a given wavelength and x_A is the mole fraction of one of the two absorbing components. Equation 3.66 is obtained in SEC mode from the total peak areas recorded at two different wavelengths by injecting copolymers of known overall composition and/or mixtures of two homopolymers, or in offline mode using a UV spectrometer.

In the case of various styrene copolymers (e.g., styrene-acrylate, styrene-methacrylate, styrene-vinylacetate) the UV detector records only UV-absorbing

units while the RI detector monitors both absorbing and non-absorbing units. The weight fraction of monomer units B (w_B) for each elution volume can be calculated using the following equation:[24]

$$w_B = \frac{(A_{RI} - A_{UV}K_2)K_1}{A_{RI}K_1 + A_{UV}K_2 - A_{UV}K_1K_2} \tag{3.67}$$

where A_{RI} and A_{UV} is the area of the ith volume slice of the chromatogram recorded by the RI and UV detectors, respectively, K_1 is the ratio of the RI detector response for homopolymer A to that for homopolymer B, and K_2 is the ratio of the RI detector response to the UV detector response for UV-absorbing homopolymer A.

Another procedure for calculating the composition across the chromatogram requires the knowledge of the extinction coefficient of the absorbing homopolymer and the specific refractive index increments of both homopolymers. The method finds an important application in the characterization of protein conjugates. Poly(ethylene glycol) (PEG) or carbohydrate are frequently used to modify the pharmacokinetic properties of protein therapeutics. By adding PEG or carbohydrate the half-life of protein can be significantly increased. If the dn/dc for protein and modifier and the protein extinction coefficient are known, it is possible to calculate the total molar mass of the conjugate and molar masses of the particular constituents and protein fraction on a slice-by-slice basis. Similar calculation can be performed for synthetic copolymers. The calculation is included in ASTRA® software (Wyatt Technology Corporation).

An online or offline infrared detector can be used to monitor chemical composition as a function of elution volume. The most important application is the determination of short-chain branching in polyethylene, which has direct impact on the end-use properties.

3.5.5 Characterization of Oligomers

Several typical examples of chromatograms of oligomers are depicted in Figures 3.28 and 3.29. Various synthetic resins (e.g., epoxies, unsaturated polyesters, urea-formaldehyde or phenol-formaldehyde condensates), are typical oligomeric materials. SEC chromatograms of some resins are that typical that the chromatogram itself can identify the type of the resin. Column efficiency and resolution increases with decreasing particle size of column packing. This fact can be fully utilized in the analysis of oligomers where flow-induced shear degradation is unlikely, and therefore 3-μm packing size should be used. Chromatograms of oligomers typically consist of several overlapping peaks corresponding to individual oligomers of low polymerization degrees. With increasing polymerization degree the resolution of particular oligomers decreases until the individual peaks become a smooth curve similar to that of polymers. Note that chromatograms of oligomers clearly demonstrate decreasing resolution of SEC with increasing molar mass. Suitable pore sizes of the column packing

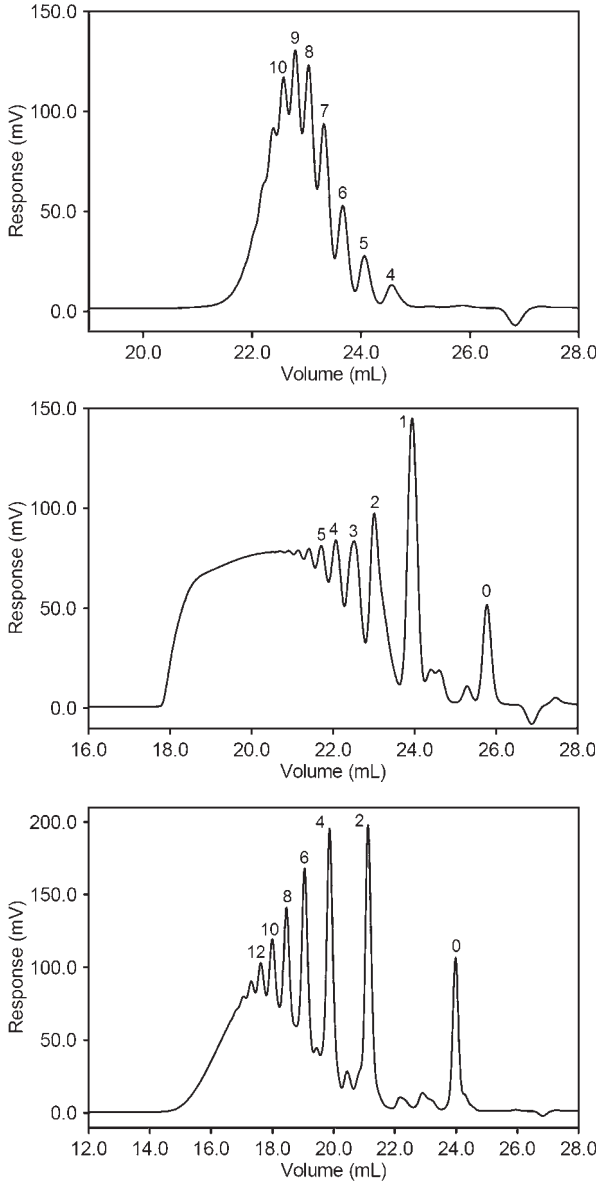

Figure 3.28 Examples of chromatograms of various oligomers: from top to bottom, polyethylene glycol (PEG) of nominal molar mass 440 g/mol, phenolic novolac, and epoxy resin based on bisphenol A prepared by reaction of low-molar-mass epoxy resin with bisphenol A. Separation conditions 3 × PLgel Mixed-E 3 μm 300 × 7.5 mm columns, THF at 1 mL/min, column temperature 40°C, inject 30 μL 0.6% w/v. PEG: $n = 4, 5, 6, \ldots$ oligomers with molar mass according to equation $M = 18 + n \times 44$. Novolac: $n = 0, 1, 2, 3, \ldots$ oligomers with molar mass according to equation $M = 94 + n \times 106$; $0 \approx$ phenol, $1 \approx$ dihydroxydiphenyl methane. Epoxy resin: $n = 0, 2, 4, \ldots$ oligomers with molar mass according to equation $M = 340 + n \times 284$; $0 \approx$ diglycidyl ether of bisphenol A.

material and high column efficiency are the most important aspects of the high resolution of oligomers.

Figure 3.30 shows the influence of column selectivity and efficiency on the resolution of oligomers. In this example, column efficiency and selectivity were controlled by number and type of SEC columns, namely PLgel Mixed-E, which

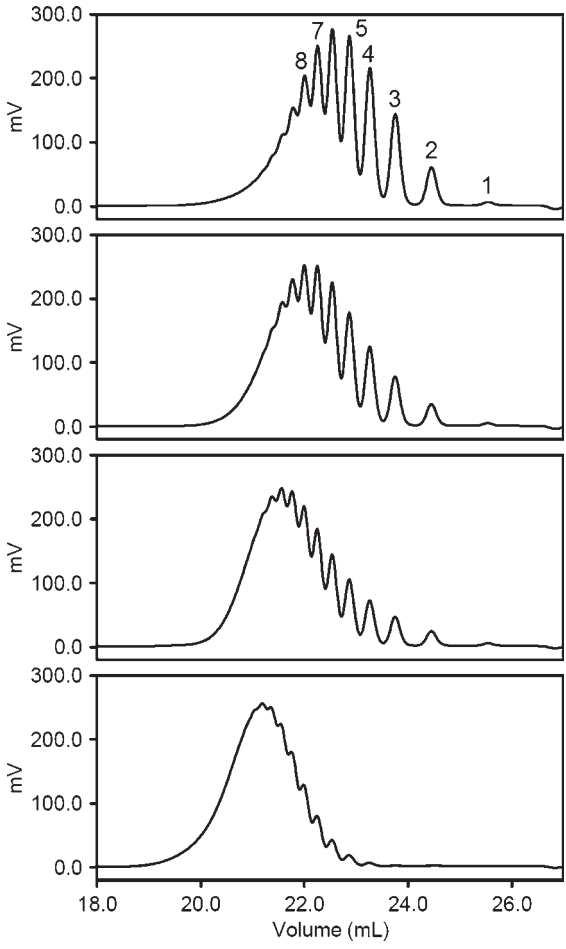

Figure 3.29 Chromatograms of oligostyrene of nominal molar mass (from top to bottom): 680 g/mol, 900 g/mol, 1050 g/mol, and 1250 g/mol, $n = 1, 2, 3, \ldots$ oligomers with molar mass $M = 58 + n \times 104$. Conditions as in Figure 3.28.

are specifically designed for the separation of oligomers, versus PLgel Mixed-C, which cover a broad molar mass range, but their selectivity in the region of lower molar masses is lower compared to the Mixed-E columns. Besides efficiency and selectivity of the SEC columns, the resolution depends on the difference of the molar masses of the two neighboring oligomers in the oligomeric series. Typically, the maximum polymerization degree for which at least partial resolution can be achieved is around ten. It must be emphasized that the resolution power of SEC concerning the ability to separate oligomers is below that of other types of HPLC. Gradient-reversed-phase HPLC can separate oligomers up to a polymerization degree of around 25.

The advantages of SEC compared to HPLC include simpler operating conditions (isocratic elution), lower demand on the purity of the mobile phase, possibility of using an RI detector, and easier identification of particular oligomers because of their explicit separation according to the hydrodynamic volume.

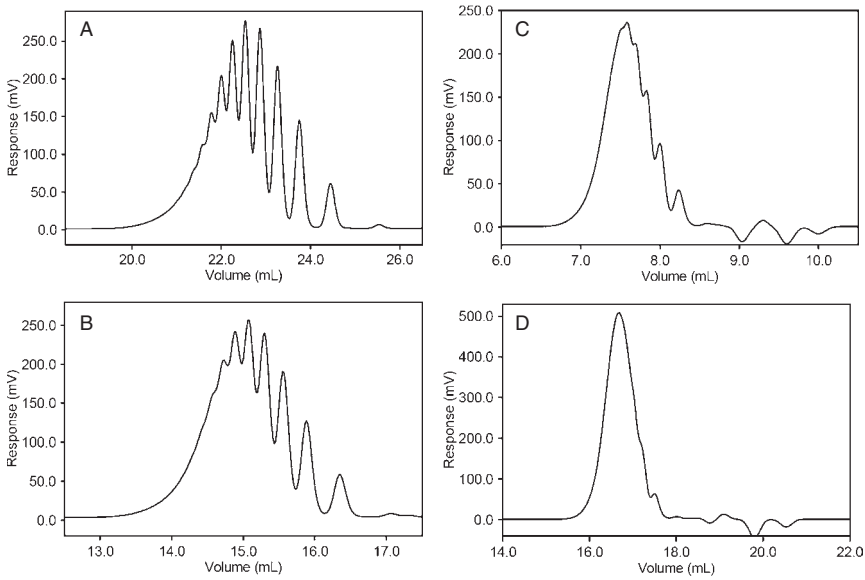

Figure 3.30 Resolution of styrene oligomers using different SEC columns: 3 × PLgel Mixed-E 300 × 7.5 mm 3 μm (A), 2 × PLgel Mixed-E 300 × 7.5 mm 3 μm (B), 1 × PLgel Mixed-E 300 × 7.5 mm 3 μm (C), 2 × PLgel Mixed-C 300 × 7.5 mm 5 μm (D).

It is also worth mentioning that it is not necessary to baseline-resolve particular oligomers in order to get the correct description of the molar mass distribution as seen in Figure 3.31.

The chromatograms of oligomers are processed in the same way as the chromatograms of polymers to get the molar mass averages and distribution curves. The procedure for the calibration of SEC columns is generally identical with that of polymers. For some oligomeric materials it is possible to separate several oligomers with low polymerization degrees and identify their peaks in a chromatogram. Then the calibration curve can be established by relating the elution volumes of oligomeric peaks with the molar masses of the corresponding oligomers. However, the calibration curve based on the oligomeric peaks is valid up to relatively low molar masses, and extrapolation toward the region of higher molar masses, where the experimental data points are missing, may be uncertain and can lead to significant errors. This is especially true if the higher oligomers are branched, such as in the case of phenol-formaldehyde polycondensates. The molar mass range of the calibration curve can be extended by the isolation of particular oligomers by semipreparative HPLC and their subsequent application for the calibration of SEC columns. The obtained calibration can be related to easily obtainable polystyrene calibration. Such a procedure is outlined in Figure 3.32, which compares the calibration curve of polystyrene with that of bisphenol A–based epoxy resin. The two calibrations are in the following

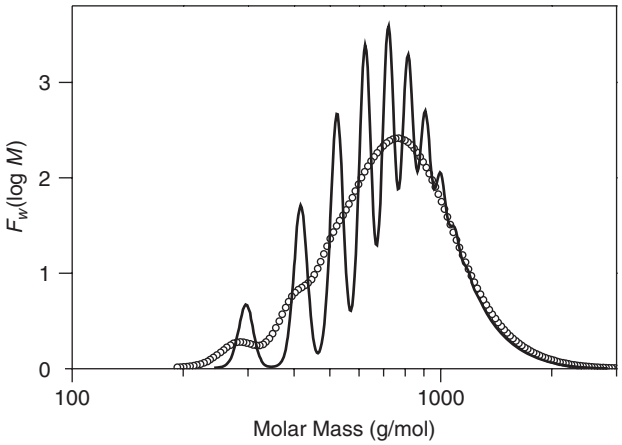

Figure 3.31 Comparison of differential distribution curves of polystyrene of nominal molar mass 680 g/mol determined using columns of different resolution: 3 × PLgel Mixed-E (solid line) versus 2 × PLgel Mixed-C (◯). M_n (g/mol) = 680 (3 × Mixed-E), 670 (2 × Mixed-C), M_w (g/mol) = 790 (3 × Mixed-E), 790 (2 × Mixed-C), M_z (g/mol) = 900 (3 × Mixed-E), 920 (2 × Mixed-C).

relation:

$$M_{EP} = 3.895 \times M_{PS}^{0.783}(25^{\circ}\text{C, THF}) \tag{3.68}$$

where subscripts *PS* and *EP* refer to polystyrene and epoxy resins, respectively. Equation 3.68 permits the transformation of the calibration obtained by polystyrene standards to the calibration valid for bisphenol A–based epoxy resins. Using SEC columns with a sufficient resolution in the oligomeric region, the

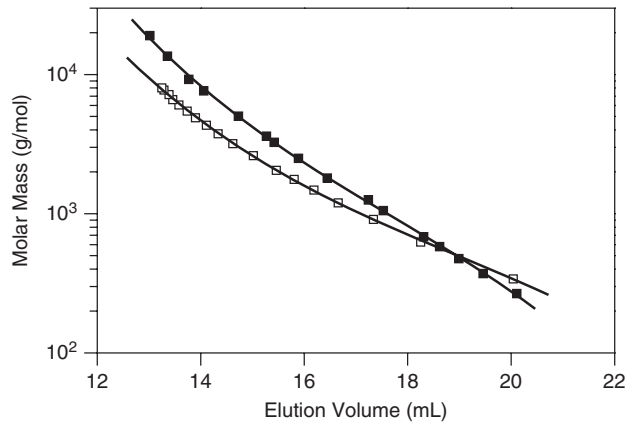

Figure 3.32 Calibration curves of polystyrene (■) and bisphenol A–based epoxy resins (□). The epoxy oligomers were isolated by semipreparative reversed-phase HPLC. Columns Microgel 100 Å, 500 Å, 1000 Å 250 × 7.8 mm, THF at 1 mL/min, room temperature.

low-molar-mass polystyrene standards are separated into several oligomers and their individual molar masses are used for the calibration. Note that polystyrene standards contain one butyl end group (from butyl lithium) and thus the molar mass of styrene oligomers is $M = 58 + n \times 104$ where n is the polymerization degree. That means the analogy for the monomer is hexylbenezene instead of ethylbenzene.

Besides the determination of molar mass distribution, content of the lowest oligomers can be easily estimated on the basis of the relative peak areas of particular peaks. The overlapping peaks are separated by vertical lines arising from the baseline to the valleys between the peaks and the weight fractions of oligomers are estimated as their relative peak areas. Exact quantitative determination of the low-molar-mass compounds available in pure form can be carried out by a procedure identical with that widely applied in other types of chromatography. The procedure is demonstrated by the determination of the lowest epoxy oligomer (diglycidyl ether of bisphenol A) in epoxy resin (Figure 3.33). Quantitative analysis by means of the *external standard* procedure involves the preparation of several solutions of the compound to be quantified at exactly known concentrations and their injections into SEC columns. The calibration graph is then established by plotting the peak area versus injected mass or concentration of the injected solutions. The calibration graph should be established using at least three data points. The sample is analyzed under the same conditions as those used for the calibration standards and the mass corresponding to the peak area is determined from the calibration graph. The procedure can be used to quantify the residual monomers, stabilizers, plasticizers, or other additives in polymers. Alternatively, the *internal standard* procedure or the procedure of *standard addition* can be applied for quantitative analysis of low-molar-mass compounds.

A potential source of errors associated with processing the chromatograms of oligomers is the dependence of the specific refractive index increment (dn/dc) or the extinction coefficient (a) on molar mass, which is typically significant at low polymerization degrees. Correction of the relative peak areas can be made if the relation between dn/dc or a and polymerization degree is known. In most practical cases the polymerization degree dependence of dn/dc or a is unknown and therefore must be neglected. The experimental results indicate that the increase of dn/dc or a with polymerization degree is negligible over molar mass of about 5,000 g/mol, and even for lower molar masses the errors caused by neglecting the molar mass dependence of dn/dc and a are mostly below 10%. Examples of the molar mass dependence of dn/dc and a can be found in the literature for polystyrene (dn/dc),[18,25] polyisobutene (dn/dc),[18] and bisphenol A–based epoxy resins (dn/dc,[25] extinction coefficient[26]). The following examples illustrate possible differences of dn/dc and a:[i]

Bispenol A–based epoxy resin, $M = 340$ g/mol: $dn/dc = 0.152$ mL/g

Bispenol A–based epoxy resin, $M_n = 1490$ g/mol: $dn/dc = 0.178$ mL/g

[i]The values are valid for THF and the wavelength of 633–690 nm (dn/dc) and 278 nm (a).

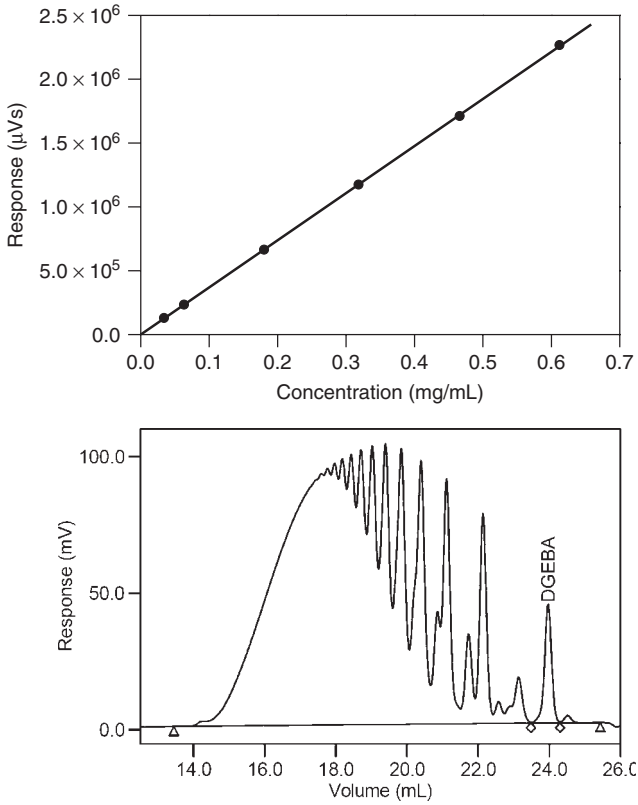

Figure 3.33 Calibration curve for diglycidyl ether of bisphenol A (DGEBA) (top) and DGEBA quantification in epoxy resin (bottom). DGEBA peak area = 613, 800 μVs; using the calibration curve the area corresponds to 0.166 mg/mL of DGEBA, concentration of injected solution = 6.06 mg/mL; that is, the concentration of DGEBA in the resin = 2.7% wt. Conditions as in Figure 3.28.

Bispenol A–based epoxy resin, $M_n = 2780$ g/mol: $dn/dc = 0.183$ mL/g
Bispenol A–based epoxy resin, $M = 340$ g/mol: $a = 10.8$ Lg^{-1} cm^{-1}
Bispenol A–based epoxy resin, $M = 1760$ g/mol: $a = 12.0$ Lg^{-1} cm^{-1}
Bispenol A–based epoxy resin, $M = 3180$ g/mol: $a = 12.1$ Lg^{-1} cm^{-1}
Bispenol A–based epoxy resin, $M > 30,000$ g/mol: $a = 12.2$ Lg^{-1} cm^{-1}
Polystyrene, $M = 580$ g/mol: $dn/dc = 0.161$ mL/g
Polystyrene, $M = 2500$ g/mol: $dn/dc = 0.182$ mL/g
Polystyrene, $M > 10^4$ g/mol: $dn/dc = 0.185$ mL/g

The differences of dn/dc and a between particular members of the oligomeric series can be assumed to be small only if their chemical composition is identical. This assumption is not always fulfilled, such as in the case of polyesters based

on a blend of aliphatic and aromatic acids, where *a* and *dn*/*dc* of the individual oligomers depend on the number of aromatic units.

Identification of the peaks in chromatograms of oligomers can be performed on the basis of expected chemical composition. Knowledge of the elution volumes of monomers or compounds of similar chemical composition as that of the analyzed oligomers can help assign particular peaks. Model oligomers synthesized using either excess or elimination of one component can be used to interpret the chromatograms of real materials. Measurements of samples taken from the batch during the course of the polyreaction can facilitate the identification of the peaks in chromatograms on the basis of changes of chromatogram pattern with reaction conversion. The expected oligomeric structure should provide good correlation of the calibration curve obtained by relating the logarithms of molar mass to the elution volumes of the peaks assigned to particular oligomers. The elution volumes of oligomers containing hydroxyl groups are influenced by the association with THF. If some of the analyzed oligomers contain hydroxyl groups and some do not, the experimental data points fit on the same curve only if multiples of THF molar mass corresponding to the number of hydroxyl groups are added to the molar masses of oligomers.[27] Another procedure for identification of chemical structure involves isolation of several oligomers and their identification by a spectral technique. A direct online application of an ESI MS detector is limited by poor ionization in THF, which is commonly used as SEC mobile phase. Applications of SEC in combination with MALDI-TOF MS were also reported.

A potentially important issue related to the analysis of oligomers arises from regulatory requirements such as REACH (Registration, Evaluation, and Authorization of Chemicals). A polymer under definition of REACH is a substance consisting of molecules characterized by the sequence of one or more types of monomer unit. Such molecules must be distributed over a range of molecular weights. In accordance with REACH, a polymer is defined as a substance meeting the following two criteria:

1. Over 50% of the weight for that substance consists of polymer molecules. A polymer molecule is a molecule that contains a sequence of at least three monomer units, which are covalently bound to at least one other monomer unit or other reactant. *Note:* In terms of polymer chemistry the requested polymerization degree is four or more.
2. The amount of polymer molecules presenting the same molecular weight must be less than 50 weight percent of the substance.

The method preferred by REACH to determine whether a substance falls under the definition of a polymer is SEC. However, performing the yes/no analysis under the REACH definition requires identification of particular oligomeric peaks in an SEC chromatogram to correctly identify their polymerization degrees. This may not be always a straightforward procedure and the proper characterization may require combination of SEC results with those obtained by other techniques such as MS or HPLC.

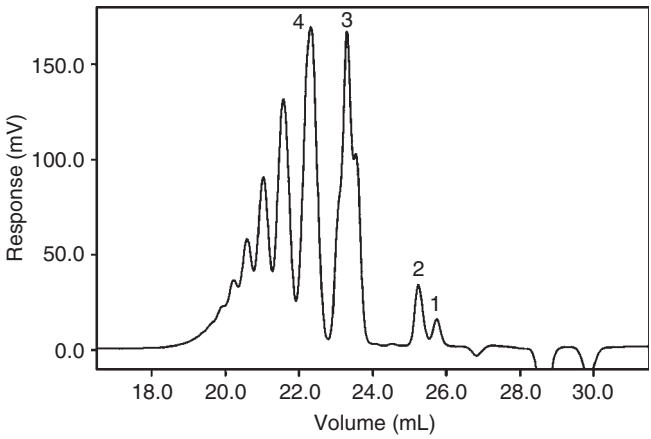

Figure 3.34 Chromatogram of oligomer prepared by glycolysis of poly(ethylene terephthalate) (PET). Composition of reaction mixture: 65% PET, 28% diethylene glycol, 7% propylene glycol. Polystyrene equivalent molar masses/relative peak areas for peaks 1, 2, 3, and 4: 146 g/mol/1.4%, 194 g/mol/3.0%, 513 g/mol/27.2%, and 793 g/mol/25.0%, respectively. Conditions as in Figure 3.28.

Let us examine whether the compound depicted in Figure 3.34 is a polymer according to the REACH classification. The investigated material is a product of glycolysis of polyethylene terephthalate (PET). The decomposition of PET in a glycolic environment is based on the transesterification of PET with glycol(s), resulting in a mixture of aromatic polyols, which can be further processed in the production of polyurethanes or unsaturated polyester resins. The obtained polyols are oligomers consisting of various numbers of terephthalate (T) units, ethylene glycol (EG) units, and units of glycol used for glycolysis (propylene glycol, PG, and diethylene glycol, DiEG, in the case of the sample shown in Figure 3.34). The procedure allows recycling of the waste PET and thus is environmentally important.

The classification of the analyzed PET alcoholysate is based on two assumptions: (1) The RI detector response of the particular oligomers is approximately identical and thus the relative peak areas can be used for the quantification, and (2) polystyrene calibration provides approximately correct determination of molar masses of terephthalic-based oligomers. An oligomer fulfilling the requirement of REACH is the reaction product PG-T-EG-T-PG with molar mass of 474 g/mol or similar oligomers with different end glycol units. The chromatogram proves that there is no oligomer in the analyzed mixture in an amount over 50%. The shape of peak #3 indicates a mixture of three compounds, most likely oligomers with different end glycol units. The polystyrene equivalent molar mass corresponding to peak #3 allows us to identify the compounds as PG-T-EG-T-PG and similar oligomers with different end units. It can be concluded that under given assumptions the compound in Figure 3.34 is a polymer according to the REACH classification.

3.5.6 Influence of Separation Conditions

Molar masses determined with conventional SEC using the traditional column calibration approach strongly depend on the calibration used for data processing. In addition, the obtained results are sensitive to several operating parameters of the SEC instrumental setup. The most important parameters are:

- Flow rate
- Column temperature
- Sample concentration and injected volume
- Column performance

It has been demonstrated in Table 3.1 that flow rate is the most essential parameter for accurate and repeatable determination of molar mass. The elution volume of polymer molecules may slightly depend on flow rate, but this dependence is not important for practical measurements because the calibration standards and polymer samples are measured at the same flow rate. SEC experiments are carried out at a fixed flow rate selected according to solvent viscosity and column specification, keeping in mind the productivity of the measurement. Using standard 8-mm-inner-diameter columns, a typical flow rate is 1 mL/min for THF and 0.5–0.8 mL/min for aqueous solvents. Lower flow rates may slightly increase efficiency. In addition, lower flow rates of about 0.3 mL/min may be beneficial from the viewpoint of possible shearing degradation of high-molar-mass fractions.

The determination of molar mass distribution is based on the assumption of efficient polymer separation according to the hydrodynamic volume. It has been stated that the resolution R_{SP} should be at least 2.5 and the parameter SP more than 6. The effect of resolution is shown in Table 3.5, which compares molar mass averages of three polydisperse polymers determined by different numbers of SEC columns. Although the molar mass averages are not entirely identical, the differences are relatively small. It is obvious that increasing the resolution by using too many columns does not benefit the obtained results. Taking into account the accuracy of measurement, run time, and solvent consumption, it can be concluded that two standard 300 × 7.5–8-mm columns packed with mixed-pore packing should be adequate for most practical applications, and even a single column would provide sufficient results when time per analysis becomes an important factor.

Column temperature is another important parameter influencing the results generated by column calibration. Unless required by limited sample solubility, SEC experiments are typically carried out at room temperature or slightly above room temperature. Figure 3.35 shows chromatograms of a mixture of polystyrene standards and corresponding calibration curves acquired at three different temperatures. The shift of the calibration curves is a result of two concurrently acting factors: a temperature expansion of the mobile phase that results in an increased flow rate, and an expansion of the hydrodynamic volume of standards

Table 3.5 Effect of Resolution on the Molar Mass Averages of Polydisperse Polystyrene

Polystyrene	M_n (10^3 g/mol)		M_w (10^3 g/mol)		M_z (10^3 g/mol)	
Sample	1 × HR5E	3 × HR5E	1 × HR5E	3 × HR5E	1 × HR5E	3 × HR5E
M1	56.9 ± 0.2	60.3 ± 0.4	283.2 ± 0.9	289.7 ± 0.7	482.3 ± 1.7	468.8 ± 0.9
M3	80.8 ± 0.8	89.3 ± 0.7	289.3 ± 1.3	296.5 ± 0.5	535.8 ± 2.4	521.0 ± 1.7
M4	42.7 ± 0.2	45.7 ± 0.2	235.4 ± 0.3	241.5 ± 0.5	483.7 ± 5.6	468.4 ± 1.6

SEC columns: 1 × versus 3 × Waters Styragel HR5E 300 × 7.8 mm, $R_{SP} = 2.4$ versus 3.3, SP = 2.6 versus 7.6 calculated for standards with M_{PEAK} 675,000 and 68,000 g/mol. *Conditions:* THF at 1 mL/min, calibration with 13 polystyrene standards $10^3 - 4.3 \times 10^6$ g/mol (concentration 0.03% w/v of each standard), sample concentration 0.25% w/v, sample injection 25 μL per column.

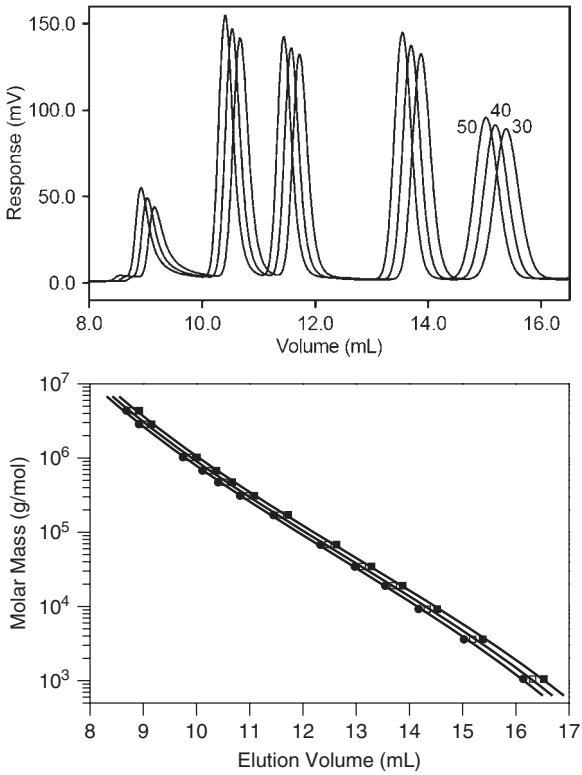

Figure 3.35 Chromatograms of polystyrene standards (top) and corresponding calibration curves (bottom) obtained at 30°C (■), 40°C (□), and 50°C (•). Columns 2 × PLgel Mixed-C 300 × 7.5 mm, THF at 1 mL/min. Standards 2,850,000 g/mol, 470,000 g/mol, 170,000 g/mol, 19,000 g/mol, and 3600 g/mol.

due to increased thermodynamic quality of the solvent. Both effects result in faster elution.

Table 3.6 shows M_w values of polydisperse polystyrene measured at temperatures of 30, 40, and 50°C using the calibration relation determined at 30°C. The decrease of elution volume due to increasing temperature results in markedly increasing M_w when the chromatograms collected at 40 and 50°C are processed

Table 3.6 Effect of Column Temperature on M_w of Polydisperse Polystyrene and the Compensation by Flow Marker

Temperature (°C)	M_w (g/mol)		Flow Marker Elution Volume (mL)
	No Flow Marker	Flow Marker	
30	273,000 ± 200	276,500 ± 600	20.25 − 20.26
40	319,700 ± 400	251,100 ± 200	19.82
50	370,900 ± 400	234,800 ± 100	19.47

Conditions: Column calibration at 30°C, THF at 1 mL/min, 2 × PLgel Mixed-C 300 × 7.5 mm columns, flow marker elution volume of calibration standards = 20.23 mL.

with the calibration curve established at 30°C. The use of a flow marker overcompensates for the effect of the increased temperature and the resulting M_w are too low. The results emphasize the necessity of using the identical temperature for column calibration and the sample measurements. The elution volume at higher temperatures can be also influenced by expansion of gel pores and decreased viscosity of the mobile phase, which consequently increases the diffusion coefficients. The temperature may also affect the secondary separation mechanisms.

Table 3.7 demonstrates the influence of injected mass on the molar mass moments of broad polystyrene. Different injected masses were achieved by different injection volumes of a sample of given concentration or by injection of the same volume of solutions of different concentration. Glancing at Table 3.7 one can see a significant decrease of molar mass with increasing injected mass. A relatively small difference in the injected mass results in a measurable difference of the molar mass.

The influence of the concentration of calibration standards on the obtained molar masses is shown in Table 3.8. Three calibration solutions were prepared as mixtures of four or five narrow polystyrene standards covering the molar mass range of $10^3 - 4.3 \times 10^6$ g/mol. The regular concentration of the calibration standards was 0.03% w/v of each of the standard. The two standards with the highest molar mass (4.34×10^6 and 2.85×10^6 g/mol) were prepared at half concentration. The calibration solutions were then prepared at concentrations lower by a factor of two and four and two and three times higher. Table 3.8 lists individual concentrations per standard and the total concentrations of all standards in the calibration solutions. The molar mass averages were calculated for sample prepared at a concentration of 0.25% w/v using calibration curves obtained for the particular concentrations of standards. The results show a negligible effect of the concentration of calibration solutions on M_n, and clearly evident impact on the higher molar mass averages. However, the influence of the concentration of polystyrene standards appears to be low over relatively broad concentration range.

Table 3.7 Effect of Injected Mass on Molar Mass Averages of Broad Polystyrene Determined by Conventional SEC

Injected Mass (mg)	Volume (μL)	Concentration (% w/v)	M_n (g/mol)	M_w (g/mol)	M_z (g/mol)
0.05	100	0.05	89,900	292,100	533,000
0.10	100	0.10	91,900	290,200	528,400
0.15	100	0.15	87,100	285,300	520,800
0.20	100	0.20	87,800	283,500	518,300
0.25	100	0.25	85,300	276,700	508,400
0.50	100	0.5	84,200	259,400	492,900
0.75	100	0.75	78,300	231,400	475,500
1.0	100	1.0	68,400	201,400	459,800
1.5	100	1.5	45,800	164,000	421,000
0.025	10	0.25	91,200	305,800	558,100
0.05	20	0.25	91,100	300,900	548,800
0.125	50	0.25	88,300	290,700	531,300
0.188	75	0.25	87,000	285,500	522,300
0.31	125	0.25	86,200	275,600	506,600
0.38	150	0.25	85,300	272,100	501,300
0.50	200	0.25	83,800	265,800	492,500
0.1	10	1.0	91,800	295,800	543,000
0.15	10	1.5	88,400	285,400	530,300
0.2	10	2.0	86,700	273,300	517,900

The concentration dependence of the elution behavior was studied by Janca et al.[28–33] Three contributions of concentration dependence of the elution volume were considered: change of the hydrodynamic size of the analyzed macromolecules, viscosity of the polymer solution in the pores of column packing, and secondary exclusion due to occupancy of a pore by another polymer molecule. The hydrodynamic volume of polymer random coils decreases with increasing concentration, which leads to the increase of elution volume. The dependence is more pronounced in thermodynamically good solvents, and the polymer dimensions become independent of concentration in theta conditions. The secondary exclusion resulting from the occupation of a part of pore volume by other polymer molecules becomes more pronounced at higher concentrations and the elution volume decreases. The viscosity effect is related to the mobility of macromolecules. The effect of the viscosity is more dominant at the region of higher molar masses.

At a certain viscosity of polymer solutions the chromatograms may become more complicated with several irregular maxima not corresponding to the true molar mass distribution. This phenomenon is called *viscous fingering* and may lead to a complete failure of SEC separation. Viscous fingering appears if the viscosity of the injected solution is markedly greater than that of the mobile phase. The high viscosity of the injected solution may result in the decreased

Table 3.8 Effect of the Concentration of Polystyrene Standards on the Molar Mass Averages of Broad Polystyrene

Concentration per Standard (% v/w)	Concentration total (% v/w)	M_n (g/mol)	M_w (g/mol)	M_z (g/mol)
0.004 or 0.008	0.026–0.034	85,500	273,300	498,400
0.008 or 0.015	0.053–0.068	85,300	274,500	501,100
0.015 or 0.030	0.105–0.135	85,600	276,900	507,000
0.030 or 0.060	0.210–0.270	85,800	282,000	520,900
0.045 or 0.090	0.315–0.405	86,300	288,300	539,200

Calibration with 13 polystyrene standards ranging from 10^3 to 4.3×10^6 g/mol, injection in three mixtures containing 4 or 5 standards.

velocity of the injected zone, whereas the faster mobile phase has a tendency to finger its way through the injected sample zone, which distorts the peak shape.

Investigation of the concentration dependence of the elution volume is facilitated by a light scattering detector capable of direct measurement of molar mass and size of the molecules eluting from SEC columns. An example of such a study is presented in Figure 3.36, which shows results obtained for different injected masses of polydisperse polystyrene. With the increasing injected mass the chromatograms are broadened and shifted to lower elution volumes. The shift of the molar mass plots toward higher elution volumes appears from a certain injected mass, below which the effect of sample concentration is negligible. The corresponding molar mass averages are listed in Table 3.9.

Comparison of Tables 3.7 and 3.9 shows significantly lower sensitivity of M_w determined by the light scattering detector to injected mass compared to M_w obtained by column calibration. In the case of conventional SEC the decrease of M_w with increasing injected mass is caused by the shift of the chromatograms toward higher elution volumes. In the case of SEC-MALS the decrease of M_w is due to neglecting the concentration dependence of the intensity of scattered light, but the effect is relatively small within the range of concentrations usually used for SEC measurements. With the MALS detector the averages M_n and M_z are determined on the assumption of the monodisperse slices, and thus the increased polydispersity within the elution volume slices due to column overloading increases M_n and decreases M_z.

It is obvious that the accuracy of the molar mass determined by SEC with column calibration depends on the injected mass of the sample and somewhat on the injected mass of the calibration solutions. To find out an optimum concentration and injected volume in order to reduce the errors caused by the concentration dependence of elution volume may not be straightforward. The concentration of the injected solution begins to change immediately after the injection as a result of sample dilution with a solvent and separation according to molar mass distribution. This effect depends on the width of the molar mass distribution,

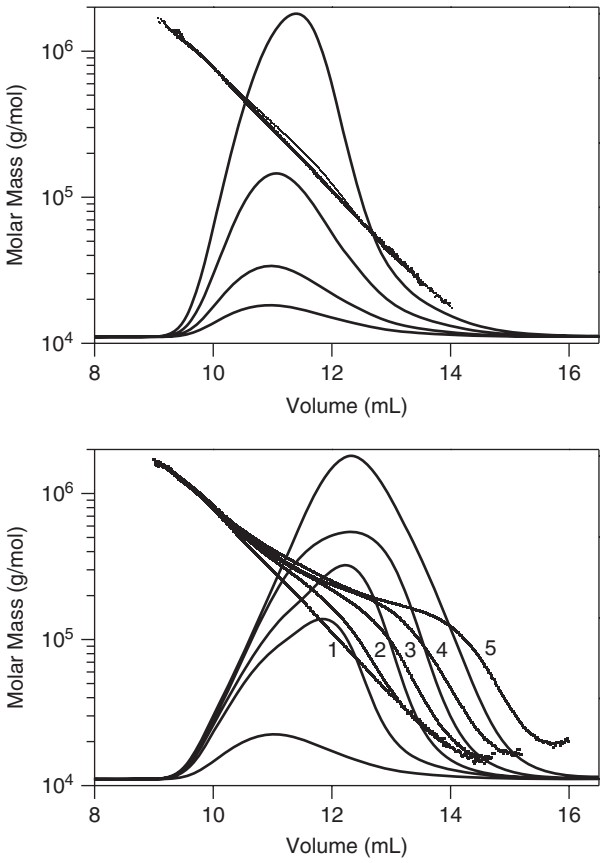

Figure 3.36 Effect of injected mass: Molar mass versus elution volume plots and RI chromatograms of polydisperse polystyrene analyzed under different injected mass. Injected mass: 0.05 mg, 0.11 mg, 0.24 mg, and 0.49 mg (top), 1 = 0.19 mg, 2 = 0.73 mg, 3 = 1.06 mg, 4 = 1.45 mg, 5 = 1.93 mg (bottom). Columns 2 × PLgel Mixed-C 300 × 7.5 mm, THF at 1 mL/min, 40°C, injected volume 100 μL. Molar mass averages are listed in Table 3.9.

Table 3.9 Effect of Injected Mass on Molar Mass Averages of Broad Polystyrene Determined by SEC-MALS

Injected mass (mg)	M_n (g/mol)	M_w (g/mol)	M_z (g/mol)
0.05	130,000	294,000	480,000
0.11	124,000	293,000	477,000
0.15	118,000	288,000	470,000
0.19	121,000	288,000	471,000
0.24	118,000	287,000	469,000
0.49	121,000	283,000	458,000
0.73	127,000	280,000	442,000
1.06	144,000	276,000	419,000
1.45	159,000	273,000	400,000
1.93	184,000	269,000	380,000

Data obtained by conventional SEC are in Table 3.7; graphical representation is in Figure 3.36.

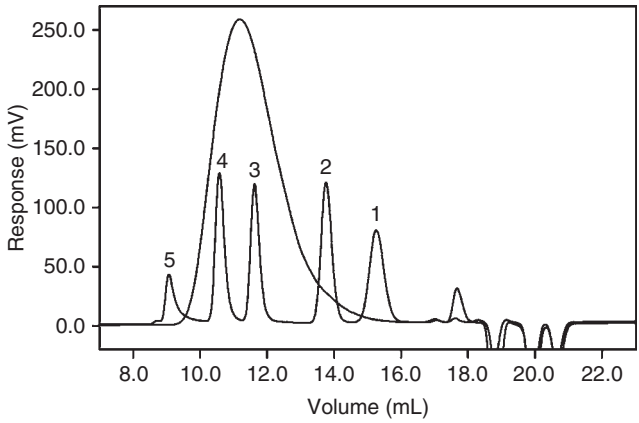

Figure 3.37 Overlay of chromatograms of a mixture of polystyrene standards and broad polystyrene. Injection: 100 μL 0.2% w/v for broad polymer, 50 μL 0.03% w/v for each of standards 1–4, and 0.015% w/v for standard 5. Molar masses of standards 1–5: 3600 g/mol, 19,000 g/mol, 170,000 g/mol, 470,000 g/mol, and 2,850,000 g/mol, respectively.

which means that broader samples are always more diluted compared to samples with narrow molar mass distribution. The dilution of polydisperse polymer in SEC columns is responsible for the fact that polymer sample concentration is mostly different from the concentration of calibration standards. The difference of the concentration of the polydisperse polymer sample from the concentration of the calibration standards varies across the peak as shown in Figure 3.37, which overlays chromatograms of a broad polymer and a mixture of narrow standards.

Several methods were proposed to eliminate the effect of the concentration of sample and calibration solutions on the molar masses determined by SEC. One of the proposed methods of reducing the concentration effect involves calibration by means of standards of different concentrations, which yields a series of calibration curves valid for different concentrations and an extrapolated curve for zero concentration. The chromatogram of a polydisperse polymer is then separated into several sections and each of them is processed using the calibration dependence valid for the concentration most appropriate to the given section. Other methods of reducing the concentration effect are an extrapolation procedure where reciprocal molar mass averages determined at various concentrations are plotted against concentration and extrapolated to zero concentration, or processing the chromatogram with the use of a calibration curve extrapolated to zero concentration. A significant disadvantage of the latter method is that it does not eliminate the concentration effect of the sample itself, which is obviously more serious than the concentration effect of the calibration standards.

It is evident that the procedures for correcting the concentration effect are not suitable for routine measurements. For example, to eliminate the concentration effect completely by using calibration curves valid for different concentrations

would require the separation of a chromatogram into a relatively high number of sections. Although the concentration effect represents a potentially serious source of inaccuracy, its reduction should not eliminate the speed and simplicity of SEC measurements. Keeping the concentration of sample and calibration standards at an appropriate level can minimize the effect of concentration. As a rule of thumb, the concentrations of the analyzed samples and calibration standards should be kept as low as possible, but achieve sufficient detector signal-to-noise ratio. The injected mass can be easily reduced by dilution of the injected sample or decreasing the injected volume. Remeasuring samples showing peak shoulders at lower injected mass can reveal multicomponent polymer blends, as demonstrated in Figure 3.38.

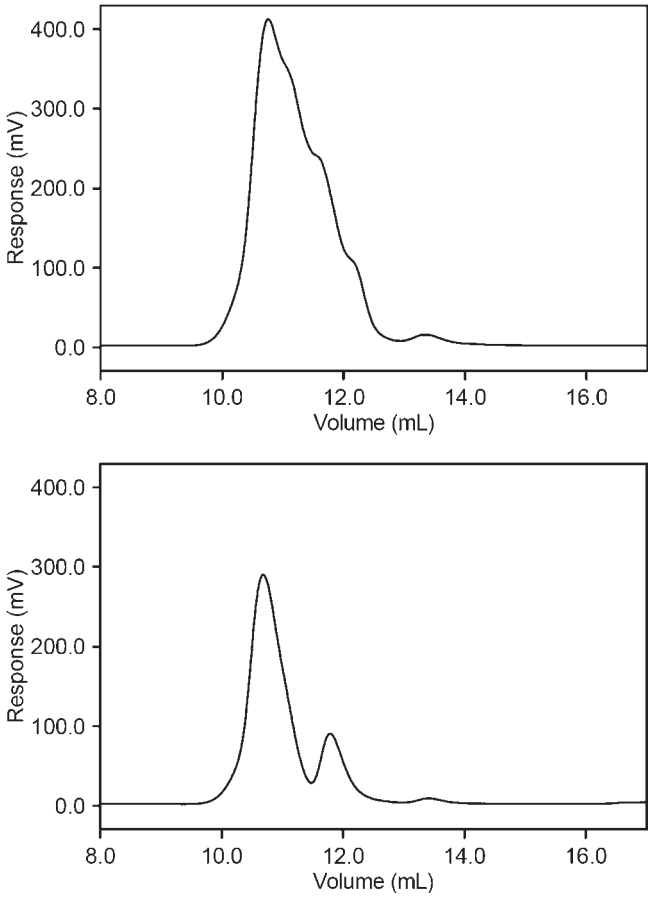

Figure 3.38 Chromatograms of polymer blend analyzed at the concentrations of 0.3% w/v (top) and 0.15% w/v (bottom). Columns 2 × PLgel Mixed-C 300 × 7.5 mm, THF at 1 mL/min, 100-μL injection.

3.5.7 Accuracy, Repeatability, and Reproducibility of SEC Measurements

The term *repeatability* (precision) refers to the variation of the experimental results generated by a single person or instrument on the same sample under identical conditions. A measurement may be considered repeatable when the variation of results is smaller than a certain agreed limit. The repeatability conditions also include measurements over a short period of time. *Reproducibility* refers to the ability of the experiment to be reproduced by someone else working independently. In contrast to repeatability, which is related to successive experiments, reproducibility is related to the agreement of experiments performed by different operators, with different apparatus and laboratory locations, or of measurements repeated in the same laboratory after a relatively long time period. Reproducibility is often confused with repeatability, and results generated in a single laboratory by a single person by multiple injections within one day are often used to demonstrate good reproducibility achievable with a given instrumentation.

Repeatability is of crucial importance for the interpretation of experimental results. When the results are at the verge of the limit of possible repeatability, the conclusions concerning the effect of synthetic conditions on molar mass, relation of molar mass with sample properties, or differences between samples might be false.

Repeatability and reproducibility are usually evaluated by the *standard deviation* defined for a large number of measurements as:

$$\sigma = \sqrt{\frac{1}{N}\sum_{i=1}^{N}(x_i - \bar{x})^2} \tag{3.69}$$

where N is the number of measurements, x_i is the result of the ith measurement, and $\overline{x}$ is the arithmetic mean (average) defined as:

$$\bar{x} = \frac{1}{N}\sum_{i=1}^{N} x_i \tag{3.70}$$

For a small number of measurements the standard deviation is estimated as:

$$\sigma = \sqrt{\frac{1}{N-1}\sum_{i=1}^{N}(x_i - \bar{x})^2} \tag{3.71}$$

Relative standard deviation is the standard deviation relative to the average. Besides standard deviation the experimental differences can be illustrated graphically as a plot of molar mass average versus laboratory number or measurement number. To estimate repeatability, standard deviation from multiple SEC runs can be calculated.

Accuracy (correctness) can be defined as agreement with the truth and can be estimated by comparison with results obtained by measurements with an absolute method or literature values. Questions related to accuracy, reproducibility, and repeatability are:

1. Do the obtained results agree with the true values?
2. Are the results comparable with those generated in other laboratories?
3. Are the results identical when the measurements are repeated after a certain period of time?

A well-characterized polymer with reliably determined molar mass averages is needed to address the first question. Molar mass averages determined by conventional SEC are compared with the results determined by light scattering and membrane osmometry for several samples in Table 3.10, which shows a tendency of SEC to yield M_n values lower than those from membrane osmometry. Note that SEC and MO have a counteracting tendency to errors in M_n. In conventional SEC the band-broadening M_n decreases, while in the case of MO the M_n may be increased due to the permeation of oligomeric fractions through the membrane. For samples containing oligomeric fractions, SEC can be a more reliable source of M_n than absolute membrane osmometry. The agreement of M_w obtained by SEC and light scattering is satisfactory and indicates that neglecting the peak-broadening correction does not affect the experimental results significantly.

Reproducibility of the measurements can be evaluated by means of *round-robin tests*, where the same samples are sent to different laboratories where they are measured using available apparatus, columns, and standards and the methodology routinely used in the laboratory. Results of ten round-robin tests[9] carried out for various polymers in the late 1980s and the 1990s showed repeatability

Table 3.10 Comparison of Molar Mass Averages Determined by Conventional SEC with Column Calibration* and Absolute Methods

	M_n (10^3 g/mol)		M_w (10^3 g/mol)		
Sample	SEC	MO	SEC	Batch MALS	SEC-MALS
PS (NIST 706)	89 ± 1	137	273 ± 1	288 ± 2	283 ± 1
PS (A)	—	—	327 ± 5	344 ± 8	326 ± 4
PS (AN)	82 ± 5	120	273 ± 7	303 ± 1	294 ± 1
PS (1)	70 ± 1	139	355 ± 1	386 ± 1	370 ± 1
PS (2)	105 ± 1	153	362 ± 1	398 ± 6	375 ± 1
PS (S)	39 ± 1	66	217 ± 1	236 ± 1	225 ± 1
PS (K)	84 ± 1	98	230 ± 1	239 ± 3	238 ± 1
PMMA (Y)	145 ± 3	185	498 ± 1	604 ± 10	558 ± 7
PMMA (J)	39 ± 1	33	84 ± 1	96 ± 1	89 ± 1

*Calibration is based on polystyrene or poly(methyl methacrylate) narrow standards.

Table 3.11 Results of Two Round-Robin Tests on Synthetic Resins (S) and Epoxy Resins (EP): Molar Mass Averages and Relative Standard Deviations

		M_n		M_w		M_z	
Sample	No. of Participants	(10^3 g/mol)	RSD (%)	(10^3 g/mol)	RSD (%)	(10^3 g/mol)	RSD (%)
S (1)	6	4.0	37	9.0	9	14.2	9
S (2)	6	3.9	49	52.2	25	320	34
EP (1)	16	1.8	16	5.0	11	—	—
EP (2)	16	4.0	13	12.4	9	—	—

and reproducibility of M_n in the ranges of 0.7–5.6% and 3.5–33.4%, respectively; and the repeatability and reproducibility of M_w in the ranges of 0.4–5.9% and 4.3–17.7%, respectively. Results of two round-robin tests organized by the author are listed in Table 3.11. Experience and round-robin tests show that:

- Repeatability is significantly better than reproducibility.
- The molar mass averages generated in two laboratories can often differ by a factor of two or more.
- The reproducibility of M_w is markedly better compared to that of M_n, which can be explained by typically higher uncertainty in the selection of the peak end.
- Reproducibility is better for well-resolved samples compared to those with high-molar-mass or low-molar-mass tails.
- Samples containing functional groups along the polymer chain show larger uncertainty of results due to interactions with the surface of the column packing.

Significantly better repeatability compared to reproducibility is true also in the same laboratory, as demonstrated in Tables 3.12 and 3.13, which compare repeatability with a long-term reproducibility generated in a single laboratory using the same SEC setup, column type, and calibration standards. It is necessary to emphasize that good repeatability may lead to self-satisfaction and overestimation of accuracy of SEC and its ability to generate comparable results when the same sample is characterized in different laboratories. An isolated operator without a confrontation with other laboratories can generate systematically shifted results.

The results of a Japanese round-robin test[34] showed significantly more favorable results when the data generated only in experienced laboratories, namely those belonging to manufacturers of SEC instrumentation and columns, were selected for calculation of standard deviations. This fact corresponds to my own experience, which is demonstrated in Table 3.14. Although Table 3.14 compares results from only two laboratories, the very good agreement is most likely not accidental, because it was obtained for five different samples. It appears that

Table 3.12 Repeatability of Molar Mass Determination of Broad Polystyrene from Ten Consecutive Runs

Run #	M_n (g/mol)	M_w (g/mol)	M_z (g/mol)
1	85,200	274,300	503,300
2	84,800	274,600	504,800
3	85,200	275,700	506,800
4	84,000	276,000	507,300
5	85,300	277,000	508,100
6	86,000	277,400	509,900
7	85,000	277,800	511,700
8	86,300	277,800	510,100
9	85,900	278,100	510,300
10	85,400	278,400	511,400
Mean	85,300	276,700	508,400
SD (g/mol)	700	1500	2800
RSD (%)	0.8	0.5	0.6

For comparison of reproducibility, see Table 3.13.
Conditions: THF at 1 mL/min, 2 × PLgel Mixed-C 300 × 7.5 mm columns, no flow marker.

SEC reproducibility is markedly better when experienced operators carry out the measurements despite using different instrumentation, columns, and calibration standards.

Relatively poor reproducibility of conventional SEC can be explained by sensitivity to many experimental and processing parameters. These are: type of columns, injection volume, concentration of injected samples and standards, type and manufacturer of calibration standards and their number, universal calibration yes/no, universal calibration parameters, fitting the calibration data, flow rate, whether flow marker is used, column temperature, sample preparation (incomplete dissolution, improper filtration), and the way of baseline and peak selection.

Regular measurements of a reference sample can address repeatability and reproducibility within a single laboratory and facilitate comparison of results acquired with a long time gap. Long-term reproducibility within a single laboratory is influenced mainly by the change in separation efficiency of the columns. Column performance usually deteriorates with time, which is indicated by decreasing plate number. Column properties may also change with respect to column interactivity (i.e., tendency to interact with polymers). Irreversibly adsorbed molecules from previous injections can occupy a part of the packing pores and thus decrease the pore volume available for sample separation. The change of the interactivity may not be revealed even by regular analysis of a control polymer, because if the chemical composition of the control polymer differs from that of samples being analyzed, then the interaction behavior is most likely different. Deviations of the pump flow rate from the nominal value are another important source of poor reproducibility within a laboratory. One

Table 3.13 Reproducibility of Molar Mass Averages of Broad Polystyrene* Measured Over a Period of One Year

Date Acquired	M_n (g/mol)	M_w (g/mol)	M_z (g/mol)
01/03	88,100	282,300	530,000
01/08	86,100	282,500	530,200
01/11	87,100	282,800	527,300
01/22	87,100	282,300	526,200
01/29	85,000	267,000	496,800
01/31	71,000	267,000	511,300
02/07	76,300	266,200	497,700
02/12	81,000	267,300	497,700
...	...	...	...
06/05	87,400	276,100	507,300
06/07	85,800	275,200	509,400
06/13	87,100	275,600	504,100
06/14	87,600	276,200	502,700
06/18	75,600	270,400	496,400
06/21	86,700	274,500	501,600
06/22	85,200	275,400	504,600
06/27	84,853	282,000	517,900
07/11	82,900	272,300	501,700
...	...	...	...
11/01	80,200	279,400	510,700
11/02	85,400	286,500	526,800
11/07	81,700	268,800	496,100
11/08	85,100	284,100	524,100
11/22	85,600	274,140	505,800
11/26	82,700	273,640	505,400
11/27	89,000	275,700	505,200
12/11	87,000	270,100	498,700
Total no. of measurements	73	73	73
Mean	82,200	272,800	506,200
SD (g/mol)	4,800	6,500	10,400
RSD (%)	5.8	2.4	2.1

*The same sample as in Table 3.12.
Conditions: THF at 1 mL/min, 2 × PLgel Mixed-C 300 × 7.5 mm columns, no flow marker, calibration before each measurement.

should not forget temperature, which may become important in laboratories without air conditioning and without a column oven.

Various round-robin tests usually did not reveal any major source of poor reproducibly. That means the variation of SEC results is due to a combination of several different factors, including the different experience and individual

Table 3.14 Molar Mass Averages of Acrylic Copolymers Determined in Two Independent, Very Experienced Laboratories: Example of Very Good Reproducibility

	M_n (g/mol)		M_w (g/mol)	
Sample No.	Laboratory #1	Laboratory #2	Laboratory #1	Laboratory #2
1	10,500	10,300	29,300	32,900
2	12,300	12,300	33,800	34,600
3	10,900	10,700	32,200	32,800
4	13,500	13,800	40,200	41,500
5	3,300	2,500	6,300	6,300

approach of operators. Reproducibility can be markedly improved by implementing proper rules and procedures. On the other hand, SEC is certainly a truly routine technique, and simplicity and ease-of-use should not be sacrificed in the name of reproducibility. It is necessary to balance between bad laboratory practices and procedures, leading to poor reproducibility, and far-too-strict rules that are difficult to fulfill and that reduce the full potential of the SEC method.

The most important measures leading to improvement of the interlaboratory reproducibility of conventional SEC results are:

- Selection of columns appropriate for samples to be analyzed, using mixed columns if possible, and using the same type of columns
- The same calibration standards from the same vendor
- The same concentration and injection volume of the calibration standards
- The same number of calibration data points and the same type of data fit, usually third-order polynomial
- The same constants of the Mark-Houwink equation if the universal calibration is applied
- The same injection volume and concentration of samples
- Recalibration before each sample series and using a flow marker if possible
- Measurement under stabilized conditions giving minimum baseline drift
- Unified methodology for finding the baseline and peak integration limits, rejecting results acquired with an unstable baseline
- Regular analysis of a common reference sample
- Using the same type of detector (mostly RI)
- Regular maintenance of the pump with respect to flow rate accuracy and repeatability

In the case of light scattering detection, some of the above parameters become far less important and the most important points are:

- A common method for the calibration of light scattering and concentration detectors

- Using identical dn/dc for the polymers being analyzed

In both conventional SEC and SEC combined with a light scattering detector, the report should contain information necessary for mutual comparison of results generated in different laboratories or within a given laboratory over a long time period. The information in the report should address the points stated above.

3.6 APPLICATIONS OF SEC

An important question to ask before characterization of polymers is what sort of information is needed, for what purpose, and in what time period. Useful information about polymers usually comes from molar mass averages, typically M_n, M_w, and M_z. However, more information can be revealed from distribution functions that yield information about the synthetic process and help us understand the structure–property relations. Therefore, the most important major application of SEC is determination of the molar mass distribution and molar mass averages. This goal can be achieved using column calibration or most effectively in combination with a light scattering detector that measures the molar mass directly.

Information about molar mass distribution is important in all areas of polymer science covering the theory, synthesis, properties, and final applications. The combination of SEC with a light scattering detector and also a viscometer can yield further information about the molecular structure. The molar mass averages are the characteristics that are easy to arrange into tables and relate with polymer properties. However, polymer properties can depend not only on the average molar masses, but also on the entire molar mass distribution and its details. Especially fractions with molar mass significantly lower or higher than the majority of polymer molecules can considerably affect the application properties. An overlay of distribution curves is especially suitable for the comparison of properties of similar samples and can explain possible differences among them. Molar mass characteristics can be used for structure–property studies, and they can be also valuable for evaluation of the reproducibility of manufacturing process and to study the influence of polymerization conditions on the molecular structure of the obtained products. In contrast to SEC, the traditional quantities such as solution or melt viscosity or content of functional groups (e.g., acid number, epoxy content) provide only an average characteristic.

Another advantage of SEC in the area of manufacturing process and quality control compared to other methods are speed and simplicity of sample preparation. The results of SEC measurement are available in very short time, which allows for taking measures before the next manufacturing batch is started.

The typical analysis time of about 30 min can be further reduced by using special columns for high-throughput analysis, which, however, provide only limited resolution. Due to the speed of the measurements, SEC can be also used for direct manufacturing process monitoring, especially in the case of polycondensation reactions. The obtained chromatograms need not be necessarily converted

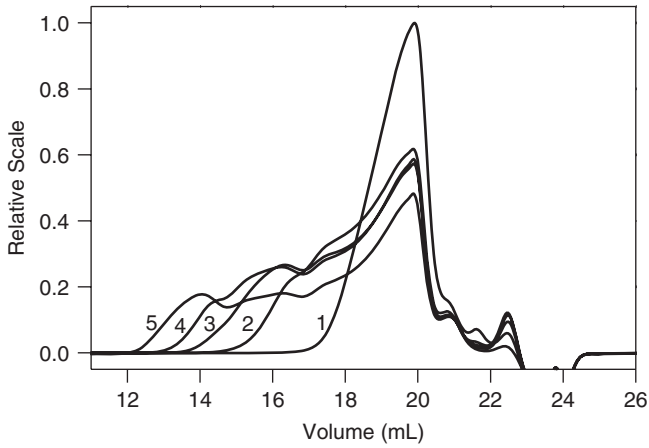

Figure 3.39 Monitoring the course of preparation of alkyd resin by a series of chromatograms of samples taken during the reaction (reaction conversion increases from sample #1 to #5).

into molar mass distribution; a simple fingerprint comparison can be sufficient for sample comparison or illustration of the growth of a polymer chain during the polyreaction or degradation process due to chemical or physical exposition. An example of the monitoring of the course of a polycondensation reaction by overlay of chromatograms is shown in Figure 3.39.

A simple fingerprint comparison of two polyols for polyurethane foams is depicted in Figure 3.40. It is evident that a simple chromatogram overlay can reveal differences between the two polyols, one containing a significant fraction of lower oligomers with the main fraction shifted to higher molar masses as compared to the other sample. The molar mass averages, although polystyrene equivalent values, correspond to the chromatograms: M_n is lower for the polyol containing the oligomeric fractions, while its M_w is higher, corresponding to the shift of the molar mass distribution to higher molar masses.

Figure 3.41 shows another example of simple interpretation of SEC data that allows us to differentiate between samples with different end-use properties.

In the case of oligomeric materials, SEC can determine the content of lower oligomers. High repeatability of SEC allows a sensitive fingerprint comparison of chromatograms of oligomeric materials such as various types of synthetic resins. Another application is the quantification of low-molar-mass additives that are added to polymers to improve their properties and to protect them against degradation. The additives include plasticizers, dyes, antioxidants, and UV stabilizers, and these can be easily quantified after the calibration of detector response.

Other low-molar-mass compounds that can be present in polymers are residual monomers, initiators, catalysts, solvents, and various side products. SEC can be used for the quantification of additives and other low-molar-mass compounds only if their molecular sizes are sufficiently different from each other. If this requirement is not fulfilled, other types of liquid chromatography must be used.

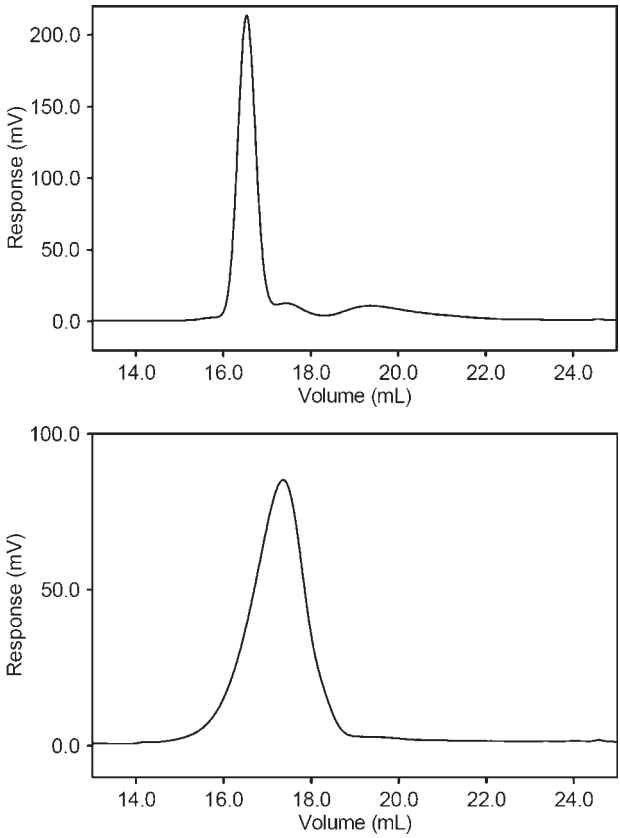

Figure 3.40 Chromatograms of polypropylene glycol–based polyols for polyurethane foams showing different molar mass distribution. Top: $M_n = 6500$ g/mol, $M_w = 9900$ g/mol, $M_w/M_n = 1.51$. Bottom: $M_n = 7100$ g/mol, $M_w = 8600$ g/mol, $M_w/M_n = 1.21$. Conditions as in Figure 3.28.

There are two different methods of determination of low-molar-mass compounds in polymers. One is the extraction of low-molar-mass compounds with a suitable solvent and subsequent SEC or HPLC analysis of the obtained extract. The extraction can be carried out by immersing a polymer film or a thin sheet in a solvent for many hours or several days or using a Soxhlet extractor. The other method is to inject the polymer solution directly into an SEC instrument with columns capable of separation of the additive from polymer. A typical example of a chromatogram of a polymer containing a low-molar-mass additive is shown in Figure 3.42.

There are also other, less-usual applications; for instance, the high repeatability of SEC has been used to identify sources of crude oil contamination on the basis of fingerprint comparison. SEC can be also used for the characterization of various low-mol-mass compounds, but the separation ability is limited compared

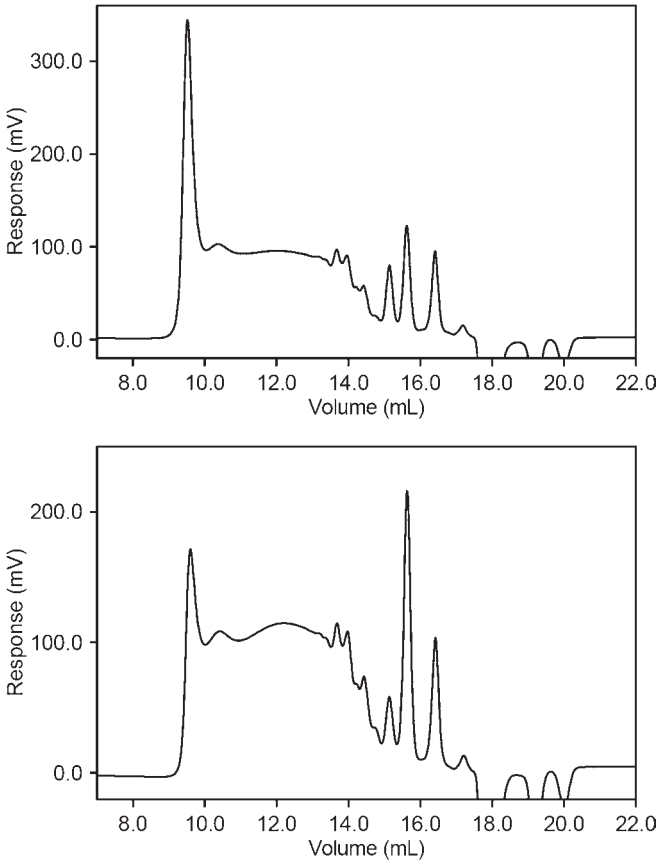

Figure 3.41 Chromatograms of two resin samples with good (top) and bad (bottom) properties obtained using columns with exclusion limit of about 30,000 g/mol. Chromatograms show presence of low-molar-mass compounds with molar mass of several hundreds as well as compounds with molar mass exceeding the exclusion limit of SEC columns. The two batches differ in the content of low-molar-mass compounds and also in the fractions with high molar mass. Columns 2 × PLgel Mixed-E 300 × 7.5 mm 3 μm, THF at 1 mL/min, injection 50 μL 0.3% w/v.

to other types of liquid chromatography. Possible applications include the characterization of crude oil, natural oil, asphalt, and tar. The obtained chromatograms may be complicated overlays of several peaks, because the complete resolution of all compounds is virtually impossible.

Special techniques include preparative, recycle, inverse, and differential SEC. Some techniques have found only limited applications, while preparative SEC may be relatively frequently used.

SEC is an important part of two-dimensional separations (2D-LC). The sequence is usually LC in the first dimension and SEC in the second dimension. The fractions separated by LC separation are transferred into the second

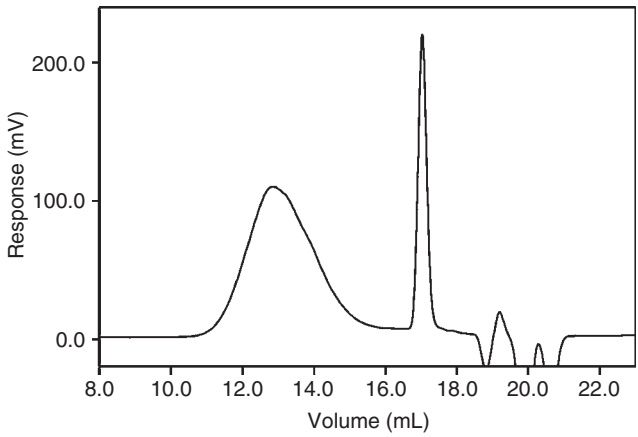

Figure 3.42 RI chromatogram of polymer containing low-molar-mass additive (copolymer styrene-methylmethacrylate-butylmethacrylate containing nonylesters of phthalic acid).

dimensions by an automatically controlled switching valve. The LC separation permits separation according to chemical composition, which is further accomplished with the determination of molar mass distribution by SEC. The reviews can be found in the literature.[35–37]

SEC plays an important role in the characterization of biomacromolecules, typically various polysaccharides (starch, dextran, pectin, hyaluronic acid) and proteins. Polysaccharides are polydisperse polymers that need to be characterized by the molar mass distribution and molar mass averages, and thus the data processing is similar to synthetic polymers. The column calibration is mostly based on pullulan standards, but it must be taken into account that polysaccharides are often branched. The use of calibration established by linear pullulan standards for branched polysaccharides provides strongly erroneous results. Pullulan calibration also yields significant errors when applied to polysaccharides bearing anionic groups (e.g., hyaluronic acid) that have expanded coil structure due to electrostatic repulsive forces. Calibration based on dextran standards may yield erroneous results even when applied to the characterization of dextran samples, because of possibly differing degrees of branching of standards and the analyzed samples.

A very important application of SEC in the area of protein characterization is the determination of oligomers and aggregates. The aggregates reduce the ability of protein to crystallize (crystals being necessary for x-ray structural studies). The quantification is usually based on the relative peak areas in RI or UV chromatograms. An example of the separation of protein oligomers is shown in Figure 3.43. Note that in protein terminology, in contrast to that used in macromolecular chemistry, *oligomer* does not refer to a lower-molar-mass polymer, but to a higher-molar-mass compound containing multiple protein molecules bonded by covalent or other chemical bonds. The term *monomer* refers

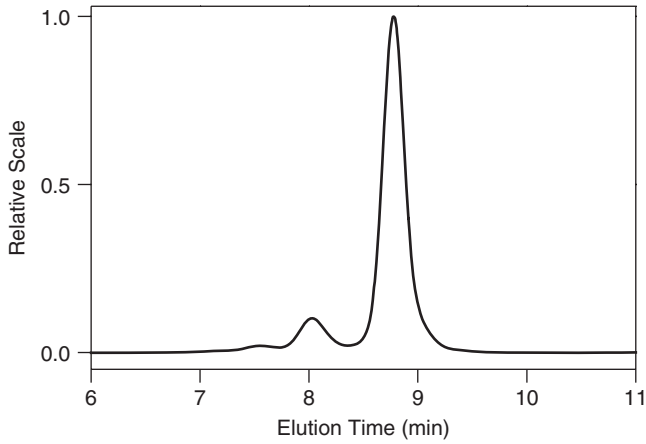

Figure 3.43 UV chromatogram of BSA showing separation of monomer, dimer, and trimer. Column Shodex Protein KW 803 300 × 8 mm, phosphate buffer, flow 0.5 mL/min, UV at 280 nm.

to a single protein molecule. That means *monomer bovine serum albumine* means the protein molecules of molar mass of 66.4×10^4 g/mol. A distinctive feature of proteins is that they are strictly monodisperse (i.e., the molar mass within each chromatographic peak is identical). The determination of molar mass of proteins and protein oligomers based on the calibration curve established by standard proteins is very inaccurate because of possibly differing protein conformation. The elution volume of proteins is also frequently affected by secondary interactions with the stationary phase. To determine the true molar mass of proteins, a light scattering detector is needed even more than in the case of other synthetic and natural polymers. For more information on SEC of proteins see the review in reference 38.

Preparative and semipreparative SEC can serve to isolate polymer fractions for their further characterization. The scale of regular analytical 300 × 8-mm columns in combination with repeated injections can provide sufficient amounts of sample for spectral analysis. To increase the loadability of SEC columns, which is proportional to the cross-sectional area of the columns, it is necessary to use wider bore semipreparative or preparative columns. The flow rate for the preparative columns must be increased proportionally to keep the same linear flow velocity and thus the run time comparable with the analytical columns. The increase of sample load can be achieved by increasing the sample concentration and injection volume. The increase of sample concentration is preferred over the increase of the injection volume, but is limited by viscosity effects of polymers containing high-molar-mass fractions. Therefore, both sample concentration and injection volume are usually increased to achieve sufficient mass injection. Peak saturation is often observed in preparative SEC, which can be addressed by decreasing detector sensitivity or using wavelengths of UV detector at which the sample absorption is minimal. The fractions are obtained in the form of

highly diluted solutions. The solvent must be evaporated using vacuum and/or elevated temperature. In the case of stabilized THF, the stabilizer (usually BHT) is concentrated and this must be taken into account for the interpretation of spectral results; otherwise, nonstabilized THF must be used. In aqueous SEC, the mobile phase typically contains salts that are concentrated in the isolated fractions. A possible application of preparative SEC is the isolation of organic contaminants from matrices for environmental analyses. The sample for environmental analysis prepared by extraction can contain compounds with higher molar mass such as fats or dyes that can be efficiently removed by SEC. That means SEC is used as a cleaning tool for agricultural products, animal fat, and soil for the determination of pesticides, polychlorobiphenyls, and polycyclic aromatic hydrocarbons.

3.7 KEYNOTES

- Size exclusion chromatography separates polymer molecules according to their hydrodynamic volume and not according to the molar mass. That means molecules of different molar mass, different chemical composition, and different degree of branching can co-elute at a common elution volume. A unimodal SEC peak does not prove the homogeneity of the chemical composition.
- SEC belongs to the group of liquid chromatography techniques. A distinctive feature of SEC is absence of enthalpic interactions between the analyzed molecules and the stationary phase. However, in real SEC, various types of interactions often play a significant role and it is necessary to minimize them by selection of suitable column packing, mobile phase, temperature, additives, or sample derivatization.
- Peak broadening in SEC columns and other parts of the instrumental setup is another undesirable phenomenon in SEC, which affects the experimentally determined molar mass distribution. However, using columns with adequate efficiency it can be neglected without serious errors in molar mass distribution.
- In order to analyze broad polymers over a wide range of molar masses it is necessary to use SEC columns with appropriate separation range. A traditional option is to use multiple columns of different pore sizes linked together in series. Another possibility is to use columns packed with a mixed-bed packing of different pore sizes at an optimized mix ratio, or a packing material composed of monodisperse particles in which a wide range of pore sizes is contained within a single particle. False molar mass distribution is obtained if the analyzed sample contains fractions with molar masses outside the separation range of the applied columns.
- In conventional mode with only a concentration detector, the SEC columns must be calibrated in order to transform elution volume to molar mass. When an adequate calibration curve is established, SEC is capable of providing correct molar mass distribution. The most accurate calibration is

achieved by a series of well-characterized narrow standards of the same chemical composition as that of the polymer under analysis. These standards are mostly unavailable and alternatively broad polymer standards or universal calibration must be used.

- For many polymers it is impossible to establish correct calibration and the true molar masses can be determined only by using the universal calibration in combination with a viscometer or by means of a light scattering detector.
- If the SEC data are evaluated by means of calibration established for a different polymer than that requiring analysis, the obtained molar mass distribution and molar mass averages are only apparent values that would have a polymer of the same chemical composition as the calibration standards and the same distribution of hydrodynamic volume as the polymer under analysis.
- A typical feature of SEC measurements is mostly very good short-term repeatability, whereas reproducibility is often significantly worse, especially when results generated in different laboratories using different instrumental conditions are compared.
- Analysis of a reference polymer should be performed along with the sample analysis to control for repeatability and reproducibility of the measurements.
- SEC results are sensitive to several experimental variables. The most important variables are flow rate, temperature, and sample concentration. Constant flow rate and column temperature can be achieved with suitable instrumentation, whereas sample concentration requires the careful attention of the operator.
- The following generic conditions can be recommended for most routine applications: two 300×8-mm mixed columns covering at least a molar mass range of $500 - 2 \times 10^6$ g/mol, sample concentration for polymers with M_w of order of magnitude of 10^5 g/mol around 0.2%, sample injection volume of 100 μL, standard concentration of 0.015–0.03% w/v, standard injection volume of 50 μL, and number of standards 10–15.
- *Modern Size-Exclusion Liquid Chromatography*[39] can be recommended to all who are interested in this technique.

3.8 REFERENCES

1. Porath, J. and Flodin, P., *Nature (London)*, **183**, 1657 (1959).
2. Moore, J. C., *J. Polym. Sci. A*, **2**, 835 (1964).
3. Tung, L. H., *J. Appl. Polym. Sci*., **10**, 375 (1966).
4. Baumgarten, J. L., Busnel, J. P., and Meira, G. R., *J. Liq. Chromatogr. Relat. Technol*., **25**, 1967 (2002).
5. van Deemter, J. J., Zuiderweg, F. J., and Klinkenberg, A., *Chem. Eng. Sci*., **5**, 271 (1956).
6. Striegel, A. M., *J. Chromatogr*., **932**, 21 (2001).
7. Kubin, M., *J. Chromatogr*., **108**, 1 (1975).

8. Tung, L. H. and Runyon, J. R., *J. Appl. Polym. Sci*., **13**, 2397 (1969).
9. Bruessau, R. J., *Macromol. Symp*., **110**, 15 (1996).
10. ISO Standard 13885-1 (1998).
11. Mottaleb, M. A., Cooksey, B. G., and Littlejohn, D., *Fresenius' J. Anal. Chem*., **358**, 536 (1997).
12. Reed, W. F., *Macromol. Chem. Phys*., **196**, 1539 (1995).
13. Yau, W. W., Gillespie, D., and Hammons, K., *International GPC Symposium 2000*, Las Vegas, October 22–25, 2000.
14. Wrobel, K., Sadi, B. B. M., Wrobel, K., Castillo, J. R., and Caruso, J. A., *Anal. Chem*., **75**, 761 (2003).
15. Szpunar, J., Pellerin, P., Makarov, A., Doco, T., Williams, P., and Lobinski, J., *J. Anal. At. Spectrom*., **14**, 639 (1999).
16. Lehmann, U. and Kohler, W. *Macromolecules*, **29**, 3212 (1996).
17. Grubisic, Z., Rempp, P., and Benoit, H., *J. Polym. Sci. B,* **5**, 753 (1967).
18. Chance, R. R., Baniukiewicz, S. P., Mintz, D., Strate, G. V., and Hadjichristidis, N., *Int. J. Polym. Anal. Character*., **1**, 3 (1995).
19. Brandrup, J., Immergut, E. H., Grulke, E. A. (editors), *Polymer Handbook*, 4th Edition, John Wiley & Sons, New York (1999).
20. Blau, K. and Halket, J. (editors), *Handbook of Derivatives for Chromatography*, John Wiley & Sons, Chichester (1993).
21. Mori, S., Kato, H., and Nishimura, Y., *J. Liq. Chrom. & Rel. Technol*., **19**, 2077 (1996).
22. Pasch, H. and Trathnigg, B., *HPLC of Polymers*, Springer-Verlag, Berlin (1999).
23. Podzimek, S., Hanus, J., Klaban, J., and Kitzler, J., *J. Liq. Chromatogr*., **13**, 1809 (1990).
24. Runyon, J. R., Barnes, D. A., Rund, J. F., and Tung, L. H., *J. Appl. Polym. Sci*., **13**, 2359 (1969).
25. Podzimek, S., in *Multiple Detection in Size-Exclusion Chromatography*, Striegel, A. M. (editor), ACS Symposium Series **893**, Washington, D.C. (2004), p. 107.
26. Braun, D. and Lee, D. W., *Angew. Makromol. Chem*., **48**, 161 (1975).
27. Podzimek, S., Dobas, I., Svestka, S., Horalek, J., Tkaczyk, M., and Kubin, M., *J. Appl. Polym. Sci*., **41**, 1161 (1990).
28. Janca, J., *J. Chromatogr*., **134**, 263 (1977).
29. Janca, J. and Pokorny, S., *J. Chromatogr*., **148**, 31 (1978).
30. Janca, J. and Pokorny, S., *J. Chromatogr*., **156**, 27 (1978).
31. Janca, J., *J. Chromatogr*., **187**, 21 (1980).
32. Janca, J., *Polym. J*., **12**, 405 (1980).
33. Janca, J., Pokorny, S., Vilenchik, L. Z., and Belenkii, B. G., *J. Chromatogr*., **211**, 39 (1981).
34. Aida, H., Matsuo, T., Hashiya, S., and Urushisaki, M., *Kobunshi Ronbunshu*, **48**, 507 (1991).
35. Berek, D., in *Handbook of Size Exclusion Chromatography and Related Techniques*, 2nd Edition, Wu, C.-S. (editor), Marcel Dekker, New York (2004), p. 501.
36. Pasch, H., in *Multiple Detection in Size-Exclusion Chromatography*, Striegel, A. M. (editor), ACS Symposium Series **893**, Washington, D.C. (2004), p. 230.
37. Teraoka, I., in *Multiple Detection in Size-Exclusion Chromatography*, Striegel, A. M. (editor), ACS Symposium Series **893**, Washington, D.C. (2004), p. 246.
38. Baker, J. O., William, S, A., Himmel, M. E., and Chen, M., in *Handbook of Size Exclusion Chromatography and Related Techniques*, 2nd Edition, Wu, C.-S. (editor), Marcel Dekker, New York (2004), p. 439.
39. Striegel, A. M., Yau, W. W., Kirkland, J. J., and Bly, D. D., *Modern Size-Exclusion Liquid Chromatography*, 2nd Edition, John Wiley & Sons, Hoboken, NJ (2009).

Chapter 4

Combination of SEC and Light Scattering

4.1 INTRODUCTION

Without separation by SEC, the light scattering measurements yield only the weight-average molar mass, the z-average RMS radius, and the second virial coefficient. Although these quantities provide valuable information about the polymer samples requiring characterization, the combination of light scattering with SEC separation brings both methods to a new qualitative level. There is an evident synergy effect of the two experimental techniques combining separation of molecules according to their hydrodynamic size with an immediate online characterization of their molecular structure. A light scattering detector connected online after the outlet from SEC columns measures molar mass from the intensity of light scattered by eluting molecules. The multi-angle light scattering (MALS) detector provides molecular size as another important piece of information that appears especially useful in relation with molar mass.[i] Since the RMS radius is determined from the angular variation of the scattered light intensity, a MALS-type light scattering detector is necessary for the determination of this quantity. In fact, the light scattering detector completely eliminates the necessity of column calibration and various SEC calibration methods may appear completely useless. However, knowledge of the calibration procedures and principles of universal calibration is necessary for understanding the basic principles of SEC itself. In addition, the universal calibration procedure can be reversed and used for the determination of some polymer characteristics such as constants of the Mark-Houwink equation or unperturbed dimensions.

The basic theory and instrumentation of light scattering are described in Chapter 2. In this chapter, the focus is on the light scattering instrument used as

[i]This chapter focuses on MALS detectors with at least three detection angles.

Light Scattering, Size Exclusion Chromatography and Asymmetric Flow Field Flow Fractionation: Powerful Tools for the Characterization of Polymers, Proteins and Nanoparticles, by Stepan Podzimek

an SEC detector and on aspects specific to the combination of light scattering and SEC. The principles that apply to the combination of light scattering with SEC are generally valid for the combination of light scattering with various techniques of flow field flow fractionation or other analytical separation techniques. The basic principles of light scattering and its combination with SEC were reviewed by Wyatt.[1,2] Despite the significant advancement in instrumentation since the date of publishing of reference 1, the paper is still a valuable source of information.

The Debye equation:

$$\frac{R_{\theta,i}}{K^* c_i} = M_i P_i(\theta) - 2A_{2,i} c_i M_i^2 P_i^2(\theta) \tag{4.1}$$

is the basis of the calculations performed in SEC-MALS. In the above equation $R_{\theta,i}$ is the excess Rayleigh ratio (cm^{-1}), c_i is the concentration of the macromolecules in mL/g, M_i is the molar mass, $A_{2,i}$ is the second virial coefficient, $P_i(\theta)$ is the particle scattering function that involves the RMS radius of scattering particles (Equation 2.12), and K^* is the optical constant including the solvent refractive index, the vacuum wavelength of the incident light, and the specific refractive index increment dn/dc (for K^* definition see Equation 2.3). The subscript i implies that the quantities are valid at the ith elution volume slice (for the sake of clarity, the subscript i is not further used). Similarly as in the case of conventional SEC the obtained chromatograms are processed at regular elution volume intervals (usually one-half, one, or two seconds). *Note:* Equation 4.1 has higher concentration terms that become significant at higher concentrations. However, these terms can be mostly safely ignored at the low concentrations that are in SEC columns.

4.2 DATA COLLECTION AND PROCESSING

For successful SEC-MALS measurements it is necessary to determine several parameters that allow proper processing of the acquired light scattering data and the calculation of correct molar masses and RMS radii. These are (1) calibration constant of the MALS photometer, (2) normalization coefficients of the MALS photometer, (3) calibration constant of the concentration detector (RI, UV), (4) volume delay between the MALS photometer and other detectors, and (5) correction for the band broadening. The meaning and the determination of the MALS and RI (UV) calibration constants and normalization coefficients are explained in Sections 2.2.1.3 and 2.6. Recall that the *MALS calibration constant* is used to transfer the voltages yielded by the photodiodes to the values of Rayleigh ratio, the *RI calibration constant* is used to calculate the absolute concentration in g/mL from the RI signal expressed in volts, and *normalization* is the process by which the various detectors' signals are related to the 90° detector signal and the MALS calibration constant. The calibration constants of MALS and RI detectors are independent of SEC mobile phase, whereas the change of mobile phase requires new normalization.

Volume delay between the MALS and other detectors consists of the volume of the tubings inside the detectors, volume of the cells, and volume of the interdetector connecting tubings and fittings. Only the volume of connecting tubings is partly under the control of the operator. Due to the volume between the detectors, the concentration, which is measured at a given time by a concentration-sensitive detector, does not match the intensity of light that is at the same time measured by the light scattering detector. The volume delay is used by the software to correct for the time that it takes fluid to transfer between the instruments so that a given light scattering intensity is matched with the appropriate concentration. Once the volume delay has been determined, there is no need to determine it again until the tubings between the instruments are changed for tubings of different length and/or inner diameter.

Note that the volume delay between UV and MALS is significantly lower than between MALS and RI. If the UV and RI detectors are used simultaneously, the sequence is UV-MALS-RI instead of MALS-UV-RI in order to minimize the delay between MALS and RI.

The delay volume is usually established by measurement of a monodisperse polymer and aligning the peaks obtained by MALS and concentration-sensitive detectors. Only in the case of monodisperse polymers the peak elution volumes of chromatograms recorded by the MALS and RI, and possibly UV and/or viscosity (VIS), detectors are identical. This is due to the different responses of various detectors to the molar mass and concentration. If the samples used to determine the volume delay are not monodisperse, the peaks will not be in alignment because the peak of a concentration detector will be at the maximum of polymer concentration, c, while the peak of a MALS detector will be at the maximum of the product of $M \times c$, and the peak of a VIS detector will correspond to the maximum of $M^a \times c$.

Proteins such as bovine serum albumin (BSA) can be used for the determination of volume delay in aqueous SEC. Polyethyleneoxide (PEO) can be alternatively used for SEC columns that retain proteins. Polydispersity of pullulan and dextran standards is usually higher than that of PEO, which results in overestimation of volume delay. Polystyrene standards are mostly used for determination of volume delay in THF and other organic solvents.

The most accurate results are obtained using a standard with molar mass approximately in the range of 200,000–400,000 g/mol. Standards with too-high molar mass are usually of higher polydispersity while low standards with molar mass in the range of several thousands can be partly separated by SEC columns and consequently the volume delay is overestimated. Standards with high molar mass can partly undergo shearing degradation, which further increases the polydispersity.

The effect of molar mass on volume delay determined by polystyrene standards is shown in Figure 4.1. The lower-molar-mass standard is separated by efficient columns and the volume difference between the RI and MALS peaks is given not only by the actual volume between the two detectors, but by the volume difference caused by standard polydispersity as well. The experience shows

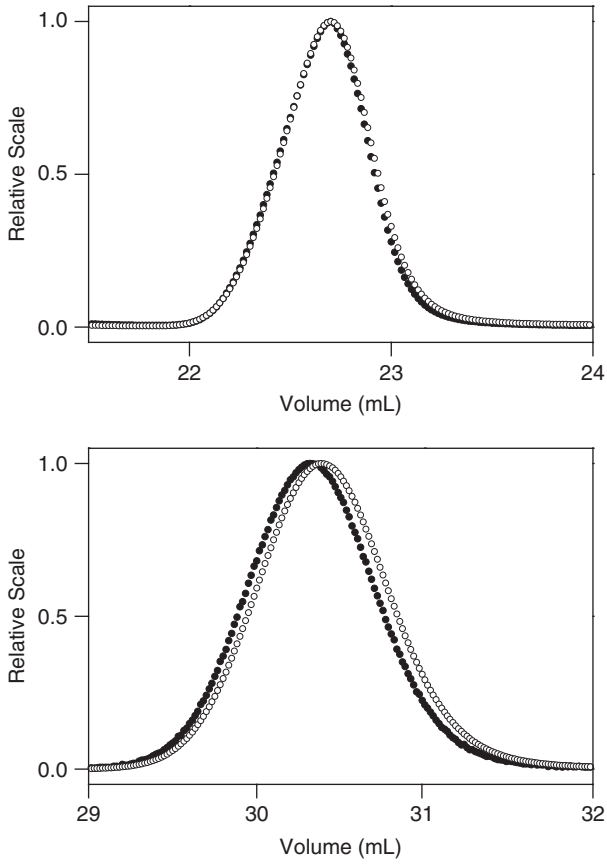

Figure 4.1 Determination of interdetector volume delay: effect of molar mass on the experimentally determined volume delay. MALS (•) and RI (○) signals of polystyrene standard with nominal molar mass of 200,000 g/mol (top) overlap while there is an additional volume difference of 0.067 mL for the peaks of 3,600 g/mol standard (bottom). Columns: 4 × PLgel Mixed-C 300 × 7.5 mm, THF at 1 mL/min. Volume delay determined by 200,000 g/mol standard = 0.217 mL, nominal $M_w/M_n = 1.05$ (3,600 g/mol standard), and 1.06 (200,000 g/mol standard). The signals are scaled to the same intensity.

that the difference in volume delays determined by 200,000 and 30,000 g/mol polystyrene standards is negligible even in the case of columns with very high resolution. For a monodisperse standard, the accurate volume delay should give an identical molar mass across the peak.

Band broadening in SEC-MALS means different phenomena than in conventional SEC. Band broadening in SEC-MALS terminology is a result of peak movement between the multiple detectors connected in series. When a peak moves along the flow path created by several detectors connected in series, each detector flow cell acts as a small mixing chamber that causes, together with axial broadening, the peak to broaden with a slight tail toward higher elution volumes. That means the peak recorded by the subsequent detector in series is broader compared with the peak recorded by the previous detector. Although peak broadening is present for all analyzed samples, it is particularly evident in the case of monodisperse samples for which the molar mass across the peak is constant. Due to peak broadening the molar mass across the peak of a monodisperse polymer is not flat, as one would expect, but has a "sad grimace" pattern.

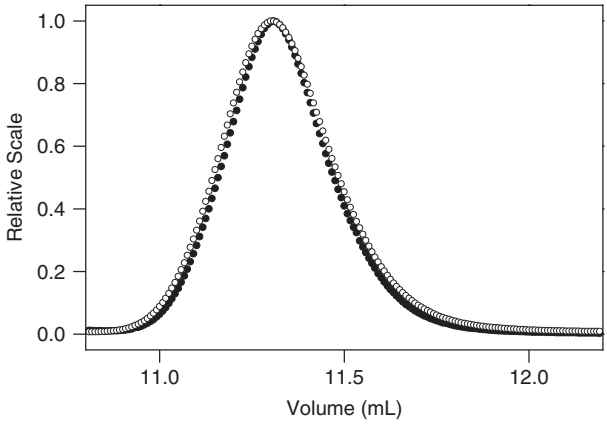

Figure 4.2 Interdetector peak broadening: signals of RI (○) detector and MALS photometer at 90° (●) for narrow polystyrene standard of nominal molar mass 200,000 g/mol. The signals are scaled to the same intensity. Columns: 2 × PLgel Mixed-C 300 × 7.5 mm columns, THF at 1 mL/min.

The peak of a monodisperse polymer recorded by the RI detector, which is always connected after the light scattering detector, is slightly broadened and tailed compared to the peak from the MALS detector, as shown in Figure 4.2. Consequently, the concentrations at particular elution volume slices do not correspond precisely to the light scattering intensities and the molar masses at the peak center are overestimated while those at the beginning and end of the peak are underestimated, which results in the "sad grimace" profile of the molar mass–versus–elution volume plot. The band-broadening effect is proportional to the interdetector volume delay and thus it is significantly less pronounced for the combination of UV-MALS as compared to the combination of MALS-RI. The peak-broadening effect is more severe for such applications where three detectors in series are used, especially in the case of combination MALS-VIS-RI. Although an average molar mass for the entire peak is usually not significantly affected, the band broadening represents at least a potential source of errors and it is also a certain "cosmetic" issue when the results for narrow or monodisperse polymers are presented. Correction for peak broadening has become a part of commercially available light scattering software ASTRA® (Wyatt Technology Corporation). To correct for the peak-broadening effect, the software expands the light scattering trace to fit the broadened RI chromatogram. The procedure may result in a slight loss of resolution, but mostly this effect is negligible. To compensate for peak broadening correctly, it is necessary to measure strictly monodisperse polymer. The requirement of monodispersity is entirely fulfilled only in the case of proteins. The measurement of narrow polymers such as polystyrene standards may result in a slight overcompensation of the broadening effect. To compensate for peak broadening by means of narrow, yet not completely monodisperse polymers, the molar mass should be roughly in the range of 200,000–400,000 g/mol.

Once the parameters for the correction of band broadening are determined utilizing a narrow polymer, they can be used for data processing of other samples. The effect of band broadening on the molar mass–versus–elution volume profile of narrow polymer standards is shown in Figure 4.3. Due to significantly lower volume delay between UV and MALS, the band-broadening effect is minimal compared with the molar mass–versus–elution volume profile obtained by the RI detector. Figure 4.3 also shows that the band-broadening effect can be eliminated by software correction. Although band broadening may have a strong effect on the molar mass–versus–elution volume plots of narrow and monodipsperse samples, the effect on the molar mass–versus–elution volume plots and distribution curves of polydisperse polymers is entirely imperceptible (Figure 4.4).

As a matter of fact, lower separation efficiency of SEC columns becomes a virtue when the determination of volume delay and/or peak-broadening correction is of interest. Since SEC resolution decreases with increasing molar mass, SEC is practically incapable of resolving slightly different molecules in a higher molar mass range. Due to the limited SEC resolution power, a narrow polymer standard of sufficiently high molar mass virtually behaves as monodisperse even if the polydispersity index is not exactly equal to unity. For this reason, a single short column (e.g., 150 × 7.5 mm) can be used to minimize the separation according to molecular size in order to increase the accuracy of the determination of the volume delay and band-broadening correction.

A typical example of chromatograms obtained by SEC-MALS analysis of a polydisperse polymer is shown in Figure 4.5, which depicts signals from the light scattering detector at 90° and the refractive index detector. Notice that the peaks given by the two detectors are of different elution volumes and shapes. As already explained, this is due to different sensitivity of particular detectors to molar mass and concentration. A typical feature of polydisperse polymers is that the peak of the MALS detector is always before the peak of the RI detector. The same elution volume of the two detectors occurs only for monodisperse or very narrow polymers; on the other hand, a large volume difference between the peaks of MALS and RI detectors is indicative of very high polydispersity. Note that the chromatograms in Figure 4.5 are scaled to the same relative intensity, but the true voltage outputs from the two detectors are not identical.

Different sensitivities of the MALS and RI detectors to molar mass and concentration is very evident from the chromatograms of narrow standards of different molar mass, as shown in Figure 4.6. Although the injected mass of 30,000 g/mol standard is double that of 200,000 g/mol standard, the signal of the MALS detector is significantly lower and only the RI detector provides true information about the concentration.

In Figures 4.5 and 4.6, only the MALS chromatogram from the 90° light scattering detector is shown. However, there are other chromatograms recorded by the MALS detector at various angles. The signals from all available light scattering detectors that are placed at different angular positions are shown in a three-dimensional plot in Figure 4.7. For molecules with RMS radius greater than about 10 nm, the light scattering signals at lower angles are greater than

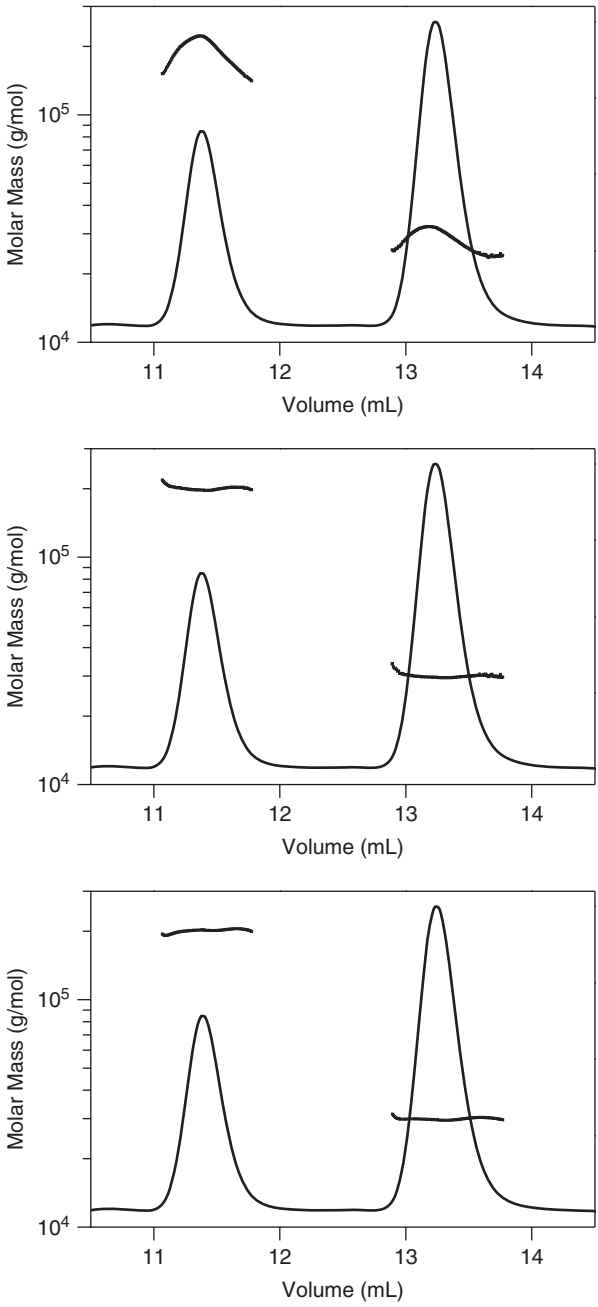

Figure 4.3 Molar mass–versus–elution volume plots for 200,000 and 30,000 g/mol polystyrene standards processed using as concentration detector RI detector (top), UV detector (center), and RI detector applying ASTRA® band-broadening correction (bottom). RI chromatogram is superimposed. M_w = 203,100 g/mol, 29,900 g/mol (top); 199,000 g/mol, 29,800 g/mol (center); 201,400 g/mol, 29,800 g/mol (bottom). Volume delays: UV to MALS = 0.017 mL, MALS to RI = 0.233 mL.

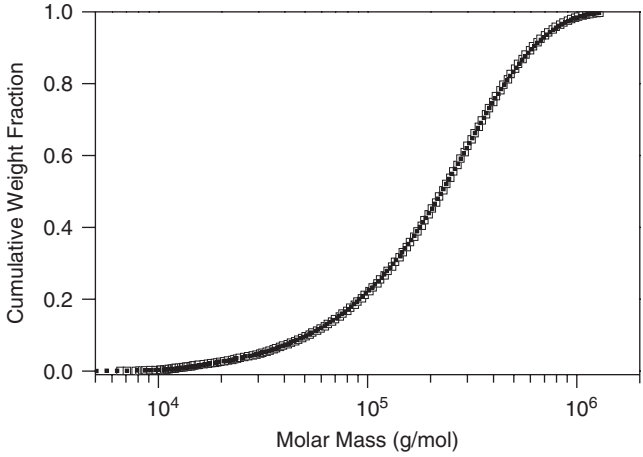

Figure 4.4 Cumulative distribution plots of a broad polymer obtained by SEC-MALS without (■) and with (□) band-broadening correction.

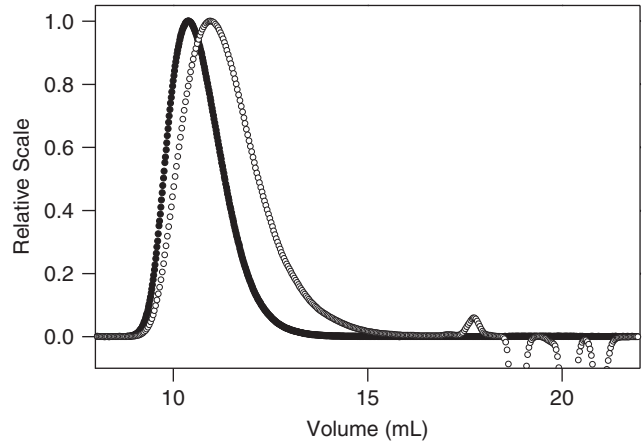

Figure 4.5 Chromatograms of polydisperse polystyrene recorded by MALS detector at 90° (•) and refractive index detector (○). Conditions: 2 × PLgel Mixed-C 300 × 7.5 columns, 100 μL 0.25% w/v, THF at 1 mL/min. The signals are scaled to the same intensity.

those at higher ones, and such angular dependence is more prominent at lower elution volumes, where the eluted molecules are larger. For small molecules with RMS radius below about 10 nm, the signals from all detectors have the same intensity and no information about the RMS radius can be obtained.

Molar mass and RMS radius of the polymer are calculated for each elution volume slice of the selected chromatographic peak by means of a so-called *Debye plot*, as depicted in Figure 4.8. The data points in the Debye plot correspond to

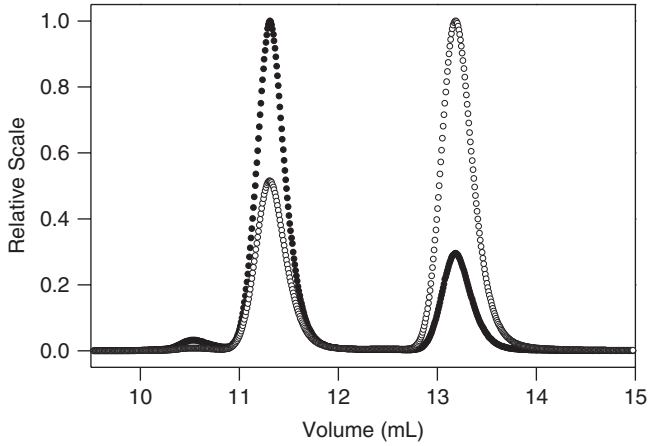

Figure 4.6 Superimposition of 90° MALS (•) and RI (○) signals of narrow polystyrene standards of nominal molar mass 200,000 g/mol and 30,000 g/mol. Conditions: 2 × PLgel Mixed-C 300 × 7.5 columns, THF at 1 mL/min injection 100 μL 0.15% w/v (200,000 polystyrene) and 0.3% w/v (30,000 polystyrene).

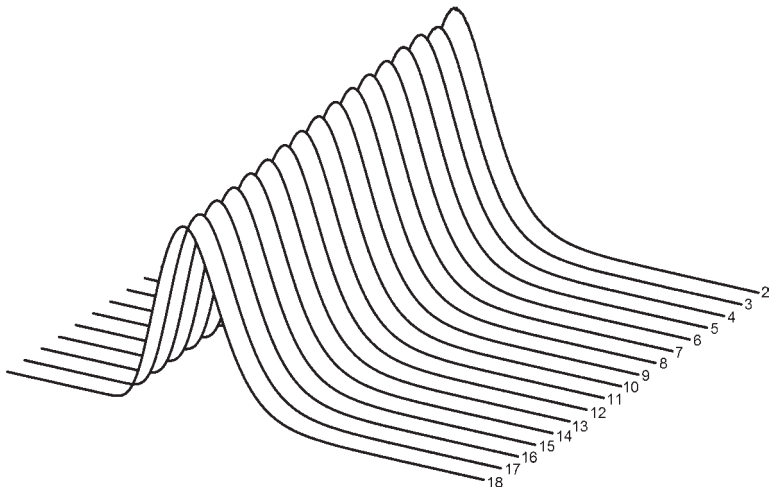

Figure 4.7 Three-dimensional view (rotation angle 30°, elevation angle 45°) of multiple MALS signals for polydisperse polystyrene: 17 scattering angles in the range of 17°–155°.

the light scattering intensities at various angles at a particular elution volume. A Debye plot, which is an arrangement of R_θ/K^*c plotted against $\sin^2(\theta/2)$, is used to extrapolate the light scattering intensities to zero scattering angle. There is no strict need to use all available data points of the MALS photometer, but some data points can be dropped and not included in the least-squares fit. Especially the lowest and partly also the highest angles are often affected by particles eluting

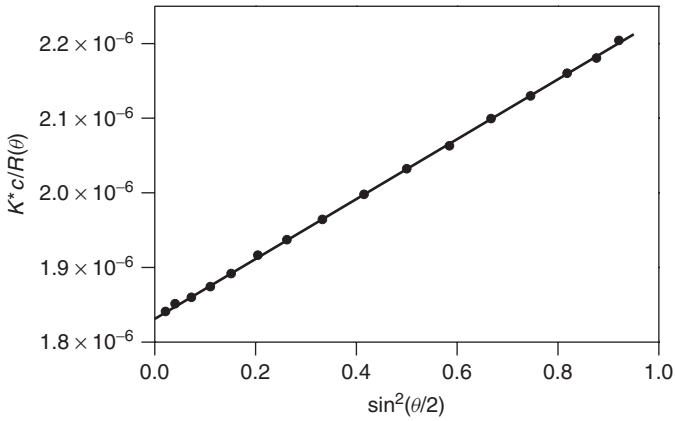

Figure 4.8 Debye plot (Zimm light scattering formalism) for one elution volume slice of Figure 4.7. $M = 546{,}000$ g/mol, $R = 31.7$ nm, $c = 5.6 \times 10^{-5}$ g/mL.

from SEC columns, incorrect normalization, or impurities in the flow cell of the MALS detector. In any event, the improper angular data points can be safely dropped without affecting the obtained results since the other data points are sufficient to derive results. This is especially true when the angular variation can be fitted by the first-order fit.

The decision whether to drop a particular angle from the calculation can be based on visual assessment of the fit and on the results uncertainty calculated by the software. A rule of thumb is that fewer data points with good fit yield more accurate results than more data points, where some of them are affected by impurities or other effects. The intercept and slope of the Debye plot at zero angle provide molar mass and RMS radius, respectively. Since the Debye plot is obtained at a single concentration, the second virial coefficient is not determined by SEC-MALS. *Note:* In principle it is possible to determine the A_2 by multiple SEC-MALS measurements by varying sample mass injections, which is supported by commercially available ASTRA® software (Wyatt Technology Corporation). However, the classical batch approach represents a more reliable way to A_2 and the SEC-MALS method of the determination of A_2 can be applied mainly for samples that are available in limited amounts. Another advantage of the online determination of A_2 is that the exact concentration of the analyzed solution need not be known, because the injected mass is determined from the signal of a concentration-sensitive detector. Variation of injected amount can be easily achieved by different injection volumes and thus a single solution can be used for the measurements. Note that for the online determination of A_2 an efficient SEC separation is not needed and the measurements can be performed using a single mixed-bed short SEC column (e.g., 150 × 7.5 mm).

Figure 4.9 plots molar mass across the peak of polydispere polymer together with corresponding RMS radius. An example of slice data is shown in Table 4.1.

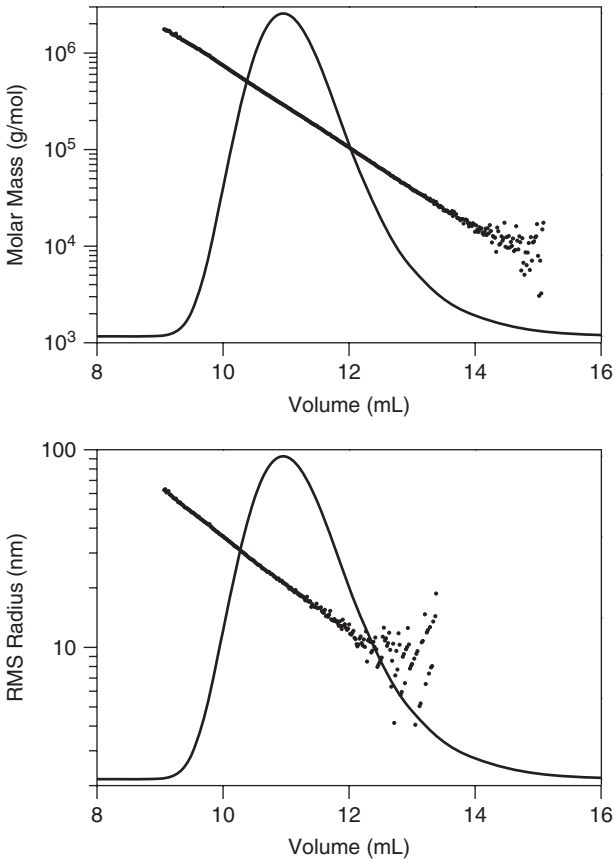

Figure 4.9 Molar mass (top) and RMS radius (bottom)–versus–elution volume plots of polydisperse polymer from Figure 4.5. RI chromatogram is superimposed in the plots.

Evenly decreasing molar mass and RMS radius across the entire chromatogram is indicative of good separation by pure size exclusion mechanism, whereas the molar mass or radius plots parallel with the elution volume axis or the rising of molar mass and radius with increasing volume indicate non–size exclusion separation, which can be due to some kind of enthalpic interactions of polymer molecules with the column packing or anchoring of branched molecules in the pores. The molar mass–versus–elution volume plot can also easily detect the presence of fractions with molar mass above the exclusion limit of the columns employed for the analysis or reveal poor column efficiency.

Figure 4.9 also demonstrates different detection limits of MALS for molar mass and RMS radius. The data points for the RMS radius become scattered as the radius approaches values of about 10 nm, but the molar mass, which is determined from the light scattering intensity, can be determined for smaller molecules. Although the SEC-MALS combined method does not require the

Table 4.1 Slice Data Obtained by SEC-MALS Analysis of Polydisperse Polymer Corresponding to Figure 4.9

Volume (mL)	M (g/mol)	R (nm)	c (g/mL)
9.050	1.875E+06	62.5	2.47E−07
9.067	1.845E+06	62.0	2.87E−07
9.083	1.815E+06	61.4	3.33E−07
9.100	1.786E+06	60.8	3.92E−07
9.117	1.757E+06	60.2	4.50E−07
9.133	1.729E+06	59.6	5.23E−07
9.150	1.701E+06	59.1	6.01E−07
9.167	1.673E+06	58.5	6.96E−07
9.183	1.646E+06	58.0	8.01E−07
9.200	1.619E+06	57.4	9.18E−07
9.217	1.593E+06	56.9	1.05E−06
9.233	1.568E+06	56.3	1.20E−06
9.250	1.542E+06	55.8	1.36E−06
9.267	1.517E+06	55.3	1.55E−06
9.283	1.493E+06	54.7	1.76E−06
9.300	1.469E+06	54.2	1.97E−06
9.317	1.445E+06	53.7	2.21E−06
9.333	1.421E+06	53.2	2.49E−06
9.350	1.398E+06	52.7	2.80E−06
9.367	1.376E+06	52.2	3.13E−06
...	...	...	...
10.867	3.173E+05	22.2	9.31E−05
10.883	3.122E+05	22.0	9.33E−05
10.900	3.072E+05	21.7	9.34E−05
10.917	3.022E+05	21.5	9.35E−05
10.933	2.973E+05	21.3	9.36E−05
10.950	2.925E+05	21.1	9.36E−05
10.967	2.878E+05	20.9	9.36E−05
10.983	2.831E+05	20.7	9.35E−05
11.000	2.786E+05	20.5	9.35E−05
11.017	2.740E+05	20.3	9.34E−05
11.033	2.696E+05	20.1	9.33E−05
11.050	2.653E+05	20.0	9.31E−05
11.067	2.610E+05	19.8	9.29E−05
11.083	2.568E+05	19.6	9.27E−05
11.100	2.526E+05	19.4	9.25E−05
11.117	2.485E+05	19.2	9.22E−05
11.133	2.445E+05	19.0	9.19E−05
11.150	2.405E+05	18.8	9.16E−05
11.167	2.367E+05	18.7	9.13E−05
11.183	2.328E+05	18.5	9.09E−05
...	...	...	...

determination of the calibration curve as in the case of conventional SEC, the calibration curve can be easily established from the acquired data and used as an additional source of information about the analyzed polymer and its SEC elution behavior. It is worth mentioning that the molar mass–versus–elution volume plot can be used for the characterization of separation efficiency on the basis of the slope of the molar mass–versus–elution volume plot.

4.2.1 Processing MALS Data

The light scattering intensity at zero angle is needed to obtain molar mass by light scattering measurements. However, the scattered intensity at zero scattering angle is not experimentally measurable. One possible solution of this problem is to measure at a very low angle by so-called low-angle light scattering, which assumes the scattering intensity at a low angle to be equal to that at zero angle. The disadvantage of the low-angle approach is that measurements at very low angles suffer from high noise generated by dust particles and other mechanical impurities in the mobile phase. Because of very high mass, the scattering intensity of dust particles is many times higher than that of significantly less dense random coils of comparable size. The effect of disturbing particles decreases with increasing angle of observation, the decrease being much steeper for compact spheres compared to random coils (compare Figures 2.7 and 2.8). In consequence, dust particles disturb light scattering signals even at trace concentrations, which is particularly true at low angles. To avoid the disturbing effect of particles in the mobile phase, the measurement is performed at multiple angles far from zero degree and the zero intensity is estimated by the extrapolation of data points from higher angles. The multi-angle approach efficiently solves the problem with noise and in addition allows the determination of the RMS radius, which can be obtained from the angular dependence close to zero angle.

Molar mass and RMS radius can be also obtained by fitting the light scattering intensities to a given particle scattering function, but a particular disadvantage of this approach is that it requires a priori knowledge of the polymer conformation (i.e., whether the molecules under investigation are random coils or another shape). In fact, this is not a serious limitation for most synthetic and natural polymers, because they generally create random coils. One possible disadvantage of the multi-angle approach is that different extrapolation methods may lead to different results, which means that careful selection and optimization of the extrapolation method is an important part of processing the experimental data.

To determine molar mass and RMS radius the experimental data can be processed in various ways that are described Sections 4.2.1.1–4.2.1.4. Note that the primary experimental results are always identical (i.e., the angular variations of light scattering intensities and concentrations collected at regular elution volume intervals across the chromatographic peak), and only the method of subsequent processing is different.

4.2.1.1 Debye Fit Method

To obtain the molar mass and the RMS radius, a Debye plot, that is, a plot of R_θ/K^*c versus $\sin^2(\theta/2)$, is constructed, and the obtained plot is fitted by a polynomial to get the intercept at zero angle R_0/K^*c and the slope at zero angle $m_0 = d(R_\theta/K^*c)/d(\sin^2(\theta/2))_{\theta\to 0}$. At angle approaching zero, the particle scattering function approaches unity and the equation becomes

$$\frac{R_{\theta\to 0}}{K^*c} = \frac{R_0}{K^*c} = M - 2A_2cM^2 \tag{4.2}$$

$$M = \frac{2\left(1 - \sqrt{1 - 8A_2c\left(\frac{R_0}{K^*c}\right)}\right)}{8A_2c} \tag{4.3}$$

or an equivalent form to avoid errors when $A_2 \to 0$:

$$M = \frac{2\left(\frac{R_0}{K^*c}\right)}{1 + \sqrt{1 - 8A_2c\left(\frac{R_0}{K^*c}\right)}} \tag{4.4}$$

and if $A_2 = 0$, then

$$M = \frac{R_0}{K^*c} \tag{4.5}$$

The mean square radius is calculated according to the equation:

$$R^2 = \frac{-3m_0\lambda^2}{16\pi^2 M(1 - 4A_2Mc)} \tag{4.6}$$

and for $A_2 = 0$:

$$R^2 = \frac{-3m_0\lambda^2}{16\pi^2 M} \tag{4.7}$$

4.2.1.2 Zimm Fit Method

The calculation according to the Zimm formalism, which is K^*c/R_θ versus $\sin^2(\theta/2)$, leads to:

$$M = \left(\frac{K^*c}{R_0} - 2A_2c\right)^{-1} \tag{4.8}$$

and

$$R^2 = \frac{3m_0\lambda^2 M}{16\pi^2} \tag{4.9}$$

where m_0 is the slope of the polynomial at angles approaching zero, $m_0 = d(K^*c/R_\theta)/d(\sin^2(\theta/2))_{\theta\to 0}$. For negligible A_2, Equation 4.8 gives molar mass as reciprocal intercept $\left(\frac{K^*c}{R_0}\right)^{-1}$.

4.2.1.3 Berry Fit Method

The molar mass and RMS radius are calculated using the Berry light scattering method, that is, a plot of $\sqrt{K^*c/R_\theta}$ versus $\sin^2(\theta/2)$, from the following equations:

$$M = \frac{4}{(\sqrt{K^*c/R_0} + \sqrt{K^*c/R_0 - 4A_2c})^2} \tag{4.10}$$

for $A_2 = 0$:

$$M = \frac{1}{(\sqrt{K^*c/R_0})^2} \tag{4.11}$$

and

$$R^2 = \frac{3\lambda^2 m_0}{8\pi^2\sqrt{M}(1/M - A_2c)} \tag{4.12}$$

for $A_2 = 0$:

$$R^2 = \frac{3\lambda^2 m_0}{8\pi^2 1/\sqrt{M}} \tag{4.13}$$

where $m_0 = d(\sqrt{K^*c/R_\theta})/d(\sin^2(\theta/2))_{\theta\to 0}$.

Note that all three methods of constructing the Debye plot differ in the quantity used on the ordinate, but the abscissa is always the same—$\sin^2(\theta/2)$. Depending on the applied method, the Debye plot appears differently and may yield different values of M and R, although it is constructed from the same data.

Note that the error of dn/dc changes both the slope and the intercept of the Debye plot, which affects the molar mass, but the RMS radius remains unchanged, because m_0 and M in Equations 4.7, 4.9 and 4.13 mutually compensate (see Figure 2.22).

4.2.1.4 Random Coil Fit Method

The random coil fit method does not fit angular variation of scattered light intensity as do the previous methods. Instead, it uses the theoretical particle scattering function for random coils (Equation 2.22), and an iterative nonlinear least-squares fit. In contrast to the previous methods, the random coil fit method assumes that the analyzed molecules are random coils. This assumption is fulfilled for most synthetic and natural polymers and thus the random coil fit method represents a suitable alternative to other methods.

4.2.1.5 Influence of Light Scattering Formalism on Molar Mass and RMS Radius

The particular light scattering formalisms for constructing the Debye plot were investigated for two different polymer shapes (homogeneous spheres and random

coils) with radii from 25 to 250 nm in reference 3. The essential conclusions obtained in reference 3 by model calculations are as follows:

1. Extrapolation to zero angle requires only the lowest angles and the data points at higher angles do not contribute significantly to the results. For a given polynomial degree more accurate results are obtained using only low angles for the extrapolation. If higher angles are used, it is necessary to use a higher-order polynomial to reach the same accuracy as for the low angles. Use of all angles is meaningful only when the experimental light scattering data are fitted to a theoretically derived particle scattering function.
2. For random coils the Berry method is superior in terms of accuracy and robustness, whereas for spheres the Debye method is superior. The Berry method should be preferred especially for large random coils. The model calculation suggested that a linear fit according to the Berry using the lowest reliable angular data is the most general procedure.
3. For molar mass determination, the extrapolation error is below 1% for all three methods in the case of small molecules (RMS radius <50 nm). With increasing size, the particular plots become more curved, which requires higher-order polynomials to fit the light scattering intensities. For large random coils ($\approx$250 nm), the error in molar mass is $<5\%$ for the Berry and Zimm method using the third- and fourth-order fit, but a fifth-order polynomial is required for the Debye method. The relative errors in RMS radius follow the same trend as for molar mass but are larger.

The above conclusions were brought about mainly by theoretical calculations. The experimental investigations published in reference 4 lead to the following conclusions:

1. The Debye fit method requires a strongly increasing polynomial degree with increasing molecular size.
2. The Zimm plot is linear up to very high molar masses, but compared to other methods it slightly overestimates molar masses and more considerably RMS radii of large molecules.
3. The Berry method is linear over a broad molar mass range.
4. The random coil method gives results quite comparable to the other methods and appears to work well even for highly compact branched molecules.

To explain the differences between particular extrapolation methods and help users make the most appropriate choice of methods in a particular situation, the data obtained for polystyrene of various molar masses are shown in Figures 4.10–4.14 and the corresponding molar masses and RMS radii are compared in Table 4.2. The plots were obtained at different elution volumes of a broad polystyrene sample or at peaks of narrow polystyrene standards. Polystyrene is well known to create random coil conformation in THF and thus the random coil

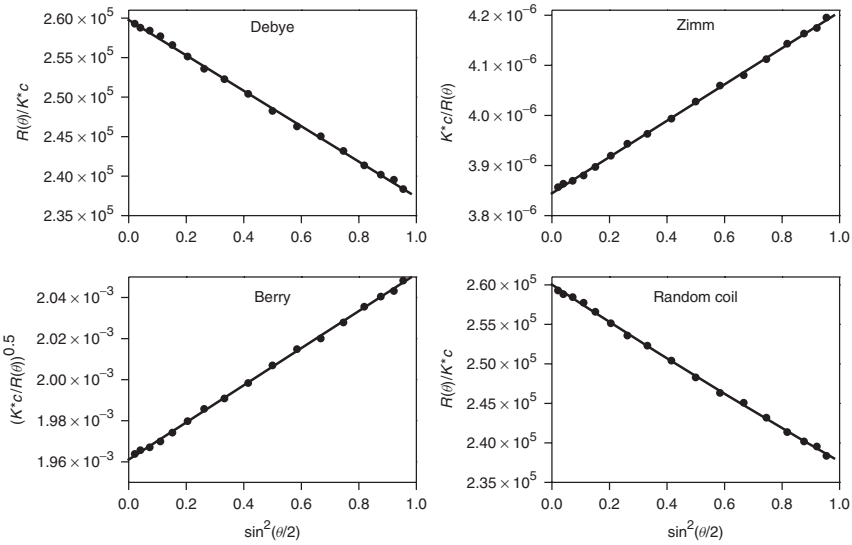

Figure 4.10 Debye plots for ≈20-nm slice of broad polystyrene using various extrapolation methods.

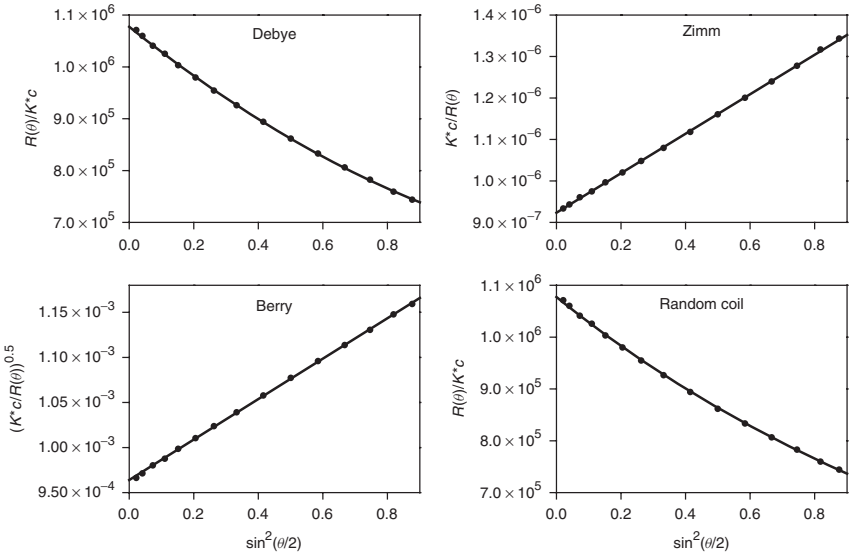

Figure 4.11 Debye plots for ≈46-nm slice of broad polystyrene using various extrapolation methods. Second-order polynomial for Debye method; first-order fits for Zimm and Berry methods.

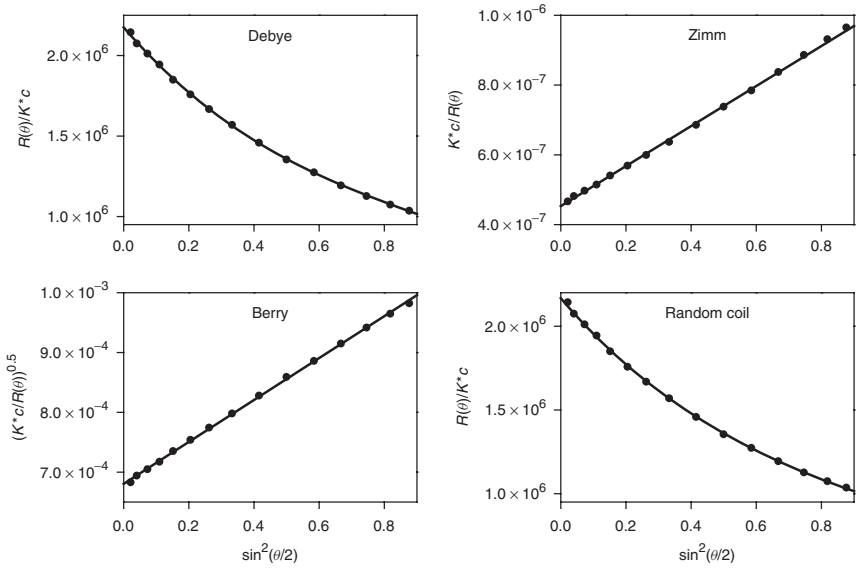

Figure 4.12 Debye plots for ≈70-nm slice of broad polystyrene using various extrapolation methods. Third-order polynomial for Debye method; first-order fits for Zimm and Berry methods.

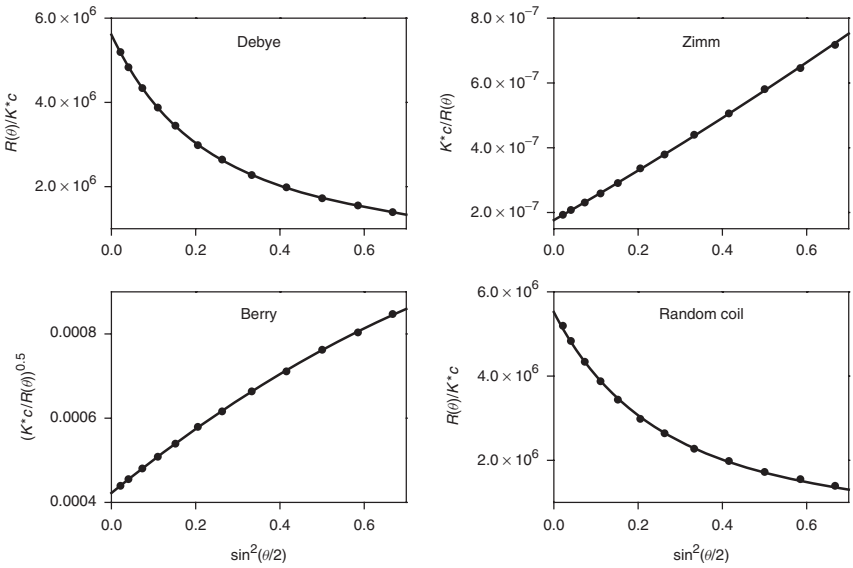

Figure 4.13 Debye plots for ≈130-nm slice of narrow polystyrene standard using various extrapolation methods. Fifth-order polynomial for Debye method; second-order fits for Zimm and Berry methods.

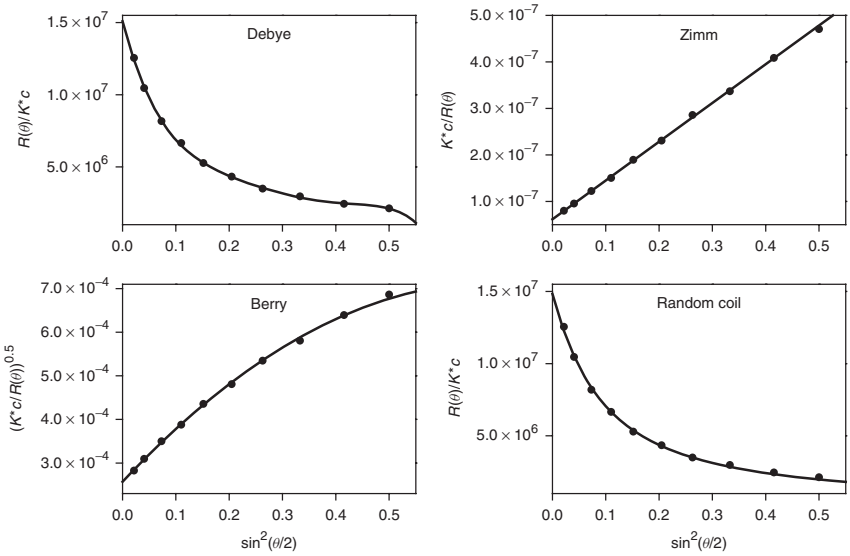

Figure 4.14 Debye plots for ≈200-nm slice of narrow polystyrene standard using various extrapolation methods. Fifth-order polynomial for Debye method; second-order fit for Berry method; first-order fit for Zimm method.

method should theoretically provide the most accurate results (assuming validity of particle scattering function outside theta temperature).

The first example (Figure 4.10) is the case where all methods work equally well and yield almost-identical molar mass and RMS radius. All available light scattering data points are used and no curvature is present in either plot. All results are associated with very low uncertainty based on the statistical consistency of the data.

The second example is for a slice with a higher molar mass, about 1 million g/mol, and RMS radius around 46 nm (Figure 4.11). In this case, the Debye method requires a second-order polynomial while the Zimm and Berry methods are still linear. All methods provide almost-identical molar masses, but the RMS radius determined by Zimm extrapolation is slightly higher than the values obtained by other methods.

This is even more evident for larger random coils of the RMS radius of about 70 nm (Figure 4.12), where Debye extrapolation needs a third-order polynomial and the overestimation of the RMS radius by the Zimm method compared to the random coil method is almost 10%. However, the agreement of molar masses is still very good for all methods. The curvature of the Debye plot further increases with increasing molecular size and a fifth-order polynomial becomes necessary for very high molecular sizes over about 100 nm (Figure 4.13 and 4.14). A second-order fit is usually needed for processing the light scattering data of such large molecules with the Berry and Zimm methods,

Table 4.2 Molar Masses and RMS Radii Corresponding to Figures 4.10–4.14 Determined Using Various Light Scattering Formalisms

	M (10^3 g/mol)				R (nm)			
Figure	Debye	Zimm	Berry	Random	Debye	Zimm	Berry	Random
4.10	259.8 ± 0.1	260.1 ± 0.1	260.0 ± 0.1	260.0 ± 0.1	19.9 ± 0.1	20.8 ± 0.1	20.6 ± 0.1	20.6 ± 0.1
4.11	1078 ± 1	1083 ± 1	1076 ± 1	1077 ± 1	46.3 ± 0.3	48.7 ± 0.1	46.3 ± 0.1	46.5 ± 0.1
4.12	2174 ± 6	2208 ± 8	2158 ± 6	2167 ± 23	70.4 ± 0.9	76.4 ± 0.3	68.9 ± 0.3	69.9 ± 0.2
4.13	5739 ± 26	5807 ± 24	5745 ± 15	5646 ± 44	133 ± 2	141 ± 1	135 ± 1	128 ± 1
4.14	$15{,}090 \pm 330$	$16{,}200 \pm 130$	$15{,}160 \pm 200$	$14{,}830 \pm 390$	208 ± 9	249 ± 1	216 ± 2	207 ± 3

but the Zimm method can still be approximated by a linear fit if the light scattering intensities acquired at high angles are dropped.

Overestimation of the RMS radii of very large molecules by the Zimm method can reach about 20%, but significantly lower error is obtained for molar mass. It is necessary to emphasize that the molecular size, not molar mass, is the relevant parameter for the curvature of the fit as illustrated in Figure 4.15 for highly compact star-branched molecules. The Debye plot is perfectly linear despite high molar mass of the analyzed molecules, which are, however, small due to the high degree of branching. The obtained results suggest that good fit of the experimental light scattering intensities can be obtained with the random coil method, which actually works well not only for linear random coils, but for highly branched molecules as well (Figure 4.16).

For processing the data of polydisperse polymers it is necessary to select the method that will be appropriate for the entire molar mass range, because the light scattering software may not allow for using different processing methods or polynomial orders for various parts of the chromatogram. In fact, this would be a simple modification of the software, but changing the extrapolation method or fit order would result in irregularities on the distribution plots. The Debye method appears the least suitable for polymers covering a broad molar mass range, because the first-order fit will not be suitable for the high molar masses, while the higher-order fits may be too high for lower molar masses.

The angular dependence of the scattering intensity can become even more complicated when smaller molecules co-elute with significantly larger molecules or even supermolecular structures. Such a situation can happen at the beginning of a chromatogram if the analyzed sample contains molecules exceeding the exclusion limit of the applied columns. In such a case the large molecules are pushed forward and mixed with smaller molecules. Another possibility is when slices at higher elution volumes are contaminated by large molecules that

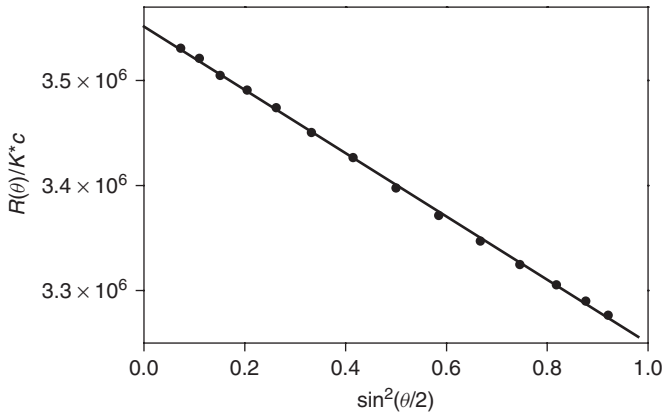

Figure 4.15 Debye plot for highly branched molecules. The plot shows no curvature despite high molar mass of 3.55 $\times 10^6$ g/mol. RMS radius = 19.8 nm.

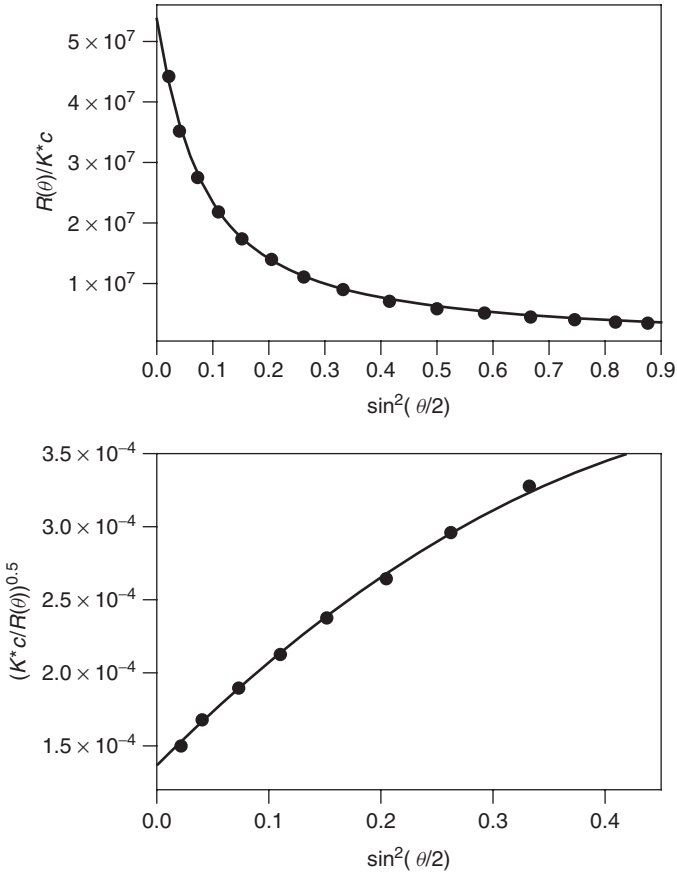

Figure 4.16 Debye plots for a slice of randomly branched polystyrene obtained by random coil (top) and Berry (bottom) formalisms: $M = 5.37 \times 10^7$ g/mol, $R = 222$ nm and $M = 5.42 \times 10^7$ $g/$ mol, $R = 228$ nm, respectively. Branching ratio $g = 0.23$.

are delayed by enthalpic interactions or, in the case of branched molecules, by anchoring in the pores of column packing. In FFF, the co-elution of small and large species can occur at the end of a fractogram when the field is switched off before complete sample elution, or due to steric separation of large species.

As shown in Figure 2.9, even a trace amount by mass of species with molar mass and size much larger than those of other molecules strongly affects the shape of the angular variation of the scattered light intensity. Investigation of the Debye plots along the elution volume axis may bring information about the separation process, as illustrated in Figure 4.17 for a sample of highly branched polystyrene. As explained in Section 6.2.1, the slices at high elution volumes consist of major parts of smaller molecules separated by steric exclusion that are contaminated by small amounts of large branched molecules.

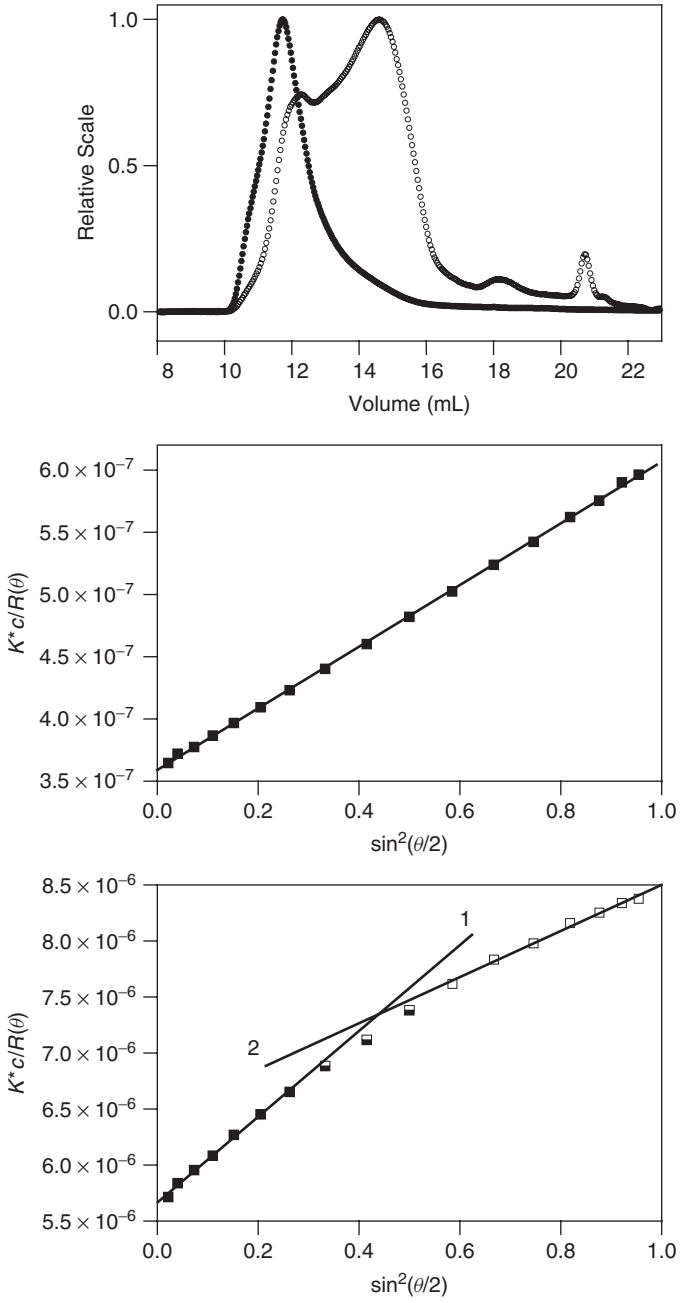

Figure 4.17 MALS (•) and RI (○) chromatograms (top) of randomly branched PS and Debye plots (Zimm formalism) taken at elution volumes of 11.7 mL (center) corresponding to $M \approx 2.8 \times 10^6$ g/mol and 14.4 mL (bottom) corresponding to $M \approx 1.8 \times 10^5$ g/mol. Lines 1 and 2 are linear fits for points (■) and (□), respectively.

Figure 4.17 shows two Debye plots obtained at two different elution volumes. A linear Debye plot at the region of lower elution volumes corresponds to the narrow fractions eluting from the column. Since the Debye plot at a higher elution volume gives a molar mass of about 180,000 g/mol, one would expect a straight plot. However, a more complicated Debye plot with two different slopes strongly resembles the plot shown in Figure 2.9, which indicates presence of a mixture of molecules of markedly different sizes. In fact the data presented in Figure 4.17 provide additional evidence about the correctness of the idea of the co-elution of smaller molecules separated by steric exclusion and large branched molecules delayed by anchoring effect.

The plot of K^*c/R_θ can also exhibit a curvature from branching. Burchard showed[5] that branching causes in Zimm plots an upturn of the angular distribution. Polydispersity reduces this upturn and in randomly branched polymers the upturn is balanced by the large polydispersity. However, in SEC-MALS the angular variation is measured for almost monodisperse polymer molecules eluting from SEC columns. The upturn in the Zimm plot is shown in Figure 4.18, where the slice from the beginning of the chromatogram of branched polystyrene (Figure 4.17) is contrasted with a slice from narrow polystyrene standard of about the same molar mass. A strong deviation from linearity suggests elution of highly branched molecules at the beginning of the chromatogram.

The following conclusions can be summarized based on the literature and experimental results shown here:

1. For small molecules (RMS radius around 20 nm), all extrapolation methods require linear fit and yield results identical with those obtained by the random coil method.
2. For medium-size molecules (up to about 70 nm), the Zimm and Berry methods are linear, whereas the Debye fit method requires a higher-order fit. The first-order Zimm extrapolation overestimates the RMS radius and the overestimation increases with increasing molecular size.
3. For molecules with RMS radius >100 nm, the Debye method typically requires a fifth-order polynomial. The Zimm and Berry methods can be fitted by the second-order polynomial and even the first-order fit may be sufficient if only lower angles are used.
4. Choice of extrapolation method has usually negligible effect on the molar mass, but it is more significant in the case of the determination of the RMS radius. The Zimm method is typically not a good choice for the determination of the conformation plot, because it often overestimates the slope, which can lead to false conclusions concerning the structure of polymer chain, because a slight decrease of the slope due to branching can be balanced by the overestimation of the slope by Zimm formalism.
5. The random coil method works well also for branched molecules with a high degree of branching.

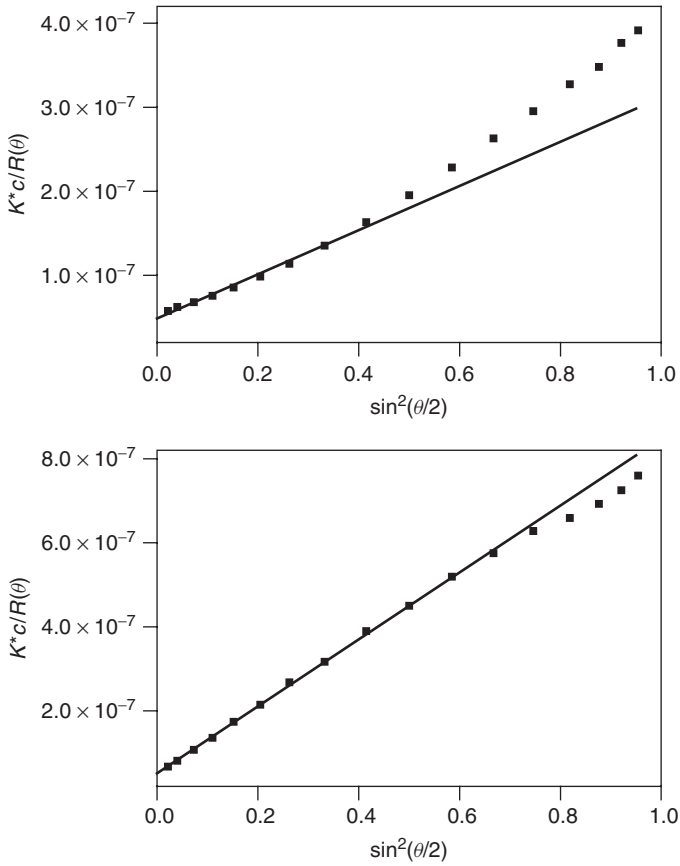

Figure 4.18 Debye plots (Zimm formalism) for a slice from the beginning of the chromatogram shown in Figure 4.17 (elution volume of 10.4 mL) (top) and for a slice of narrow polystyrene standard (bottom). $M \approx 2 \times 10^7$ g/mol for both plots. An upturn on the Zimm plot indicates a high degree of branching of molecules eluting at the beginning of the chromatogram.

6. In the case of large molecules of RMS radius around 100 nm and more, processing the light scattering data should be always based on carefully and critically evaluated Debye plots.
7. Zero-order fit, that is, line parallel with $\sin^2(\theta/2)$ axis, can be used for small polymers with negligible angular variation of scattered light intensity. The zero-order fit calculates an average intensity measured at particular angles.
8. The Berry fit method appears to be the most universal extrapolation method for polymers of various conformation over a broad molar mass range.

4.2.2 Determination of Molar Mass and RMS Radius Averages and Distributions

Regardless of the light scattering formalisms used for data processing, the SEC-MALS measurement yields for each slice of elution volume V_i the molar mass M_i and the mean square radius R_i^2. In fact, the molar mass is the weight-average and the mean square radius is the z-average, but the primary assumption for all SEC-MALS calculations is that the polydispersity within the elution volume slice can be neglected, and that both quantities are just molar mass M_i and the mean square radius R_i^2. Although efficient SEC separation is crucial for the determination of molar mass and RMS radius distributions and moments, it must be emphasized that even if SEC resolution is poor (for whatever reason), the M_w and R_z are always correct, because they are measured by the fundamental principle of light scattering independently of separation performance. On the other hand, the averages M_n, M_z, R_n, and R_w are correct only if the volume slices are truly monodisperse. Consequently, SEC-MALS has a tendency to overestimate M_n and underestimate M_z values.

Using the slice values of molar mass and mean square radius together with the concentrations determined by a concentration-sensitive detector, it is possible to calculate the molar mass and RMS radius moments according to the following equations:

Number-average molar mass:

$$M_n = \frac{\sum c_i}{\sum \frac{c_i}{M_i}} \tag{4.14}$$

Weight-average molar mass:

$$M_w = \frac{\sum c_i M_i}{\sum c_i} \tag{4.15}$$

Z-average molar mass:

$$M_z = \frac{\sum c_i M_i^2}{\sum c_i M_i} \tag{4.16}$$

Number-average mean square radius:

$$R_n^2 = \frac{\sum \frac{c_i}{M_i} R_i^2}{\sum \frac{c_i}{M_i}} \tag{4.17}$$

Weight-average mean square radius:

$$R_w^2 = \frac{\sum c_i R_i^2}{\sum c_i} \tag{4.18}$$

Z-average mean square radius:

$$R_z^2 = \frac{\sum c_i M_i R_i^2}{\sum c_i M_i} \tag{4.19}$$

The quantities M_i, R_i^2, and c_i in the above equations are the molar mass, the mean square radius, and the concentration, respectively, and the subscript i indicates the ith elution volume slice. All sums are typically taken over one chromatographic peak. The RMS radius moments are obtained as the square roots of the appropriate mean square radii. The SEC-MALS measurement yields the weight-average molar mass and the z-average RMS radius, which are obtainable by a batch light scattering experiment. That means the values of M_w and R_z from the SEC-MALS experiment should equal those determined in batch mode. This is typically well fulfilled as demonstrated in Table 4.3. A discrepancy in SEC-MALS and batch MALS results indicates problems with chromatography, such as shearing degradation of molecules with ultra-high molar mass or adsorption of part of the analyzed sample in the columns.

Note that the molar mass averages in Equations 4.14–4.16 are true molar mass moments (i.e., higher powers of M_i are used in the successive moments). On the other hand, the RMS radius moments in Equations 4.17–4.19 are different, because they use the same power of R_i^2. That means the radius averages are not true moments of the radius distribution. For example, the true z-average mean square radius is defined as:

$$R_z^2 = \frac{\sum \frac{c_i}{M_i} (R_i^2)^3}{\sum \frac{c_i}{M_i} (R_i^2)^2} \tag{4.20}$$

Table 4.3 Weight-Average Molar Masses and z-Average RMS Radii Determined by Batch and SEC-MALS

	M_w (10^3 g/mol)		R_z (nm)	
Sample	Batch MALS	SEC-MALS	Batch MALS	SEC-MALS
PS (A)	344 ± 8	326 ± 4	34.4 ± 0.6	36.2 ± 0.8
PS (AN)	303 ± 1	294 ± 3	29.5 ± 0.1	30.1 ± 0.1
PS (NIST 706)	288 ± 2	285 ± 3	27.9 ± 0.2	28.4 ± 0.2
PS (1)	386 ± 1	370 ± 2	40.3 ± 0.4	42.7 ± 0.4
PS (2)	398 ± 6	375 ± 1	39.5 ± 0.4	43.3 ± 0.4
PS (K)	239 ± 3	238 ± 1	27.2 ± 1.0	27.9 ± 0.6
PS (S)	236 ± 1	225 ± 1	27.3 ± 0.4	27.2 ± 0.8
PMMA (J)	96 ± 1	89 ± 1	13 ± 1	13 ± 2
PMMA (Y)	604 ± 10	558 ± 7	41.3 ± 0.5	44.3 ± 0.1
EP (1)	3.5 ± 0.1	3.4 ± 0.1	—	—
EP (2)	8.3 ± 0.1	8.1 ± 0.1	—	—

Note: Results uncertainty is based on repeated experiments and/or uncertainty calculated by ASTRA software.

where c_i/M_i is the molar amount n_i of molecules having the mean square radius R_i^2. A similar equation can be written for the average R_w that would be the true moment of radius distribution. However, the average RMS radius that is obtained by the batch light scattering measurement of a polydisperse polymer is that defined by Equation 4.19 and not by Equation 4.20 (compare Equation 2.20). Although the SEC-MALS experiment permits calculation of true R_z, the calculation according to Equation 4.19 provides a result that is consistent with the batch measurement.

The physical meaning of the mean square radius defined by Equation 4.19 is that it is the mean square radius of molecules having the z-average molar mass as evident from the following: For a random coil polymer in theta conditions, the mean square radius is proportional to the molar mass ($R^2 = A \times M$). For a polydisperse random coil polymer, the mean square radius of each species is proportional to the molar mass of that species. That means that using Equation 4.19 one gets:

$$R_z^2 = \frac{\sum c_i A M_i^2}{\sum c_i M_i} = A \times M_z \tag{4.21}$$

where A is the proportionality constant. Equations 4.17 and 4.18 are equivalent and yield the RMS radii corresponding to the number- and weight-average molar masses, respectively. The values of R_n and R_w permit comparison of RMS radius averages with the same types of molar mass averages, but their applicability for polymer characterization appears rather limited. In addition, the accuracy of R_n is often affected by the presence of small molecules for which the RMS radius cannot be directly determined and can be only estimated by the extrapolation procedure, as will be shown later.

Besides molar mass and RMS radius moments, the SEC-MALS data allow for the determination of differential and cumulative distributions using a similar procedure as in the case of conventional SEC. In contrast to conventional SEC, the combination of SEC-MALS also allows the determination of the distribution of RMS radius and relation between the RMS radius and molar mass. The latter relation is often called a *conformation plot*,[i] because it can provide information about the conformation and architecture of polymer chains. The values of the slopes of the conformation plots for linear random coils in theta solvents, rods, and compact spheres are 0.5, 1.0, and 0.33, respectively. Due to the expansion of polymer chains in thermodynamically good solvents, the slopes of the conformation plots of linear random coils are typically 0.58–0.60, and larger values indicate expansion of polymer chain due to chain rigidity or repulsive electrostatic forces. On the other hand, the decrease of the slope to lower values indicates a more compact molecular structure, usually due to the presence of branched

[i]The term *conformation* is related to the spatial arrangement of a polymer chain that results from the rotation of its segments about single bonds. However, the relation RMS radius versus molar mass (conformation plot) is typically used with respect to linearity or branching. That means the term *conformation* is often incorrectly associated with polymer branching.

macromolecules. The assumption of monodisperse slices is even more serious in the case of a conformation plot than in the case of molar mass distribution, because the z-average RMS radius is more sensitive to polydispersity than the weight-average molar mass. That means that if the conformation plot of a linear polymer in a thermodynamically good solvent is perfectly linear with the slope around the value of 0.58, the separation performance of SEC columns can be considered appropriate.

If the polydispersity of the slices is increased due to secondary separation mechanisms or low column performance, the conformation plots become distorted. The non–size exclusion separation usually increases the polydispersity at higher elution volumes and the conformation plots show a typical upswing at the region of lower molar masses. The upswing is given by the higher sensitivity of the z-average RMS radius to polydispersity. The presence of molecules with molar masses above the exclusion limit increases the polydispersity at the beginning of the chromatogram and the upswing may appear at the region of high molar masses, but the upswing at the region of lower molar masses is usually more evident.

4.2.3 Chromatogram Processing

Data processing in SEC-MALS is generally identical with that in conventional SEC and involves setting the baseline and peak limits. In addition, one has to decide which formalism and fit degree are appropriate for the acquired light scattering data. To process the SEC-MALS data, the signals from both MALS and RI detectors must be considered and their different responses to molar mass and concentration taken into account. In contrast to conventional SEC, the baseline has to be set for signals corresponding to all scattering angles. This procedure can be performed using the autobaseline feature of the light scattering software. The baseline for other detectors (RI, UV, viscometer) should be set independently because of their different shapes and sensitivities to chromatographic conditions. For example, the RI detector often shows positive and negative solvent and impurity peaks at the end of the chromatogram that are completely unseen by the light scattering detector. A typical feature of the MALS detector is almost no drift of the light scattering signals, which is due to very low sensitivity to temperature and pump fluctuations and slight changes of the mobile phase composition during column stabilization. As in the case of conventional SEC, moving the starting and ending points of the baseline backward or forward should have negligible impact on the obtained results. To select the peak limits it is necessary to take into account the signals from at least two detectors of different sensitivity to molar mass and concentration. Besides the most frequent combination MALS-RI, this can often be UV-MALS-RI or MALS-VIS-RI, and other detector combinations are possible as well. Detection of the peak beginning is usually easier than detection of the peak end. Issues concerning the determination of the end of the RI chromatogram are discussed in Section 3.5.2. If a polymer sample contains a low

level of oligomers causing the tailing of the RI chromatogram, the light scattering signal at the peak end can drop below the detection limit.

A typical example of RI and MALS chromatograms for a polymer containing an oligomeric tail is shown in Figure 4.19. The determination of the peak beginning in this particular example is straightforward while the determination of the peak end is complicated by a long oligomeric tail showing weak RI and almost no MALS response. No appreciable signal is obtained by the light scattering detector beyond about 15 mL, although the RI detector signal remains evident. The low signal from MALS results in inaccurate molar masses and consequently typical scattering of molar mass data points.

The accuracy of the determination of molar mass can be improved by the extrapolation of the molar mass–versus–elution volume relation from the high-concentration region toward the end of the chromatogram, where the data are scattered due to low concentration, as demonstrated in Figure 4.19. In this particular example, the peak end is established at the elution volume corresponding to about 1,000 g/mol, which yields reasonable M_n in good correlation with the value obtained by conventional SEC (compare Table 3.4). The extrapolation uses the molar masses determined in the region where the signals from both detectors are high to establish the relation between the molar mass and elution volume (i.e., SEC calibration for a given polymer under given SEC conditions) to calculate the molar masses in the region where the detector signal is weak and the data are uncertain. The extrapolation procedure can be also used to improve the determination of lower moments of RMS radius. The values determined for NIST SRM 706 polystyrene are shown in the caption of Figure 4.19. It is worth mentioning that the obtained R_n and R_w agree well with the experimental values of M_n and M_w. Using the relation $R = 0.014 \times M^{0.585}$ for linear polystyrene in THF, the M_n and M_w calculated from the values of R_n and R_w are 72,000 g/mol and 277,000 g/mol, respectively.

The region of reliable M is usually limited by the sensitivity of the RI detector at the high-molar-mass part of the chromatogram and by the sensitivity of the MALS detector at the low-molar-mass part. The extrapolation of molar mass and RMS radius can improve accuracy of measurements at the peripheral regions of the chromatogram where the signal of the MALS or RI detector is low. However, the peak limits should not be extended to the regions where signals of both detectors drop to baseline. In such a case the software calculates solely randomly scattered data points associated with zero concentration of eluting molecules. It is also important to keep in mind that any extrapolation behind the region of experimental values is always an uncertain procedure and the extrapolated data should not go too far behind the experimental ones. The *data extrapolation* should not be confused with the *results fitting*, when all data points, including those determined from weak detector signals, are taken into account. When too many scattered points are included, the fit may become incorrect. The user should get familiar with the features and possibilities of a particular software package.

Although results extrapolation or results fitting may improve the accuracy of the M_n and the low-molar-mass part of the molar mass distribution to a great

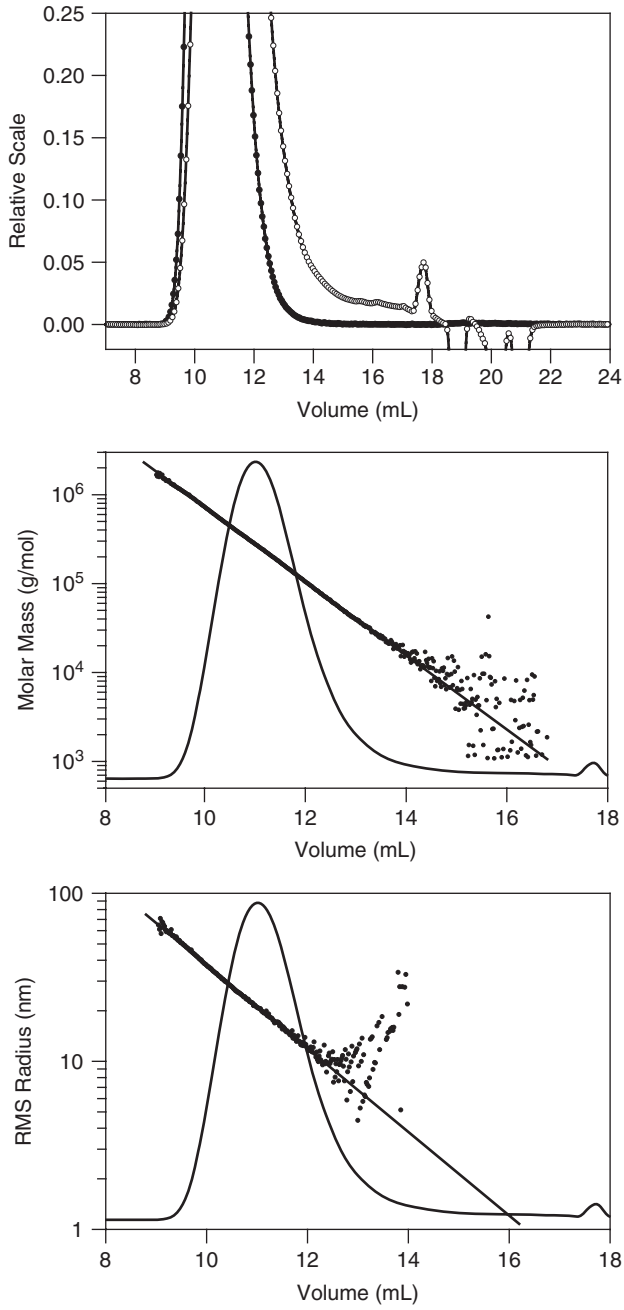

Figure 4.19 MALS at 90° (•) and RI (○) chromatograms of polystyrene NIST SRM 706 (top) and the extrapolation of molar mass (center) and RMS radius (bottom) toward high elution volumes. $M_n = 66{,}000$ g/mol, $R_n = 9.7$ nm, $R_w = 21.4$ nm.

extent, the more reliable way to get correct results is to improve the signal-to-noise ratio. It must be emphasized at this point that the electronic noise generated by a light scattering photometer is far below the noise generated from the chromatography system by particles from the mobile phase or bleeding from the column packing.

Although samples that show an imperceptible MALS signal at the end of the chromatogram, but still an evident signal of the RI detector, are more frequent, the reverse situation can occur at the beginning of chromatograms of samples containing trace amounts of high-molar-mass species. For such samples the strong difference in sensitivities between the RI detector and the light scattering detector results in an intensive signal of MALS and a barely detectable signal of the RI detector, as shown in Figure 4.20. Note that even if the weak RI signal does not allow for the determination of reliable molar mass, the RMS radius can still be determined accurately from the angular variation of the light scattering intensity. If the concentration signal is very close to zero, noise can make the concentrations randomly positive and negative, and the Debye plots may look confusing. If this happens, it is possible to manually adjust the baseline for the concentration detector to be slightly below the baseline, thus insuring that all concentration values are positive regardless of being incorrect. This procedure will drastically affect the molar masses, but they are incorrect anyway. Manually adjusting the RI baseline has no effect on the accuracy of the RMS radii.

Since the molar mass is calculated from the responses of both the light scattering and RI detectors, a random fluctuation of the RI signal can lead to upward or downward curvature of the molar mass at the beginning of a chromatogram, as shown in Figure 4.21. Since the RMS radius is calculated independently of the signal of the RI detector, the RMS radius–versus–elution volume plot can

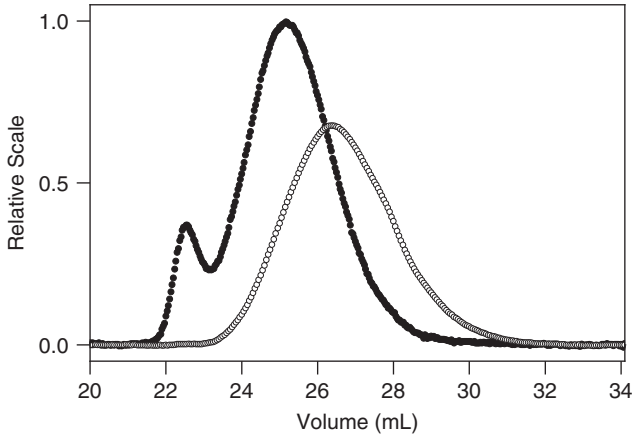

Figure 4.20 MALS at 90° (●) and RI (○) chromatograms of NIST SRM 1476 polyethylene showing intensive light scattering signal at the beginning of the chromatogram.

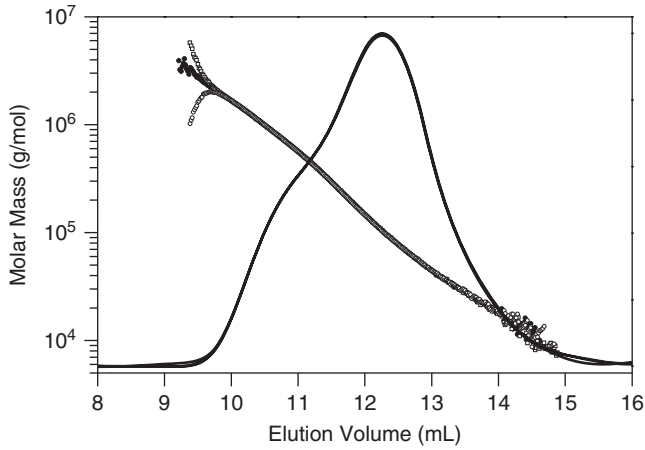

Figure 4.21 Molar mass–versus–elution volume plots and RI chromatograms from three consecutive SEC-MALS runs of broad polystyrene. The discrepancy of the plots at the beginning of chromatograms is caused by random fluctuation of RI signal.

reveal that the curvature is an artifact and does not give a true picture of the polymer separation.

The effect of random noise level on the accuracy of molar masses and RMS radii determined by SEC-MALS was studied by Tackx and Bosscher,[6] who theoretically simulated MALS and RI chromatograms and showed systematic deviations of molar mass in the region of low and high elution volumes. They showed that in the low-molar-mass region of the chromatogram the log molar masses are too high, while in the high-molar-mass region they are systematically too low. This was explained by the random noise in the MALS and RI signals. When the noise level becomes too high, positive and negative molar masses are obtained, but only the logarithm of positive molar masses has mathematical meaning. Therefore, all the negative points are omitted in the log M–versus–elution volume plot. According to my own experience, the majority of polymer samples show no (or negligible) systematic deviation at the region of lower molar masses.

The calculation at reference 6 starts way before the real beginning of MALS and RI chromatograms. Also in the region of high elution volumes the integration limit seems to go too far after the real end of the RI chromatogram. Although the explanation given in reference 6 appears reasonable, it remains unclear why this systematic deviation is not observed for all samples. For instance, the molar masses in Figures 4.9 or 4.19 evidently do not show any strong systematic deviation. Experience also suggests, but does not directly prove, that the systematic deviations on molar mass plots appear more often when older SEC columns are used, which might be caused by release of previously retained impurities due to a slight pressure pulse created by sample injection.

4.2.4 Influence of Concentration and Second Virial Coefficient

The calculation of molar mass in SEC-MALS commonly neglects the concentration effect; that is, the term with the second virial coefficient in Equations 4.4, 4.8, and 4.10 is considered to be small enough to be neglected without a significant effect on molar mass. In principle, the concentration effect can be easily corrected for by using appropriate values of A_2. However, the relation between A_2 and molar mass is generally unknown for most polymers requiring analysis. In addition, light scattering software may not allow for using different values of A_2 at different elution volumes (i.e., for different molar masses). Nevertheless, since A_2 varies only weakly with M for most polymers, an average value corresponding to M_w can be used for polydisperse polymers. The procedure is that the sample under analysis is first processed using $A_2 = 0$ mol mL/g^2, then the obtained M_w is used to calculate $A_2 =$ from Equation 2.4 and the obtained value is used to recalculate the data. Nevertheless, the differences in the obtained results are mostly negligible.

According to Equation 4.2, the product $2A_2cM \ll 1$; then $\frac{R_0}{K^*c} = M$. That means the effect of A_2 must be considered with respect to the concentration of molecules eluting at a given elution volume and their molar mass. Table 4.4 shows the effect of A_2 on the molar masses determined across the peak of typical polydisperse polymer. The molar mass at each volume slice was at first determined using $A_2 = 0$ mol mL/g^2, and then for each molar mass the A_2 was calculated according to Equation 2.5 and used to calculate the true molar mass.

The data in Table 4.4 show that the concentration of injected solution is diluted by a factor of at least 25 and that neglecting the concentration effect results in an error of about 2% at maximum. The molar mass error is equal to $100 \times 2A_2cM\,(\%)$, which means the only parameter directly influencing the molar mass correctness is the concentration, which should be therefore kept as low as possible, though without sacrificing the signal-to-noise ratios of the applied detectors. It is obvious that the concentration-related errors strongly decrease with decreasing molar mass and thus that the concentration is typically not an important parameter in the case oligomers, when solutions of about 10 times higher concentrations than those used for the analysis of higher-molar-mass polymers can be used in order to assure an intensive light scattering signal.

4.2.5 Repeatability and Reproducibility

It has been shown that flow rate is an absolutely key parameter for the accurate determination of molar mass by conventional SEC with column calibration and that the obtained results are also strongly affected if the temperature used for the analysis deviates from that used for the column calibration. Very low sensitivity of MALS detection to both flow rate and temperature deviations results in significantly improved repeatability and reproducibility of the measurements

Table 4.4 Influence of the Second Virial Coefficient on Molar Masses of Polydisperse Polymer Determined by SEC-MALS (Injection 100 μL 0.2% w/v)

Volume (mL)	Concentration (g/mL)	$M\,(A_2 = 0)$ (g/mol)	A_2 (mol mL/g^2)	$M_{\text{corrected}}$ (g/mol)	Error (%)
9.0	1.24e−6	2.316e+6	2.56e−4	2.320e+6	0.17
9.1	2.25e−6	2.028e+6	2.65e−4	2.033e+6	0.25
9.3	6.20e−6	1.631e+6	2.79e−4	1.640e+6	0.55
9.4	9.59e−6	1.466e+6	2.87e−4	1.478e+6	0.81
9.5	1.41e−5	1.329e+6	2.95e−4	1.344e+6	1.12
9.6	1.95e−5	1.204e+6	3.02e−4	1.221e+6	1.39
9.7	2.55e−5	1.083e+6	3.10e−4	1.102e+6	1.72
9.8	3.17e−5	9.753e+5	3.18e−4	9.948e+5	1.96
9.9	3.75e−5	8.739e+5	3.27e−4	8.930e+5	2.14
10.0	4.28e−5	7.806e+5	3.36e−4	7.985e+5	2.24
10.1	4.76e−5	6.972e+5	3.46e−4	7.135e+5	2.28
10.2	5.18e−5	6.247e+5	3.56e−4	6.394e+5	2.30
10.3	5.56e−5	5.619e+5	3.65e−4	5.751e+5	2.30
10.4	5.90e−5	5.053e+5	3.75e−4	5.169e+5	2.24
10.5	6.22e−5	4.562e+5	3.85e−4	4.664e+5	2.19
10.6	6.51e−5	4.136e+5	3.94e−4	4.226e+5	2.13
10.8	7.04e−5	3.404e+5	4.14e−4	3.473e+5	1.99
11.0	7.48e−5	2.801e+5	4.35e−4	2.853e+5	1.82
11.2	7.79e−5	2.315e+5	4.56e−4	2.354e+5	1.66
11.4	7.89e−5	1.904e+5	4.79e−4	1.932e+5	1.45
11.6	7.70e−5	1.565e+5	5.03e−4	1.584e+5	1.20
11.8	7.15e−5	1.281e+5	5.29e−4	1.294e+5	1.00
12.0	6.30e−5	1.061e+5	5.54e−4	1.068e+5	0.66
12.2	5.30e−5	8.630e+4	5.83e−4	8.680e+4	0.58
12.5	3.77e−5	6.420e+4	6.28e−4	6.440e+4	0.31
12.8	2.42e−5	4.760e+4	6.77e−4	4.770e+4	0.21

compared with conventional SEC. The negligible impact of the temperature and the flow rate on the molar mass determined by the MALS detector is demonstrated in Table 4.5. Repeatability and reproducibility are illustrated in Table 4.6. Considerably better repeatability and reproducibility of the SEC-MALS method should be of interest even for those who demand only mutual comparison of samples of equal chemical composition and molecular structure and does not require absolute molar mass values, and such may consider the light scattering detector for their applications needless. Note that very good reproducibility is found especially for M_w values that are determined by the MALS detector alone and are not affected by SEC resolution.

Table 4.5 Effect of Flow Rate and Column Temperature on M_w of Broad Polystyrene Determined by SEC-MALS

Temperature (°C)	M_w (10^3 g/mol)	Flow Rate (mL/min)	M_w (10^3 g/mol)
20	332	1.00	337
24	333	1.01	338
28	333	1.03	337
32	333	1.05	336
35	333	1.07	337
—	—	1.10	336

Note: Compare Tables 3.1 and 3.6.

Table 4.6 Repeatability and Reproducibility of M_w of Broad Polystyrene Determined by SEC-MALS

Measurements	Number	M_w (10^3 g/mol)	RSD (%)
One day, single SEC-MALS setup	12	329	0.2
22 months, single SEC-MALS setup	34	332	1.7
17 months, 10 MALS and 4 RI detectors in various combinations	28	331	1.6

Note: Wyatt Technology Corporation miniDAWN™ and DAWN® EOS photometers were used for the study.

4.2.6 Accuracy of Results

Random errors are caused by accidental noise in detector signals (in the MALS signal mostly due to randomly eluting dust particles; in RI due to flow rate and temperature fluctuations), run-to-run variations of the SEC separation process, and drift of the baseline (the MALS drift is usually negligible while the RI detectors are more apt to drift). Systematic errors include calibration constants of MALS, RI, and UV detectors; physical constants such as refractive index and especially dn/dc values; errors from improper normalization; errors of interdetector delay volume; errors caused by interdetector band broadening; errors due to improper type of light scattering formalisms and/or polynomial fit degree; and baseline selection and peak integration limits. MALS detector calibration and normalization and dn/dc accuracy are discussed in Sections 2.2.1.3 and 2.4. Errors due to the interdetector volume determination are specific for SEC with combined detectors. Although the determination of the interdetector volume appears straightforward, the obtained values can be affected by polydispersity of standard used for alignment, and flow rate deviations, as well as by errors due to the subjective approach of the operator. The effect of errors of interdetector volume on the exponents of the Mark-Howink and conformation plots can be

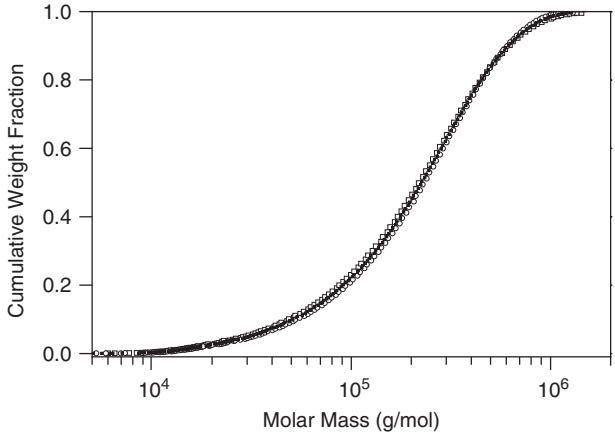

Figure 4.22 Cumulative distribution curves of broad polystyrene obtained using correct (■) interdetector volume, and values incorrect by +10% (○) and −10% (□). Molar mass moments: M_n = 112,000 g/mol, 116,000 g/mol, 108,000 g/mol; M_w = 289,000 g/mol, 289,000 g/mol, 289,000 g/mol; M_z = 485,000 g/mol, 466,000 g/mol, 507,000 g/mol for correct volume delay, and values incorrect by + 10% and −10%, respectively.

quite significant, whereas the impact on the molar mass distribution curves is usually negligible.

Figure 4.22 shows the influence of interdetector volume errors on the molar mass distribution and the molar mass moments. Of note is the fact that errors in the interdetector volume do not appreciable affect the determination of M_w and that errors within about 10% will have only a moderate effect on the molar mass distribution and the moments M_n and M_z.

Figure 4.23 shows a typical effect of interdetector volume on the RMS radius–versus–molar mass plot. It is evident that a relatively small error in the interdetector volume results in a relatively significant change of the slope of the conformation plot and for some samples may even lead to false estimation of polymer conformation and branching, especially if, for instance, the increase of the slope caused by using Zimm formalism is combined with that given by incorrect volume delay.

4.3 APPLICATIONS OF SEC-MALS

4.3.1 Determination of Molar Mass Distribution

Let us at first ignore the problems associated with polymer blends and heterogeneous copolymers, whose dn/dc values may vary significantly from slice to slice, and whose slice concentrations cannot be obtained from the signal of RI detector. The primary application of SEC-MALS is the determination of molar mass averages and molar mass distribution. This kind of information is needed in all

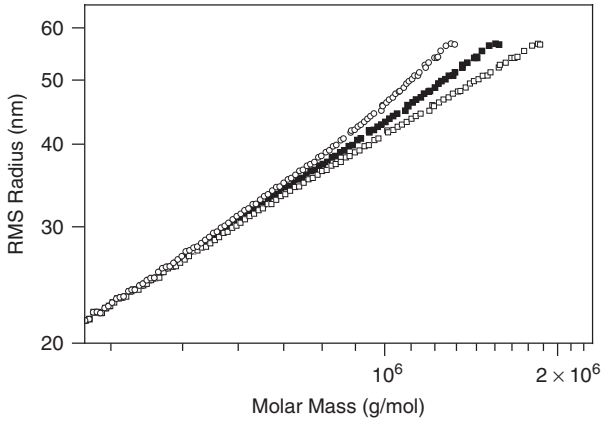

Figure 4.23 Effect of interdetector volume on shape of conformation plot. Data for broad polystyrene. Conformation plots obtained using correct (■) interdetector volume, and values incorrect by +10% (○) and −10% (□). Slopes of the plots = 0.58; 0.64 and 0.53 for correct volume delay, and values incorrect by +10% and −10%, respectively.

areas of polymer science covering fundamental research and theoretical considerations, manufacturing quality control, control of properties, and final applications. In contrast to conventional SEC, the use of a MALS detector yields true molar mass averages and molar mass distribution and eliminates errors resulting from improper calibration. Although the results obtained by the SEC-MALS technique typically differ by several tens or even hundreds percent from the values generated by conventional SEC with improper calibration, incidental agreement between conventional SEC and SEC-MALS can happen even in the case of obscure calibration procedure.

For curiosity's sake, let me relate an experience that happened many years ago in my laboratory. The goal was to determine the molar mass averages of polyelectrolyte based on sodium salts of acrylic and maleic acids. The only available columns allowing the analysis of aqueous polymers were those based on bare silica gel, which could be also used in THF. Since the laboratory had no suitable water-soluble standards, the columns were at first calibrated by polystyrene standards in THF and then flushed with water and finally with aqueous sodium sulphate. The polyelectrolyte samples were analyzed and processed by means of the polystyrene calibration determined in THF. The obtained molar masses were considered to be far from the true ones, but they were useful for sample comparison and allowed us to optimize the polymerization process. Surprisingly, almost-identical results were determined after several years when the same polymers were analyzed by SEC-MALS.

Accuracy of M_n can be questioned due to limited resolution of SEC columns. The values of M_n of several polydisperse polymers determined by SEC-MALS and membrane osmometry are compared in Table 4.7. The differences are not

Table 4.7 Number-Average Molar Masses of Polydisperse Polymers Determined by Membrane Osmometry and SEC-MALS

	M_n (10^3 g/mol)	
Sample	SEC-MALS	MO
PS (AN)	118 ± 2	120
PS (1)	121 ± 2	139
PS (2)	108 ± 4	153
PS (S)	49 ± 2	66
PS (K)	92 ± 1	98
PMMA (Y)	184 ± 4	185
PMMA (J)	43 ± 2	33

unusually large considering the results from substantially different methods are compared. The results listed in Table 4.7 may be to some extent overestimated due to the polydispersity of volume slices in SEC-MALS and permeation of small amounts of oligomeric fractions through the membrane in membrane osmometry,[i] but it is obvious that SEC-MALS can yield M_n values with the same accuracy as traditionally used, but more laborious and currently less common, membrane osmometry. Results published in reference 4 for a series of 17 oligomeric compounds with molar mass covering 200–5,800 g/mol showed very good agreement of M_n values determined by SEC-MALS with those obtained by VPO, NMR, or HPLC. Favorable results of experiments comparing M_n and M_w of oligomers determined by SEC-MALS with those obtained by NMR, VPO, MALDI, and supercritical fluid chromatography were also reported in references 7 and 8. Taking into account the limitations of absolute methods of the determination of M_n, that is, errors due to permeation of oligomeric fractions in MO and very high sensitivity to even trace amounts of low-molar-mass compounds in the case of VPO, and laboriousness of the measurements (both osmometric methods require measurements at multiple exactly known concentrations), SEC-MALS appears to be a fast and reliable technique for determination of M_n.

The low-molar-mass limit for which SEC-MALS can be used is a frequent question that users and potential users of SEC-MALS ask. As already discussed, the response of the MALS detector is proportional to the molar mass and concentration and thus the MALS detector yields several orders of magnitude lower response for oligomers than for polymers. A typical concentration for the SEC-MALS analysis of polymers is around 0.2% w/v. In the case of oligomers the concentration can be safely increased by a factor of 10 to 25 without significant impact on the error caused by neglecting the term with the second virial coefficient, because for very low molar masses the term $2A_2cM \ll 1$ even for high concentrations.

[i]As a matter of fact, both SEC-MALS and membrane osmometry have a tendency to overestimate M_n, though for different reasons.

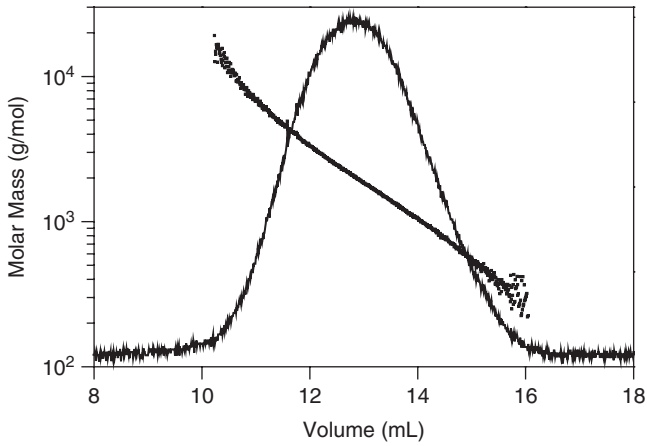

Figure 4.24 Molar mass–versus–elution volume plot and 90° MALS signal for polybutandiol. Injection 200 μL 5% w/v, $dn/dc = 0.069$ mL/g, M_n (SEC-MALS) = 950 g/mol, M_n (HPLC) = 940 g/mol.[9] Columns: 2 × PLgel Mixed-E 300 × 7.5 mm, THF at 1 mL/min.

An example in Figure 4.24 shows that an acceptable signal-to-noise ratio of a light scattering detector and consequently reliable molar mass can be measured down to a few hundreds g/mol in spite of relatively low dn/dc of the analyzed sample. Despite high injected mass, the data show good separation without noticeable signs of column overloading. In a given example, the highest concentration of the eluting molecules was about 3 mg/mL at molar mass of about 1,200 g/mol. That means the error caused by neglecting the concentration term is most likely well below 3% unless the second virial coefficient is unusually high. It has been explained that the lower the angle of measurement, the more likely the signal will show light scattered by impurities or dust. This is of particular importance for oligomers, which generally yield low light scattering signal. However, since no information can be obtained from the measurement of the angular variation of light scattering intensity for small molecules, the lower angles can be safely dropped and only those angles showing the minimum noise can be used for the molar mass calculation. A zero-fit degree (i.e., line parallel with $\sin^2(\theta/2)$ axis) can be used for processing the data of oligomers since they scatter light equally in all angles. In the case of poor signal-to-noise ratio, only a 90° detector, which usually shows the lowest noise level, can be used to process the data of oligomers.

The only assumptions for the determination of true molar mass distribution by SEC-MALS of homopolymers are negligible polydispersity of the elution volume slices, that is, negligible band broadening in the columns and other parts of chromatographic setup, and negligible concentration effects. Both assumptions are usually fulfilled to a great extent and thus SEC-MALS can be considered a reliable and fast method for characterization of molar mass distribution with precision limited only by the correctness of the MALS calibration constant,

normalization coefficients, calibration constant of the concentration detector, and dn/dc. More complicated polymers for the SEC-MALS measurements are heterogeneous copolymers, polymer blends, and branched polymers, where the obtained results may be negatively affected by sample heterogeneity and limited separation efficiency of SEC.

A challenge may be estimation of molar mass distribution of narrow polymers, because possible inaccuracies arising from interdetector peak broadening are significantly more serious than for the polydisperse polymers. Since the calculation of the RMS radius is independent of concentration, the RMS radius can be used instead of molar mass to assess the sample polydispersity. Once the RMS radius distribution is established, it can be converted to molar mass distribution using the RMS radius–versus–molar mass relation. However, the determination of polydispersity of narrow polymers of higher molar mass is limited by SEC resolution.

4.3.2 Fast Determination of Molar Mass

One possible application of SEC-MALS is combination with so-called high-throughput, fast or rapid SEC columns of reduced dimension (e.g., 150 × 7.5 mm or 100 × 10 mm). A serious weakness of the fast columns, which recently achieved a certain popularity, is their lower selectivity and efficiency. This fact is of particular importance for conventional SEC, where the calculation of molar mass distribution is based on the assumption of negligible peak broadening. The application of a MALS detector at least partly eliminates the reduced separation efficiency of the fast columns. It has been already explained that determination of M_n, M_z, and the entire molar mass distribution by means of SEC-MALS is based on the assumption of almost monodisperse elution volume slices. However, determination of M_w and R_z is based on the fundamental principle of light scattering and as a matter of fact does not require sample fractionation at all. Therefore, the M_w and R_z values determined by SEC-MALS do not depend on the SEC resolution and are always correct even if other molar mass averages and molar mass distribution are affected by poorer SEC separation efficiency.

Molar mass averages determined by fast SEC-MALS measurements are compared with those obtained by regular SEC column sets in Table 4.8. According to the expectation, differences in M_w are negligible for all column systems, but the use of a single high-throughput column results in a slight overestimation of M_n and underestimation of M_z, which corresponds to decreased resolution and increased polydispersity within the elution volume slices. The graphical comparison of regular and high-throughput analysis of two polymers covering different molar mass range is presented in Figures 4.25 and 4.26. The obtained data indicate slight differences in the molar mass distribution especially at the margins of molar mass distribution. However, it is apparent that high-throughput SEC-MALS analysis can evidently provide not only correct M_w and R_z, but also an acceptable estimation of molar mass distribution, and can be used especially in applications that require short analysis times.

Table 4.8 Molar Mass Averages Obtained by SEC-MALS Analysis Using Four and Two Regular Columns (4R, 2R) and a Single High-Throughput Column (1H)

	M_n (10^3 g/mol)			M_w (10^3 g/mol)			M_z (10^3 g/mol)		
Sample	4R	2R	1H	4R	2R	1H	4R	2R	1H
PES	1.56	1.57	1.81	2.49	2.56	2.54	3.66	3.83	3.44
EP (1)	1.58	1.56	1.80	3.40	3.42	3.45	5.83	5.99	5.49
EP (2)	3.20	3.24	3.58	8.20	8.22	8.15	19.0	18.9	16.2
PMMA (J)	48.7	47.8	50.3	89.2	88.9	88.4	137.8	140.3	127.5
Alkyd	5.90	5.77	6.38	151.3	151.7	151.0	1003	1023	904
PS (AN)	117.0	111.9	120.5	292.6	289.5	287.6	484.5	487.2	441.7

Regular columns: 300 × 7.5 mm PLgel Mixed-C; *high-throughput column:* 150 × 7.5 mm PLgel HTS-C; THF at 1 mL/min; *injection volume:* 200, 100, and 25 μL for four, two, and single columns, respectively. *Samples:* PES = polyester, EP = epoxy resin, PMMA = poly(methyl methacrylate), PS = polystyrene.

The fastest SEC measurement happens when the separation is minimized to the separation of polymer from low-molar-mass compounds, such as solvents, additives, and impurities. This type of measurement, sometimes called *FIPA* (flow injection polymer analysis), provides M_w and R_z. In addition, the analysis can be completed by the measurement of the average intrinsic viscosity by an online viscometer. The SEC-MALS measurement with only a guard column yields the same type of information that can be obtained by a classical batch light scattering experiment. However, a classical light scattering experiment involves measurements of a series of solutions of different concentrations, which is rather a laborious procedure that requires precise concentrations of all solutions. In the case of fast SEC-MALS with a guard column, the polymer is separated from the low-molar-mass compounds and the concentration of polymer molecules eluting from the guard column is measured online by a concentration detector, which means the accurate concentration of the measured solution need not be known. The results can be obtained by a single injection in an analysis time of less than three minutes, which makes the method uniquely suitable for industrial applications for the control of polymerization processes.

Other advantages are very low consumption of solvent and very low system backpressure. The RI signal yields the total injected mass, which allows determination of polymer concentration in the analyzed sample as additional information that is important, for example, in the case of samples taken from the reactor during the manufacturing process. For linear polymers the M_z value can be estimated from R_z provided the relation between the RMS radius and molar mass is known for the polymer under investigation. Knowledge of M_z is important from a practical viewpoint, because comparison of M_z and M_w permits estimation of sample polydispersity. Comparison of results obtained by guard column measurements compared with those determined by means of regular SEC columns or other techniques is shown in Table 4.9.

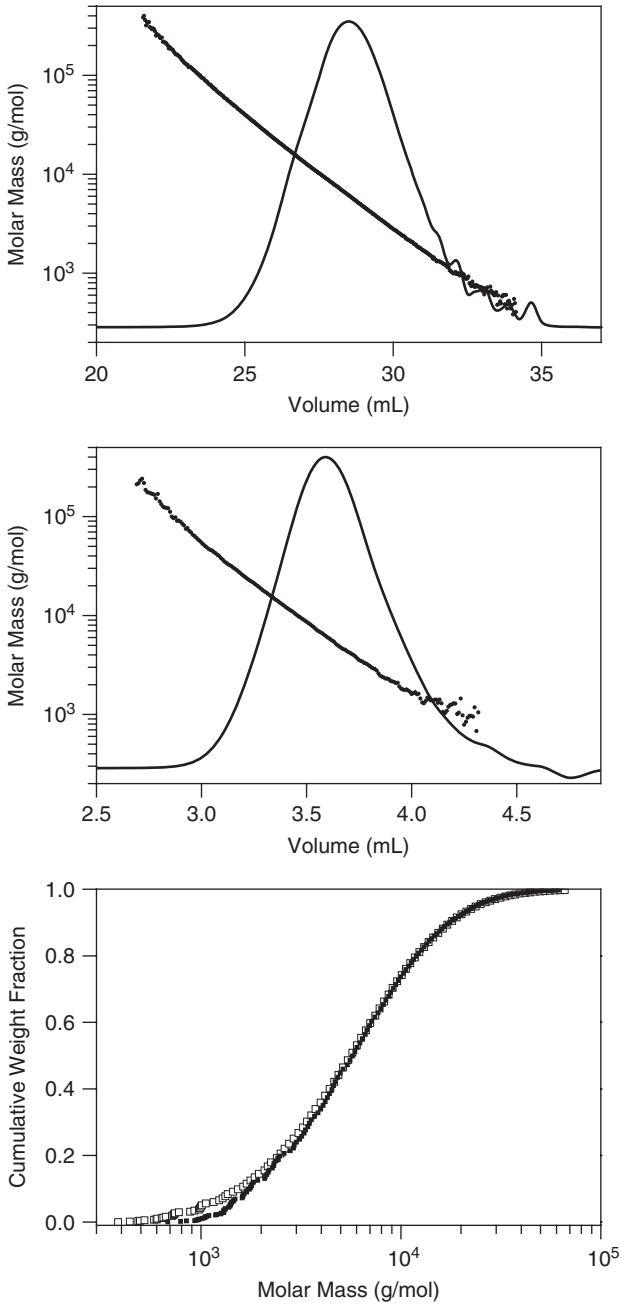

Figure 4.25 Molar mass–versus–elution volume plots and RI chromatograms obtained by 4 × PLgel Mixed-C 300 × 7.5-mm columns (top) and a single PLgel HTS-C 150 × 7.5-mm high-throughput column (center). Overlay of cumulative distribution plots (bottom) obtained with four columns (□) and a single high-throughput column (■). Sample: epoxy resin.

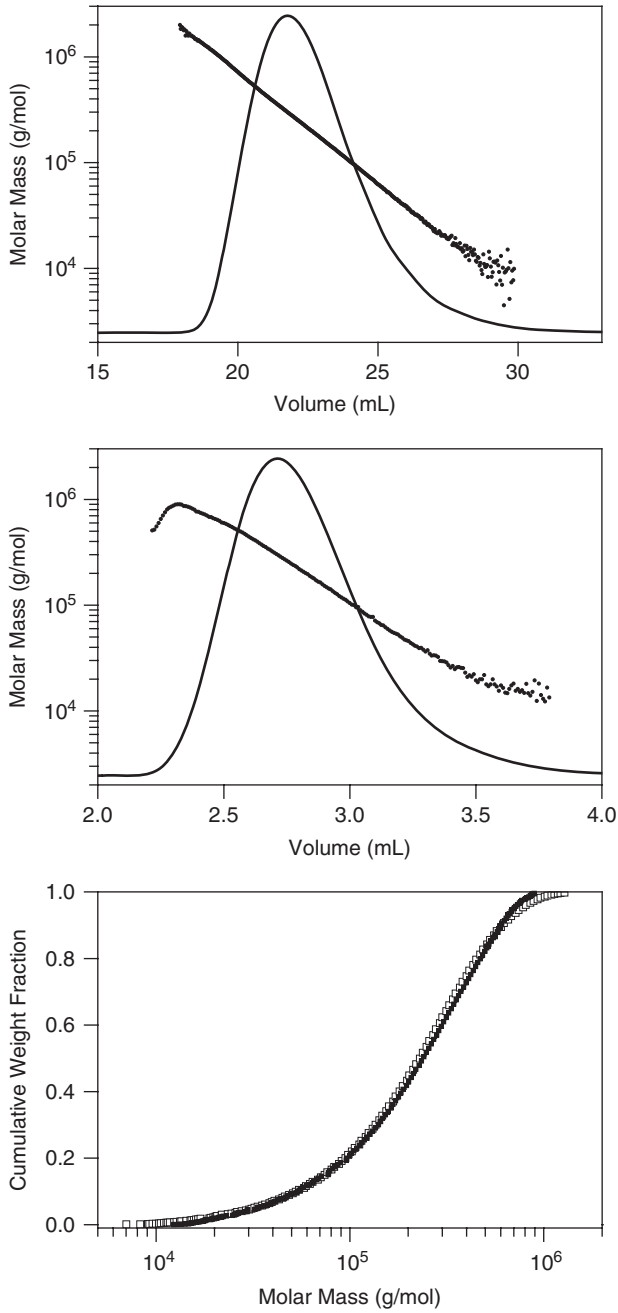

Figure 4.26 Molar mass–versus–elution volume plots and RI chromatograms obtained by 4 × PLgel Mixed-C 300 × 7.5-mm columns (top) and a single PLgel HTS-C 150 × 7.5-mm high-throughput column (center). Overlay of cumulative distribution plots (bottom) obtained with four columns (□) and a single high-throughput column (■). Sample broad polystyrene.

Table 4.9 Comparison of Results Obtained by Fast SEC-MALS Analysis with a Single Guard Column with Nominal (N) Values and Results Obtained by Means of Batch MALS and SEC-MALS Using Regular Columns

	Guard column		M_z from R_z	Two 300 × 8 mm columns		M_w
Sample	M_w (10^3 g/mol)	R_z (nm)	(10^3 g/mol)	M_w (g/mol)	M_z (nm)	(10^3 g/mol)
EP (1)	3.46	—	—	3.42	—	3.50^{MALS}
Narrow PS	208	18.2	210	204	—	200^{N}
PS (NIST 706)	281	27.5	426	283	421	288^{MALS} 285^{N}
PS (A)	326	33.9	609	326	644	344^{MALS}
PBZMA (38)	418	27.5	679	399	660	—
PMMA (Y)	544	41.7	1185	558	1051	612^{MALS}

4.3.3 Characterization of Complex Polymers

Although the experimental results indicate that the slices of linear homopolymers are almost monodisperse, the situation may be significantly less favorable in the case of branched polymers and heterogeneous copolymers, where molecules of identical hydrodynamic volume, but different molar mass, can co-elute within the elution volume slices. Increasing SEC performance does not help since the slices may be perfectly monodisperse with respect to the hydrodynamic volume, yet polydisperse from the viewpoint of molar mass. To assess polydispersity within the elution volume slice one can, at least theoretically, compare the number-average molar mass determined by SEC-MALS with that measured by membrane osmometry. Significantly higher M_n obtained by SEC-MALS compared to that from MO would indicate increased slice polydispersity. However, such a comparison would be relatively laborious and unfortunately also uncertain due to the drawbacks of membrane osmometry, that is, penetration of oligomeric fractions through the membrane and low sensitivity to high-molar-mass fractions. It may be worth noting that due to the polydispersity within elution volume slices, the slice molar masses obtained by MALS detection are the weight-averages, while the combination of an online viscometer with the universal calibration yields the number-averages.

4.3.3.1 Branched Polymers

Branching of any kind results in the reduction of molecular dimensions, which are typically expressed in terms of RMS radius, hydrodynamic radius, or intrinsic viscosity. With the exception of regular branched structures, such as perfect stars composed of the same number and length of arms, most natural and synthetic branched polymers have random structure, which means they consist of

molecules of different molar masses, different numbers of branch units, and different branch lengths and topologies. Since the separation of polymers by SEC is controlled by hydrodynamic volume and not by molar mass or molecular architecture, molecules eluting at a given elution volume from the columns are polydisperse with respect to their molar mass and branching characteristics. However, if the band-broadening effect is negligible, they are monodisperse with respect to the hydrodynamic volume.

Note that this kind of polydispersity is different from that resulting from delayed elution of large-branched molecules due to their anchoring in the pores of SEC column packing. In the case of polydisperse slices the MALS detection yields M_w and R_z that are valid for a given elution volume (hydrodynamic volume). The weight-average calculated from Equation 4.15 by entering $M_{w,i}$ instead of M_i provides the weight-average, and the same is true for R_z. However, using $M_{w,i}$ in Equations 4.14 and 4.16 results in overestimation of M_n and underestimation of M_z and the polydispersity M_w/M_n. The entire molar mass distribution is shifted to higher (in the lower-molar-mass region) and lower (in the higher-molar-mass region) molar masses.

The authors of reference 10 defined a distribution function $N(M, V_h)$, the number of chains with molar mass M and hydrodynamic volume V_h, which was suggested to be used to reveal mechanistic information about polymer synthesis. They showed how true M_w and M_n can be obtained from processing the hydrodynamic volume distribution. Although reference 10 can serve as an important source of the theory of characterization of complex branched polymers using multiple detection, practical application is limited by the fact that commercially available SEC-MALS-VIS software assumes that the polydispersity within the elution volume slices is negligible. This assumption, although rarely completely fulfilled, significantly simplifies the processing and interpretation of the experimental data. My experience indicates that the SEC-MALS and SEC-MALS-VIS results obtained under the simplifying assumption of negligible slice polydispersity mostly provide a valuable characterization of various branched polymers, and that the characterization of branching is often affected by other limitations of the same significance.

4.3.3.2 Copolymers and Polymer Blends

In the most favorable, and also unusual, case of homogeneous copolymers (i.e., when all molecules present in the sample have identical chemical composition), one can use the weighted average of dn/dc of parent homopolymers to determine the molar mass at each elution volume. In the case of heterogeneous copolymers the chain dimensions depend not only on the molar mass, but also on the chemical composition. Molecules of different composition and molar mass may have the same hydrodynamic volume. Consequently, in SEC separation of chemically heterogeneous copolymers a given elution volume slice can consist of molecules of different molar mass and chemical composition (different dn/dc). Changing the dn/dc along the elution volume axis is theoretically possible, but mostly would

be of little use, because the composition as a function of molar mass is unknown for most polymers being analyzed. Therefore, an average *dn*/*dc* calculated on the basis of bulk copolymer composition or determined experimentally must be used for processing the entire peak.

In contrast to branched homopolymers, where branching affects the polydispersity within the elution volume slice but the *dn*/*dc* remains constant, the chemical heterogeneity also affects *dn*/*dc* at a given elution volume and consequently the concentration obtained by the RI detector and the molar mass calculated from the light scattering intensity. That means, in contrast to branched polymers, even M_w cannot be considered to be correct. The influence of chemical heterogeneity of copolymers on the separation process in SEC was studied theoretically by Netopilik et al.[11] with these two main conclusions:

1. The molar mass of a chemically heterogeneous copolymer at a given elution volume may vary with the chemical composition to a considerable extent (e.g., by about 30%).
2. Significant deviations of experimental molar mass averages obtained by SEC with light scattering detection from the true values due to the effect of composition heterogeneity may be expected only for significantly different *dn*/*dc* of the parent homopolymers.

The results published in reference 4 for blends of polystyrene, poly(methyl methacrylate), and poly(benzyl methacrylate) showed acceptable accuracy of M_n and M_w determined by SEC-MALS. The blends were processed using an average *dn*/*dc* calculated on the basis of composition. However, the investigated polymers were of almost overlapping molar mass distribution. In such a case, where the molar mass of one polymer is overestimated due to the incorrect *dn*/*dc*, the molar mass of the other polymer is underestimated and thus the total error is at least partly compensated. If the molar mass distributions of particular polymers are not completely overlapping, there is at least one region of the chromatogram where molecules of only one chemical composition elute. Using an average *dn*/*dc* results in over- or underestimation of molar mass that is not compensated by molecules of another chemical composition.

In the case of copolymers, the actual heterogeneity is usually significantly lower compared to the polymer blends, which represents the ultimate example of chemically heterogeneous systems. Consequently, the deviations of the average *dn*/*dc* from the true values for molecules of particular chemical composition will be lower. Another parameter to consider is the difference in *dn*/*dc* of parent homopolymers, which is in many practical cases small. For example, for various acrylic copolymers the differences in *dn*/*dc* of parent homopolymers are relatively low.

It can be concluded that chemically heterogeneous copolymers cannot be accurately characterized by SEC-MALS and the possible errors may be considerable. Errors of molar mass are less serious in the case of moderately heterogeneous samples and/or where the differences between the *dn*/*dc* values of parent

homopolymers are low. The combination of RI and UV detection can be applied for copolymers if one of the monomers is UV absorbing.

4.3.4 Conformation Plots

The conformation plot relates RMS radii and molar masses obtained at particular elution volumes. The ability to relate the RMS radius to the molar mass is important for polymer characterization and also permits testing of polymer theories. The conformation plots may be affected by the light scattering formalism utilized for data processing. The conformation plots obtained for a linear polydisperse polymer using various light scattering formalisms are depicted in Figure 4.27. The plots show typical behavior, and similar results have been obtained for other polymers. It can be concluded that the slopes obtained by the Zimm method are usually overestimated, especially if the sample contains large molecules more than about 100 nm. The Berry and random coil methods yield almost identical conformation plots. The slopes of the conformation plots obtained by the Debye methodology with the first-order fit are underestimated, and the underestimation increases strongly toward high molar masses.

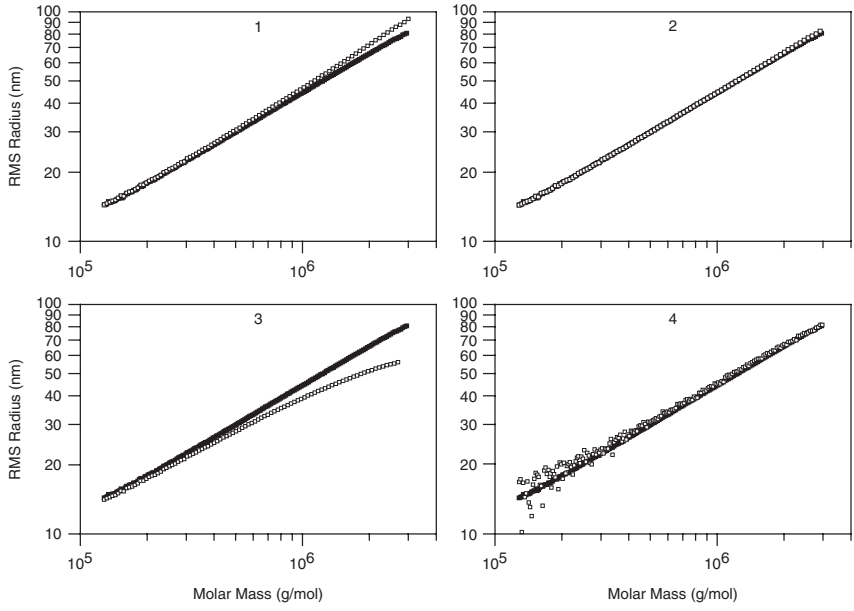

Figure 4.27 Conformation plots of broad linear polystyrene obtained by different processing methods. (1) Berry (■) versus Zimm (□), slopes = 0.57 and 0.60, respectively; (2) Berry (■) versus random coil (□), slope = 0.57; (3) Berry (■) versus Debye first-order fit (□), slope = 0.49; (4) Berry (■) versus Debye third-order fit (□), slope = 0.55.

The application of the first-order Debye formalism to large molecules can easily lead to false conclusions about polymer conformation, because even for linear random coils in thermodynamically good solvent the first-order Debye fit can yield a slope below 0.5 (i.e., characteristic value for branched macromolecules). By fitting a higher-degree polynomial to the Debye formalism, more accurate data providing a reliable slope of the conformation plot are obtained. However, a higher-order fit increases the scattering of the data points in the region of lower molar masses, because the extrapolation becomes very sensitive to data containing random errors. Although a difference in the slope of several hundredths may appear negligible, it may play an important role in the identification of branching, since, for example, a slope equal to 0.58 is typical for linear molecules in thermodynamically good solvents, while a slope of 0.54 may indicate the presence of a certain amount of branched molecules. Both slopes can be easily obtained for a polymer under investigation by just changing from the Zimm processing method to the Berry or random coil method. Conclusions based on the slope of the conformation plot should therefore be made with caution, always considering the accuracy of the M and R from which the conformation plot is constructed and the limitations of particular processing methods. This is of particular importance for very large scattering species where the differences between the particular processing methods are greater.

Although in principle the slope of the conformation plot itself is sufficient for making conclusions about conformation and branching, the risk of misinterpretation is significantly reduced if a model linear counterpart is available. Since the slope of the conformation plot is very sensitive to the processing method used to determine the molar mass and RMS radius, for polymer samples covering very broad molar mass range it may be beneficial to divide the chromatogram into several sections and evaluate each section separately using the most appropriate processing method. Alternatively, the particular data points of the conformation plot can be obtained by means of individually evaluated Debye plots, where the most appropriate angular intervals and fit orders are used for each volume slice. The molar mass and RMS radius pairs obtained for a sufficient number of slices can be processed and plotted by Excel or Origin software.

Besides sensitivity to the light scattering method used for data processing, the conformation plots can be affected by delayed elution of branched polymers (see Section 6.2.1) and resolution of SEC columns. And as already mentioned, errors in the interdetector volume delay can affect the accuracy of the slope (see Figure 4.23).

4.3.5 Mark-Houwink Plots

Intrinsic viscosity is one of the most fundamental quantities in polymer science. It has had considerable historical importance in establishing the very existence of polymer molecules, and can still provide considerable insight into polymer structure and behavior. A modern way to generate Mark-Houwink plots is to

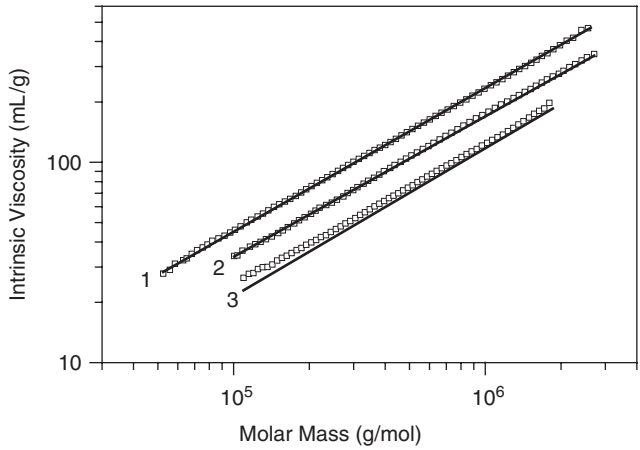

Figure 4.28 Mark-Houwink plots of (1) polystyrene, (2) poly(methyl methacrylate), and (3) poly(benzyl methacrylate) determined by SEC-MALS-VIS (symbols) compared with the literature Mark-Houwink equations (solid lines): $[\eta]_{PS} = 0.0117 \times M^{0.717}$, $[\eta]_{PMMA} = 0.0107 \times M^{0.70}$, $[\eta]_{PBZMA} = 0.00438 \times M^{0.738}$ (references12-14, respectively), THF at room temperature.

couple an SEC instrument to an online viscometer and a light scattering detector. The hyphenated SEC-MALS-VIS technique yields molar masses and intrinsic viscosities for narrow fractions eluting from SEC columns with the limitations discussed in relation to complex polymers.

Figure 4.28 compares Mark-Houwink plots obtained by SEC-MALS-VIS with those generated by classical measurements using a capillary viscometer. The results confirm that at least for homopolymers the SEC-MALS-VIS hyphenated technique represents a reliable and fast way to obtain the Mark-Howink plots.

Figure 4.28 shows excellent agreement for polystyrene and poly(methyl methacrylate), where the classical determination of Mark-Houwink parameters was performed using narrow PS and PMMA standards, whereas a slight discrepancy in the plots for poly(benzyl methacrylate) may be due to using fractions isolated by precipitation fractionation (i.e., samples of larger polydispersity than that of narrow SEC standards). The polydispersity within the elution volume slice due to co-elution of molecules of the same hydrodynamic volume, but different structure and molar mass, or due to band broadening in the SEC columns, is in most cases lower than the polydispersity of the fractions prepared by classical methods of polymer fractionation. Consequently, the Mark-Houwink parameters determined by means of SEC-MALS-VIS may often be more accurate than the values listed in the older scientific references.

Similarly as in the case of determination of the conformation plot, polydisperse samples covering at least one order of magnitude of molar mass are needed. The Mark-Houwink and conformation plots are affected by low signal intensities, and thus the beginning and end regions of the chromatogram with randomly scattered data points should be eliminated from the calculation.

The effect of the erroneous interdetector volume delay is similar to that in the case of the conformation plot; this issue is even more serious because of generally larger interdetector volumes between the viscometer and other detectors.

4.4 KEYNOTES

- MALS detection in SEC provides absolute molar mass distribution and molar mass moments, and completely eliminates the need for constructing the calibration curves with standards. A MALS photometer also yields the RMS radius distribution.
- The dependence of the RMS radius on molar mass (conformation plot) yields information about the molecular conformation of polymers in solution. The conformation plot is the most direct method for detection and characterization of branching.
- SEC-MALS data acquired at particular elution volume slices are processed by means of Debye plots. The processing can be performed using various light scattering formalisms. The selection of the processing method is typically not critical for smaller polymers, but it becomes more and more important with increasing molecular size.
- Combination of MALS detection with an online viscometer is a fast and accurate method for determination of a Mark-Houwink plot.
- The determination of molar mass distribution, conformation plot, and Mark-Houwink plot assumes efficient SEC separation yielding almost monodisperse fractions within the elution volume slice. However, the M_w and R_z values determined by SEC-MALS are based on the fundamental principle of light scattering and are completely independent of the efficiency of SEC separation.
- One of the important advantages of SEC-MALS compared to conventional SEC is significantly reduced sensitivity to operation variables such as flow rate, temperature, or column performance, which assures very good repeatability and reproducibility.

4.5 REFERENCES

1. Wyatt, P. J., *Analytica Chimica Acta*, **272**, 1 (1993).
2. Wyatt, P. J., in *Handbook of Size Exclusion Chromatography and Related Techniques*, 2nd Edition, Wu, C.-S. (editor), Marcel Dekker, New York (2004), p. 623.
3. Andersson, M., Wittgren, B., and Wahlund, K.-G., *Anal. Chem*., **75**, 4279 (2003).
4. Podzimek, S., in *Multiple Detection in Size-Exclusion Chromatography*, A. M. Striegel (editor), ACS Symposium Series **893**, Washington, D.C. (2004), p. 109.
5. Burchard, W, *Macromolecules*, **10**, 919 (1977).
6. Tackx, P. and Bosscher, F., *Analytical Communications*, **34**, 295 (1997).
7. Xie, T., Penelle, J., and Verraver, M., *Polymer*, **43**, 3973 (2002).

8. Saito, T., Lusenkova, M. A., Matsuyama, S., Shimada, K., Itakura, M., Kishine, K., Sato, K., and Kinugasa, S., *Polymer*, **45**, 8355 (2004).
9. Rissler, K., Socher, G., and Glockner, G., *Chromatographia*, **54**, 141 (2001).
10. Gaborieau, M, Gilbert, R. G., Gray-Weale, A., Hernandez, J. M., and Castignolles, P., *Macromol. Theory Simulations*, **16**, 13 (2007).
11. Netopilik, M., Bohdanecky, M., and Kratochvil, P., *Macromolecules*, **29**, 6023 (1996).
12. Kolinsky, M. and Janca, J., *J. Polym. Sci.: Polym. Chem. Ed*., **12**, 1181 (1974).
13. Podzimek, S., *J. Appl. Polym. Sci*., **54**, 91 (1994).
14. Podzimek, S. and Vlcek, T., *J. Appl. Polym. Sci*., **82**, 454 (2001).

Chapter 5

Asymmetric Flow Field Flow Fractionation

5.1 INTRODUCTION

The history of *field flow fractionation* (FFF) started with the work of Giddings[1] of the University of Utah in Salt Lake City. He and his team invented the principle of FFF, derived fundamental theory, developed various types of FFF, and constructed the first instruments. Although invented in the same decade when the first *size-exclusion chromatography* (SEC) instruments became commercially available, FFF suffered for a long time from the fact that reliable instruments were not commercially available and the work concentrated in several research groups working with their own instrumentation. For several decades, academic works concerning theoretical aspects of separation by various kinds of FFF prevailed over real applications; FFF did not become a widely applied and routine analytical tool. SEC thus became the dominant method used for the characterization of molar mass distribution of synthetic and natural polymers. Further progress in SEC occurred with the development of advanced detector systems such as online viscometers, which allowed full usage of the principles of universal calibration, and especially light scattering detectors that completely eliminated the need for column calibration. However, despite wide application range and versatility, SEC sometimes suffers from serious drawbacks that can be significantly reduced or even completely eliminated by the application of FFF.

This chapter focuses on *asymmetric flow field flow fractionation* (A4F), which currently represents the most instrumentally developed type of FFF with readily available instrumentation and numerous applications covering synthetic polymers, natural polymers, colloidal particles, proteins, vaccines, various biological materials, and environmental samples. Due to the recent development of a new generation of A4F instruments, the method has finally achieved the mature state

Light Scattering, Size Exclusion Chromatography and Asymmetric Flow Field Flow Fractionation: Powerful Tools for the Characterization of Polymers, Proteins and Nanoparticles, by Stepan Podzimek

where it can be used as routinely as SEC; especially in combination with a multi-angle light scattering (MALS) detector A4F represents a powerful method of polymer analysis and characterization with several advantages over traditionally used SEC.

One of the most serious limitations of SEC is the possibility of shearing degradation of polymer molecules with molar mass above about 10^6 g/mol.[2] Since most synthetic and natural polymers are polydisperse, many samples contain fractions running into the molar mass range of several millions g/mol, and for such samples the experimenter often does not know whether the high-molar-mass region of the molar mass distribution curve provides a true picture of the real molar mass distribution, or whether it was affected by shearing degradation. Finding out whether shearing degradation has occurred requires analysis under different conditions (flow rate, particle size of column packing) or crosschecking with batch light scattering. The critical molar mass at which shearing degradation occurs can be to a certain extent controlled by SEC separation conditions. The use of columns packed with 20-μm packing at a flow rate of 0.2–0.5 mL/min can especially extend the shearing degradation limit far beyond 10^6 g/mol. However, the possibility of shearing degradation in SEC columns can never be completely eliminated. The likelihood of shearing degradation is significantly reduced in A4F, where the system backpressure is several times lower than in SEC columns. For example, two 300 × 8-mm columns packed with 5-μm packing at room temperature with THF at 1 mL/min yield pressure of about 60 bar, whereas the pressure in the A4F channel is mostly below 10 bar; thus the method can be supposed to be relatively nondestructive.

Another very important advantage of A4F is that the lack of stationary phase strongly eliminates the enthalpic interactions of macromolecules with column packing. Various polymers containing polar functional groups have a strong tendency to interact with SEC columns and thus to suppress the size-based separation. Proteins and various polyelectrolytes are other examples of important polymers that often show non–size exclusion separation mechanisms. Although the macromolecules analyzed by A4F are in contact with the semipermeable membrane of the accumulation wall, the total contact surface is much lower compared to the packed porous SEC columns and thus enthalpic interactions are significantly less likely. The SEC separation according to hydrodynamic size is also affected in the case of branched polymers due to their specific elution behavior (see Section 6.2.1). This problem does not exist in A4F separation.

The characterizations of (1) ultra-high-molar-mass polymers, supermolecular structures, and particles, (2) polymers having a tendency to enthalpic interactions with SEC columns, and (3) branched polymers represent the key application areas of A4F. However, the method offers other advantages that are outlined in the following.

The injection volume in SEC is limited to a maximum of about 200 μL per 300 × 8-mm column, and actually lower injection volumes in the range of 50–100 μL should be preferred. Injection of, for example, 200-μL solution at 1-mL/min flow rate takes 12 seconds. That means the molecules injected into the

column at the end of injection are 12 s delayed after the molecules injected at the beginning. Using two regular 300 × 7.5-mm columns, the polymer molecules elute in the range of about 8–17 minutes. That means the 12 s injection time is obviously acceptable because the molecules have enough time to "catch" each other and sort out according to their hydrodynamic size. However, this simple example shows that it is impossible to significantly increase the injected volume without excessive contribution to the peak broadening. On the other hand, in A4F the injected molecules do not start their passage through the channel immediately after the injection; they stay close to injection inlet and are focused after the injection to a common starting line. This allows for increasing the injection volume to several milliliters without affecting the resolution. The possibility of large-volume injections may be useful for the analysis of samples that can be prepared only at very low concentrations (e.g., environmental samples) or that are available as a small drop. The drop can be diluted to a larger volume that can be easily handled and injected.

In SEC, resolution can be controlled mainly by using different numbers of columns or columns of different particle size and/or porosity. In A4F, resolution can be controlled by separation conditions and thus polymer samples of extremely broad molar mass range of $\approx 10^4 - 10^9$ g/mol can be analyzed using the same separation device.

Changing the solvent in SEC requires many hours to replace the solvent completely and to stabilize the baseline of the RI detector because typical SEC packing is swollen gel and thus it takes a long time for the old solvent to be completely replaced by the new solvent. The solvent change in A4F is fast because of low total system volume and no stationary phase. In addition, absence of stationary phase also eliminates possible column bleeding, which disturbs the signal of a light scattering detector.

SEC columns are relatively delicate devices that can be damaged by improper use (e.g., solvent evaporation during storage, use of incompatible solvent, injection of samples containing insoluble matters or sample precipitation in the columns, excessive pressure, or mechanical shocks). In addition, supermolecular structures and molecules interacting with column packing can be irreversibly retained in SEC columns, which not only causes loss of information about the sample under analysis, but also shortens column lifetime. The A4F channel is practically indestructible, and channel membrane, when contaminated, can be easily replaced at a cost that is a small fraction of that of an SEC column.

5.2 THEORY AND BASIC PRINCIPLES

Fundamental FFF theory can be found in the articles of Giddings and Wahlund and their coworkers,[3–6] books such as references 7 and 8, or the *FFF Handbook*,[9] which may be also used as sources of further references. In the context of A4F, one must point out the article in reference 6, which represents the fundamental description of theory related to the asymmetric channel.

Although by the applications and instrumentation A4F resembles liquid chromatography, there is a principal difference from any kind of liquid chromatography that is due to the absence of stationary phase. The separation in A4F is achieved with no stationary phase, solely by a flow in an empty channel where a perpendicular flow force is applied. The channel consists of two plates jointed together that are separated by a spacer. The bottom plate is permeable, made of porous frit covered by a semipermeable membrane with a typical cutoff of 5 or 10 kDa (kg/mol). The membrane is permeable for the molecules of eluent (the term *carrier* is often used in FFF literature), but impermeable for the polymer molecules and colloidal particles and therefore keeps the sample in the channel so that it is directed by flow to the channel outlet.

In the originally developed symmetrical design, the channel with both walls permeable to cross flow was used and the field was generated by the solvent being pumped into the channel through the upper wall and leaving the channel through the accumulation wall. An obvious disadvantage of this configuration is that it requires two HPLC pumps, which increases the cost of the apparatus as well as maintenance requirements and probability of system breakdown. In the asymmetric A4F equipment, the upper plate is impermeable and only the bottom plate is permeable. This design permits making all flows with a single pump.

A typical asymmetric channel and its main parts are depicted in Figure 5.1. In contrast to SEC, the sample is not injected directly into the main stream, but the channel has a separate inlet for sample injection. The channel spacer is cut out of a thin plastic (e.g., Teflon) sheet (Figure 5.2) of usual thickness of 350 μm, which is sandwiched between two blocks to create a ribbon-like channel. The cross section of the channel is rectangular and usually decreases from the channel inlet toward the channel outlet. The laminar flow of the carrier creates a parabolic flow profile within the channel (Figure 5.3); that is, the carrier moves more slowly closer to the channel walls compared to the channel center. The analyzed molecules and particles are driven by the cross flow toward the bottom wall of the channel. Diffusion creates a counteracting motion due to which smaller particles, which have higher diffusion coefficients, move closer to the channel center, where the axial flow is faster. The velocity gradient inside the channel separates the molecules and particles according to their hydrodynamic size in such a way that smaller molecules elute before the larger ones. This means that A4F separation is the opposite of SEC separation, in which the large molecules elute first.

The schematic view of the separation channel used in A4F is in Figure 5.3. The axial (longitudinal, channel) flow velocity profile is parabolic, with the axis of symmetry located in the center of the channel:[10]

$$v(x) = 6\langle v\rangle \left(\frac{x}{w} - \frac{x^2}{w^2}\right) \tag{5.1}$$

where x is the distance from the bottom (accumulation) wall, w is the channel thickness (i.e., distance between the accumulation wall and upper wall), and $\langle v\rangle$ is the average cross-sectional carrier velocity (cm/s) along the axis of the channel.

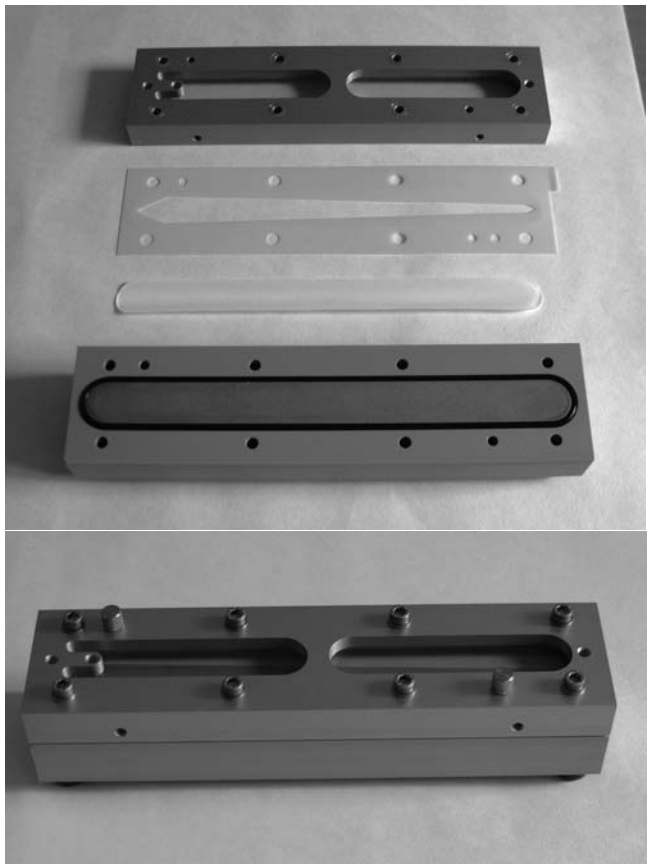

Figure 5.1 Components of A4F channel (top) and assembled channel (bottom). Components (from top to bottom): upper block consisting of metal part and transparent polycarbonate inlay, spacer, semipermeable membrane; bottom block with a frit and sealing o-ring. Dimensions: 290 × 70 × 50 mm.
Source: Courtesy of Wyatt Technology Europe.

The equations given in the following text describe the main parameters of the separation process.[6] They can be used as guidelines for understanding the experimental results and optimizing the experimental variables such as channel flow rate, cross flow rate, channel length and thickness, and temperature.

The cross flow velocity (cm/s) as a function of the distance from the accumulation wall is:

$$u(x) = u_0 \left(1 - \frac{3x^2}{w^2} + \frac{2x^3}{w^3}\right) \tag{5.2}$$

where u_0 is the cross flow velocity at the accumulation wall. The cross flow velocity is zero at the upper wall and increases toward the bottom wall, as

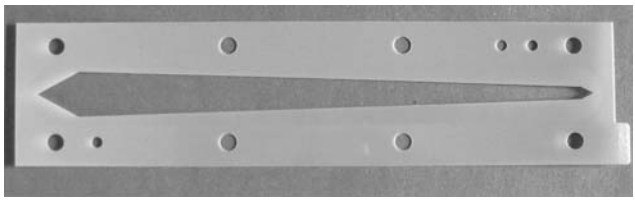

Figure 5.2 Top view of A4F spacer (trapezoidal shape). Tip-to-tip length = 265 mm, length of the triangular tapered inlet = 20 mm, length of the triangular tapered outlet = 5 mm, breadth at the widest point of the tapered inlet = 22 mm, breadth at the widest point of the tapered outlet = 6 mm, area ≈ 36 cm^2.
Note: This channel shape and 5-kDa regenerated cellulose membrane were used to collect the experimental results presented in this chapter.
Source: Courtesy of Wyatt Technology Europe.

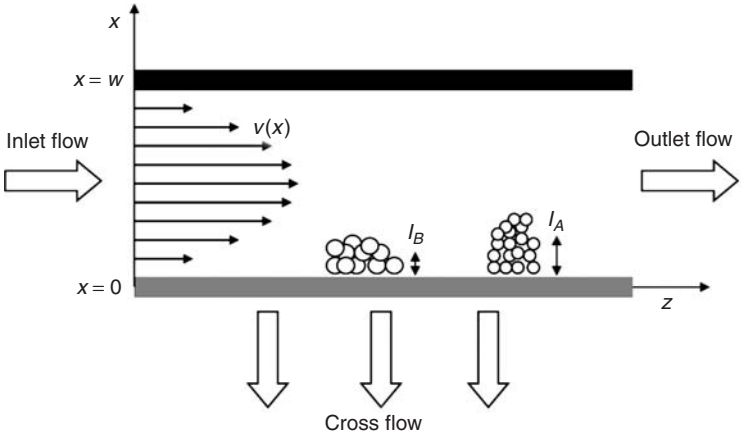

Figure 5.3 Schematic illustration of side view of A4F channel with zones of compounds A and B flowing in the direction of longitudinal axis z; w is the channel thickness; $v(x)$ is the flow velocity as a function of distance from the channel bottom (accumulation wall); l_A and l_B are the centers of gravity of zones of compounds A and B.

shown in Figure 5.4. The change of the cross flow velocity with the distance from the accumulation wall is a principal difference from the symmetrical flow FFF, where the cross flow velocity is constant across the channel.

It is worth noting that close to the accumulation wall the cross flow velocity is approximately constant, which means that for highly retained samples the separation can be described in the same way as in symmetrical flow FFF. As shown in reference 11, the cross flow velocity does not change along the longitudinal axis of the channel.

The longitudinal flow velocity as a function of axis z decreases linearly according to relation 5.3:[6]

$$\langle v \rangle = \langle v \rangle_0 - \frac{u_0}{w} z \tag{5.3}$$

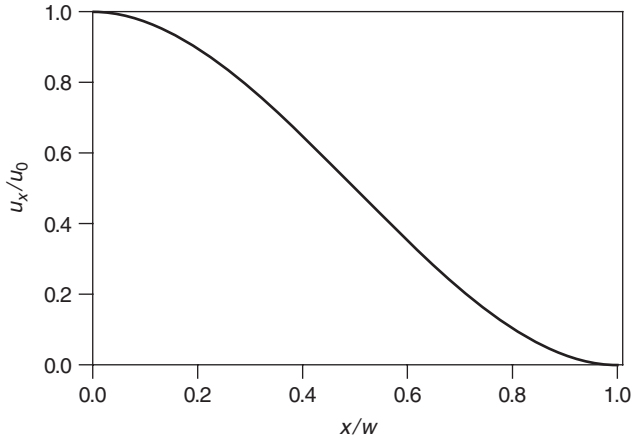

Figure 5.4 Cross flow velocity related to the cross flow velocity at the accumulation wall (u_0) as a function of distance x from the accumulation wall related to total channel thickness w (Equation 5.2).

where $\langle v \rangle_0$ is the average longitudinal flow velocity at the channel inlet. For a given channel thickness the steepness of the decrease of the longitudinal flow velocity is controlled by the cross flow velocity at the accumulation wall. Note that using the trapezoidal channel (see Figure 5.2) the decrease of the longitudinal flow velocity is compensated by the decreasing channel cross section. Comparison of velocity gradients in the rectangular and trapezoidal channels was published in paper[12]. The obtained results favor the trapezoidal channel over the rectangular one, and also the asymmetrical versus the symmetrical channel.

The concentration profile of the analyzed sample with respect to the distance from the accumulation wall can be approximated by:[6]

$$c = c_0 e^{-\frac{x}{l}} \tag{5.4}$$

where c_0 is the concentration at the channel accumulation wall and l is the distance of the center of the sample layer from the accumulation wall, equal to:

$$l = \frac{D}{u_0} \tag{5.5}$$

and D is the sample diffusion coefficient (cm^2/s). To account for different channel dimensions, the distance l is related to the channel thickness:

$$\lambda = \frac{l}{w} \tag{5.6}$$

Retention parameter λ defines the distance between the accumulation wall and the center of gravity of the sample zone relative to the channel thickness. As seen

from Equations 5.5 and 5.6, the retention parameter is related to the properties of the analyzed molecules, the strength of the cross flow, and the channel thickness.

Assuming the usual cross flow of 3 mL/min and membrane area of about 36 cm^2, the corresponding $u_0 \approx 0.0014$ cm/s. The diffusion coefficients of polystyrene molecules of molar masses of 10^4 g/mol, 2×10^5 g/mol, and 2×10^6 g/mol are approximately 2×10^{-6} cm^2/s, 4×10^{-7} cm^2/s, and 1.2×10^{-7} cm^2/s, respectively. The distances l corresponding to these molar masses are 14.3 μm, 2.9 μm, and 0.9 μm, respectively; that is, assuming channel thickness of 300 μm the corresponding retention parameters λ are about 0.048, 0.010, and 0.003. It is evident that even for relatively small molecules with molar mass close to the cutoff of membrane the center of the sample layer is in close proximity to the channel bottom.

The concentration profiles for polystyrene molecules of different molar mass are shown in Figure 5.5. The curves illustrate how the sample concentration is distributed across the channel and how it depends on the diffusion coefficient. The injected sample forms a layer whose thickness is determined by the diffusion coefficient and the cross flow velocity.

The effect of the cross flow on the concentration profile is demonstrated in Figure 5.6. The concentration of monodisperse molecules in the layer decreases exponentially with the distance from the accumulation wall. For a polydisperse sample, the total concentration profile is a superimposition of the profiles of individual species in the sample and the molecules are distributed within the layer according to their diffusion coefficients. It has been shown in reference 6 that for identical λ the concentration profile in the asymmetrical channel is less compressed against the accumulation wall than that in the symmetrical channel, but the difference is negligible for λ less than about 0.1.

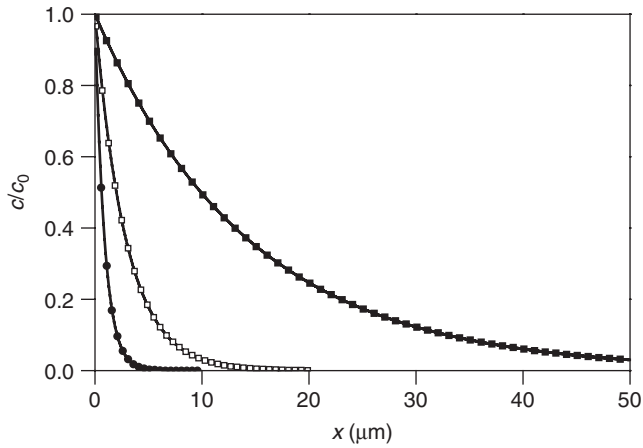

Figure 5.5 Concentration profiles for three polystyrene molecules of molar mass 10^4 g/mol (■), 200×10^3 g/mol (□), and 2×10^6 g/mol (•). Centers of sample layers $l = 14.3$ μm (■), 2.9 μm (□), and 0.9 μm (•). Cross flow = 3 mL/min, accumulation wall area = 36 cm^2.

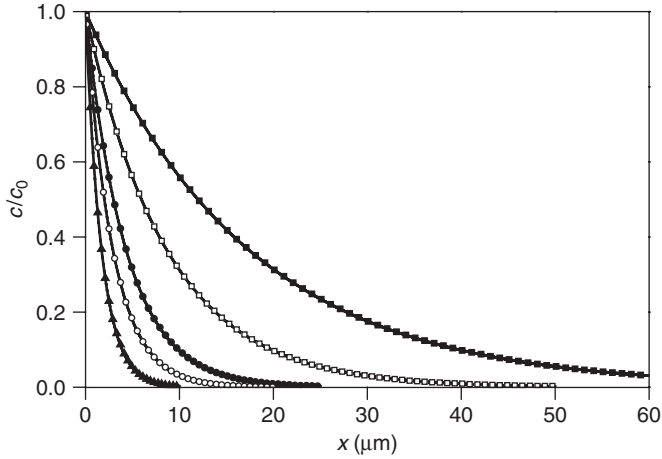

Figure 5.6 Concentration profiles for polystyrene of molar mass of 200,000 g/mol at various cross flow rates: 0.5 mL/min (■), 1 mL/min (□), 2 mL/min (●), 3 mL/min (○), and 5 mL/min (▲). Accumulation wall area = 36 cm^2.

In real experiments, the volumetric flow rates in mL/min are measured instead of velocities in cm/s:

$$u_0 = \frac{\dot{V}_c}{bL} \tag{5.7}$$

$$\langle v \rangle_0 = \frac{\dot{V}_{in}}{bw} \tag{5.8}$$

$$V_0 = bLw \tag{5.9}$$

where V_0 is the channel volume; $\dot{V}_c$ and $\dot{V}_{in}$ are the volumetric cross flow and the volumetric inlet flow (at $z = 0$), respectively; and L, b, and w are the channel length, the channel breadth, and the channel thickness, respectively. The product Lb equals the membrane surface, but for a channel with uneven channel breadth the membrane surface must be calculated according to a given spacer shape. All the flow rates can be easily measured directly and their mutual relation is:

$$\dot{V}_{in} = \dot{V}_c + \dot{V} \tag{5.10}$$

where $\dot{V}$ is the volumetric channel outlet flow (detector flow) at $z = L$. Substituting Equations 5.7 and 5.9 into the expressions for the retention parameter (Equations 5.5 and 5.6) we get:

$$\lambda = \frac{DV_0}{w^2 \dot{V}_c} \tag{5.11}$$

Equation 5.11 can be rearranged using the expression for the channel volume to the form:

$$\lambda = \frac{DbL}{\dot{V}_c w} \tag{5.12}$$

Retention ratio, which describes the retention of the molecules of given diffusion coefficient compared to the molecules that are under given experimental conditions unretained by the applied cross flow, is defined as:

$$R = \frac{v}{\langle v \rangle} \tag{5.13}$$

where v is the migration velocity of given molecules and $\langle v \rangle$ is the average longitudinal carrier velocity. The retention ratio can range from unity for an unretained sample to zero for a completely retained sample. The retention ratio can be expressed as follows:[13]

$$R = 6\lambda \left(coth \frac{1}{2\lambda} - 2\lambda \right) \tag{5.14}$$

The bracketed function of hyperbolic cotangent approaches unity with decreasing λ and thus for many practical cases the retention can be described by the simple relationship:

$$R = 6\lambda \tag{5.15}$$

or

$$R = 6\lambda - 12\lambda^2 \tag{5.16}$$

Equation 5.15 is accurate within 5% when $\lambda < 0.02$; Equation 5.16 is accurate within 2% when $\lambda < 0.2$. The above equations show that retention is exclusively controlled by the retention parameter, that is, by the diffusion coefficient related to the cross flow velocity and channel thickness. The term *retention* refers to the fact that the particles are retained by forcing them close to the channel bottom into streamlines that move with slower velocity than the average. Alternatively, the retention ratio can be expressed as:

$$R = \frac{t_0}{t_R} \tag{5.17}$$

where t_0 is the void time of unretained component travelling with the average carrier velocity, t_R is the retention time of the investigated component. The retention time in A4F can be approximated by the following expressions:[6]

$$t_R = \frac{w^2}{6D} \ln \left(1 + \frac{\dot{V}_c}{\dot{V}} \right) = \frac{w^2 \pi \eta R_h}{kT} \ln \left(1 + \frac{\dot{V}_c}{\dot{V}} \right) \tag{5.18}$$

$$t_R = \frac{w^2}{6D} \ln \left(\frac{z_f/L - \dot{V}_{in}/\dot{V}_c}{1 - \dot{V}_{in}/\dot{V}_c} \right) = \frac{w^2 \pi \eta R_h}{kT} \ln \left(\frac{z_f/L - \dot{V}_{in}/\dot{V}_c}{1 - \dot{V}_{in}/\dot{V}_c} \right) \tag{5.19}$$

where w is the channel thickness, D is the diffusion coefficient related with the hydrodynamic radius R_h by Stokes-Einstein relation, k is the Boltzmann's constant, T is the absolute temperature, η is the viscosity of the carrier, z_f is the position of the focusing point, and $\dot{V}_{in}$, $\dot{V}_c$ and $\dot{V}$ are the inlet flow rate, the cross flow rate and the detector flow rate, respectively. Equation 5.18 applies for the case when sample elution starts directly at the channel inlet, i.e., $z_f = 0$. Note that for given experimental conditions, the sample components are separated solely according to their hydrodynamic radius, since R_h is the only quantity in Equations 5.18 and 5.19 that is characteristic of the analyzed molecules. Molar mass, which is a far more desirable quantity for the characterization of polymer samples, is related to the diffusion coefficient by Equation 1.20.

The A4F analysis consists of three steps: (1) *injection*, (2) *focusing* and *relaxation*, and (3) *elution*. During the first two steps, injection and focusing, the flow delivered by the HPLC pump is split, enters the channel from the inlet and outlet, and is balanced to meet near the injection port. At this step the eluent moves only in cross direction, permeates the membrane, and exits from the cross outlet of the channel. The sample moves and becomes focused at a certain distance from the channel inlet as a narrow line, from which the elution begins after the flow is switched into the elution mode. The focusing step can be visualized by injection of a colored polymer (blue dextran can be used for this purpose; see Figure 5.7). After complete injection of the sample solution, the injection flow is stopped and the sample is focused for several additional minutes before the third step (elution), when the eluent flows from the channel inlet to the channel outlet that is connected to detectors. Sample focusing is the transport of the injected sample axially to the focusing line. The time needed for this step (focusing time t_f) was derived in reference 6:

$$t_f \approx \frac{w^2 \ln(1-f)}{-6D} \tag{5.20}$$

where f is the factor <1 (e.g., 0.99). Equation 5.20 shows that the focusing time is independent of the flow rate, and it is directly proportional to the square of channel thickness and indirectly proportional to the diffusion coefficient. It is evident that for high-molar-mass components with low diffusion coefficients the focusing time might range from minutes to hours. The position of the focusing line can be controlled by the ratio of the flow rates entered into the channel inlet and outlet:

$$z_f = L\frac{\dot{V}_{in,f}}{\dot{V}_{in,f} + \dot{V}_{out,f}} \tag{5.21}$$

where z_f is the position of the focusing line, L is the channel length, $\dot{V}_{in,f}$ is the flow rate that enters the channel inlet and $\dot{V}_{out,f}$ is the flow rate that enters the channel from the outlet, and the index f refers to the focusing and

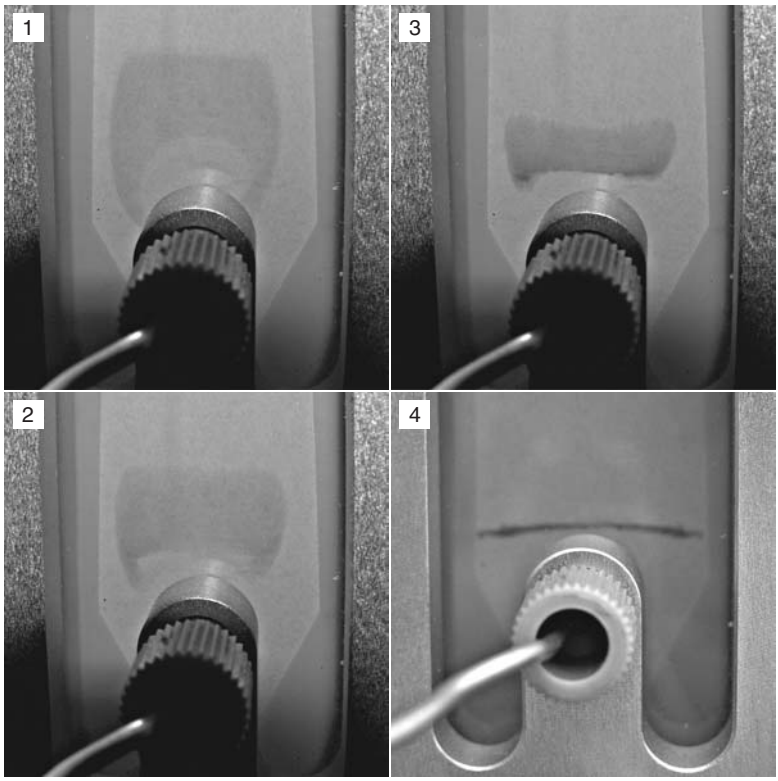

Figure 5.7 Images taken during the focusing of blue dextrane at approximately (from 1 to 4) 3 min, 5 min, 7 min, and 18 min after the injection. Channel thickness ≈300 μm.

relaxation process. To maximize the length of the channel for elution and separation, the focusing point should be near the channel inlet (i.e., a few millimeters from the injection inlet toward the channel outlet; see (Figure 5.7). In order to achieve the position of the focusing point near the channel inlet, $\dot{V}_{out,f}$ must be $\gg \dot{V}_{in,f}$.

Simultaneously with the focusing, the sample is concentrated near the accumulation wall. At the time of injection into the channel the sample is distributed across the entire channel thickness. After the injection, the sample moves toward the accumulation wall with a velocity equal to that of the cross flow; the focus flow during the sample injection and subsequent focusing period causes the sample relaxation. Relaxation means establishing the concentration equilibrium against the accumulation wall. The relaxation time (τ) needed for complete sample relaxation in symmetric flow FFF is given by the ratio $V_0/\dot{V}_c$. Since in asymmetric flow FFF the cross flow velocity decreases with increasing distance from the accumulation wall and approaches zero at the upper wall, the species close to the upper wall would require very long times to be transported across

the channel; that is, a part of the injected sample would create an almost stagnant layer at the proximity of the upper wall. However, even the molecules that are situated very close to the upper wall do not stay there indefinitely, because they are driven from this stagnant layer by diffusion. The combination of both cross flow and diffusion can be described by the following equation:[6]

$$\tau \approx \left(\frac{V_0}{3\dot{V}_c}\right)^{\frac{2}{3}} \left(\frac{w^2}{mD}\right)^{\frac{1}{3}} \tag{5.22}$$

where m is a constant of order unity. For example, for polystyrene molecules of $M = 2 \times 10^6$ g/mol, using a typical channel of $V_0 \approx 1$ mL, $w \approx 300$ μm, and $\dot{V}_c = 3$ mL/min, the relaxation time is roughly 70 sec.

5.2.1 Separation Mechanisms

The major A4F separation mechanism is called *normal* or *Brownian separation* and governs submicrometer colloidal particles and macromolecules. The normal mode is based on the transport of relatively small particles driven by the cross flow toward the accumulation wall and their concentration in the proximity of the wall. The increase of concentration near the wall creates a concentration gradient that causes the diffusion away from the wall. As the transport of molecules continues and the concentration gradient increases, the counteracting diffusion increases proportionally until it balances the cross flow–driven transport toward the wall. The balance of the two counteracting transport processes forms a cloud of particles having an equilibrium concentration distribution. The concentration of particles decreases exponentially with distance from the accumulation wall and different components have different concentration profiles (Figure 5.5). The separation in normal mode is based on the fact that particles of different diffusion coefficients form layers of different thickness and different mean elevation above the accumulation wall. In parabolic flow profile the thickest layers flow fastest, followed by layers that are more and more compressed to the accumulation wall. Thus the normal elution order is from the smallest to the largest particles.

In the case of much larger particles with diameter approximately above 1 μm, the diffusion coefficients are very low, the Brownian motion becomes negligible, and the diffusion does not create a sufficient counteracting force against the flow force. The large particles are driven by the cross flow directly to the accumulation wall and stay there in direct contact with the wall. The layer thickness in this case is controlled solely by the geometrical dimensions of the particles; the larger particles extend further into the faster flowing streamlines of the channel. This is called *steric separation*, and the separation order is inverted compared to the normal separation (i.e., larger particles elute before the smaller ones). This idealized model of steric separation is affected by hydrodynamic lift forces that disturb direct contact of particles with the wall. The hydrodynamic forces increase

with increasing channel flow rate as well as with increasing particle size. The hydrodynamic lift forces are oriented from the wall and thus they move the particles away from the accumulation wall. The movement of the particles from the wall is counteracted by the cross flow until equilibrium is reached. As a consequence of the balance of hydrodynamic lift forces and cross flow, particles of different sizes form narrow bands at different elevations above the wall. This mechanism is called *hyperlayer separation*. Retention in hyperlayer A4F is given by the ratio of the cross flow strength and the counteracting lift forces. The elution order is identical as in the case of steric separation.

Both separation modes are illustrated in Figure 5.8. In real experiments, it is practically impossible to distinguish between steric and hyperlayer separation, because they are closely related and produce similar separation results. Also the inversion point between the normal and steric-hyperlayer separation cannot be expected to be sharp. The steric-hyperlayer separation mode can occur simultaneously with the normal separation. This can happen in the case of polydisperse samples with a broad size distribution that spans across the steric inversion diameter. In the case of such samples the smaller components elute in the normal mode and the larger in the steric-hyperlayer mode. The co-elution of normally and sterically migrating components of a polydisperse sample increases the polydispersity of fractions eluting at a given time from the channel.

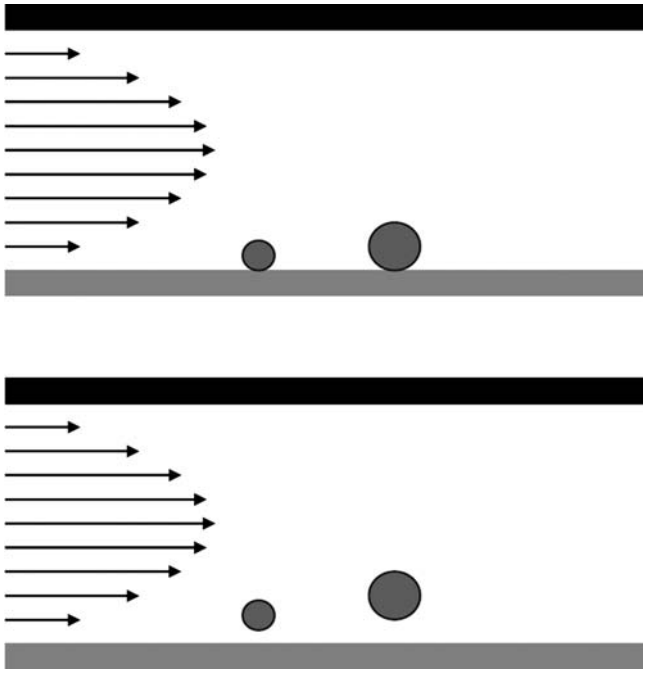

Figure 5.8 Schematic illustration of steric separation (top) and hyperlayer separation (bottom).

The steric inversion diameter, at which the transition between the normal and steric-hyperlayer modes occurs, has been reported between 0.3–3 μm. [14,15] It can be shifted by changing experimental conditions.[16] For polymers, the separation conditions are mostly chosen so as to work completely in the normal separation mode before the inversion point. When steric-hyperlayer separation becomes active for high-molar-mass fractions, the normal mode can be enhanced by raising the temperature, that is, intensifying Brownian movement, using channels of larger thickness (i.e., making the molecules relatively smaller), or decreasing $\dot{V}$ and $\dot{V}_c$. Although the steric-hyperlayer mode is usually unwanted in the case of separation of polydisperse polymers, it can be effectively used for the separation of larger particles.

For midsized particles, where both separation mechanisms play role in retention, the retention ratio can be written as:[14]

$$R = 6\lambda + 3\frac{\gamma d}{w} \tag{5.23}$$

where γ is the dimensionless steric correction parameter of the order of unity and d is the diameter of the particles. For small particles, the second term of the above equation becomes negligible and the retention can be approximated by Equation 5.15. For very large particles, the retention parameter becomes insignificant because of very slow diffusion, while the ratio d/w becomes significant. The factor γ can be set as unity to simplify the above expression. The values of $\gamma > 1$ apply to hyperlayer separation when hydrodynamic lift forces lift the particles away from the wall.

5.2.2 Resolution and Band Broadening

As with SEC, the A4F technique is often used to separate and characterize the molar mass distribution of polydisperse polymers. The *selectivity* of the separation process can be defined in the same way as in SEC by the slope of molar mass–versus–retention (elution) time dependence. This slope reflects how well a separation device (A4F channel, SEC column) can separate monodisperse polymers of different molar mass. The selectivity of the separation process can be defined as:

$$S = \left| \frac{d(\log t_R)}{d(\log M)} \right| \tag{5.24}$$

where the absolute value reflects the fact that retention time increases (in A4F) or decreases (in SEC) with molar mass. Selectivity according to Equation 5.24 is based on molar mass. Alternatively, selectivity can be defined in terms of size:

$$S = \left| \frac{d(\log t_R)}{d(\log d)} \right| \tag{5.25}$$

where d is the particle diameter. Indexes M or d can be used to distinguish the selectivity based on molar mass or size, respectively.

The relation between selectivity and sample retention is given by the following equation:[17]

$$S = \left| 3\left(\frac{R}{36\lambda^2} + 1 - \frac{1}{R} \right) \right| \left| \frac{d(\ln \lambda)}{d(\ln M)} \right| \tag{5.26}$$

The above relation shows that the value of S increases as R decreases and approaches its maximum value S_{max} at low R (high retention) when Equation 5.15 becomes a true approximation of the relation between R and λ. The maximum selectivity:

$$S_{max} = \left| \frac{d(\ln \lambda)}{d(\ln M)} \right| \tag{5.27}$$

equals the exponent β of the molar mass dependence of diffusion coefficient as evident from Equation 5.11 and molar mass dependence of diffusion coefficient (Equation 1.20). That means the selectivity depends on the conformation of the sample being analyzed and thermodynamic quality of the solvent and typically varies in the range of about 0.3–0.7. The dependence of selectivity on molecular conformation indicates that selectivity will decrease with increasing degree of branching. Generally, the typical selectivity of A4F is markedly more than that of SEC (generally around 0.1).

A graphical illustration of Equation 5.26 is shown in Figure 5.9. The comparison of selectivity of A4F and of SEC obtained for a typical polydisperse polymer measured under typical A4F and SEC experimental conditions is shown in Figure 5.10. The data were obtained by a MALS detector and a commercially

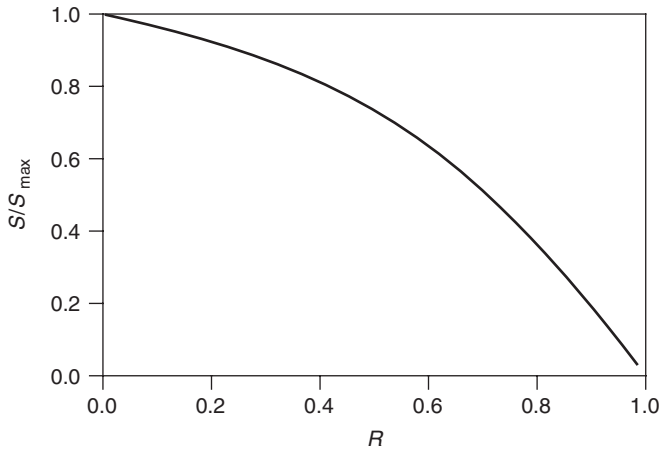

Figure 5.9 A4F selectivity as a function of retention. S_{max} is the selectivity in the limit of very high retention that equals the exponent β in the molar mass dependence of diffusion coefficient.

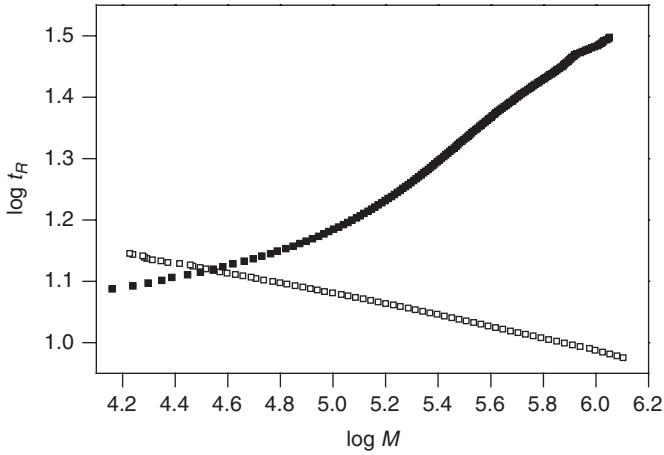

Figure 5.10 Selectivity plot log t_R versus log M for broad linear polystyrene analyzed by SEC-MALS (□) and A4F-MALS (■) using typical separation conditions. SEC: 2 × 300 × 7.5 mm PLgel Mixed-C 5-μm columns, injection 100 μL 0.25% w/v, THF at 1 mL/min, 35°C; A4F: detector flow 1 mL/min, cross flow 3 mL/min to 0.15 mL/min within 30 min plus 5 min at 0.15 mL/min, injection 100 μL 0.25% w/v, 350 μm spacer, temperature 60°C. SEC/A4F slopes = 0.08/0.10, 0.08/0.21, 0.09/0.35, and 0.1/0.30 for log M range of 4.3–4.8, 4.8–5.2, 5.2–5.6, 5.6–6.0, respectively.

available A4F channel and high-performance SEC columns. Selectivity for a certain molar mass range is determined as the slope of the plot log t_R versus log M. Selectivity can also be estimated from the plot of log M versus log t_R (i.e., SEC calibration curve). Then a decrease of the slope indicates increased selectivity.

High selectivity means that there is a significant change of retention time with a small change of molar mass or particle size. However, the quantity that describes the quality of separation of two components is the *resolution* that takes into account both selectivity and *efficiency* (i.e., *band-broadening* effects).

The resolution of the two components can be expressed as:[18]

$$R_S = \frac{\Delta t_R}{4\bar{\sigma}} = \frac{1}{4}\frac{\Delta R}{\bar{R}}\left(\frac{L}{\bar{H}}\right)^{\frac{1}{2}} \tag{5.28}$$

where Δt_R is the difference in retention time of the two components, $\bar{\sigma}$ is the average standard deviation of the two peaks, ΔR is the difference of retention ratio, $\bar{R}$ and $\bar{H}$ are the average values of R and H for the two components, and L is the channel length. This equation shows that resolution increases with $N^{1/2}$. Band broadening (also called *zone broadening*, *zone dispersion*, *zone spreading*, *axial dispersion*) is expressed in terms of *plate height* (H) or number of theoretical plates $N = L/H$. High selectivity means high resolution only if zone broadening is small, because high selectivity can be distorted by excessive band broadening.

There are several contributions to H, for example, axial diffusion, nonequilibrium, polydispersity, instrumental effects (channel irregularities, reversible adsorption of components on the accumulation wall, overloading), and contributions outside the channel such as spreading in connecting tubings and detector cells. Note that unlike SEC the contribution caused by injection of finite sample volume is eliminated by sample focusing.

The contribution of the axial diffusion can be expressed as:

$$H_d = \frac{2D}{R\langle v \rangle} \tag{5.29}$$

where R is the retention ratio, D is the diffusion coefficient, and $\langle v \rangle$ is the average carrier velocity. The effect of axial diffusion increases with increasing sample retention. However, the contribution of H_d is usually negligible because polymers have generally low diffusion coefficients.

For highly retained components (small λ) the nonequilibrium contribution to plate height can be approximated as:[19]

$$H_n = 24\lambda^3(1 - 8\lambda + 12\lambda^2)\frac{w^2\langle v \rangle}{D} \tag{5.30}$$

In the case of lower retention levels, the above equation includes more complicated functions of λ, while for $\lambda \rightarrow 0$ the bracketed term in Equation 5.30 can be neglected. Nonequilibrium is the most important source of band broadening in A4F, which originates from the fact that particular molecules of the sample layer flow in the channel at different velocities. The molecules of identical hydrodynamic radius do not form a thin layer at a given streamline, but they protrude from the wall to streamlines of different velocity (see Figure 5.5). As a consequence of that, molecules of a given kind do not move toward the channel outlet with the same velocity, but they move with the velocity given by the distance x of a particular streamline from the accumulation wall. Different velocities of different streamlines spread the sample axially, because the molecules located closer to the channel center forerun those located closer to the bottom wall. The concentration gradients created by spreading are counteracted by tangential diffusion so that the rapidly moving sample components diffuse toward the accumulation wall while slowly moving components diffuse away from the wall.

The way to reduce nonequilibrium dispersion is to reduce λ, that is, to form more compact sample layers by increased cross flow. The nonequilibrium dispersion is also reduced by using small channel thickness w and low carrier velocity. Note that in A4F $\langle v \rangle$ changes along the longitudinal axis and the time-average carrier velocity $\langle \bar{v} \rangle$ must be used in the relations for plate height.

A significant contribution to plate height is caused by sample polydispersity. In contrast to other plate height contributions, this broadening actually represents the separation process and is not destructive. In fact, sample polydispersity is not a true broadening factor; H_p represents band broadening as a result of true sample separation. Typically, the polydispersity term of plate height is nonnegligible

even for samples of low polydispersity, which indicates the high resolving power of A4F. For samples of low-to-moderate polydispersity, the contribution of polydispersity to plate height is:[20]

$$H_p = LS^2\left(1 - \frac{1}{\mu}\right) \tag{5.31}$$

where μ is polydispersity M_w/M_n, and selectivity S can be calculated from the average retention ratio via Equation 5.26, or determined experimentally from the slope of log t_R–versus–log M relation.

The general expression for the plate height is given as the sum of individual contributions:

$$H = H_d + H_n + H_p + \Sigma H_i \tag{5.32}$$

where subscripts d, n, p, and i indicate contributions of axial diffusion, nonequilibrium, polydispersity, and the sum of other contributions, respectively. The nonequilibrium term shows a significant dependence on carrier velocity (Equation 5.30). That means extrapolation of H to zero velocity eliminates the nonequilibrium contribution to the plate height. Then, assuming H_d and ΣH_i to be negligible, one can determine H_p from the intercept at zero velocity and thus calculate the sample polydispersity from Equation 5.31. The determination of plate height can be performed by the usual procedure based on peak retention time and baseline width or half-height width.

Another parameter describing the separation in A4F is *fractionating power*, which can be defined on the basis of diameter (d) or molar mass (M):[21]

$$F_d = \frac{R_S}{dd/d} = \frac{d}{4\sigma}\frac{dt_R}{dd} = \frac{t_R}{4\sigma}S_d \tag{5.33}$$

$$F_M = \frac{R_S}{dM/M} = \frac{M}{4\sigma}\frac{dt_R}{dM} = \frac{t_R}{4\sigma}S_M \tag{5.34}$$

where d is the particle diameter, M is the molar mass, dt_R/dd and dt_R/dM are the changes in retention time with d or M, respectively, and σ is the standard deviation of the peak. According to the above equations the fractionating power can be understood as the resolution between particles whose diameters differ by the relative increment dd/d, or whose molar masses differ by the relative increment dM/M.

5.3 INSTRUMENTATION

In asymmetric flow FFF instruments, splitting the main flow delivered by a chromatographic pump into the channel generates the cross flow. The A4F instrumentation is currently manufactured by Wyatt Technology Europe and Postnova. The Postnova AF2000 system utilizes (along with the main pump) a second

syringe pump, which withdraws liquid from the channel cross flow outlet, and a third, separate pump that is used for sample injection. The Wyatt Technology Europe Eclipse™ A4F system is based on a single HPLC pump to generate three separate flow streams (detector flow, cross flow, and injection flow). The Eclipse™ system is based on an Agilent or a Shimadzu HPLC pump. Using a single pump from a renowned HPLC manufacturer benefits the reliability and maintenance requirements.

The Eclipse™ A4F separation system consists of a channel and a control chassis that includes a CoriFlow device, a LiquiFlow device, two software-controlled motor-driven needle valves, two Rheodyne switching valves, and two pressure sensors. The cross flow generates at the channel inlet; that is, the flow entering the channel flows in two directions: channel (detector) direction and cross direction. The motor-driven switching valves are used to direct the flow during the three phases of the separation process (focusing and relaxation, injection, and elution). To achieve sufficient and stable cross flow the backpressure in the detector direction must be several times higher than the backpressure across the membrane. The pressure in the channel is also useful for extending the boiling temperature of volatile solvents such as THF, which can be safely used up to a temperature of about 90°C.

A simplified scheme of the single-pump Eclipse™ A4F instrument is shown in Figure 5.11. In the focusing mode, the flow delivered by the HPLC pump flows through tubing 1 and splits into lines 2, 3, and 4. The inject needle valve is closed and the channel is entered from the inlet (line 2) and from the outlet (line 3). The split of the focusing flow into the channel inlet and outlet is adjusted with a software-controlled motor-driven focus needle valve. During the injection mode, the inject system (consisting of a needle valve and a LiquiFlow measuring device) is opened and flow is controlled at specified flow rate (usually 0.2 mL/min), which delivers the sample from the loop of autosampler or manual injector into the channel inject port (line 5). When the injection is completed, the inject system is closed while the flow remains flowing in lines 2, 3, and 4 for sample focusing and relaxation.

Note that in the focusing mode the detector flow actually bypasses the channel. During the elution mode the inject line is closed and the solvent flows from the pump via line 1 into the channel inlet (line 2) and the channel outlet flows through lines 3 and 4 into detectors. The cross flow rate (line 6) is controlled and measured by a CoriFlow device. If a cross flow gradient is applied, the flow from the pump is gradually decreased along with the equivalent decrease of the flow through the CoriFlow controller to keep the detector flow constant.

In general, an A4F instrumental setup is similar to that used in SEC, only SEC columns are replaced by a channel and a chassis. Similarity between SEC and A4F allows shearing the pump, injector, detectors, and measuring and processing software. In other words, an A4F instrumental setup can be easily converted to an SEC setup by disconnecting the channel and chassis and connecting columns instead. This is a simple procedure than can be done manually in a few minutes. In addition, the Eclipse™ A4F system offers a GPC option, which allows easy

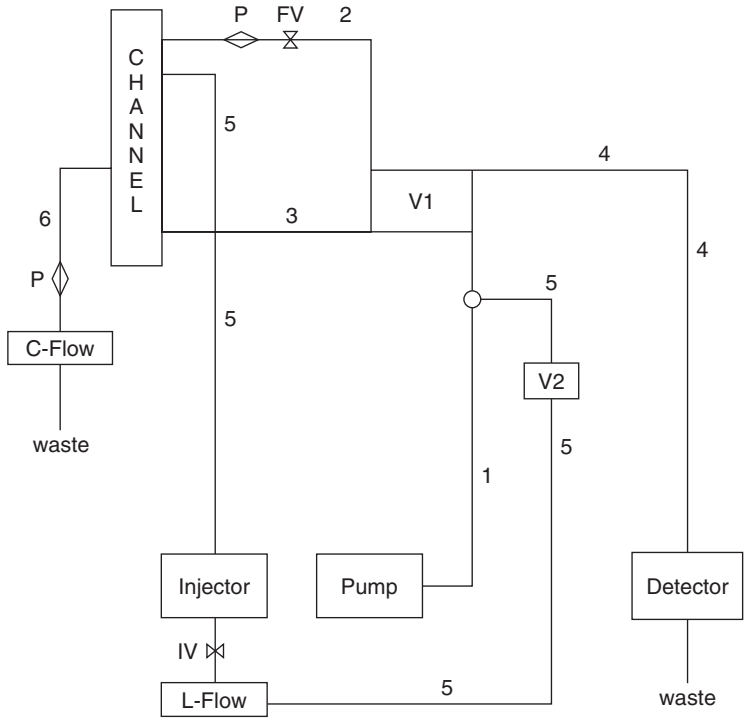

Figure 5.11 Simplified scheme of A4F instrument Eclipse™ utilizing a single HPLC pump to generate all flows. C-Flow = CoriFlow Coriolis style mass flow meter/mass flow controller, L-Flow = LiquiFlow liquid flow meter operating on a thermal through-flow measuring principle, P = pressure sensor, FV = focus valve, IV = injection valve, V1, V2 = Rheodyne valves. *Source:* Courtesy of Wyatt Technology Europe.

switching between the channel and columns using an additional switching valve controlled by the software. When SEC columns are not being used, they can be continuously flushed by an additional pump connected to the chassis.

The profile of the channel is cut in the spacer. The channel shape is usually a trapezoid with two tapered ends. Due to the trapezoidal shape the channel breadth decreases toward the outlet, which maintains the longitudinal flow velocity despite the loss of the carrier through the membrane. In addition, peak dilution is reduced compared to a rectangular channel. The channel parameters are tip-to-tip length, thickness, length of the triangular tapered inlet, length of the triangular tapered outlet, breadth at the widest point of the tapered inlet, and breadth at the widest point of the tapered outlet.

The top and bottom channel walls must be parallel to assure a uniform parabolic flow profile across the channel breadth. It is also necessary that the walls are smooth, even though the membrane surface is always sort of irregular concerning porosity and roughness. An ultrafiltration membrane made of regenerated

cellulose can be used for both aqueous and organic solvent applications. Other membrane materials include, for example, polyethersulfone or cellulose acetate.

The membrane must be compatible with the carrier and must not swell or dissolve. The membrane must not interact with the sample since the interactions would affect retention. The interactions depend on the membrane surface chemical composition, composition of the sample, and eluent properties. Although sample–membrane interactions represent an issue for some samples, interactions-related problems are significantly less frequent compared to SEC. The most important parameter of the membrane is cutoff, which must be low enough to keep the sample in the channel. The typical membrane cutoffs are 5 kDa, 10 kDa, or 30 kDa. The nominal cutoffs provide only a rough estimation of real molar masses that will be retained by the membrane, because the critical parameter is sample size. Thus various polymers will have different molar mass cutoffs according to their actual chain dimensions. The semipermeable membrane consists of a thin skin with very fine, regular pores that is supported by a significantly thicker layer with large pores. It is important to make sure that the thin, polished side of the membrane faces the channel. The membrane is supported by a frit; when the channel is mounted together the membrane is compressed by the spacer, whereas in the area where the membrane is not in contact with the spacer it maintains its original thickness. As a result of compression by the spacer, the membrane protrudes into the channel and the effective channel thickness is less than the nominal spacer thickness.

Membrane compression can be easily measured by a micrometer after channel disassembly. The experience shows that the regenerated cellulose membrane is typically compressed by 60–90 μm. When the actual channel thickness is of interest, as in the case of the determination of retention ratios or λ parameters (and consequently diffusion coefficients and hydrodynamic radii), it can be determined from the retention time of a compound of well-known diffusion coefficient and Equation 5.19. The proteins bovine serum albumin or ferritin in aqueous solvents and narrow polystyrene standards in organic solvents can be used for the determination of the actual channel thickness. However, when the A4F system is coupled with a MALS detector the exact channel thickness is actually not needed.

As already mentioned, an A4F instrument is similar to an SEC (HPLC) instrument with the only difference that of using channels instead of columns. Although the HPLC pump, injector, connecting tubings, and detectors are identical with those used in SEC, the channel pressure is substantially lower than in SEC columns. Most HPLC pumps require a certain backpressure for proper check-valve operation. Nevertheless, this requirement is usually fulfilled since pump pressure for the entire system from injector to detector is usually sufficient (for THF and detector flow of 1 mL/min the pressure is around 20 bar and more when the cross flow is applied). When needed for the sake of proper cross flow, a short piece of 0.13-mm ID tubing connected before the detector can be used to increase the pressure in the detector direction (1 m of 0.13-mm ID tubing at 1-mL/min THF yields pressure of about 12 bar).

Submicrometer particles in the carrier can completely disturb any information obtainable from the MALS detector. SEC columns are a potential source of particles bleeding from the packing material, but when the column system gets flushed and stabilized, the SEC columns actually serve as an efficient eluent filter. Since the packing material is not used in A4F, both effects are missing. The channel is usually not a serious source of particles, but on the other hand, the filtration effect is missing. Therefore, the carrier must be filtered with an online filter placed between the pump and injector. When aqueous buffers are used, pre-filtration with 0.1 μm should be performed. However, the pre-filtration is not needed in the case of organic solvents such as THF. As a result of using two flows, the cross flow being usually several times higher than the detector flow, the solvent consumption is significantly higher than in SEC. That means the solvent reservoirs and waste bottles should be of larger volume than those regularly used in SEC.

Similarly as in SEC, refractive index (RI) and UV detectors are the most frequently used concentration-sensitive detectors in A4F (the principles of particular detectors are described in Section 3.3.3). Other detectors for polymer analysis include online viscometer or evaporative light scattering detectors, and in principle other HPLC detectors can be used. An interesting application is the characterization of aquatic colloids in natural water using an ICP-MS (inductively coupled plasma-mass spectrometry) detector.[22,23]

5.4 MEASUREMENTS AND DATA PROCESSING

The first step in an A4F experiment is sample preparation, which is similar to that used for SEC (Section 3.5.1). As in SEC, the major requirement of successful determination of molar mass distribution is sample solubility. Although A4F can measure particles up to several tens of micrometers, filtration of polymer solutions before injecting into the A4F system is strongly recommended. The filtration can remove any large particles or swollen gels that might block connecting or inner-detector tubings. Some polymer samples can contain trace amounts of fractions with ultra-high molar mass and size beyond the steric inversion diameter, which can co-elute with the main polymer peak and disturb the light scattering signal by intensive spikes. The co-elution of very large particles with the main polymer peak occurs due to inversion of the separation mechanism from normal to steric when particles become too large. If the species disturbing the light scattering signal cannot be completely separated from the polymer peak, they can be removed prior to analysis by filtration using a filter size that is large enough for polymer molecules and small enough for the components that are intended to be removed.

Figure 5.12 shows the smoothing effect of filtration on the light scattering signal without noticeable effect on the molar mass distribution. However, the filtration step can strongly affect the molar mass distribution, as demonstrated in Figure 5.13. Selection of an appropriate filter size may not always be straightforward and samples containing high-molar-mass fractions should be filtered with

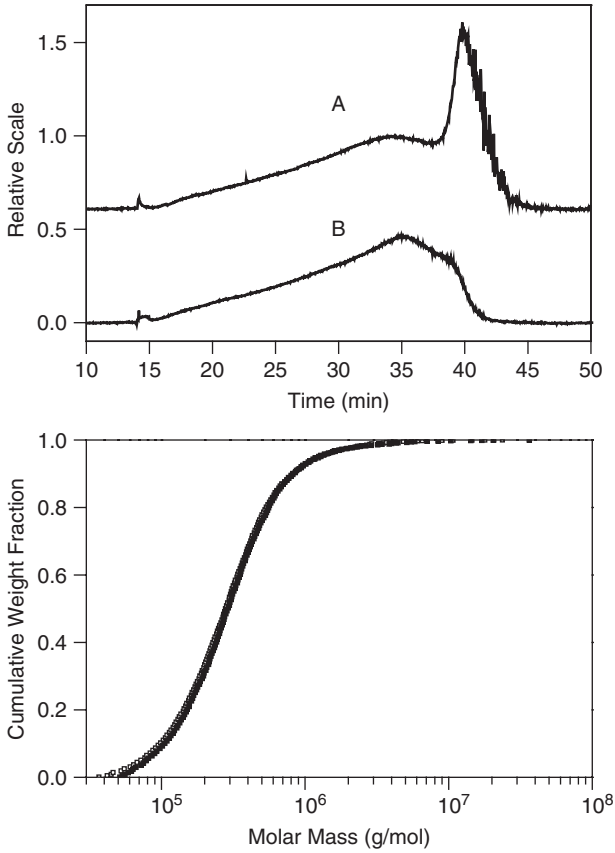

Figure 5.12 Effect of sample filtration: light scattering fractograms (top) and cumulative distribution curves (bottom) for a sample of polybutadiene rubber. Sample solution filtered with 0.45-μm (□, B) or 1-μm (■, A) filter.

different filters in order to select a suitable filter porosity that will not corrupt the molar mass distribution, but will remove the species disturbing the light scattering signal. Since one of the strong features of A4F lies in the analysis of polymers containing ultra-high-molar-mass species, the filtration step of sample preparation represents a generally more important issue than in the case of SEC, where filtration with a 0.45-μm filter is usually appropriate.

In contrast to SEC, the A4F separation technique allows measurement of insoluble particles. In this case the sample must be completely dispersible in the carrier with no aggregation and sedimentation when left in a vial for several hours.

In the simplest case, the measurements are carried out solely with the concentration-sensitive detector and the direct comparison of fractograms from similar samples measured under identical conditions is used to determine qualitative

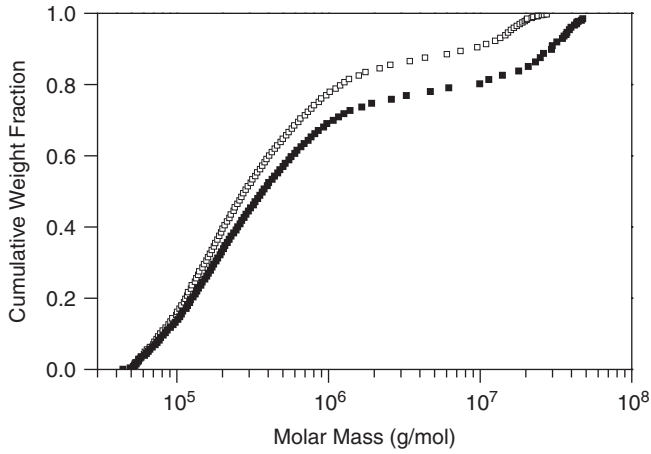

Figure 5.13 Effect of sample filtration: molar mass distribution plots of styrene-butadiene rubber determined by A4F-MALS with sample filtration using 0.45-μm (□) or 5-μm (■) filter.

differences among samples. For example, one can identify the presence of high-molar-mass fractions, polymer blends, or nanoparticles used as polymer modifiers. For more detailed analysis, the retention time axis must be converted to molar mass or particle size. The particle size can be theoretically determined directly from the retention data and molar mass can be calculated from the relation between the molar mass and diffusion coefficient. Alternatively, calibration curves can be established on the basis of standard materials (i.e., polymer narrow standards or particle size standards). However, direct measurement of molar mass by a MALS detector is undoubtedly the most accurate and reliable way to obtain molar mass, molecular size, and conformation information. Determination of molar mass and RMS radius distribution with a MALS detector is identical with that described in Chapter 4.

Similarly as in SEC-MALS, the M_w results are independent of the separation efficiency, while other molar mass averages, molar mass distribution curves, and conformation plots are calculated on the basis of the assumption that each data slice is monodisperse. Thus it is important to choose separation conditions that provide sufficient resolution for the sample to be analyzed. Data processing, that is, setting the baseline and peak integration limits, follows the same rules as those applied in SEC and SEC-MALS. Since oligomeric portions of polymer samples are lost through the accumulation membrane, the RI peaks do not show oligomeric tail or the peaks of low-molar-mass impurities, and the determination of the peak beginning is typically easier than the determination of the peak end in SEC. In contrast to SEC, the RI signal may be affected by switching from focusing to elution and by cross flow gradient. This RI baseline instability can be eliminated by subtraction of a blank signal from the run signal, as demonstrated in Figure 5.14. The blank signal is obtained by injection of pure solvent under identical conditions as those used for the sample analysis.

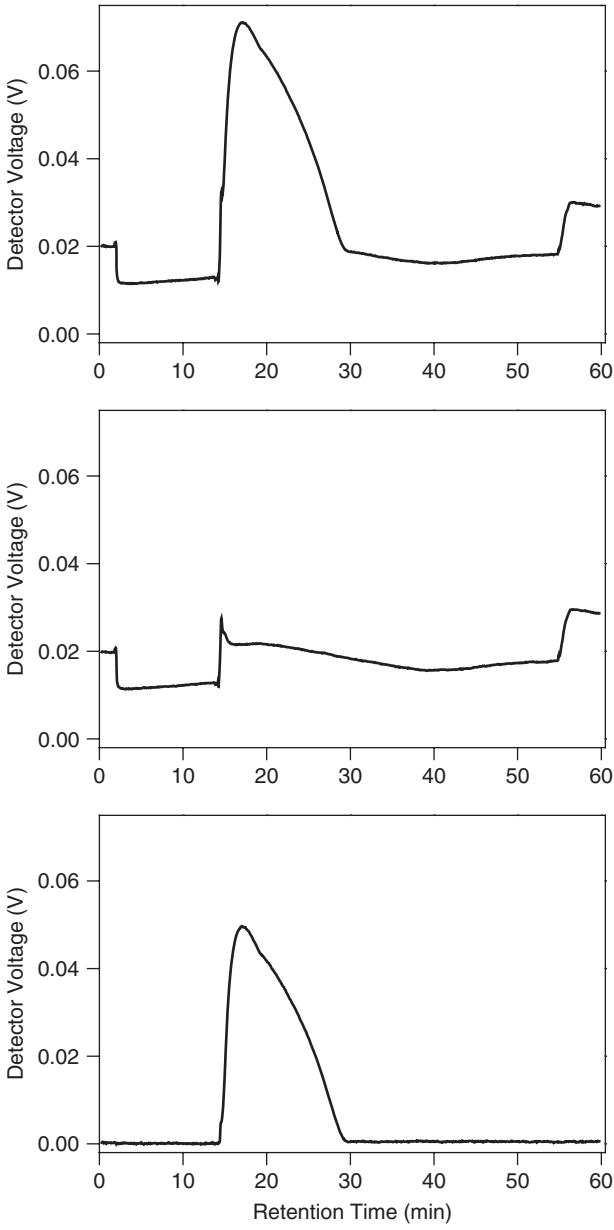

Figure 5.14 RI fractograms from analysis of polydisperse polystyrene. From top to bottom: raw signal, blank signal, and difference obtained by subtraction of the blank from the raw. Cross flow: 3 mL/min for 5 min and then linear gradient to 0.1 mL/min within 20 min + 10 min at 0.1 mL/min, 6 min at 0 mL/min, and 5 min at 3 mL/min. Elution starts at 14 min.

The extent of RI signal instability may depend on solvent, gradient type, and membrane cutoff. For successful baseline subtraction it is recommended to perform the sample sets in sequence, sample–blank injection–sample–blank injection, and so forth, instead of using just a single blank for subtraction from several sample runs. A certain disadvantage of this approach is that it actually doubles the run time per sample. For THF it is beneficial to use helium sparging to prevent chemical changes brought about by the presence of oxygen. The use of both vacuum degassing together with helium sparging was found to yield the most stable baseline and accurate RI signal subtraction.

As in SEC, the results should be reported together with instrumental details necessary for their interpretation and/or remeasurement. In addition to the parameters stated in Section 3.5.3, the membrane material, channel dimensions, detector flow, cross flow, and cross flow gradient (when applied) should be reported with the experimental results. Since part of a sample can be lost through the membrane, mass recovery should be stated with the reported results. Mass recovery is calculated from the injected mass and the mass calculated from the RI detector response and sample dn/dc. For polydisperse polymers, mass recovery less than 100% usually indicates presence of oligomeric fractions that were lost through the membrane. In such a case, additional SEC analysis can be performed in order to characterize the lower-molar-mass portion of the sample. Although a 100% mass recovery is ideal, partial recovery may be acceptable for analytical purposes assuming that sample loss does not occur selectively to specific size or molar mass range.

5.4.1 Influence of Separation Conditions

The experimental variables that control the separation process are the cross flow rate, the axial flow (detector flow) rate, the temperature, and the channel dimensions. Equations 5.28, 5.30, 5.33 and 5.34 for resolution, plate height, and fractionating power can be expressed in terms of variables that can be used to control the A4F experiments:

$$R_S = 0.051 \left(\frac{\Delta R}{\bar{R}}\right) \left(\frac{w^2}{\bar{D} V_0}\right) \left(\frac{\dot{V}_c^3}{\dot{V}}\right)^{1/2} \tag{5.35}$$

$$H_n = 24 \frac{LD^2 V_0^2}{w^4} \frac{\dot{V}}{\dot{V}_c^3} \tag{5.36}$$

$$F_{d,M} = S_{d,M} \frac{0.051}{bLD} \frac{w \dot{V}_c^{3/2}}{\dot{V}^{1/2}} \tag{5.37}$$

Subscripts d and M in Equation 5.37 refer to the diameter or molar mass–based parameters. The above equations were derived for the symmetrical channel where $\langle v \rangle$ can be expressed as $\dot{V} L / \dot{V}_0$ In A4F the detector flow rate does not

equal to the longitudinal flow rate in the channel, which depends on the position z and on the cross flow rate. However, the two flow rates are directly proportional and such the equations can be used to demonstrate the effect of experimental variables on the separation process in A4F as well. A general goal is to keep the resolution and fractionating power high, whereas plate height should be low. An increase of cross flow rate has a strong enhancing effect on resolution because of 1.5-power dependence. On the other hand, an increase of the detector flow decreases resolution, but at a lower rate of 0.5-power. Consequently, simultaneous increase of $\dot{V}_c$ and $\dot{V}$ will increase the resolution without affecting retention time. Low detector flow rate will reduce peak broadening and may also be beneficial in high-molar-mass polymer analysis because of decreased probability of shearing degradation. Fractionating power increases with the rate of cross flow and channel thickness and decreases with the rate of detector flow. However, simultaneous increase of both flow rates yields an increase in fractionating power.

Fractionating power is also inversely proportional to the channel bottom area bL. This is because at a given $\dot{V}_c$ the linear velocity cross flow (i.e., actual strength of the flow field) increases. Smaller channels may therefore provide better separation, but there is also a limit of channel pressure and small channels are also more prone to overloading effects. Also the total number of plates will decrease with decreasing channel length. Small channels may be efficient for the separation of some compounds, such as proteins, when samples are available in very low quantities. An additional advantage of small channels is lower consumption of eluent, because of generally lower cross flow rates.

The strength of the cross flow field is probably the most important separation variable; it has a strong effect on resolution and can be varied widely and rapidly without need to change the channel geometry. Note that cross flow and detector flow rates are limited by the HPLC pump and pressure in the channel (for Eclipse™ the maximum pressure in the channel is 30 bar). Although the cross flow has a positive effect on the resolution, excessive cross flow may push the sample through the membrane and thus increase the sample loss. Too-high cross flow may also promote interactions of sample with the membrane, sample aggregation, or mutual entanglement of macromolecules, because the molecules are pushed to a thin, concentrated layer near the accumulation wall.

Temperature of the channel is an often-overlooked experimental variable. A4F experiments are traditionally carried out at ambient temperatures. However, the entire channel can be placed into a sufficiently large HPLC oven or another suitable thermostating device. The retention time decreases with increasing temperature. Although temperature has generally negative impact on A4F separation, because it decreases resolution and fractionation power and increases plate height via increase of diffusion coefficient, it may be beneficial for polymer samples containing fractions with very high molar mass. For such a sample, the elevated temperature increases the steric inversion diameter and thus extends the range of normal separation. The elevated temperature can also hasten the elution of large, slowly eluting sample components.

Another experimental variable that can be used to control the separation is channel thickness. A certain disadvantage of this parameter is that its change requires manual disassembly of the channel. Thick channels decrease the probability of overloading and occurrence of steric separation and thus are suitable for polymer samples containing ultra-high-molar-mass fractions. On the other hand, thin channels can be used when steric separation of larger particles is of interest.

5.4.1.1 Isocratic and Gradient Experiments

The detector flow rate is usually constant throughout the injection, focusing, and elution steps. The cross flow can be either kept constant during the entire experiment or programmed to decay over the course of analysis to speed up the elution of strongly retained components. Programmed cross flow may also improve detectability, because isocratic runs of highly polydisperse polymers may result in very broad peaks and consequently weak detector response, especially at the end of fractograms.

A possible advantage of the isocratic run is reduction in baseline drift of the RI detector, which is sensitive to minor pressure changes due to decay of the cross flow. Also the prediction of retention time or estimation of the diffusion coefficient from retention data may be easier from the isocratic measurements. Isocratic experiments are usually sufficient for the separation of simple mixtures such as proteins containing dimer and trimer without the presence of large aggregates. However, for most polydisperse polymers, measurements using the cross flow gradient should be preferred. The cross flow can be decreased in a linear or exponential way. The speed and the pattern of the decay depend on the sample type and also on requested information.

A rule of thumb is to start the gradient at a cross flow that assures sufficient retention of early-eluting components; then the cross flow is decreased, either linearly or in an exponential pattern. Linear cross flow decay is obtained by setting the initial cross flow and the ramp time to reach the final cross flow rate. During the gradient run the channel inlet flow rate and the flow of one flow stream are accurately controlled, which assures control of the second stream as well.

Let us give a concrete example: When the starting cross flow of 3 mL/min and detector flow of 1 mL/min are required, the HPLC pump must generate a flow rate of 4 mL/min. Since the backpressure in the detector direction is significantly more than that in the cross direction, the liquid has a tendency to flow in the cross direction, which is regulated by the CoriFlow device to 3 mL/min, and thus the remaining flow of 1 mL/min must flow in the detector direction. To achieve the cross flow gradient, the flow stream generated by the pump is decreased at the same rate as the cross flow is decayed such that the outlet flow is maintained at 1 mL/min. When the A4F software can generate only the linear cross flow gradients, the exponential cross flow decay can be approximated by a series of consecutive linear segments. However, linear cross flow decay with possibly one

or two isocratic sections is usually sufficient for the separation of even extremely broad polymers.

When the cross flow reaches zero value while part of the sample is still in the channel, the remaining sample is swept out without further separation, which may result in underestimation of molar mass and size distribution in the high-molar-mass region. To avoid this effect, the cross flow gradient is programmed in such a way that the cross flow reaches a small non-zero value that is maintained for a certain period of time in order to reduce the possibility of some large species being eluted unfractionated. On the other hand, the "swept effect" can help to detect small amounts of high-molar-mass species. The presence of high-molar-mass fractions in the sample is evident from the MALS signal shortly after the cross flow is switched to zero.

5.4.1.2 Overloading

Overloading in thermal and flow FFF analysis was theoretically described and experimentally studied by Caldwell et al.[24] A rule of thumb is to take caution in A4F measurements when injecting larger masses of samples. For most samples the separation takes place in a relatively thin layer near the accumulation wall. During the sample relaxation the local concentrations of molecules can become very high and sample components may start to affect each other. At very high concentrations, the mutual interference between the particles may result in a steric effect; that is, there is not enough room for the particles to reach equilibrium. Consequently, the relaxation equilibrium in the channel may not be fully reached, which can result in the shift of the retention time and perturbation of the shape of the fractogram. Other possible effects resulting from too-high injected mass are aggregation of particles, entanglement of macromolecular chains, or repulsion forces between macromolecules or particles.

The major factors that affect the amount of sample that can be injected into the channel are channel volume, sample molar mass, polydispersity, cross flow, and ionic strength in the case of aqueous solvents. The cross flow determines the extent at which the sample is concentrated near the wall. The sample amount that can be injected into the channel without overloading decreases as the molar mass increases, and narrow distribution samples should be injected at lower amounts compared to the broad samples. The injected amount can increase with the channel volume (channel breadth, length and thickness). For aqueous solvents the injected mass can usually increase as the ionic strength increases. In routine experimental practice, it is necessary to balance the injected amount with the response from the light scattering and concentration detectors. Especially the latter detector may show weak response in the case of polymers with high molar mass that require analysis under low sample load.

Unknown samples should be analyzed at different injected amounts. Overloading is missing if there is no significant change of retention time and peak shape; in particular, the absence of overloading is proved by the consistency of distribution curves obtained with different sample loads. Although keeping

sample concentration as low as possible is generally advantageous, one has to keep in mind that in the A4F channel, after initial sample concentration during the relaxation process, elution is accompanied by a significant sample dilution. As a general rule, a sample mass of 0.2–0.3 mg can be safely injected without overloading for polydisperse polymers of M_w up to about 5×10^5 g/mol, with possibly higher amounts for polymers with $M_w < 1 \times 10^5$ g/mol and lower amounts if $M_w > 5 \times 10^5$ g/mol (for the channel outlined in Figure 5.2 and 350-μm spacer).

5.4.2 Practical Measurements

In contrast to SEC, in A4F there are several experimental parameters that can be readily adjusted to control the separation. This feature makes the method more flexible and powerful, but it requires a certain amount of development to optimize the conditions in order to get appropriate separation within an acceptable time. The experimental variables to consider are $\dot{V}$, $\dot{V}_c$, w, channel dimensions, temperature, and to some extent also the eluent. In order to get a first impression of an unknown sample, one can start with a 350-μm spacer and the generic conditions outlined in Figure 5.15. In this particular example the analysis starts with two-minute elution and focusing steps that stabilize the system; then the sample is injected for three minutes into the channel, and after the injection is completed the focusing is kept for an additional five minutes in order to allow the sample to focus and relax.

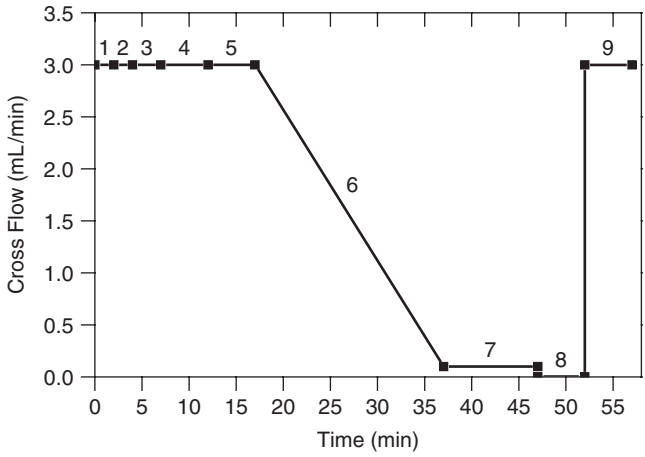

Figure 5.15 Generic conditions for separation of polydisperse polymers by A4F. Step: 1 = elution, 2 = focusing, 3 = focusing + inject, 4 = focusing, 5 to 9 = elution.
Note: Unless otherwise stated, the focus flow identical with the cross flow at the beginning of elution was used to obtain results presented in this chapter.

Note that length of the injection step depends on the injection volume and inject flow. The injection must be long enough not only to flush the sample loop, but also to transfer the sample from the injector through the A4F chassis into the channel. It is possible to use a few minutes' longer inject time than the minimum value in order to flush the inject line properly. The elution starts with a five-minute isocratic step to improve the separation of the lower-molar-mass components. After the isocratic elution, the cross flow decays linearly within 20 minutes to 0.1 mL/min, which is kept for an additional ten minutes to separate possibly occuring fractions with very high molar mass. Then the cross flow is completely stopped and the channel is flushed for five minutes. During this flush period there is typically no sample elution, but some samples may contain aggregates or other large species that are retained in the channel and released when no cross flow is applied. The final step is returning back to the initial cross flow that will be used for the next measurement. After collecting the first results, the conditions can be adjusted to increase retention of the lower-molar-mass fractions, to hasten elution of the high-molar-mass fractions, or to diminish steric separation.

The effect of particular experimental variables on the separation of a typical polydisperse polymer is illustrated in Figures 5.16–5.24. With the exception of Figure 5.22, the data were obtained by the measurements of the same broad polystyrene. The results depicted in these figures are mostly self-explanatory and can be used for planning your own experiments. The general message from this comparison is that once an appropriate separation is achieved, further increase of resolution does not lead to a significant difference in the obtained molar mass distribution plots. Almost identical molar mass distribution curves can be determined using different separation conditions. However, when too-low cross flow is used (Figure 5.17), the local polydispersity within the elution volume slices becomes significant and consequently the low-molar-mass part of the distribution is shifted to higher molar masses while the high-molar-mass part of the distribution is shifted to lower molar masses; that is, M_n values are overestimated and M_z values are underestimated and the sample appears virtually narrower.

If too-low focusing flow is applied (Figure 5.19), the lower-molar-mass fractions are swept immediately after switching to elution mode and appear unresolved as the intensive void peak at the beginning of fractogram. Note also the positive effect of temperature on the separation of high-molar-mass fractions as shown in Figure 5.22, where the elevated temperature shifted the steric inversion point to larger molecules and maintained normal separation over an extremely broad molar mass range. It can be concluded that the molar mass distribution of a polydisperse polymer will not be affected by a minor change of operational conditions (i.e., the A4F-MALS method is highly robust). This is, however, true only in the case of online use of a MALS detector, where retention time is not a principal parameter used for sample characterization.

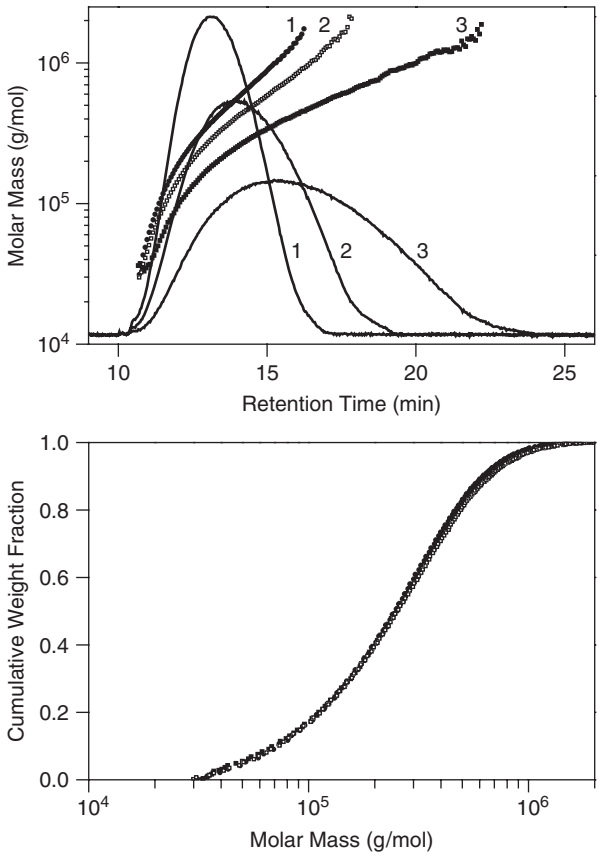

Figure 5.16 Effect of cross flow for isocratic separation: light scattering fractograms and molar mass–versus–retention time plots (top) and molar mass distribution curves (bottom) obtained by A4F-MALS measurements of broad polystyrene using isocratic cross flow of 1.5 mL/min (1,•), 2 mL/min (2,□), and 3 mL/min (3,■). A4F conditions: THF, detector flow 1 mL/min, injection 25 μL 0.25% w/v, spacer 250 μm, channel temperature 80°C. Elution starts at 10 min.

5.5 A4F APPLICATIONS

In contrast to SEC, which is strongly limited to soluble polymers, A4F is applicable to samples that can be not only dissolved, but also suspended in the carrier. Originally, FFF was developed to determine the diffusion coefficient and consequently hydrodynamic radius calculated on the basis of the retention data. That means it served as a separation and characterization method simultaneously. Although A4F theory allows the calculation of hydrodynamic radius from the retention time, significantly more detailed characterization can be achieved with a MALS detector, which allows the calculation of molar mass and RMS radius directly from the intensity of scattered light (see Chapter 2). The MALS detector can be equipped with a QELS option for direct measurement of hydrodynamic radius and thus RMS and hydrodynamic radii can be measured simultaneously.

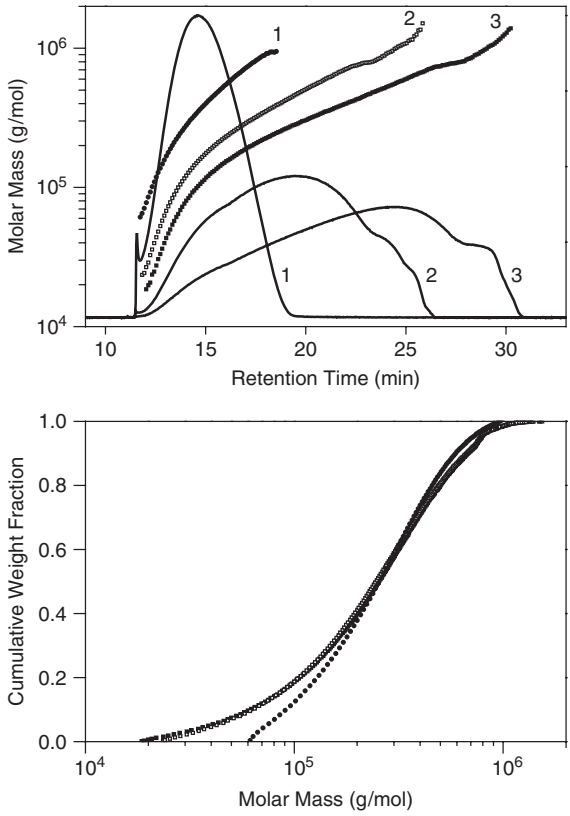

Figure 5.17 Effect of beginning cross flow for gradient separation: light scattering fractograms and molar mass–versus–retention time plots (top) and molar mass distribution curves (bottom) obtained by measurements of broad polystyrene using cross flow starting at 1 mL/min (1,•), 2 mL/min (2,□), and 3 mL/min (3,■), linear gradient to 0.1 mL/min within 20 minutes. A4F conditions: THF, detector flow 1 mL/min, injection 100 μL 0.25% w/v, spacer 350 μm, channel temperature 80°C. Elution starts at 11 min.

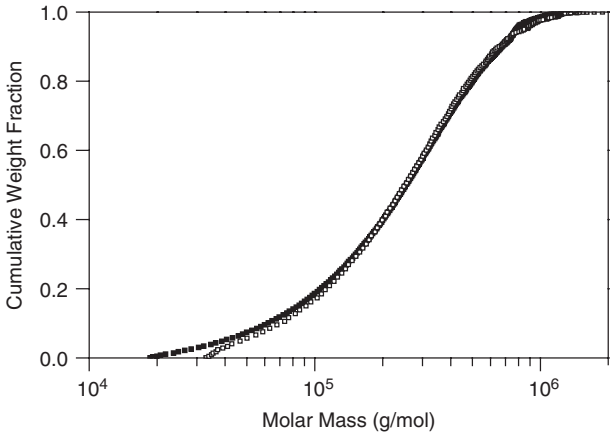

Figure 5.18 Distribution curves of polydisperse polystyrene determined by isocratic (□) and gradient (■) experiments using cross flow 3 mL/min (see Figures 5.16 and 5.17).

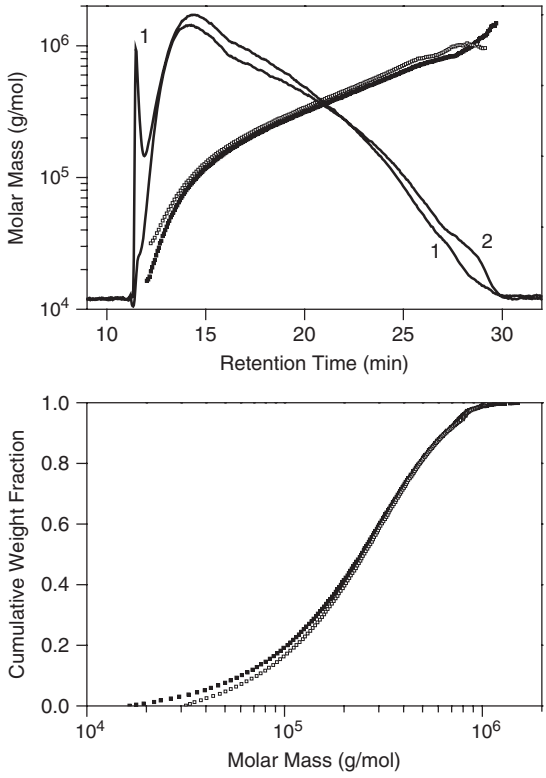

Figure 5.19 Effect of focus flow: RI fractograms and molar mass versus retention time plots (top) and molar mass distribution curves (bottom) obtained by measurements of broad polystyrene using focus flow 1 mL/min (1,□) and 3 mL/min (2,■). A4F conditions: THF, detector flow 1 mL/min, cross flow 3 mL/min for 5 min and then linear decay to 0.1 mL/min within 20 min plus 10 min at 0.1 mL/min, injection 100 μL 0.25% w/v, spacer 350 μm, channel temperature 60°C. Elution starts at 11 min.

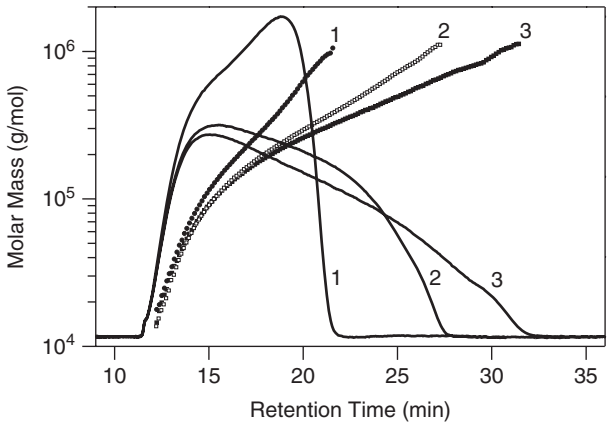

Figure 5.20 Effect of gradient decay time: RI fractograms and molar mass–versus–retention time plots (top) and molar mass distribution curves (bottom) obtained by A4F-MALS measurements of broad polystyrene using linear cross flow gradient with different decay time. A4F conditions: THF, detector flow 1 mL/min, cross flow 3 mL/min to 0.15 mL/min within 10 min (1,•), 20 min (2,□), and 30 min (3,■) plus 5 min at 0.15 mL/min, injection 100 μL 0.25% w/v, 350 μm spacer, channel temperature 60°C. Elution starts at 11 min.

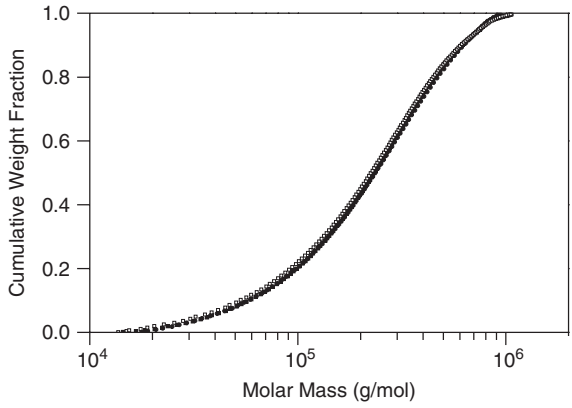

Figure 5.20 (*Continued*)

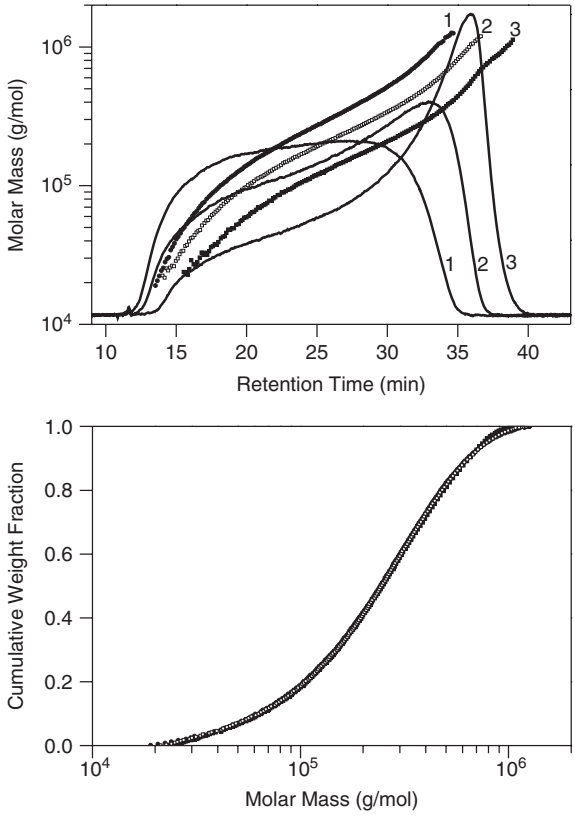

Figure 5.21 Effect of temperature: RI fractograms and molar mass–versus–retention time plots (top) and molar mass distribution curves (bottom) obtained by A4F-MALS measurements of broad polystyrene at channel temperature 25°C (3,■), 60°C (2,□), and 90°C (1,•). A4F conditions: THF, detector flow 1 mL/min, cross flow 3 mL/min for 5 min and then linear gradient to 0.1 mL/min within 20 min plus 10 min at 0.1 mL/min, injection 100 μL 0.25% w/v, spacer 490 μm. Elution starts at 12 min.

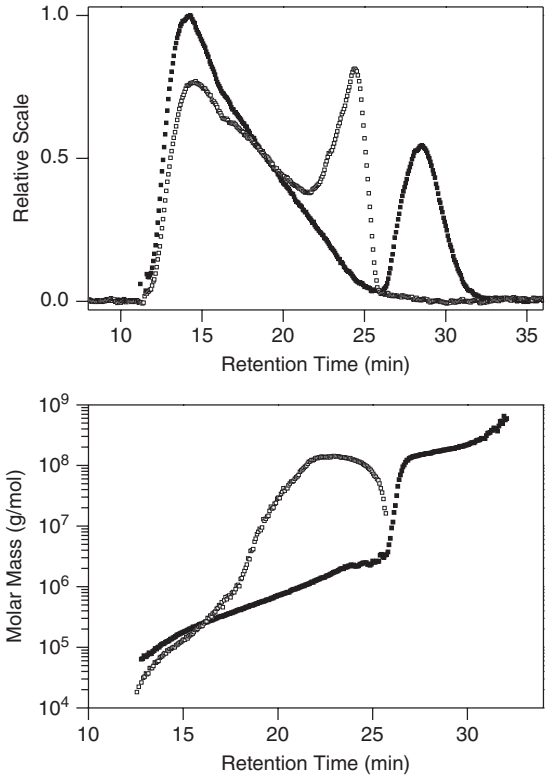

Figure 5.22 Effect of temperature: RI fractograms (top) and molar mass–versus–retention time plots (bottom) obtained by A4F-MALS measurements of bimodal acrylic copolymer using channel temperatures 60°C (□) and 80°C (■). A4F conditions: THF, detector flow 1 mL/min, cross flow 3 mL/min for 5 min and then linear gradient to 0.1 mL/min within 10 min plus 15 min at 0.1 mL/min, injection 50 μL 0.25% w/v, spacer 350 μm. Elution starts at 11 min. $M_w \approx 37 \times 10^6$ g/mol, $M_w/M_n \approx 140$.

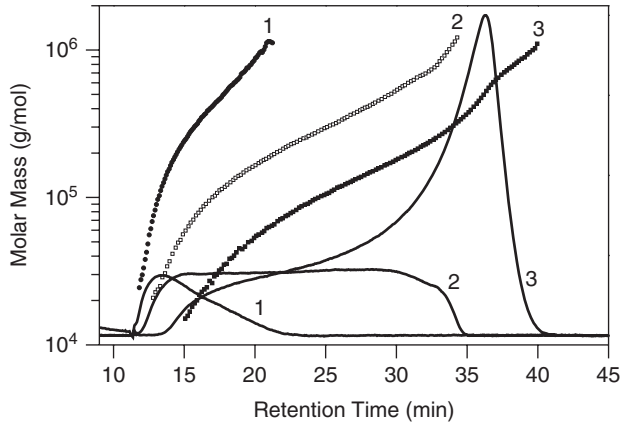

Figure 5.23 Effect of channel thickness: RI fractograms and molar mass–versus–retention time plots (top) and molar mass distribution curves (bottom) obtained by A4F-MALS measurements of broad polystyrene using spacer thickness of 250 μm (1,●), 350 μm (2,□), and 490 μm (3,■). A4F conditions: THF, detector flow 1 mL/min, cross flow 3 mL/min for 5 min and then linear gradient to 0.1 mL/min within 20 min plus 10 min at 0.1 mL/min, injection 25 μL, 100 μL, and 200 μL 0.25% w/v for increasing spacer thickness. Elution starts at 11 min.

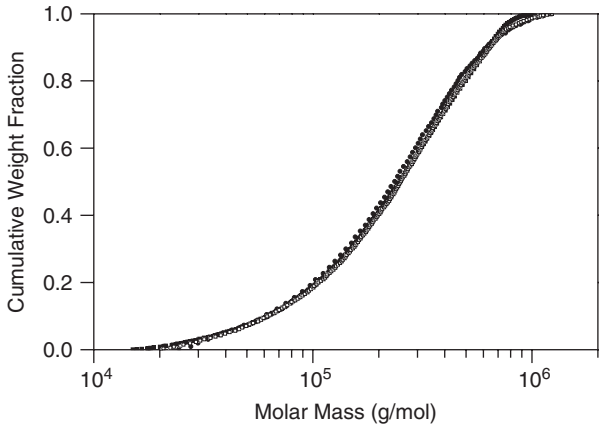

Figure 5.23 (*Continued*)

The QELS option also allows confrontation of directly measured hydrodynamic radii with those obtained from the retention time.

The main applications of the A4F-MALS method are the determination of molar mass distribution, characterization of polymer branching, detection and characterization of aggregates in proteins and polymers, and determination of particle size distribution. The materials that can be characterized by means of flow FFF include synthetic polymers, both water soluble[25,26] and organic

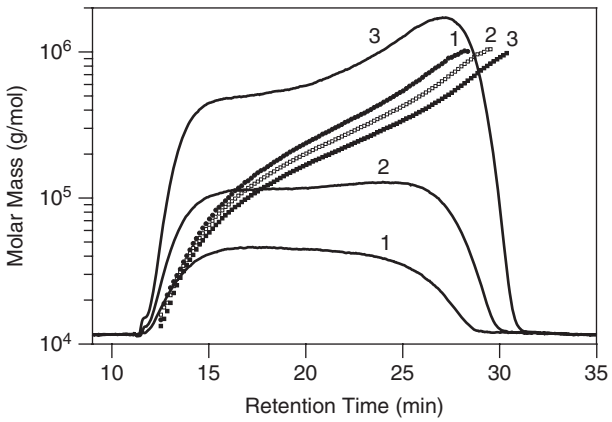

Figure 5.24 Effect of injected mass: RI fractograms and molar mass–versus–retention time plots (top) and molar mass distribution curves (bottom) obtained by A4F-MALS measurements of broad polystyrene using different injected mass: 125 μg (1,•), 250 μg (2,□), and 500 μg (3,■). A4F conditions: THF, detector flow 1 mL/min, cross flow 3 mL/min to 0.15 mL/min within 20 min plus 10 min at 0.15 mL/min, injection 50 μL, 100 μL, and 200 μL 0.25% w/v, spacer 350 μm, ambient temperature. Elution starts at 11 min.

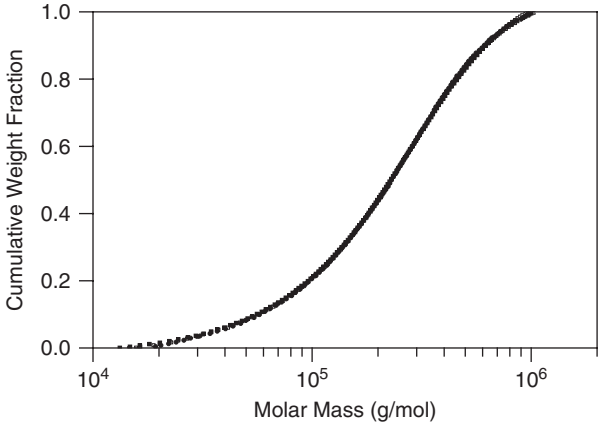

Figure 5.24 (*Continued*)

soluble,[27,28] natural polymers,[29–32] proteins[33–35] and protein conjugates, DNA,[36] antibodies,[37,38] viruses,[39–41] ribosomes,[42] liposomes,[43–45] micelles,[46] polymer latexes,[47] nanoparticles,[48–51] and natural colloids.[52]

Determination of molar mass distribution is the major application of A4F-MALS for the characterization of synthetic and natural polymers. Not only does successful application of A4F-MALS benefit from the A4F separation advantages when analysis of SEC-difficult polymers is requested; the method should provide comparable results with SEC-MALS even for samples that can be characterized by SEC-MALS without considerable problems. A typical separation of polydisperse polymer with A4F-MALS is demonstrated on NIST SRM 706 polystyrene in Figure 5.25, which also compares the corresponding molar mass distribution plot with that determined by SEC-MALS (see SEC separation in Figure 4.19). The molar mass distribution determined by A4F-MALS misses the oligomeric part below roughly 10^4 g/mol, which was lost by permeation through the semipermeable membrane. In addition, the molar mass distribution in the region of low molar masses may be affected by low retention of low-molar-mass fractions. Nevertheless, the agreement of the two distribution plots is quite acceptable. It is worth noting that the M_n value determined by A4F-MALS is in excellent agreement with that determined initially by membrane osmometry, that is, when the result was similarly affected by the permeation of oligomeric fractions through the membrane of a membrane osmometer.

Acceptable agreement between M_n values determined by A4F-MALS and MO was found also for other samples, as shown in Table 5.1. Although for the determination of molar mass distribution of regular polymers A4F does not provide significant improvement over SEC, the power of the method appears when the SEC separation is affected by non-SEC mechanisms. This is presented in Figure 5.26, which compares SEC-MALS and A4F-MALS data for randomly branched polystyrene for which the lower-molar-mass part of the distribution is affected by abnormal SEC elution (see Section 6.2.1). In this case, A4F provides

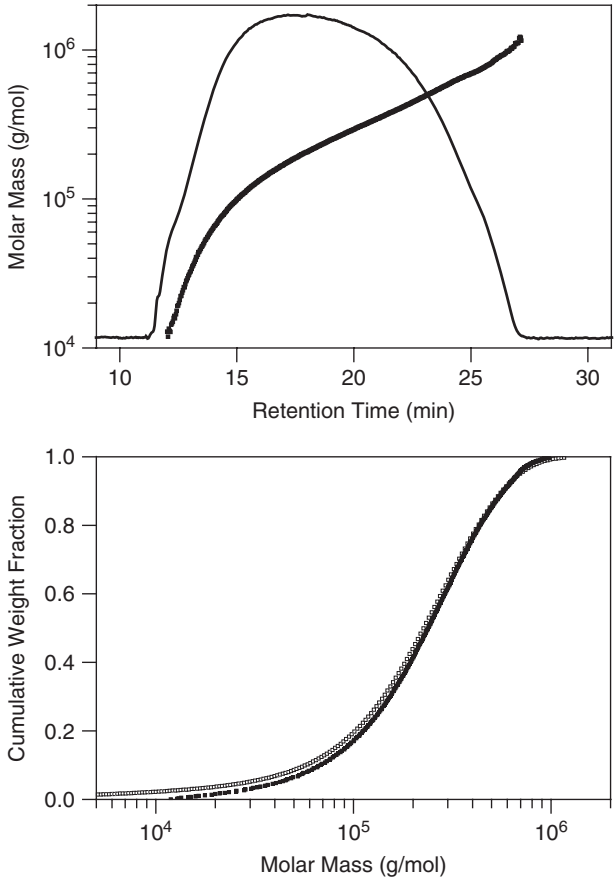

Figure 5.25 Molar mass–versus–retention time plot and RI fractogram for NIST SRM 706 PS determined by A4F-MALS (top) and comparison of cumulative molar mass distribution plots determined by SEC-MALS (□) and A4F-MALS (■) (bottom). SEC-MALS: $M_n = 66{,}000$ g/mol; $M_w = 279{,}000$ g/mol; $M_z = 442{,}000$ g/mol. A4F-MALS: $M_n = 137{,}000$ g/mol; $M_w = 284{,}000$ g/mol; $M_z = 423{,}000$ g/mol. SEC conditions: 2 × PLgel Mixed-C 300 × 7.5-mm columns, THF at 1 mL/min, injection 100 μL 0.25% w/v. A4F conditions: THF, detector flow 1 mL/min, cross flow from 3 to 0.15 mL/min within 20 min, injection 100 μL 0.25% w/v, spacer 350 μm, channel temperature 60°C. Elution starts at 11 min. For SEC separation, see Figure 4.19.

a more accurate description of molar mass distribution; the higher M_n from SEC can be attributed to abnormal SEC elution while the lower M_z indicates either shearing degradation of fractions with very high molar mass or poor SEC resolution of high-molar-mass fractions exceeding the total exclusion limit.

Figure 5.27 presents another example where A4F provides better separation compared to SEC, namely analysis of polymer containing amine functionality resulting in strong polymer interaction with SEC column packing. No indication of interactions is found for the data obtained by A4F-MALS.

Table 5.1 Number-Average Molar Masses of Polydisperse Polymers Determined by A4F-MALS and Membrane Osmometry

	M_n (g/mol)	
Sample	A4F-MALS	MO
PS (AN)	135 ± 9	120
PS (1)	138 ± 2	139
PS (2)	145 ± 3	153
PS (S)	82 ± 2	66
PS (K)	117 ± 3	98
PMMA (Y)	225 ± 5	185
PMMA (J)	62 ± 1	33

A4F is particularly suited for the separation and characterization of ultra-high-molar-mass polymers and polymers containing supermolecular structures. Shear degradation of ultra-high-molar mass fractions in the A4F channel is minimized due to mild conditions. In contrast to SEC, where the separation range is limited by total exclusion limit, there is no exclusion limit in A4F, and as for the molar mass the method is practically unlimited.

An example of the analysis of a polymer with molar mass range spanning over four orders of magnitude and polydispersity of about 25 is presented in Figure 5.28. The molar mass–versus–retention time plot shows separation up to molar masses over 10^8 g/mol. Such separation is typically impossible with SEC, because these molar masses are over the separation range of regularly available SEC columns and they are also highly prone to shearing degradation. Figure 5.28 also demonstrates the ability of A4F to yield conformation plots with no artifacts caused by abnormal SEC elution.

Another example of polymer containing fractions with ultra-high molar mass is presented in Figure 5.29. In this example, the ultra-high-molar-mass fractions are present at very low concentrations, yielding almost no RI detector signal; nevertheless, they are baseline separated from the main polymer peak due to the high separation power of A4F and no filtration and shearing effect, and are sensitively detected by the MALS detector.

Proteins and protein-related materials represent another important application area of the A4F-MALS technique. A typical property of proteins is their ability to form aggregates by association of protein molecules. Detection and characterization of protein aggregates is a common goal in protein science. In the pharmaceutical industry, the protein aggregation is strongly related to drug activity and undesirable side effects. The protein aggregation can be a major limitation in the development of protein-based drugs and thus understanding these phenomena is important for development of new products. The protein samples can range from single molecules to insoluble precipitates, which makes AF4 an ideal separation tool. SEC is conventionally used for the characterization of various proteins, but the effects of shear and adsorption can affect the obtained

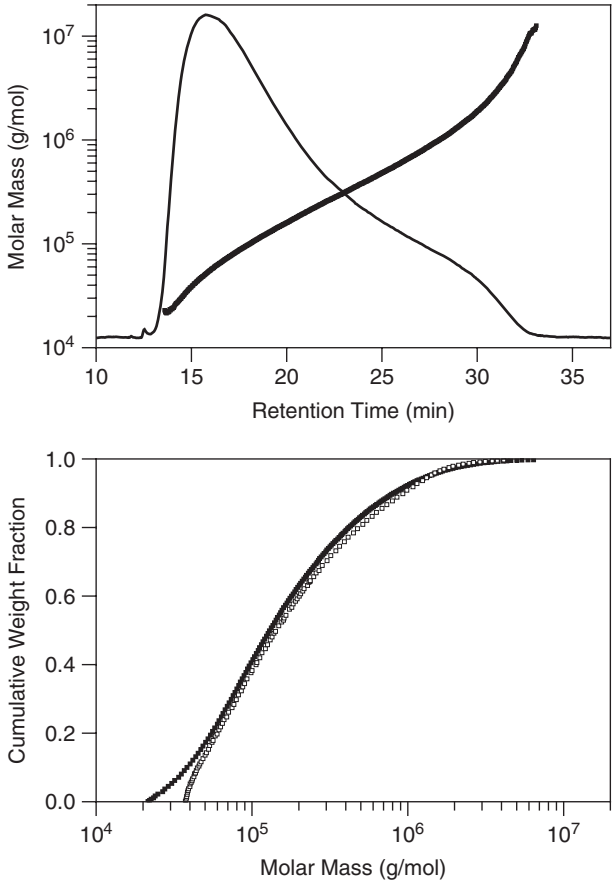

Figure 5.26 Plot of molar mass–versus–retention time with RI fractogram for randomly branched polystyrene obtained by A4F-MALS (top) and comparison of cumulative molar mass distribution plots determined by SEC-MALS (□) and A4F-MALS (■) (bottom). SEC-MALS: $M_n = 108{,}000$ g/mol; $M_w = 353{,}000$ g/mol; $M_z = 1.2 \times 10^6$ g/mol. A4F-MALS: $M_n = 92{,}000$ g/mol; $M_w = 350{,}000$ g/mol; $M_z = 1.9 \times 10^6$ g/mol. SEC conditions: 2 × PLgel Mixed-C 300 × 7.5-mm columns, THF at 1 mL/min, injection 100 μL 0.2% w/v. A4F conditions: THF, detector flow 1 mL/min, cross flow from 3 to 0.2 mL/min within 20 min + 10 min at 0.2 mL/min, injection 100 μL 0.35% w/v, spacer 350 μm, ambient channel temperature. Elution starts at 12 min. For SEC separation, see Figure 6.2.

results. In addition, regulatory bodies may request verification of the absence of aggregates by an additional analytical technique.

Most protein-based samples are water soluble and the most common A4F carriers include phosphate buffer or sodium nitrate solution. Because pH and ionic strength affect protein association and denaturation, they can be adjusted to match the pH and ionic strength of the sample solution. Figure 5.30 shows a

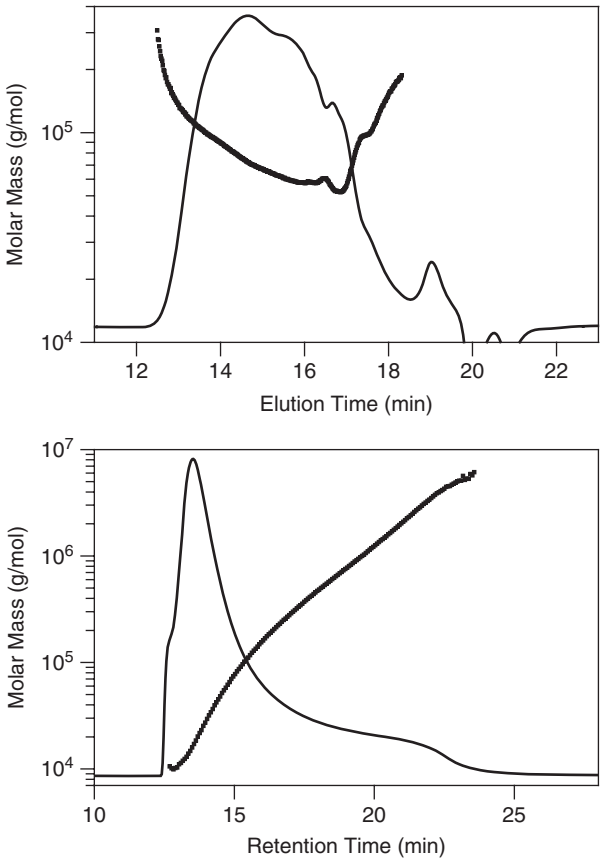

Figure 5.27 RI signals and molar mass–versus–retention time plots from SEC-MALS (top) and A4F-MALS (bottom) analysis of polymer containing amine functionality. SEC conditions: 2 × PLgel Mixed-C 300 × 7.5-mm columns, THF at 1 mL/min, injection 100 μL 1% w/v. A4F conditions: THF, detector flow 1 mL/min, cross flow from 3 to 0.15 mL/min within 10 min + 10 min at 0.15 mL/min, injection 100 μL 1% w/v, ambient channel temperature. Elution starts at 12 min.

typical protein fractogram. The concentrations of protein monomer, dimer, and trimer can be determined from the relative peak areas of the fractogram recorded by the RI or UV detector and the molar mass of protein molecules is determined directly by the MALS detector.

5.6 KEYNOTES

- A4F is an alternative to SEC with its main advantages including ability to analyze polymers up to ultra-high molar masses and significantly reduced possibility of shearing degradation and enthalpic interactions. The method has been proven to be very efficient for the separation of branched polymers.
- Besides analysis of soluble polymers the A4F method is capable of separating particles up to the micrometer scale.

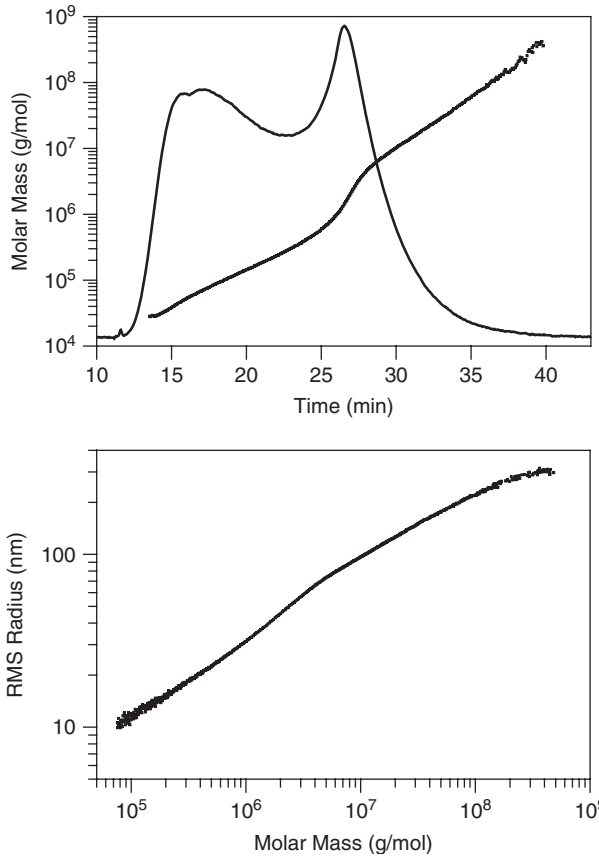

Figure 5.28 Molar mass distribution along the retention time axis overlaid on the RI response (top) and conformation plot (bottom) for a branched polystyrene sample of very broad molar mass distribution. $M_n = 134{,}000$ g/mol; $M_w = 3.3 \times 10^6$ g/mol; $M_z = 64.7 \times 10^6$ g/mol. A4F conditions: THF, detector flow 1 mL/min, cross flow 3 mL/min for 5 min and then linear decay to 0.1 mL/min within 10 min + 40 min at 0.1 mL/min, injection 200 μL 0.2% w/v, spacer 490 μm, ambient channel temperature. Elution starts at 11 min.

- The principal difference of A4F compared to SEC is its lack of stationary phase. Separation is achieved by flow in an empty channel where perpendicular cross flow is applied.
- Separation power of A4F is adjustable by operational variables.
- Separation of soluble macromolecules and particles in the nanoscale range is based on the equilibrium of the cross flow field and diffusion, and is called *normal* or *Brownian*. The separation mechanisms for micrometer-sized particles is based on either the steric effect of the particles pressed closely to the bottom wall or the equilibrium of the cross flow force and hydrodynamic lift forces.
- The main contributions to plate height in A4F are nonequilibrium and sample polydispersity. However, the polydispersity contribution is actually given by the real sample separation.
- Selectivity of A4F is usually significantly higher than that of SEC.

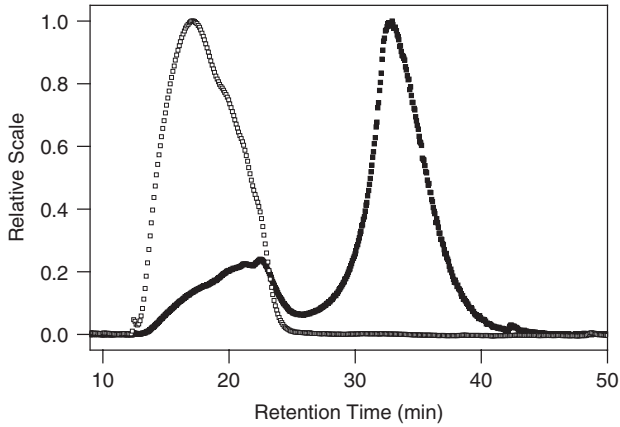

Figure 5.29 RI (□) and MALS (■) fractograms of polymer containing trace amounts of ultra-high-molar-mass fractions. A4F conditions: THF, detector flow 1 mL/min, cross flow from 3 mL/min to 0.2 mL/min within 20 min + 10 min at 0.2 mL/min, injection 200 μL 0.2% w/v, spacer 490 μm, ambient channel temperature. Elution starts at 12 min.

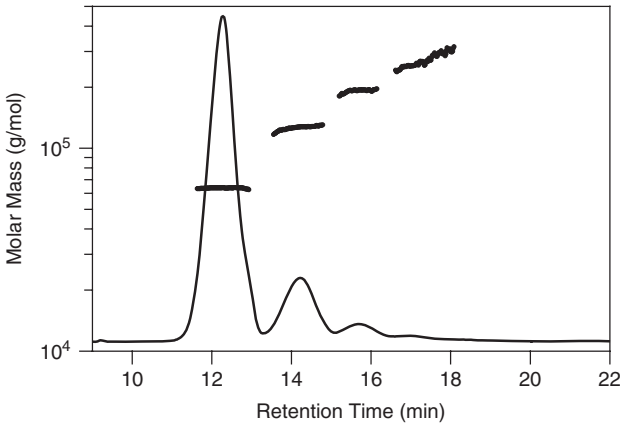

Figure 5.30 RI fractogram and molar mass for particular peaks of BSA. A4F conditions: 50 mM sodium nitrate aqueous solution, detector flow 1 mL/min, isocratic cross flow 5 mL/min, focus flow 3 mL/min, injection 15 μL 0.2% w/v, spacer 350 μm, ambient channel temperature, beginning of elution at 6 min. Relative peak area = 76.1% (monomer), 17.1% (dimer), 4.6% (trimer), and 2.2% (tetramer + higher).

5.7 REFERENCES

1. Giddings, J. C., *Separation Sci*., **1**, 123 (1966).
2. Barth, H. G. and Carlin, F. J., *J. Liq. Chromatogr*., **7**, 1717 (1984).
3. Giddings, J. C., Yang, F. J., and Myers, M. N., *Science*, **193**, 1244 (1976).
4. Giddings, J. C., Yang, F. J., and Myers, M. N., *Anal. Chem*., **48**, 1126 (1976).

5. Wahlund, K.-G., Winegarner, H. S., Caldwell, K. D., and Giddings, J. C., *Anal. Chem*., **58**, 573 (1986).
6. Wahlund, K.-G. and Giddings, J. C., *Anal. Chem*., **59**, 1332 (1987).
7. Janca, J., *Field-Flow Fractionation: Analysis of Macromolecules and Particles*, Marcel Dekker, New York (1988).
8. Janca, J., *Microthermal Field-Flow Fractionation*, HNB P, New York (2008).
9. Schimpf, M. S., Caldwell, K., and Giddings, J. C. (editors), *Field-Flow Fractionation Handbook*, Wiley-Interscience, New York (2000).
10. Giddings, J. C., *J. Chem. Ed*., **50**, 667 (1973).
11. Giddings, J. C., *Sep. Sci. Technol*., **21**, 831 (1986).
12. Litzen, A. and Wahlund, K.-G., *Anal. Chem*., **63**, 1001 (1991).
13. Giddings, J. C., Myers, M. N., Caldwell, K. D., and Fisher, S. R., *Methods of Biochemical Analysis*, Glick, D. (editor), John Wiley & Sons, New York (1980), Vol. **26**, p. 79.
14. Lee, S. and Giddings, J. C., *Anal. Chem*., **60**, 2328 (1988).
15. Ratanathanawongs, S. K. and Giddings, J. C., *Chromatography of Polymers: Characterization by SEC and FFF*, ACS Symposium Series **521**, Provder, T. (editor), American Chemical Society, Washington D.C. (1993), Chapter 2.
16. Jensen, K. D., Williams, S. K. R., and Giddings, J. C., *J. Chromatogr. A*, **746**, 137 (1996).
17. Caldwell, K. D., *Modern Methods of Polymer Characterization*, Barth, H. G. and Mays, J. W. (editors), John Wiley & Sons, New York (1991), Chapter 4.
18. Giddings, J. C., Martin, M., and Myers M. N., *J. Chromatogr*., **158**, 419 (1978).
19. Giddings, J. C., Yoon, U. H., Caldwell, K. D., Myers. M. N., and Hovingh, M. E., *Sep. Sci*., **10**, 447 (1975).
20. Smith, L. K., Myers, M. N., and Giddings, J. C., *Anal. Chem*., **49**, 1750 (1977).
21. Giddings, J. C., Williams, P. S., and Beckett, R., *Anal. Chem*., **59**, 28 (1987).
22. Dubascoux, S., Hecho, I. Le, Gautier, M. P., and Lespes, G., *Talanta*, **77**, 60 (2008).
23. Siripinyanond, A., Worapanyanond, S., and Shiowatana, J., *Environ. Sci. Technol*., **39**, 3295 (2005).
24. Caldwell, K. C., Steven, L. B., Gao, Y., and Giddings, J. C., *J. Appl. Polym. Sci*., **36**, 703 (1988).
25. Leeman M., Islam, M. T. Haseltine, W. G., *J. Chromatogr. A*, **1172**, 194 (2007).
26. Benincasa, M.-A. and Caldwell, K. D., *J. Chromatogr. A*, **925**, 159 (2001).
27. Mes, E. P. C., de Jonge, H., Klein, T., Welz, R. R., and Gillespie, D. T., *J. Chromatogr. A*, **1154**, 319 (2007).
28. Bang D. Y., Shin D. Y., Lee, S., and Moon, M. H., *J. Chromatogr. A*, **1147**, 200 (2007).
29. Kwon, J. H., Hwang, E., Cho, I.-H., and Moon, M. H., *Anal. and Bioanal. Chem*., **395**, 519 (2009).
30. Benincasa, M.-A., Cartoni, G., and Delle Fratte, C., *J. Chromatogr. A*, **967**, 219 (2002).
31. Wittgren, B. and Wahlund, K.-G., *J. Chromatogr. A*, **760**, 205 (1997).
32. Leeman, M., Wahlund, K.-G., and Wittgren, B., *J. Chromatogr. A*, **1134**, 236 (2006).
33. Giddings, J. C., Yang, F. J., and Myers, M. N., *Anal. Biochem*., **81**, 395 (1977).
34. Min-Kuang Liu, Ping Li, and Giddings J. C., *Protein Science*, **2**, 1520 (2008).
35. Silveira, J. R., Hughson, A. G., and Caughey, B., *Methods Enzymol*., **412**, 21 (2006).
36. Liu, M.-K. and Giddings, J. C., *Macromolecules*, **26**, 3576 (1993).
37. Hawe, A., Friess, W., Sutter, M., and Jiskoot, W., *Anal. Biochem*., **378**, 115 (2008).
38. Gabrielson, J. P., Brader, M. L., Pekar, A. H., Mathis, K. B., Winter, G., Carpenter, J. F., and Randolph, T. W., *J. Pharmaceutical Sci*., **96**, 268 (2007).
39. Giddings, J. C., Yang, F. J., and Myers, M. N., *J. Virology*, **21**, 131 (1977).
40. Citkowicz, A., Petry, H., Harkins, R. N., Ast, O., Cashion, L., Goldmann, C., Bringmann, P., Plummer, K., and Larsen, B. R., *Anal. Biochem*., **376**, 163 (2008).
41. Pease, L. F., Lipin, D. I., Tsai, D.-H., Zachariah, M. R., Lua, L. H. L., Tarlov, M. J., and Middelberg, A. P. J., *Biotechnology and Bioengineering*, **102**, 845 (2009).
42. Nilsson, M., Birnbaum S., and Wahlund, K.-G., *J. Biochem. Biophys. Methods*, **33**, 9 (1996).
43. Arifin, D. R. and Palmer, A. F., *Biotechnology Progress*, **19**, 1798 (2003).

44. Hupfeld, S., Ausbacher, D., and Brandl, M., *J. Sep. Sci*., **32**, 1465 (2009).
45. Hupfeld, S., Ausbacher, D., and Brandl M., *J. Sep. Sci*., **32**, 3555 (2009).
46. Wittgren, B., Wahlund, K.-G., Derand, H., and Wesslen, B., *Macromolecules*, **29**, 268 (1996).
47. Frankema, W., van Bruijnsvoort, M., Tijssen, R., and Kok, W. T., *J. Chromatogr. A*, **943**, 251 (2002).
48. Lesher, E. K., Ranville, J. F., and Honeyman, B. D., *Environmental Science and Technology*, **43**, 5403 (2009).
49. Zattoni, A., Rambaldi, D. C., Reschiglian, P., Melucci, M., Krol, S., Garcia, A. M. C., Sanz-Medel, A., Roessner, D., and Johann C., *J. Chromatogr. A*, **1216**, 9106 (2009).
50. Kang, D. Y., Kim, M. J., Kim, S. T., Oh, K. S., Yuk, S. H., and Lee, S., *Anal. Bioanal. Chem*., **390**, 2183 (2008).
51. Dubascoux, S., Kammer, F. V. D., Le Hecho. I., Gautier, M. P., and Lespes, G., *J. Chromatogr. A*, **1206**, 160 (2008).
52. Bouby, M., Geckeis, H., and Geyer, F. W., *Anal. Bioanal. Chem*., **392**, 1447 (2008).

Chapter 6

Characterization of Branched Polymers

6.1 INTRODUCTION

Branching of polymeric chains is one type of polymer nonuniformity. It is one of the most important molecular parameters that determines various physical, mechanical, and end-use properties of synthetic and natural polymers. Polymer properties affected by branching include glass transition temperature, mechanical properties (e.g., strength, tack, peel), viscoelastic properties, ability to crystallize, thermodynamic behavior (A_2 or θ-temperature), solubility, chemical resistance, phase separation of polymer mixtures, solution viscosity, melt viscosity, melt elasticity, rheological behavior of solutions and melts, workability, curing behavior of synthetic resins, and ability to swell. This last property can be of primary importance for drug delivery systems since the drug release rate can be controlled by the degree of branching of a polymer used as a drug carrier. Indeed, various branched polymers, such as branched polylactides, are of great interest for medical, biomedical, and pharmaceutical applications.

The effect of branching on polymer properties can be either negative or positive, depending on particular circumstances and polymer applications. For some properties the effect of branching may not be straightforward. For example, branching increases glass transition temperature (T_g) as a consequence of decreased mobility of polymer segments; on the other hand, increased concentration of chain ends increases free volume and thereby contributes to the decrease of the T_g. Similarly as for molar mass it may be necessary to find optimum values of branching, because positive effects on one property may result in negative effects on another property. The relation between type and degree of branching and polymer properties can be studied experimentally by means of model branched polymers or derived theoretically. Although it

Light Scattering, Size Exclusion Chromatography and Asymmetric Flow Field Flow Fractionation: Powerful Tools for the Characterization of Polymers, Proteins and Nanoparticles, by Stepan Podzimek

may be difficult to predict properties of branched polymer unambiguously due to the variety of possible branching structures and the fact that many branching reactions occur in a random fashion, branching in polymers is undoubtedly an important structural variable that can be used to modify the processing and application properties of polymers. Some properties of specific branched polymers (e.g., dendrimers) are unachievable by means of linear polymers.

Some properties of branched polymers are very attractive. For example, branching is an efficient means of inhibition of polymer crystallization. That is because branching discourages the chains from fitting closely together so that the structure is amorphous with relatively large amounts of empty space, whereas structures with little or no branching allow the polymer chains to fit closely together, forming a crystalline structure. Another result of branching is that it reduces the molecular size. Consequently, branching is an effective way of reduction of solution viscosity. Some polymers may be easily melt-processable, but favorable processability may be associated with bad mechanical properties. Improvement in mechanical properties may cause processsability to deteriorate, and branching of polymer chains may help to balance the two counteracting properties. The impact of branching on shear thinning (i.e., decrease of viscosity with increasing rate of shear stress) may play an important role in extrusion and injection molding. The impact on polymer dielectric properties may improve breakdown voltage and energy loss of capacitors. Various types of polyethylene play an important role as engineering polymers and thus the influence of long-chain branching on flow properties is of primary interest in the polyolefin industry. For instance, long-chain branches in polyethylene lead to significantly improved processing behavior due to increased shear thinning and strain hardening in elongation flow. An important fact is that even a very low level of branching can improve processing behavior in a sufficient manner.

One of the most important properties in rheology of polymer melts is the temperature dependence of the viscosity (Equation 1.89). The higher the activation energy E, the more temperature sensitive is the polymer melt. The value of E varies from polymer to polymer depending on chain composition. From a certain minimum value of molar mass (equal to the entanglement molar mass), E is independent on molar mass, but increases with the amount of long-chain branches. Branching is not only important from the viewpoint of structure–property and structure–property–processing relationships, but it brings valuable information about the polymerization mechanisms and extent and type of side reactions.

The term *degree of branching* refers to number of branch units in a macromolecule or number of arms in a starlike macromolecule. A *branched polymer* is a polymer containing at least one *branch unit* (branch point, junction point), that is, a small group of atoms from which more than two long chains emanate. A branch point from which f linear chains emanate is called an f-functional branch point. A distinguishing feature of branched polymers compared to linear polymers is presence of more than two chain ends. A branch is an oligomeric or polymeric offshoot from a macromolecular chain. An oligomeric branch is called

a *short-chain branch* while a polymeric branch is termed a *long-chain branch*. If the addition or removal of one or a few structural units has a negligible effect on the molecular properties, then the material can be considered to be a polymer and a branch can be considered to be a long-chain branch. Alternatively, if the branch length is comparable to the length of the backbone, the branched polymer can be termed as long-chain. However, the line between short-chain and long-chain is never explicit.

Branched molecules can be of varied structures, namely randomly branched molecules, combs, stars, dendrimers, and hyperbranched molecules. Even unusual branched structures such as centipedes or barbwire molecules have been reported in the literature. Branched molecules can arise as a result of various side reactions or can be prepared purposefully by simple or sophisticated synthetic pathways. Chain transfer to polymer, addition of water and glycols on double bonds during the synthesis of unsaturated polyesters, reaction of epoxy groups with aliphatic hydroxyl groups in epoxy resins, or polymerization of the second double bond in polyisoprene or polybutadiene are examples of side reactions leading to branching.

Free radical polymerization of a monovinyl monomer (e.g., styrene, acrylates, methacrylates) with the addition of a small amount of a divinyl monomer[i] (e.g., divinyl benzene, ethyleneglycol dimethacrylate) represents the simplest example of the synthesis of branched polymers. The reaction technique is very straightforward and typically involves addition of free radical initiator to solution of monomers in a suitable solvent and polymerization at a temperature appropriate to the initiator. The resulting polymer has randomly (statistically) branched structure. At early stages of polymerization, predominantly only one of the vinyl groups of the divinyl monomer reacts and thus branch units appear at higher conversions. The length and number of branches can be partly controlled by the reaction temperature; varying the concentrations of divinyl monomer, initiator, and solvent; and using transfer agent.

Depending on the conversion and concentration of a polyfunctional monomer, the branching reaction can reach the gel point, that is, the stage when an infinitesimal fraction of indefinite structure appears in the system. At the gel point the weight-average molar mass reaches infinite value while the number-average molar mass is finite. With increasing reaction conversion after the gel point, the fraction of infinite insoluble structure (gel) increases while the amount of soluble fraction (sol) decreases and the M_w of sol decreases as well. A typical feature of a polymer prepared by free radical polymerization of a mixture of mono and divinyl monomers is a large fraction of linear molecules even at the proximity of gel point.

Another characteristic of randomly branched polymers is a presence of high-molar-mass tail and broadening of the molar mass distribution in comparison to the distribution that would arise under identical reaction conditions without

[i]In free radical polymerization, each vinyl group is difunctional (i.e., divinyl monomer is tetrafunctional).

presence of polyfunctional monomer. The probability that a randomly selected molecule will contain a branch unit increases with increasing molar mass and thus the degree of branching increases with increasing molar mass.

Randomly branched macromolecules can also arise by the radical polymerization of vinyl monomers due to the chain transfer to polymer. In contrast to the polymerization of monovinyl and divinyl monomer mixture, the resulting branch units are trifunctional. Another synthetic way to prepare randomly branched polymers is polycondensation of difunctional (e.g., hydroxy acid, mixture of dicarboxylic acids and glycols) and polyfunctional monomers (e.g., glycerol, pentaerythritol), which leads to polymers of equivalent structure to those prepared by radical polymerization with the exception of the presence of relatively high levels of oligomeric fractions even at high conversions. Other reactions leading to randomly branched polymers are heat treatment or irradiation of linear polymers. Branched macromolecules may be also formed during polymer aging.

Special synthetic methods can lead to branched polymers with well-defined structure compared to randomly branched polymers. Anionic polymerization is particularly suited for the preparation of branched polymers with controlled architecture. The technique yields polymers that retain their active chain ends even after all monomer has been consumed. These living polymers can react with multifunctional linking agents under formation of starlike polymers with the number of arms equivalent to the functionality of the linking agent. Possible heterogeneity is given by formation of stars containing different numbers of arms, as in the case of the reaction of poly(styryl)lithium with silicon tetrachloride, which usually leads to a mixture of three-arm and four-arm stars. Another synthetic way to form starlike polymers is living polymerization using multifunctional initiators.

Group transfer polymerization (GTP) is a technique applicable to the polymerization of methacrylic monomers, which in contrast to anionic polymerization yields living polymers at room temperature. The technique applies special initiators that enable synthesis of various polymethacrylates with controlled molecular structure. GTP synthesis of branched polymers involves two steps. Living arms from methacrylate are prepared in the first step, and then in the second step they react with a dimethacrylate monomer (e.g., ethyleneglycol dimethacrylate, EGDMA), which can react with up to four arms and partly also with itself. The resulting polymer consists of a dense EGDMA center from which numerous arms protrude. The method can provide starlike polymers with up to hundreds of arms and possibly functional groups located at the arm ends or in the arm chains. The properties can be further modified by the preparation of arms consisting of block copolymer.

Dendrimers are highly branched well-defined macromolecules with a branch point at each monomer unit, resembling the structure of trees. Their synthesis consists of numerous protection/deprotection and purification steps leading to products of increasing generation and molar mass. Dendrimers of higher generations of eight to ten reach the molar mass of several hundreds of thousands g/mol. Many interesting potential applications of dendrimers are based on their

molecular uniformity, highly dense structure, and multifunctional surface. On the other hand, the extreme laboriousness of their preparation, which requires multiple steps, is a serious limitation on their broader application.

Hyperbranched polymers represent a simpler alternative to dendrimers. They are prepared by a single-step polycondensation of AB_x ($x \geq 2$) monomers with different types of functional groups A and B capable of reacting with each other (e.g., dimethylol propionic acid, dimethylol butanoic acid). Hyperbranched polymers are expected to be highly branched like dendrimers; however, experimental results often indicate the presence of significant amounts of linear segments.

Macromonomers, that is, polymeric or oligomeric monomers with polymerizable functional groups at one end, can be used for the preparation of comb-shaped branched polymers with the distance between the branch units controllable with a regular low-molar-mass comonomer. In principle, macromonomers enable synthesis of polymers with a very high branch density.

6.2 DETECTION AND CHARACTERIZATION OF BRANCHING

In most branched polymers the distribution of degree of branching coexists with the distribution of molar mass and possibly with the distribution of other characteristics such as chemical composition. In addition, branched polymers are typical in variety of branching topology, as can be seen from the following simple example. Let us imagine a polymer molecule with two trifunctional branch units. The two branches can protrude from the backbone or one branch can protrude from the other, and they can have various positions with respect to the chain ends. If the branches are located close to the backbone ends, then the entire molecule virtually behaves as a linear molecule. This simple example shows that a branched molecule of a given molar mass and branching degree can occur in numerous positional isomers.

Another reaction complicating the architecture of branched polymers is the possible formation of intramolecular rings due to the reaction that occurs between two segments of the same macromolecule. Branched polymers mostly consist of molecules of different molar mass and degree of branching, which is particularly true in the case of randomly branched polymers. Molecules of identical molar mass can differ in the number of branch units, and macromolecules of identical molar mass and number of branch units can differ in the position of branch units in a polymer chain.

Thorough characterization of branched polymers involves not only the determination of the distribution of molar mass, but also the distribution of branching degree. However, there is no experimental technique that would enable separation of polymer molecules purely according to the degree of branching and regardless of their molar mass. The temperature rising elution fractionation (TREF) and crystallization analysis fractionation (CRYSTAF) techniques utilize the different crystallizability brought in by short-chain and long-chain branches to fractionate

polymer on the basis of the branching degree. In principle, this mechanism permits characterization of the branching distribution, but the applicability of both methods is limited mainly for the analysis of polyethylene and polyethylene-based copolymers. In addition, although the separation is expected to be according to the degree of branching, there is also simultaneous separation on the basis of molar mass. In a conventional arrangement with a concentration detector only (infrared detector) there is no information about the molar mass of fractions eluting from the TREF/CRYSTAF system, and the obtained fractions must be further characterized.

Another method attempting the separation of molecules according to their branching degree has been reported by Meunier et al.[1] The method is based on the idea of anchoring of branched molecules in porous matrix, described in reference 2. It uses monolithic columns to create a tortuous path where the flow-through channels have size of the order of polymer molecular dimensions. Because the long-chain branched molecules are retained more than linear molecules of the same size, the method can be used to separate branched chains from linear molecules. The method may succeed in separating simple branched polymers, such as mixtures consisting of four-arm and three-arm stars and residual linear molecules. However, it is unlikely that the method would allow efficient separation of complex branched polymers solely according to the branching degree.

Two-dimensional chromatography may offer another possible approach in the more detailed characterization of various branched polymers, where fractions of identical hydrodynamic volume obtained by SEC in the first step can be further separated according to the branching degree by a suitable type of interaction chromatography in the second step.

Currently, the only really measurable branching distribution is the degree of branching as a function of molar mass. In fact, the branching ratio determined at a given molar mass is an average for all molecules having this molar mass, because the molecules may have different degrees of branching at the same molar mass. That means molecules of a given molar mass consist of molecules with a certain distribution of branching degree. Another complicating fact is that the available analytical separation techniques separate on the basis of hydrodynamic volume and not molar mass. Consequently, the molecules eluting from the separation system at a given elution time have the same hydrodynamic volume, but different degrees and topologies of branching and also different molar masses. In a rigorous manner the obtained result is the relation between the average branching degree (average for a given average molar mass) and the average molar mass (average for a given hydrodynamic volume).

Various methods providing relationships between branching degree and molar mass will be described in this chapter. Taking into account the complexity of branched polymers with respect to their molar mass distribution, number of branch units per molecule, and branching topology, a detailed description of branching is virtually impossible. In reality, detection of the presence of branched molecules and estimation of the degree of branching as a function of molar mass

and the determination of an average branching characteristic for the entire sample is the only obtainable information for most branched polymers.

The characterization of branching is often complicated by the impossibility of preparing well-defined branched model polymers. Although sophisticated synthetic routes can yield well-defined stars or combs, the preparation of well-defined models for randomly branched polymers is impossible. For some polymers even the preparation of a linear counterpart of identical chemical composition is impossible, as in the case of various synthetic resins (e.g., alkyds, phenol-formaldehyde resins, epoxies). Also the tendency of various acrylates (not methacrylates) to chain transfer to polymer is so strong that it may be difficult to prepare purely linear homopolymers by free radical polymerization.

It may be noted that structure and number of branches in a polymer sample can be revealed from the rheological measurements.[3,4] Rheological experiments conducted on irradiated polypropylene were shown[4] to be more sensitive with respect to long-chain branching than characterization by means of SEC-MALS. However, rheological measurements are not applicable to all kinds of branched polymers and the obtained results are merely average characteristics with no information about branching distribution. Although the presence of branch units can be in principle detected by spectral techniques, the level of long-chain branching is often that low that it cannot be detected by standard analytical methods. Branched molecules can be detected and characterized indirectly by the measurement of dilute solution properties. A review of solution properties of branched macromolecules can be found in reference 5.

The fundamental principle of detection and characterization of branching is based on the fact that at a given molar mass the molecular size decreases with increasing degree of branching. In other words, branching reduces the molecular size and increases the compactness of the macromolecules. This means that to get branching information it is necessary to determine both molar mass and molecular size. The analytical methods commonly applicable for the investigation of branching can be divided into two categories: (1) characterization methods, mainly light scattering, dynamic light scattering, and viscometry, and (2) separation methods, mainly SEC and field flow fractionation techniques. The characterization methods can be used in batch mode or in combination with a separation technique.

A numerical description of the degree of branching can be achieved by the parameter defined by Zimm and Stockmayer:[6]

$$g = \left(\frac{R_{br}^2}{R_{lin}^2} \right)_M \tag{6.1}$$

where R^2 is the mean square radius of a branched (br) and a linear (lin) macromolecule of the same molar mass (M). The parameter g is called *branching ratio* (*branching index*, *branching parameter*, or *contraction factor*) and is equal to unity for linear polymers and decreases with increasing extent of branching. For polymers with a very high degree of branching, the ratio g approaches values around 0.1, but never zero. It is also evident from the definition of g that it is never larger than 1.

Branching frequency (λ), defined as the number of branch units per 1,000 repeat units, is another parameter that can be used for the description of branched polymers and is frequently used in the analysis of polyolefins. Branching ratio itself can serve for the characterization of branching degree, and it can be used for further calculations. As shown by Zimm and Stockmayer, the branching ratio g allows calculation of number of branch units per molecule or number of arms in starlike molecules. Various theoretical equations describing the structure of branched polymers can be found in the literature.[6–11] The most frequently stated relations are those derived by Zimm and Stockmayer for randomly branched and star-branched polymers.[6]

For randomly branched polymers with tri- or tertafunctional branch units, the ratio g is given by the equations:

$$g_3 = \left[\left(1 + \frac{m}{7}\right)^{\frac{1}{2}} + \frac{4m}{9\pi}\right]^{-\frac{1}{2}} \tag{6.2}$$

$$g_4 = \left[\left(1 + \frac{m}{6}\right)^{\frac{1}{2}} + \frac{4m}{3\pi}\right]^{-\frac{1}{2}} \tag{6.3}$$

where m is the average number of branch units per molecule and subscripts 3 and 4 refer to trifunctional and terafunctional branch units. For instance, the polymerization of vinyl monomers with an addition of a small amount of a divinyl monomer results in tetrafunctional branch units while chain transfer to polymer creates trifunctional branch units. In a given example, both functionalities can occur simultaneously, the former being relatively easily controllable by the amount of divinyl monomer and conversion, the latter being indirectly controllable by reaction conditions. Simultaneous existence of branch units of different functionality may be also expected in the case of polyfunctional monomers, for instance in polycondensation of a mixture of difunctional monomers with addition of a tetrafunctional monomer, which can undergo reaction completely, giving tetrafunctional branch units, or incompletely, giving trifunctional branch units. Trifunctional randomly branched topology can be assumed in branched polymers formed by irradiation, because formation of branch points with higher functionality is statistically improbable.

Equations 6.2 and 6.3 were derived for the case where a material of heterogeneous molar mass containing randomly distributed branch units is fractionated into a series of samples, each of them being monodisperse but of different molar mass, and the branch units in each fraction are still randomly distributed. As a matter of fact, these conditions approximately correspond to the situation occurring in SEC or FFF. Since m is the average number of branch units (actually the number-average), the ratio g given by Equations 6.2 and 6.3 is the average value valid for molecules of the same molar mass but different numbers of branch units.

The expressions for polymers heterogeneous with respect to molar mass are:

$$g_{3,w} = \frac{6}{n_w}\left[\frac{1}{2}\left(\frac{2+n_w}{n_w}\right)^{\frac{1}{2}} \ln\left(\frac{(2+n_w)^{\frac{1}{2}} + n_w^{\frac{1}{2}}}{(2+n_w)^{\frac{1}{2}} - n_w^{\frac{1}{2}}}\right) - 1\right] \tag{6.4}$$

and

$$g_{4,w} = \frac{\ln(1+n_w)}{n_w} \tag{6.5}$$

where n_w is the weight-average number of branch units per molecule and the subscripts indicate functionality of the branch unit and the fact that the ratios are the weight-averages.

For the z-average values of g, the formulas derived in reference 6 are:

$$g_{3,z} = \frac{1}{1+\frac{n_w}{3}} \tag{6.6}$$

and

$$g_{4,z} = \frac{1}{1+n_w} \tag{6.7}$$

For stars with f arms of random length, the branching ratio is given by the equation:[6]

$$g = \frac{6f}{(f+1)(f+2)} \tag{6.8}$$

And for regular stars with arms of equal length:

$$g = \frac{3f-2}{f^2} \tag{6.9}$$

Note that for the linear molecules, $f = 2$ or $m = 0$, the above formulas yield the value unity. The graphical representation of Equations 6.2, 6.3, and 6.8 is shown in Figure 6.1.

It must be emphasized that the above equations were derived assuming unperturbed chain statistics for both linear and branched macromolecules, that is, assuming no excluded volume effect. However, the real measurements are mostly carried out in thermodynamically good solvents where the molecules expand due to intensive interactions between polymer molecules and solvent. The expansion of a polymer chain is more pronounced in the case of linear molecules, and thus the ratio g determined in thermodynamically good solvent is smaller than it would be in theta solvent and the branching degree is overestimated. The correction for the excluded volume effect yields equations that are complicated, with several parameters generally unknown or at least uncertain. In reality, the effect of the excluded volume is probably lower than experimental and other uncertainties and thus can be neglected. The selection of an appropriate equation relating g with a parameter characteristic for a given branched structure may not

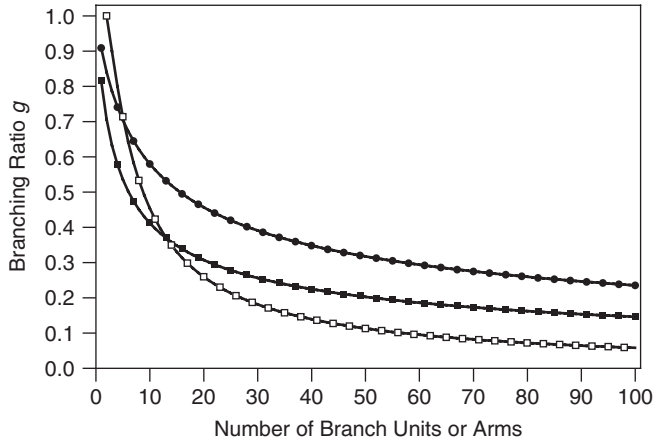

Figure 6.1 Branching ratio as a function of number of branch units per molecule for three (•) and four (■) functional branch units in randomly branched polymer and number of arms (□) in star-branched polymer (Equations 6.2, 6.3, and 6.8).

be always straightforward, because the functionality of branch unit or the type of branched structure may not be known. In addition, the theoretical equations were typically not verified by experiments due to lack of well-defined branched standards.

Although the application of theoretical equations may not provide an absolutely accurate description of a branched polymer, especially when the measurement is carried out far from θ-conditions, the equations can yield an estimate of m or f, mutual comparison of various samples with respect to their branching degree, and indicate the effectiveness of synthetic techniques with respect to their ability to yield branched polymers of desired structure. The equations relating g with the number of branch units or arms are only one part of branching characterization; before they can be applied, a reliable value of g must be determined by a suitable experimental technique. The main objective of this chapter is to show the most important methods available for the characterization of branching and discuss their advantages and limitations. The focus is on methods that have general applicability and that are relatively easy to apply.

As described in Chapter 2, the molar mass and the root mean square radius, which are necessary to characterize branched molecules by parameter g, can be obtained by multi-angle light scattering. One serious limitation of MALS is that when applied on unfractionated polymer sample it yields M and R of different moments, namely the weight-average molar mass and the z-average RMS radius. The two averages are of different sensitivities to high-molar-mass species; consequently, batch MALS usually can provide branching information only for monodisperse or very narrow polymers. Combination of MALS with a separation method overcomes this limitation to a great extent since M and R are measured for narrow fractions eluting from the separation device.

Traditional methods of polymer fractionation, such as precipitation fractionation, are of limited applicability due to their laboriousness and low efficiency with respect to the polydispersity of obtained fractions. SEC and A4F, or other FFF techniques, are separation methods that can be used in combination with MALS for the characterization of branched polymers. However, in comparison to linear polymers, where the local slice polydispersity is given solely by the band broadening in the SEC columns or A4F channel and can be reduced by optimization of separation conditions, branching represents another contribution to the polydispersity of fractions eluting from an SEC or AF4 system. Since both methods separate molecules according to their hydrodynamic volume, in a given elution volume all molecules eluting from the separation device have identical hydrodynamic volume (assuming absence of band broadening), but different molar masses, numbers of branch units, and chain architectures. Consequently, a MALS detector does not measure the molar mass and RMS radius, but their averages. Nevertheless, as there is no simple method providing information about the polydispersity of fractions eluting from SEC columns or A4F channel, the polydispersity effect must be neglected and the molar masses and RMS radii must be treated as if they were determined for monodisperse fractions. This is a basic assumption that one has to accept at least for routine characterization.

Characterization of branching on the basis of RMS radius is also limited by the fact that RMS radius cannot be determined for smaller polymer molecules with RMS radii below about 10 nm, which roughly corresponds to molar mass of 10^5 g/mol. That means the size of many branched polymers cannot be determined by elastic light scattering. There are two alternative techniques that can be used for the determination of size below 10 nm: dynamic light scattering and viscometry of dilute solutions. The latter one is especially efficient for the determination of size of polymer molecules covering broad molar mass range. The intrinsic viscosity, $[\eta]$, describes the size of polymer molecules in a dilute solution. An alternative branching ratio was defined as the ratio of the intrinsic viscosities of a branched (br) and a linear (lin) macromolecule of identical molar mass:[12]

$$g' = \left(\frac{[\eta]_{br}}{[\eta]_{lin}} \right)_M \tag{6.10}$$

The mutual relationship of the two branching ratios can be expressed by a simple relation:

$$g' = g^e \tag{6.11}$$

where e is a parameter related to drainability of a polymer chain, the values of which are usually assumed to vary from 0.5 to 1.5. The value of e depends on solvent, molar mass, temperature, and branching. An important advantage of intrinsic viscosity is that it can be accurately determined even for small polymer molecules with molar masses down to about a thousand g/mol with practically no upper limit. In contrast to RMS radius, the weight-average intrinsic viscosity, $[\eta]_w$, is measured for an unfractionated sample and therefore the combination of MALS with a capillary viscometer can be used for the determination of average

g' by batch measurements. However, considerably more information can be obtained by means of an online viscometer combined with an SEC-MALS setup.

6.2.1 SEC Elution Behavior of Branched Polymers

As already mentioned, the polydispersity of elution volume slices in SEC separation of branched polymers is generally larger compared to linear polymers separated under the same separation conditions because of co-elution of molecules of the same hydrodynamic volume, but different molar masses and branching. However, for many branched polymers there is an additional, substantially more serious contribution that increases the local polydispersity within the elution volume slices. Many branched polymers show the SEC elution that is demonstrated in Figure 6.2, which depicts plots of molar mass and RMS radius versus elution volume for a randomly branched polymer. At lower elution volumes both molar mass and RMS radius decrease evenly with increasing elution volume, as is typical of SEC separation. At a certain point in the chromatogram both quantities

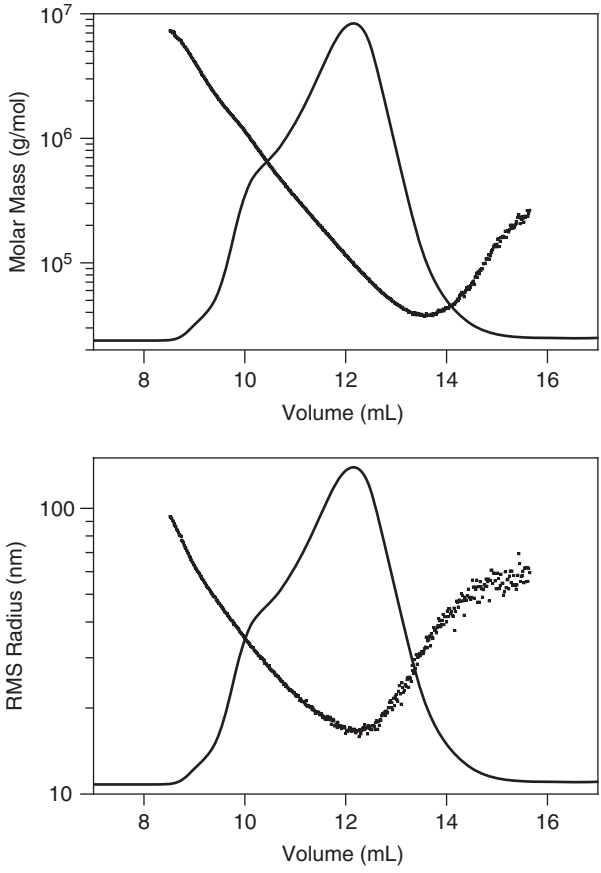

Figure 6.2 Abnormal SEC elution of branched polymer: Molar mass–versus–elution volume (top) and RMS radius–versus–elution volume (bottom) plots of randomly branched polymer. RI chromatogram is also shown here.

start to increase with increasing volume. For the RMS radius this upturn appears at a lower elution volume than for the molar mass. Although this SEC elution behavior is not observed for all branched polymers, it is frequent and becomes more pronounced with increasing degree of branching.

This behavior was reported by several authors and explained in different ways. It was systematically studied in reference 2, where the influence of various experimental parameters (e.g., flow rate, column type, temperature) on the pattern of molar mass and RMS radius plots was investigated. The most important finding was that the abnormal elution behavior was not found in the separation by thermal FFF, which was afterward repeatedly verified by separation using A4F, as shown later in this chapter.

On the basis of the obtained results, the abnormal SEC elution was explained by the entanglement of large, highly branched molecules in the pores of column packing. Since the previously used term *entanglement* is also used with respect to the concentration at which the polymer chains in solution start to overlap, the term *anchoring* will be used in this book to avoid confusion of the two phenomena. Anchoring is where particular parts of large branched molecules can behave as separate molecules, penetrate into the pores, and anchor the entire molecules.

This anchoring idea is sketched in Figure 6.3. Due to the anchoring effect some large molecules are delayed and elute at higher elution volumes than would correspond to their hydrodynamic volumes. The fractions eluting from SEC columns at the region of high elution volumes consist of smaller molecules separated by a purely SEC mechanism and very large branched molecules that were delayed by the anchoring effect. In such a case, the assumption of monodisperse fractions eluting from the SEC columns is not valid, the local polydispersity cannot be neglected, and the MALS detector yields values of M_w and R_z instead of values of M and R. The R_z is more sensitive to the presence of small amounts of fractions with very high molar mass than the M_w, and thus the upswing on the RMS plot appears at a lower elution volume compared to the molar mass. Simple estimation leads to the conclusion that the concentration of contaminating large molecules is rather low. For example, taking data from Figure 6.2 it is possible to estimate that the fractions of smaller macromolecules eluting at about

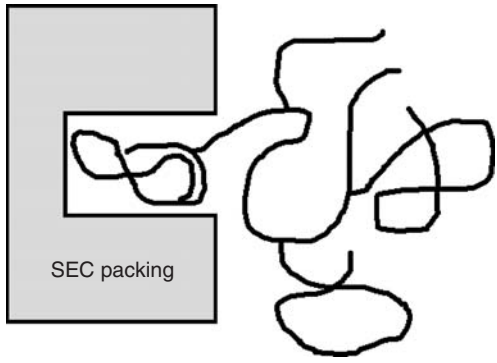

Figure 6.3 Illustration of the anchoring of a large branched molecule in a pore of column packing by a part of the polymer chain.

15 mL have molar mass around 10,000 g/mol. This number can be obtained by extrapolation of a molar mass–versus–elution volume plot from the region of low elution volumes to the high elution volumes. The molar mass measured by the MALS detector at this elution volume is about 140,000 g/mol. Assuming that the delayed molecules are of molar mass of the order of magnitude of 5×10^6 g/mol, that is, approximately the molar mass measured at the beginning of the chromatogram, one can estimate the fraction of the delayed molecules as follows:

$$140{,}000 = w_1 \times 10{,}000 + (1 - w_1) \times 5 \times 10^6$$

where w_1 is the weight fraction of molecules with molar mass 10,000 g/mol and $(1 - w_1) = w_2$ is the weight fraction of molecules with molar mass 5×10^6 g/mol. For this particular example, we get $w_2 = 0.026$; that is, delayed macromolecules represent approximately 2.6% of eluting molecules. The reality is certainly more complicated; co-eluting macromolecules are of different molar mass and the upturn on the molar mass and RMS radius plots can be caused by a trace level of ultra-high-molar-mass, highly branched fractions. For some highly branched polymers the anchoring effect is so strong that the light scattering signal tails to the elution volumes beyond the limit of total permeation of SEC columns. That means the molecules are delayed by anchoring for a relatively long time and they elute at very low concentrations detectable only by a light scattering detector.

An unwelcome consequence of the anchoring effect is the upswing on the conformation plot, as shown in Figure 6.4. It must be emphasized that the upswing on the conformation plot from SEC-MALS is totally virtual; that is, there are no molecules in the analyzed sample that would have two different radii at the same molar mass as one can see at the lower-molar-mass part of the conformation plot in Figure 6.4. The upswing is caused by the nonnegligible polydispersity of the fractions eluting at the end of the chromatogram and the higher sensitivity of R_z to the polydispersity compared to M_w.

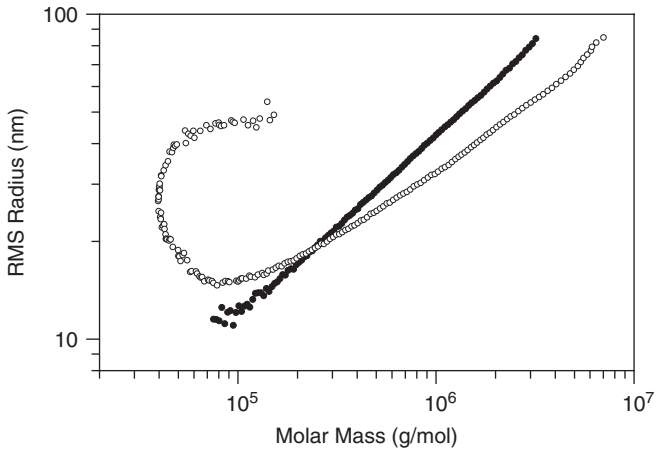

Figure 6.4 Conformation plots for linear (•) and randomly branched (○) polystyrene determined by SEC-MALS. The same polymer as in Figure 6.2.

6.2.2 Distribution of Branching

Branching distribution is usually characterized by the relation between the branching ratio and molar mass and consequently the relation between the number of branch units and molar mass. As already explained, this is usually the only measurable branching distribution, because the available separation techniques separate according to hydrodynamic volume and there is no generally working separation technique separating primarily on the basis of branching degree. The acquisition of requested experimental data requires hyphenation of an analytical separation technique and characterization methods capable of providing molar mass and molecular size. The characterization of branching distribution is based on the assumption of almost monodisperse fractions eluting from a separation system. That means an efficient separation analytical technique is crucial for accurate branching characterization.

Although the separation of branched polymers is generally less efficient than the separation of corresponding linear polymers, the experimental results for many branched polymers suggest that SEC and especially A4F are usually sufficient to provide useful branching information. For routine characterization of branched polymers, the slice polydispersity is neglected and the effort is focused on optimization of separation conditions, especially in the sense of minimizing the undesirable anchoring effect. Generally, there are three methods that can be used for determination of ratio g as a function of molar mass: (1) *radius method* (calculation of g from R at the same M), (2) *mass method* (calculation of g from M at the same elution volume), and (3) *viscosity method* (calculation of g' from $[\eta]$ at the same molar mass).

Figures 6.4–6.6 show typical results obtained by SEC-MALS or SEC-MALS-VIS analysis of a branched polymer and a corresponding linear counterpart. They are: (1) RMS radius–versus–molar mass plot (radius method

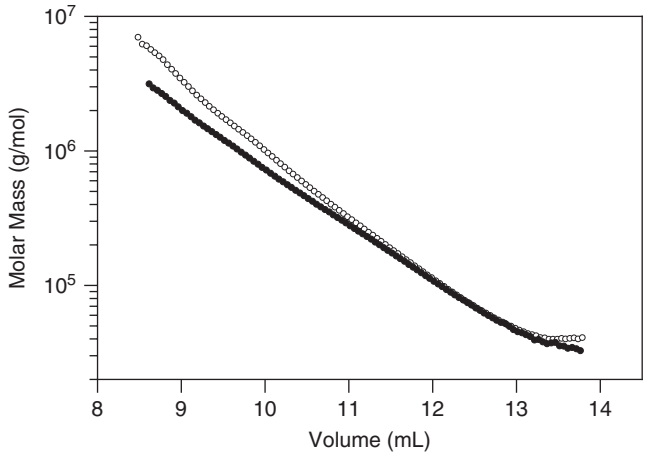

Figure 6.5 Molar mass–versus–elution volume plots for linear (•) and randomly branched (○) polystyrene (conformation plots are in Figure 6.4).

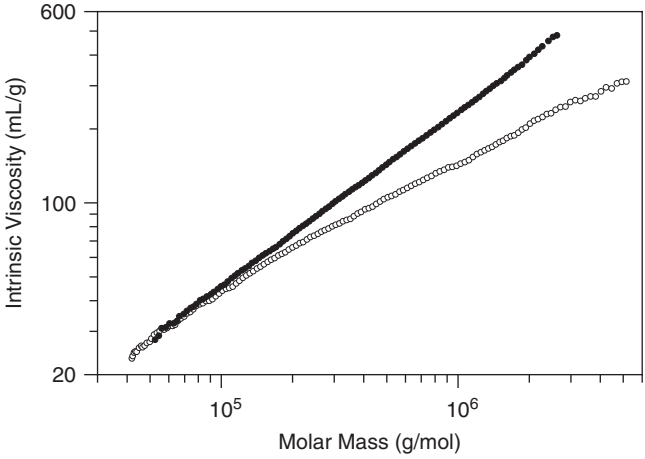

Figure 6.6 Mark-Houwink plots for linear (•) and randomly branched (○) polystyrene (conformation plots are in Figure 6.4).

of calculation of g), (2) molar mass–versus–elution volume plot (mass method), and (3) Mark-Houwink plot (viscosity method). All three plots relate the size information with the molar mass. The first two plots can be obtained using only SEC-MALS; the determination of the Mark-Houwink plot requires coupling the SEC-MALS instrument with an online viscometer.

The relation between the RMS radius and molar mass (*conformation plot*) is one of the basic tools for detection and characterization of branching. The conformation plots of linear polymers in thermodynamically good solvents are linear with the slopes around 0.58. In the case of branched polymers the slope of the conformation plot decreases with increasing degree of branching. Some conformation plots show leveling off toward high molar masses. The conformation plot can prove the presence or absence of branching even if the linear counterpart is unavailable. However, the decrease of the slope at low branching degrees is small (for example, from 0.58 to 0.55), which makes the detection of branching without a linear counterpart uncertain.

The slope of the conformation plot can be also influenced by the light scattering formalisms used for data processing (see Section 4.3.4) and possibly also by the separation range of the SEC columns. If the sample contains molecules with molar mass over the exclusion limit of the SEC columns, these molecules elute nonseparated at the beginning of the chromatogram and the MALS detector measures for that region M_w and R_z, which may result in the increase of the slope of the conformation plot. In such a case, the data from the beginning of the chromatogram should not be used for the determination of the slope; the same is true for the data points at the end of the chromatogram, which are often scattered due to the low concentration and molar mass of eluting molecules.

As already discussed, the conformation plots from SEC-MALS of many branched polymers show a noticeable upswing at the region of lower molar

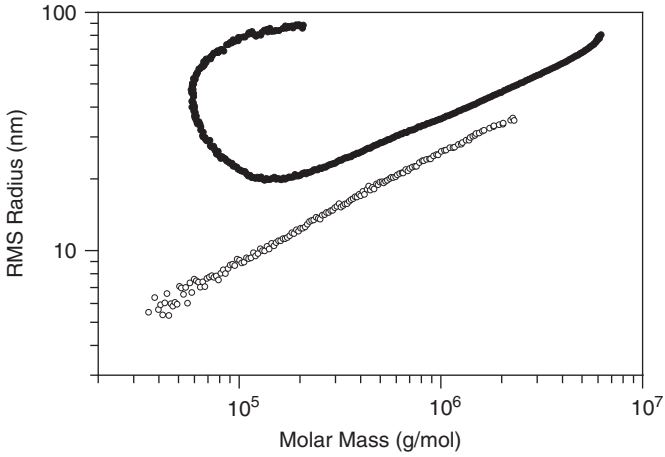

Figure 6.7 Conformation plots of two different branched samples with and without upswing. M_w, g_{M_z} and g'_{M_w} are listed in Table 6.1 for PS B2 (●) and PS 20 (○).

masses. In fact, the upswing is so typical that it may serve as evidence of the presence of branching. It has been explained that the upswing is a consequence of the anchoring of branched macromolecules in the pores of column packing during their flow through the SEC columns.

Although the upswing on the conformation plot is quite frequent, it may be missing on the conformation plots of some branched polymers as shown in Figure 6.7. The upswing is negligible especially in the case of polymers with lower degree of branching, branched samples that do not contain molecules with very high molar masses or polymers with relatively short branches. This is because smaller branched molecules or molecules with relatively short branches cannot be anchored in the way shown in Figure 6.3. The upswing also becomes less pronounced with decreasing sample polydispersity.

The intensity of the upswing is also related to the type of SEC columns used for the separation, as demonstrated in Figure 6.8, which shows that the upswing is more pronounced when SEC columns with smaller particle size and smaller pore size are used for the SEC separation. The upswing can be also partly eliminated using very low flow rates such as 0.1 mL/min. However, working at such low flow rates increases run time and the change in the flow rate typically results in increased noise level of a MALS detector due to release of particles from SEC columns. Stabilization of the signal at a very low flow rate takes a long time, and thus working at extremely low flow rates appears impractical. The only effective solution to the anchoring problem is change of the separation technique.

The upswing is completely eliminated when A4F is applied instead of SEC, as shown in Figure 6.9. The comparison of SEC-MALS and A4F-MALS results for various branched polymers proved unambiguously A4F to be a more efficient separation technique for branched polymers. This is certainly true mainly for

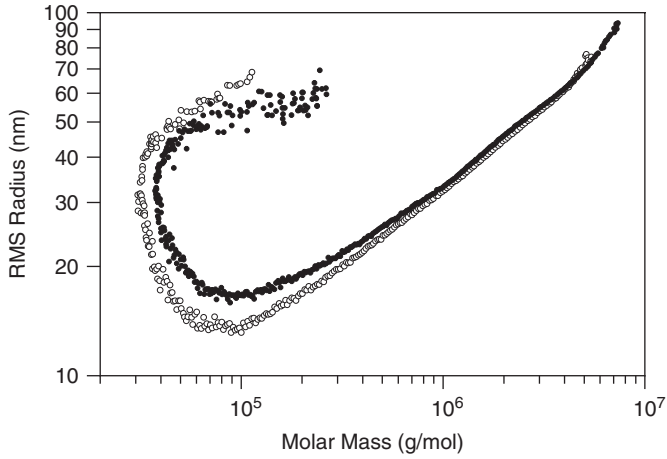

Figure 6.8 Conformation plots of randomly branched PS obtained by two different columns: 2 × Plgel Mixed-C (•) and 2 × Plgel Mixed-B (○). Mixed-C is 5-μm particle size column packing with operating range 200–2 × 10^6 g/mol; Mixed-B is 10-μm packing with operating range 500–10^7 g/mol.

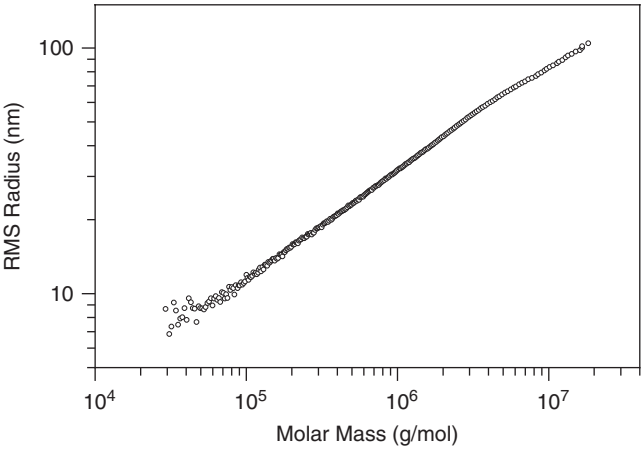

Figure 6.9 Conformation plot of branched polystyrene determined by A4F-MALS. (For comparison with SEC-MALS, see Figure 6.4).

large polymers with a tendency to anchor in the SEC column packing, whereas for smaller molecules SEC usually provides satisfactory results.

SEC elution volume is related to molecular size and therefore the relation between the molar mass and elution volume can be used for branching studies. Using the approach of Yu and Rollings,[13] the molar mass–versus–elution volume plots of a branched polymer and a linear polymer of the same chemical composition measured under identical separation conditions can yield the branching

ratio according to the equation:

$$g = \left(\frac{M_{lin}}{M_{br}}\right)_V^{\frac{1+a}{e}} \tag{6.12}$$

where M is the molar mass of linear (lin) and branched (br) molecules eluting at the same elution volume V, a is the exponent of the Mark-Houwink equation of a linear polymer in a given solvent and at a given temperature, and e is the draining parameter.

Calculation of g from the molar mass–versus–elution volume plots appears to be the least appropriate method of branching characterization, because it strongly depends on separation conditions and has no general validity. It requires knowledge of two parameters, a and e, which may not be always known. On the other hand, the molar mass–versus–elution volume plot is applicable over a broad molar mass range including oligomers. The molar mass–versus–elution volume plots can be valuable for mutual graphical comparison of samples measured under identical separation conditions. The mass method does not require the measurement of RMS radius, which makes it less sensitive to anchoring phenomena. Since the molecular size is not measured directly, but merely estimated from the elution volume, the method is highly sensitive to any kind of non-SEC separation.

In contrast to the molar mass–versus–elution volume plot, the conformation plot and the Mark-Houwink plot relate absolute quantities obtained by MALS and VIS detectors. They do not require concurrent measurement of a linear counterpart, but previously established relationships R versus M or $[\eta]$ versus M for a corresponding linear polymer can be used for branching detection and characterization.

An important finding is the significantly lower sensitivity of the Mark-Houwink plot to the anchoring effect. The explanation is that in the case of poor SEC separation the conformation plot relates R_z with M_w, whereas the Mark-Houwink plot relates $[\eta]_w$ with M_w, and thus the effect of poor separation is at least partly eliminated because both quantities are equally affected by increased polydispersity.

Figure 6.10 compares branching ratios g and g' obtained from the data depicted in Figure 6.4 and Figure 6.6. Branching ratio g' starts at about unity and decreases with increasing molar mass. This is typical behavior for randomly branched polymers, because the probability that a randomly selected macromolecule contains a branch unit increases with increasing polymerization degree. Consequently, in randomly branched polymers the fractions with lower molar mass are mostly linear while the fractions with higher molar mass are more branched. The branching ratio g calculated from the RMS radius shows different behavior. At the region of high molar masses it goes approximately parallel with g', while at the region of lower molar masses it goes for above unity, which is a maximum value of this parameter. As already explained, this is caused by increased polydispersity of fractions eluting at the region of higher elution volumes.

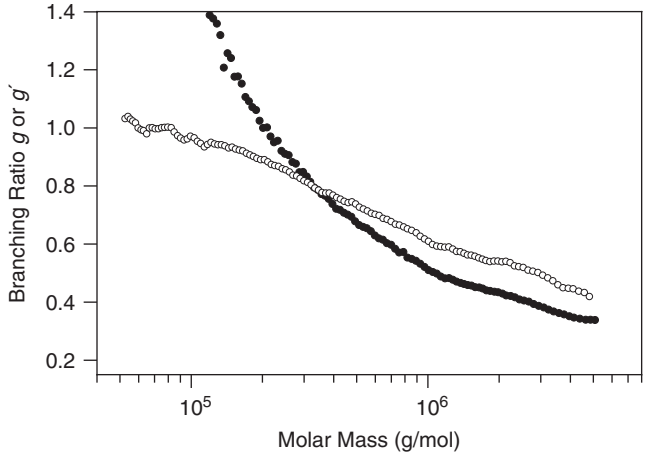

Figure 6.10 Molar mass dependence of branching ratios g (•) and g'(○) calculated using the data from Figures 6.4 and 6.6.

To avoid misunderstanding, it must be stressed that g of branched polymers is always smaller than unity if the branched and linear molecules are compared at the same molar mass or at the same molar mass moment. It has been shown in reference14 that g of a branched polymer can be larger than unity in the case of an unfractionated sample when the RMS radii are compared at the same M_w, which is exactly the case in SEC-MALS when some elution slices are polydisperse due to the anchoring effect.

Figure 6.11 contrasts the parameter g–versus–molar mass plots determined by A4F-MALS and by SEC-MALS. The two plots overlap at the region of

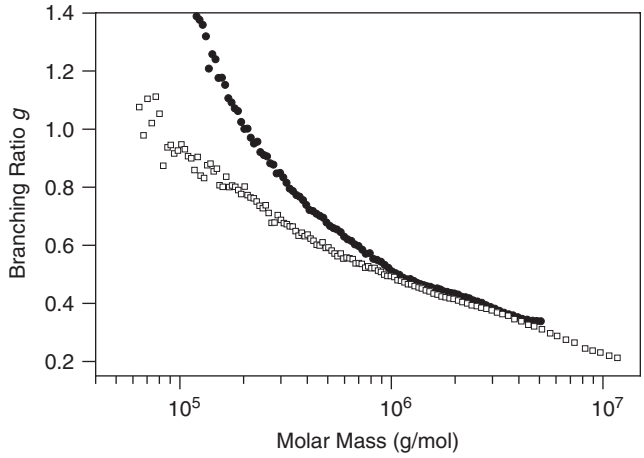

Figure 6.11 Branching ratio g–versus–molar mass plots of randomly branched polystyrene determined by SEC-MALS (•) and A4F-MALS (□).

high molar masses, where the anchoring effect in SEC is imperceptible and elution slices are narrow, and deviate toward lower molar masses due to the rising polydispersity of the SEC slices. The contamination with large branched molecules decreases toward lower elution volumes and obviously there is no contamination at the very beginning of the chromatogram. It may be noted that the anchoring affects not only the ability of SEC-MALS to characterize branching, but also the ability to determine the molar mass distribution and molar mass averages. Since light scattering measures M_w and R_z by its first principle, these two quantities are correct even in the case of poor SEC separation. On the other hand, the value of M_n is affected strongly, because the lower-molar-mass fractions are the most contaminated. As the contamination effect is small at the beginning of the chromatogram, the value of M_z that counts strongly the high-molar-mass fractions can be considered to be almost correct (assuming no shearing degradation).

The distribution of branching along the molar mass axis (i.e., plots of g versus M or m versus M) can be overlaid with the molar mass distribution curve as shown in Figure 6.12. Such a plot permits the determination of branching distribution with respect to the molar mass. Using the data presented in Figure 6.12 one can see that molecules with molar mass below about 10^5 g/mol are linear. This represents almost 40% of molecules in the given sample. The fraction of molecules with molar mass over 10^6 g/mol represents about 8%, which means about 8% of molecules in the sample have more than seven branch units on average.

Figure 6.13 compares branching results obtained by means of radius and viscosity methods. It shows the relation between g obtained directly from the

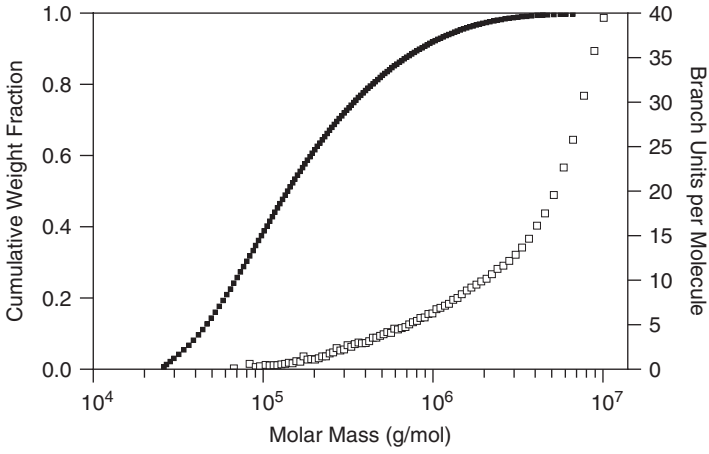

Figure 6.12 Cumulative molar mass distribution plot of randomly branched polystyrene (■) and number of branch units per molecule (□). Branch units calculated from g determined by A4F-MALS (see Figure 6.11).

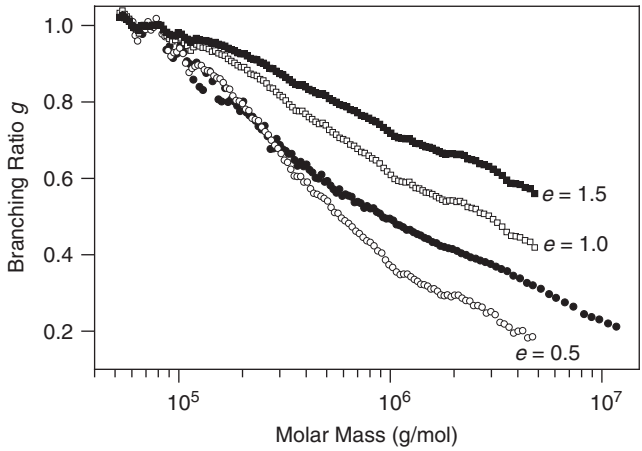

Figure 6.13 Molar mass dependence of branching ratio g determined by radius method (•) and calculated from g' using different values of draining parameter e.

conformation plot (Figure 6.9), and calculated from the Mark-Houwink plot (Figure 6.6) using Equations 6.10 and 6.11 with various values of draining parameter. None of the boundary values of e provide good agreement of results generated from the RMS radii and intrinsic viscosities. The best agreement of the two plots is obtained using e of about 0.7. However, since the parameter e depends on the properties of polymer chain and experimental conditions, no general validity of this value can be assumed.

The comparison of results obtained by the radius and mass methods is depicted in Figure 6.14. Similarly as in the viscosity method, the

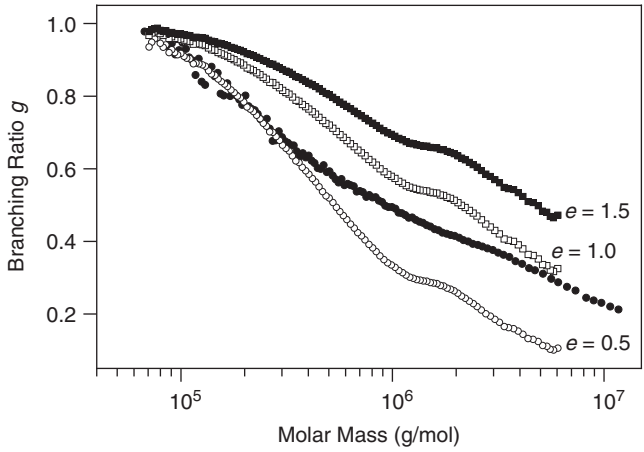

Figure 6.14 Molar mass dependence of branching ratio g determined by radius method (•) and mass method using different draining parameters e.

obtained results strongly depend on the draining parameter and the best agreement of the mass method with the radius method is achieved for e around 0.7.

Although g calculated by means of viscosity and mass methods depends on the value of parameter e and generally does not concur with g obtained by the radius method, with the same e the viscosity and mass methods yield consistent results, as demonstrated in Figure 6.15.

Despite uncertainty of the calculation of g from the intrinsic viscosity due to the commonly unknown parameter e, the intrinsic viscosity has the great advantage of the possibility of measurement of relatively small branched molecules for which the RMS radius cannot be determined. Characterization of lower-molar-mass polymers is demonstrated in Figure 6.16 for star poly(DL-lactic acid) with tripentaerythritol as a branching agent. The RMS radius of such polycondensates is below the detection limit of elastic light scattering and thus the intrinsic viscosity appears as a suitable alternative. The Mark-Houwink plot allows clear detection of branching in the analyzed sample. As molar mass increases, the difference of the intrinsic viscosity between the branched molecules and the linear reference increases, which indicates that molecules of higher molar mass consist of more arms.

Although more detailed analysis of the obtained experimental data regarding the number of arms is limited by the uncertainty of draining parameter e, the data undoubtedly prove the presence of branched macromolecules, and allow mutual comparison of different samples, as well as give a certain feeling of the number of arms. Figure 6.16 also presents the molar mass–versus–elution volume plot that can serve as a simple alternative for branched oligomers when a viscometer is not available.

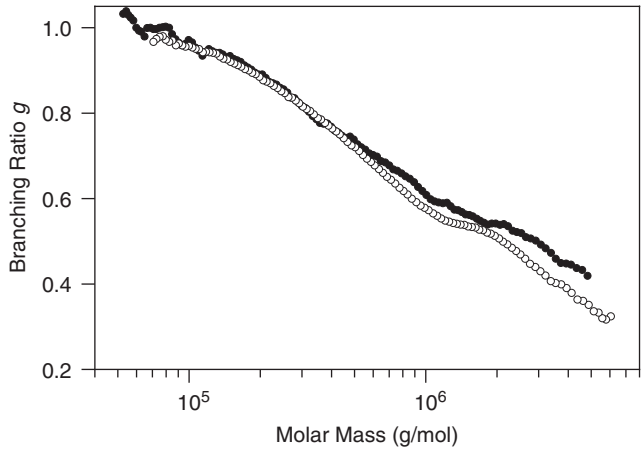

Figure 6.15 Molar mass dependence of branching ratio g determined by viscosity method (•) and mass method (○) using $e = 1$.

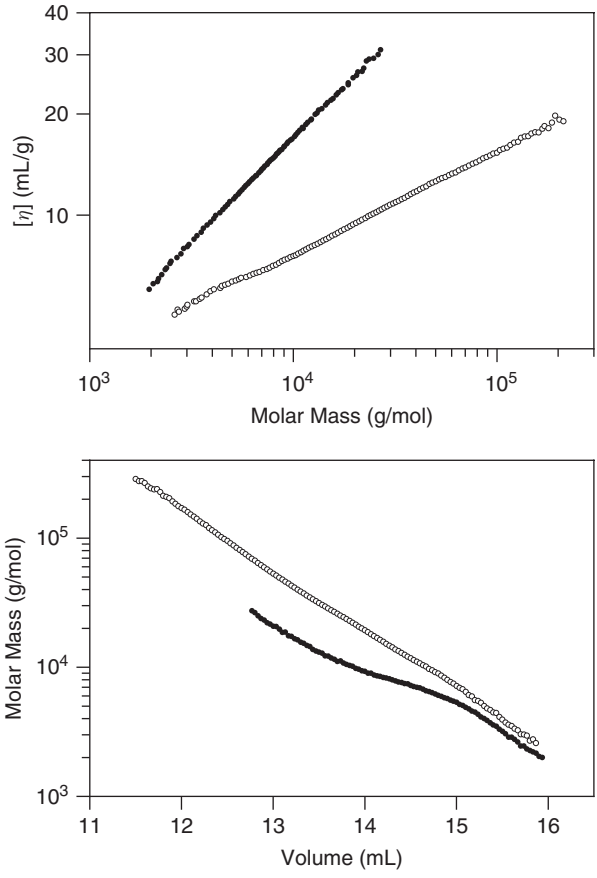

Figure 6.16 Branching analysis of lower-molar-mass polymer: Mark-Houwink plots (top) and molar mass–versus–elution volume plots (bottom) of linear (•) and branched (○) poly(DL-lactic acid).

6.2.3 Average Branching Ratios

A possible advantage of the average branching ratios is that some of the needed information can be obtained by the batch measurements of an unfractionated sample, namely M_w and R_z by classical light scattering and $[\eta]_w$ by a capillary viscometer. Moreover, these averages are not at all or only negligibly affected by the anchoring effect during the SEC separation. The average branching ratios are (1) average branching ratio g_{M_z} calculated for the same M_z, and (2) average branching ratio g'_{M_w} calculated at the same M_w.

The calculation of the average g_{M_z} at the same M_z requires knowledge of R_z and M_z. The former quantity can be obtained by a classical light scattering experiment in the batch mode or by SEC-MALS; the latter can be determined by SEC-MALS. It has been explained that the classical light scattering experiment provides R_z by its fundamental principle and consequently the value of R_z is not influenced by the anchoring effect in SEC column packing. The anchoring effect

on M_z is relatively small, because this quantity counts mainly the high-molar-mass fractions that are not contaminated by molecules delayed by anchoring. In addition to the experimentally determined R_z and M_z the relation between RMS radius and molar mass for the linear polymer of the identical chemical composition must be known. Let us illustrate the calculation on the branched polystyrene (see conformation and Mark-Houwink plots in Figures 6.9 and 6.6, respectively). The experimental results obtained by SEC-MALS are as follows:

$R_z = 37.0$ nm

$M_z = 1.24 \times 10^6$ g/mol

The relation RMS radius versus molar mass $R = 0.014 \times M^{0.585}$ can be found in the literature.[15] Using this relation and experimental M_z one can calculate R_z of a linear polymer of the same M_z as that of branched polymer: $R_z = 0.014 \times (1.24 \times 10^6)^{0.585} = 51.4$ nm, which yields average branching ratio $g_{M_z} = 0.52$.

A similar calculation leads to the average branching ratio g'_{M_w} at the same M_w:

$[\eta]_w = 68.4$ mL/g

$M_w = 370{,}000$ g/mol

Using the literature[16] Mark-Houwink equation $[\eta] = 0.0117 \times M^{0.717}$, the intrinsic viscosity of a linear polymer having the same M_w as the branched polymer is 115.0 mL/g and consequently average branching ratio g'_{M_w} for the entire sample is 0.59. Note that the average g'_{M_w} can be determined solely by batch measurements with no influence of chromatography separation.

A possible drawback of g_{M_z} is that a part of fractions with very high molar mass can be retained in SEC columns and/or undergo shearing degradation. The R_z and M_z determined by A4F for our branched polystyrene can be used for the sake of demonstration:

$R_z = 43.7$ nm

$M_z = 2.27 \times 10^6$ g/mol

Significantly larger R_z and M_z determined by A4F and smaller average g_{M_z} of 0.36 indicate that some of the high-molar-mass fractions were degraded by shear or retained in SEC columns.

Comparison of g_{M_z} and g'_{M_w} for several branched polymers is shown in Table 6.1. It is worth mentioning that the two average ratios are not supposed to be identical, because they are based on different molar mass averages with different sensitivities to the fractions with very high molar mass, and they are mutually related with the draining parameter e, which is generally not equal to unity. It must be also pointed out that g_{M_z} and g'_{M_w} are not true moments of their distribution, and especially g_{M_z} reflects mainly the branching degree of the most-branched fractions (i.e., those with the highest molar mass).

The calculation of the average branching ratios as well as the determination of the relation between g and M require log-log relations R versus M and $[\eta]$ versus

Table 6.1 Comparison of g_{M_z} and g'_{M_w} for Various Branched Polymers Obtained by SEC-MALS-VIS

Polymer	M_w (10^3 g/mol)	g_{M_z}	g'_{M_w}
Randomly branched PS (8)	180	0.71	0.81
Randomly branched PS (9)	220	0.63	0.77
Randomly branched PS (42)	270	0.53	0.71
Randomly branched PS (B1)	250	0.53	0.80
Randomly branched PS (10)	370	0.52	0.59
Randomly branched PS (19)	55	0.49	0.80
Randomly branched PS (40)	330	0.47	0.64
Randomly branched PS (B2)	540	0.45	0.60
Randomly branched PS (20)	80	0.42	0.67
Star PBZMA (197/1)	2,900	0.09	0.09
Star PBZMA (199/1)	2,100	0.09	0.08
Star PS 8-arm	350	0.32	0.51
Brush PS	7,200	0.07	0.04

M for linear polymer of the same chemical composition as the branched polymer under investigation. The latter can be found in the literature for many polymer solvent systems. The published data are not always consistent and careful selection of the literature values and if possible their experimental verification should be carried out. Published relations R versus M are significantly less frequent.

Table 6.2 lists parameters of conformation plots for several common polymers. The determination of the conformation and Mark-Houwink plots requires measurements of a series of narrow standards or a broad polymer sample with polydispersity $M_w/M_n \approx 2$ and more. Narrow standards can be measured either in batch or online mode, whereas broad polymers require online measurement. The necessary condition is that the data cover a sufficiently broad range of molar mass of at least one order of magnitude. It must be noted that measurement of a single narrow polymer can lead to false results and conclusions about branching.

Table 6.2 Constants of Relation $R = k \times M^b$

Polymer	k	b
Polystyrene	0.014	0.585
Poly(methyl methacrylate)	0.012	0.583
Poly(benzyl methacrylate)	0.0114	0.580
Polybutadiene	0.016	0.597
Polyisobutylene	0.0145	0.581
Polyisoprene	0.012	0.611
Polyethylene	0.0186	0.596

Note: THF and room temperature with exception of PE (TCB at 135°C).

6.2.4 Other Methods for the Identification and Characterization of Branching

A certain limitation of the conformation plot based on the RMS radius is the impossibility of characterizing smaller polymers with a majority of molecules with RMS radii below 10 nm. Since the hydrodynamic radius can be accurately determined down to about 1 nm, the relation between the hydrodynamic radius and molar mass (i.e., R_h conformation plot) may become a suitable alternative.

Figure 6.17 shows the conformation plot for a relatively small polymer. Due to the scattering of RMS radii the slope of the conformation plot is determined with high uncertainty. In contrast, the R_h conformation plot appears significantly more reliable and allows accurate determination of the slope. In fact, the same information about the molecular structure can be obtained from the Mark-Houwink plot. However, the R_h conformation plot is a closer equivalent of the RMS radius conformation plot with the slope approximately equal to that based on the RMS radius.

A possible advantage of the R_h conformation plot over that based on the RMS radius is low sensitivity to abnormal SEC elution, as demonstrated in Figure 6.18. In addition, the R_h conformation plot is less sensitive to the light scattering formalisms used for data processing than the RMS radius conformation plot. A conformation plot based on R_h can be determined by SEC-MALS-VIS or SEC-MALS-DLS.

Comparison of the slopes of the conformation plots based on the RMS radius and hydrodynamic radius is shown in Table 6.3, which also includes the slopes of the Mark-Houwink plots. It may be noted that larger differences of the slopes of Mark-Houwink plots of linear and branched polymers compared

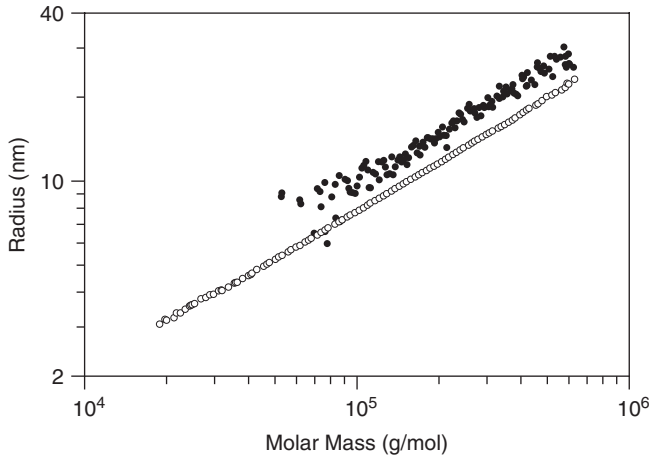

Figure 6.17 RMS radius (•) and hydrodynamic radius (○)–versus–molar mass plots of linear poly(isobutyl methacrylate) determined by SEC-MALS-VIS.

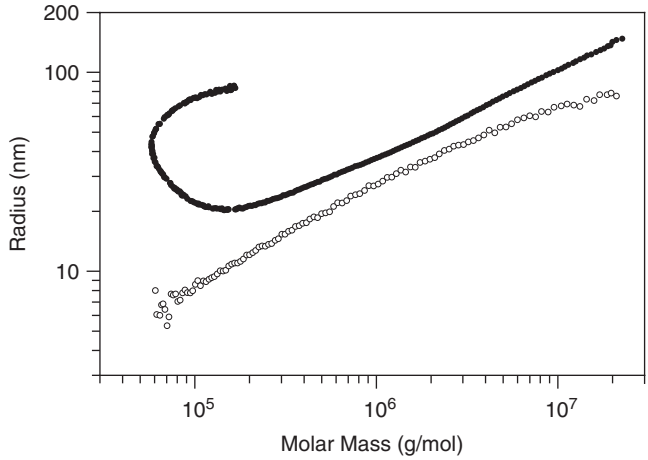

Figure 6.18 RMS radius (•) and R_h (○) conformation plots of randomly branched polystyrene determined by SEC-MALS-DLS.

Table 6.3 Slopes of Conformation Plots Based on RMS Radius and Hydrodynamic Radius and Exponents of Mark-Houwink Relation for Linear and Branched Polymers

Polymer	Slope of Conformation Plot Based on		Mark-Houwink Exponent
	RMS Radius	Hydrodynamic Radius	
Linear PS	0.57	0.57	0.70
Linear PS (NIST 706)	0.57	0.57	0.70
Linear PMMA (Y)	0.57	0.57	0.71
Linear PBZMA (38)	0.57	0.57	0.70
Linear PIBMA	—	0.57	0.73
Randomly branched PS (10)	0.46	0.50	0.51
Randomly branched PS (40)	0.46	0.50	0.50
Randomly branched PS (42)	0.45	0.51	0.51
Star PBZMA (197/1), high f	0.49	0.39	0.15
Star PIBMA, high f	—	0.36	≈ 0

to the differences of the slopes of conformation plots confirm higher sensitivity of the Mark-Houwink plot to detect and differentiate branching.

Burchard et al.[14] suggested the characterization of branching on unfractionated samples and derived theoretical equations for various branched structures. In contrast to g, where the radii are compared either at the same molar mass (in the case of narrow fractions eluting from a separation device) or at the same z-average molar mass (in the case of unfractionated polymer), they came with the definition of g on the basis of R_z at the same weight-average molar mass. A potential advantage of this approach is given by the fact that the quantities R_z and M_w are directly measured by a batch light scattering experiment, while the

z-average molar mass is not directly accessible by light scattering and requires an online fractionation. In contrast to g defined at the same molar mass or M_z, where g decreases with the branching degree and is always smaller than unity, the g defined at the same M_w can be larger than unity and increase with the increasing number of branch units. The explanation of this behavior is that polydispersity causes a larger increase of R_z than the corresponding increase of M_w. The g value is then a result of two counteracting effects: polydispersity, which causes an increase, and branching, which causes a decrease. A typical feature of randomly branched polymers is very high polydispersity, which overwhelms the decrease due to the branching.

Another quantity for the characterization of branching suggested by Burchard et al. is the dimensionless ratio ρ:[14]

$$\rho = \frac{R_z}{R_{h,z}} \tag{6.13}$$

where $R_{h,z}$ is the z-average hydrodynamic radius obtained by dynamic light scattering. A potential advantage of the ratio ρ is that it does not require data for linear chains as reference.

The ratio ρ is readily measurable by combination of static and dynamic light scattering. In addition, with the combination of SEC-MALS-DLS(VIS) or A4F-MALS-DLS the ratio ρ can be measured across the molar mass distribution of polymers and thereby indicate the change of polymer architecture along the molar mass axis. The values of the dimensionless ratio ρ were derived for various polymer architectures in theta and thermodynamically good solvents.[5,14]

The ability of the dimensionless ratio ρ to detect and characterize branching is based on the fact that the two radii are of different definitions and reflect different properties, namely distribution of mass around the center of gravity and the hydrodynamic dimensions. Comparison of RMS radii and hydrodynamic radii of linear polystyrene is presented in Figure 6.19. It may be noted that the difference of R_h based on diffusion coefficient and intrinsic viscosity is small and that the molar mass dependencies of R and R_h are parallel.

Graphical representation of ratio ρ as a function of molar mass for a linear polymer, a randomly branched polymer, and a star polymer with a large number of arms is shown in Figure 6.20. Almost constant values of ρ across the molar mass distribution for the linear chains indicate identical molecular architecture across the molar mass distribution. Decreasing ρ for randomly branched molecules toward high molar masses indicate change of the molecular structure with molar mass as is typical of randomly branched polymers. However, it is not clear why the parameter ρ for the fractions with lower molar mass is larger than in the case of linear molecules. The lowest ρ for the stars consisting of large numbers of arms can be interpreted as a consequence of highly compact molecular structure.

Branching information can be also revealed from the pattern of particle scattering function. Functions $P(\theta)$ for various branched structures can be found in

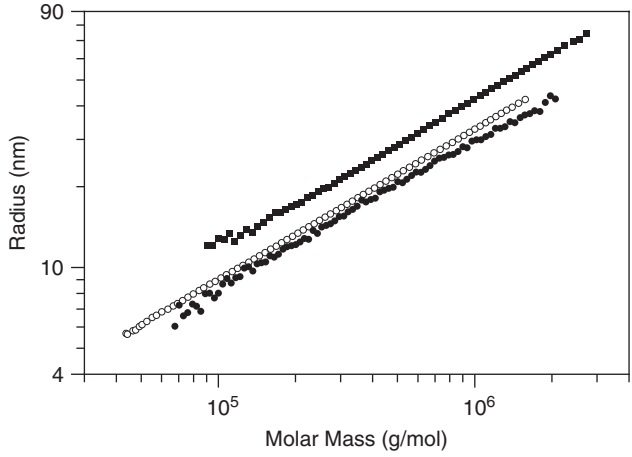

Figure 6.19 Molar mass dependence of RMS radius (■) and hydrodynamic radius determined by DLS (●) and viscometry (○) for linear polystyrene.
Data obtained by SEC-MALS-DLS and SEC-MALS-VIS, THF at 25°C.

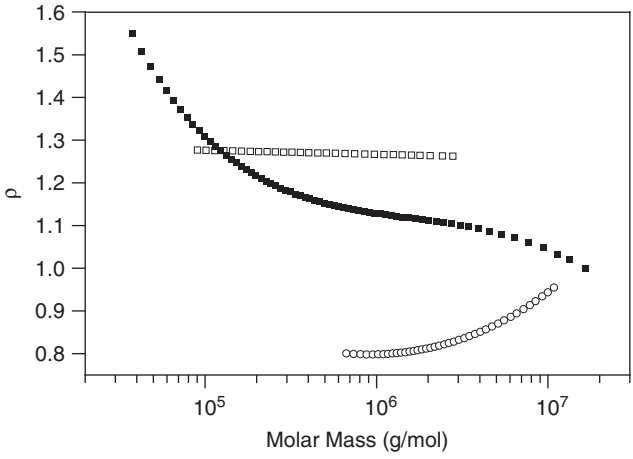

Figure 6.20 Ratio $\rho = R/R_h$ as a function of molar mass for linear polystyrene (□), randomly branched polystyrene (■), and star poly(benzyl methacrylate) of large f (○).

the literature.[14,17] In order to infer branching information the molecules must have large dimensions, which represents a significant limitation of applicability.

Another possible parameter characterizing the branching degree is the ratio of the weight-average molar mass determined by conventional SEC, M_w(SEC), to the true M_w determined by light scattering. Both M_w(SEC) and M_w can be obtained in a single SEC-MALS experiment when the obtained RI signal is processed also using the column calibration. The ratio M_w(SEC)/M_w is certainly the least fundamental parameter describing the degree of branching that has no direct

relation to the number of branch units or arms in branched macromolecules. However, it may appear useful especially in the case of smaller branched polymers that are characterized by SEC-MALS without a viscometer. Since SEC separates molecules according to their hydrodynamic volume, the elution volume itself bears information about the molecular size, and consequently the M_w(SEC) calculated from a calibration curve is related to the average hydrodynamic size. If polystyrene calibration is used for data processing, the M_w(SEC) can be interpreted as the weight-average molar mass of a hypothetical sample of polystyrene having the same distribution of hydrodynamic volume as a polymer under investigation. Similarly to g and g', the ratio M_w(SEC)/M_w decreases with increasing degree of branching. However, depending on the relation between the calibration applied for data processing and the true calibration for a polymer under investigation, the ratio M_w(SEC)/M_w for a linear polymer may be larger or smaller than unity.

6.3 EXAMPLES OF CHARACTERIZATION OF BRANCHING

It has been shown that there are several possible methods useful for the characterization of polymer branching. Some of them are of rather theoretical applicability and their real ability to provide information about the branching seems to be limited. That is the case with the particle scattering function, which can provide structural information only for very large macromolecules. Additional experimental data may be needed to further verify the usability of parameter ρ, because not all results appear as straightforward as those shown in Figure 6.20. Some methods are purely empirical and have no direct relation to branched structure, such as the ratio M_w(SEC)/M_w. However, simplicity and applicability over broad molar mass range is the great advantage of this ratio, which can be readily determined by combination of conventional SEC and SEC-MALS.

The conformation plot appears to be the soundest way to obtain branching information, but it is significantly restricted by the impossibility of studying smaller molecules and moreover by frequently poor SEC separation of large, highly branched macromolecules. Consequently, the combination of A4F with MALS appears to be the most efficient method for branching studies of larger macromolecules, while for smaller branched molecules SEC-MALS-VIS will usually be the best choice. However, there is no general method for branching characterization. The results obtained by the particular methods need not be identical, but they should provide the same trends. The combination of results obtained by different methods may confirm the presence or absence of branching and indicate the structure of branched molecules. For successful branching investigation it is important to understand the limits and realize that really detailed characterization is usually impossible, and that any obtainable information may be valuable. The purpose of this chapter is to show several typical examples of data for various branched polymers, which should facilitate proper interpretation of the reader's own experimental results and help avoid making false conclusions.

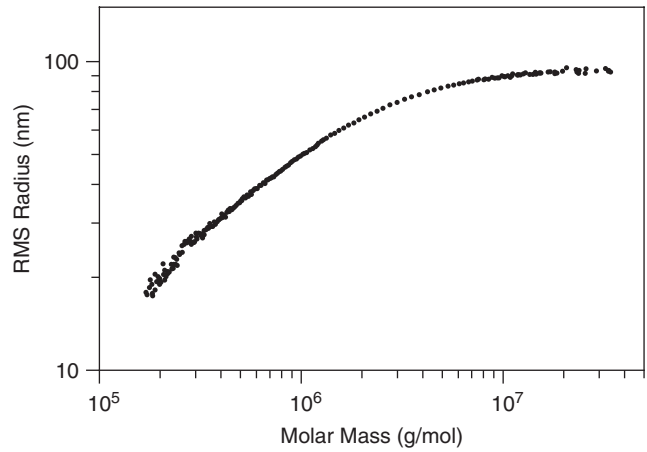

Figure 6.21 Conformation plot of randomly branched polymer with slope leveling off toward high molar masses.

Figure 6.21 is an example of a conformation plot with the slope decreasing toward high molar masses. At the high-molar-mass end, the conformation plot reaches a plateau, which means that a further increase of molar mass is absorbed inside the polymer coil without increase of molecular size. This pattern of conformation plot is typical for randomly branched polymers containing high-molar-mass fractions with high degree of branching.

Figure 6.22 shows an example of Mark-Houwink plot for a linear oligomer. The slope of about 0.5 could lead to a false conclusion of the presence of branching. However, the slope of the Mark-Houwink plots of linear oligomers is close to 0.5 even in thermodynamically good solvents, since the excluded volume

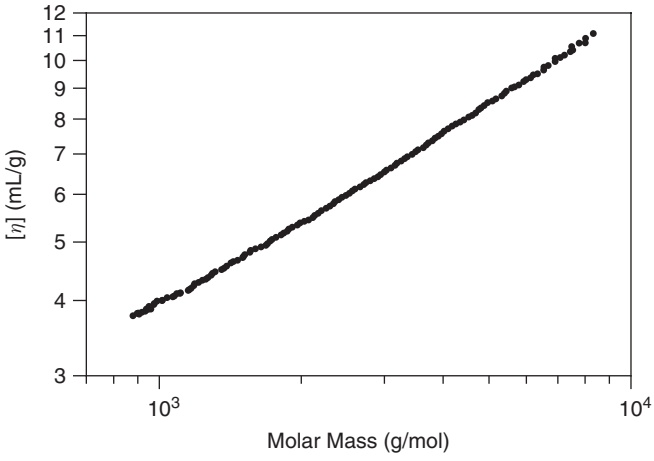

Figure 6.22 Mark-Houwink plot of linear oligoester: Mark-Houwink exponent $a = 0.48$.

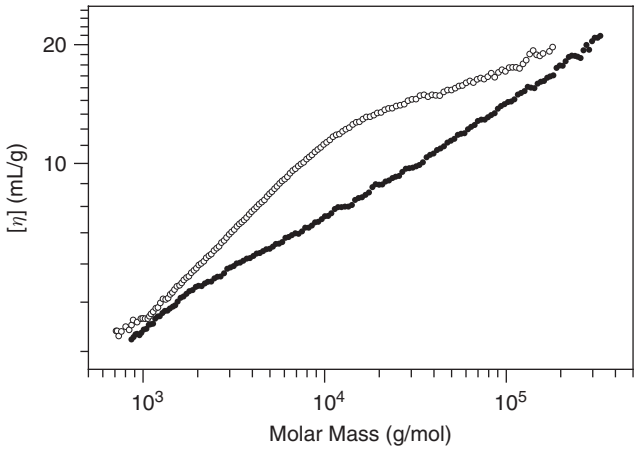

Figure 6.23 Mark-Houwink plots of unsaturated polyester resins of different distributions of branching.

effect is absent in the case of oligomeric chains that are too short to obey the intramolecular self-avoiding behavior.

Figure 6.23 depicts Mark-Houwink plots for two unsaturated polyester (UP) resins. One of the UP resins prepared from difunctional monomers (○) shows different slopes of the Mark-Houwink plot. The slope up to the molar mass of about 10,000 g/mol is roughly 0.5, which is in good agreement with the Mark-Houwink exponents for model UP resins that were prepared with maleic anhydride replaced with succinic acid that has no double bond capable of side reactions. Above a molar mass of about 10,000 g/mol the slope is significantly lower (≈ 0.16),

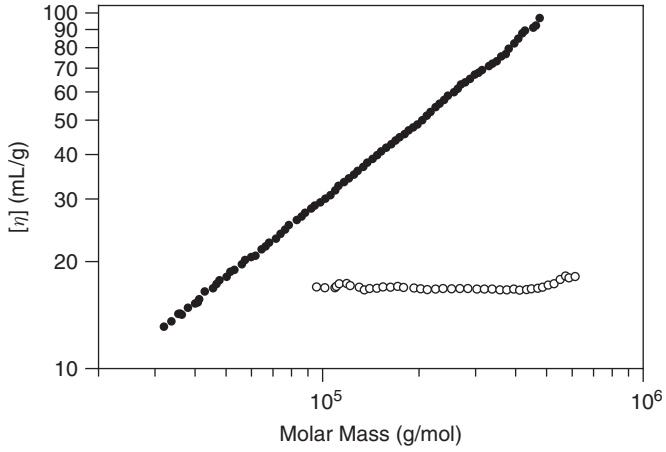

Figure 6.24 Mark-Houwink plots of linear (•) and star high-*f* (○) poly(isobutyl methacrylate). Zero slope indicates compact sphere-like structure of star macromolecules.

which can be explained by side reactions of double bonds of maleic anhydride leading to formation of branched molecules. The second UP resin (•), which was prepared with an addition of six-functional dipentaerythritol, shows a markedly lower Mark-Houwink exponent of ≈ 0.26 from the region of low molar masses. In this resin the addition of polyfunctional monomer resulted in the formation of branched molecules from the beginning of molar mass distribution.

Figure 6.24 compares the Mark-Houwink plot of linear poly(isobutyl methacrylate), PIBMA, with that of star-branched PIBMA with high numbers of arms prepared by GTP. The plot of linear PIBMA is linear as is characteristic of linear polymer with typical slope of ≈ 0.7, while the slope of the star PIBMA is close to zero, which indicates a highly compact molecular structure resembling compact spheres.

Another example of Mark-Houwink plots with the slopes in proximity to zero is shown in Figure 6.25 for a series of high-*f* star-branched polymers. The mutual shift of the plots along the axis of intrinsic viscosity indicates different compactness of the sphere-like macromolecules. It is worth noting that the Mark-Houwink

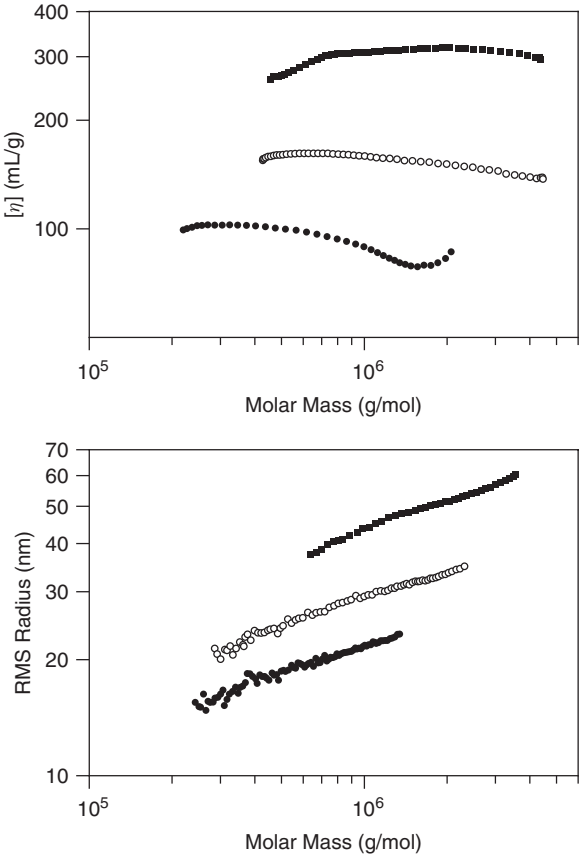

Figure 6.25 Mark-Houwink plots with the slopes close to zero for highly branched sphere-like polymers (top) and the corresponding conformation plots obtained by A4F-MALS (bottom). Slopes of the conformation plots ≈ 0.23.

plots show regions of decrease of the intrinsic viscosity with increasing molar mass. Such behavior was described for dendrimers[18] and explained as due to the polymer growing faster in density than in radial growth, when the intrinsic viscosity initially increases with molar mass, reaches a maximum, and then steadily decreases with increasing molar mass. The Mark-Houwink plots are completed by the corresponding conformation plots with the slopes confirming compact sphere-like structure of the analyzed molecules.

Figure 6.26 shows conformation and branching ratio g–versus–molar mass plots for starlike poly(benzyl methacrylate) prepared by GTP. Unlike the g-versus-M plot of randomly branched polymers (e.g., Figure 6.11), the plot in this figure starts at very low g and further decreases with increasing molar mass. This indicates that the sample does not contain, with the exception of residual unreacted arms that are not included in the plot, linear molecules. That is a significant difference compared to randomly branched polymers that typically contain a large part of linear molecules of lower molar mass. According to

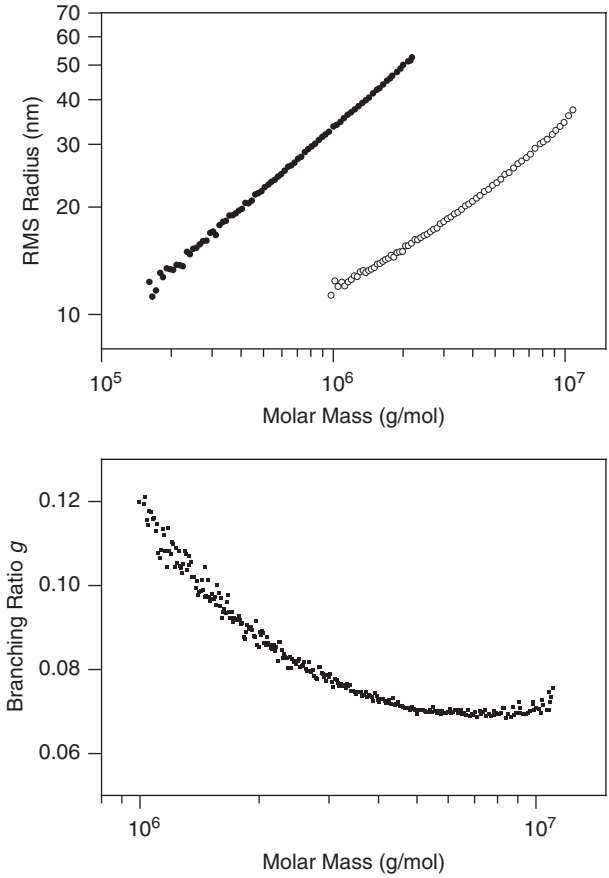

Figure 6.26 Conformation plots of linear (•) and star high-f (○) poly(benzyl methacrylate) (top) and branching ratio–versus–molar mass plot (bottom).

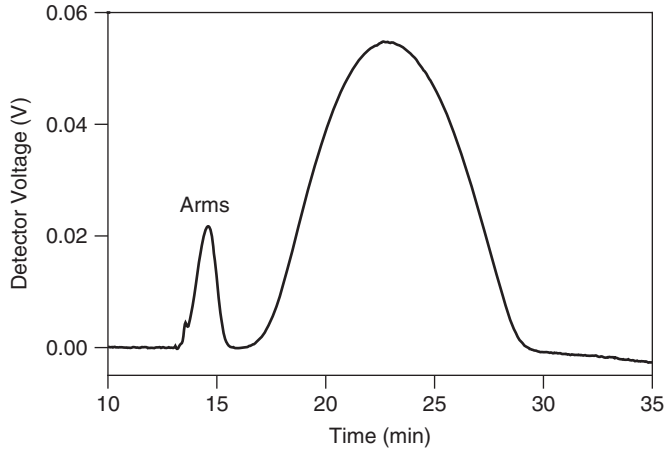

Figure 6.27 A4F RI fractogram showing separation of unreacted arms from stars for poly(benzyl methacrylate) prepared by GTP. Conformation and g-versus-M plots are shown in Figure 6.26.

Equation 6.8, the branching ratio g of 0.1–0.07 corresponds to about 60–80 arms. The presence of unreacted arms (see Figure 6.27) in the sample and the determination of their molar mass allow the estimation of number of arms by dividing M_n of stars and arms. This results in an average number of about 70 arms, which is in very good agreement with the value estimated from g.

Figure 6.28 compares conformation plots of two branched polystyrene samples. The plot of one of the samples is shifted to lower RMS radii, which can be explained by higher branching degree and thus higher polymer coil density. The

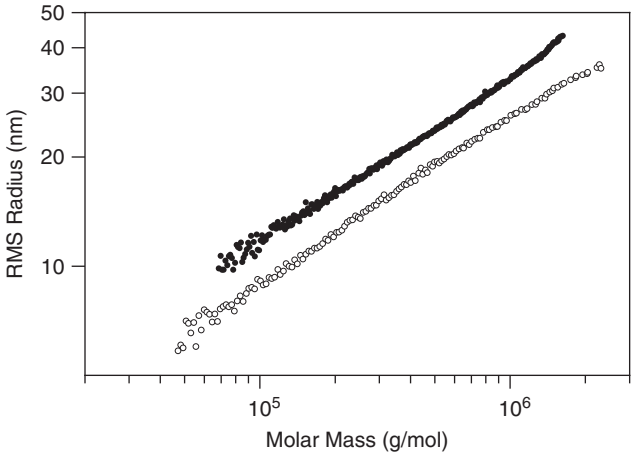

Figure 6.28 Conformation plots of two randomly branched polystyrene samples prepared using identical amounts of divinylbenzene (0.5% wt), but different initiator concentrations, namely 0.1% (•) and 1% (○). Conversion: 26% and 63% for initiator concentration of 0.1% and 1%, respectively.

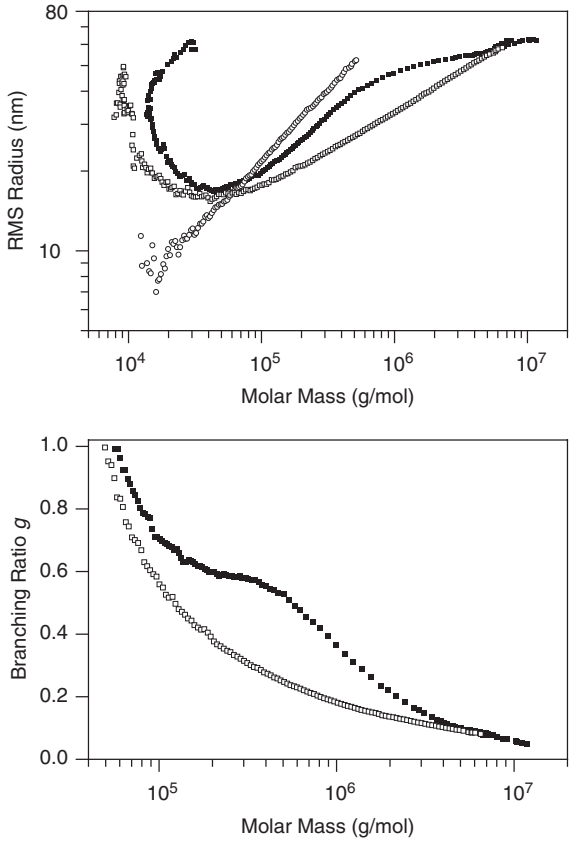

Figure 6.29 Conformation plots (top) and g-versus-M plots (bottom) of linear polyethylene NIST SRM 1475 (o) and two branched polyethylenes: NIST SRM 1476 (■) and a commercial sample (□). Columns 3× PLgel Mixed-B, TCB at 1 mL/min, 160°C.

samples were prepared using identical levels of branching co-monomer (divinylbenzene), but different concentrations of initiator of radical polymerization. The higher radical concentration resulted in higher conversion of divinylbenzene (i.e., higher number of branch units), and also shorter chains due to termination by recombination of growing radicals.

Figure 6.29 contrasts conformation plots of three polyethylenes and the branching ratios of the two branched samples. The conformation plots of both branched samples cross that of linear polyethylene and show typical upturn in the region of lower molar masses. Except for the upturn, the conformation plot of standard NIST SRM 1476 polyethylene (■) can be separated into two regions with different slopes suggesting different branching topology, while the slope of the commercial sample (□) is approximately constant. The obtained data indicate that up to molar mass of about 5×10^6 g/mol, NIST SRM 1476 is less branched than the commercial sample since its conformation plot is shifted to higher RMS radii and the branching ratio is larger. At the region of high molar masses the

plots of the two branched polyethylenes meet each other, which indicates similar degree of branching.

6.4 KEYNOTES

- The fundamental principle of branching characterization is based on the fact that branching reduces molecular size.
- The molar mass and a parameter characterizing molecular size are necessary to determine the degree of branching.
- The effect of long-chain branching on the size of branched macromolecules in dilute solution is characterized with parameter g, which is defined as the ratio of the mean square radius of a branched molecule to that of a linear molecule at the same molar mass. The parameter g decreases with increasing degree of branching and can be used to calculate the number of branch units or number of arms in branched molecules. An alternative branching ratio g' is defined as the ratio of the intrinsic viscosity of a branched molecule divided by the intrinsic viscosity of a liner molecule at the same molar mass. The branching ratios g and g' are related via the draining parameter e, whose values are supposed to be in the range 0.5–1.5. However, the exact e values are usually unknown.
- SEC-MALS, A4F-MALS, and SEC-MALS-VIS data can be processed in three different ways to detect the presence of branched molecules and get information about the distribution of branching with respect to molar mass. The branching ratio g can be obtained from (1) conformation plot, (2) molar mass–versus–elution volume plot, and (3) Mark-Houwink plot.
- Two average branching characteristics g_{M_z} and g'_{M_w} can be calculated, the latter being obtainable even without chromatographic separation. In addition, the ratio $M_w(\text{SEC})/M_w$ can be used as a simple parameter capable of identifying branching and differentiating branching degree of polymers of identical chemical composition.
- The conformation plot, which is the most direct way to obtain parameter g and further branching characteristics, is often affected by the anchoring of branched molecules in the pores of SEC column packing. Anchoring increases the polydispersity of slices at the region of higher elution volumes. Since polydispersity causes a larger increase of the z-average RMS radius compared to the weight-average molar mass, the conformation plots become upward at the region of lower molar masses.
- A crucial requirement for the determination of a true conformation plot is that the molecules eluting from the separation device are almost monodisperse. For many large branched polymers this requirement is not fulfilled using SEC due to the anchoring effect in the pores of column packing. The anchoring effect is totally eliminated in the case of A4F, where the separation occurs in an empty channel and such highly efficient separation

of branched molecules is achieved resulting in perfectly linear conformation plots with no artifacts. Another requirement for the determination of accurate conformation plot is avoiding the marginal scattered data points.

- Lower sensitivity to the anchoring effect and the possibility of characterizing small branched polymers are advantages of the SEC-MALS-VIS measurements.

6.5 REFERENCES

1. Meunier, D. M., Smith, P. B., and Baker, S. A., *Macromolecules*, **38**, 5313 (2005).
2. Podzimek, S., Vlcek, T., and Johann, C., *J. Appl. Polym. Sci*., **81**, 1588 (2001).
3. Trinkle, S., Walter, P., and Fredrich, C., *Rheol. Acta*, **41**, 103 (2002).
4. Auhl, D., Stange, J., Munstedt, H., Krause, B., Voigt, D., Lederer, A., Lappan, U., and Lunkwitz, K., *Macromolecules*, **37**, 9465 (2004).
5. Burchard, W., *Adv. Polym. Sci*., **143**, 113 (1999).
6. Zimm, B. H. and Stockmayer, W. H., *J. Chem. Phys*., **17**, 1301 (1949).
7. Orofino, T. A., *Polymer*, **2**, 305 (1961).
8. Kurata, M. and M. Fukatsu, *J. Chem. Phys*., **41**, 2934 (1964).
9. Burchard, W., *Macromolecules*, **10**, 919 (1977).
10. Burchard, W., *Adv. Polym. Sci*., **48**, 1 (1983).
11. Stockmayer, W. H. and Fixman, M., *Ann. N.Y. Acad. Sci*., **57**, 334 (1953).
12. Zimm, B. H. and Kilb, R. W., *J. Polym. Sci*., **37**, 19 (1959).
13. Yu, L. P. and Rollings, J. E., *J. Appl. Polym. Sci*., **33**, 1909 (1987).
14. Burchard, W., Schmidt, M., and Stockmayer, W. H., *Macromolecules*, **13**, 1265 (1980).
15. Podzimek, S., *J. Appl. Polym. Sci*., **54**, 91 (1994).
16. Kolinsky, M. and Janca, J., *J. Polym. Sci.: Polym. Chem. Ed*., **12**, 1181 (1974).
17. Burchard, W., *Macromolecules*, **5**, 604 (1972); **7**, 835, 842 (1974); **10**, 919 (1977).
18. Mourey, T. H., Turner, S. R., Rubinstein, M., Frechet, J. M. J., and Wooley, K. L., *Macromolecules*, **25**, 2401 (1992).

Symbols

A	Absorbance
A	Peak area, slice area
A_2	Second virial coefficient
A_3	Third virial coefficient
a	Exponent of Mark-Houwink equation
a	Extinction coefficient
a	Parameter of Schulz-Zimm distribution
a	Radius of sphere
b	Channel breadth
b	Exponent of the molar mass dependence of the root mean square radius
b	Parameter of Schulz-Zimm distribution
C_∞	Asymptotic value of the characteristic ratio C_n
c	Concentration
c_0	Concentration at accumulation wall
c^*	Critical concentration
D	Diffusion coefficient
D	Sphere diameter
d	Density
d	Particle diameter
dn/dc	Specific refractive index increment
E	Flow activation energy
e	Draining parameter
F_d	Fractionating power based on particle diameter
F_M	Fractionating power based on molar mass
$F_w(\log M)$	Weigh-differential molar mass distribution in logarithmic scale
f	Functionality of branch unit
f	Instrumental constant of light scattering photometer
f	Monomer functionality

Light Scattering, Size Exclusion Chromatography and Asymmetric Flow Field Flow Fractionation: Powerful Tools for the Characterization of Polymers, Proteins and Nanoparticles, by Stepan Podzimek

f	Number of arms
$f_n(M)$	Number-differential molar mass distribution
$f_w(M)$	Weigh-differential molar mass distribution
$G(V)$	Detector signal (chromatogram)
g	Branching ratio (branching index) based on the root mean square radius
g	Gravitational acceleration (9.81 m/s^2)
g'	Branching ratio based on the intrinsic viscosity
$g(V)$	Normalized detector signal (normalized chromatogram)
$g(\tau)$	Autocorrelation function
H	Plate height
H	Peak or slice height
H_d	Contribution of axial diffusion to plate height
H_n	Contribution of nonequilibrium to plate height
H_p	Contribution of polydispersity to plate height
IP	Inlet pressure
$I_n(M)$	Number-cumulative molar mass distribution
$I_w(M)$	Weight-cumulative molar mass distribution
I_0	Intensity of the incident radiation
I_θ	Intensity of scattered radiation at angle θ
K	Constant of Mark-Houwink equation
K_d	SEC distribution coefficient
K^*	Optical constant
k	Boltzmann's constant (1.38065×10^{-23} JK^{-1})
k	Capacity factor in liquid chromatography
k	Proportionality constant of molar mass dependence of root mean square radius
k_H	Huggins constant
k_K	Kraemer constant
L	Channel length
L	Column length
L	Flow cell length
L	Length of tube
L	Rod length
l	Segment length
l	Distance of sample layer center from the accumulation wall
M	Molar mass
M_n	Number-average molar mass
M_{PEAK}	Molar mass at peak
M_v	Viscosity-average molar mass
M_w	Weight-average molar mass
M_z	z-average molar mass
M_{z+1}	$z+1$-average molar mass
M_w/M_n	Polydispersity
M_0	Mass of monomeric unit
M_0	Parameter of log-normal distribution

m	Mass
m	Average number of branch units per molecule
m	Relative refractive index of scattering molecules
m_0	Slope of the angular variation of scattered light intensity at zero angle
N	Number of measurements
N	Number of theoretical plates
N_A	Avogadro's number (6.022×10^{23} mol^{-1})
n	Number of moles
n	Number of segments
n	Refractive index of polymer solution
n_w	Weight-average number of branch units per molecule
n_0	Solvent refractive index
P	Polymerization degree
P_n	Number-average polymerization degree
P_w	Weight-average polymerization degree
ΔP	Pressure difference
$P(\theta)$	Particle scattering function
p	Hydrostatic pressure
Q	Volumetric flow rate
q	Reaction conversion
R	Correction factor based on nominal and experimental polydispersity
R	Gas constant (8.314 JK^{-1} mol^{-1})
R	Inner radius of capillary
R	Retention ratio
R	Root mean square radius (radius of gyration)
RF_{UV}	Response factor of UV detector
R_h	Hydrodynamic radius
R_n	Number-average root mean square radius
R_S	Resolution
R_{SP}	Specific resolution
R_w	Weight-average root mean square radius
R_z	z-average root mean square radius
R_θ	Excess Rayleigh ratio at angle θ
R^2	Mean square radius
$R(\theta)$	Excess Rayleigh ratio at angle θ
$\langle R^2 \rangle$	Mean square radius
$\langle R^2 \rangle^{\frac{1}{2}}$	Root mean square radius (radius of gyration)
r	Inner radius of column
r	Molar ratio of monomers A and B
$r_{1,2}$	Relative retention in liquid chromatography
$\langle r \rangle^2$	Mean square end-to-end distance
$\langle r^2 \rangle^{1/2}$	Root mean square end-to-end distance
$\langle r^2 \rangle_0^{1/2}$	Root mean square end-to-end distance in theta conditions

S	Selectivity
s	Peak symmetry
s	Sedimentation coefficient
T	Temperature
T_g	Glass transition temperature
t	Time
t_R	Retention time
t_0	Retention time of unretained component
u_0	Cross flow velocity at the accumulation wall
$u(x)$	Cross flow velocity at distance x from the accumulation wall
V	Volume
V	Elution volume
V_c	Volume of SEC column, $V_c = V_0 + V_i + V_g$
V_e	Elution volume
V_g	Volume of SEC packing matrix
V_h	Hydrodynamic volume
V_i	Volume of the solvent inside the pores of SEC packing
V_i	Voltage at the ith elution volume slice
V_R	Retention volume
V_t	Total solvent volume in SEC column, $V_t = V_0 + V_i$
V_0	Channel volume
V_0	Volume of the mobile phase outside the SEC packing particles
$\dot{V}$	Volumetric flow rate
$\dot{V}$	Volumetric detector flow rate
$\dot{V}_c$	Volumetric cross flow rate
$\dot{V}_{in}$	Volumetric channel inlet flow rate
V_R'	Net retention volume
ΔV	Slice elution volume (volume between two data points)
v	Migration velocity of sample molecules
$v(x)$	Carrier velocity at distance x from the accumulation wall
$\langle v \rangle$	Average cross-sectional carrier velocity
W	Peak width at the baseline
$W_{1/2}$	Peak width at half height
w	Channel thickness
w	Weight fraction
x	Distance from the accumulation wall
x	Molar (number) fraction
$\bar{x}$	Arithmetic average
z	Axial dimension of channel
z_f	Position of focusing line
α	Expansion factor based on the root mean square end-to-end distance
α	Calibration constant of RI detector
α_R	Expansion factor based on the root mean square radius
α_η	Expansion factor based on the intrinsic viscosity
β	Exponent of the molar mass dependence of diffusion coefficient

β	Parameter of log-normal distribution
β	Signal amplitude of the autocorrelation function
γ	Shear rate
δ	Solubility parameter
ε	Parameter in Ptitsyn-Eizner equation
η	Viscosity (dynamic viscosity)
η_{inh}	Inherent viscosity
η_{red}	Reduced viscosity (viscosity number)
η_{rel}	Relative viscosity
η_{sp}	Specific viscosity
$[\eta]$	Intrinsic viscosity
ϑ	Exponent of the molar mass dependence of the second virial coefficient
λ	Branching frequency
λ	Retention parameter
λ	Wavelength of light in medium
λ_0	Vacuum wavelength of light
μ	Scattering vector
μ	Polydispersity M_w/M_n
$\bar{v}$	Partial specific volume
π	Osmotic pressure
ρ	Ratio of R to R_h
σ	Standard deviation
σ	Steric factor
σ^2	Variance of the chromatographic peak
τ	Delay time
τ	Relaxation time
Φ	Flory constant after correction for non-theta conditions
Φ_0	Flory constant
φ	Volume fraction of polymer in solution

Abbreviations

A4F	Asymmetric flow field flow fractionation
BHT	2,6-Ditert-butyl-4-hydroxy toluene
BSA	Bovine serum albumin
CRYSTAF	Crystallization analysis fractionation
DGEBA	Diglycidyl ether of bisphenol A
DLS	Dynamic light scattering
DMF	N,N-dimethyl formamide
DMSO	Dimethyl sulfoxide
DNA	Deoxyribonucleic acid
DRI	Differential refractive index
DVB	Divinylbenzene
EGDMA	Ethyleneglycol dimethacrylate
ELSD	Evaporative light scattering detector
EP	Epoxy resin
ESI	Electrospray ionization
FFF	Field flow fractionation
GPC	Gel permeation chromatography
GTP	Group transfer polymerization
HA	Hyaluronic acid
HEMA	Hydroxyethyl methacrylate
HFIP	Hexafluoroisopropanol (1,1,1,3,3,3-Hexafluoro-2-propanol)
HPLC	High-performance liquid chromatography
ICP	Inductively coupled plasma
IR	Infrared
LALLS	Low-angle laser light scattering
LC	Liquid chromatography
MALDI	Matrix-assisted laser desorption ionization
MALS	Multi-angle light scattering

Light Scattering, Size Exclusion Chromatography and Asymmetric Flow Field Flow Fractionation: Powerful Tools for the Characterization of Polymers, Proteins and Nanoparticles, by Stepan Podzimek

MO	Membrane osmometry
MS	Mass spectrometry
NMP	N-methylpyrrolidone
NMR	Nuclear magnetic resonance
NIST	National Institute of Standards and Technology
PBZMA	Poly(benzyl methacrylate)
PDA	Photodiode array
PE	Polyethylene
PEG	Poly(ethylene glycol)
PES	Polyester
PET	Poly(ethylene terephthalate)
PIBMA	Poly(isobutyl methacrylate)
PMMA	Poly(methyl methacrylate)
PTFE	Polyetetrafluoro ethylene (Teflon)
PS	Polystyrene
QELS	Quasielastic light scattering
RALS	Right-angle light scattering
REACH	Registration, Evaluation, and Authorization of Chemicals
RGD	Rayleigh-Gans-Debye
RI	Refractive index
RMS	Root mean square
RSD	Relative standard deviation
SD	Standard deviation
SEC	Size-exclusion chromatography
SP	Separation performance
SRM	Standard reference material
TCB	1,2,4-Trichlorobenzene
THF	Tetrahydrofuran
TOF	Time-of-flight mass analyzer
TREF	Temperature-rising elution fractionation
UC	Ultracentrifugation
UP	Unsaturated polyester
UV	Ultraviolet
VIS	Viscometry (viscosity detection)
VPO	Vapor pressure osmometry (vapor-phase osmometry)

Index

Light Scattering, Size Exclusion Chromatography and Asymmetric Flow Field Flow Fractionation: Powerful Tools for the Characterization of Polymers, Proteins and Nanoparticles, by Stepan Podzimek